PO Box 2345, Beijing 100023, China
www.wjgnet.com
wjg@wjgnet.com

ELSEVIER

World J Gastroenterol 2005;11(44):6899-6904
World Journal of Gastroenterology ISSN 1007-9327

Clinicopathological study of cardiac tamponade due to pericardial metastasis originating from gastric cancer

Michiya Kobayashi, Takehiro Okabayashi, Ken Okamoto, Tsutomu Namikawa, Keijiro Araki

Michiya Kobayashi, Takehiro Okabayashi, Ken Okamoto, Tsutomu Namikawa, Keijiro Araki, Department of Tumor Surgery, Kochi Medical School, Nankoku 783-8505, Japan
Supported by KOBAYASHI MAGOBE Memorial Medical Foundation
Correspondence to: Michiya Kobayashi, MD, PhD, Department of Tumor Surgery, Kochi Medical School, Oko-cho, Nankoku, Kochi 783-8505, Japan. kobayasm@kochi-ms.ac.jp
Telephone: +81-888-80-2370 Fax: +81-888-80-2371
Received: 2005-05-02 Accepted: 2005-07-19

Key words: Gastric cancer; Pericarditis carcinomatosa; Cardiac tamponade; Chemotherapy

Kobayashi M, Okabayashi T, Okamoto K, Namikawa T, Araki K. Clinicopathological study of cardiac tamponade due to pericardial metastasis originating from gastric cancer. *World J Gastroenterol* 2005; 11(44): 6899-6904
http://www.wjgnet.com/1007-9327/11/6899.asp

Abstract

AIM: To review the cases reported in the literature, examined their clinicopathological features, and evaluated the efficacy of different therapeutic modalities for this rare condition.

METHODS: A search of the MEDLINE database revealed 16 cases of pericarditis carcinomatosa (PC) originating from GC reported in the literature between 1982 and 2005. Additional detailed data were obtained from the authors of these studies for subsequent clinicopathological investigation. We have also described about a case study from our own clinic.

RESULTS: The mean age of cases with pericarditis carcinomatosa originating from GC was 54 years. Females were diagnosed at a younger age (46.3 years) compared to males (58 years). The mean survival period after diagnosis was 4.5 mo. No statistical differences in the length of survival time were found between different therapeutic modalities, such as drainage, and local and/or systemic chemotherapy after drainage. However, three cases who underwent systemic chemotherapy survived for more than 10 mo. Cases that developed metachronous cardiac tamponade for more than 2 years after the diagnosis of GC generally survived for a longer period of time, although this was not statistically significant. Multivariate analysis revealed that low levels of carcinoembryonic antigen (CEA), and CEA and/or cancer antigen 19-9 (CA 19-9) were associated with longer survival.

CONCLUSION: Cases with low levels of CEA, and CEA and/or CA 19-9 should undergo systemic chemotherapy with or without local chemotherapy after drainage.

INTRODUCTION

Malignant pericardial effusion typically develops slowly and can spontaneously regress or remain stable. Some cases, however, may progress to cardiac tamponade[1]. Pericardial effusion can be caused by common primary malignancies that metastasize to the pericardium, such as lung cancer, lymphoma, breast cancer, and leukemia[2-4]. Cardiac tamponade due to pericarditis carcinomatosa (PC) originating from a primary gastric cancer (GC) is a rare condition. It is usually detected during the terminal stages of GC; however, it is also detected during cardiac emergencies. There are several reports of cardiac tamponade due to GC; however, most of them are only case reports. Due to the limited number of cases seen in a single institute, we performed a clinicopathological study of the cases of PC originating from GC reported in the literature, including a case from our hospital, and investigated the best therapeutic modality for this rare condition.

MATERIALS AND METHODS

A search of the MEDLINE database revealed 16 cases of PC originating from GC reported in the literature and meeting proceedings between 1982 and 2005 (Table 1)[5-15]. Cases in which PC was synchronous with GC and its recurrence were included. In addition, we asked the authors of these studies to review the available medical records to obtain more information about the cases.

A 36-year-old female patient, diagnosed with Kruckenberg's tumor, who consulted our clinic for further examination, was included in this case study. Endoscopic examination revealed GC of the antrum. The patient underwent distal gastrectomy with lymph node dissection. Histological examination showed that signet-ring cell carcinoma was mostly confined within the mucosal layer and had slightly invaded the muscular layer. Histology also showed lymph node metastases in a wide area with

Table 1 Reported cases of cardiac tamponade due to pericarditis carcinomatosa from gastric cancer.

Case	Author	Year	Sex	Age	Hist[1]	T	ly	v	n	Time interval[2]	Symptom	AST	ALT	ALP	LDH	CEA	CA19-9	Treatment[3]	Survival[4]
1	Ohtomo	1982	F	33	ud	2	3	NA	NA	0	Cough	31	26	297	365	NA	NA	D	5.0
2	Koide	1984	M	67	NA	NA	NA	NA	NA	NA	NA	NA	NA	NA	NA	NA	NA	D	2.0
3		1984	F	65	NA	NA	NA	NA	NA	NA	NA	NA	NA	NA	NA	NA	NA	D	5.0
4	Usami	1989	F	44	NA	NA	NA	NA	NA	NA	NA	NA	NA	NA	NA	NA	NA	L	1.3
5	Moriyama	1995	M	64	por	>2	NA	NA	>1	2.5 mo	Chest pain	38	11	4.2KA	832	240.1	26.7	S + L	1.5
6	Orihata	1996	M	51	sig	2	0	0	0	27.5 mo	Dyspnea	417	283	281	921	2.3	1 100	L	3.0
7	Sakusabe	1998	M	42	por	2	2	0	0	77 mo	Hypotension	25	35	142	154	0.6	2.7	L	3.5
8	Unno	1998	F	48	sig	NA	NA	NA	NA	7 mo	Dyspnea	51	56	503	235	0.7	47	L	1.5
9	Sakai	1999	M	45	sig	1	3	NA	3	0	Dyspnea	14	18	299	211	1.7	8.6	D	2.5
10	Kobayashi	2000	M	44	sig	1	2	1	2	19 mo	Dyspnea	22	94	456	216	2.5	56	S + L	5.0
11	Hiramatsu	2002	M	51	por	2	2	1	2	26 mo	Fatigue	1 224	1 087	NA	NA	3.0	27.9	S	10.0
12	Saitoh	2003	M	68	tub1	1	2	0	2	4 mo	Hypotension	NA	NA	NA	NA	12.5	238	S	2.5
13		2003	M	69	sig	2	3	3	2	50 mo	Cough	44	58	307	377	3.6	15.5	S + L	14.0
14	Sakusabe	2005	M	69	tub1	2	1	2	0	13 mo	Dyspnea	NOR	NOR	NOR	NOR	5.7		S	2.5
15	Suto	2003	F	52	sig	2	3	2	1	26 mo	Dyspnea	N	N	N	N	N	178.4	D	4.0
16		2003	M	68	tub2	3	3	2	3	32 mo	Dyspnea	N	N	N	N	41.6	894.1	D	1.0
17	Author		F	36	sig	2	2	1	2	27.5 mo	Vomit	95	152	312	272	0.76	9.78	S + L	13.0

NA: data not available, NOR: within normal range

[1]Hist: Histology, ud: undifferentiated carcinoma, por: poorly differentiated adenocarcinoma, sig: signet-ring cell carcinoma, tub1: well differentiated tubular adenocarcinoma, tub2: moderately differentiated tubular adenocarcinoma

[2]Time interval: time interval from the diagnosis of gastric cancer to the onset of cardiac tamponade

[3]D: drainage only, L: local chemotherapy, S: systemic chemotherapy

[4]Survival: survival after onset of cardiac tamponade (months)

Cases 11, 13 and 14 were cited from meeting proceedings.

massive permeation into the lymphatic vessels. The patient underwent postoperative chemotherapy of sequential methotrexate plus 5-fluorouracil. Twenty-seven and a half months after the operation, she developed nausea and laboratory data showed elevated levels of aspartate aminotransferase (95 IU/L), alanine aminotransferase (152 IU/L) and alkaline phosphatase (312 IU/L). An abdominal CT scan revealed massive pericardial effusion and left pleural effusion. The patient underwent pericardiocentesis and left pleural centesis. Cytological examination of the fluid revealed signet-cell carcinoma. After drainage, 10 mg of cisplatin was infused into the pericardial space. The pericardial effusion subsequently disappeared. She underwent injection chemotherapy into the pleural space (135 mg cisplatin) and systemic chemotherapy (cisplatin and sequential methotrexate plus 5-fluorouracil) until the pericardial effusion reappeared 9.5 mo later. Pericardiocentesis was performed again and 150 mg cisplatin was infused into the pericardial space. She also underwent systemic chemotherapy, however, died 13 months after the onset of PC.

Survival curves were generated using the Kaplan-Meier method and compared using the log-rank test. Multivariate Cox regression analysis was used to identify factors independently associated with mortality. For multivariate analysis, all factors were dichotomized: gender (male, female), time interval between diagnosis of gastric cancer and diagnosis of cardiac tamponade (<24 mo including synchronous cases, >24 mo), carcinoembryonic antigen (CEA) levels (<5.0, >5.0 ng/mL), cancer antigen 19-9 (CA 19-9, <40 U/mL, >40 U/mL), and systemic chemotherapy (done, not done). Using the Pearson's χ^2 test, differences in proportions were evaluated. $P<0.05$ was considered statistically significant.

RESULTS

The clinicopathological features of cardiac tamponade due to PC originating from GC are presented in Table 2. More than half of the patients were males, an occurrence similar to that generally seen in GC. The mean age of the 17 cases was 54 years (range, 33-69 years). Females diagnosed with cardiac tamponade tended to be younger (mean, 46.3 years; range, 33-65 years) as compared with the males (mean, 58 years; range, 42-69 years). Of the 17 cases, 14 died within 6 mo of diagnosis. Figure 1 shows the Kaplan-Meier survival curve for all the 17 cases. The mean survival after the diagnosis of PC was 4.5 mo (range: 1.0-14.0 mo). Histological data was obtained for 12 of the cases. Of these, 11 were of the less differentiated type. Eleven of the twelve cases also showed lymphatic permeation, and nine showed lymph node metastasis.

The different treatments used after the diagnosis of cardiac tamponade and the survival of the corresponding cases are shown in Table 3. Six cases underwent pericardiocentesis only, and the mean survival after the diagnosis of cardiac tamponade was 3.3 mo. Eleven cases underwent local infusion chemotherapy targeting the pericardial space and/or systemic chemotherapy following pericardiocentesis. The mean survival periods of the cases treated with local chemotherapy, systemic chemotherapy, and combined local and systemic chemotherapy were

Table 2 Clinicopathological analysis of cardiac tamponade due to PC from GC

Male:female	11:6
Mean age (yr; *n* = 17)	54.0 (range: 33-6)
Male	58.0 (range: 42-69)
Female	46.3 (range: 33-65)
Histological types (*n* = 14)	
sig	7
por	3
ud	1
tub	3
T (*n* = 13)	
1	3
2	9
3	1
ly (*n* = 12)	
0	1
1	1
2	5
3	5
v (*n* = 10)	
0	3
1	3
2	3
3	1
n (*n* = 12)	
0	3
1	2
2	5
3	2

The histological types, "T", "ly", "v", and "n", are defined in the General Rules for the Gastric Cancer Study by Japanese Research Society for Gastric Cancer[26]. sig: signet-ring cell carcinoma; por: poorly differentiated carcinoma; ud: undifferentiated carcinoma; and tub: tubular adenocarcinoma.

For T which represents depth of cancer invasion, 1: mucosal and submucosal layer; 2: proper muscular and subserosal layer; 3: expose to serosal layer; and 4: invasion to the adjacent organ.

For ly and v which represent lymphatic permeation and venous permeation, respectively, 0: none; 1: slight; 2: moderate; and 3: massive.

Table 3 Treatment and corresponding mean survival time after the diagnosis of cardiac tamponade

Modalities	*n*	Mean survival (mo)
Drainage only	6	3.3
Drainage+chemotherapy		
Local only	4	2.3
Systemic+local	4	8.4
Systemic only	3	5.0

Local: local infusion chemotherapy into pericardial space.

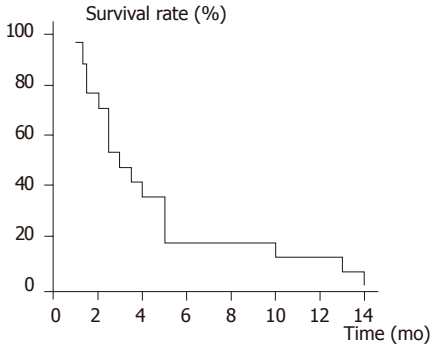

Figure 1 Kaplan-Meier survival curve of all cases (*n* = 17).

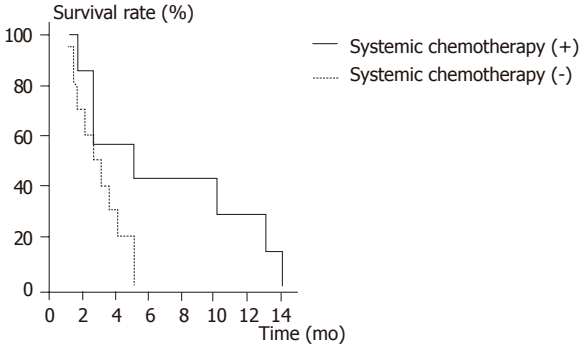

Figure 2 Kaplan-Meier survival curve according to administration of systemic chemotherapy. The cases treated with systemic chemotherapy were more likely to survive longer (*P* = 0.0579) than those who were not treated with systemic chemotherapy.

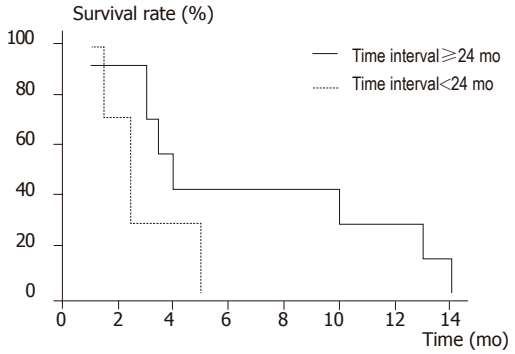

Figure 3 Kaplan-Meier survival curve according to time period between the diagnosis of gastric cancer and diagnosis of cardiac tamponade. The cases in whom cardiac tamponades were diagnosed for more than 24 mo after the diagnosis with gastric cancer were more likely to survive longer than those in whom cardiac tamponade was diagnosed for less than 24 mo after the initial diagnosis of gastric cancer. However, there was no statistical difference between the two groups (*P* = 0.1130).

2.3, 5.0, and 8.4 mo, respectively. All the three cases who had survived for more than 10 mo underwent systemic chemotherapy (two cases: local and systemic; one case: systemic only).

Statistical analyses of the prognostic factors are presented in Table 4. Cases treated with systemic chemotherapy tended to survive longer (6.9 mo) than those who were not treated with systemic chemotherapy (*P* = 0.0579; Figure 2). The mean survival period of the cases that developed cardiac tamponade within 2 years after the diagnosis of primary GC, including one synchronous case, was 2.9 mo. This was shorter than the cases in which the onset of cardiac tamponade occurred 2 years after the diagnosis of GC (6.9 mo). However, there were no statistical differences between the two groups (*P* = 0.1130; Figure 3). The mean

Table 4 Clinical characteristics of cardiac tamponade due to pericarditis carcinomatosa from GC

Characteristics	*n*	Survival rate (%) 1 mo	5 mo	10 mo	Median survival in months (range)	*P* values
Overall	17	94.2	17.7	11.8	4.5 (1.0-14.0)	
Gender						
Male	11	90.9	18.2	9.1	4.3 (1.0-14.0)	
Female	6	-	16.7	-	5.0 (1.3-13.0)	0.7614
Time interval						
<24 mo	7	-	0.0	0.0	2.9 (1.5-5.0)	
>24 mo	7	85.7	-	28.5	6.9 (1.0-14.0)	0.1130
CEA (ng/mL)						
<5	9	-	-	22.2	6.3 (1.5-14.0)	
>5	4	75.0	0.0	0.0	1.9 (1.0-2.5)	0.0071
CA 19-9 (U/mL)						
<40	6	-	33.3	16.7	7.4 (1.5-14.0)	
>40	6	-	0.0	0.0	2.8 (1.0-5.0)	0.1074
CEA and/or CA 19-9						
Normal	5	-	0.0	0.0	8.6 (2.5-14.0)	
High	8	87.5	0.0	0.0	2.6 (1.0-5.0)	0.0244
Systemic chemotherapy						
Done	7	-	42.9	28.6	6.9 (1.5-14.0)	
Not done	7	90.0	0.0	0.0	2.8 (1.0-5.0)	0.0579

Table 5 Relative risk of death as analyzed by Cox proportional Hazards model

Variables	*B* value	Relative risk (95%CI)	*P* values
CEA			
<5.0 ng/mL			
>5.0 ng/mL	1.9	6.7 (1.2–36.6)	0.029
CEA and/or CA-19-9			
<5.0 ng/mL, <40 U/mL			
>5.0 ng/mL, >40 U/mL	1.6	4.9 (1.0-23.7)	0.049

95%CI: confidence interval.

survival periods of cases with high levels (>5.0 ng/mL) and normal levels (<5.0 ng/mL) of CEA were 6.3 and 1.9 months, respectively (P = 0.0071; Figure 4). The mean survival periods of cases with high levels (>40 U/mL) and normal levels (<40 U/mL) of CA 19-9 were 2.8 and 7.4 months, respectively (P = 0.1074). The cases in which either CEA and/or CA 19-9 were elevated at the time of cardiac tamponade had shorter survival periods (2.6 mo) as compared with the cases without CEA and/or CA 19-9 elevation (8.6 mo) (P = 0.0244). Multivariate analysis also revealed that high levels of CEA and CEA and/or CA 19-9 were associated with poor survival (P = 0.029 and 0.049, respectively; Table 5).

DISCUSSION

Secondary tumors of the heart and/or pericardium are rarely diagnosed in clinical practice. However, it is not uncommon to find these during autopsy cases. Secondary cardiac metastases most frequently arise from primary lung tumors. Primary GC rarely metastasize to the heart, with 4.3-7.7%[16-19] reported from autopsy investigations.

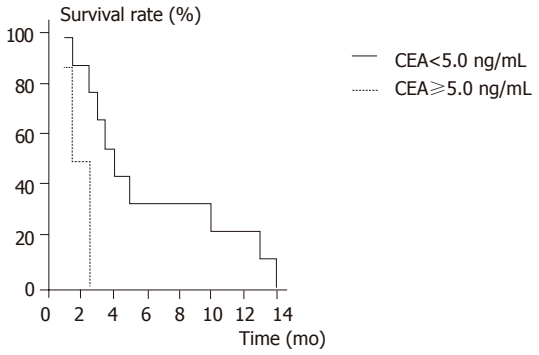

Figure 4 Kaplan-Meier survival curve according to CEA levels. The cases with normal CEA levels had a longer survival period as compared to those with high CEA levels (P = 0.0071).

We investigated 17 reported cases of cardiac tamponade due to PC originating from GC, and observed several characteristics specific to this condition. The mean age of the patients was 54 years, which was slightly younger than the average age reported for GC. Females tended to be diagnosed at a younger age than males. Histopathological results of 11 out of the 12 cases showed less differentiated tumors with massive lymphatic involvement. Raven[20] and Hanfling[21] reported that the hematogenous route was the most common metastatic pathway to the heart, while Warren and Gates[22] and Kline[23] believed that the cardiac lymphatic system was the major metastatic pathway to the heart. The fact that almost all cases showed massive lymphatic permeation suggested that the mechanism of pericardial metastasis might be through the lymphatic system.

There is no defined therapy for pericardial metastasis. Most reports describing therapeutic modalities for cardiac tamponade due to malignant pericarditis were based on cases in which lung cancer was the primary tumor. Drainage of the malignant effusion either by percutaneous pericardiocentesis or by pericardiectomy should be performed if this condition is diagnosed. The prognosis of cardiac tamponade caused by malignant pericarditis is grave and survival is limited. Fraser *et al*.[24] reported the prognosis of 21 cases and more than half of the 21 cases originated from lung cancer. Seven patients treated with pericardiocentesis and provided with supportive care had a median survival time of 3 wk. Eight patients treated with pericardiocentesis and either radiotherapy and/or intrapericardial or systemic chemotherapy had a median survival period of 3.5 mo. Six patients treated with pericardiocentesis and pericardiectomy with or without radio- or chemotherapy had a median survival period of 6 mo. Moreover, Appelqvist *et al*.[1] reported the prognosis of three cases of pericardiectomy. Among them, two cases had primary lung cancer, while the primary tumor was of unknown origin in the third case. The case who did not undergo treatment only survived for 5 wk, the case treated with radiotherapy survived for 7 wk, and the case treated with systemic chemotherapy survived for 9 mo[1].

To our knowledge, there are no reports investigating the different therapeutic modalities available for the treatment of cardiac tamponade originating from GC. Our review of the literature showed that the therapeutic modalities in 6 cases were only the drainage of malignant effusion, while the 10 cases underwent chemotherapy after the drainage. In addition, the chemotherapy treatment varied in the cases with the routes of administration of anti-cancer agents (e.g., intrapericardial infusion and/or systemic administration), the type of anti-cancer agents, and the dose of anti-cancer agents. More than half of the cases treated with local chemotherapy received various doses of cisplatin. We found that there were no complications caused by local chemotherapy in our review of the literature, and cisplatin was the most frequently used agent for local chemotherapy. The agents used for local chemotherapy should be less irritable to the heart. As the number of cases was limited, we were unable to determine which treatment was the most effective for this condition. However, we did find that cases treated with systemic chemotherapy tended to survive longer than those who were not ($P = 0.0579$).

The period of time from the diagnosis of gastric cancer to the onset of cardiac tamponade may influence prognosis. When the time period was less than 2 years, the survival was 2.9 mo, and if the time period was over 2 years, the survival increased to 6.9 mo. The cases with high levels of either of the tumor markers CEA or CA 19-9 had a shorter survival period than those with low levels of either of these markers.

Honda *et al*.[25] reported a case of cardiac tamponade originating from lung cancer, in which the malignant cardiac effusion was controlled by weekly paclitaxel therapy. Sakusabe *et al*.[15] also reported that weekly administration of paclitaxel was effective for the control of malignant pericardial effusion originating from GC. There are many reports demonstrating that malignant ascites arising from GC can be controlled by paclitaxel in patients diagnosed with peritonitis carcinomatosa of GC. We confirmed that the level of paclitaxel in malignant ascites remained effective until 72 h after systemic administration (submitted for publication). Paclitaxel may, therefore, be a promising agent for systemic chemotherapy, and should be considered for the treatment of malignant pericardial effusion.

In summary, we were unable to reveal which therapy was the best for extending the life expectancy in cases of PC originating from GC. However, the cases with systemic chemotherapy survived for a longer period of time compared to the cases treated with drainage only or with local chemotherapy. The cases that developed cardiac tamponade due to PC arising from GC more than 2 years after the diagnosis, and the cases in which the levels of CEA and CA 19-9 were not elevated may have a possibility of surviving for a longer period of time. Such cases should undergo chemotherapy following emergency pericardiocentesis. While a specific chemotherapeutic strategy has not yet been developed for these cases, the use of paclitaxel for systemic, and cisplatin for local chemotherapy may be promising for the treatment of cardiac tamponade caused by PC arising from GC.

REFERENCES

1 **Appelqvist P,** Maamies T, Gröhn P. Emergency pericardiotomy as primary diagnostic and therapeutic procedure in malignant pericardial tamponade: report of three cases and review of the literature. *J Surg Oncol* 1982; **21:** 18-22

2 **Thurber DL,** Edwards JE, Achor RW. Secondary malignant tumors of the pericardium. *Circulation* 1962; **26:** 228-241

3 **Kusnoor VS,** D'Souza RS, Bhandarkar SD, Golwalla AF. Malignant pericardial effusion. Report of 2 cases. *J Assoc Physicians India* 1973; **21:** 101-104

4 **Theologides A.** Neoplastic cardiac tamponade. *Semin Oncol* 1978; **5:** 181-192

5 **Ohtomo T,** Sakanaka M, Urano S, Shimizu I, Kitamura H, Kunishige H, Andachi H. Superficial spreading carcinoma of the stomach presenting as neoplastic cardiac tamponade: report of a case with autopsy findings. *Matsushita Med J* 1982; **20:** 28-35

6 **Koide S,** Kawada S, Inoue H, Ogawa J, Fukuda T, Inamura S. Shohtsu A, Hoshiai M. Cardiac tamponade - especially with subxiphoid pericardial window. *Heart* 1984; **16:** 504-511

7 **Usami I,** Kato M, Hayashi Y, Kuroki H, Hanaki H, Furutani M, Yamada Y, Takeuchi T. Local treatment of cancerous pericarditis by cisplatin. *Jpn J Lung Cancer* 1989; **29:** 127-131

8 **Moriyama A,** Murata I, Kuroda T, Yoshikawa I, Tabaru A, Ogami Y, Otsuki M. Pericardiac metastasis from advanced gastric cancer. *J Gastroenterol* 1995; **30:** 512-516

9 **Orihata M,** Hata M, Hase Y, Nakagawa H, Kidokoro T, Yamanaka O, Sagawa F. A case of cardiac tamponade induced by cardiac metastasis of a gastric cancer two years after a surgical treatment. *J Jpn Surg Assoc* 1996; **57:** 862-866

10 **Unno J,** Yasunami T, Ishiko T, Koizumi M, Ichikawa K, Arai S, Okuyama H, Hayashida N, Kouda S, Tadokoro M. A case study of gastric carcinoma presenting as carcinomatous pericarditis and meningeal carcinomatosis. *Gan no Rinsho* 1998; **44:** 1555-1559

11 **Sakusabe M,** Yoshioka H, Niwa M. A case of cardiac tamponade secondary to gastric cancer after curative gastrectomy. *J Jpn Surg Assoc* 1998; **59:** 2578-2581

12 **Sakai Y,** Minouchi K, Ohta H, Annen Y, Sugimoto T. Cardiac tamponade originating from primary gastric signet ring cell carcinoma. *J Gastroenterol* 1999; **34:** 250-252

13 **Hiramatsu K,** Matsuura Y, Kono H, Kitagawa Y, Yamanaka H. A recurrent case of gastric cancer presented with carcinomatous pericarditis. *J Jpn Surg Assoc* 2002; **63:** 333-336

14 **Suto K,** Ichikawa W, Tsuji Y, Arai E, Shimizu M, Hirayama R. Two cases of pericardial metastasis from gastric cancer with cardiac tamponade. *J Jpn Surg Assoc* 2003; **64:** 2414-2417

15 **Sakusabe M,** Ouchi S, Seki H, Kumagai Y, Kamata S, Kotanagi H. A case of effective weekly paclitaxel administration for gastric cancer recurrence with carcinomatous pericarditis. *Gan To Kagaku Ryoho* 2005; **32:** 77-79

16 **Tabata Y,** Nakato H, Nakamura Z, Sasaki A, Shoji K, Yokoyama H, Tanji Y, Saito K, Uehara H. Metastatic cancer to the heart: a clinicopathological analysis of 64 autopsy cases. *Respir Circ* 1983; **31:** 569-573

17 **Klatt EC,** Heitz DR. Cardiac metastases. *Cancer* 1990; **65:** 1456-1459

18 **Nakayama R,** Yoneyama T, Takatani O, Kimura K. A study of metastatic tumors to the heart, pericardium and great vessels. I. Incidences of metastases to the heart, pericardium and great vessels. *Jpn Heart J* 1966; **7:** 227-234

19 **Mukai K,** Shinkai T, Tominaga K, Shimosato Y. The incidence of secondary tumors of the heart and pericardium: a 10-year study. *Jpn J Clin Oncol* 1988; **18:** 195-201

20 **Raven RW.** Secondary malignant disease of the heart. *Br J*

Cancer 1948; **2:** 1-7
21 **Hanfling SM.** Metastatic cancer to the heart. Review of the literature and report of 127 cases. *Circulation* 1960; **22:** 474-483
22 **Warren S,** Gates O. Lung Cancer and Metastasis. *Arch Pathol* 1964; **78:** 467-473
23 **Kline IK.** Cardiac lymphatic involvement by metastatic tumor. *Cancer* 1972; **29:** 799-808
24 **Fraser RS,** Viloria JB, Wang NS. Cardiac tamponade as a presentation of extracardiac malignancy. *Cancer* 1980; **45:** 1697-1704
25 **Honda K,** Oura S, Hirai I, Yoshimasu T, Kokawa Y, Sasaki R, Okamura Y. Successful management of malignant pericardial effusion with weekly paclitaxel therapy in a lung adenocarcinoma patient. *Gan To Kagaku Ryoho* 2003; **30:** 1317-20
26 **Japanese Gastric Cancer Association.** Japanese classification of gastric carcinoma -2nd English edition-. *Gastric Cancer* 1998; **1:** 10-24

Science Editor Kumar M and Guo SY **Language Editor** Elsevier HK

PO Box 2345, Beijing 100023, China
www.wjgnet.com
wjg@wjgnet.com

ELSEVIER

World J Gastroenterol 2005;11(44):6905-6909
World Journal of Gastroenterology ISSN 1007-9327

Significance of a novel sucrose permeability test using serum in the diagnosis of early gastric cancer

Tadayuki Shishido, Taketo Yamaguchi, Takeo Odaka, Masanori Seimiya, Hiromitsu Saisho, Fumio Nomura

Tadayuki Shishido, Taketo Yam aguchi, Takeo Odaka, Hiromitsu Saisho, Department of Medicine and Clinical Oncology, Graduate School of Medicine, Chiba University, 1-8-1 Inohana, Chuo-ku, Chiba-city, Chiba 260-8677, Japan
Masanori Seimiya, Fumio Nomura, Department of Molecular Diagnosis, Graduate School of Medicine, Chiba University, 1-8-1 Inohana, Chuo-ku, Chiba-city, Chiba 260-8677, Japan
Correspondence to: Taketo Yamaguchi, Department of Medicine and Clinical Oncology, Graduate School of Medicine, Chiba University, 1-8-1 Inohana, Chuo-ku, Chiba-city, Chiba 260-8677, Japan. yamaguch-cib@umin.ac.jp
Telephone: +43-226-2083 Fax: +43-226-2088
Received: 2005-04-25 Accepted: 2005-05-24

Abstract

AIM: To investigate the usefulness of sucrose permeability test using serum in the diagnosis of gastric diseases, with special reference to early gastric cancer (EGC).

METHODS: A total of 63 subjects, including 11 patients with gastric ulcer, 20 patients with gastric cancer (13, early; 7, advanced) and 32 healthy controls, were studied. Blood and urine samples were collected repeatedly for 5 h before and after the sucrose loading. Sucrose levels were measured by a newly developed enzymatic method.

RESULTS: Serum sucrose levels started to increase 15 min after loading, and peaked at 60 min in the gastric disease groups. The levels for gastric ulcer, EGC and advanced gastric cancer (AGC) at 60 min were significantly higher than that in the healthy controls (26.9±2.4, 34.4±5.0, and 71.8±15.6 *vs* 7.9±0.7 mol/L, respectively, $P<0.01$). The cut-off level set at 15.4 mol/L (60 min) offered the best distinction between EGC patients and healthy controls; and the sensitivity and specificity were 92.3% and 93.8%, respectively, while those of the urine method were 76.9% and 93.8%, respectively.

CONCLUSIONS: The gastric permeability test using serum is reliable for the detection of EGC, and this test can provide results much earlier than the conventional urine method. This test may offer a useful alternative to more invasive tests for EGC.

Key words: Sucrose test; Gastric permeability; Early gastric cancer; Advanced gastric cancer; Gastric ulcer

Shishido T, Yamaguchi T, Odaka T, Seimiya M, Saisho H, Nomura F. Significance of a novel sucrose permeability test using serum in the diagnosis of early gastric cancer. *World J Gastroenterol* 2005; 11(44): 6905-6909
http://www.wjgnet.com/1007-9327/11/6905.asp

INTRODUCTION

In 1993, Meddings *et al.*[1], proposed the sucrose permeability test as a new non-invasive test for evaluating gastroduodenal injury. This test is based on the principle that sucrose does not permeate the healthy gastric mucosa and is rapidly dissolved in the small intestine, whereas it permeates and is absorbed through sites of injury in the stomach, enters the bloodstream and is excreted into the urine. It is reported that this test is useful for diagnosing gastric ulcer or gastroduodenal injury caused by NSAIDs or steroids[2-6]. Furthermore, it has been demonstrated that sucrose permeability is elevated by infection with *H pylori* or celiac disease, reflecting mucosal injury associated with inflammatory cell infiltration; thus, the usefulness of this test in evaluating gastroduodenal injury has been established[4,7,8].

However, the conventional method is not practical for outpatients or for health screenings because urine must be collected for 5 h or longer after the sucrose loading. If the sucrose test could be done in a shorter period of time, its clinical usefulness would increase.

We recently developed a novel enzymatic assay that is sensitive enough to determine serum levels of sucrose accurately[9]. The changes of serum sucrose levels after ingestion in patients with gastric diseases, as in healthy subjects, are unknown. Therefore, the first aim of this study was to investigate the changes of serum sucrose levels in healthy subjects, patients with gastric ulcer and gastric cancer. The second aim was to identify the most suitable time to collect serum samples for the detection of gastric disease.

There are reports that gastric mucosal permeability is elevated in patients with advanced gastric cancer (AGC), but none regarding those with early gastric cancer (EGC). The third aim of this study was to evaluate the diagnostic value of the sucrose test using serum in patients with EGC.

MATERIALS AND METHODS

Patients

The subjects studied included: (1) 32 healthy volunteers (HV: 15 men and 17 women; mean age 51.0 years, range 35-65 years) without symptoms or a history of gastrointestinal disease, who had not been prescribed any medicine that might have affected the gastrointestinal system; and (2) a gastric disease patient group composed of 31 patients, including 11 with gastric ulcers (GU: 5 men and 6 women; mean age 55.5 years, range 24-80 years; mean long diameter 1.4 cm, range 0.8-2.0 cm), 13 with EGC (11 men and 2 women; mean age 73.5 years, range 61-87 years; depth of invasion Tis in 11, T1 in 2; mean long diameter 1.55 cm, range 0.8-3.5 cm), and 7 with AGC (3 men and 4 women; mean age 65.0 years, range 48-75 years; depth of invasion T2 in 3, T3 in 2, and unknown in 2; mean long diameter 7.7 cm, range 4.3 cm-whole stomach). The depth of invasion of the gastric cancer was judged by pathological exploration of the resected mucosal specimens and the surgical specimens (Table 1).

Table 1 Clinical data of subjects studied

	HV (n = 32)	GU (n = 11)	EGC (n = 13)	AGC (n = 7)
Age (yr)	51 (35-65)	55.5 (24-80)	73.5 (61-87)	65 (48-75)
Gender (M:F)	17:15	5: 6	11: 2	3: 4
Size (cm)	-	1.4 (0.8-2.0)	1.55 (0.8-3.5)	7.7 (4.3-whole stomach)
Invasive Depth	-	-	Tis:T1=11:2	T2:T3:unknown = 3:2:2

HV: healthy volunteers, GU: Gastric ulcers, EGC: early gastric cancers, AGC: advanced gastric cancers.
Tis = mucosa, T1 = submucosa, T2 = proper muscle and subserosa, T3 = serosa.

The gastric mucosa was resected in patients with EGC, when considered, on the basis of endoscopic diagnosis including endoscopic ultrasonography, to be an intramucosal lesion. In two cases of EGC that were judged to have invaded as far as the deep submucosa, and in five cases of AGC, surgery was performed, while the remaining two cases were treated non-surgically. Two cases in which the depth of invasion could not be determined histopathologically were diagnosed endoscopically as AGC. Patients with diabetes mellitus or reduced renal function were excluded.

Informed consent was obtained from every subject. This study was performed with the approval of the Ethical Committee of Chiba University School of Medicine, Japan.

Gastric permeability

After an overnight fast, patients and HV were given a solution composed of 100 g sucrose and 450 mL water for 15 min. Blood samples were collected before and at 15, 30, 45, 60, 75, 90, 120, 180, 240, and 300 min after the sucrose loading. The blood samples were immediately centrifuged and the sera were obtained. Simultaneously, urine was collected for over a period of 5 h after the sucrose loading and the amount of sucrose excreted during the 5-h period was obtained from the volume of urine and the concentration of sucrose. Sera and urine were stored at -20 °C until the assay.

Assay

Sucrose was phosphorylated by the action of sucrose phosphorylase. The subsequent reaction in the presence of phosphoglucomutase and glucose-1, 6-diphosphate formed glucose-6-phosphate. Finally, the sucrose of the monad formed the dyad thio-NADPH. The reaction was monitored by changes in absorbance at 405 nm. The details of the assay procedures are published elsewhere[9].

Statistical analysis

Data were expressed as mean±SE. Using ANOVA, the serum sucrose concentration before and after the administration of sucrose in each group was compared. Serum sucrose concentrations at each sampling time within each group and comparison by the urine collection method within each group were compared using Tukey's method. Comparison of diagnostic ability based on areas under the receiver operator characteristics (ROC) curve at each sampling point was carried out using Hanley's method[10]. Cut-off points based on the ROC curve at each time point were set to obtain sensitivity, specificity, and accuracy. The surface area of GC was calculated using the formula (1/4×π×long diameter×short diameter) on the assumption that the tumor was elliptical. The relationship between the surface area of EGC and the serum sucrose level was determined. A two-sided P value <0.05 was considered statistically significant.

RESULTS

Baseline serum sucrose concentrations were 2.4±0.4, 2.9±0.8, 1.4±0.7, and 1.6±1.4 μmol/L for the HV, GU, EGC and AGC, respectively, which showed no significant intergroup differences. The peak serum sucrose level for the HV was 8.5±0.8 μmol/L at 120 min after the sucrose loading. Serum sucrose levels for the GU, EGC and AGC, which increased 15 min after the sucrose loading (P<0.01), peaked between 45 and 120 min, and then gradually decreased (Figure 1). Serum sucrose levels for GU, EGC and AGC showed a significant difference from the HV (P<0.01) between 60 and 240 min. Between 15 and 300 min, serum sucrose levels for AGC showed a significant difference from those for EGC or GU (P<0.01). However, there was no significant difference between the serum sucrose levels for EGC and GU at any time point from 15 to 300 min.

The amounts of sucrose excreted into the urine in HV, GU, EGC and AGC were 50.5±4.4, 172.9±19.1, 165.1±27.2, and 464.5±78.9 mg, respectively, showing significantly higher values in GU, EGC and AGC as compared to the HV. In addition, the amount of sucrose excreted into the urine in AGC showed a significantly higher value than that

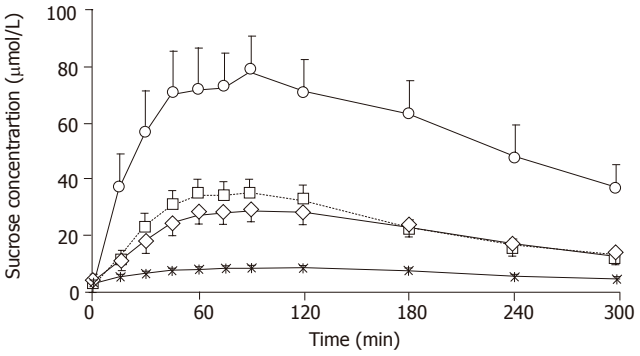

Figure1 Changes in serum sucrose level in HV, GU, EGC, and AGC groups (mean ±SE). The serum sucrose level in EGC group (□) showed a significant difference between 30 and 300 min after the sucrose loading as compared to the HV group (⁎) between 30 and 240 min (P<0.01) and 30 and 300 min (P<0.05). The serum sucrose level of AGC (○) patients showed a significant difference from HV (⁎) between 15 and 300 min after sucrose loading, GU (◇) and EGC (□) (P<0.01). GU patients (◇) showed a significant difference from the HV group ( ) between 45 and 240 min after sucrose loading (45 min, P<0.05; from 60 to 240 min, P<0.01). However, there was no significant difference in serum sucrose level in HV group from 15 to 300 min after loading as compared with either EGC (◇) or GU (□) group.

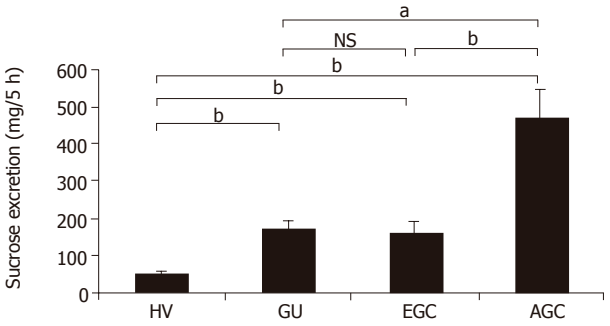

Figure 2 Amounts of sucrose excreted into urine in HV, GU, EGC and AGC groups (mean±SE). Even in the urine collection method, the amount of sucrose excreted in GU, EGC and AGC groups showed a significant difference (^bP<0.01) as compared with the HV group, and AGC group showed a significant difference (^bP<0.01) from both GU and EGC groups. However, no significant difference was seen in either EGC; NS: no significant difference.

in GU or EGC (Figure 2).

The diagnostic value of the sucrose test in gastric disease (GU, EGC and AGC) in relation to HV was compared between the serum method and the urine collection method using ROC curves (Figure 3). The areas under the curve (AUC) in the serum method at 15 and 60 min, and in the urine collection method were 0.876 (95%CI 0.783-0.968), 0.992 (95%CI 0.978-1.006), and 0.980

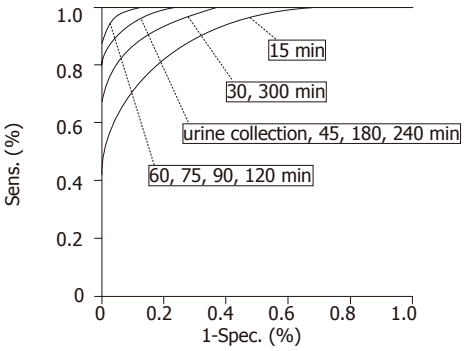

	AUC	SE	95% CI	
			Lower limit	Upper limit
Urine (5 h)	0.98	0.014	0.953	1.006
0 min	0.366	0.072	0.226	0.506
15 min	0.876	0.047	0.783	0.968
30 min	0.951	0.024	0.904	0.998
45 min	0.979	0.014	0.952	1.005
60 min	0.992	0.007	0.978	1.006
75 min	0.994	0.006	0.983	1.005
90 min	0.993	0.006	0.981	1.006
120 min	0.989	0.01	0.97	1.008
180 min	0.971	0.017	0.937	1.005
240 min	0.973	0.016	0.941	1.004
300 min	0.959	0.022	0.917	1.002

Figure 3 Receiver operator characteristics (ROC) curve and AUC of ROC curve. Comparison of the ROC curve of the sucrose test and AUC at each time point. There was no significant difference between the urine collection method and the serum method from 30 to 300 min. AUC: Area under the ROC curve; SE: standard error; CI: confidence interval.

(95%CI 0.953-1.006), respectively (Figure 3). Comparison of the AUC between the urine collection method and the serum method at every time point showed no significant difference. The diagnostic values of the urine collection method and the serum method were comparable from 30 min onward at each sampling time.

Cut-off points for the detection of gastric disease at each sampling time in the serum method were obtained from the ROC curves, and the diagnostic value of this method was also obtained. Similarly, cut-off points and diagnostic values were obtained by the urine collection method (Table 2). The cut-off points for the detection of gastric disease by the serum method over 60 min was 15.4 μmol/L and that of the urine collection method was 95 mg. Serum sucrose levels of the four studied groups at 60 min are shown in Table 3.

The sensitivity, specificity, and overall accuracy of the urine collection method for detecting gastric disease were 90.3%, 93.8%, and 92.1%, respectively, while those

Table 2 Cut-off points and diagnostic values of sucrose test at each time point for detection of gastric disease (gastric ulcer and gastric cancer)

Time (min)	Urine	15	30	45	60	75	90	120	180	240	300
Cut-off points[1]	95	7.4	10.2	11.8	15.2	16.8	16	14	11	8.2	6.5
Sensitivity (%)	90.3	80.6	83.9	93.5	96.8	96.8	96.8	96.8	93.5	93.5	90.3
Specificity (%)	93.8	87.5	93.8	90.6	93.8	96.9	93.8	93.8	90.6	90.6	90.6
Accuracy (%)	92.1	84.1	88.9	92.1	95.2	96.8	95.2	95.2	92.1	92.1	90.5

[1] Cut-off points: Urine as mg/5 h, Serum as μmol/L

Table 3 Sucrose concentrations at 60 min of the 4 groups

	HV	GU	EGC	AGC
Mean (μmol/L)	7.6	26.9	34.4	71.8
SE (μmol/L)	0.7	2.4	5.0	15.6

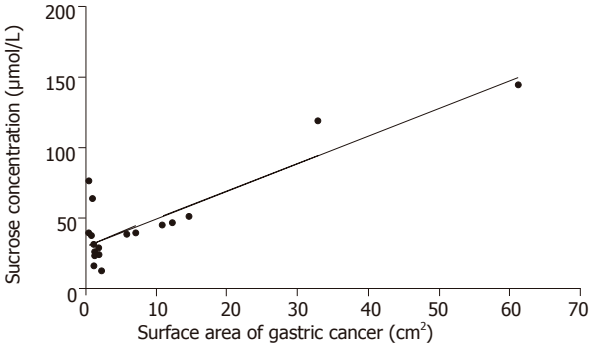

Figure 4 Relationship between serum sucrose level at 60 min and surface area of gastric cancer. The serum sucrose level at 60 min was closely correlated with the surface area of the gastric cancer (r = 0.83, P<0.01).

for the serum method (over 60 min) were 96.8%, 93.8%, and 95.2% (Table 4), indicating that the serum method was superior to the urine collection method, but not so significantly.

Sensitivity in detecting GU and AGC was 100% by using both the methods. Sensitivity in detecting EGC was 76.9% by the urine collection method, but 92.3% by the serum method (60 min), which was relatively high, but again without a significant difference.

There was a significant correlation between the surface area of GC and the serum sucrose level (60 min) (r = 0.83) (Figure 4).

DISCUSSION

The sucrose permeability test is a valuable noninvasive test for detecting gastroduodenal injury[1-8,11-13]. The conventional method involves measuring the amount of sucrose excreted into the urine for over a period of as long as 5 h following the administration of sucrose. If this test could be done more quickly, its clinical usefulness would increase greatly.

Vinet *et al*.[14] reported that the serum concentrations of sucrose after sucrose loading in volunteers whose stomachs had been injured by NSAIDs or alcohol clearly increased, and that this occurred only after 15-45 min. We considered that it might be useful in clinical practice to measure the sucrose concentration in the serum instead of the urine. However, the pattern of the changes of serum sucrose levels after sucrose ingestion either in healthy subjects or in patients with gastric diseases was unknown. Moreover, the appropriate time point for collecting serum samples was not known, nor was the usefulness of serum testing for detecting gastric diseases. We conducted this fundamental study for these reasons.

We took advantage of a novel enzymatic method that we had recently developed for measuring serum sucrose levels. Previously, the concentration of sucrose in biological fluids was measured by high-performance liquid chromatography (HPLC) with an electrochemical technique for detection[1-7,11], or by an enzymatic assay[8,14,15] in which invertase hydrolyzes sucrose to fructose and glucose, and then the glucose is measured using a hexokinase procedure with reduced nicotinamide adenine dinucleotide phosphate formation. But the invertase method is not applicable to serum samples because of interference by the glucose in the samples. The HPLC method is accurate and widely used, but is labor-intensive, costly, and time-consuming.

We collected blood specimens at 11 different sampling times from 63 individuals and examined the changes in serum sucrose and the time point appropriate for the detection of mucosal injury. There was no significant difference in diagnostic value between the urine collection method and the serum method at any determined time point between 30 and 300 min. Thus, it may be possible to detect a gastroduodenal injury using serum at any determined point between 30 and 300 min after sucrose loading. In particular, because the accuracy at 60, 75, 90, and 120 min was greater than 95%, which was higher than that for the urine collection method, it should be satisfactory to carry out sampling for the serum method only at 60 min in order to obtain more reliable results more quickly. On the basis of these results, we were able to shorten the sucrose test, and to increase its diagnostic accuracy.

All cases of GU were detected when the serum method was carried out for 60 min. Although GU is a benign disease, medical treatment is essential, and GU must be distinguished from cancer. In this respect, the high detection rate of GU by the serum method will not reduce the significance of this test for the screening of gastric cancer.

The average age of patients with GC in this study was higher than those of HV and GU patients, but there was no significant age-related difference in the sucrose level within each group (data not shown), because the inter-group age differences had little effect on the outcome.

Table 4 Sensitivity of sucrose permeability test for each gastric disease

Time (min)	Urine	15	30	45	60	75	90	120	180	240	300
Cut-off points[1]	95	7.4	10.2	11.8	15.2	16.8	16	14	11	8.2	6.5
GU	100	72.7	81.8	100	100	100	100	100	100	100	90.9
EGC	84.6	76.9	76.9	84.6	92.3	92.3	92.3	92.3	92.3	84.6	84.6
AGC	100	100	100	100	100	100	100	100	100	100	100

[1]Cut-off points: Urine, as mg/5 h; serum, as μmol/L

We observed a significant relationship between the surface area of the gastric cancer and sucrose permeability even in cases without ulcer formation. This observation is exceedingly interesting and indicates some process of active absorption of sucrose through unhealthy gastric mucosa. This finding should be tested *in vitro*.

Using the conventional urine collection test for sucrose permeability, Kawabata *et al*.[11] reported an abnormally high sucrose permeability in 11 of 12 patients with advanced gastric cancer, which was significantly higher than that of a healthy control group. However, the diagnostic significance of this test for patients with early gastric cancer has not been elucidated. The results of our study clearly demonstrated that the sucrose test can detect not only AGC but also EGC.

When early gastric cancers are limited to the mucosal layer, they are frequently subjected to endoscopic submucosal dissection (ESD), and can be treated without conventional surgery[16,17]. In this study, 10 of the 11 patients who underwent ESD showed positive results with the sucrose test.

Gastric cancer is the second largest cause of cancer death throughout the world[18]. Contrast-enhanced upper gastrointestinal radiography has been widely used as the screening test for gastric cancer in Japan, but its diagnostic value regarding EGC is considered to be low[19]. The serum pepsinogen method is a new screening test for gastric cancer, but it was reported that the test failed to detect a considerable proportion of patients with advanced gastric cancer[19,20]. In this study, our results clearly demonstrated that the sucrose test on the serum had a higher sensitivity rate for EGC than any other non-invasive test reportedly used for screening purposes. Furthermore, the diagnostic sensitivity of the test for AGC was 100%.

In conclusion, the sucrose test conducted on the serum is a very promising screening test for gastric cancer. Since the serum method can be performed much more easily with an automatic analyzer, it can be used for mass screening of a large number of samples. Confirmatory large-scale prospective studies comparing this method with other methods used in mass screenings are still needed before definite recommendations can be made regarding the significance of the test in screening for gastric cancer, especially EGC.

ACKNOWLEDGMENTS

We thank Shino-Test Corporation for the supply of enzymatic assay reagents.

REFERENCES

1 **Meddings JB,** Sutherland LR, Byles NI, Wallace JL. Sucrose: a novel permeability marker for gastroduodenal disease. *Gastroenterology* 1993; **104:** 1619-1926
2 **Sutherland LR,** Verhoef M, Wallace JL, Van Rosendaal G, Crutcher R, Meddings JB. A simple, non-invasive marker of gastric damage: sucrose permeability. *Lancet* 1994; **343:** 998-1000
3 **Meddings JB,** Kirk D, Olson ME. Noninvasive detection of nonsteroidal anti-inflammatory drug-induced gastropathy in dogs. *Am J Vet Res* 1995; **56:** 977-981
4 **Rabassa AA,** Goodgame R, Sutton FM, Ou CN, Rognerud C, Graham DY. Effects of aspirin and Helicobacter pylori on the gastroduodenal mucosal permeability to sucrose. *Gut* 1996; **39:** 159-163
5 **Smecuol E,** Bai JC, Sugai E, Vazquez H, Niveloni S, Pedreira S, Maurino E, Meddings J. Acute gastrointestinal permeability responses to different non-steroidal anti-inflammatory drugs. *Gut* 2001; **49:** 650-655
6 **Kiziltas S,** Imeryuz N, Gurcan T, Siva A, Saip S, Dumankar A, Kalayci C, Ulusoy NB. Corticosteroid therapy augments gastroduodenal permeability to sucrose. *Am J Gastroenterol* 1998; **93:** 2420-2425
7 **Goodgame RW,** Malaty HM, el-Zimaity HM, Graham DY. Decrease in gastric permeability to sucrose following cure of Helicobacter pylori infection. *Helicobacter* 1997; **2:** 44-47
8 **Vogelsang H,** Oberhuber G, Wyatt J. Lymphocytic gastritis and gastric permeability in patients with celiac disease. *Gastroenterology* 1996; **111:** 73-77
9 **Seimiya M,** Osawa S, Hisae N, Shishido T, Yamaguchi T, Nomura F. A sensitive enzymatic assay for the determination of sucrose in serum and urine. *Clin Chim Acta* 2004; **343:** 195-199
10 **Hanley JA,** McNeil BJ. The meaning and use of the area under a receiver operating characteristic (ROC) curve. *Radiology* 1982; **143:** 29-36
11 **Kawabata H,** Meddings JB, Uchida Y, Matsuda K, Sasahara K, Nishioka M. Sucrose permeability as a means of detecting diseases of the upper digestive tract. *J Gastroenterol Hepatol* 1998; **13:** 1002-1006
12 **Fukuda Y,** Bamba H, Okui M, Tamura K, Tanida N, Satomi M, Shimoyama T, Nishigami T. Helicobacter pylori infection increases mucosal permeability of the stomach and intestine. *Digestion* 2001; 63 (*Suppl*) **1:** 93-96
13 **Gotteland M,** Cruchet S, Verbeke S. Effect of Lactobacillus ingestion on the gastrointestinal mucosal barrier alterations induced by indometacin in humans. *Aliment Pharmacol Ther* 2001; **15:** 11-17
14 **Vinet B,** Panzini B, Boucher M, Massicotte J. Automated enzymatic assay for the determination of sucrose in serum and urine and its use as a marker of gastric damage. *Clin Chem* 1998; **44:** 2369-2371
15 **Birnberg PR,** Brenner ML. A one-step enzymatic assay for sucrose with sucrose phosphorylase. *Anal Biochem* 1984; **142:** 556-561
16 **Noda M,** Kodama T, Atsumi M, Nakajima M, Sawai N, Kashima K, Pignatelli M. Possibilities and limitations of endoscopic resection for early gastric cancer. *Endoscopy* 1997; **29:** 361-365
17 **Ono H,** Kondo H, Gotoda T, Shirao K, Yamaguchi H, Saito D, Hosokawa K, Shimoda T, Yoshida S. Endoscopic mucosal resection for treatment of early gastric cancer. *Gut* 2001; **48:** 225-229
18 **Hohenberger P,** Gretschel S. Gastric cancer. *Lancet* 2003; **362:** 305-315
19 **Miki K,** Morita M, Sasajima M, Hoshina R, Kanda E, Urita Y. Usefulness of gastric cancer screening using the serum pepsinogen test method. *Am J Gastroenterol* 2003; **98:** 735-739
20 **Kitahara F,** Kobayashi K, Sato T, Kojima Y, Araki T, Fujino MA. Accuracy of screening for gastric cancer using serum pepsinogen concentrations. *Gut* 1999; **44:** 693-697

Science Editor Kumar M and Guo SY **Language Editor** Elsevier HK

PO Box 2345, Beijing 100023, China
www.wjgnet.com
wjg@wjgnet.com

ELSEVIER

World J Gastroenterol 2005;11(44):6910-6919
World Journal of Gastroenterology ISSN 1007-9327

Bifunctional chimeric SuperCD suicide gene -YCD: YUPRT fusion is highly effective in a rat hepatoma model

Florian Graepler, Marie-Luise Lemken, Wolfgang A Wybranietz, Ulrike Schmidt, Irina Smirnow, Christine D Groß, Martin Spiegel, Andrea Schenk, Hansjörg Graf, Ulrike A Lauer, Reinhard Vonthein, Michael Gregor, Sorin Armeanu, Michael Bitzer, Ulrich M. Lauer

Florian Graepler, Marie-Luise Lemken, Wolfgang A. Wybranietz, Ulrike Schmidt, Irina Smirnow, Christine D. Groß, Martin Spiegel, Andrea Schenk, Michael Gregor, Sorin Armeanu, Michael Bitzer, Ulrich M. Lauer, Department of Internal Medicine I, University Clinic Tübingen, Tübingen D-72076, Germany
Hansjörg Graf, Ulrike A. Lauer, Section of Experimental Radiology, University Clinic Tübingen, Tübingen D-72076, Germany
Reinhard Vonthein, Department of Medical Biometry, University Clinic Tübingen, Tübingen D-72076, Germany
Supported by grants from German Research Foundation (LA649-20-2), Federal Ministry of Education, Science, Research and Technology (Fö. 01KS9602, Fö. 01KV9532), Interdisciplinary Clinical Research Center (IZKF) Tübingen, and the fortüne-program of the Medical Faculty of Eberhard-Karls-University Tübingen (F.1281127). W.A.W. supported by a scholarship from Pinguin Foundation (Henkel KGaA)
Correspondence to: Dr Florian Graepler, Department of Internal Medicine I, Medical University Clinic Tübingen, Otfried-Müller-Str. 10, Tübingen D-72076,
Germany. florian.graepler@uni-tuebingen.de
Telephone: +49-7071-2980651 Fax: +49-7071-294630
Received: 2005-04-26 Accepted: 2005-05-24

Abstract

AIM: To investigate the effects of catalytically superior gene-directed enzyme prodrug therapy systems on a rat hepatoma model.

METHODS: To increase hepatoma cell chemosensitivity for the prodrug 5-fluorocytosine (5-FC), we generated a chimeric bifunctional SuperCD suicide gene, a fusion of the yeast cytosine deaminase (YCD) and the yeast uracil phosphoribosyltransferase (YUPRT) gene.

RESULTS: *In vitro* stably transduced Morris rat hepatoma cells (MH) expressing the bifunctional SuperCD suicide gene (MH SuperCD) showed a clearly marked enhancement in cell killing when incubated with 5-FC as compared with MH cells stably expressing YCD solely (MH YCD) or the cytosine deaminase gene of bacterial origin (MH BCD), respectively. *In vivo*, MH SuperCD tumors implanted both subcutaneously as well as orthotopically into the livers of syngeneic ACI rats demonstrated significant tumor regressions ($P<0.01$) under both high dose as well as low dose systemic 5-FC application, whereas MH tumors without transgene expression (MH naïve) showed rapid progression. For the first time, an order of *in vivo* suicide gene effectiveness (SuperCD>> YCD>>BCD>>>negative control) was defined as a result of a direct *in vivo* comparison of all three suicide genes.

CONCLUSION: Bifunctional SuperCD suicide gene expression is highly effective in a rat hepatoma model, thereby significantly improving both the therapeutic index and the efficacy of hepatocellular carcinoma killing by fluorocytosine.

Key words: YCD/YUPRT fusion; Cytosine deaminase; GDEPT; Suicide gene therapy; Hepatoma therapy

Graepler F, Lemken ML, Wybranietz WA, Schmidt U, Smirnow I, Groß CD, Spiegel M, Schenk A, Graf H, Lauer UA, Vonthein R, Gregor M, Armeanu S, Bitzer M, Lauer UM. Bifunctional chimeric SuperCD suicide gene -YCD: YUPRT fusion is highly effective in a rat hepatoma model. *World J Gastroenterol* 2005; 11(44): 6910-6919
http://www.wjgnet.com/1007-9327/11/6910.asp

INTRODUCTION

Suicide gene therapy involves the transfer of genes into tumor cells to render them specifically sensitive to prodrugs that are relatively nontoxic to normal tissues. Cytosine deaminase (CD) enzyme is found in many bacteria, yeast and fungi, where it deaminates cytosine to uracil[1]. It also deaminates the relatively nontoxic prodrug 5-fluorocytosine (5-FC) to the highly toxic chemotherapeutic compound 5-fluorouracil (5-FU), used in the treatment of malignant tumors (Figure 1A)[2]. Transduction of the CD gene into tumor cells combined with systemic administration of 5-FC has been shown to have anticancer effects in various animal models[3-7]. Due to their inherent bystander effect, toxic 5-FU metabolites (Figure 1A) also reach non-transduced neighboring cells[8-10]. In contrast to the herpes simplex virus type 1 thymidine kinase/ganciclovir system, this bystander effect does not depend on gap junctional intercellular communication channels[11].

In this work, we focused on the optimization of the CD suicide gene system for hepatoma treatment. We

compared both *in vitro* and *in vivo* therapeutic efficiency of stable expression of: (1) a new bifunctional chimeric SuperCD suicide gene, composed of the yeast cytosine deaminase (YCD) suicide gene directly fused to a 5'-terminally deleted yeast uracil phosphoribosyltransferase (YUPRT) gene[12]; (2) YCD suicide gene; and (3) bacterial cytosine deaminase (BCD) suicide gene in the MH 3924A animal model[13].

MATERIALS AND METHODS

Retroviral vector construction

Genomic DNA of *Saccharomyces cerevisiae*, strain KFY159 (kindly provided by K.-U. Fröhlich, Physiologisch-Chemisches Institut, Eberhard-Karls-University, Tübingen, Germany), was employed to amplify YCD and YUPRT using polymerase chain reaction technique. YCD (*S. cerevisiae* gene FCY-1) was amplified with primers: 5'-G GGGTACCGCCACCATGGTGACAGGGGGAAT GGCAAG-3' (primer #1) and 5'-GGGCGGCCGCCT CACTCACCAATATCTTCAAA CCAATC-3' (primer #2). Alternatively, primer #3 (5'-GGGAATTCTCACC AATATCTTCAAACCAATC-3') was used as a reverse primer in combination with primer #1 to amplify the yeast FCY-1 gene. The latter YCD fragment was subsequently joined to a PCR product amplifying the yeast FUR-1 gene (YUPRT). While omitting the N-terminal domain, the remaining domains of the YUPRT open reading frame, enzymatically sufficient for efficiently transferring the phosphoribosyl residue to the deaminated 5-FC[14], were amplified with primers: 5'-CCGAATTCGGAACCATTTA AGAACGTC-3' (primer #4) and 5'-CCGCGGCCGCCTT AAACACAGTAGTATCTGTCACC-3' (primer #5). Both PCR fragments were purified for subsequent ligation as recently described elsewhere[15]. Subsequently, both YCD and YUPRT PCR amplification products were combined in a three-fragment ligation procedure employing a pUC-based cloning vehicle as a backbone. This intermediate construct was used to remove the *Eco*RI site between the YCD and YUPRT sequences and at the same time to generate the bifunctional SuperCD suicide fusion gene employing a site-directed mutagenesis using the Promega QuikChange method (Promega, Mannheim, Germany). With sense and anti-sense mutagenesis primers (sense sequence: 5'-ATGGTTTCCGAAGCCTCACCAATAT CT-3'), the two enzymatic moieties were joined in-frame, resulting in an Ala residue linking the two yeast ORFs (now with the YUPRT gene starting at the natural S38 codon). Subsequently, the following retroviral constructs were generated (Figure 1B): (1) pLXSN-BCD contains the *E. coli* cytosine deaminase (BCD) suicide gene under the control of the retroviral 5´LTR in basic retroviral vector pLXSN[16] (kindly provided by R.M. Blaese, NIH, Bethesda, MD, USA; originally denominated as pCD2)[17]; (2) pLXSN-YCD harboring the YCD suicide gene was generated by the insertion of the YCD PCR amplification product into basic vector pLXSN-GreeN (derivative of vector pLXSN, in which we exchanged the neo^r gene by a bifunctional EGFP/neo^r fusion gene); (3) pLXSN-SuperCD harboring the bifunctional SuperCD suicide fusion gene was generated by insertion of the YCD/YUPRT in-frame fusion fragment into basic vector pLXSN-GreeN.

Cell culture

Morris hepatoma (MH 3924A) cells were purchased from the German Cancer Research Center (DKFZ) Tumor Collection, Heidelberg, Germany, and maintained in DMEM supplemented with 50 mL/L fetal calf serum (FCS) in a humidified incubator containing 50 mL/L CO_2 at 37 °C.

Generation of stable BCD, YCD and SuperCD expressing Morris hepatoma 3924A cell lines

For the generation of suicide gene transducing retroviral particles, 5×10^5 PE501 ecotropic packaging cells were seeded on 60-mm diameter petri dishes. After 24 h, using lipofectAMINE reagent (Invitrogen), cells were transiently transfected with 3 μg of each retroviral vector DNA. Forty-eight hours later, the supernatant was employed for transduction of 3×10^5 naïve MH cells. Following G418 selection (600 μg/mL), resistant clones were analyzed for EGFP marker gene expression by fluorescence microscopy, followed by functional characterization of suicide gene expression in the sulforhodamin B (SRB) cytotoxicity assay. Cell clones exhibiting the highest cytotoxic effect were selected and named as MH BCD, MH YCD, and MH SuperCD.

Western blot analysis

Cells were lysed in SDS sample buffer and proteins were separated on 100 g/L SDS-PAGE and transferred to PVDF membranes[18]. Polyclonal rabbit antiserum directed against YCD (a generous gift from Transgene SA, Strasbourg, France), a polyclonal rabbit anti-BCD antibody (a generous gift from C. Richards, Glaxo-Wellcome, RTP, NC, USA)[19] and goat anti-rabbit IgG-horseradish peroxidase conjugates (BioRad, München, Germany) were used. Detection of reactive bands was facilitated using horseradish peroxidase-linked secondary conjugate and ECL detection reagents (Amersham Pharmacia, Freiburg, Germany).

SRB cytotoxicity assay

MH (naïve) as well as MH BCD, MH YCD, MH SuperCD cells were seeded in 24-well plates (1×10^4 cells/well). The next day 5-FC containing medium was added (a generous gift from Roche, Basel, Switzerland) and the cells were incubated for 4 d in order to allow untreated cells to reach confluence. Growth inhibition was evaluated by the SRB cytotoxicity assay[20] using a microtiter plate reader (Dynatech MR7000, Denkendorf, Germany) at 550 nm.

In vivo experiments

All animal experiments were performed in concordance with the laws of the German Government concerning the conduction of animal experimentation. Surgical and imaging procedures were performed under intraperitoneally applied anesthesia with ketamine hydrochloride (Ketanest,

Parke-Davis, Berlin, Germany; 100 mg/kg body weight) and xylazine hydrochloride (Rompun, Bayer, Leverkusen, Germany; 10 mg/kg body weight).

The subcutaneous MH naïve and MH SuperCD tumors were established by injecting 1×10^7 cells (in 70 μL PBS) at the dorsum of 6-wk-old male syngeneic ACI rats (Harlan Winkelmann, Borchen, Germany). Eleven days later the rats were randomized into two groups (3 rats/group), and were treated twice daily with ip injections of 5-FC (283 mg/kg body weight) or saline (0.9% NaCl) for 7 d. Tumor sizes were measured with calipers. Tumor volumes were calculated in cubic centimeter using the formula recommended by Carlsson *et al*.[21]: tumor volume (mm^3)=largest diameter (mm)×[smallest diameter (mm)]^2/2.

In order to monitor 5-FC serum levels by HPLC quantification, blood was taken via tail vein puncture on d 5 of the 5-FC application period. On d 8 of the treatment period, the animals were killed, and tumors were explanted and measured for tumor weight and volume. Tumor samples were analyzed for (1) the presence of SuperCD DNA and (2) the endurance of the SuperCD suicide gene functional activity. For PCR analysis, tumor sample DNA was extracted using DNeasy Tissue Kit (Qiagen, Hilden, Germany). MH SuperCD DNA was amplified using primers 5'-CGACCCCGCCTCGATCCTCC-3' (primer #6) and 5'-CTGCTGGGGAGCCTGGGGAC-3' (primer #7). PCR products were separated by electrophoresis on a 10 g/L agarose gel. For the functional testing of continuous suicide gene presence following the *in vivo* growth period of MH SuperCD tumors, tumor tissues were minced, placed into six-well plates and cultivated in DMEM medium containing 50 mL/L FCS, supplemented with 1% penicillin-streptomycin. Three days later, stably transduced MH SuperCD cells were selected by continuous addition of G418 (600 μg/mL). Two weeks later, the cells were analyzed for functional SuperCD gene activity employing the SRB cytotoxicity assay.

Orthotopic tumor implantation within the liver was performed as described elsewhere[13]. Twenty-one days later, tumor sizes were measured by magnetic resonance imaging (MRI). Subsequently, the rats were randomized into two groups (six rats/group) and were treated twice daily with ip injections of 5-FC (283 mg/kg body weight) or saline. On d 31, tumor sizes were again measured by MRI. Animals were killed, livers explanted and analyzed macroscopically for the presence of tumor tissue.

MRI measurements

Monitoring of tumor growth was performed by sequential MRI studies, using a 1.5 Tesla MR tomograph (VISION, Siemens, Erlangen, Germany). A turbospinecho sequence was applied to acquire T2 weighed images using the following parameters: 3.5 s repetition time, 96 ms echo time, field of view of 200 mm×100 mm. Fifteen slices with an in-plane resolution of 0.75 mm×0.75 mm, a slice thickness of 2 mm and a gap of 0.3 mm between the slices were acquired with six signal averages. Maximum areas of the tumors were determined by the identification of the tumor slice exhibiting largest diameters (main diameter *a* and minor diameter *b*), followed by the calculation of the respective area ($a/2\times b/2\times\pi$).

Statisticial analysis

Viability was explained by cell line, 5-FU concentration, and their interaction in analyses of variance. Square roots of counts were used as Box-Cox analyses and normal quantile-plots of residuals suggested so. Means and 95% confidence intervals were transformed back and divided by the fitted value of MH naïve cells. The *in vivo* experiment with four cell lines was analyzed by the analysis of covariance of logarithms of tumor sizes (considered censored at 30 mm² when below) with variable time factors, cell line and individual and different slopes for the cell lines. The hypotheses were: all four mean growth rates are equal, and mean growth rates of YCD and SuperCD cells are equal. As intra-individual comparison of cell lines was possible, all six possible combinations were implanted as in a balanced incomplete block plan. Sample size was planned to guarantee multiple power of more than 0.8 at effect size 30% and coefficient of variation 30%, while the multiple significance level was 0.05.

RESULTS

Through its toxic metabolites, 5-FU kills cells by binding to the thymidylate synthase, thereby causing a blockade of DNA synthesis as well as by directly interfering with the cellular RNA metabolism (Figure 1A). Because 5-FU is able to diffuse passively through cell membranes, it not only affects transduced cells, but also neighboring cells (so-called bystander cells). However, the conversion of 5-FU to 5-FUMP constitutes a rate-limiting step at least in some tumor cells[22]. In the context of suicide gene transfer, it is hypothesized that an additional encoding of the UPRT gene not only enhances tumor cell sensitivity to 5-FU, but also augments the sensitivity of tumor cells to 5-FC, when such cells are enabled to simultaneously express a CD gene (Figure 1A). Since also low tumor transduction efficiencies are recognized as a major limitation in liver tumor suicide gene therapy[23,24], 5-FC/CD/UPRT-based suicide gene systems could not only help to improve the effectiveness of 5-FC toxification, but also enhance the effectiveness of bystander killing, thereby helping to compensate for currently still low efficiencies of direct liver tumor suicide gene transfer. In this work, we therefore investigated whether hepatoma cell chemosensitivity for 5-FC could be enhanced by simultaneously addressing the two major steps of 5-FC metabolism. For this purpose, we first generated a so-called SuperCD fusion gene which combines the (1) enzymatic function of yeast CD (YCD) with (2) YUPRT-mediated phosphorylation of 5-FU to 5-FUMP (Figures 1A and B).

Construction of SuperCD/YCD/BCD suicide gene expressing retroviral vectors, and analysis of stably transduced Morris rat hepatoma cells

We employed genomic DNA of *S. cerevisiae* to amplify both yeast CD as well as yeast UPRT genes by PCR[22].

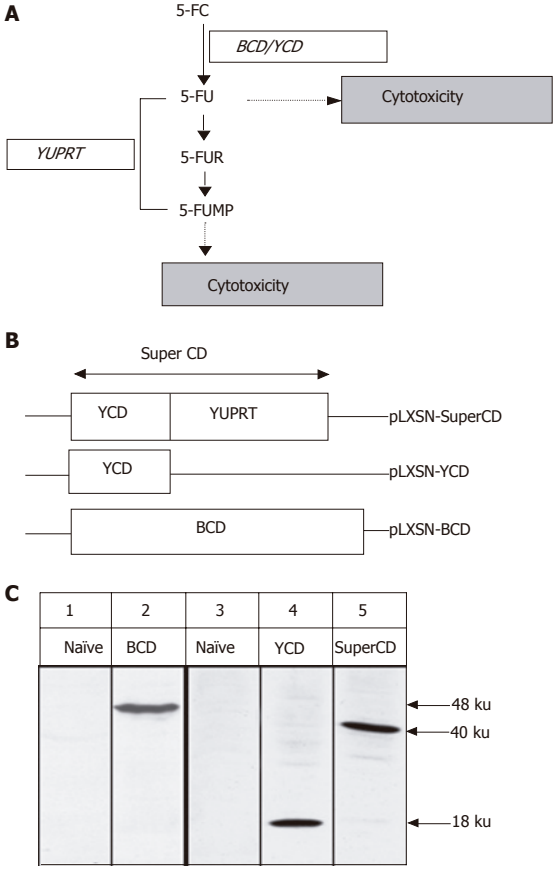

Figure 1 Mode of action of SuperCD (YCD::YUPRT) fusion. Panel **A**: Schematic representation of biological pathways resulting in cytotoxicity following cytosine deaminase/uracil phosphoribosyltransferase (UPRT)-mediated toxification of the prodrug 5-FC. 5-FC: 5-fluorocytosine; 5-FU: 5-fluorouracil; 5-FUR: 5-fluorouridine; 5-FUMP: 5-fluorouridine 5'-monophosphate; CD: cytosine deaminase; YUPRT: yeast uracil phosphoribosyltransferase. Panel **B**: Schematic representation of retroviral vectors used, in which suicide gene expression was placed under the retroviral 5' LTR. Panel **C**: Western blot detection of suicide gene expression in retrovirally generated stable SuperCD/YCD/BCD-expressing Morris hepatoma (MH) cell lines employing polyclonal rabbit antisera directed against BCD (lanes 1 and 2) and YCD (for detection of both SuperCD and YCD; lanes 3-5). Lane 1: MH naïve cells (negative control); lane 2: MH BCD cells, exhibiting a 48-ku band specific for BCD; lane 3: MH naïve cells (negative control); lane 4: MH YCD cells, exhibiting a 18-ku band specific for YCD; lane 5: MH SuperCD cells, exhibiting a 40-ku band specific for the YCD::YUPRT fusion, i.e. SuperCD. Numbers on the right hand side indicate the sizes of the expected proteins.

Subsequently, both genes were linked in-frame using a site-directed mutagenesis scheme, resulting in generation of a bifunctional suicide fusion gene which was named as SuperCD. Next, the SuperCD DNA sequence was inserted into basic retroviral vector pLXSN[16], resulting in generation of pLXSN-SuperCD (Figure 1B, upper construct), in which transgene expression is driven by the retroviral 5´LTR. For comparison of cytotoxic effectiveness, we likewise generated retroviral vectors pLXSN-YCD (Figure 1B, middle construct; solely encoding the YCD cDNA) and pLXSN-BCD (Figure 1B, lower construct; solely encoding the BCD cDNA)[25]. Employing all three constructs, PE501 ecotropic packaging cells were transiently transfected. Subsequently, respective

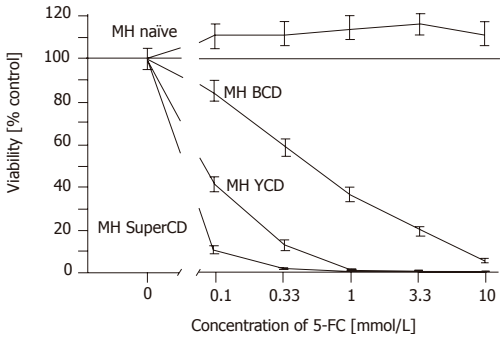

Figure 2 SRB cytotoxicity assay with stable BCD, YCD, SuperCD expressing Morris hepatoma (MH) cell lines generated by retroviral transduction. Untransduced MH3924A cells (MH naïve) and stably transduced Morris hepatoma cell lines (MH BCD, MH YCD, MH SuperCD) were seeded on 24-well plates. After 4 d of 5-FC treatment, the growth inhibition was determined by SRB staining and measured at 550 nm. All values were referred to that of the untransduced control cells without the addition of 5-FC and are given as percentage of surviving cells (control: 100%). All experiments were carried out at least in quadruplicate. Viability values plotted represent fitted medians and 95%CI.

supernatants containing recombinant retroviruses were used for transduction of MH 3924A cells. G418 selection gave rise to neo^r resistant clones (MH SuperCD, MH YCD, and MH BCD), which stably expressed suicide genes SuperCD, YCD, or BCD at comparable levels as detected by Western blotting (Figure 1C). Next, a SRB cytotoxicity assay was performed to compare the suicidal efficiencies of the different transgenes in the context of stable cell lines. As shown in Figure 2, a clear order of efficacy of the different suicide transgenes was found: in the SuperCD expressing cell line (MH SuperCD) even at a 5-FC concentration as low as 0.1 mmol/L, a very low cell survival of only 8% was observed. In contrast, sole expression of YCD (MH YCD) was much less efficient, resulting in a nearly 5-fold higher cell survival (38% at 0.1 mmol/L 5-FC). Finally, sole expression of BCD had only a minor cytotoxic effect (>80% cell survival at 0.1 mmol/L 5-FC). Thereby, convincing *in vitro* evidence was provided that the YUPRT component implemented within the SuperCD fusion gene is highly functional in the context of hepatoma cells. This corresponds to observations made by others with cell lines derived from non-liver tumor tissues (e.g. human colon cancer cells, human pancreas tumor cells, human breast cancer cells, human glioblastoma cells)[22,26]. The efficacy of much lower 5-FC doses has to be regarded as an important finding when transferring the 5-FC/SuperCD system to the preclinical/clinical situation: in the mammalian organism, 5-FC is also metabolized by the bacteria of the gut flora. An increased intestinal production of 5-FU can lead to dramatic unwanted side effects which are feared greatly in the context of 5-FU chemotherapeutic regimes[27].

Subcutaneously implanted MH SuperCD tumors demonstrate a complete tumor regression under systemic 5-FC application

A first *in vivo* testing of the SuperCD-enhanced suicide

gene effect was performed in six animals who received two sc tumor cell injections each: (1) MH SuperCD cells into the right dorsum; and (2) as a control in the same animals MH naïve cells into the left dorsum. On d 11, when tumors had reached a measurable size, rats were randomized into two groups and treated for one week with twice daily ip injections of 5-FC or saline (control group). 5-FC serum levels of treated animals as determined by HPLC ranged from 1 to 2.6 μg/mL, whereas control animals receiving saline displayed background levels only (data not shown). During the treatment period, tumor volume increased constantly in the saline-treated negative control group, irrespectively of the tumor type implanted. In contrast, in all the three 5-FC treated animals, the MH SuperCD tumors disappeared completely, whereas the MH naïve tumors grown on the opposite dorsum further increased in volume until d 18, when the animals were killed (Table1). At post mortem examination of 5-FC-treated animals, no residual tumor tissue was found on the right dorsum in which the MH SuperCD tumors originally had grown, whereas large MH SuperCD tumors, weighing between 1.8 and 2.7 g, were found in the saline-treated animals. As expected, all animals displayed large MH naïve tumors on the opposite site, independent of 5-FC or saline treatment.

Molecular and functional analysis of subcutaneously grown control tumors explanted on d 18

In vivo selective pressure for transgene-negative tumor cells and silencing of transgenes by methylation events are well-known phenomena[28]. We, therefore, extracted DNA from subcutaneously grown xenograft tumors for PCR analysis. In all three SuperCD tumor samples obtained from saline-treated animals, a 1 143-bp SuperCD-specific PCR amplification product was detected (Figure 3A, lanes #1-#3). Thus, *in vivo* passage of SuperCD-expressing tumor cells does not cause a relevant selective pressure against the presence of the SuperCD transgene. From the same subcutaneously grown tumors explanted at d 18, we further performed a functional analysis on recultured tumor cells (saline-treated MH SuperCD/MH naïve tumors) by applying the SRB cytotoxicity assay (Figure 3B). A 4-d treatment with 5-FC had no toxic effect on *in vivo* passaged MH naïve cells (control). However, all three MH SuperCD cell cultures (#1-#3) obtained after *in vivo* passage demonstrated a profound 5-FC-induced cytotoxic effect (Figure 3B, lower curves). The cytotoxic effect following *in vivo* passage was found to be comparable with MH tumor cells that had not undergone an *in vivo* passage (compared with Figure 2). These results demonstrated that, irrespective of an 18-d *in vivo* passage, MH SuperCD tumor cells continuously exerted a strong suicide gene effect at low 5-FC prodrug levels, which is of importance for further preclinical and clinical suicide gene therapy approaches.

Orthotopically implanted MH SuperCD tumors demonstrate a profound tumor regression under systemic 5-FC application

Based on the overwhelming efficacy of 5-FC treatment

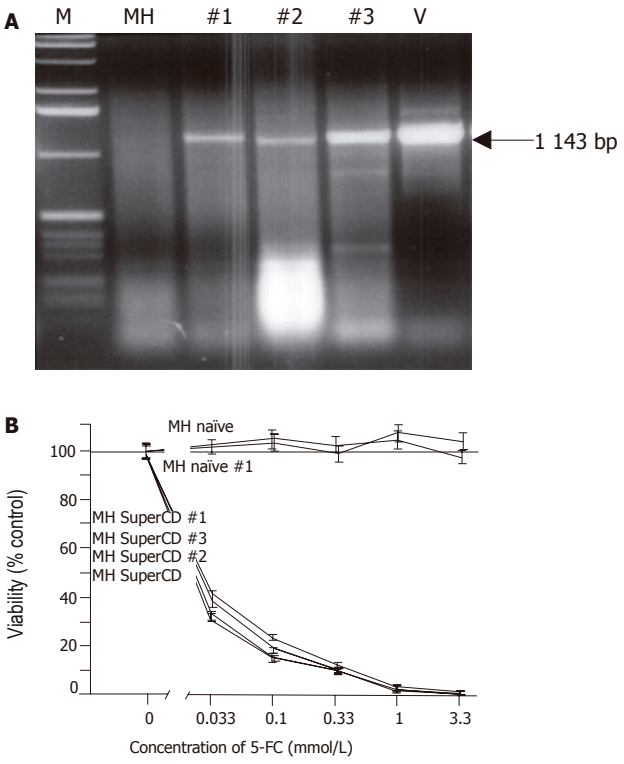

Figure 3 Molecular and functional analysis of subcutaneously grown control tumors explanted on d 18 (saline-treated MH SuperCD/MH naïve tumors).
A: Agarose gel electrophoresis of SuperCD DNA-specific PCR products. Lane M: marker DNA ladder; lane MH: MH parental cell line (no transgene; negative control; PCR performed with 1 μg of DNA); lanes 1-3: PCR amplifications performed on MH SuperCD tumor tissues of animals 1, 2, 3 (PCR performed with 1–3 μg of DNA); lane V: vector control lane (PCR performed with 1 pg of pLXSN-SuperCD). Arrow: indicates 1 143-bp SuperCD-specific amplification product. **B:** SRB cytotoxicity assay with recultured tumor cells explanted after 18 d of subcutaneous growth. As in Figure 2, cytotoxicity was measured after 5-FC treatment for 4 d *in vitro*. MH naïve: negative control with MH parental cell line (no transgene; no animal passage); MH naïve, #1: MH naïve tumor explanted from a saline-treated animal (control); MH SuperCD, cell line: MH SuperCD parental cell line (control; no animal passage); MH SuperCD 1, 2, 3, tumor passage: MH SuperCD tumors explanted from saline-treated animals 1, 2, 3. All values were referred to that of the untransduced control cells and are given as percentage of surviving cells (control: 100%). All experiments were carried out in quadruplicate. Viability values plotted represent fitted medians and 95%CI.

observed in subcutaneously grown MH SuperCD tumors, we next treated orthotopic liver tumors in the same rat hepatoma model in a larger number of animals, thereby investigating the statistical relevance of SuperCD suicide protein expression. As caliper measurement of small intrahepatic tumors is impossible, this study was based on non-invasive MRI imaging. Twenty-one days after the implantation of solitary MH SuperCD tumors into the livers of recipient animals, a first MRI was performed. Maximum tumor areas were analyzed. Rats with tumor areas ranging from 20 to 156 mm^2 (representative day 21 MRI images shown in Figures 4B and C, respectively, column 1 "untreated") were then randomized into two groups with six rats in each, and treated twice daily with ip injections of 5-FC or saline for 10 d.

MRI-based measurement of tumor sizes at the end of

Table 1 Effect of 5-FC treatment on subcutaneous MH tumor growth

		Suicide gene	
		None (control)	SuperCD
Treatment	5-FC	1.4 g	n.d.
		3.2 g	n.d.
		1.8 g	n.d.
	Saline (control)	2.5 g	1.8 g
		2.9 g	1.9 g
		3.7 g	2.7 g

Six animals received two sc tumor cell injections (1×10^7 cells in 70 μL PBS/animal). On d 11, tumor-bearing rats were randomized into two groups and treatment started with twice daily ip injections of 5-FC (283 mg/kg body weight) or saline (control). At the end of 5-FC treatment (d 18), animals were killed, tumors were harvested and weighed. Complete regression of tumors was observed only in the 5-FC-treated SuperCD tumors (n.d.: no detectable tumors).

the treatment (d 31) revealed a persistent orthotopic tumor growth for saline-treated control animals (Figure 4A, solid lines). In contrast, all six animals treated systemically for 10 d with 5-FC exhibited a clear decline of tumor sizes, either complete regressions or dramatic reductions (Figure 4A, broken lines). Ranking area differences revealed a significant difference between the untreated and the treated groups (*U*-test, $P = 0.0051$). Thus, bifunctional SuperCD suicide gene expression was found to be highly effective against a rat hepatoma model under both subcutaneous and orthotopic implantation conditions.

Low dose 5-FC application found to be sufficient to achieve complete tumor regressions of orthotopically implanted MH SuperCD cells

Anticipating an enhanced SuperCD suicide gene effect, we already had started to administer twice daily with 5-FC dosage of 283 mg/kg body weight, which is only half of the dosage of about 500 mg/kg body weight used by others[6,29-33]. Since this prodrug dosing regimen was found to be highly efficient for the eradication of both subcutaneous (Table 1) and orthotopic (Figure 4) MH SuperCD hepatomas, we aimed next at further decreasing the 5-FC dose by reducing the application frequency. Thereby, side effects due to 5-FU metabolites resulting from unwanted routes of "collateral" gut toxification could be even further reduced.

We tested this hypothesis on three animals with small MH SuperCD liver tumors (#7, #8, #9) having received saline only as control animals during the first treatment period. The other animals had to be euthanized due to their tumor burden. In these animals, low dose treatment was started on d 31 with only twice weekly ip injections of 5-FC (283 mg/kg body weight) for 28 d. When MRI was again performed at d 59, all MH SuperCD tumors had completely disappeared (Figure 5, right column). In none of these three animals, any solid tumor tissue was found at autopsy. Instead, only small yellowish fatty "scars" were visible. Thereby, bifunctional SuperCD suicide gene expression was found to be highly effective in a rat hepatoma model under both subcutaneous and orthotopic growth conditions, even when a strongly reduced 5-FC dosing regime was applied.

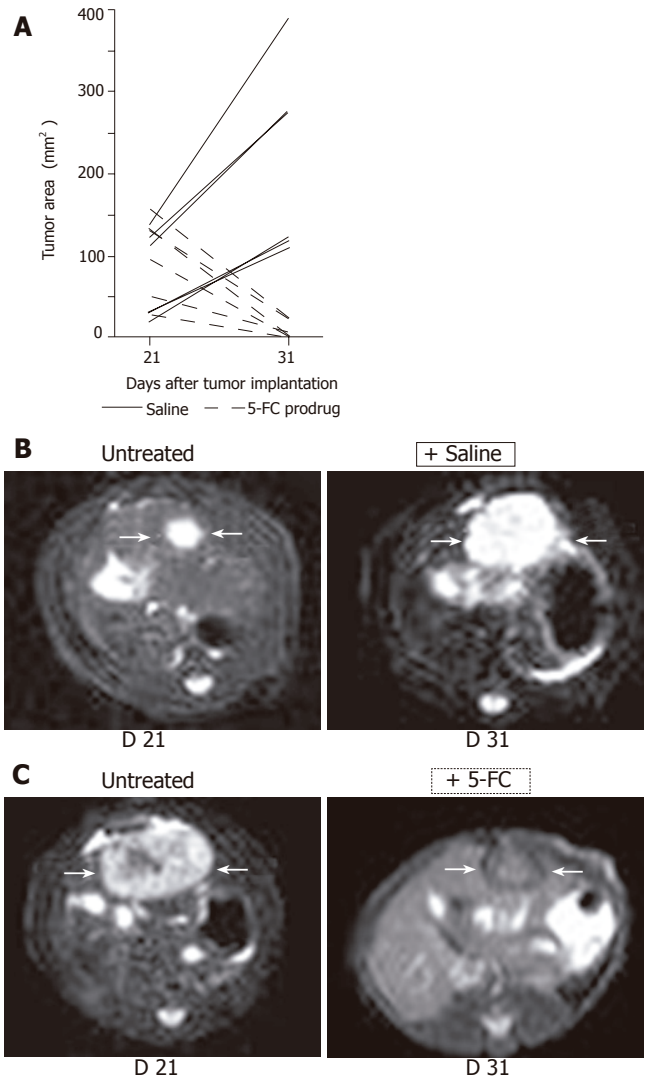

Figure 4 Non-invasive MRI detection of tumor growth of orthotopically implanted MH SuperCD hepatomas (saline *vs* 5-FC prodrug treatment). Animals with MRI detectable liver tumors in T2 weighed images were randomized into two groups (6 rats/group) and treated twice daily with ip injections of saline or 5-FC (283 mg/kg body weight) over a 10-d period. Panel A: Maximum tumor areas (mm^2) at d 21 and d 31; solid lines: tumor growth of control animals (saline-treated); broken lines: tumor regression of serum animals (5-FC-treated). Panel B: Representative MRI tumor images of the saline-treated control animal exhibiting the smallest tumor area at d 21 (left); and a dramatic tumor growth was observed at d 31 (right). Panel C: Representative MRI tumor images of the serum animal (treated with 5-FC) exhibiting the largest tumor area at d 21 (left); and a dramatic tumor regression was measured at d 31 (right).

Determination of in vivo suicide gene effectiveness by direct in vivo comparison of suicide genes SuperCD vs YCD vs BCD

Until now, no study encompassing a direct *in vivo* comparison of different suicide genes (SuperCD *vs* YCD *vs* BCD) has been performed. Therefore, 1×10^7 cells of the four cell-lines (1) MH naïve (negative control), (2) MH BCD, (3) MH YCD, and (iv) MH SuperCD were injected subcutaneously into ACI rats. In this course, each animal

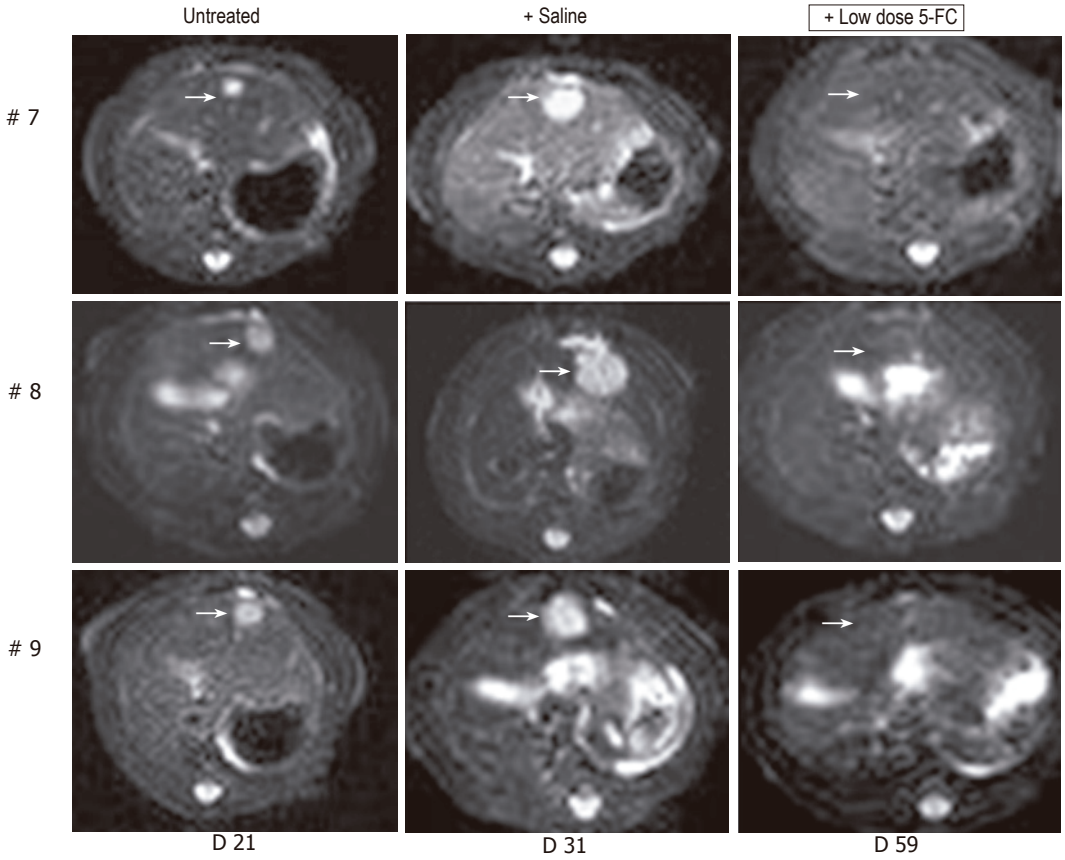

Figure 5 MRI detection of tumor growth of orthotopically implanted MH SuperCD hepatomas treated under a low-dose 5-FC regimen. Animals #7, #8, #9 (column 1: tumor size at d 21), which first had been treated with saline only for over a 7-d period and thereafter, uniformly exhibiting a substantial tumor growth (column 2: tumor size at d 31), were then treated by a low-dose 5-FC regimen [twice weekly ip injections of 5-FC (283 mg/kg body weight)] over a 28-d period until d 59. Analysis of subsequent MRI sections did not reveal any MH SuperCD tumors (column 3, d 59: +low dose 5-FC); T2 weighed images are depicted; arrows in column 3 point out to places of former tumor localizations before the onset of 5-FC treatment.

received two injections with two different cell-lines, one inoculated at the left dorsum, and the other one at the right dorsum. Based on a balanced incomplete block plan, the six possible pairs of cell lines were implanted into six groups, each comprising eight animals. Tumor volumes were determined by caliper measurement. At d 15 after hepatoma cell inoculation, prodrug therapy with twice weekly ip injections of 283 mg 5-FC/kg body weight (low dose regime) was started. Interestingly, 8 out of 18 MH SuperCD tumors on d 28 and 11 out of 18 MH SuperCD-tumors on d 31 had shrunken to an immeasurable size (Figure 6A, right panel). A subsequent analysis of covariance of log tumor volumes revealed a significant reduction in median tumor volumes under our low dose 5-FC application scheme only for the MH SuperCD tumors. The reduction in median tumor volume was almost complete (95%CI for the reduction between d 14 and 31 from 98.7% to 99.6%) (Figure 6B). The maximum likelihood ratio χ^2 test of the global hypothesis was significant $\chi^2 = 264$; 3 df; $P = 6\times10^{-57}$). Thus, for the first time *in vivo* evidence was provided demonstrating that the SuperCD *in vivo* suicide gene effect might be superior to the one of YCD ($P < 10^{-10}$), which itself was superior to BCD (Figures 6A and B).

DISCUSSION

Although the study described here demonstrated that the expression of YCD and YUPRT as a fusion protein with 5-FC administration exerted a striking antitumor effect on solid tumors like hepatomas, further improvements are needed for clinical applications. Current limitations of *in vivo* liver tumor transduction efficiencies could be further compensated with the help of intercellular cargo proteins (e.g. VP22, our own work[18,34], and Refs. [35,36]). At the moment, we are evaluating the properties of VP22-SuperCD/SuperCD-VP22 fusion proteins to further potentiate suicide gene therapy efficiencies in our rat hepatoma model, thereby improving the intratumoral distribution of enzymatically enhanced suicide genes. Other promising approaches rely on the employment of strong hepatoma-specific promoters which are suitable to achieve high levels of hepatoma-specific SuperCD expression *in vivo* (e.g. the cell growth-related midkine promoter)[37]. Most importantly, gene transfer systems have to be identified, which are suitable to provide a significant increase of the accessibility of liver tumor cells to systemically applied gene transfer vectors. In a recent study, herpes thymidine kinase suicide gene transducing liposomes, based on the hemagglutinating

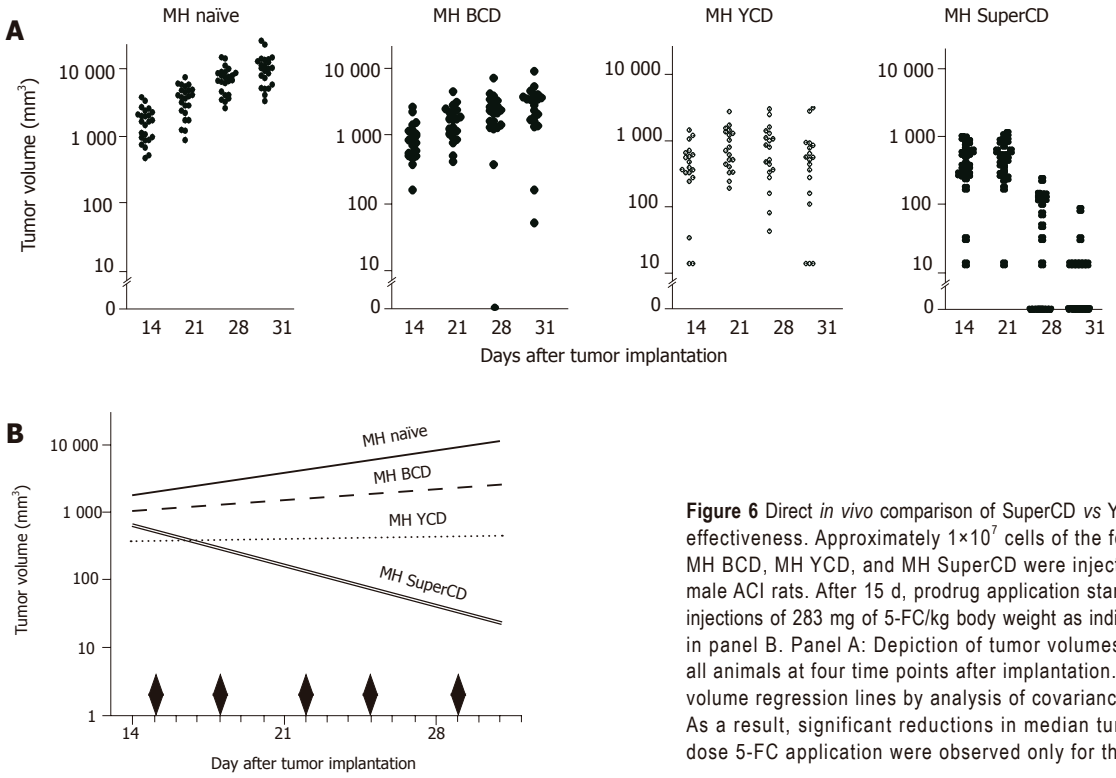

Figure 6 Direct *in vivo* comparison of SuperCD *vs* YCD *vs* BCD suicide gene effectiveness. Approximately 1×10^7 cells of the four cell-lines MH naïve, MH BCD, MH YCD, and MH SuperCD were injected subcutaneously into male ACI rats. After 15 d, prodrug application started with twice weekly ip injections of 283 mg of 5-FC/kg body weight as indicated by black diamonds in panel B. Panel A: Depiction of tumor volumes of all four cell lines in all animals at four time points after implantation. Panel B: Median tumor volume regression lines by analysis of covariance of log tumor volumes. As a result, significant reductions in median tumor volumes under low dose 5-FC application were observed only for the MH SuperCD tumors.

virus of Japan, were injected directly into the portal vein of severe combined immunodeficiency mice, and reported to be as an efficient tool for the transduction of multilocalized HUH7 human hepatocellular carcinomas in this animal model[38]. Thus, transduction properties of hemagglutinating virus of Japan (also defined as Sendai virus) seem to favor transduction of liver tumors. Concluding from this, also recombinant Sendai virus vectors[39,40] encoding optimized suicide genes might be suitable to overcome the liver tumor transduction barrier[41,42]. HIV-derived lentiviral vectors have also been successfully used for suicide gene therapy in hepatocellular carcinoma[43]. In addition, newly developed replication-competent vectors/oncolytic vectors[42,44-47] could be used to cope with the liver tumor transduction barrier.

Concerning our current knowledge on severe gene therapeutic side effects employing state-of-the-art retroviral[48], adenoviral[49], or adeno-associated virus vectors[50], a reduction of vector dosages might become possible with the SuperCD suicide gene. This would constitute an important additional safety factor for further clinical gene therapy applications. Subsequent *in vivo* studies will compare application of the therapeutic SuperCD suicide gene by virtue of direct (injection), systemic (iv) or regional (ia) gene transfer and treatment with 5-FC.

In summary, a combination of synergistic strategies as described above may allow a further enhancement of the suicide gene effect in the near future. Thus, further refinements may help to make suicide gene therapy a feasible treatment modality for solid malignant tumors in human beings.

REFERENCES

1 **Danielsen S,** Kilstrup M, Barilla K, Jochimsen B, Neuhard J. Characterization of the Escherichia coli codBA operon encoding cytosine permease and cytosine deaminase. *Mol Microbiol* 1992; **6:** 1335-1344
2 **Austin EA,** Huber BE. A first step in the development of gene therapy for colorectal carcinoma: cloning, sequencing, and expression of Escherichia coli cytosine deaminase. *Mol Pharmacol* 1993; **43:** 380-387
3 **Kanai F,** Lan KH, Shiratori Y, Tanaka T, Ohashi M, Okudaira T, Yoshida Y, Wakimoto H, Hamada H, Nakabayashi H, Tamaoki T, Omata M. *In vivo* gene therapy for alpha-fetoprotein-producing hepatocellular carcinoma by adenovirus-mediated transfer of cytosine deaminase gene. *Cancer Res* 1997; **57:** 461-465
4 **Ohwada A,** Hirschowitz EA, Crystal RG. Regional delivery of an adenovirus vector containing the Escherichia coli cytosine deaminase gene to provide local activation of 5-fluorocytosine to suppress the growth of colon carcinoma metastatic to liver. *Hum Gene Ther* 1996; **7:** 1567-1576
5 **Richards CA,** Austin EA, Huber BE. Transcriptional regulatory sequences of carcinoembryonic antigen: identification and use with cytosine deaminase for tumor-specific gene therapy. *Hum Gene Ther* 1995; **6:** 881-893
6 **Adachi Y,** Tamiya T, Ichikawa T, Terada K, Ono Y, Matsumoto K, Furuta T, Hamada H, Ohmoto T. Experimental gene therapy for brain tumors using adenovirus-mediated transfer of cytosine deaminase gene and uracil phosphoribosyltransfer ase gene with 5-fluorocytosine. *Hum Gene Ther* 2000; **11:** 77-89
7 **Miller CR,** Williams CR, Buchsbaum DJ, Gillespie GY. Intratumoral 5-fluorouracil produced by cytosine deaminase/5-fluorocytosine gene therapy is effective for experimental human glioblastomas. *Cancer Res* 2002; **62:** 773-780
8 **Uckert W,** Kammertons T, Haack K, Qin Z, Gebert J, Schendel DJ, Blankenstein T. Double suicide gene (cytosine deaminase and herpes simplex virus thymidine kinase) but not single

gene transfer allows reliable elimination of tumor cells *in vivo*. *Hum Gene Ther* 1998; **9:** 855-865

9 **Hirschowitz EA,** Ohwada A, Pascal WR, Russi TJ, Crystal RG. *In vivo* adenovirus-mediated gene transfer of the Escherichia coli cytosine deaminase gene to human colon carcinoma-derived tumors induces chemosensitivity to 5-fluorocytosine. *Hum Gene Ther* 1995; **6:** 1055-1063

10 **Huber BE,** Austin EA, Richards CA, Davis ST, Good SS. Metabolism of 5-fluorocytosine to 5-fluorouracil in human colorectal tumor cells transduced with the cytosine deaminase gene: significant antitumor effects when only a small percentage of tumor cells express cytosine deaminase. *Proc Natl Acad Sci USA* 1994; **91:** 8302-8306

11 **Trinh QT,** Austin EA, Murray DM, Knick VC, Huber BE. Enzyme/prodrug gene therapy: comparison of cytosine deaminase/5-fluorocytosine versus thymidine kinase/ganciclovir enzyme/prodrug systems in a human colorectal carcinoma cell line. *Cancer Res* 1995; **55:** 4808-4812

12 **Tiraby M,** Cazaux C, Baron M, Drocourt D, Reynes JP, Tiraby G. Concomitant expression of E. coli cytosine deaminase and uracil phosphoribosyltransferase improves the cytotoxicity of 5-fluorocytosine. *FEMS Microbiol Lett* 1998; **167:** 41-49

13 **Trubenbach J,** Graepler F, Pereira PL, Ruck P, Lauer U, Gregor M, Claussen CD, Huppert PE. Growth characteristics and imaging properties of the morris hepatoma 3924A in ACI rats: a suitable model for transarterial chemoembolization. *Cardiovasc Intervent Radiol* 2000; **23:** 211-217

14 **Kern L,** de Montigny J, Jund R, Lacroute F. The FUR1 gene of Saccharomyces cerevisiae: cloning, structure and expression of wild-type and mutant alleles. *Gene* 1990; **88:** 149-157

15 **Wybranietz WA,** Lauer U. Distinct combination of purification methods dramatically improves cohesive-end subcloning of PCR products. *Biotechniques* 1998; **24:** 578-580

16 **Miller AD,** Rosman GJ. Improved retroviral vectors for gene transfer and expression. *Biotechniques* 1989; **7:** 980-982, 984-986, 989-990

17 **Mullen CA,** Kilstrup M, Blaese RM. Transfer of the bacterial gene for cytosine deaminase to mammalian cells confers lethal sensitivity to 5-fluorocytosine: a negative selection system. *Proc Natl Acad Sci USA* 1992; **89:** 33-37

18 **Wybranietz WA,** Prinz F, Spiegel M, Schenk A, Bitzer M, Gregor M, Lauer UM. Quantification of VP22-GFP spread by direct fluorescence in 15 commonly used cell lines. *J Gene Med* 1999; **1:** 265-274

19 **Rogulski KR,** Kim JH, Kim SH, Freytag SO. Glioma cells transduced with an Escherichia coli CD/HSV-1 TK fusion gene exhibit enhanced metabolic suicide and radiosensitivity. *Hum Gene Ther* 1997; **8:** 73-85

20 **Skehan P,** Storeng R, Scudiero D, Monks A, McMahon J, Vistica D, Warren JT, Bokesch H, Kenney S, Boyd MR. New colorimetric cytotoxicity assay for anticancer-drug screening. *J Natl Cancer Inst* 1990; **82:** 1107-1112

21 **Carlsson G,** Gullberg B, Hafstrom L. Estimation of liver tumor volume using different formulas - an experimental study in rats. *J Cancer Res Clin Oncol* 1983; **105:** 20-23

22 **Erbs P,** Regulier E, Kintz J, Leroy P, Poitevin Y, Exinger F, Jund R, Mehtali M. *In vivo* cancer gene therapy by adenovirus-mediated transfer of a bifunctional yeast cytosine deaminase/uracil phosphoribosyltransferase fusion gene. *Cancer Res* 2000; **60:** 3813-3822

23 **Maron DJ,** Tada H, Moscioni AD, Tazelaar J, Fraker DL, Wilson JM, Spitz FR. Intra-arterial delivery of a recombinant adenovirus does not increase gene transfer to tumor cells in a rat model of metastatic colorectal carcinoma. *Mol Ther* 2001; 4: 29-35

24 **Yoon SK,** Armentano D, Wands JR, Mohr L. Adenovirus-mediated gene transfer to orthotopic hepatocellular carcinomas in athymic nude mice. *Cancer Gene Ther* 2001; **8:** 573-579

25 **Mullen CA,** Kilstrup M, Blaese RM. Transfer of the bacterial gene for cytosine deaminase to mammalian cells confers lethal sensitivity to 5-fluorocytosine: a negative selection system. *Proc Natl Acad Sci United States* 1992; **89:** 33-37

26 **Kievit E,** Nyati MK, Ng E, Stegman LD, Parsels J, Ross BD, Rehemtulla A, Lawrence TS. Yeast cytosine deaminase improves radiosensitization and bystander effect by 5-fluorocytosine of human colorectal cancer xenografts. *Cancer Res* 2000; **60:** 6649-6655

27 **Diasio RB,** Lakings DE, Bennett JE. Evidence for conversion of 5-fluorocytosine to 5-fluorouracil in humans: possible factor in 5-fluorocytosine clinical toxicity. *Antimicrob Agents Chemother* 1978; **14:** 903-908

28 **Roncarolo MG,** Levings MK, Mangia P, Bordignon C, Marktel S, Bonini C, Traversar C. Characterization and modulation of the undesirable T cell-mediated responses to transgenes. *Mol Ther* 2002: S399

29 **Kanyama H,** Tomita N, Yamano T, Aihara T, Miyoshi Y, Ohue M, Sekimoto M, Sakita I, Tamaki Y, Kaneda Y, Senter PD, Monden M. Usefulness of repeated direct intratumoral gene transfer using hemagglutinating virus of Japan-liposome method for cytosine deaminase suicide gene therapy. *Cancer Res* 2001; **61:** 14-18

30 **Kievit E,** Bershad E, Ng E, Sethna P, Dev I, Lawrence TS, Rehemtulla A. Superiority of yeast over bacterial cytosine deaminase for enzyme/prodrug gene therapy in colon cancer xenografts. *Cancer Res* 1999; **59:** 1417-1421

31 **Chung-Faye GA,** Chen MJ, Green NK, Burton A, Anderson D, Mautner V, Searle PF, Kerr DJ. *In vivo* gene therapy for colon cancer using adenovirus-mediated, transfer of the fusion gene cytosine deaminase and uracil phosphoribosyltransferase. *Gene Ther* 2001; **8:** 1547-1554

32 **Hamstra DA,** Rice DJ, Fahmy S, Ross BD, Rehemtulla A. Enzyme/prodrug therapy for head and neck cancer using a catalytically superior cytosine deaminase. *Hum Gene Ther* 1999; **10:** 1993-2003

33 **Block A,** Freund CT, Chen SH, Nguyen KP, Finegold M, Windler E, Woo SL. Gene therapy of metastatic colon carcinoma: regression of multiple hepatic metastases by adenoviral expression of bacterial cytosine deaminase. *Cancer Gene Ther* 2000; **7:** 438-445

34 **Wybranietz WA,** Gross CD, Phelan A, O'Hare P, Spiegel M, Graepler F, Bitzer M, Stahler P, Gregor M, Lauer UM. Enhanced suicide gene effect by adenoviral transduction of a VP22-cytosine deaminase (CD) fusion gene. *Gene Ther* 2001; **8:** 1654-1664

35 **Liu CS,** Kong B, Xia HH, Ellem KA, Wei MQ. VP22 enhanced intercellular trafficking of HSV thymidine kinase reduced the level of ganciclovir needed to cause suicide cell death. *J Gene Med* 2001; **3:** 145-152

36 **Ford KG,** Souberbielle BE, Darling D, Farzaneh F. Protein transduction: an alternative to genetic intervention? *Gene Ther* 2001; **8:** 1-4

37 **Tomizawa M,** Yu L, Wada A, Tamaoki T, Kadomatsu K, Muramatsu T, Matsubara S, Watanabe K, Ebara M, Saisho H, Sakiyama S, Tagawa M. A promoter region of the midkine gene that is frequently expressed in human hepatocellular carcinoma can activate a suicide gene as effectively as the alpha-fetoprotein promoter. *Br J Cancer* 2003; **89:** 1086-1090

38 **Hirano T,** Kaneko S, Kaneda Y, Saito I, Tamaoki T, Furuyama J, Tamaoki T, Kobayashi K, Ueki T, Fujimoto J. HVJ-liposome-mediated transfection of HSVtk gene driven by AFP promoter inhibits hepatic tumor growth of hepatocellular carcinoma in SCID mice. *Gene Ther* 2001; **8:** 80-83

39 **Yonemitsu Y,** Kitson C, Ferrari S, Farley R, Griesenbach U, Judd D, Steel R, Scheid P, Zhu J, Jeffery PK, Kato A, Hasan MK, Nagai Y, Masaki I, Fukumura M, Hasegawa M, Geddes DM, Alton EW. Efficient gene transfer to airway epithelium using recombinant Sendai virus. *Nat Biotechnol* 2000; **18:** 970-973

40 **Sedlmeier R,** Neubert WJ. The replicative complex of

paramyxoviruses: structure and function. *Adv Virus Res* 1998; **50:** 101-139

41 **Bilbao R,** Bustos M, Alzuguren P, Pajares MJ, Drozdzik M, Qian C, Prieto J. A blood-tumor barrier limits gene transfer to experimental liver cancer: the effect of vasoactive compounds. *Gene Ther* 2000; **7:** 1824-1832

42 **Shayakhmetov DM,** Li ZY, Ni S, Lieber A. Targeting of adenovirus vectors to tumor cells does not enable efficient transduction of breast cancer metastases. *Cancer Res* 2002; **62:** 1063-1068

43 **Gerolami R,** Uch R, Faivre J, Garcia S, Hardwigsen J, Cardoso J, Mathieu S, Bagnis C, Brechot C, Mannoni P. Herpes simplex virus thymidine kinase-mediated suicide gene therapy for hepatocellular carcinoma using HIV-1-derived lentiviral vectors. *J Hepatol* 2004; ***40:*** 291-297

44 **Ohashi M,** Kanai F, Tateishi K, Taniguchi H, Marignani PA, Yoshida Y, Shiratori Y, Hamada H, Omata M. Target gene therapy for alpha-fetoprotein-producing hepatocellular carcinoma by E1B55k-attenuated adenovirus. *Biochem Biophys Res Commun* 2001; **282:** 529-535

45 **Rogulski KR,** Wing MS, Paielli DL, Gilbert JD, Kim JH, Freytag SO. Double suicide gene therapy augments the antitumor activity of a replication-competent lytic adenovirus through enhanced cytotoxicity and radiosensitization. *Hum Gene Ther* 2000; **11:** 67-76

46 **Bitzer M,** Lauer UM. [Oncolytic viruses for genetic therapy of gastrointestinal tumors] *Z Gastroenterol* 2003; **41:** 667-674

47 **Kirn D,** Martuza RL, Zwiebel J. Replication-selective virotherapy for cancer: Biological principles, risk management and future directions. *Nat Med* 2001; **7:** 781-787

48 **Hacein-Bey-Abina S,** Le Deist F, Carlier F, Bouneaud C, Hue C, De Villartay JP, Thrasher AJ, Wulffraat N, Sorensen R, Dupuis-Girod S, Fischer A, Davies EG, Kuis W, Leiva L, Cavazzana-Calvo M. Sustained correction of X-linked severe combined immunodeficiency by ex vivo gene therapy. *N Engl J Med* 2002; **346:** 1185-1193

49 **Somia N,** Verma IM. Gene therapy: trials and tribulations. *Nat Rev Genet* 2000; **1:** 91-99

50 **Arruda VR,** Fields PA, Milner R, Wainwright L, De Miguel MP, Donovan PJ, Herzog RW, Nichols TC, Biegel JA, Razavi M, Dake M, Huff D, Flake AW, Couto L, Kay MA, High KA. Lack of germline transmission of vector sequences following systemic administration of recombinant AAV-2 vector in males. *Mol Ther* 2001; **4:** 586-592

Science Editor Kumar M and Guo SY **Language Editor** Elsevier HK

PO Box 2345, Beijing 100023, China
www.wjgnet.com
wjg@wjgnet.com

ELSEVIER

World J Gastroenterol 2005;11(44):6920-6925
World Journal of Gastroenterology ISSN 1007-9327

Role of blood AFP mRNA and tumor grade in the preoperative prognostic evaluation of patients with hepatocellular carcinoma

Umberto Cillo, Alessandro Vitale, Filippo Navaglia, Daniela Basso, Umberto Montin, Marco Bassanello, Francesco D'Amico, Francesco Antonio Ciarleglio, Alberto Brolese, Giacomo Zanus, Vito De Pascale, Mario Plebani, Davide Francesco D'Amico

Umberto Cillo, Alessandro Vitale, Umberto Montin, Marco Bassanello, Francesco D'Amico, Francesco Antonio Ciarleglio, Alberto Brolese, Giacomo Zanus, Davide Francesco D'Amico, Clinica Chirurgica I, Dipartimento di Scienze Chirurgiche e Gastroenterologiche, Università degli Studi di Padova, Italy
Filippo Navaglia, Daniela Basso, Mario Plebani, Dipartimento di Medicina di Laboratorio, Università degli Studi di Padova, Italy
Vito De Pascale, Dipartimento Assistenziale di Chirurgia Generale ed Emergenze Chirurgiche, II Università degli Studi di Napoli, Italy
Correspondence to: Alessandro Vitale, MD, Clinica Chirurgica I - Dipartimento di Scienze Chirurgiche e Gastroenterologiche - Università degli Studi di Padova - Via Giustiniani 2, Policlinico III piano, 35128 Padova, Italy. alessandro.vitale@unipd.it
Telephone: +39-49-8212210 Fax: +39-49-656145
Received: 2005-02-17 Accepted: 2005-04-26

Abstract

AIM: To explore the potential prognostic role of preoperative tumor grade and blood AFP mRNA in a cohort of patients with hepatocellular carcinoma (HCC) eligible for radical therapies according to a well-defined treatment algorithm not including nodule size and number as absolute selection criteria.

METHODS: Fifty patients with a diagnosis of HCC were prospectively enrolled in the study. Inclusion criteria were: (1) histological assessment of tumor grade by means of percutaneous biopsies; (2) determination of AFP mRNA status in the blood; (3) patient's eligibility for radical therapies.

RESULTS: At preoperative evaluation, 54% of the study group had a well-differentiated HCC, 42% had AFP mRNA in the blood, 40% had a tumor larger than 5 cm and 56% had more than one nodule. Surgery (resection or liver transplantation) was performed in 29 patients, while 21 had percutaneous ablation procedures. After a median follow-up of 28 mo, 12-, 24-, and 36-mo survival rates were 78%, 58%, and 51%, respectively. Surgical therapy, performance status and three tumor-related variables (AFP mRNA, HCC grade and gross vascular invasion) resulted as significant survival predictors at univariate analysis. Nodule size and number did not perform as significant prognosticators. Multivariate study selected only surgical therapy and a biologically early HCC profile (AFP mRNA negative and well-differentiated tumor without gross vascular invasion) as independent survival variables.

CONCLUSION: The preoperative determination of tumor grade and blood AFP mRNA status may potentially refine the prognostic evaluation of HCC patients and improve the selection process for radical therapies.

Key words: Hepatocellular carcinoma; Prognosis; Treatment policy; Biomarker; Tumor biology

Cillo U, Vitale A, Navaglia F, Basso D, Montin U, Bassanello M, D'Amico F, Ciarleglio FA, Brolese A, Zanus G, De Pascale V, Plebani M, D'Amico DF. Role of blood AFP mRNA and tumor grade in the preoperative prognostic evaluation of patients with hepatocellular carcinoma. *World J Gastroenterol* 2005; 11(44): 6920-6925
http://www.wjgnet.com/1007-9327/11/6920.asp

INTRODUCTION

Liver transplantation (LT), hepatic resection and percutaneous treatments[1-3] are commonly considered as potential radical therapies for patients with hepatocellular carcinoma (HCC). Macroscopic tumor characteristics detected by imaging studies (nodule size and number) undoubtedly identify a subgroup of HCC patients at an early stage of hepatic disease (single nodule <5 cm, <3 nodules, and <3 cm) able to achieve long-term survival figures when radically treated[4,5]. Large pathologic retrospective studies[6-9], however, have shown that these macro-morphological features are indirect markers of specific tumor histological characteristics such as grade of differentiation and microscopic vascular invasion which have therefore the potential to refine the HCC prognostic assessment[10-12]. On the other hand, many molecular biological factors have been studied and related to the HCC biological aggressiveness[13]. However, preoperatively detectable biomarkers (histological and/or hematic) have not yet been introduced in the

routine HCC prognostic evaluation. In our experience, the preoperative determination of the HCC grade by means of percutaneous biopsy performed as a valid tool in the selection of unresectable HCC patients for transplantation[14]. Moreover, we retrospectively showed that some patients with morphologically advanced but well-differentiated HCC may benefit of potentially radical therapies[15]. Among the proposed HCC molecular markers, alpha-fetoprotein messenger RNA (AFP mRNA), detected in the blood by reverse-transcription polymerase chain reaction (RT-PCR), has been the most diffusely studied in last years[16-19]. Our preliminary experience with this marker showed its significance and promising correlation with HCC invasiveness parameters[16]. However, the prognostic utility of AFP mRNA when detected before the treatment remains controversial[20-22]. In this prospective study, a group of HCC patients were selected for radical therapies according to a precise treatment schedule. In addition to conventional HCC parameters, their preoperative study also included the determination of tumor grade and AFP mRNA status in the blood. The enrolled patients were prospectively followed in order to identify the main preoperative predictors of survival.

MATERIALS AND METHODS

Patient enrolment

Between April 2001 and October 2002, 50 patients with a diagnosis of HCC were prospectively enrolled in the study. Patients were eligible for inclusion if they met the following criteria: (1) HCC diagnosis histologically confirmed by the examination of liver specimens obtained by percutaneous biopsies. Pathological grading was contextually assessed in all the patients according to Edmonson's classification; (2) patient's informed consent to provide blood samples for AFP mRNA determination; (3) patient's eligibility for radical therapies according to a published schedule[14,23].

Hepatic resection was considered for HCC patients with preserved liver function (Child-Pugh A-B) and a technically resectable liver tumor without extra hepatic metastasis. If resection was not feasible, patients were considered for LT. The following exclusion criteria for LT were established as previously reported[14]: general contraindications to transplant (age, severe extrahepatic diseases, recent malignancies, and compliance), extra hepatic spread or gross vascular invasion (preoperatively evident or suspected), poorly-differentiated HCC (G3) at pre-OLT percutaneous biopsy. Size and number of nodules were not considered as absolute selection criteria. Patients not fulfilling the criteria for any surgical procedure were assessed for other loco-regional treatments such as percutaneous radiofrequency (RF) or ethanol injection (PEI), and transarterial chemoembolization (TACE).

After discharge, the patients were followed up regularly according to the main treatment received. To detect tumor recurrence after surgery, patients received clinical and laboratory assessment every month, and US and CT every 3rd and 6th mo, respectively. When HCC recurrence was noted, patients were further treated with the most appropriate procedure according to our treatment schedule. After PEI, RF or TACE, dynamic CT examinations were performed to determine therapy efficacy and, when residual staining was noted, these procedures were repeated and the outcome was examined. None of the enrolled patients were lost during follow-up or died within 30 d after first observation or treatment. Therefore, all the 50 patients initially entering the study were available for the survival analysis.

Detection of AFP mRNA in nucleated cells

The AFP mRNA status in the blood was determined in each enrolled patient within 3 mo from treatment application. In brief, total RNA was extracted from 7 mL of peripheral blood and converted to complementary DNA. A nested polymerase chain reaction (PCR) protocol was performed as previously reported[16]. Positive results were evidenced as a 282-bp band in agarose gel stained with ethidium-bromide. As a positive control, cDNA obtained from human hepatocyte was used in each run. Negative controls for each step were also always included.

Statistical analysis

All variables were described by statistical characteristics: categorical data were described by frequency and percentage, whereas continuous data by median (range). Comparison between groups was done by using the χ^2 test or the Fisher's exact test for qualitative variables and the logistic regression for quantitative variables. Follow-up length and survival are expressed as median (range). Recruitment of follow-up data was closed on December 31, 2004. Twenty-four preoperative variables were assessed in the univariate survival analysis: age, sex, performance status, presence of cirrhosis, etiology of cirrhosis, clinical evidence of portal hypertension (presence of esophageal varices, splenomegaly with a platelet count <100 000/mm^3, or ascites), Child-Pugh's classification[24], bilirubin, albumin, prothrombin activity, alkaline phosphatase, gamma-glutamyl transpeptidase, creatinin, aspartate, and alanine aminotransferase, AFP, AFP mRNA blood-status, tumor morphology at preoperative imaging study (TNM, bilobarity, number and size of nodules, gross vascular invasion), differentiation degree at preoperative liver biopsy, and type of treatment. For continuous variables, the cut-off level was their median value. Univariate survival analysis was performed including each variable in a Cox regression model and calculating its related likelihood-ratio of χ^2 and *P* value. Survival curves were calculated using the Kaplan-Meier method and compared by means of the log-rank test. All variables significantly influencing survival in the univariate analysis were analyzed together in a Cox's proportional hazard regression model (multivariate analysis) with the aim of studying the independent contribution of each variable in explaining survivorship. The results of the Cox regression were expressed using both the risk ratios with its related confidence interval and the likelihood ratio of χ^2 with its related *P* value. Analyses were performed using the SAS Institute statistical package

(JMP). Differences were considered significant at $P<0.05$.

RESULTS

The main characteristics of the study group are shown in Table 1. At presentation, only 20% of patients had a compromised general condition due to cancer-related symptoms (PST ⩾1), 63% had a Child B-C cirrhosis and 62% had a clinically relevant portal hypertension. As for tumor characteristics, 52% of patients had a T3-T4 HCC; the tumor was larger than 5 cm in 20 patients (40%), while 28 (56%) had more than one nodule; macroscopic vascular invasion was detected in 12 patients (24%) and 27 patients (54%) had a well-differentiated HCC. AFP mRNA was found in the blood of 21 HCC patients (42%). As previously reported[16], the presence of AFP mRNA in blood was significantly related to cholestatic indices, gross vascular invasion, nodule size, and G2-G3 tumors (Table 1). Surgery was performed in 29 patients (58%), including 22 liver resections and 7 OLT, while 21 patients (42%) had percutaneous ablation procedures eventually associated with TACE.

Survival analysis

As at December 31st 2004, the median follow-up for the whole HCC group (50 patients) was 28 months (range 1-45 mo). Overall mortality was 48% (24 cases) and 12-, 24-, and 36-mo survival rates were 78%, 58%, and 51%, respectively (Figure 1A). Five out of the twenty-four variables had predictive prognostic value for survival in the univariate analysis (Table 1): PST, AFP mRNA, gross vascular invasion, histological grade, and surgical therapy.

A first multivariate study including these five variables selected only surgical treatment as independent survival predictor (Table 2, Figure 1B). Taking into account the strict correlation between AFP mRNA, vascular invasion and HCC grade in the study group[16], in a further analysis we combined these three tumor-related variables in a single parameter defined early HCC (AFP mRNA negative and well-differentiated tumor without gross vascular invasion). This second multivariate study selected tumor early biological status as the most important prognostic factor (Table 2 and Figure 1C).

DISCUSSION

Prognostic prediction and therapeutic decision for HCC patients are currently based in most centers on macroscopic tumor characteristics detected by imaging studies (nodule size and number). In the last decade, an empirical rule

Table 1 Preoperative characteristics of the 50 enrolled HCC patients and univariate survival analysis

Variables	Study group (50 patients)	Likelihood-ratio χ^2 (*P* value)
Median age (yr)	62 (22-88)	2.23 (NS)
Sex (M/F)	41/9	1.35 (NS)
Performance status (PST) ⩾1	10	4.06 (.0438)
Cirrhosis	43	1.12 (NS)
Etiology: HCV/HBV/alcohol/other	29/6/5/10	
viral	35	1.7 (NS)
Portal hypertension	31	0.17 (NS)
Child-Pugh score (A/B/C)	16/24/3	2.31 (NS)
Analytical data		
Bilirubin (μmol/L)	20 (7-233)	0.02 (NS)
Serum albumin (g/L)	35 (21-46)	0.49 (NS)
Prothrombin activity (%)	77 (39-109)	0.02 (NS)
[1]Alkaline phosphatase (U/L)	113 (42-395)	1.33 (NS)
[1]GGT (U/L)	64 (21-864)	3.25 (NS)
Creatinin (μmol/L)	83 (63-166)	1.47 (NS)
AST (U/L)	95 (20-492)	0.48 (NS)
ALT (U/L)	78 (12-469)	0.19 (NS)
Median AFP level (ng/L)	17 (4-1 400)	0.69 (NS)
Positive AFP mRNA	21	5.96 (0.0146)
TNM T3/T4	26	2.8 (NS)
Bilobar	7	2.38 (NS)
Number of nodules (1/2 or 3/>3)	22/23/5	
Multinodular	28	0.99 (NS)
[1]Median nodule size (cm)	4 (1-18)	2.76 (NS)
Nodule >5 cm	20	1.62 (NS)
[1]Gross vascular invasion	12	4.42 (0.0354)
[1,2]Histological grade (I/II/III)	27/16/7	
II-III	23	4.10 (0.0490)
Type of treatment		
Resection/LT/loco-regional therapies	22/7/21	
Surgery	29	16.40 (0.0001)

HCV: hepatitis C virus; HBV: hepatitis B virus; AFP: alpha-fetoprotein; TNM: tumor node metastasis classification; LT: liver transplantation.
[1]Variables significantly related to the presence of AFP mRNA in blood. [2]I: well; II: moderately; and III: poorly differentiated HCC.

Table 2 Multivariate survival analysis in the 50 enrolled HCC patients. Only variables significantly influencing survival at univariate analysis were introduced in the Cox proportional hazard model

Variables	RR (95%CI)	Likelihood-ratio χ^2	*P*
Assessing single variables			
Surgery	2.72 (1.59-5.03)	14.07	0.0002
AFP mRNA	2.00 (0.90-4.82)	2.83	NS
Moderately or poorly differentiated grade	1.20 (0.55-2.41)	0.23	NS
Gross vascular invasion	0.86 (0.48-1.59)	0.24	NS
Performance status >1	1.21(0.64-2.46)	0.31	NS
Combining tumor related variables			
Surgery	5.84 (2.23-17.32)	13.23	0.0003
[1]Early HCC	5.84 (2.23-17.32)	13.60	0.0002
Performance status >1	1.18 (0.41-3.09)	0.11	NS

RR: risk ratio; CI: confidence interval.

[1]AFP mRNA negative and well-differentiated HCC without gross vascular invasion.

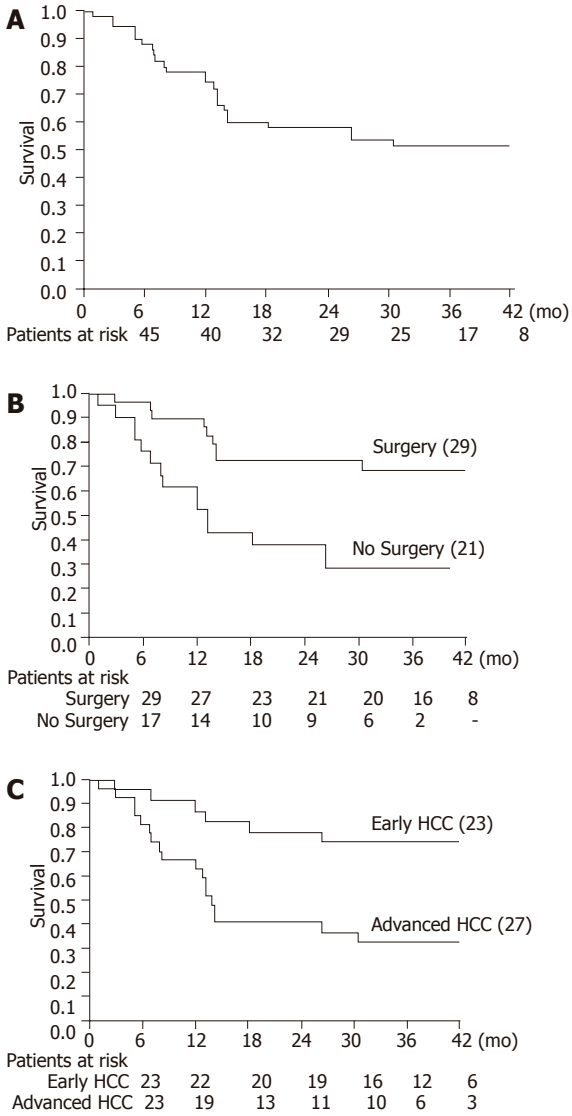

Figure 1 Subject **A:** Overall probability of survival of the 50 enrolled HCC patients; **B:** Overall probability of survival of the 50 enrolled HCC patients, dividing them in the two main treatment groups (surgery *vs* no surgery). Log rank test = 0.0015; **C:** Overall probability of survival of the 50 enrolled HCC patients, dividing them according to tumor biological status (early *vs* advanced HCC). Log rank test = 0.0042. Early HCC = AFP mRNA negative and well-differentiated HCC without gross vascular invasion.

of single nodule smaller than 5 cm in diameter and of multiple nodules (2 or 3) smaller than 3 cm has been used to define early HCC, reflecting the excellent outcomes achieved after LT[25,26]. Although the use of these strict selection criteria for the treatment has undoubtedly improved survival rates of a subgroup of HCC patients in the previous years[4,5], such a diffuse therapeutic policy has dramatically reduced the use of potentially radical therapies for those HCC patients not meeting the same criteria. In virtue of such a tight selection philosophy, on one hand it has obtained an important reallocation of resources but on the other it has faced the concrete risk that a considerable proportion of HCC patients have been unfairly excluded from radical treatment[6-8]. In this context, the identification of new reliable prognostic factors may play a crucial role in improving the treatment criteria process of HCC patients[27].

This study was designed to identify prospectively the main preoperative HCC predictors of survival with particular reference to the prognostic utility of preoperative AFP mRNA and tumor grade. In order to avoid the bias associated to predefined selection criteria, less restrictive enrollment criteria for radical treatment in terms of both tumor status and liver function were deliberately used. If on one hand such a selection policy may account for the relatively unsatisfactory outcome of the 50 enrolled patients (Figure 1A), on the other it allowed us to develop an effective analysis of predictive factors for survival. Moreover, in spite of the relatively low number of enrolled patients, our study has the advantage of a monocentric, prospective analysis in which a well-defined treatment algorithm was used[14,23].

According to other studies[28,29], tumor biological parameters appeared as the most relevant prognostic factors selecting those patients achieving the best survival outcome when radically treated (Tables 1 and 2). In the present study, macro-morphological parameters failed in defining early HCC, since they showed a marginal impact on survival in our group of patients (Table 1). On the contrary, other tumor characteristics such as AFP mRNA in the blood, histological grade and vascular involvement served as more adequate markers of HCC biological

aggressiveness.

In this context, the independent prognostic power of surgical treatment (Table 2 and Figure 1B) may not be misinterpreted as a therapeutic disadvantage in using other loco-regional options. It is not the aim of the present study, in fact, to make a comparison between treatment options since such an analysis may be correctly performed only in the experimental setting of a randomized clinical trial.

This study, in fact, showed that some HCC biological features such as grading, AFP mRNA status in the blood and gross vascular invasion influence patient prognosis independently from the type of adopted therapy (Table 2). A prognostic stratification of the study group in two main tumor stages according to significantly predictive variables was obtained (Figure 1C). A favorable biological picture of HCC (AFP mRNA negative, well-differentiated and without gross vascular invasion) appeared hierarchically as the most relevant factor in determining patient prognosis. Conversely, liver function parameters, such as Child-Pugh classification, bilirubin and portal pressure, did not reach a significant impact on survival in our small study group suggesting a secondary prognostic role when compared to tumor features. In this view, our study does not claim to provide a new definition of early HCC but it wants to simply and strongly underline the urgent need to readdress the focus of the HCC patients selection process for radical treatment more on tumor biological aggressiveness rather than on size and number of tumor nodules.

Concerning the single HCC parameters selected from survival analysis, tumor grade is a well recognized prognostic factor for HCC patients as showed by many large retrospective pathological analyses[1,6,11]. There are, however, no studies evaluating the prognostic role of preoperative determined HCC grading in a prospective setting.

Previous experiences exploring the prognostic role of preoperative AFP mRNA showed controversial results[30-32]. It is likely that this biologic HCC parameter alone does not reach an adequate prognostic power in highly selected populations undergoing radical therapies. In this view, the present study suggests that in the context of a larger population basis, AFP mRNA may be probably useful in identifying morphologically advanced HCC suitable for radical therapies. The introduction of appropriate molecular methods to quantify AFP mRNA in the blood in perspective will further improve the prognostic power of this promising biomarker.

In conclusion, this study showed that the preoperative determination of tumor grade and blood AFP mRNA may potentially refine the prognostic evaluation of HCC patients. On a purely preliminary basis, these two parameters may probably help the treatment decision process for that group of HCC patients suitable for radical therapies consequently improving the currently used restrictive selection criteria.

REFERENCES

1 **Jonas S,** Bechstein WO, Steinmuller T, Herrmann M, Radke C, Berg T, Settmacher U, Neuhaus P. Vascular invasion and histopathologic grading determine outcome after liver transplantation for hepatocellular carcinoma in cirrhosis. *Hepatology* 2001; **33:** 1080-1086

2 **Ikeda K,** Saitoh S, Tsubota A, Arase Y, Chayama K, Kumada H, Watanabe G, Tsurumaru M. Risk factors for tumor recurrence and prognosis after curative resection of hepatocellular carcinoma. *Cancer* 1993; **71:** 19-25

3 **Koda M,** Murawaki Y, Mitsuda A, Ohyama K, Horie Y, Suou T, Kawasaki H, Ikawa S. Predictive factors for intrahepatic recurrence after percutaneous ethanol injection therapy for small hepatocellular carcinoma. *Cancer* 2000; **88:** 529-537

4 **Bruix J,** Llovet JM. Prognostic prediction and treatment strategy in hepatocellular carcinoma. *Hepatology* 2002; **35:** 519-524

5 **Befeler AS,** Di Bisceglie AM. Hepatocellular carcinoma: diagnosis and treatment. *Gastroenterology* 2002; **122:** 1609-1619

6 **Klintmalm GB.** Liver transplantation for hepatocellular carcinoma: a registry report of the impact of tumor characteristics on outcome. *Ann Surg* 1998; **228:** 479-490

7 **Poon RT,** Fan ST, Ng IO, Wong J. Prognosis after hepatic resection for stage IVA hepatocellular carcinoma: a need for reclassification. *Ann Surg* 2003; **237:** 376-383

8 **Regimbeau JM,** Farges O, Shen BY, Sauvanet A, Belghiti J. Is surgery for large hepatocellular carcinoma justified? *J Hepatol* 1999; **31:** 1062-1068

9 **Vauthey JN,** Lauwers GY, Esnaola NF, Do KA, Belghiti J, Mirza N, Curley SA, Ellis LM, Regimbeau JM, Rashid A, Cleary KR, Nagorney DM. Simplified staging for hepatocellular carcinoma. *J Clin Oncol* 2002; **20:** 1527-1536

10 **Ercolani G,** Grazi GL, Ravaioli M, Del Gaudio M, Gardini A, Cescon M, Varotti G, Cetta F, Cavallari A. Liver resection for hepatocellular carcinoma on cirrhosis: univariate and multivariate analysis of risk factors for intrahepatic recurrence. *Ann Surg* 2003; **237:** 536-543

11 **Esnaola NF,** Lauwers GY, Mirza NQ, Nagorney DM, Doherty D, Ikai I, Yamaoka Y, Regimbeau JM, Belghiti J, Curley SA, Ellis LM, Vauthey JN. Predictors of microvascular invasion in patients with hepatocellular carcinoma who are candidates for orthotopic liver transplantation. *J Gastrointest Surg* 2002; **6:** 224-232; discussion 232

12 **Yao FY,** Ferrell L, Bass NM, Watson JJ, Bacchetti P, Venook A, Ascher NL, Roberts JP. Liver transplantation for hepatocellular carcinoma: expansion of the tumor size limits does not adversely impact survival. *Hepatology* 2001; **33:** 1394-1403

13 **Qin LX,** Tang ZY. The prognostic molecular markers in hepatocellular carcinoma. *World J Gastroenterol* 2002; **8:** 385-392

14 **Cillo U,** Vitale A, Bassanello M, Boccagni P, Brolese A, Zanus G, Burra P, Fagiuoli S, Farinati F, Rugge M, D'Amico DF. Liver transplantation for the treatment of moderately or well-differentiated hepatocellular carcinoma. *Ann Surg* 2004; **239:** 150-159

15 **Bassanello M,** Cillo U, Vitale A, Lumachi F, Ciarleglio FA, Boccagni P, Brolese A, Zanus G, D'Amico F, Senzolo M, D'Amico DF. Multimodal approach and its impact on survival for patients with hepatocellular carcinoma. *Anticancer Res* 2003; **23:** 4047-4053

16 **Cillo U,** Navaglia F, Vitale A, Molari A, Basso D, Bassanello M, Brolese A, Zanus G, Montin U, D'Amico F, Ciarleglio FA, Carraro A, Bridda A, Burra P, Carraro P, Plebani M, D'Amico DF. Clinical significance of alpha-fetoprotein mRNA in blood of patients with hepatocellular carcinoma. *Clin Chim Acta* 2004; **347:** 129-138

17 **Matsumura M,** Niwa Y, Kato N, Komatsu Y, Shiina S, Kawabe T, Kawase T, Toyoshima H, Ihori M, Shiratori Y. Detection of alpha-fetoprotein mRNA, an indicator of hematogenous spreading hepatocellular carcinoma, in the circulation: a possible predictor of metastatic hepatocellular carcinoma. *Hepatology* 1994; **20:** 1418-1425

18 **Funaki NO,** Tanaka J, Seto SI, Kasamatsu T, Kaido T,

Imamura M. Hematogenous spreading of hepatocellular carcinoma cells: possible participation in recurrence in the liver. *Hepatology* 1997; **25:** 564-568

19 **Louha M,** Poussin K, Ganne N, Zylberberg H, Nalpas B, Nicolet J, Capron F, Soubrane O, Vons C, Pol S, Beaugrand M, Berthelot P, Franco D, Trinchet JC, Brechot C, Paterlini P. Spontaneous and iatrogenic spreading of liver-derived cells into peripheral blood of patients with primary liver cancer. *Hepatology* 1997; **26:** 998-1005

20 **Matsumura M,** Shiratori Y, Niwa Y, Tanaka T, Ogura K, Okudaira T, Imamura M, Okano K, Shiina S, Omata M. Presence of alpha-fetoprotein mRNA in blood correlates with outcome in patients with hepatocellular carcinoma. *J Hepatol* 1999; **31:** 332-339

21 **Minata M,** Nishida N, Komeda T, Azechi H, Katsuma H, Nishimura T, Kuno M, Ito T, Yamamoto Y, Ikai I, Yamaoka Y, Fukuda Y, Nakao K. Postoperative detection of alpha-fetoprotein mRNA in blood as a predictor for metastatic recurrence of hepatocellular carcinoma. *J Gastroenterol Hepatol* 2001; **16:** 445-451

22 **Ijichi M,** Takayama T, Matsumura M, Shiratori Y, Omata M, Makuuchi M. alpha-Fetoprotein mRNA in the circulation as a predictor of postsurgical recurrence of hepatocellular carcinoma: a prospective study. *Hepatology* 2002; **35:** 853-860

23 **Cillo U,** Bassanello M, Vitale A, Grigoletto FA, Burra P, Fagiuoli S, D'Amico F, Ciarleglio FA, Boccagni P, Brolese A, Zanus G, D'Amico DF. The critical issue of hepatocellular carcinoma prognostic classification: which is the best tool available? *J Hepatol* 2004; **40:** 124-131

24 **Pugh RN,** Murray-Lyon IM, Dawson JL, Pietroni MC, Williams R. Transection of the oesophagus for bleeding oesophageal varices. *Br J Surg* 1973; **60:** 646-649

25 **Bismuth H,** Chiche L, Adam R, Castaing D, Diamond T, Dennison A. Liver resection versus transplantation for hepatocellular carcinoma in cirrhotic patients. *Ann Surg* 1993; **218:** 145-151

26 **Mazzaferro V,** Regalia E, Doci R, Andreola S, Pulvirenti A, Bozzetti F, Montalto F, Ammatuna M, Morabito A, Gennari L. Liver transplantation for the treatment of small hepatocellular carcinomas in patients with cirrhosis. *N Engl J Med* 1996; **334:** 693-699

27 **Cillo U,** Vitale A, Bassanello M, Grigoletto F, Burra P, D' Amico DF. The two faces of HCC prognostic evaluation: 'observational' or 'pragmatic' approach? *J Hepatol* 2004; **40:** 1042-1043

28 **Llovet JM,** Bru C, Bruix J. Prognosis of hepatocellular carcinoma: the BCLC staging classification. *Semin Liver Dis* 1999; **19:** 329-338

29 **Bruix J,** Sherman M, Llovet JM, Beaugrand M, Lencioni R, Burroughs AK, Christensen E, Pagliaro L, Colombo M, Rodes J. Clinical management of hepatocellular carcinoma. Conclusions of the Barcelona-2000 EASL conference. European Association for the Study of the Liver. *J Hepatol* 2001; **35:** 421-430

30 **Lemoine A,** Le Bricon T, Salvucci M, Azoulay D, Pham P, Raccuia J, Bismuth H, Debuire B. Prospective evaluation of circulating hepatocytes by alpha-fetoprotein mRNA in humans during liver surgery. *Ann Surg* 1997; **226:** 43-50

31 **Witzigmann H,** Geissler F, Benedix F, Thiery J, Uhlmann D, Tannapfel A, Wittekind C, Hauss J. Prospective evaluation of circulating hepatocytes by alpha-fetoprotein messenger RNA in patients with hepatocellular carcinoma. *Surgery* 2002; **131:** 34-43

32 **Sheen IS,** Jeng KS, Shih SC, Wang PC, Chang WH, Wang HY, Shyung LR, Lin SC, Kao CR, Tsai YC, Wu TY. Does surgical resection of hepatocellular carcinoma accelerate cancer dissemination? *World J Gastroenterol* 2004; **10:** 31-36

Science Editor Guo SY **Language Editor** Elsevier HK

PO Box 2345, Beijing 100023, China
www.wjgnet.com
wjg@wjgnet.com

ELSEVIER

World J Gastroenterol 2005;11(44):6926-6931
World Journal of Gastroenterology ISSN 1007-9327

Etiology and functional status of liver cirrhosis by ^{31}P MR spectroscopy

Monika Dezortova, Pavel Taimr, Antonin Skoch, Julius Spicak, Milan Hajek

Monika Dezortova, Antonin Skoch, Milan Hajek: MR Unit, Department of Diagnostic and Interventional Radiology; Institute for Clinical and Experimental Medicine, Prague, Czech Republic
Pavel Taimr, Julius Spicak: Department of Hepatogastroenterology; Institute for Clinical and Experimental Medicine, Prague, Czech Republic
Supported by grant from Ministry of Health IGA 7853-3, and MZO 00023001, Czech Republic
Correspondence to: Monika Dezortova, PhD, MR-Unit, ZRIR, IKEM, Videnska 1958/9, 140 21 Prague 4,
Czech Republic. mode@medicon.cz
Telephone: +420-241717729 Fax: +420-241717729
Received: 2005-03-03 Accepted: 2005-04-08

Abstract

AIM: To assess the functional status and etiology of liver cirrhosis by quantitative ^{31}P magnetic resonance spectroscopy (MRS).

METHODS: A total of 80 patients with liver cirrhosis of different etiology and functional status described by Child-Pugh score were examined and compared to 11 healthy volunteers. MR examination was performed on a 1.5 T imager using a ^{1}H/^{31}P surface coil by the 2D chemical shift imaging technique. Absolute concentrations of phosphomonoesters (PME), phosphodiesters (PDE), inorganic phosphate (Pi) and adenosine triphosphate (ATP) were measured.

RESULTS: MRS changes reflected the degree of liver dysfunction in all the patients as well as in individual etiological groups. The most important change was a decrease of PDE. It was possible to distinguish alcoholic, viral and cholestatic etiologies based on MR spectra. Alcoholic and viral etiology differed in PDE (alcoholic, viral, controls: 6.5±2.3, 6.5±3.1, 10.8±2.7 mmol/L, P<0.001) and ATP (alcoholic, viral, controls: 2.9±0.8, 2.8 ±0.9, 3.7±1.0 mmol/L, P<0.01) from the control group. Unlike viral etiology, patients with alcoholic etiology also differed in Pi (alcoholic, controls: 1.2±0.4, 1.6±0.6 mmol/L, P<0.05) from controls. No significant changes were found in patients with cholestatic disease and controls; nevertheless, this group differed from both alcoholic and viral groups (cholestatic, alcoholic, viral: 9.4 ±2.7, 6.5±2.3, 6.5±3.1 mmol/L, P<0.005) in PDE.

CONCLUSION: ^{31}P MRS can significantly help in non-invasive separation of different etiological groups leading to liver cirrhosis. In addition, MRS changes reflect functional liver injury.

Key words: Liver cirrhosis; ^{31}P MR spectroscopy; Absolute concentration; Child-Pugh score; Etiology

Dezortova M, Taimr P, Skoch A, Spicak J, Hajek M. Etiology and functional status of liver cirrhosis by ^{31}P MR spectroscopy. *World J Gastroenterol* 2005; 11(44): 6926-6931
http://www.wjgnet.com/1007-9327/11/6926.asp

INTRODUCTION

Cirrhosis is the final stage of various liver diseases. Regardless of etiology (i.e., viral, alcoholic, autoimmune, metabolic and others), the liver injury leads to the excessive accumulation of extracellular matrix and to nodular regeneration of parenchyma. Information about the etiology and degree of liver derangement is indispensable and usually needs to be verified by means of liver biopsy. This procedure is invasive, uncomfortable for the patient and sometimes not without serious complications. Therefore, efforts have been made to non-invasively obtain information concerning liver injury.

Additional important information is the degree of functional limitation of the liver. In clinical settings, this is usually described by a Child-Pugh score (CPS), which is calculated from clinical and laboratory tests[1-3]. As clinicians need to determine the specific etiological diagnosis of liver cirrhosis, all possible additional information is valuable in clinical practice to find an appropriate treatment[4]. Imaging examinations, which are capable of improving the diagnostic process, are very helpful.

One of the promising techniques is the application of magnetic resonance (MR) spectroscopy[5]. Phosphorus (^{31}P) MR spectroscopy has been used to study liver metabolism *in vivo* for several years[6-9]. It enables the observation of energy metabolism and intracellular compartmentation through the signals of phosphomonoesters (PME), phosphodiesters (PDE), inorganic phosphate (Pi) and nucleotide triphosphates, mainly adenosine triphosphate (ATP). The PME and PDE signals are multicomponent with phosphorylcholine and phosphorylethanolamine which are the main contributors to PME as well as

glycerophosphorylcholine and glycerophosphorylethanola mine which are the main contributors to PDE [10]. The final typical signal of ^{31}P MR spectra *in vivo* is phosphocreatine (PCr). Although it is a dominant signal in muscles, it is not readily observable in spectra of the liver because of its low contribution to hepatic metabolic processes. Its presence indicates some contribution of signals from abdominal wall muscle as a partial volume effect.

In this study we investigated whether quantitative ^{31}P MR spectroscopy can distinguish different etiologies of liver cirrhosis and assess the functional severity of liver injury. The main goal of the study was to describe the relationship between the concentration of phosphorylated metabolites in the liver and the different etiological groups of liver cirrhosis.

METHODS

Subjects

A group of 80 patients (49.7 ± 11.5 years) with confirmed liver cirrhosis of different etiology (alcoholic cirrhosis in 33 cases, viral hepatitis in 22 cases (B virus in three cases, C virus in 17 cases, combined B+C in two cases), cholestatic liver disease in 16 cases (primary biliary cirrhosis in six cases, one case of secondary biliary cirrhosis, primary sclerosing cholangitis in eight cases and one case of biliary atresia), and other etiologies in nine cases (one Budd-Chiari, two congenital fibrosis, two autoimmune, and four cryptogenic cases) were examined. The last nine patients were excluded from etiological evaluations because of their etiological diversity and small number. Patients with combined etiologies (especially viral and alcoholic) were strictly excluded from the study as well as another 19 patients with insufficient resolution or low signal to noise ratio due to technical problems. Results were compared to those of a group of 11 healthy volunteers (40.5 ± 10.9 years). Liver biopsy was performed in all cirrhotic patients except for those whose clinical, laboratory, endoscopic and imaging studies (abdominal ultrasound and CT) were typical and without any doubt for severe liver cirrhosis. Etiological diagnosis was made using standard diagnostic rules. All alcoholic patients admitted had a previous regular drinking of alcohol more than 80 g/d, patients with viral hepatitis B and C were confirmed by specific antibodies and/or PCR DNA/RNA positivity. Patients with primary biliary cirrhosis were AMA positive, patients with primary sclerosing cholangitis had typical cholangiography, all cholestatic patients were confirmed by liver biopsy. Similarly strict criteria were used for other etiologies. All patients were originally examined for the liver transplantation program and six-month alcohol abstinence in alcoholic patients was proved by independent observers, i.e. family members, primary care physicians and psychiatrists trained in substance abuse treatment. All subjects, including the healthy volunteers, abstained from alcohol during 48 h before MR examination and underwent standard clinical biochemical testing just before the MR examination which was performed in early morning after an overnight fast (at least 8 h of fasting). A Child-Pugh score [1-3] was obtained in all patients (mean CPS = 9.3) and patients were distributed into groups A, B, and/or C for statistical evaluation. MELD score was not used because of its main application in donor allocations. The subjects were fully informed and signed the protocol of the examination in accordance with rules approved by the ethical committee, which conform to the ethical guidelines of the 1975 Declaration of Helsinki.

MR examination

MR examination was performed on a Siemens Vision (Erlangen, Germany) whole-body MR imager operating at 1.5 Tesla equipped with a commercial dual ^{1}H/^{31}P surface coil. The subjects were examined in a prone position with the liver centered on the surface coil. Neither ECG nor breathing monitoring due to this position was found to be necessary. No tremor because of encephalopathy which might also influence the quality of MR examination was observed. Basic MR images in all orientations were obtained for the localization of voxels (Figure 1). ^{31}P MR spectra were measured using a standard two-dimensional chemical shift imaging (CSI) technique[5] in the transversal plane with the following parameters: TR = 323 ms, TE = 2.3 ms, matrix 16 × 16, field of view (FOV) = 480 mm, flip angle = 90º, slice thickness = 4 cm, voxel volumes were 3 cm × 3 cm × 4 cm, 12 acquisitions, acquisition time = 16 min.

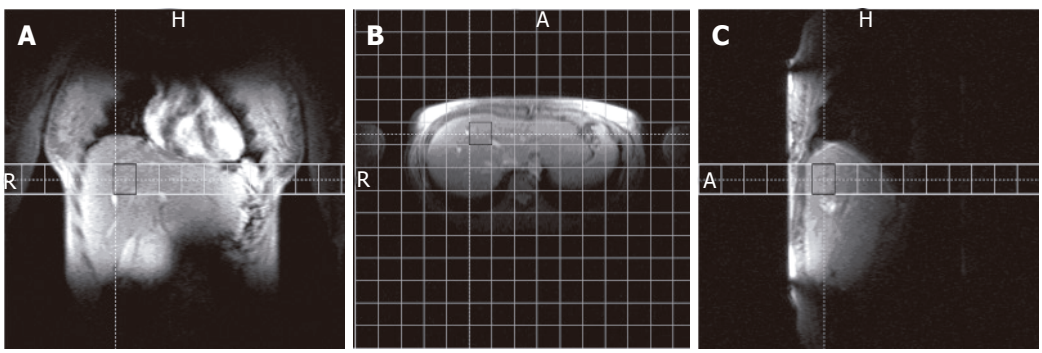

Figure 1 MR images of a healthy volunteer in all orientations with selected matrix for spectroscopic measurement and indicated volume of interest for spectra evaluation.

Spectra evaluation

Approximately 12 voxels (in the normal size of the liver) were selected from a whole CSI matrix (256 voxels). The most appropriate voxel for the quantitative evaluation[11] had to fulfill two conditions: (1) no visible PCr signal characterizing the presence of abdominal muscles; (2) no visible large intrahepatic blood vessels (portal vein truncus and its left and right lobar branches, inferior vena cava and large branches of hepatic veins). Such voxel was chosen using a standard postprocessing method (the movement of the whole CSI matrix) and considered as volume of interest (VOI) for quantitative evaluation. However, the contribution of small hepatic veins to measured signal intensities could not be excluded.

Spectra were evaluated using standard Siemens Numaris software (Gauss apodization with halfwidth = 30 ms, manual phase and spline baseline correction, Fourier transformation and curve fitting with the assumption of Gaussian line shapes). We used Pi chemical shift = 5 ppm as a standard frequency for the assignment of observed signals. Signal intensities of PME, Pi, PDE and β ATP (αATP and γATP signals were not used for the evaluation because of overlap with signals of other compounds) were used for the measurement of absolute molar concentrations. The methodology of the absolute quantification using the CSI sequence was published previously[11,12]. The signal intensity ratios were not used because of the signal intensity dependence on the distance of the VOI from the center of the surface coil.

Statistical analysis

The comparison of several neighboring voxels from different places in the liver was performed and a VOI of 36 mL was found to be large enough to disregard structural heterogeneities. All data represented three independent evaluations and were expressed as mean ± SD unless otherwise indicated.

Statistical analysis was performed using paired *t* tests and the technique of "contrast analysis" in the ANOVA module of STATISTICA 6[13] for multiple comparisons. Pattern recognition analysis of data was performed by principal component analysis (PCA) using the Multivariate Explanatory Techniques module of the STATISTICA software and by linear and nonlinear discriminant analyses (LDA and NDA, respectively)[14] using MaZda B11[15].

A Levene's test of homogeneity of variances in groups confirmed that there was no effect at $P<0.05$. This means data had the same variance and could be compared by standard t test. The null hypothesis H_0 (group means are not different from the control group) was rejected if $P<0.05$ (5 % error level).

RESULTS

Figure 2 shows typical examples of phosphorus spectra from healthy and cirrhotic liver tissue. The altered hepatic phosphorus metabolism in cirrhosis could be described by calculated molar concentrations of selected compounds in the liver tissue. The spectroscopic data of patients and controls together with Child-Pugh score are summarized in Table 1. Compared to controls, molar concentrations of PDE and ATP were significantly lower in all patients with liver cirrhosis. We divided patients into three groups according to CPS, independent of etiology. In this case, no significant differences were found between controls and patients with mild cirrhosis status (CPS-A) whereas groups CPS-B and CPS-C showed statistical differences to the control group in PDE ($P<0.001$) and ATP ($P<0.02$). If groups of patients were compared to each other, differences in patients within the CPS-A grouping increased for PDE as CPS worsened, no statistical differences were found in ATP. The relationship between calculated molar concentrations and the known etiology of liver cirrhosis is summarized in Table 2.

Spectroscopic data (PME, Pi, PDE and ATP concentrations) were also evaluated by various pattern recognition methods. We found similar levels of misclassification of subjects by using PCA, LDA and NDA procedures[15]. For demonstration and graphical output we used PCA plots from STATISTICA software[13], LDA and NDA results were not shown. To distinguish the different etiology and functional status of the liver cirrhosis from the controls, we highlighted individual subgroups of patients in PCA plots. If individual etiological groups were projected together with a control group, trends demonstrating the functional status of the liver were highlighted, i.e. the distance from the control area directly depended on CPS. The alcoholic group differed from

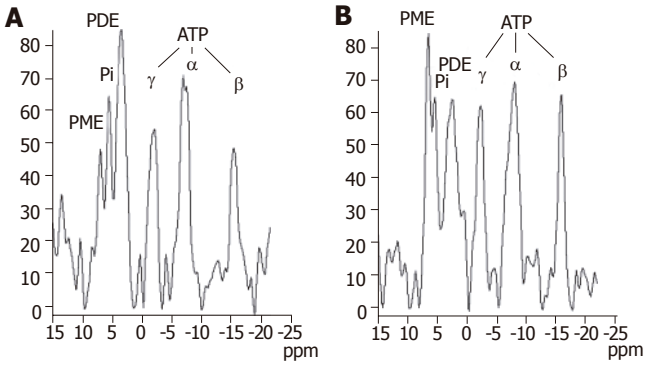

Figure 2 ^{31}P MR spectra of the liver in a healthy volunteer (**A**) and in a patient with liver cirrhosis (**B**). PME - phosphomonoesters; Pi - inorganic phosphate; PDE - phosphodiesters; γATP, αATP, βATP - γ, α and β phosphates of adenosine triphosphate.

Table 1 Concentrations of ^{31}P visible metabolites (mmol/L) in the liver according to the degree of liver injury

	n	PME	Pi	PDE	ATP
Controls	11	3.09±1.45	1.63±0.55	10.83±2.68	3.72±0.99
All patients	80	3.53±1.45	1.33±0.61	7.16±2.88[d]	2.95±0.84[b]
CPS-A	18	3.64±1.68	1.37±0.56	9.16±2.32	3.24±0.85
CPS-B	25	3.60±1.31	1.31±0.57	7.31±2.62[d]	2.93±0.78[a]
CPS-C	37	3.44±1.46	1.33±0.66	6.07±2.80[d,f]	2.83±0.87[b]

[a]$P<0.05$, [b]$P<0.01$, [d]$P<0.001$ *vs* the control group; [f]$P<0.01$ *vs* the CPS-A group.

Table 2 Concentrations (mmol/L) of ^{31}P visible metabolites in the liver according to different etiologies and CPS

	n	PME	Pi	PDE	ATP	CPS	*n*	PME	Pi	PDE	ATP
Controls	11	3.09±1.45	1.63±0.55	10.83±2.68	3.72±0.99	-	-	-	-	-	-
Alcohol	33	3.48±1.53	1.19±0.39[a,c]	6.52±2.29[d,f]	2.86±0.80b	A	5	3.87±2.05	1.17±0.32	8.35±1.26	3.43±0.53
						B	6	3.50±1.32	1.17±0.35	6.22±2.01[c]	2.92±0.55
						C	22	3.38±1.51	1.21±0.43a	6.18±2.40[c]	2.71±0.87[b]
Viral	22	3.64±1.55	1.57±0.77[c]	6.47±3.13[d,f]	2.84±0.92b	A	7	3.47±1.92	1.54±0.69	8.95±2.37	3.27±1.20
						B	8	3.99±1.51	1.51±0.63	6.23±2.72[c]	2.59±0.74[b]
						C	7	3.40±1.41	1.66±1.04	4.26±2.66c	2.69±0.74[a]
[1]Cholestatic	16	3.59±1.31	1.43±0.63	9.36±2.70	3.27±0.90	A	2	-	-	-	-
						B	10	3.44±1.26	1.26±0.66	8.94±2.34	3.24±0.89
						C	4	-	-	-	-

[a]P<0.05, [b]P<0.01, [d]P<0.001 *vs* the control group; [c]P<0.05 between alcohol and viral etiological groups; [f]P<0.001 *vs* the cholestatic group.
[1]The cholestatic group was not divided into subgroups reflecting CPS because of the insufficient number in groups CPS-A and CPS-C.

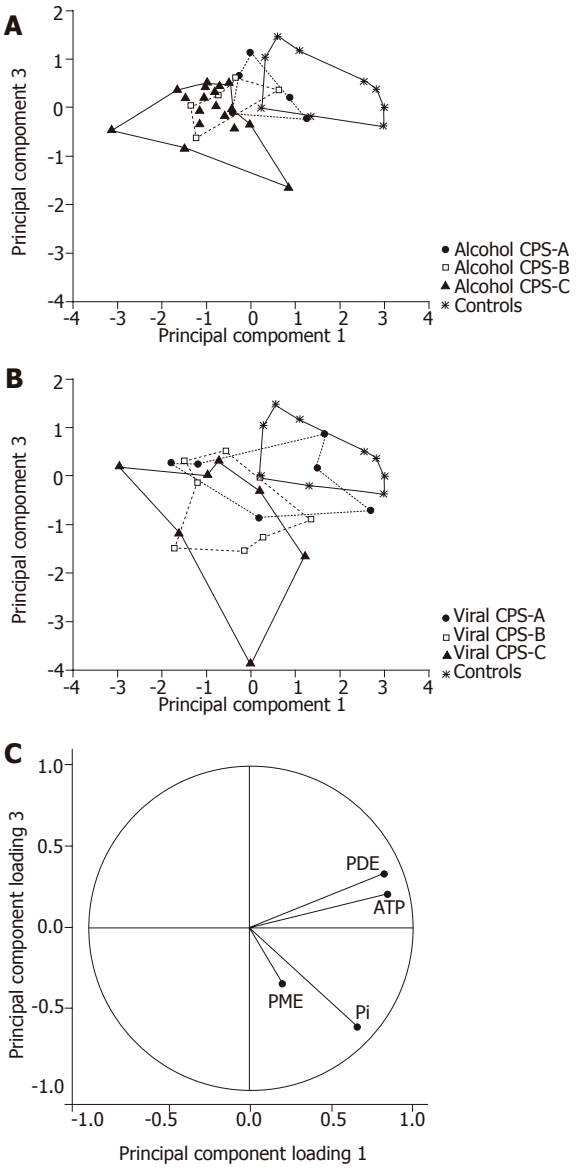

Figure 3 Results of principal component analysis (CPS). Individual positions of spectra displayed on the PCA scatterplots. Principal components are standardized (centered and scaled to unit variance). Principal component 1 explains 47 % of total variance, principal component explains 3 16% of total variance. (**A**) Patients with only alcoholic etiology and controls; (**B**) patients with only viral etiology and controls. Child-Pugh score subgroups (**A, B,** and **C**) and controls are bounded. (**C**) Projection of the principal component loadings on the planes 1 and 3.

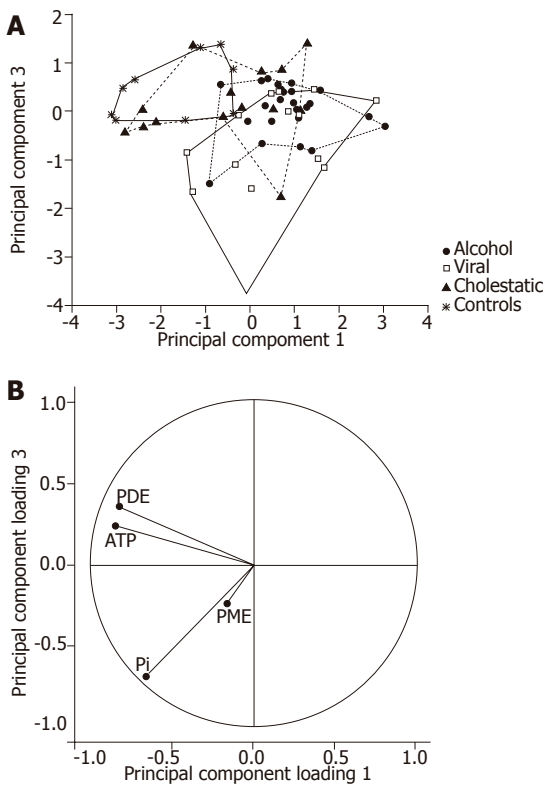

Figure 4 Results of principal component analysis (etiology). (**A**) Individual positions of spectra of patients with CPS-B and C together with a control group are displayed on the PCA plot. Etiological groups (alcoholic, viral and cholestatic) and controls are bounded. Principal component 1 explains 46 % of total variance, principal component 3 explains 17% of total variance; (**B**) Projection of the principal component loadings on the planes 1 and 3.

controls in the CPS-C area, whereas the viral group differed in the CPS-B area (Figure 3). Because of the insufficient number of cholestatic patients in the CPS-A and CPS-C groups, that plot was not presented.

As data from the CPS-A groups overlapped with controls, we used patients with CPS-B or CPS-C liver status for another statistical analysis (Figure 4). In this case, principal component analysis confirmed clear separation of viral patients from controls. Partial overlap was seen between alcoholic patients and controls. Finally, the group

of cholestatic patients overlapped all groups.

By comparing differences in ^{31}P MR spectra of patients to controls we could distinguish alcoholic, viral and cholestatic etiologies of liver cirrhosis. Patients with alcoholic and viral etiology differed in PDE and ATP from the control group. Unlike viral etiology, patients with alcoholic etiology also differed from the control group in Pi (P<0.05). No significant changes were found in patients with cholestatic disease and the control group; however, this group differed from both alcoholic and viral groups in PDE.

DISCUSSION

Diagnosis of liver cirrhosis is mainly based on invasive methods such as liver biopsy, laparoscopy, various radiological examinations and other clinical tests. The functional severity of liver cirrhosis is usually described by CPS which is partially based on subjective parameters. Thus, this description is not fully sufficient and can impair accuracy. On the other hand, signals from ^{31}P MR spectroscopy reflect intracellular and membrane metabolism *in vivo* non-invasively and they are objective parameters[6,7,8,10].

From our data above, we are able to conclude: (1) three basic etiologies can be distinguished by using correlation with metabolite concentrations; (2) there exists a correlation between the Child-Pugh score and the concentration of PDE and ATP, which is also observable in single etiologies.

The majority of published ^{31}P MR spectroscopic studies have dealt with quantification of relative signal intensities characterized by ratios such as PCr/Pi, Pi/ATP etc. Unlike previous studies, where only relative signal ratios were used, we measured absolute concentration of the metabolites[11]. Absolute quantification of metabolites in mmol/L is not often used because of technical problems[12,16]. However, we believe that only relative quantification using signal intensity ratios cannot fully describe metabolic changes and absolute quantification should be taken into account even if a number of correction factors must be calculated. For example, if two or more compounds increase or decrease together, only the absolute quantification of independent metabolites accurately describes the event as signal ratios may remain unchanged.

PCA analysis of PME, Pi, PDE and ATP concentrations showed different localization of the etiological groups and trends in accordance with the CPS (Figures 3 and 4). Projection of the variables confirmed the similarities of ATP and PDE spectroscopic parameters. The best separation was obtained in the projection on the principal component-planes 1 and 3 despite losing some information available in the projections 1 and 2. The principal component 2 correlated specifically with PME. Nevertheless, in our study PME had high variation so that we did not use the projection on the component-plane 1 and 2.

Standard statistic tests confirmed the trends observable in PCA graphs. Data show a mean decrease of about 23% in ATP in patients with alcohol etiology versus the control group. A similar decrease of ATP concentration was also observed in the group of patients with viral etiology. In both groups we found that the decrease strongly depend on the CPS. Nevertheless, the higher difference was foud between CPS group A and CPS groups B and C. A very small difference was observed between CPS groups B and C which could be explained by the overall severity of hepatocyte dysfunction. Contrary to the alcoholic and viral groups, no statistically significant changes were found in ATP concentration in the cholestatic group.

Our findings in the group of alcoholic patients correspond to the results of animal studies. A number of reports show decreased levels of ATP in the liver of animals chronically fed ethanol. ATP levels could be measured using the intragastric feeding model[17,18]. In rats feeding a high-fat, low protein diet plus alcohol (similar to the diet of malnourished human alcoholics) levels of ATP decreased and remained constant at 35 % lower than levels of ATP in control animals. Hypoxia resulted in a decrease in hepatic levels of ATP in both ethanol-fed and control rats, but the magnitude of the decrease was significantly greater in the ethanol-fed group. Levels of adenosine monophosphate (AMP) and adenosine diphosphate (ADP) were not changed.

The most important change was a decreased concentration of PDE which is considered to be an indicator of membrane phospholipids and catabolic processes. The rate of PDE change was different in various etiologies. When etiological groups were compared to the control group regardless of CPS status (Table 2), mean PDE values were found to be about 60% in alcoholic and viral patients (P<0.001 to controls, and P<0.005 compared to the cholestatic group) and about 86% in the cholestatic group (without statistical significance). Moreover, in CPS-C groups, PDE concentration decreased to 39% of the control value in viral patients (58% in CPS-B) whereas in alcoholic patients PDE did not further decrease (57% of control PDE value in CPS-B and CPS-C). The fact that the changes are already significant in milder stages of cirrhosis (CPS-B) can improve the diagnostic effectiveness of this method. Unlike a previous study[9], our results were more pronounced in more severely affected patients.

We also studied PME concentration, which mainly represents intermediates on the phospholipid biosynthesis pathway. Although some other studies describe an increased PME signal[7,9,19-21], our data only show a statistically non-significant trend.

The last measured concentration - inorganic phosphate Pi - has been found to change only in alcoholic patients (P<0.05). Thus, inorganic phosphate concentration could be used to separate patients with alcoholic and viral etiology.

Observed signals in ^{31}P MR spectra describe many metabolites in intra and extracellular liver tissue. It is known that many types of cells (hepatocytes, cholangiocytes, vascular wall cells, hepatic stellate cells macrophages and others) contribute to liver metabolism depending on their status. Changes in extracellular matrix also influence the concentration of energetic metabolites. Although ^{31}P MR signals from the liver represent whole parenchymal tissue, the results of our study have confirmed previous

findings that metabolic changes in energetic phospholipid metabolism are observable by ^{31}P MRS in patients with decompensated cirrhosis in contrast to patients with compensated cirrhosis. In addition, different concentrations of metabolites in various etiologies indicate different damages of liver parenchyma.

In conclusion, according to differences in ^{31}P MR spectra of patients and controls, we can differentiate various etiologies of liver cirrhosis, i.e. alcoholic, viral and cholestatic. Patients with alcoholic etiology differed in all selected metabolites except for PME from the control group. Patients with viral etiology differed from controls only in PDE and ATP, and no significant changes were found in patients with cholestatic disease. We suppose that this reflects different pathophysiological mechanisms of various liver diseases.

The importance of a larger, multicentric study to delineate ranges, borders and significant parameters for different cirrhotic groups (etiological and/or functional) in the nearest future is advisable. That will be the only way to assess the clinical relevance and usefulness of ^{31}P MRS in liver cirrhosis. The application of this noninvasive method in liver patients will increase. The ultimate goal is the use of ^{31}P MRS as a standard tool in the armamentarium of clinical hepatologists.

ACKNOWLEDGMENTS

The authors thank Dr Karoly Heberger, Chemical Research Center, Hungarian Academy of Sciences, for the helpful discussion of the results.

REFERENCES

1 **Child CG,** Turcotte JG. Surgery and portal hypertension. In child CG. The liver and portal hypertension. 1st ed. Philadelphia. WB Saunders Co. 1968: 50-72
2 **Pugh RN,** Murray-Lyon IM, Dawson JL, Pietroni MC, Williams R. Transection of the oesophagus for bleeding oesophageal varices. *Br J Surg* 1973; **60:** 646-649
3 **Christensen E,** Schlichting P, Fauerholdt L, Gluud C, Andersen PK, Juhl E, Poulsen H, Tygstrup N. Prognostic value of Child-Turcotte criteria in medically treated cirrhosis. *Hepatology* 1984; **4:** 430-435
4 **Montgomery Bissel D,** Maher JJ. Hepatic fibrosis and cirrhosis. In: Zakim D, Boyer TD. Hepatology, a textbook of liver disease. 4th ed. Philadelphia: Saunders, 2002: 395-416
5 **de Graff RA.** In vivo NMR Spectroscopy: Principles and Techniques. 1st ed. Chichester: John Wiley & Sons, 1998
6 **Meyerhoff DJ,** Boska MD, Thomas AM, Weiner MW. Alcoholic liver disease: quantitative image-guided P-31 MR spectroscopy. *Radiology* 1989; **173:** 393-400
7 **Munakata T,** Griffiths RD, Martin PA, Jenkins SA, Shields R, Edwards RH. An in vivo 31P MRS study of patients with liver cirrhosis: progress towards a non-invasive assessment of disease severity. *NMR Biomed* 1993; **6:** 168-172
8 **Angus PW,** Dixon RM, Rajagopalan B, Ryley NG, Simpson KJ, Peters TJ, Jewell DP, Radda GK. A study of patients with alcoholic liver disease by 31P nuclear magnetic resonance spectroscopy. *Clin Sci (Lond)* 1990; **78:** 33-38
9 **Menon DK,** Sargentoni J, Taylor-Robinson SD, Bell JD, Cox IJ, Bryant DJ, Coutts GA, Rolles K, Burroughs AK, Morgan MY. Effect of functional grade and etiology on in vivo hepatic phosphorus-31 magnetic resonance spectroscopy in cirrhosis: biochemical basis of spectral appearances. *Hepatology* 1995; **21:** 417-427
10 **Taylor-Robinson SD,** Sargentoni J, Bell JD, Saeed N, Changani KK, Davidson BR, Rolles K, Burroughs AK, Hodgson HJ, Foster CS, Cox IJ. In vivo and in vitro he patic 31P magnetic resonance spectroscopy and electron microscopy of the cirrhotic liver. *Liver* 1997; **17:** 198-209
11 **Tosner Z,** Dezortova M, Tintera J, Hajek M. Application of two-dimensional CSI for absolute quantification of phosphorus metabolites in the human liver. *MAGMA* 2001; **13:** 40-46
12 **Murphy-Boesch J,** Jiang H, Stoyanova R, Brown TR. Quantification of phosphorus metabolites from chemical shift imaging spectra with corrections for point spread effects and B1 inhomogeneity. *Magn Reson Med* 1998; **39:** 429-438
13 http://www.statsoft.com/textbook/stathome.html
14 **Meloun M,** Militky J. Statisticka analyza experimentalnich dat. (Cz) (Statistical analysis of experimental data.) 1st ed. Academia, 2004
15 http://www.eletel.P.lodz.pl/cost/cost_project.html
16 **Sijens PE,** Dagnelie PC, Halfwerk S, van Dijk P, Wicklow K, Oudkerk M. Understanding the discrepancies between 31P MR spectroscopy assessed liver metabolite concentrations from different institutions. *Magn Reson Imaging* 1998; **16:** 205-211
17 **Miyamoto K,** French SW. Hepatic adenine nucleotide metabolism measured in vivo in rats fed ethanol and a high fat-low protein diet. *Hepatology* 1988; **8:** 53-60
18 **Corbin IR,** Buist R, Peeling J, Zhang M, Uhanova J, Minuk GY. Hepatic 31P MRS in rat models of chronic liver disease: assessing the extent and progression of disease. *Gut* 2003; **52:** 1046-1053
19 **Jalan R,** Taylor-Robinson SD, Hodgson HJ. In vivo hepatic magnetic resonance spectroscopy: clinical or research tool? *J Hepatol* 1996; **25:** 414-424
20 **Kiyono K,** Shibata A, Sone S, Watanabe T, Oguchi M, Shikama N, Ichijo T, Kiyosawa K, Sodeyama T. Relationship of 31P MR spectroscopy to the histopathological grading of chronic hepatitis and response to therapy. *Acta Radiol* 1998; **39:** 309-314
21 **Lim AK,** Patel N, Hamilton G, Hajnal JV, Goldin RD, Taylor-Robinson SD. The relationship of in vivo 31P MR spectroscopy to histology in chronic hepatitis C. *Hepatology* 2003; **37:** 788-794

Science Editor Wang XL and Guo SY **Language Editor** Elsevier HK

PO Box 2345, Beijing 100023, China
www.wjgnet.com
wjg@wjgnet.com

ELSEVIER

World J Gastroenterol 2005;11(44):6932-6935
World Journal of Gastroenterology ISSN 1007-9327

• *COLORECTAL CANCER* •

Three-dimensional computed tomography in laparoscopic surgery for colorectal carcinoma

Hiroshi Ohtani, Kohei Ohta, Yuichi Arimoto, Eui-Chul Kim, Hiroko Oba, Kenji Adachi, Shoichi Terakawa, Mitsuo Tsubakimoto

Hiroshi Ohtani, Kohei Ohta, Yuichi Arimoto, Eui-Chul Kim, Department of Surgery, Osaka City Sumiyoshi Hospital, 1-2-16 Higashikagaya, Suminoe-ku, Osaka 559-0012, Japan
Hiroko Oba, Kenji Adachi, Department of Gastroenterology, Osaka City Sumiyoshi Hospital, 1-2-16 Higashikagaya, Suminoe-ku, Osaka 559-0012, Japan
Shoichi Terakawa, Mitsuo Tsubakimoto, Department of Radiology, Osaka City Sumiyoshi Hospital, 1-2-16 Higashikagaya, Suminoe-ku, Osaka 559-0012, Japan
Co-first-author: Hiroshi Ohtani
Co-correspondence: Hiroshi Ohtani
Correspondence to: Dr Hiroshi Ohtani, Department of Surgery, Osaka City Sumiyoshi Hospital, 1-2-16 Higashikagaya, Suminoe-ku, Osaka 559-0012, Japan. m5051923@msic.med.osaka-cu.ac.jp
Telephone: +81-6-6681-1000 Fax: +81-6-6686-1547
Received: 2005-04-24 Accepted: 2005-05-24

Abstract

AIM: To evaluate the usefulness of three-dimensional computed tomography (3DCT) in laparoscopic surgery for colorectal carcinoma.

METHODS: Seventy-two patients with colorectal cancer who underwent curative operation at our hospital were enrolled in this study. They were classified into two groups by operative procedures. Sixteen patients underwent laparoscopic surgery, laparoscopic group (LG), while 56 patients underwent conventional open surgery, open group (OG). At our institution, contrast-enhanced CT is routinely performed as part of intra-abdominal screening and the 3D images of the major regional vessels are described. We have previously described about the preoperative visualization of the inferior mesenteric artery (IMA) by 3DCT. This time we newly acquired 3D images of the superior mesenteric artery (SMA)/superior mesenteric vein (SMV), ileocecal artery (ICA), middle colic artery (MCA), and inferior mesenteric vein (IMV). We have compared our two study groups with regard to five items, including clinical anastomotic leakage. We have discussed here the role of 3DCT in laparoscopic surgery for colorectal carcinoma.

RESULTS: The mean length of the incision in LG was 4.625±0.89 cm, which was significantly shorter than that in OG (P<0.001). The association between ICA and SMV and SMA was described in the right-sided colectomy. The preoperative imaging of IMA and IMV was created in the rectosigmoidectomy. There was no significant difference in anastomotic leakage between the two groups, but no patients in LG experienced anastomotic leakage.

CONCLUSION: Most of the patients are satisfied with the shorter incisional length following laparoscopic surgery. Preoperative visualization of the major regional vessels may be helpful for the secure treatment of the anastomosis in laparoscopic surgery for colorectal carcinoma.

Key words: Three-dimensional computed tomography; Laparoscopic colorectal surgery; Colorectal cancer

Ohtani H, Ohta K, Arimoto Y, Kim EC, Oba H, Adachi K, Terakawa S, Tsubakimoto M. Three-dimensional computed tomography in laparoscopic surgery for colorectal carcinoma. *World J Gastroenterol* 2005; 11 (44): 6932-6935
http://www.wjgnet.com/1007-9327/11/6932.asp

INTRODUCTION

Laparoscopic colectomy has been generally accepted, and the instruments and techniques have been developed considerably. The advantages of laparoscopic approaches include shorter hospital stay, quicker return of gastrointestinal function, less pain, fewer wound complications, and quicker recovery[1-6]. However, laparoscopic colorectal surgery for malignancies requires the use of advanced surgical techniques that entail a long learning curve[7,8]. In right-sided colon cancer, the regional anatomy is relatively complicated[9]. In the lymph node dissection around the surgical trunk, it is important to recognize two patterns in the relationship between the ileocecal artery (ICA) and the superior mesenteric vein (SMV). One pattern is that the ICA is in front of SMV (Type A), and the other is that ICA is in back of SMV (Type B)[10]. A previous study have described about the risk of more anastomotic leakage in the converted laparoscopic colorectal surgery compared to the conventional open surgery[11]. In laparoscopic colorectal surgery, understanding of the anatomical orientation, including the regional vessels, is important. We have previously reported that preoperative visualization of the inferior mesenteric artery (IMA) by three-dimensional computed tomography (3DCT) is useful in colorectal surgery[12]. In this study, we have described about the three-dimensional (3D) images of the other major visceral vessels, such as the superior mesenteric artery (SMA), SMV, ICA, middle colic artery (MCA), and inferior mesenteric vein (IMV). Here, we have

evaluated the efficacy of 3DCT in performing laparoscopic colorectal surgery for carcinoma.

MATERIALS AND METHODS

Patients

Between April 2002 and March 2005, 72 patients with colorectal cancer underwent curative surgery at our hospital. Operative procedures were laparoscopic colorectal surgery [laparoscopic group (LG); 16 patients: 5 men and 11 women] and open colorectal surgery [open group (OG); 56 patients: 32 men and 14 women]. The mean age was 66.6±7.4 years (range, 52-83 years) in LG and 68.2±11.3 years (range, 36-91 years) in OG. The following data were examined and compared between LG and OG: (1) patient's age and gender; (2) Duke's staging; (3) presence of the postoperative ileus; (4) length of incision for exteriorization and resection of the specimen; (5) wound infection; and (6) clinical anastomotic leakage.

Methods

Contrast-enhanced CT is routinely performed to screen for intra-abdominal malignancies before the surgery at our hospital. Dual-phase helical CT was performed with a high-speed scanner [multi-detector CT (MDCT); Aquilion M8, Toshiba Medical Systems Co., Ltd, Tokyo, Japan] on the patients. During each phase, scanning was performed in a single breath-hold. Dual-phase helical CT data were then transferred to a Zio M900 workstation (Ziosoft, Inc., Morgan Hill, CA, USA), and 3DCT images of the major visceral vessels, such as SMA, SMV, ICA, IMA, and IMV, were reconstructed. The detailed imaging techniques have been described in the previous literatures[12,13]. In right-sided colectomy, the association between ICA and SMV, the variation of the right colic artery (RCA) and the image of the middle colic artery were confirmed by 3DCT before the surgery. In the resectioning of advanced sigmoid colon and rectal cancer, we routinely dissect the lymph nodes around the root of IMA while preserving the left colic artery (LCA), because resection of the root of IMA occasionally causes ischemia of the oral side of the sigmoid colon, sometimes leading to anastomotic leakage[12].

Statistical analysis

Data were expressed as the mean±SD. Statistical analysis was performed using Mann-Whitney *U* test, χ^2 and Student's *t*-test. *P* values of less than 0.05 were considered statistically significant.

RESULTS

There was no significant difference in age, gender, Duke's staging, presence of the postoperative ileus or wound infection between the LG and the OG (Tables 1 and 2). The mean length of incision in the LG (4.625± 0.885 cm) was significantly shorter, than that in OG (15.91 ±2.51 cm, $P<0.001$). Three patients in OG experienced anastomotic leakage, while no patients in LG experienced it. However, there was no statistically significant difference in anastomotic leakage between these two groups. Two of the three patients undergoing anastomotic leakage in OG suffered from advanced rectal cancer. The root of IMA was resected because of the wide-ranging lymph node metastasis. In one of the two patients, lymph node metastasis spread around the marginal vessels of the sigmoid colon.

Table 1 Characteristics of patients in the two groups

	LG (*n* = 16)	OG (*n* = 56)	*P*
Age (yr)	66.6±7.4 (52–83)	68.2±11.3 (36–91)	NS
Male/female	5/11	32/14	NS
Duke's staging			NS
A	7	12	
B	6	24	
C	3	20	

NS: not statistically significant

Table 2 Complications of surgery

	LG (*n* = 16)	OG (*n* = 56)	*P*
Postoperative ileus	0	5	NS
Wound infection	2	13	NS
Anastomotic leakage	0	3	NS

Preoperative visualization of the ICA in front of the SMV (Type A) and that in back of the SMV (Type B) is shown in Figures 1A and 2A, respectively. The variation of the RCA and MCA was evaluated. Intraoperative findings of the association between ICA and SMV are shown in Figures 1B, 2B and C. Figure 3 shows the MCA diverging at a more peripheral portion of SMA than usual. The image of IMA and LCA to be preserved can be seen (Figure 4A). The intraoperative findings are shown in Figure 4B. Preoperative visualization of the essential vessels was described in all the patients undergoing contrast-enhanced CT.

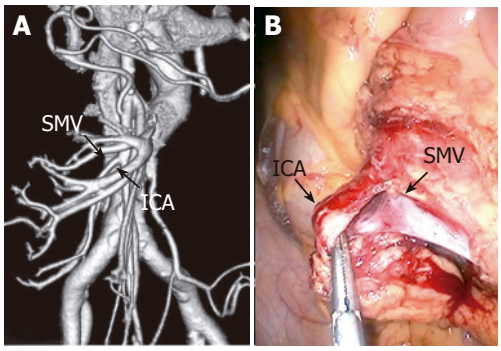

Figure 1 ICA situated in front of SMV at 3DCT (**A**) and at intraoperative findings (**B**).

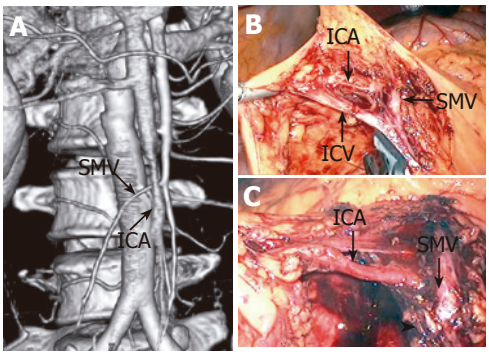

Figure 2 ICA situated in back of SMV at 3DCT (**A**) and at intraoperative findings (**B**); **C**: ICA existed after the ileocecal vein (ICV) had been resected. The arrow head shows the cut end of the ICV.

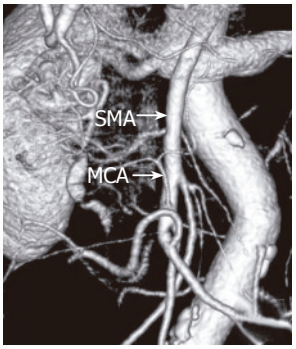

Figure 3 Preoperative visualization of the SMA showing the MCA to branch at a more peripheral portion of the SMA than usual.

DISCUSSION

Laparoscopic approaches have been widely applied, but laparoscopic colorectal surgery for carcinoma is not yet a proven operation[1]. There exists some controversies about the safety of the operation[14,15], the oncological results[16,17] and the long-term survival rate[18]. Recently, a number of studies have shown a favorable outcome of laparoscopic surgery for colon cancer[19-23]. There appears to be no significant differences in perioperative complications between laparoscopic and open colorectal surgery[24]. In our study, we acquired the same results in the presence of postoperative ileus and wound infection. The mean length of the wound used for the extraction of specimens in LG was significantly shorter than that in OG. Most of the patients in LG were satisfied with the shortness of the incisional length during the perioperative period and the subtlety of the incisional scar during the follow-up period, as they had said[25]. In addition, laparoscopic surgery has been found to be associated with significantly decreased intraoperative blood loss and postoperative complications[19,26]. The anastomotic leak rate reported in a larger series of laparoscopic anterior resection was considerably less than 10%, which was comparable to that of conventional open anterior resection[18,27]. To date, the laparoscopic approach for colorectal surgery is not associated with a higher risk of anastomotic leaks[28].

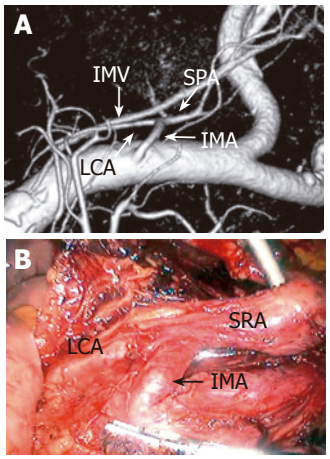

Figure 4 Three-dimensional images of the IMA, the IMV, the LCA and the superior rectal artery (SRA) were obtained (**A**) and were helpful in resecting the SRA (**B**).

In a previous report, four instances (25%) of clinical anastomotic leakage occurred in patients in whom the laparoscopic dissection had been difficult[11]. For the prevention of leakage, it is essential that there is a good supply to the colorectal anastomosis site[29]. Therefore, we preserve the LCA when dissecting lymph nodes around the root of IMA. Understanding the vascular anatomy of the regional vessels is important[12]. Preoperative visualization of SMA/SMV, ICA, MCA or IMA/IMV is crucial when performing a right-sided colectomy or a rectosigmoidectomy. Recently, a new generation of MDCT has been used in clinical practice[30]. At our hospital, MDCT has been performed not only to examine intra-abdominal malignancies, but also to provide preoperative visualization of the regional vessels. At our institution, no patients in LG had experienced anastomotic leakage, while three patients in OG experienced so. Ischemia of the oral side colon may have caused anastomotic leakage. There was no significant difference in anastomotic leakage between LG and OG, suggesting that preoperative visualization in laparoscopic surgery may be helpful in the prevention of anastomotic leakage. MDCT scanning is performed in a single breath-hold during each phase. In the past, there was a significant delay before roentgen engineers could show us the 3D images of the regional vessels, but now they are able to provide 3D images promptly after CT scanning. Having 3D images of SMA/SMV, ICA, MCA, and IMA/IMV lead to a more secure treatment of the regional vessels in laparoscopic surgery for carcinoma.

In conclusion, we suggest that preoperative visualization of the major regional vessels may have advantages in laparoscopic surgery for colorectal carcinoma.

REFERENCES

1 **Kieran JA,** Curet MJ. Laparoscopic colon resection for colon cancer. *J Surg Res* 2004; **117:** 79-91
2 **Franklin ME Jr,** Rosenthal D, Abrego-Medina D, Dorman JP, Glass JL, Norem R, Diaz A. Prospective comparison of

open vs. laparoscopic colon surgery for carcinoma. Five-year results. *Dis Colon Rectum* 1996; **39:** S35-46
3 **Hoffman GC,** Baker JW, Doxey JB, Hubbard GW, Ruffin WK, Wishner JA. Minimally invasive surgery for colorectal cancer. Initial follow-up. *Ann Surg* 1996; **223:** 790-798
4 **Milsom JW,** Bohm B, Hammerhofer KA, Fazio V, Steiger E, Elson P. A prospective, randomized trial comparing laparoscopic versus conventional techniques in colorectal cancer surgery: a preliminary report. *J Am Coll Surg* 1998; **187:** 46-55
5 **Stocchi L,** Nelson H. Laparoscopic colectomy for colon cancer: trial update. *J Surg Oncol* 1998; **68:** 255-267
6 **Falk PM,** Beart RW Jr, Wexner SD, Thorson AG, Jagelman DG, Lavery IC, Johansen OB, Fitzgibbons RJ Jr. Laparoscopic colectomy: a critical appraisal. *Dis Colon Rectum* 1993; **36:** 28-34
7 **Bennett CL,** Stryker SJ, Ferreira MR, Adams J, Beart RW Jr. The learning curve for laparoscopic colorectal surgery. Preliminary results from a prospective analysis of 1194 laparoscopic-assisted colectomies. *Arch Surg* 1997; **132:** 41-45
8 **Agachan F,** Joo JS, Sher M, Weiss EG, Nogueras JJ, Wexner SD. Laparoscopic colorectal surgery. Do we get faster? *Surg Endosc* 1997; **11:** 331-335
9 **Zheng MH,** Feng B, Lu AG, Li JW, Wang ML, Mao ZH, Hu YY, Dong F, Hu WG, Li DH, Zang L, Peng YF, Yu BM. Laparoscopic versus open right hemicolectomy with curative intent for colon carcinoma. *World J Gastroenterol* 2005; **11:** 323-326
10 **Okuda J,** Tanigawa N. [Laparoscopic surgery for rectal and sigmoid colon cancer] *Nippon Rinsho* 2003; 61**:** 391-395
11 **Slim K,** Pezet D, Riff Y, Clark E, Chipponi J. High morbidity rate after converted laparoscopic colorectal surgery. *Br J Surg* 1995; **82:** 1406-1408
12 **Ohtani H,** Kawajiri H, Arimoto Y, Ohno K, Fujimoto Y, Oba H, Adachi K, Hirano M, Terakawa S, Tsubakimoto M. Efficacy of multislice computed tomography for gastroenteric and hepatic surgeries. *World J Gastroenterol* 2005; **11:** 1532-1534
13 **Kim T,** Murakami T, Hori M, Takamura M, Takahashi S, Okada A, Kawata S, Cruz M, Federle MP, Nakamura H. Small hypervascular hepatocellular carcinoma revealed by double arterial phase CT performed with single breath-hold scanning and automatic bolus tracking. *AJR Am J Roentgenol* 2002; **178:** 899-904
14 **Larach SW,** Patankar SK, Ferrara A, Williamson PR, Perozo SE, Lord AS. Complications of laparoscopic colorectal surgery. Analysis and comparison of early vs. latter experience. *Dis Colon Rectum* 1997; **40:** 592-596
15 **Degiuli M,** Mineccia M, Bertone A, Arrigoni A, Pennazio M, Spandre M, Cavallero M, Calvo F. Outcome of laparoscopic colorectal resection. *Surg Endosc* 2004; **18:** 427-432
16 **Yamamoto S,** Watanabe M, Hasegawa H, Kitajima M. Oncologic outcome of laparoscopic versus open surgery for advanced colorectal cancer. *Hepatogastroenterology* 2001; **48:** 1248-1251
17 **Braga M,** Vignali A, Zuliani W, Radaelli G, Gianotti L, Toussoun G, Carlo V. Training period in laparoscopic colorectal surgery. *Surg Endosc* 2002; **16:** 31-35
18 **Scheidbach H,** Schneider C, Huegel O, Barlehner E, Konradt K, Wittekind C, Kockerling F. Laparoscopic sigmoid resection for cancer: curative resection and preliminary medium-term results. *Dis Colon Rectum* 2002; **45:** 1641-1647
19 **Hasegawa H,** Kabeshima Y, Watanabe M, Yamamoto S, Kitajima M. Randomized controlled trial of laparoscopic versus open colectomy for advanced colorectal cancer. *Surg Endosc* 2003; **17:** 636-640
20 **Leung KL,** Kwok SP, Lam SC, Lee JF, Yiu RY, Ng SS, Lai PB, Lau WY. Laparoscopic resection of rectosigmoid carcinoma: prospective randomised trial. *Lancet* 2004; **363:** 1187-1192
21 **Braga M,** Vignali A, Gianotti L, Zuliani W, Radaelli G, Gruarin P, Dellabona P, Di Carlo V. Laparoscopic versus open colorectal surgery: a randomized trial on short-term outcome. *Ann Surg* 2002; **236:** 759-767
22 **Stage JG,** Schulze S, Moller P, Overgaard H, Andersen M, Rebsdorf-Pedersen VB, Nielsen HJ. Prospective randomized study of laparoscopic versus open colonic resection for adenocarcinoma. *Br J Surg* 1997; **84:** 391-396
23 Clinical Outcomes of Surgical Therapy Study Group.A comparison of laparoscopically assisted and open colectomy for colon cancer. *N Engl J Med* 2004; **350:** 2050-2059
24 **Tomita H,** Marcello PW, Milsom JW. Laparoscopic surgery of the colon and rectum. *World J Surg* 1999; **23:** 397-405
25 **Adachi Y,** Sato K, Kakisako K, Inomata M, Shiraishi N, Kitano S. Quality of life after laparoscopic or open colonic resection for cancer. *Hepatogastroenterology* 2003; **50:** 1348-1351
26 **Lacy AM,** Garcia-Valdecasas JC, Delgado S, Castells A, Taura P, Pique JM, Visa J. Laparoscopy-assisted colectomy versus open colectomy for treatment of non-metastatic colon cancer: a randomised trial. *Lancet* 2002; **359:** 2224-2229
27 **Pera M,** Delgado S, Garcia-Valdecasas JC, Pera M, Castells A, Pique JM, Bombuy E, Lacy AM. The management of leaking rectal anastomoses by minimally invasive techniques. S*urg Endosc* 2002; **16:** 603-606
28 **Kockerling F,** Rose J, Schneider C, Scheidbach H, Scheuerlein H, Reymond MA, Reck T, Konradt J, Bruch HP, Zornig C, Barlehner E, Kuthe A, Szinicz G, Richter HA, Hohenberger W. Laparoscopic colorectal anastomosis: risk of postoperative leakage. Results of a multicenter study. Laparoscopic Colorectal Surgery Study Group (LCSSG). *Surg Endosc* 1999; **13:** 639-644
29 **Wu WX,** Sun YM, Hua YB, Shen LZ. Laparoscopic versus conventional open resection of rectal carcinoma: A clinical comparative study. *World J Gastroenterol* 2004; **10:** 1167-1170
30 **Zheng XH,** Guan YS, Zhou XP, Huang J, Sun L, Li X, Liu Y. Detection of hypervascular hepatocellular carcinoma: Comparison of multi-detector CT with digital subtraction angiography and Lipiodol CT. *World J Gastroenterol* 2005; **11:** 200-203

Science Editor Kumar M and Guo SY **Language Editor** Elsevier HK

PO Box 2345, Beijing 100023, China
www.wjgnet.com
wjg@wjgnet.com

ELSEVIER

World J Gastroenterol 2005;11(44):6936-6940
World Journal of Gastroenterology ISSN 1007-9327

Fibrinogen-like protein 2 fibroleukin expression and its correlation with disease progression in murine hepatitis virus type 3-induced fulminant hepatitis and in patients with severe viral hepatitis B

Chuan-Long Zhu, Wei-Ming Yan, Fan Zhu, Yong-Fen Zhu, Dong Xi, De-Ying Tian, Gary Levy, Xiao-Ping Luo, Qin Ning

Chuan-Long Zhu, Wei-Ming Yan, Fan Zhu, Yong-Fen Zhu, Dong Xi, De-Ying Tian, Xiao-Ping Luo, Qin Ning, Tongji Hospital of Tongji Medical College, Huazhong University of Science and Technology, Wuhan 430030, Hubei Province, China
Gary Levy, Toronto General Hospital of University of Toronto, Toronto M5G 2N2, Canada
Supported by the National Natural Science Foundation of China for Distinguished Young Scholars, No. 30225040 for Dr Ning Q, No. 30123019 for Dr Luo XP
Co-first-authors: Chuan-Long Zhu and Wei-Ming Yan
Correspondence to: Dr Qin Ning, Laboratory of Infectious Immunology and Department of Infectious Disease, Tongji Hospital, 1095 Jie Fang Avenue, Wuhan 430030, Hubei Province, China. qning@tjh.tjmu.edu.cn
Telephone: +86-27-83662391 Fax: +86-10-85381893
Received: 2005-04-28 Accepted: 2005-05-25

Abstract

AIM: To evaluate the expression of fibrinogen-like protein 2 (fgl2) and its correlation with disease progression in both mice and patients with severe viral hepatitis.

METHODS: Balb/cJ or A/J mice were infected intraperitoneally (ip) with 100 PFU of murine hepatitis virus type 3 (MHV-3), liver and serum were harvested at 24, 48, and 72 h post infection for further use. Liver tissues were obtained from 23 patients with severe acute chronic (AOC) hepatitis B and 13 patients with mild chronic hepatitis B. Fourteen patients with mild chronic hepatitis B with cirrhosis and 4 liver donors served as normal controls. In addition, peripheral blood mononuclear cells (PBMC) were isolated from 30 patients (unpaired) with severe AOC hepatitis B and 10 healthy volunteers as controls. Procoagulant activity representing functional prothrombinase activity in PBMC and white blood cells was also assayed. A polyclonal antibody against fgl2 was used to detect the expression of both mouse and human fgl2 protein in liver samples as well as in PBMC by immunohistochemistry staining in a separate set of studies. Alanine aminotransferase (ALT) and total bilirubin (TBil) in serum were measured to assess the severity of liver injury.

RESULTS: Histological changes were found in liver sections 12-24 h post MHV-3 infection in Balb/cJ mice. In association with changes in liver histology, marked elevations in serum ALT and TBil were observed. Mouse fgl2 (mfgl2) protein was detected in the endothelium of intrahepatic veins and hepatic sinusoids within the liver 24 h after MHV-3 infection. Liver tissues from the patients with severe AOC hepatitis B had classical pathological features of acute necroinflammation. Human fgl2 (hfgl2) was detected in 21 of 23 patients (91.30%) with severe AOC hepatitis B, while only 1 of 13 patients (7.69%) with mild chronic hepatitis B and cirrhosis had hfgl2 mRNA or protein expression. Twenty-eight of thirty patients (93.33%) with severe AOC hepatitis B and 1 of 10 with mild chronic hepatitis B had detectable hfgl2 expression in PBMC. No hfgl2 expression was found either in the liver tissue or in the PBMC from normal donors. There was a positive correlation between hfgl2 expression and the severity of the liver disease as indicated by the levels of TBil. PCA significantly increased in PBMC in patients with severe AOC hepatitis B.

CONCLUSION: The molecular and cellular results reported here in both mice and patients with severe viral hepatitis suggest that virus-induced hfgl2 prothrombinase/fibroleukin expression and the coagulation activity associated with the encoded fgl2 protein play a pivotal role in initiating severe hepatitis. The measurement of hfgl2/fibroleukin expression in PBMC may serve as a useful marker to monitor the severity of AOC hepatitis B and a target for therapeutic intervention.

Key words: Viral hepatitis; Fgl2; Murine hepatitis virus; Gene expression

Zhu CL, Yan WM, Zhu F, Zhu YF, Xi D, Tian DY, Levy G, Luo XP, Ning Q. Fibrinogen-like protein 2 fibroleukin expression and its correlation with disease progression in murine hepatitis virus type 3-induced fulminant hepatitis and in patients with severe viral hepatitis B. *World J Gastroenterol* 2005; 11(44): 6936-6940
http://www.wjgnet.com/1007-9327/11/6936.asp

INTRODUCTION

Viral hepatitis remains a major public health problem and the most common type of liver disease worldwide[1,2]. There are an increasing number of patients with chronic hepatitis B who develop acute hepatitis on chronic condition (AOC) and die of acute hepatic failure both as a result of our lack of understanding of the pathogenesis of the disease and lack of effective treatment[3]. The hallmark of AOC is the extreme rapidity of the necro-microinflammatory process resulting in widespread or total hepatocellular necrosis in weeks or even in days[3]. Our previous studies have shown that macrophage activation and expression of fgl2, encoding a serine protease capable of directly cleaving prothrombin to thrombin, result in widespread fibrin deposition within the liver and hepatocyte necrosis[3-6]. The present study was designed to assess the expression of fgl2 and its correlation with disease progression in both mice and patients with severe viral hepatitis.

MATERIALS AND METHODS

Virus

MHV-3 was purchased from the American Type Culture Collection (ATCC), plaque was purified on monolayers of DBT cells and grown to a titer of 1×10^6 PFU/mL in 17 CL cells. Viral titers were determined on monolayers of L2 cells by a standard plaque assay as described elsewhere[5].

Animals

Female Balb/cJ mice, 8-10 wk of age and weighing 20-22 g, were purchased from Hubei Provincial Institute of Science and Technology. Female A/J mice, 8-10 wk of age and weighing 20-22 g, were purchased from Jackson Laboratory (Bar Harbor, ME, USA).

Main reagents

The affinity-purified polyclonal antibody to both murine and human fgl2 prothrombinases was produced by 21 repeated injections into rabbits with a 14-amino-acid hydrophilic peptide (CKLQADDHRDPGGN) from exon 1 of the fgl2 prothrombinase coupled to keyhole limpet hemocyanin. Rabbit brain thromboplastin was purchased from Sigma Chemical Company (St. Louis, MO, USA).

Murine hepatitis model

All animal experiments were carried out according to the guidelines of the Chinese Council on Animal Care and approved by the Tongji Hospital of Tongji Medical College Committees on Animal Experimentation. The research protocol was reviewed and approved by the Hospital Institutional Review Board of Tongji Hospital, Huazhong University of Science and Technology, Wuhan, China. All mice were housed in the animal facility in Tongji Hospital. Mice received 100 PFU of MHV-3 by intraperitoneal injection. The liver and serum were collected from both Balb/cJ and A/J mice 0, 24, 48, and 72 h after intraperitoneal injection of MHV-3.

Patients

Biochemical, histological, and clinical features were used to define patients with severe AOC hepatitis B or mild chronic viral hepatitis B and compensated cirrhosis. The patients with chronic viral hepatitis B were evaluated on the basis of a thorough history and physical examination with special emphasis on risk factors for co-infection (with hepatitis C, D, or HIV), alcohol use, family history of viral hepatitis B and liver cancer. Liver tissues were obtained by biopsies from patients in 1995-2001, including 23 severe AOC hepatitis B patients (20 males and 3 females, 36.0±7.8 years on average with a mortality of 82% ALT 586.0±570.2 IU/L, TBil 452.9±227.2 μmol/L, and PT 35±10 s), 13 mild chronic hepatitis B patients (11 males and 2 females, 43.8±5.6 years on average, ALT 300.5±325.2 IU/L, TBil 78.3±175.4 μmol/L, and PT 12±1 s), 14 compensated cirrhosis hepatitis B patients (all males, 45.0±8.6 years on average, ALT 265.3±215.8 IU/L and TBil 46.6±27.6 μmol/L, PT 14±2 s). All mild chronic hepatitis B and compensated cirrhotic hepatitis B patients recovered from the disease. There were no significant differences in HBV DNA levels among different groups of patients. Liver biopsies were performed within 30 min after the patients died of acute hepatic failure. Liver samples were also obtained from four liver donors as normal controls. PBMCs were freshly isolated from 30 patients (all males, 37.7±9.1 years on average) with severe AOC hepatitis B, elevated ALT (108.9±75.2 IU/L) and TBil (389.3±116.9 μmol/L), elevated PT (40±31 s). Ten mild chronic hepatitis B patients (8 males and 2 females, 34.0±10.5 years on average) had normal ALT and TBil. The isolated PBMCs were smeared on slides and kept at -80 ℃ for further study. Liver tissue histological sections were stained with hemotoxylin and eosin.

Immunohistochemical staining

Immunohistochemical staining was performed with a rabbit polyclonal antibody against the fgl2 prothrombinase as described previously[3,6].

Procoagulant activity (PCA)

PBMC and white blood cells (WBC) were evaluated for functional PCA in a one-stage clotting assay. Freshly isolated PBMC and WBC were washed twice with PBS (pH 7.0) and resuspended at a concentration of 10^6/mL. Samples were assayed for the ability to shorten the spontaneous clotting time of normal citrated human platelet-poor plasma. Milliunits of PCA were assigned by reference to a standard curve generated with serial log dilutions of a standard rabbit brain thromboplastin as described previously[2].

Statistical analysis

Quantitative data were expressed as mean±SD. Statistical analysis was carried out by one-way analysis of variance. $P<0.05$ was considered statistically significant.

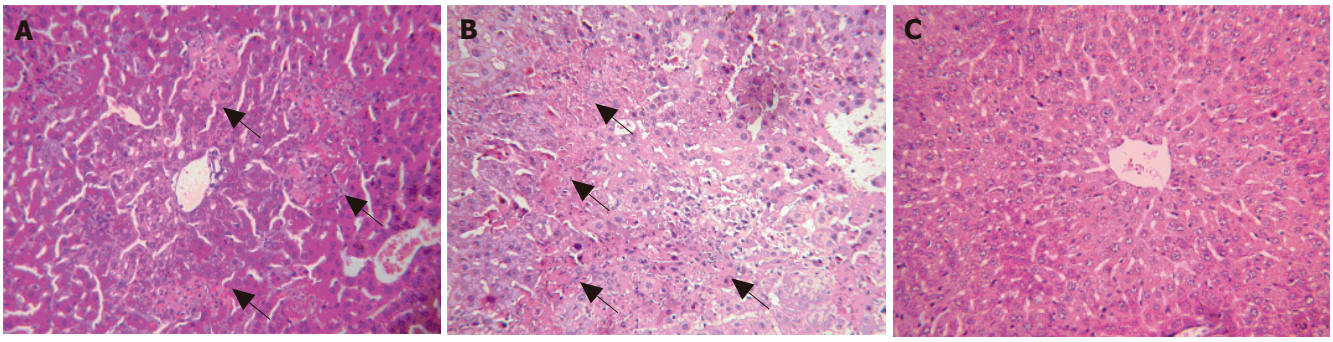

Figure 1 HE staining of liver tissue 48 h (**A**) and 72 h (**B**) after MHV-3 infection in Balb/cJ mice and 72 h (**C**) after MHV-3 infection in A/J mice. Arrows represent areas of hepatocyte necrosis.

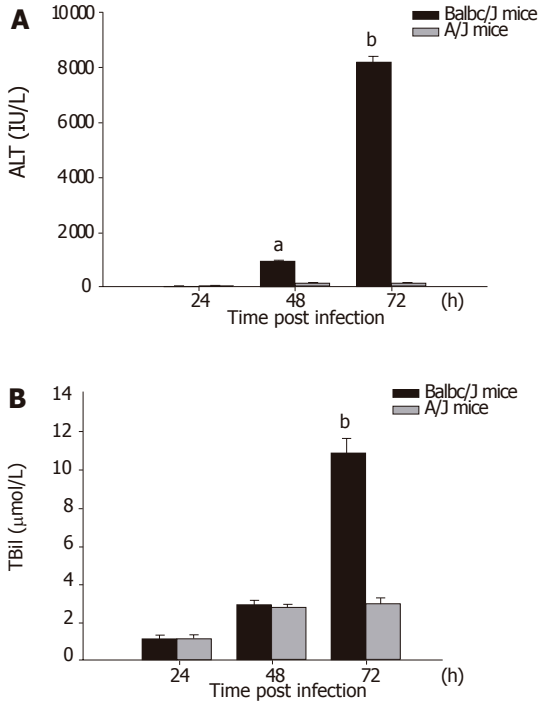

Figure 2 Serum ALT (**A**) and TBil (**B**) levels in MHV-3 infected Balb/cJ and A/J mice. $^{b}P<0.01$ *vs* A/J mice group.

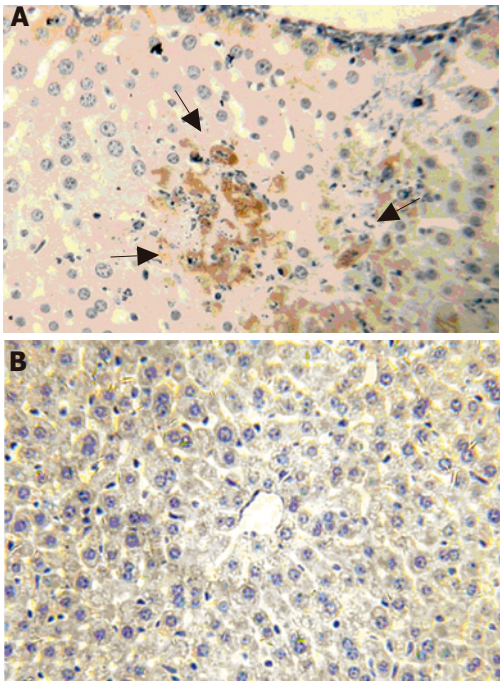

Figure 3 Mfgl2 expression in liver 24 h after MHV-3 infection Balb/cJ (**A**) and A/J (**B**) mice by immunohistochemical staining. Arrows represent mfgl2 positive cells.

RESULTS

Peritoneal administration of MHV-3-induced fulminant viral hepatitis in Balb/cJ mice

Small and discrete foci of necrosis with sparse polymorphonuclear leukocyte infiltrates were seen 12-24 h after MHV-3 infection. After 48 h, the area of these lesions enlarged and became confluent necroses (Figures 1A and 1B). There was no evidence of necrosis in the livers of MHV-3 infected A/J mice (Figure 1C). In Balb/cJ mice, serum ALT and TBil levels increased after 16-24 h, peaked at 72 h and remained elevated thereafter, while there were no significant ALT and TBil changes in MHV-3-infected A/J mice (Figures 2A and 2B).

Elevated expression of mfgl2 prothrombinase in MHV-3-infected Balb/cJ mice

mfgl2 prothrombinase expression increased in MHV-3-infected Balb/cJ mice starting from 12 to 24 h (Figure 3A) and was sustained until the animals died days after infection (data not shown). There was no evidence of mfgl2 staining in normal Balb/cJ mice (data not shown) or MHV-3-infected A/J mice (Figure 3B).

Increased hfgl2 prothrombinase and PCA in patients with severe AOC hepatitis B

Hfgl2 was detected in 21 of 23 patients (91.30%) with severe AOC hepatitis B (Figure 4A), while only 1 of 13 patients (7.69%) with mild chronic hepatitis B and cirrhosis (no evidence of active disease) had hfgl2 mRNA or protein expression. Twenty-eight of thirty patients with severe AOC hepatitis B (93.33%) and 1 of 10 with mild chronic hepatitis B had detectable hfgl2 expression in PBMC (Figure 4C). There was no hfgl2 expression either in the liver tissue or in the PBMC from the normal donors.

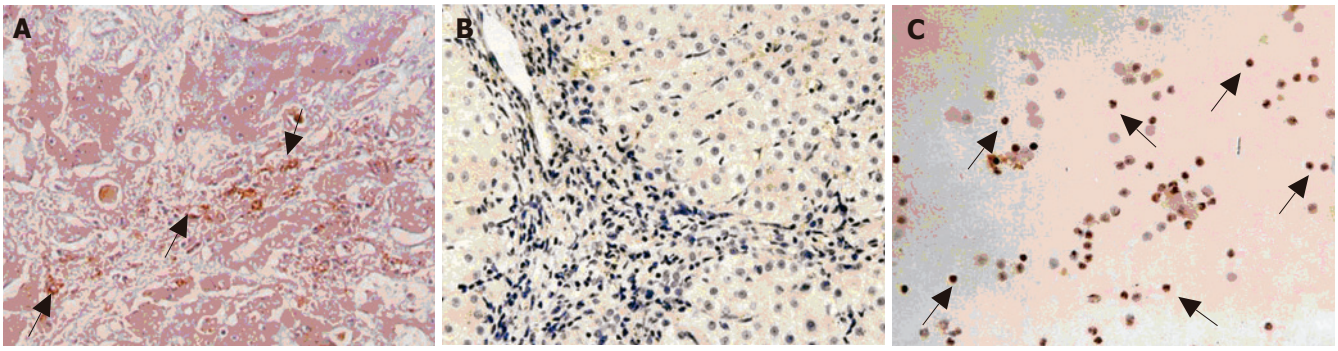

Figure 4 Immunohistochemical staining of hfgl2 in liver of patients with server AOC hepatitis B (**A**) and mild chronic hepatitis B (**B**) or in PBMC of patients with severe AOC hepatitis B (**C**). Arrows represent hfgl2 positive cells.

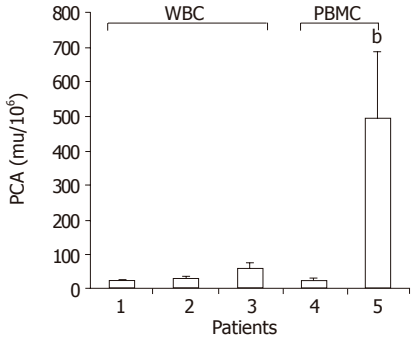

Figure 5 PCA levels in PBMC and WBC of patients.1. Healthy control; 2. patients with mild chronic hepatitis B; 3. patients with severe AOC hepatitis B; 4. healthy control; 5. patients with severe AOC hepatitis B. $^{b}P<0.01$ *vs* group 4

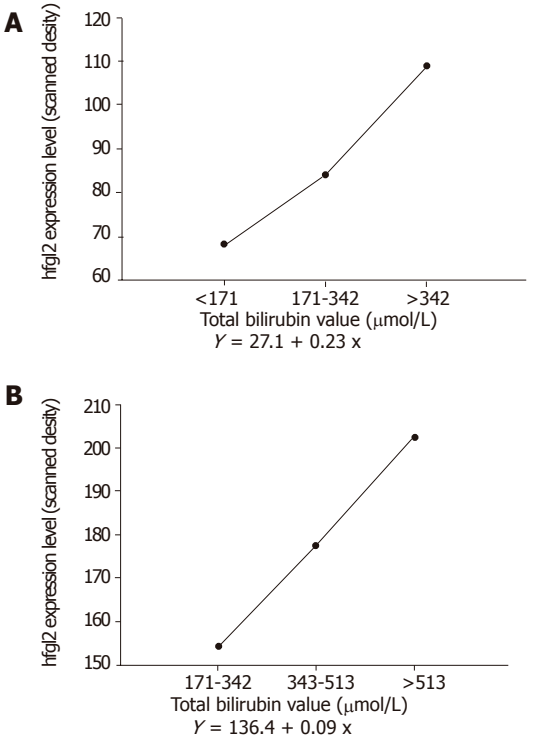

Figure 6 Correlation of hfgl2 expression in liver (**A**) and PBMC (**B**) with serum TBil level.

There was a significant increase in PCA activity in patients with serve AOC hepatitis B compared to patients with mild chronic hepatitis B, while there was no significant difference in PCA in various groups of patients (Figure 5).

Expression of hfgl2 prothrombinase correlates with the severity of hepatitis B

Hfgl2 expression both in liver and in PBMC was semi-quantified by a MPIAS-500 scanning analysis system. The data indicated that there was a close correlation between hfgl2 expression and the severity of the disease as shown in Figures 6A and 6B.

DISCUSSION

The inability to propagate human hepatitis viruses in culture and the lack of suitable animal models have impeded the determination of the pathological mechanisms of fulminant hepatic failure (FHF). However, animal models of FHF induced by murine hepatitis virus strain 3[4,7], transgenic models of hepatitis B virus infection[8,9] and clinical cases of FHF have provided insights into the pathogenesis of viral FHF[3,6]. MHV-3 produces a broad spectrum of diseases, including pneumonitis, encephalitis, enterocolitis, nephritis, and hepatitis[10,11]. This report demonstrated that Balb/cJ mice after MHV-3 infection developed fulminant viral hepatitis. HE staining showed infiltration of lymphocytes and massive hepatic necrosis in association with mfgl2 expression in the endothelial cells of hepatic sinusoids and in areas of focal necrosis. The serum ALT and bilirubin levels reflected the damage of liver tissue in MHV-3-induced FHF in Balb/cJ mice. In contrast, there was no or only minor hepatocyte injury with no mfgl2 in MHV-3-infected A/J mice. Therefore, these results further demonstrate that though MHV-3 replicates in tissues of both resistant and susceptible animals, suggesting that host factors may be more critical than viral replication in the pathogenesis of MHV-induced hepatitis. Our previous study have demonstrated that MHV-3 infection of macrophages results in transcription of host inflammatory cytokines, including TNF-α, IL-1, and superoxides[4]. Cytokines can play an important role in the course of inflammatory injury *in vivo*, and interference

with their action can alter the course of inflammatory diseases[12-15]. The importance of mfgl2 prothrombinase in the pathogenesis of MHV-3 infection is supported by the observation that a neutralizing antibody to this protein prevents fibrin deposition and protects mice from the lethality of MHV-3 infection. Furthermore, mfgl2 knockout mice lack fibrin deposition and liver necrosis and survival increased from 0% to 33%[3,16].

To address the relevance of hfgl2 in human chronic viral hepatitis, we studied patients with both minimal and severe AOC hepatitis B. We detected robust expression of hfgl2 near or within the areas of hepatic necrosis and elevated levels of hfgl2 were seen in PBMC isolated from patients with severe AOC hepatitis B. These findings are in contrast to the lack of expression of hfgl2 in the livers and PBMC of patients with minimal chronic hepatitis B. Functional assay of hfgl2 prothrombinase in PBMC showed a robust increase of PCA in patients with severe AOC hepatitis B compared to patients with minimal chronic hepatitis B. Semiquantitative analysis of hfgl2 expression both in liver tissue and PBMC showed a close correlation with the severity of the disease as indicated by elevations in serum bilirubin levels. There was no significant difference in terms of HBeAg level and HBV DNA level between different groups of patients, further supporting that host factors may be critical in the pathogenesis of severe hepatitis.

In conclusion, MHV-3-induced hfgl2 prothrombinase/fibroleukin expression and the potent function of the protein it encodes play a pivotal role in initiating both acute and fulminant hepatitis on chronic liver injury. The measurement of hfgl2 expression in PBMC may serve as a useful marker to monitor the severity of AOC hepatitis B and a target for therapeutic intervention.

REFERENCES

1 **Fattovich G.** Natural history and prognosis of hepatitis B. *Semin Liver Dis* 2003; **23:** 47-58

2 **Levy GA,** Liu M, Ding J, Yuwaraj S, Leibowitz J, Marsden PA, Ning Q, Kovalinka A, Phillips MJ. Molecular and functional analysis of the human prothrombinase gene (HFGL2) and its role in viral hepatitis. *Am J Pathol* 2000; **156:** 1217-1225

3 **Marsden PA,** Ning Q, Fung LS, Luo X, Chen Y, Mendicino M, Ghanekar A, Scott JA, Miller T, Chan CW, Chan MW, He W, Gorczynski RM, Grant DR, Clark DA, Phillips MJ, Levy GA. The Fgl2/fibroleukin prothrombinase contributes to immunologically mediated thrombosis in experimental and human viral hepatitis. *J Clin Invest* 2003; **112:** 58-66

4 **Ding JW,** Ning Q, Liu MF, Lai A, Leibowitz J, Peltekian KM, Cole EH, Fung LS, Holloway C, Marsden PA, Yeger H, Phillips MJ, Levy GA. Fulminant hepatic failure in murine hepatitis virus strain 3 infection: tissue-specific expression of a novel fgl2 prothrombinase. *J Virol* 1997; **71:** 9223-9230

5 **Ning Q,** Brown D, Parodo J, Cattral M, Gorczynski R, Cole E, Fung L, Ding JW, Liu MF, Rotstein O, Phillips MJ, Levy G. Ribavirin inhibits viral-induced macrophage production of TNF, IL-1, the procoagulant fgl2 prothrombinase and preserves Th1 cytokine production but inhibits Th2 cytokine response. *J Immunol* 1998; **160:** 3487-3493

6 **Chen Y,** Ning Q, Wang BJ, Zhang DS, Yan FM, Sun Y, Xi D, Yan WM, Hao LJ. Expression of human fibroleukin gene acute on chronic hepatitis B and its clinical significance. *Zhonghua Yi Xue Za Zhi* 2003; **83:** 446-450

7 **Ning Q,** Berger L, Luo X, Yan W, Gong F, Dennis J, Levy G. STAT1 and STAT3 alpha/beta splice form activation predicts host responses in mouse hepatitis virus type 3 infection. *J Med Virol* 2003; **69:** 306-312

8 **Guidotti LG,** Morris A, Mendez H, Koch R, Silverman RH, Williams BR, Chisari FV. Interferon-regulated pathways that control hepatitis B virus replication in transgenic mice. *J Virol* 2002; **76:** 2617-2621

9 **Guidotti LG,** McClary H, Loudis JM, Chisari FV. Nitric oxide inhibits hepatitis B virus replication in the livers of transgenic mice. *J Exp Med* 2000; **191:** 1247-1252

10 **Ning Q,** Luo XP, Wang ZM, Han MF, Yan WM, Liu MF, Levy G. The study of cis-element HNF4 in the regulation of mfg12 prothrombinase/fibroleukin gene expression in response to nucleocapsid protein of MHV-3. *Zhonghua Yi Xue Za Zhi* 2003; **83:** 678-683

11 **Lai MM.** RNA recombination in animal and plant viruses. *Microbiol Rev* 1992; **56:** 61-79

12 **Thimme R,** Wieland S, Steiger C, Ghrayeb J, Reimann KA, Purcell RH, Chisari FV. CD8(+) T cells mediate viral clearance and disease pathogenesis during acute hepatitis B virus infection. *J Virol* 2003; **77:** 68-76

13 **Major ME,** Dahari H, Mihalik K, Puig M, Rice CM, Neumann AU, Feinstone SM. Hepatitis C virus kinetics and host responses associated with disease and outcome of infection in chimpanzees. *Hepatology* 2004; **39:** 1709-1720

14 **McClary H,** Koch R, Chisari FV, Guidotti LG. Relative sensitivity of hepatitis B virus and other hepatotropic viruses to the antiviral effects of cytokines. *J Virol* 2000; **74:** 2255-2264

15 **Wieland SF,** Vega RG, Muller R, Evans CF, Hilbush B, Guidotti LG, Sutcliffe JG, Schultz PG, Chisari FV. Searching for interferon-induced genes that inhibit hepatitis B virus replication in transgenic mouse hepatocytes. *J Virol* 2003; **77:** 1227-1236

16 **Li C,** Fung LS, Chung S, Crow A, Myers-Mason N, Phillips MJ, Leibowitz JL, Cole E, Ottaway CA, Levy G. Monoclonal antiprothrombinase (3D4.3) prevents mortality from murine hepatitis virus (MHV-3) infection. *J Exp Med* 1992; **176:** 689-697

Science Editor Wang XL and Guo SY **Language Editor** Elsevier HK

PO Box 2345, Beijing 100023, China
www.wjgnet.com
wjg@wjgnet.com

ELSEVIER

World J Gastroenterol 2005;11(44):6941-6947
World Journal of Gastroenterology ISSN 1007-9327

• *BASIC RESEARCH* •

Clinical significance of telomerase and its associate genes expression in the maintenance of telomere length in squamous cell carcinoma of the esophagus

Chung-Ping Hsu, Li-Wen Lee, Sen-Ei Shai, Chih-Yi Chen

Chung-Ping Hsu, Li-Wen Lee, Sen-Ei Shai, Chih-Yi Chen, Division of Thoracic Surgery, Department of Surgery, Taichung Veterans General Hospital, Taichung, Taiwan, China
Chung-Ping Hsu, School of Medicine, National Yang-Ming University, Taipei, Taiwan, China
Supported by grant from NSC (NSC-92-2314-B-075A-011), Taipei, Taiwan, China
Correspondence to: Chung-Ping Hsu, MD, FCCP, Division of Thoracic Surgery, Taichung Veterans General Hospital, No. 160, Sec. 3, Taichung-Kang Road, Taichung, Taiwan, China. cliff@vghtc.gov.tw
Telephone: +886-4-23592525-2692 Fax:+886-4-23594065
Received: 2005-03-08 Accepted: 2005-07-08

Abstract

AIM: To observe the interaction between the expression of telomerase activity (TA) and its associate genes in regulation of the terminal restriction fragment length (TRFL) in esophageal squamous cell carcinoma (SCC).

METHODS: Seventy-four specimens of esophageal SCC were examined. The TA was measured by telomeric repeat amplification protocol (TRAP) assay, and the associated genes [human telomerase-specific reverse transcriptase (hTERT), hTERC, TP1, c-Myc, TRF1, and TRF2] were detected using RT-PCR method. The TRFL was measured by Telomere Length Assay Kit and Southern blotting. The correlations between the expression of telomerase and its associated genes with the TRFL and survivals were examined.

RESULTS: Expressions of the TA, hTERT, hTERC, TP1, c-Myc, TRF1, and TRF2 genes were observed in 85.1%, 64.9%, 79.7%, 100.0%, 94.6%, 82.4%, and 91.9% of the tumor tissues, respectively. The TRFL of the tumor and normal esophageal tissues were 2.70±1.42 and 4.93 ±1.74 kb, respectively (P<0.0001). The TRFL of the telomerase positive and telomerase negative tumor tissues were 2.72±1.44 and 2.58±1.32 kb, respectively (P = 0.767). The TRFL ratios (TRFLR) of the telomerase positive and telomerase negative tumor tissues were 0.55±0.22 and 0.59±0.41, respectively (P = 0.742). The expression rates of h-TERT (P = 0.0002), hTERC (P<0.0001), and TRF1 (P = 0.002) in the tumor tissues are higher than those of the normal paired tissues. Though TA is markedly activated in tumor tissues (P<0.0001), its expression is not related to clinicopathological parameters including gender, tumor differentiation, and TNM stages. The cumulative 4-year survival rates of telomerase positive and telomerase negative cases were 35.86% and 31.2%, respectively (P = 0.8442). The cumulative 4-year survival rates of patients with their TRFLR ≤85% and >85% were 38.7% and 15.7%, respectively (P = 0.1307).

CONCLUSION: Though telomerase expression is not related to tumor stages and prognosis, our data support that the TA increased as the TRFL decreased, probably under the control of hTERT, hTERC, and TRF1. When telomerase expression was activated, only TRF2 overexpression persisted to stabilize T-loop formation. Furthermore, as the TRFLR decreased to 85%, a trend of better prognosis was observed. Cox model analysis indicates a higher t/n TRFLR and distant metastasis are independent poorer prognostic factors (P = 0.035 and P = 0.042, respectively).

Key words: Telomere; Telomerase; hTERT; Terminal restriction fragment length; Esophageal cancer

Hsu CP, Lee LW, Shai SE, Chen CY. Clinical significance of telomerase and its associate genes expression in the maintenance of telomere length in squamous cell carcinoma of the esophagus. *World J Gastroenterol* 2005; 11(44): 6941-6947
http://www.wjgnet.com/1007-9327/11/6941.asp

INTRODUCTION

Telomerase is a ribonucleoprotein, which is responsible for the synthesis and maintenance of the telomeric repeats at the distal ends of human chromosomes. These end structures, named telomeres, serve as protective caps and consist of specific tandem repeats (5'-TTAGGG-3') with an average length of 5-20 kb[1-3]. Upon each cell division, the chromosomal ends shorten at a rate of 50-200 bp[4] This molecular erosion sets a physical limit to the potential number of cell divisions and serves as a "mitotic clock" defining the lifespan of somatic cells. Unlike somatic cells, new telomeric repeats are added to the chromosomal end of the germline cells to maintain their stability and also preserve their full genomic information for the next

generation[5]. Similarly, immortalized cell lines and more than 85% of the cancer cells can prevent the telomere from progressive shortening by telomerase activation. This phenomenon is regulated by a length-sensing feedback mechanism when the critical point is reached[6]. Telomerase contains a catalytic human telomerase-specific reverse transcriptase (hTERT) and a RNA template (hTERC) for the telomere, provides the cancer cells unlimited replicative capacity and prevents lethal chromosomal instability. Other telomerase-independent mechanism called as alternative lengthening of telomeres (ALT) may ensure the same chromosome ends replication functions.

Normally, the 3' DNA terminal protein-DNA complexes of the telomeres form capping structures to stabilize chromosomal ends and prevent them from being recognized as DNA double-strand breaks by the cells. The current model for chromosome capping is that telomeres form a higher-order chromatin structure that physically hides the 3'-chromosome end from cellular activities. This protective structure could be provided by the ability of the 3'-overhang to fold back and invade the double-strand region of the telomere forming the so-called T-loop and D-loop with the help of TRF1 and TRF2[7,8]. If these checkpoints fail, chromosomal instability may ensue leading to oncogenic mutations.

Since 1994, the telomeric repeat amplification protocol (TRAP) assay was extensively used for the detection of TA. Our previous report has demonstrated good correlations between the expressions of hTERT (not telomerase) and its associated genes such as c-Myc, TRF1 and TRF2[9]. We also found that the expression of the TA may indicate poorer prognosis[10]. A tumor-to-normal telomere restriction fragment length ratio (t/n TRFLR) $\leq$ 75% indicates a better prognosis[11]. In addition, we found a negative linear correlation between the t/n TRFLR and expression of TA, suggesting a negative feedback mechanism in the maintenance of TRFL[11]. In this study, we investigated for correlations between the changes of t/n TRFLR and expression of the telomerase associated genes including c-Myc, TRF1 and TRF2 in squamous cell carcinoma of the esophagus.

MATERIALS AND METHODS

Patients and follow-up

Between June 1999 and December 2003, we included 74 cases of squamous cell carcinoma of the esophagus who underwent surgical resection in this prospective study. Patients who received pre-operative chemotherapy or radiotherapy were excluded. Whole body bone scan and liver sonography were performed for all of the patients to rule out systemic metastasis. The tumor differentiation included well-differentiated carcinoma in none, moderately differentiated carcinoma in 49, and poorly differentiated carcinoma in 25. Tumor staging was performed according to the AJCC (6th edition) criteria[12]. The p-TNM stages included stage I in 2, stage II in 25, stage III in 33, and stage IV in 14. The clinicopathological characteristics of the patients are summarized in Table 1.

Table 1 Clinical characteristics of 74 patients with esophageal cancer

	Numbers of patients
Age (mean), years	36-79 (59.5)
Sex	
Male	71
Female	3
Differentiation	
Well	0
Moderate	49
Poor	25
Tumor site	
T1	3
T2	10
T3	50
T4	11
Lymph node	
N0	24
N1	50
Metastasis	
M0	60
M1	14
Stage	
I	2
II	25
III	33
IV	14

Preparation of cell extracts

Twenty milligrams of frozen tissue samples were lysed with 200 μL lysis buffer and homogenized by polytron. Samples were then incubated in ice for 30 min and the lysate was centrifuged at 16 000 g at 4 °C for 20 min. The supernatant was transferred to a fresh tube and the protein concentration was determined by the Bradford assay (Bio-Rad Protein Assay Kit, Bio-Rad Lab., Hercules, CA, USA).

DNA isolation from tissues

Twenty-five milligrams of fresh frozen tissue was lysed with 800 μL lysis buffer containing 0.5% sodium dodecyl sulfate (SDS), 2 mmol/L EDTA, 0.5 mol/L NaCl, 10 mmol/L $MgCl_2$, 10 mmol KCl and 10 mmol Tris-HCl (pH 76), and digested with proteinase K at 50 μg/mL at 50 °C for at least 2 h. High molecular weight DNA was extracted with phenol/chloroform.

Assay for telomerase activity

TA was measured twice in independent experiments using 1-3 μg of total protein. Assays were performed using Telomerase PCR ELISA Kit (Boehringer Mannheim GmbH, Mannheim, Germany) including TRAP assay and detection by ELISA in two steps. In the first step, using TRAP, cell extracts were incubated with biotinylated telomerase substrate oligonucleotide (P1-TS) at 25 °C for 30 min, followed by 94 °C for 10 min to inactivate the telomerase. The extended products were amplified by PCR using Taq polymerase, the P1-TS, P2 primers and nucleotides. The PCR conditions were 33 cycles of 94 °C for 30 s on a DNA thermocycler (GeneAmp PCR System 9700, Perkin Elmer, Norwalk, CT, USA). In the second step, using the ELISA method, the amplified products

were immobilized onto streptavidin-coated microtiter plates via biotin-streptavidin interaction, and then detected by anti-digoxigenin (DIG) antibody conjugated to peroxidase. After the addition of the peroxidase substrate (3,3',5,5'-tetramethyl benzidine), the amount of TRAP products were determined by measurement of their absorbance at 450 nm (with a reference wavelength of 690 nm). Negative control reactions were performed by incubating cell extracts with 1 μg/μL RNase for 20 min at 37 °C. The results were interpreted as negative, 1+, 2+, and 3+ when the optic density (OD) values were <0.2, 0.2-1, 1-2, and >2, respectively.

Moreover, to confirm the ELISA results, amplified products were systemically run on 15% non-denaturing polyacrylamide gel. After transferring the PCR products onto a positively charged nylon membrane, Southern blotting was performed by the semi-dry electrophoretic blotting instrument (Multiphore II NovaBlot Unit, Amersham Pharmacia Biotech, Buckinghamshire, UK). The membrane was then incubated with a streptavidin alkaline phosphatase conjugate (1:5 000 dilute in blocking solution), and after rinsing, blotted products were visualized by Biotin Luminescence Detection Kit (Boehringer Mannheim). In addition, all telomerase-negative tumor specimens were re-checked by additional TRAP assay using a 150 bp internal telomerase assay standard to exclude the possibility of Taq DNA polymerase inhibition in the tumor extracts[13].

Reverse transcription-polymerase chain reaction (RT-PCR) for telomerase-associated genes

Total RNA was isolated from tissue by SV Total RNA Isolation System (Promega Corporation, USA). First strand complementary DNA (cDNA) was synthesized using 5 mg of total cellular RNA with reverse transcriptase (Invitrogen Tech-Line SM, USA) and random primers (Protech Technology Enterprise Co. Ltd). PCR was performed using RT-MPCR* Kits for Human Telomerase Genes (Maxim Biotech, Inc., USA). RTMPCR* Kits included PCR primers for human 18S (hTELS-18S, 554 bp), PCR primers for human TRF-1 (hTELS-TRF1, 433 bp), PCR primers for human c-Myc (hTELS-MYC, 381 bp), PCR primers for human TRF-2 (hTELS-TRF2, 337 bp), PCR primers for human TP-1 (hTELS-TP1, 292 bp), PCR primers for hTERT (hTELS-TERT, 255 bp), and PCR primers for human TER (hTELS-TER, 191 bp). PCR reaction mixture contained RT-MPCR buffer, 200 mM each of dATP, dCTP, dTTP, and dGTP, 5U Taq DNA polymerase and 1 mL primers. The thermal cycles of PCR were performed as follows: 3 cycles at 95 °C for 1 min and 56 °C for 4 min followed by 30 cycles at 94 °C for 1 min and 55 °C for 2.5 min and then an extension of 1 cycle at 70 °C for 10 min. PCR products were subjected to electrophoresis through 3% agarose gel stained with ethidium bromide.

Terminal restriction fragment (TRF) length measurement and tumor-to-normal TRFL ratio (t/n TRFLR)

TRFL measurement was performed using TeloTAGGG Telomere Length Assay Kit (Roche, Mannheim, Germany). Eight micrograms of genomic DNA was digested with each 30U Hinf 1/Rsa l at 37 °C for 16 h. The resulting fragments were fractionated by electrophoresis on 0.8% agarose gel and transferred to nylon membrane using Southern blotting. After transfer, the transferred DNA was fixed on the membrane by UV-crosslinking (120 mJ). The membrane was first pre-hybridized at 42 °C for 30 min and then hybridized with telomere-specific DIG-labeled probe at 42 °C for 3 h. After washing the membrane in 2× SSC, the membrane was incubated with anti-DIG-alkaline phosphatase (1:5 000 dilute in blocking solution). Finally, the immobilized telomere probe was visualized by alkaline phosphatase metabolizing CDP-Star, a highly sensitive chemiluminescent substrate. The membrane was then exposed to X-ray film, and the average TRFL was determined by comparing the signals relative to a molecular weight standard (using BIO-PROFIL Bio-1D Software, Version 99, Vilber Lourmat, France), and the mean of three measured TRFLs deducted by 2.5 kb was used as the presented telomere length[14,15]. Furthermore, the TRFLR was defined as the ratio between the length of tumor tissue TRF (t-TRF) and their paired normal tissue TRF (n-TRF) from the same patient.

Statistical analysis

All probabilities were two-tailed, with a *P*-value less than 0.05 regarded as statistically significant. The statistical calculations were conducted with SPSS software (v10.5, SPSS Inc., Chicago, IL, USA).

RESULTS

Expression of telomerase activity and its associated genes

Positive TAs were observed in 63 of 74 (85.1%) tumor tissue samples, and 24 of 74 (32.4%) normal tissue samples, respectively. Expressions of hTERT, hTERC, TP1, c-Myc, TRF1 and TRF2 genes were observed in 64.9%, 79.7%, 100.0%, 94.6%, 82.4%, and 91.9% of the tumor tissues, respectively. Representative samples showing the expression of the TA by TRAP assay, and the associated genes in paired tumor (T) and normal (N) tissues are shown in Figure 1. Expression of TA according to the patient's clinicopathological characteristics are listed in Table 2. Expression of the telomerase associate genes in normal and tumor tissues are listed in Table 3. Expression of the telomerase associate genes in tumor tissues according to the TA are listed in Table 4.

Terminal restriction fragment (TRF) length and tumor-to-normal TRFL ratio (t/n TRFLR)

The mean TRFL of the tumor and normal esophageal tissues were 2.70±1.42 and 4.93±1.74 kb, respectively (P<0.0001). The mean TRFL of the telomerase positive and telomerase negative tumor tissues were 2.72±1.44 and 2.58±1.32 kb, respectively (P = 0.767). The TRFLR of the telomerase positive and telomerase negative tumor tissues were 0.55±0.22 and 0.59±0.41, respectively (P = 0.742). The mean TRFL were 3.04±0.42 kb in stage I tumor, 2.65±1.44 kb in stage II tumor, 2.83±1.44 kb in stage III

Table 2 Expression of telomerase activity according to the clinicopathological characteristics of 74 esophageal cancer patients

	Telomerase (+)	Telomerase (-)	*P* value[1]
Gender			1.0
Female	3	0	
Male	60	11	
Differentiation			0.492
Well to moderate	20	5	
Poor	43	6	
Tumor Size			1.0
T_1+T_2	11	2	
T_3+T_4	52	9	
Lymph node			0.321
N_0	19	5	
N_1	44	6	
Metastasis			0.110
M_0	49	11	
M_1	14	0	
Stage			0.194
I+II	21	6	
III+IV	42	5	

[1]Fisher's exact test (if expectation<5) or Yate's correction of contingency.

Table 3 Expression of telomerase associate genes of the tumor and normal tissues in 74 esophageal cancer patients

Expression	Positive	Negative	*P*-values[1]
TRF1			0.002
Tumor	61	13	
Normal	43	31	
TRF2			1.0
Tumor	68	6	
Normal	67	7	
c-Myc			0.160
Tumor	70	4	
Normal	64	10	
hTERT			0.0002
Tumor	48	26	
Normal	24	50	
hTERC			<0.0001
Tumor	59	14	
Normal	30	44	
TP1			N/A
Tumor	74	0	
Normal	74	0	
Tissue			0.288
Tumor	63	11	
Normal	24	50	<0.0001

[1]Pearson's χ^2-test.

Table 4 Expression of telomerase associate genes of the tumor tissues according to the telomerase activity in 74 esophageal cancer patients

	Telomerase (+)	Telomerase (-)	*P*-value[1]
hTERT			0.737
Positive	40	8	
Negative	23	3	
hTERC			0.684
Positive	51	8	
Negative	12	3	
c-Myc			0.103
Positive	61	9	
Negative	2	2	
TRF1			0.396
Positive	53	8	
Negative	10	3	
TRF2			0.039[1]
Positive	60	8	
Negative	3	3	
TP1			N/A
Positive	63	11	
Negative	0	0	

[1]Fisher's exact test (if expectation<5) or Yate's correction of contingency.

Table 5 TRFL and t/n TRFLR of the tumor tissues according to the telomerase expression and TNM stages

Variables	TRFL	*P*- values	t/n TRFLR	*P*- values
Tissues		<0.0001[1]		
Normal	4.93±1.74 kb			
Tumor	2.70±1.42 kb			
Telomerase		0.767[1]		0.742[2]
Positive	2.72±1.44 kb		0.55±0.22	
Negative	2.58±1.32 kb		0.59±0.41	
Tumor stages		0.936[2]		0.867[2]
Stage I	3.04±0.42 kb		0.818±0.019	
Stage II	2.65±1.44 kb		0.686±0.184	
Stage III	2.83±1.44 kb		0.729±0.265	
Stage IV	2.41±1.49 kb		0.649±0.185	
Total	2.70±1.42 kb		0.73±0.24	

P values: [1]Paired *t*-test, [2]Independent *t*-test.

tumor, and 2.41±1.49 kb in stage IV tumor, respectively (stage I+II *vs* stage III+IV, $P = 0.936$). The t/n TRFLR were 0.818±0.019 in stage I tumor, 0.686±0.184 in stage II tumor, 0.729±0.265 in stage III tumor, and 0.649±0.185 in stage IV tumor, respectively (stage I+II vs stage III+IV, $P = 0.867$). Table 5 lists the TRFL and t/n TRFLR data of our patients. The representative samples showing TRFL in paired T and N tissues are shown in Figure 2.

Survival analysis

The influence of TA expression was evaluated by cumulative survival period. The 5-year cumulative survival

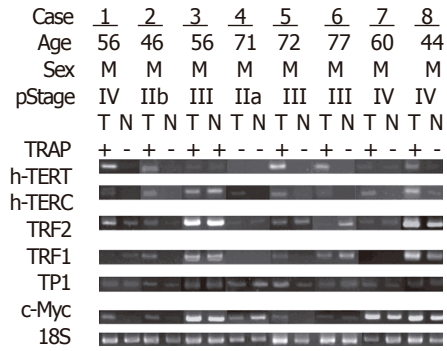

Figure 1 Representative samples showing expression of the telomerase activity by TRAP assay, and the associated genes in paired tumor (T) and normal (N) tissues.

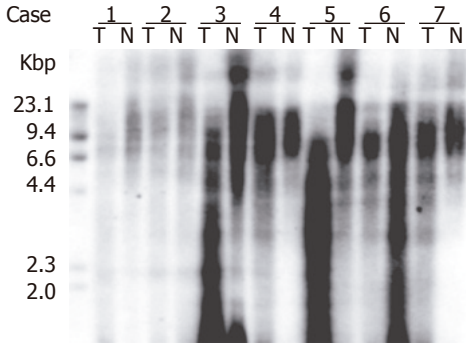

Figure 2 Representative samples showing TRFL by telomere length assay kit in paired tumor (T) and normal (N) tissues are shown.

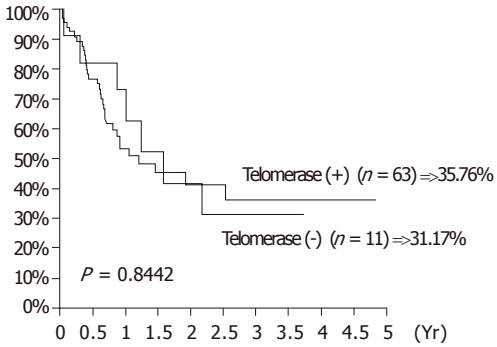

Figure 3 Cumulative survival rates according to the expression of telomerase activity in 74 SCC of esophagus.

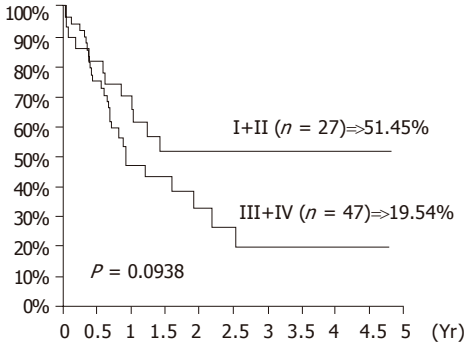

Figure 4 Cumulative survival rates according to the TNM stages in 74 SCC of esophagus.

rates of the patients by tumor stages and presence of distant metastasis are shown in Figures 3 and 4. As shown in Figure 5, the 4-year cumulative survival rates of telomerase-positive and telomerase-negative patients were 35.8, and 31.2%, respectively (P = 0.8442). When survival analyses were performed based on the change of TRFL in the tumor tissues, a cut-off value of 50% demonstrated a trend in survival difference. As shown in Figure 6, the 4-year cumulative survival rates of lower t/n TRFLR (≤85%) and higher t/n TRFLR (>85%) patients were 38.7, and 15.7%, respectively (P = 0.1307). Multivariate survival analysis using Cox proportional hazards model revealed

Table 6 Multivariate survival analysis for Cox proportional hazards model

Risk factors (# Patients)	Coefficients (SE)	Relative risk (95%CI)	*P*-values[1]
t/n TRFLR	0.78 (0.37)	(1.06-4.48)	0.035
≤85% (*n* = 57)		1	
>85% (*n* = 17)		2.18	
T-status	1.17 (0.78)	(0.70-15.06)	0.134
T1+T2 (*n* = 13)		1	
T3+T4 (*n* = 61)		3.24	
N-status	1.06 (0.66)	(0.79-10.48)	0.108
N0 (*n* = 24)		1	
N1+N2 (*n* = 50)		2.88	
M-status	0.87 (0.43)	(1.03-5.49)	0.042
M0 (*n* = 60)		1	
M1 (*n* = 14)		2.38	
Stage	-0.90 (0.78)	(0.09-1.89)	0.251
I+II (*n* = 27)		1	
III+IV (*n* = 47)		0.41	
Differentiation	0.33 (0.35)	(0.70-2.76)	0.352
W+M (*n* = 25)		1	
P (*n* = 49)		1.39	
Telomerase expression	-0.11 (0.46)	(0.36-2.22)	0.811
Negative (*n* = 11)		1	
Positive (*n* = 63)		0.90	

[1]Wald statistic

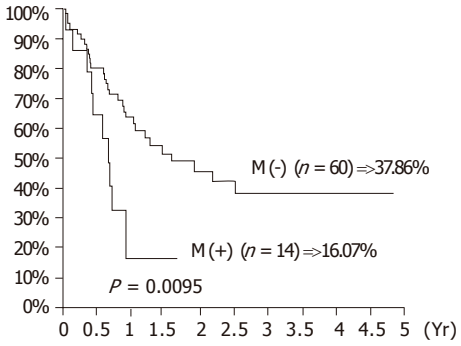

Figure 5 Cumulative survival rates according to the distant metastasis in 74 SCC of esophagus.

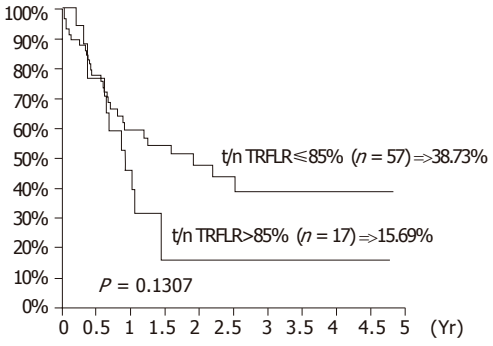

Figure 6 Cumulative survival rates according to the t/n TRFLR in 74 SCC of esophagus.

independent prognostic factors that includes t/n TRFLR (P = 0.035), and M-status (P = 0.042) of the tumor (Table 6).

DISCUSSION

Cell numbers are vigorously controlled within the body and, in human adults, only a few cell types are capable of continued division. Cultured cells *in vitro* can undergo only a limited number of cell divisions, known as the Hayflick limit, before entering a state of senescence where they remain metabolically active but have lost their capacity to replicate (M1 crisis). Reduction in telomere length could provide the signal to cause growth arrest. Cultured cells can be induced to continue to divide beyond the Hayflick limit by inactivation of p53 or p16INK4a genes. During this process of oncogenesis, their telomeres continue to shorten with each division and at a certain point cells enter a crisis where the majority will die (M2 crisis). Rare immortalized clones that emerge from crisis express the enzyme telomerase[16]. The regulation of TA is a complex issue, involving the transcriptional activity of the hTERC (telomerase RNA component gene), and the hTERT, as well as the interaction of telomerase with other telomerase-associated proteins, such as TP1/c-Myc/TRF1/TRF2/ Tankyrase. TP1, which is expressed ubiquitously, may play a role in coordinating telomerase holoenzyme tertiary or/and quaternary structures and/or serve as a docking/ scaffold protein in recruiting telomerase regulatory factors. The ability of c-Myc to function as a transcription factor has been shown to depend upon its dimerization with the protein Max[17]. In addition to the formation of stable complexes with c-Myc, Max also heterodimerizes with proteins of the Mad(Mxi1) family[18]. These Mad/Max complexes act in an antagonistic manner to c-Myc/Max-induced transactivation and result in potent repression of gene expression. Two proteins that bind to the double-stranded region of mammalian telomeres have been identified: TTAGGG repeat binding factor 1 (TRF1) and factor 2 (TRF2). These proteins are related and have a similar domain organization. Both proteins are associated with telomeres throughout the cell cycle and bind to the cognate telomeric sequence as homodimers using a carboxy-terminal myb-type DNA binding domain. TRF1 regulates telomere length and TRF2 protects chromosome ends. These two paralogs bind to double stranded telomeric DNA with high affinity, but no interaction between TRF1 and TRF2 has been observed so far[19,20]. However, TRF1 and TRF2 interact with other proteins in regulating telomeric repair. Together with tankyrase, TRF1 is involved in telomere length regulation via negative feedback mechanism; overexpression results in shortened telomeres, and mutation of telobox causes elongated telomeres[20,21]. Removal of TRF2 from the telomere results in the loss of the 3'-overhang, covalent fusion of telomeres, and the induction of ATM and p53 dependent apoptosis. Overexpression of TRF2 in telomerase negative cells prevents critically short telomeres from fusion and delays the onset of senescence[19] .

The expression rates of telomerase and hTERT were 85.1% and 64.9%, which were consistent with other reports. We also found telomerase expression in 32.4% of the paired normal esophageal mucosa. This had been attributed to actively dividing basal layer cells[22,23] or submucosal tumor infiltration[24]. A higher telomerase and hTERT expression rate in the normal esophageal mucosa makes it a distinct finding as compared with other digestive tract mucosa[25]. The telomerase expression of the tumor is not related to the clinicopathological parameters including gender, tumor differentiation, and TNM stages of the patients (see Table 2). Controversy in interpretation of the clinical significance of telomerase expression may be related to the presence of the alternative telomere lengthening (ATL) mechanism. ALT cells have long heterogeneous telomeres thought to be generated by a recombination-based mechanism[26]. Interestingly, tumor cells may simultaneously obtain both telomerase and ATL mechanisms in maintaining telomere length[27]. This will cause more complexity in analyzing the relation between the telomerase expression, telomere maintenance, and their impact on prognosis.

In a previous study in non-small cell lung cancers, we found that c-Myc, TRF1, and TRF2 expression was closely related to hTERT expression, although there was no association with telomerase expression[9]. We also found that when the TRFL decreased to a critical level, the TA could be elicited[11]. This hypothesis was further confirmed by the establishment of a negative linear association between the t/n TRFLR and the expression of TA in NSCLC tumor tissues[11] In the current study, we found a higher expression rate of the hTERT, hTERC, and TRF1 in the tumor tissues (Table 3). This suggests that hTERT, hTERC, and TRF1 are incorporated in the regulation of telomerase expression in the tumor tissues as the TRFL becomes progressively shortened. However, once the telomerase expression was activated, TRF1 expression becomes suppressed to prevent interference with telomerase binding. Instead, TRF2 overexpression persisted (see Table 4), which increases the number of TRF2 molecules binding on the telomeric DNA, and subsequently leads to more efficient and stable T-loop formation as described in the *in vitro* study[28]. Therefore, it is not only the telomere length, but also the TRF2 that determines whether senescence ensues or not.

Though a decreased TRFL was observed in the tumor tissues, there were no significant changes in TRFL between different tumor stages or different telomerase expression. Also, the t/n TRFLR did not change accordingly in different tumor stages. But when the t/n TRFLR decreased to a critical level ($\leqslant 85\%$), a better survival was observed (Figure 6). This may be due to the failure of the tumor cells to regain an adequate telomere length, which subsequently triggers the apoptosis pathway. Cox model analysis also confirmed t/n TRFLR as an independent prognostic factor in addition to distant metastasis.

In summary, our data suggest that telomerase expression in esophageal cancers is not related to tumor stages and patient's prognosis. This may be due to a high telomerase expression in the normal esophageal mucosa which makes telomerase not a reliable biomarker in esophageal tumors. However, TA can be elicited as the TRFL decreased in the tumor tissues, probably under the control of hTERT, hTERC, and TRF1 (but not TRF2).

Once the telomerase expression was elicited, TRF1 expression becomes suppressed to prevent interference with telomerase binding. Instead, TRF2 overexpression persisted, which increases the number of TRF2 molecules binding on the telomeric DNA, and subsequently leads to more efficient and stable T-loop formation. Moreover, as the t/n TRFLR decreased to 85%, a trend of poorer prognosis was observed. These findings further confirm our previous proposal using the t/n TRFLR as an indicator of chromosome ends replication ability[11]. The complex interweaving of the regulatory pathway for telomere maintenance and the mechanism involved in the detection of telomere loss by tumor cells, which subsequently activates telomerase expression require further study.

ACKNOWLEDGMENTS

The authors thank Ms SW Tang, and Ms HC Ho (Biostatistics Task Force of Taichung Veterans General Hospital) for their assistance in tissue preparation, data recording, and statistical analysis.

REFERENCES

1 **Allshire RC,** Dempster M, Hastie ND. Human telomeres contain at least three types of G-rich repeat distributed non-randomly. *Nucleic Acids Res* 1989; **17:** 4611-4627
2 **Moyzis RK,** Buckingham JM, Cram LS, Dani M, Deaven LL, Jones MD, Meyne J, Ratliff RL, Wu JR. A highly conserved repetitive DNA sequence, (TTAGGG)n, present at the telomeres of human chromosomes. *Proc Natl Acad Sci U S A* 1988; **85:** 6622-6626
3 **Cross SH,** Allshire RC, McKay SJ, McGill NI, Cooke HJ. Cloning of human telomeres by complementation in yeast. *Nature* 1989; **338:** 771-774
4 **Vaziri H,** Schachter F, Uchida I, Wei L, Zhu X, Effros R, Cohen D, Harley CB. Loss of telomeric DNA during aging of normal and trisomy 21 human lymphocytes. *Am J Hum Genet* 1993; **52:** 661-667
5 **Buchkovich KJ,** and Greider CW. Telomerase regulation during entry into the cell cycle in normal human T cells. *Mol Biol Cell* 1996; **7:** 1443-1454
6 **Harley CB.** Telomere loss: mitotic clock or genetic time bomb? *Mutat Res* 1991; **256:** 271-282
7 **Stansel RM,** de Lange T, Griffith JD. T-loop assembly in vitro involves binding of TRF2 near the 3' telomeric overhang. *EMBO J* 2001; **20:** 5532-5540
8 **Griffith JD,** Comeau L, Rosenfield S, Stansel RM, Bianchi A, Moss H, de Lange T. Mammalian telomeres end in a large duplex loop. *Cell* 1999; **97:** 503-514
9 **Hsu CP,** Miaw J, Hsia JY, Shai SE, Chen CY. Concordant expression of the telomerase-associated genes in non-small cell lung cancer. *Eur J Surg Oncol* 2003; **29:** 594-599
10 **Wu TC,** Lin P, Hsu CP, Huang YJ, Chen CY, Chung WC, Lee H, Ko JL. Loss of telomerase activity may be a potential favorable prognostic marker in lung carcinomas. *Lung Cancer* 2003; **41:** 163-169
11 **Hsu CP,** Miaw J, Shai SE, Chen CY. Correlation between telomerase expression and terminal restriction fragment length ratio in non-small cell lung cancer--an adjusted measurement and its clinical significance. *Eur J Cardiothorac* Surg 2004; **26:** 425-431
12 **Greene FL,** Page DL Fleming ID Fritz AG Balch CM Haller DG Morrow M. AJCC Cancer Staging Handbook. 6th ed. New York, Springer-Verlag Inc, 2002: 191-203
13 **Wright WE,** Shay JW, Piatyszek MA. Modifications of a telomeric repeat amplification protocol (TRAP) result in increased reliability, linearity and sensitivity. *Nucleic Acids Res* 1995; **23:** 3794-3795
14 **de Lange T,** Shiue L, Myers RM, Cox DR, Naylor SL, Killery AM, Varmus HE. Structure and variability of human chromosome ends. *Mol Cell Biol* 1990; **10:** 518-527
15 **Counter CM,** Avilion AA, LeFeuvre CE, Stewart NG, Greider CW, Harley CB, Bacchetti S. Telomere shortening associated with chromosome instability is arrested in immortal cells which express telomerase activity. *EMBO J* 1992; **11:** 1921-1929
16 **Wright WE,** Shay JW. Cellular senescence as a tumor-protection mechanism: the essential role of counting. *Curr Opin Genet Dev.* 2001; **11:** 98-103
17 **Schreiber-Agus N,** DePinho RA. Repression by the Mad(Mxi1)-Sin3 complex. *Bioessays* 1998; **20:** 808-818
18 **Ayer DE,** Kretzner L, Eisenman RN. Mad: a heterodimeric partner for Max that antagonizes Myc transcriptional activity. *Cell* 1993; **72:** 211-222
19 **van Steensel B,** Smogorzewska A, de Lange T. TRF2 protects human telomeres from end-to-end fusions. *Cell* 1998; **92:** 401-413
20 **van Steensel B,** de Lange T. Control of telomere length by the human telomeric protein TRF1. *Nature* 1997; **385:** 740-743
21 **Smith S,** Giriat I, Schmitt A, de Lange T. Tankyrase, a poly(ADP-ribose) polymerase at human telomeres. *Science* 1998; **282:** 1484-1487
23 **Ikeguchi M,** Unate H, Maeta M, Kaibara N. Detection of telomerase activity in esophageal squamous cell carcinoma and normal esophageal epithelium. *Langenbecks Arch Surg* 1999; **384:** 550-555
24 **Koyanagi K,** Ozawa S, Ando N, Kitagawa Y, Ueda M, and Kitajima M. Clinical significance of telomerase activity in peripheral blood of patients with esophageal squamous cell carcinoma. *Ann Thorac Surg* 2002; **73:** 927-932
25 **Koyanagi K,** Ozawa S, Ando N, Kitagawa Y, Ueda M, Kitajima M. Clinical significance of telomerase activity in peripheral blood of patients with esophageal squamous cell carcinoma. *Ann Thorac Surg* 2002; **73:** 927-932
26 **Bryan TM,** Englezou A, Gupta J, Bacchetti S, Reddel RR. Telomere elongation in immortal human cells without detectable telomerase activity. *EMBO J* 1995; **14:** 4240-4248
27 **Bryan TM,** Englezou A, Dalla-Pozza L, Dunham MA, Reddel RR. Evidence for an alternative mechanism for maintaining telomere length in human tumors and tumor-derived cell lines. *Nat Med* 1997; **3:** 1271-1274
28 **Karlseder J,** Smogorzewska A, de Lange T. Senescence induced by altered telomere state, not telomere loss. *Science* 2002; **295:** 2446-2449

Science Editor Guo SY **Language Editor** Elsevier HK

PO Box 2345, Beijing 100023, China
www.wjgnet.com
wjg@wjgnet.com

ELSEVIER

World J Gastroenterol 2005;11(44):6948-6953
World Journal of Gastroenterology ISSN 1007-9327

• *BASIC RESEARCH* •

Relationship between body surface area and ALT normalization after long-term lamivudine treatment

Makoto Nakamuta, Shusuke Morizono, Yuichi Tanabe, Eiji Kajiwara, Junya Shimono, Akihide Masumoto, Toshihiro Maruyama, Norihiro Furusyo, Hideyuki Nomura, Hironori Sakai, Kazuhiro Takahashi, Koichi Azuma, Shinji Shimoda, Kazuhiro Kotoh, Munechika Enjoji, Jun Hayashi: Kyushu University liver Disease Study Group

Makoto Nakamuta, Kazuhiro, Shusuke Morizono, Kotoh, Munechika Enjoji, Department of Medicine and Bioregulatory Science, Graduate School of Medical Sciences, Kyushu University, Japan
Norihiro Furusyo, Jun Hayashi, Department of Environmental Medicine and Infectious Diseases, Graduate School of Medical Sciences, Kyushu University, Japan
Shinji Shimoda, Department of Medicine and Biosystemic Science, Graduate School of Medical Sciences, Kyushu University, Japan
Koichi Azuma, Department of Medicine and Clinical Science, Graduate School of Medical Sciences, Kyushu University, Japan
Yuichi Tanabe, Department of Medicine, Fukuoka City Hospital, Fukuoka, Japan
Eiji Kajiwara, Department of Internal Medicine, Nippon Steel Yawata Memorial Hospital, Kitakyushu, Japan
Junya Shimono, Department of Medicine, Yahata Saiseikai Hospital, Kitakyushu, Japan
Akihide Masumoto, Department of Clinical Research, National Hospital Organization Kokura Hospital, Kitakyushu, Japan
Toshihiro Maruyama, Department of Medicine, Kitakyushu Municipal Medical Center, Kitakyushu, Japan
Hideaki Nomura, Department of Internal Medicine, Shin-Kokura Hospital, Kitakyushu, Japan
Hironori Sakai, Department of Gastroenterology, National Hospital Organization Kyushu Medical Center, Fukuoka, Japan
Kazuhiro Takahashi, Department of Medicine, Hamanomachi Hospital, Fukuoka, Japan
Correspondence to: Makoto Nakamuta, Department of Medicine and Bioregulatory Science, Graduate School of Medical Sciences, Kyushu University, 3-1-1 Maidashi, Higashi-ku, Fukuoka 812-5282, Japan. nakamuta@intmed3.med.kyushu-u.ac.jp
Telephone: +81-92-6425282 Fax: +81-92-6425287
Received: 2005-04-20 Accepted: 2005-05-12

Abstract

AIM: To further evaluate the relationship between BSA and the effects of lamivudine in a greater number of cases and over a longer period of observation than in our previous evaluation.

METHODS: We evaluated 249 patients with chronic hepatitis B. The effects of treatment for one year (n = 249), two years (n = 147), and three years (n = 72) were evaluated from the levels of serum ALT and HBV-DNA, as biological and virological effects (undetectable levels by PCR), respectively. Moreover, several variables that could influence the response to treatment, including ALT, albumin, bilirubin, platelet counts, BSA, HBV-DNA, and HBeAg were analyzed.

RESULTS: For 1-year treatment, multivariate analysis revealed that BSA (P = 0.0002) was the only factor for the biological effect, and that ALT (P = 0.0017), HBV-DNA (P = 0.0004), and HBeAg (P = 0.0021) were independent factors for the virological effect. For 2-year treatment, multivariate analysis again showed that BSA (P = 0.0147) was the only factor for the biological effect, and that ALT (P = 0.0192) and HBeAg (P = 0.0428) were independent factors for the virological effect. For 3-year treatment, multivariate analysis, however, could not reveal BSA (P = 0.0730) as a factor for the normalization of ALT levels.

CONCLUSION: BSA is a significant predictor for the normalizing the effect of lamivudine therapy on ALT for an initial 2-year period, suggesting that lamivudine dosage should be based on the individual BSA.

Key words: Lamivudine; Hepatitis B virus; Body surface area; Dose; Long-term treatment

Nakamuta M, Morizono S, Tanabe Y, Kajiwara E, Shimono J, Masumoto A, Maruyama T, Furusyo N, Nomura H, Sakai H, Takahashi K, Azuma K, Shinji S, Kotoh K, Enjoji M, Hayashi J. Kyushu University liver Disease Study Group. Relationship between body surface area and ALT normalization after long-term lamivudine treatment. *World J Gastroenterol* 2005; 11(44): 6948-6953
http://www.wjgnet.com/1007-9327/11/6948.asp

INTRODUCTION

Chronic hepatitis B is an important cause of morbidity and mortality resulting from cirrhosis-related liver failure and hepatocellular carcinoma (HCC)[1-3]. Lamivudine is an oral nucleoside analog approved for the treatment of chronic hepatitis B. It inhibits viral DNA replication by means of chain termination, and competitively inhibits viral polymerase. A daily dosage of lamivudine of 100 mg has been accepted worldwide for the treatment for chronic hepatitis B, since early studies showed that there was no

significant difference in the effect of lamivudine at doses of 100 and 300 mg[4,5]. However, to establish ideal dosages in those studies, efficacy was mainly evaluated by measuring hepatitis B virus (HBV)-DNA, and the assay used was much less sensitive than the polymerase chain reaction (PCR) assay. Studies in which HBV-DNA was measured by PCR assay reported an additional viral suppressive activity with high doses (300 mg) of lamivudine for 24 wk[6]. In addition to the limits imposed by the assay methods that were used, the observation periods in the studies on lamivudine doses of 100-300 mg were limited to a period of 12[4] or 24 wk[5]. Although the effect of doses greater than 100 mg on the emergence of YMDD mutants has not been evaluated, baseline body mass index has been reported to be significantly related to the emergence of HBV mutants during lamivudine treatment in patients co-infected with HBV and human immunodeficiency virus-1 (HIV-1)[7]. In a previous study of 134 patients treated for 23.1 mo(mean observation period), body surface area (BSA) was shown to be an independent factor contributing to the effects of lamivudine treatment[8]. In the present study, to further confirm these results, we evaluated the relationship between BSA and the effects of lamivudine effects in a greater number of patients and for longer observation periods than those in the previous report.

MATERIALS AND METHODS

Patients

Criteria for entry into this study were as follows: (a) the patients had not been treated with lamivudine previously; (b) they had chronic hepatitis caused by HBV, and persistent abnormal levels of alanine aminotransferase (ALT); and (c) patients with HCC were excluded. A total of 249 patients with chronic hepatitis B were evaluated. They had been treated with 100 mg of lamivudine for more than 1 year at Kyushu University Hospital and its affiliated hospitals (Table 1). For all the patients, the existence of serum HBV-DNA was confirmed by transcription-mediated nucleic acid amplification (TMA) assay ($10^{3.7}$-$10^{8.7}$ genome equivalents/mL; 3.7-8.7 log genome equivalents [LGE]/mL) (Chugai Diagnostic Science, Tokyo, Japan) or by a Roche Monitor kit ($10^{2.6}$-$10^{7.6}$ copies/mL; 2.6-7.6 log copies/mL) (Roche Diagnostics, Tokyo, Japan) before the treatment. None of the patients dropped out and all were treated with 100 mg/d lamivudine until the end of the observation period. After the start of medication, basic hepatic function and serum levels of HBV-DNA were measured at least every 3 mo for all the patients. The efficacy of lamivudine was evaluated from the serum levels of ALT and HBV-DNA, as biological and virological effects, respectively. The categories for the biological evaluation based on serum ALT were as follows: (1) sustained responder (SR) ALT: the serum levels of ALT decreased and remained at less than 30 U/L continuously during the observation period; and (2) non-responder (NR) ALT: the serum ALT was more than 30 U/L at the end of the observation. Similarly, the categories for the virological evaluation based on HBV-DNA were: (1) SR-HBV: serum HBV-DNA decreased to levels undetectable by PCR (<2.6 log copies/mL) and remained negative continuously during the observation period; and (2) NR-HBV: serum HBV-DNA was detectable at the end of the observation period (>2.6 log copies/mL). BSA was calculated using the method of DuBois.

Statistical analysis

The baseline characteristics of the patients prior to the beginning of the lamivudine therapy are expressed as mean±SD for the quantitative variables. In order to determine the contribution of these variables to the effect of the treatment, univariate and multivariate logistic analyses were performed. For multivariate logistic analysis, we analyzed BSA as an independent factor contributing to the effects of lamivudine treatment variables that showed χ^2 values of more than 1.0 in the univariate logistic

Table 1 Baseline characteristics of patients treated for 1 year[1]

	Total (range)	SR-ALT	NR-ALT	SR-DNA	NR-DNA
n	249	150	99	183	66
Male/female	180/67	99/51	82/17	127/54	53/13
ALT (U/L)	211.1±402.4 (16-4491)	242.1±424.2	163.6±363.6	240.3±462.2	128.8±88.1
Albumin (g/dL)	3.8±0.6 (2.2-4.9)	3.8±0.6	3.8±0.6	3.8±0.6	3.9±0.6
Bilirubin (mg/dL)	1.3±1.7 (0.1-12.9)	1.4±1.8	1.2±1.5	1.4±1.9	1.0±1.1
Platelet (10^4/mL)	14.1±6.1 (2.6-35.5)	14.2±5.8	14.0±6.5	13.9±6.2	14.9±5.6
BSA (m^2)	1.70±0.20 (1.25-2.17)	1.66±0.17	1.75±0.18	1.69±0.18	1.73±0.18
HBV-DNA					
≤5 (LEG/mL)	31	20	11	29	2
5< ≤6	33	18	15	27	6
6< ≤7	68	41	27	52	16
7<	117	71	46	75	42
HBeAg +/-	135/110	83/64	52/46	84/96	51/14
Age (yr)	48.6±11.6 (19-73)				
CH/LC [Child A/B/C]	162/87 [61/11/15]				

[1]Data are shown as mean±SD.

model. *P* value less than 0.05 was considered statistically significant.

RESULTS

The effects of lamivudine for 1 year were analyzed in a total of 249 patients (Table 1), of which 150 (60.2%) were identified as SR-ALT and 99 (39.8%) as NR-ALT, and 183 (73.5%) were identified as SR-DNA and 66 (26.5%) as NR-ALT (Table 1). To evaluate the contribution of the variables to the effect of treatment, univariate and multivariate logistic analyses were performed. In the univariate logistic analysis, BSA and ALT in the biological evaluation, and ALT, albumin, bilirubin, platelet count, BSA, HBV-DNA, and HBeAg in the virological evaluation, had χ^2 values of more than 1.0 (Table 2). Therefore, we used these factors as variables for multivariate logistic analysis. The results of multivariate analysis revealed that BSA was the only significant factor for the improvement of ALT levels (χ^2 = 14.3, P = 0.0002), and ALT, albumin, HBV-DNA and HBeAg were independent factors for the disappearance of serum HBV-DNA (ALT: χ^2 = 9.8, P = 0.0017; albumin: χ^2 = 5.1, P = 0.0238; HBV-DNA: χ^2 = 12.6, P = 0.0004; and HBeAg: χ^2 = 9.5, P = 0.0021) (Table3).

The effects of 2-year therapy were evaluated in 147 patients (Table 4). Of these patients, 75 (51.0%) were identified as SR-ALT and 72 (49.0%) as NR-ALT, while 85 (57.8%) were identified as SR-DNA and 62 (42.2%) as NR-ALT (Table 5). In the univariate logistic analysis, bilirubin, platelet count and BSA in the biological evaluation, and ALT, bilirubin, platelet, BSA and HBeAg in the virological evaluation, were selected (χ^2>1.0) (Table 5). Multivariate analysis revealed that BSA was the only significant factor in the biological effects (χ^2 = 5.6, P = 0.0147), and ALT and HBeAg were independent factors in the virological effects (ALT: χ^2 = 5.5, P = 0.0192; and HBeAg: χ^2 = 4.1, P = 0.0428) (Table 6).

Finally, the effects of 3-year therapy were evaluated in 72 patients (Table 7). Of these patients, 33 (45.8%) were identified as SR-ALT and 39 (54.2%) as NR-ALT, while

Table 2 Univariate analysis of the effects of lamivudine treatment for 1 year

Variables	χ^2	P
Biological effects		
ALT (U/L)	2.963405	0.0852
Albumin (g/dL)	0.230408	0.6312
Bilirubin (mg/dL)	0.934082	0.3338
Platelet count (10^4/mL)	0.097459	0.7549
BSA (m^2)	15.96269	<0.0001
HNV-DNA (LEG/mL)	0.000983	0.9750
HBeAg	0.275000	0.6000
Virological effects		
ALT (U/L)	8.293809	0.0040
Albumin (g/dL)	3.353949	0.0670
Bilirubin (mg/dL)	3.258437	0.0711
Platelet count (10^4/mL)	1.331910	0.2485
BSA (m^2)	2.586640	0.1078
HNV-DNA (LEG/mL)	14.38010	0.0001
HBeAg	19.51400	<0.0001

Table 3 Multivariate analysis on the effects of lamivudine treatment for 1 year

Variables	χ^2	P
Biological effects		
ALT (U/L)	1.921529	0.1657
BSA (m^2)	15.96269	0.0002
Virological effects		
ALT (U/L)	9.797455	0.0017
Albumin (g/dL)	5.106762	0.0238
Bilirubin (mg/dL)	0.450406	0.5021
Platelet count (10^4/mL)	0.009626	0.9218
BSA (m^2)	2.222164	0.1360
HNV-DNA (LEG/mL)	12.64904	0.0004
HBeAg	9.476967	0.0021

Table 4 Baseline characteristics of patients treated for 2 years[1]

	Total (range)	SR-ALT	NR-ALT	SR-DNA	NR-DNA
n	147	75	72	85	62
Male/female	112/35	52/23	60/12	62/23	50/12
ALT (U/L)	221.6±493.5 (17-4491)	258.9±548.5	182.3±428.2	291.3±626.3	122.2±132.0
Albumin (g/dL)	3.8±0.6 (2.2-4.9)	3.8±0.5	3.8±0.6	3.8±0.5	3.9±0.6
Bilirubin (mg/dL)	1.5±2.1 (0.3-12.9)	1.7±2.5	1.3±1.7	1.7±2.6	1.0±1.1
Platelet (10^4/mL)	13.8±6.2 (3.4-33.6)	12.9±5.4	14.6±6.8	13.1±5.5	14.9±5.6
BSA (m^2)	1.71±0.18 (1.30-2.17)	1.67±0.18	1.76±0.17	1.70±0.18	1.73±0.18
HBV-DNA					
≤5 (LEG/mL)	18	11	7	12	6
5< ≤6	20	7	13	11	9
6< ≤7	42	23	19	26	16
7<	69	35	34	38	31
HBeAg +/–	82/65	41/34	41/31	41/45	41/20
Age (yr)	48.9±11.4 (19-73)				
CH/LC [Child A/B/C]	95/54 [43/3/8]				

[1] Data are shown as mean±SD.

38 (52.8%) were identified as SR-DNA and 34 (47.2%) as NR-DNA (Table 8). In the univariate logistic analysis, albumin, platelet count, BSA, and HBeAg in the biological evaluation, and no variables in the virological evaluation, were selected (χ^2>1.0) (Table 8). Multivariate analysis did not reveal BSA as a factor for predicting the biological efficacy of lamivudine therapy $\chi^2 = 3.2$, $P = 0.0730$) (Table 9).

DISCUSSION

In this present study, we found that BSA was a significant factor that could contribute to the normalization of serum ALT (biological response) after the treatment with lamivudine for an initial 2-year period. Body weight was also a significant factor contributing to the effects of lamivudine treatment (data not shown). Because χ^2 values of BSA were higher than those of body weight and BSA is determined with body weight and height, we used BSA as a variable for statistical analysis. We initially reported that BSA was an independent factor contributing to both the biological and virological responses[8]. The difference in the contribution to the virological response between the present and the previous study might be attributed to the differences in the criteria used to evaluate treatment effects. In our previous study, we used a third category in addition to SR and NR transient responder (TR) which included patients with serum ALT levels that initially decreased to less than 30 U/L but increased to more than 30 U/L during the subsequent observation period (TR-ALT), and the patients in whom serum HBV-DNA initially decreased to undetectable levels (<2.6 log copies/mL) but became positive again during the subsequent observation period (TR-DNA). Regardless of the differences in evaluation criteria, both studies clearly demonstrated that BSA independently contributed to the normalization of ALT in the patients treated with lamivudine for an initial 2-year period. Because the pharmacokinetics of lamivudine correlate with body weight, as is the case with many other drugs[9], it is reasonable to conclude that patients with lower BSA would have achieved higher blood concentrations

Table 5 Univariate analysis of the effects of lamivudine treatment for 2 years

Variables	χ^2	*P* values
Biological effects		
ALT (U/L)	0.962196	0.3266
Albumin (g/dL)	0.279331	0.5971
Bilirubin (mg/dL)	1.384215	0.2394
Platelet count (10^4/mL)	2.943368	0.0862
BSA (m^2)	8.339371	0.0039
HNV-DNA (LEG/mL)	0.009964	0.9205
HBeAg	0.077000	0.7810
Virological effects		
ALT (U/L)	8.990505	0.0027
Albumin (g/dL)	0.643271	0.4225
Bilirubin (mg/dL)	3.176521	0.0747
Platelet count (10^4/mL)	2.064207	0.1508
BSA (m^2)	1.060739	0.3030
HNV-DNA (LEG/mL)	0.546020	0.4598
HBeAg	5.595000	0.0180

Table 6 Multivariate analysis of the effects of lamivudine treatment for 2 years

Variables	χ^2	*P* values
Biological effects		
Bilirubin (mg/dL)	0.496757	0.4809
Platelet count (10^4/mL)	0.572997	0.4491
BSA (m^2)	2.263849	0.0147
Virological effects		
ALT (U/L)	5.482584	0.0192
Bilirubin (mg/dL)	0.983777	0.3212
Platelet count (10^4/mL)	1.098891	0.2945
BSA (m^2)	0.714246	0.3980
HNV-DNA (LEG/mL)	0.592857	0.4413
HBeAg	4.101478	0.0428

Table 7 Baseline characteristics of patients treated for 3 years

	Total (range)	SR-ALT	NR-ALT	SR-DNA	NR-DNA
n	72	33	39	38	34
Male/female	53/19	21/12	32/7	27/11	26/8
ALT (U/L)	198.6±437.2 (18-3545)	200.0±229.0	197.5±562.1	191.2±218.0	207.2±602.6
Albumin (g/dL)	3.8±0.5 (2.5-4.9)	3.7±0.4	4.0±0.5	3.8±0.5	3.9±0.5
Bilirubin (mg/dL)	1.5±2.1 (0.3-12.9)	1.6±2.2	1.5±2.3	1.6±2.2	1.5±2.4
Platelet (10^4/mL)	13.8±6.2 (3.9-33.6)	11.6±4.6	15.1±6.9	13.3±5.8	13.8±6.5
BSA (m^2)	1.71±0.18 (1.30-2.17)	1.75±0.17	1.66±0.19	1.69±0.17	1.73±0.20
HBV-DNA					
≤5 (LEG/mL)	7	4	3	4	3
5< ≤6	15	4	11	6	9
6< ≤7	17	11	6	13	4
7<	33	14	19	15	18
HBeAg +/–	41/31	21/12	20/19	22/16	19/15
Age (yr)	49.5±11.1 (21-73)				
CH/LC [Child A/B/C]	43/29 [25/0/4]				

[1] Data are shown as mean±SD.

Table 8 Univariate analysis of the effects of lamivudine treatment for 3 years

Variables	χ^2	*P* values
Biological effects		
ALT (U/L)	0.000598	0.9805
Albumin (g/dL)	5.541899	0.0186
Bilirubin (mg/dL)	0.100733	0.7510
Platelet count (10^4/mL)	6.242535	0.0125
BSA (m^2)	4.393544	0.0361
HNV-DNA (LEG/mL)	0.001477	0.9693
HBeAg	1.113000	0.2915
Virological effects		
ALT (U/L)	0.023922	0.8771
Albumin (g/dL)	0.565446	0.4315
Bilirubin (mg/dL)	0.010128	0.9198
Platelet count (10^4/mL)	0.137799	0.7105
BSA (m^2)	0.805305	0.3695
HNV-DNA (LEG/mL)	0.065438	0.7981
HBeAg	0.030000	0.8633

Table 9 Multivariate analysis of the effects of lamivudine treatment for 3 years

Variables	χ^2	*P* values$_\chi$
Biological effects		
Albumin (g/dL)	0.865354	0.3522
Platelet count (10^4/mL)	2.391260	0.1220
BSA (m^2)	3.213451	0.0730
HBeAg	1.252959	0.2630

of lamivudine, although we did not actually monitor the concentration of lamivudine. Recent reports suggest that the baseline body mass index is significantly related to the emergence of HBV mutation during lamivudine treatment (300 mg/d, >6 mo) in patients co-infected with HBV and HIV-1[7]. Therefore, the results of our studies again question whether a lamivudine dosage of 100 mg/d is adequate, particularly for long-term treatment.

The standard lamivudine dose of 100 mg daily was based on early studies in which doses of 25, 100, and 300 mg were compared for 12[4] or 24 wk[5]. Because there were no significant differences reported in the rates of non-detection of HBV-DNA and normalization of ALT levels between the 100 and 300 mg doses, the dose of 100 mg has become a well-accepted therapeutic standard[4,5]. However, several factors should be considered when evaluating the results of these studies, including the number of patients, duration of treatment, emergence of lamivudine-resistant mutants over long-term treatment, and detection limits for HBV-DNA.

In the present study, we found that there was a significant difference in the contribution of BSA to the biological effect, although the differences in the mean values of BSA between SR-ALT and NR-ALT were relatively small. Therefore, it is possible that previous studies failed to detect a significant contribution of BSA to the effects of lamivudine because of the smaller number of patients examined. The major drawback of lamivudine monotherapy is the emergence of resistant HBV with mutations of the tyrosine-methionine-aspartate-aspartate (YMDD) motif. The incidence of these mutants rises from 15-20% in the first year of therapy to 40% by the second year, and to 67% by the fourth year[10]. In some cases, fatal liver failure subsequent to the emergence of the mutant was reported[11]. Therefore, observation periods of 24 wk may not be adequate for detecting the emergence of lamivudine-resistant mutants. In our evaluation of HBV-DNA, the rates of NR-DNA were found to be 26.5%, 42.2%, and 57.2% in patients who were positive for HBV-DNA (>2.6 log copies/mL) by the first, second, and third year, respectively. Although we did not confirm YMDD mutation in all cases of NR-DNA, the increase in NR-DNA ratio might be attributable to the emergence of mutants. Concomitant with the increases in HBV-DNA seen over the 3-year period, the NR-ALT ratio rose from 39.8% in the first year to 49.0% by the second year and to 54.8% by the third year in the present study, suggesting that the emergence of mutants could abolish the contribution of BSA to biological effects in the third year. Further studies will be needed to confirm whether BSA affects the incidence of YMDD mutants.

In previous studies that showed no difference in the effects of 100 and 300 mg lamivudine on HBV-DNA levels (as aforementioned)[4,5], HBV-DNA was measured quantitatively by liquid hybridization assay (Abbott Laboratories), which has a detection limit of 10^7 geq/mL[12]. Honkoop *et al*.[6] studied the efficacy of 100 and 300 mg lamivudine in viral suppression for 24 wk using a semi-quantitative PCR method with a detection limit of 10^2-10^3 geq/mL. In the present study, we used a Roche Monitor kit, which has detection limit of 2.6 log copies/mL, and could not find a significant relationship between BSA and the virological effect of lamivudine. Chun *et al*.[13], reported that there was no significant correlation between viral replication and liver damage in chronic hepatitis B. Hence, it seems reasonable that we did not find a contribution of BSA to the virological effects of treatment. Further study will be needed to evaluate dose-dependent lamivudine effects on viral suppression including the emergence of mutants which could directly affect the viral load.

In conclusion, we have shown that BSA is a statistically significant and potentially important factor for predicting the efficacy of lamivudine therapy for chronic hepatitis B. A noteworthy finding in our study was that small differences in BSA might significantly influence the effect of lamivudine treatment, suggesting that a small increase in lamivudine dose might markedly increase its therapeutic efficacy. We believe that a long-term clinical trial with higher-dose lamivudine treatment in a large number of cases is warranted, since lamivudine will continue to be a first-line treatment for HBV.

REFERENCES

1 **Ganem D,** Prince AM. Hepatitis B virus infection--natural history and clinical consequences. *N Engl J Med* 2004; **350:** 1118-1129

2 **Lai CL,** Ratziu V, Yuen MF, Poynard T. Viral hepatitis B.

Lancet 2003; **362:** 2089-2094
3 **Qin LX,** Tang ZY. Hepatocellular carcinoma with obstructive jaundice: diagnosis, treatment and prognosis. *World J Gastroenterol* 2003; **9:** 385-391
4 **Dienstag JL,** Perrillo RP, Schiff ER, Bartholomew M, Vicary C, Rubin M. A preliminary trial of lamivudine for chronic hepatitis B infection. *N Engl J Med* 1995; **333:** 1657-1661
5 **Nevens F,** Main J, Honkoop P, Tyrrell DL, Barber J, Sullivan MT, Fevery J, De Man RA, Thomas HC. Lamivudine therapy for chronic hepatitis B: a six-month randomized dose-ranging study. *Gastroenterology* 1997; **113:** 1258-1263
6 **Honkoop P,** de Man RA, Niesters HG, Main J, Nevens F, Thomas HC, Fevery J, Tyrrell DL, Schalm SW. Quantitative hepatitis B virus DNA assessment by the limiting-dilution polymerase chain reaction in chronic hepatitis B patients: evidence of continuing viral suppression with longer duration and higher dose of lamivudine therapy. *J Viral Hepat* 1998; **5:** 307-312
7 **Wolters LM,** Niesters HG, Hansen BE, van der Ende ME, Kroon FP, Richter C, Brinkman K, Meenhorst PL, de Man RA. Development of hepatitis B virus resistance for lamivudine in chronic hepatitis B patients co-infected with the human immunodeficiency virus in a Dutch cohort. *J Clin Virol* 2002; **24:** 173-181
8 **Nakamuta M,** Kotoh K, Tanabe Y, Kajiwara E, Shimono J, Masumoto A, Maruyama T, Furusyo N, Nomura H, Sakai H, Takahashi K, Azuma K, Shimoda S, Enjoji M, Hayashi J. Body surface area is an independent factor contributing to the effects of lamivudine treatment. *Hepatol Res* 2005; **31:** 13-17
9 **Johnson MA,** Moore KH, Yuen GJ, Bye A, Pakes GE. Clinical pharmacokinetics of lamivudine. *Clin Pharmacokinet* 1999; **36:** 41-66
10 **Liaw YF,** Leung NW, Chang TT, Guan R, Tai DI, Ng KY, Chien RN, Dent J, Roman L, Edmundson S, Lai CL. Effects of extended lamivudine therapy in Asian patients with chronic hepatitis B. Asia Hepatitis Lamivudine Study Group. *Gastroenterology* 2000; **119:** 172-180
11 **Kagawa T,** Watanabe N, Kanouda H, Takayama I, Shiba T, Kanai T, Kawazoe K, Takashimizu S, Kumaki N, Shimamura K, Matsuzaki S, Mine T. Fatal liver failure due to reactivation of lamivudine-resistant HBV mutant. *World J Gastroenterol* 2004; **10:** 1686-1687
12 **Zaaijer HL,** ter Borg F, Cuypers HT, Hermus MC, Lelie PN. Comparison of methods for detection of hepatitis B virus DNA. *J Clin Microbiol* 1994; **32:** 2088-2091
13 **Chun YK,** Kim JY, Woo HJ, Oh SM, Kang I, Ha J, Kim SS. No significant correlation exists between core promoter mutations, viral replication, and liver damage in chronic hepatitis B infection. *Hepatology* 2000; **32:** 1154-1162

Science Editor Wang XL and Guo SY **Language Editor** Elsevier HK

PO Box 2345, Beijing 100023, China
www.wjgnet.com
wjg@wjgnet.com

ELSEVIER

World J Gastroenterol 2005;11(44):6954-6959
World Journal of Gastroenterology ISSN 1007-9327

• *BASIC RESEARCH* •

Excessive portal flow causes graft failure in extremely small-for-size liver transplantation in pigs

Hong-Sheng Wang, Nobuhiro Ohkohchi, Yoshitaka Enomoto, Masahiro Usuda, Shigehito Miyagi, Takeshi Asakura, Hiroo Masuoka, Takashi Aiso, Keisuke Fukushima, Tomohiro Narita, Hideyuki Yamaya, Atsushi Nakamura, Satoshi Sekiguchi, Naoki Kawagishi, Akira Sato, Susumu Satomi

Hong-Sheng Wang, Yoshitaka Enomoto, Masahiro Usuda, Shigehito Miyagi, Takeshi Asakura, Hiroo Masuoka, Takashi Aiso, Keisuke Fukushima, Tomohiro Narita, Hideyuki Yamaya, Atsushi Nakamura, Satoshi Sekiguchi, Naoki Kawagishi, Akira Sato, Susumu Satomi, Division of Advanced Surgical Science and Technology, Graduate School of Medicine, Tohoku University, 1-1 Seiryo-machi, Aoba-ku, Sendai 980-8574, Japan

Nobuhiro Ohkohchi, Department of Surgery, Graduate School of Comprehensive Human Science, University of Tsukuba, 1-1-1 Tennoudai, Tsukuba 305-8577, Japan

Supported by Grants-in-Aid for Scientific Research from the Ministry of Education, Science, and Culture of Japan, the Ministry of Welfare of Japan, and by a grant from Graduate School of Medicine, Tohoku University

Co-correspondent: Hong-Sheng Wang

Correspondence to: Nobuhiro Ohkohchi, Department of Surgery, Graduate School of Comprehensive Human Science, University of Tsukuba, 1-1-1 Tennoudai, Tsukuba 305-8577, Japan. nokuchi3@md.tsukuba.ac.jp

Telephone: +81-29-8353221 Fax: +81-29-8353222

Received: 2005-04-28 Accepted: 2005-06-09

Abstract

AIM: To evaluate the effects of a portocaval shunt on the decrease of excessive portal flow for the prevention of sinusoidal microcirculatory injury in extremely small-for-size liver transplantation in pigs.

METHODS: The right lateral lobe of pigs, i.e. the 25% of the liver, was transplanted orthotopically. The pigs were divided into two groups: graft without portocaval shunt (n = 11) and graft with portocaval shunt (n = 11). Survival rate, portal flow, hepatic arterial flow, and histological findings were investigated.

RESULTS: In the group without portocaval shunt, all pigs except one died of liver dysfunction within 24 h after transplantation. In the group with portocaval shunt, eight pigs survived for more than 4 d. The portal flow volumes before and after transplantation in the group without portocaval shunt were 118.2±26.9 mL/min/100 g liver tissue and 270.5±72.9 mL/min/100 g liver tissue, respectively. On the other hand, in the group with portocaval shunt, those volumes were 124.2±27.8 mL/min/100 g liver tissue and 42.7±32.3 mL/min/100 g liver tissue, respectively (P<0.01). As for histological findings in the group without portocaval shunt, destruction of the sinusoidal lining and bleeding in the peri-portal areas were observed after reperfusion, but these findings were not recognized in the group with portocaval shunt.

CONCLUSION: These results suggest that excessive portal flow is attributed to post transplant liver dysfunction after extreme small-for-size liver transplantation caused by sinusoidal microcirculatory injury.

Key words: Hyperperfusion syndrome; Liver regeneration; Portocaval shunt; Postoperative liver dysfunction; Sinusoidal microcirculatory injury; Small-for-size liver transplantation

Wang HS, Ohkohchi N, Enomoto Y, Usuda M, Miyagi S, Asakura T, Masuoka H, Aiso T, Fukushima K, Narita T, Yamaya H, Nakamura A, Sekiguchi S, Kawagishi N, Sato A, Satomi S. Excessive portal flow causes graft failure in extremely small-for-size liver transplantation in pigs. *World J Gastroenterol* 2005; 11(44): 6954-6959
http://www.wjgnet.com/1007-9327/11/6954.asp

INTRODUCTION

Since the first successful living donor liver transplantation (LDLT) in a child[1] patient and an adult[2] patient, LDLT has become the established method to reduce the number of patients on the waiting list and is considered as an alternative to standard liver transplantation[3-7]. The survival rate of adults is significantly lower than that in children[8] and the key to a successful LDLT, especially in adult recipients, is the adequacy of the size of the graft that can be safely harvested from the donor[9-11]. In some cases, graft weight ratio of the recipient native liver weight (GWRLW) of 30% or less has been transplanted successfully, but in general, graft weight per recipient's body weight (GWBW) less than 0.8% or GWRLW less than 40% has been considered marginal or small-for-size. These small-for-size grafts are associated with an increased incidence of complications and graft failure[9-12]. A small-for-size graft cannot supply the metabolic demand of an adult recipient in the early posttransplant period. Poor early graft function is characterized by protracted

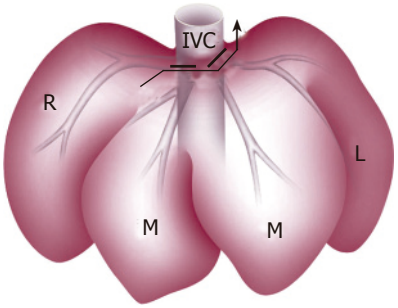

Figure 1 Anterior view of left tri-segmentectomy. Bold line indicates the left and middle hepatic veins ligated by transfixing suture; arrow indicates parenchymal transection of the left lobe and right paramedian lobe; L: left lateral lobe; M: median lobe; R: right lateral lobe; IVC: inferior vena cava.

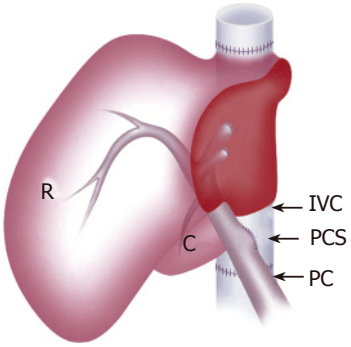

Figure 2 Schematic view of the liver graft with PCS placed by side-to-side anastomosis of PV and IVC. R: right lateral lobe; C: caudate lobe; PV: portal vein; IVC: inferior vena cava; PCS: portocaval shunt.

cholestasis, coagulopathy and ascites, and these findings are proposed to be the essential symptoms of small-for-size syndrome[13]. However, the precise mechanism for this dysfunction remains unclear.

Previously, we have reported that portal hypertension after reperfusion is one of the most important factors aggravating the microcirculatory injury of the graft[14]. In the present study, we hypothesized that the increment of portal flow played a major role in graft injury and poor function of small-for-size grafts, and investigated the effects of portocaval shunt (PCS) on the excessive portal flow for the prevention of the sinusoidal microcirculatory injury after extremely small-for-size liver transplantation using pigs.

MATERIALS AND METHODS

Animals

Landrace white pigs, weighing 18-28 kg, were used as donors and recipients. All experiments were conducted according to Principles of Laboratory Animal Care (NIH publication No. 86-23, revised in 1985). Food was withheld for 24 h before the operation. Anesthesia was induced by intramuscular administration of ketamine (5 mg/kg) and atropine sulfate (1.0 mg/body) followed by endotracheal intubation and maintenance with oxygen and isoflurane by positive pressure mechanical ventilation. A catheter was placed in the internal jugular vein for fluid administration and central venous pressure (CVP) monitoring and fixed at the back of the neck for postoperative venous sampling. A carotid arterial line was also placed for intraoperative blood sampling and monitoring mean arterial pressure (MAP). In recipients, an opposite internal jugular vein was used for the venovenous bypass from the portal vein and femoral vein. Eleven transplantations were carried out in each group.

Donor operation

After laparotomy, the left hepatic artery supplying the left lateral and left median lobes was ligated and divided. Glisson's sheaths of the left lobe and the right median lobe were identified and resected. After mobilization of the liver, by dissecting all ligamentous attachments, the left and middle hepatic veins were ligated with transfixing sutures (Figure 1). Parenchymal transection of the left lobe and the right median lobe was performed and finally left tri-segmentectomy of the liver was done.

Following intravenous administration of heparin, catheters were cannulated in the lower abdominal aorta and splenic vein. The diaphragm was widely opened and the supradiaphragmatic aorta was divided and encircled. Cold University of Wisconsin (UW) solution (4℃) was flushed in from both the aorta and the splenic vein after aortic clamp. The right lateral lobe was removed and preserved in UW solution.

Back table operation

In the group with shunt, the PCS was made on the back table and placed by means of side-to-side anastomosis between the portal vein and the infra-hepatic inferior vena cava (IVC) (Figure 2). The diameter of the PCS was 6 mm. The graft was weighed after the back table preparation.

Recipient operation

Total hepatectomy was performed under ilioportaljugular venovenous bypass[15]. The reduced-size graft with or without PCS was implanted orthotopically with end to end vascular anastomosis of the suprahepatic IVC, the portal vein, the infra-hepatic IVC, and the hepatic artery. Before anastomosis of the portal vein, rinse solution was perfused into the portal vein of the graft. Hepatic arterial reconstruction was performed under a microscope. A catheter was inserted into the common bile duct for bile drainage.

After transplantation, the pigs were placed in a warmed cage with free access to water and food. FK506 (0.1 mg/kg • d) was injected for immunosuppression from postoperative day (POD) 1-7. When recipients died, autopsy was performed to exclude the possibility of technical complications and to confirm the patency of all anastomoses. Liver grafts were also weighed.

Monitoring

Systemic hemodynamic monitoring of MAP and CVP was carried out continuously during the operation, as well as portal vein pressure was monitored. Portal flow

and hepatic arterial flow (HAF) were measured before hepatectomy in donors and after arterial reperfusion in recipients using ultrasound transit time flow probes and a flow meter (Transonic Systems Inc., Ithaca, NY, USA). The diameter of the probe was 8 mm for the portal vein and 3 mm for the artery. Total liver blood flow (TLBF) was calculated as the sum of portal flow and HAF. Liver biopsies were performed before hepatectomy, after reperfusion, and on every other day up to POD 7, and tissue specimens were examined under light microscope and Ki-67 staining was performed for the determination of proliferating hepatocytes. Transmission electron microscopical findings were also investigated in the specimen after reperfusion. Arterial blood samples were obtained hourly for gas analysis during the operation and determining alanine aminotransferase (ALT), aspartate aminotransferase (AST), total bilirubin (T-Bil), and anti-thrombin III (AT-III) before the operation, at 3 and 6 h after reperfusion and on every POD up to POD 7.

The graft weight at the time of transplantation expressed as a percentage of GWRLW and GWBW was calculated.

Statistical analysis

Values of parameters were expressed as mean±SD. Statistical significance was determined by Student's *t*-test. The survival rate was calculated by the Kaplan-Meier method. Values between the two groups were statistically analyzed by generalized Wilcoxon test. *P* values less than 0.05 were regarded as statistically significant.

RESULTS

Graft volume and operation time

Body weight, graft volume, and operation time are shown in Table 1. The graft volume was approximately 25% of the recipient native liver volume, and 0.6% of the recipient body weight in both groups. The cold ischemic time in the group with PCS was slightly longer than that in the group without PCS because of the time required for the PCS at the back table, but there was no statistical difference. There was no significant difference in MAP or CVP between the two groups (data not shown).

Table 1 Graft characteristics (mean±SD)

Parameters	Group without PCS (n = 11)	Group with PCS (n = 11)
DBW (kg)	21.8±2.7	20.8±1.1
RBW (kg)	22.8±1.2	22.1±2.6
GW (g)	131.8±18.3	139.3±32.0
RLW (g)	525.4±41.4	548.3±63.8
GWRLW (%)	25.1±2.7	25.4±3.4
GWBW (%)	0.58±0.09	0.63±0.13
Anhepatic time (min)	43±2	41±4
Operation time (min)	261±28	263±44
Total ischemic time (min)	151±51	161±20

DBW: donor body weight; RBW: recipient body weight; GW: liver graft weight at implantation; RLW: recipient native liver weight; GWRLW: percentage of GW to the recipient native liver weight; GWBW: percentage of GW to the recipient body weight.

Survival rate

In the group without PCS, all pigs except one died of liver dysfunction within 24 h after reperfusion. On the other hand, in the group with PCS, eight pigs survived for more than 4 d and the remaining three died of portal vein thrombosis at the anastomotic site of PCS or perforated gastric ulcer within 3 d. The PCS significantly improved the survival rate of the animals in comparison to the animals without the shunt after transplantation (P<0.05) (Figure 3).

Portal pressure

There were no significant differences in portal vein pressures at laparotomy in both groups. However, after reperfusion, portal vein pressures significantly increased up to 2.2±0.7 KPa in the group without PCS and 1.6±0.6 KPa in the group with PCS (Figure 4).

Hepatic hemodynamics

Hepatic hemodynamic parameters including portal flow, HAF and TLBF at laparotomy and after reperfusion in both groups are shown in Table 2. The portal flow after reperfusion in the group without PCS increased significantly more than that at laparotomy, whereas it decreased in the group with PCS (P<0.01). The HAF after reperfusion decreased compared to that at laparotomy in the group without PCS, while it increased more than that at laparotomy in the group with PCS (P<0.05).

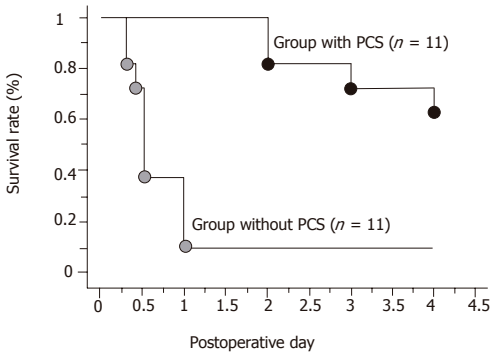

Figure 3 Survival rates. [b]P<0.01 *vs* the group without PCS.

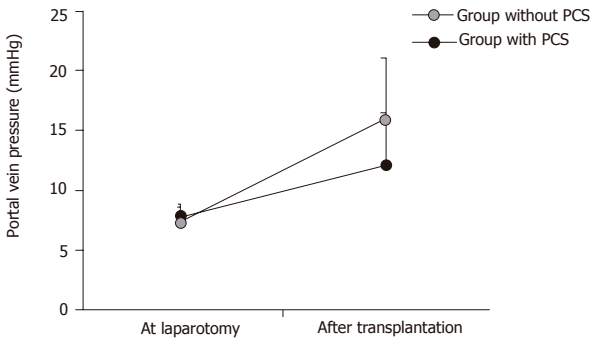

Figure 4 Changes of portal vein pressure (n = 11). [a]P<0.05 *vs* the group with PCS.

Table 2 Changes of hepatic hemodynamics (mean±SD)

Parameters	Group	At laparotomy	After transplantation
Portal flow	Group without PCS	118.2±26.9	270.5±72.9[b,a]
(mL/min/100 g liver tissue)	Group with PCS	124.2±27.8	42.7±32.3[a]
Hepatic arterial flow	Group without PCS	50.1±8.3	37.7±21.0[a]
(mL/min/100 g liver tissue)	Group with PCS	50.5±11.6	75.1±39.5
Total liver blood flow	Group without PCS	168.3±30.9	308.2±52.8[b,a]
(mL/min/100 g liver tissue)	Group with PCS	174.8±29.1	117.8±42.1[c]
Ratio of PF/TLBF (%)	Group without PCS	70.2±4.2	87.8±8.2[b,a]
	Group with PCS	71.1±4.9	36.3±19.5[a]

PF: portal flow; TLBF: total liver blood flow.

[b]P<0.01 *vs* the group with PCS; [a]P<0.01 *vs* at laparotomy; [a]P<0.05 *vs* the group with PCS; [c]P<0.05 *vs* at laparotomy.

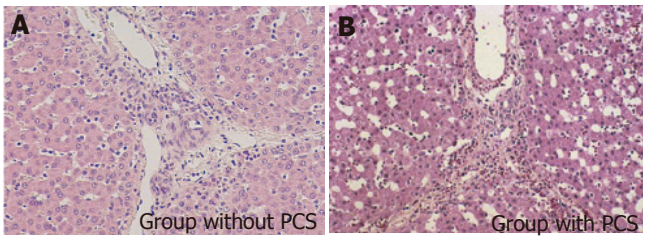

Figure 5 Histological findings of hepatic tissues after reperfusion (×100).

The TLBF after reperfusion increased significantly higher than that at laparotomy in the group without PCS, whereas the TLBF slightly decreased after reperfusion in the group with PCS. After reperfusion, the TLBF in the group without PCS was significantly greater than that in the group with PCS (P<0.01). In the group without PCS, the contribution of portal flow to TLBF increased from 70.2% to 87.8%, while in the group with PCS the contribution of the portal flow to TLBF decreased from 71.1% to 36.3%.

Histological findings

The light microscopical findings of the liver graft after reperfusion are shown in Figure 5. In the group without PCS, enlargement of the sinusoidal lumen and bleeding in the peri-portal triads were observed but these abnormal findings were not recognized in the group with PCS.

Transmission electron microscopic findings of the sinusoid after reperfusion are shown in Figure 6. In the group without PCS, the sinusoidal endothelial cells were destroyed and detached into the sinusoidal space with destruction of the Disse's spaces, while in the group with PCS the sinusoidal endothelial cells were well preserved, the Disse's spaces were intact, and the structure of endothelial lining was well preserved.

Liver regeneration in the group with PCS

The graft weight in the recipients who survived for more than 4 d (n = 8) increased to 87.3% of the recipient native liver. Ki-67 labeling index before and after transplantation is shown in Figure 7. The Ki-67 labeling index showed only 1.0% of hepatocytes at laparotomy. However, it increased abruptly after transplantation, reaching a peak value of approximately 60% at POD 2, and decreasing to 30% on POD 4.

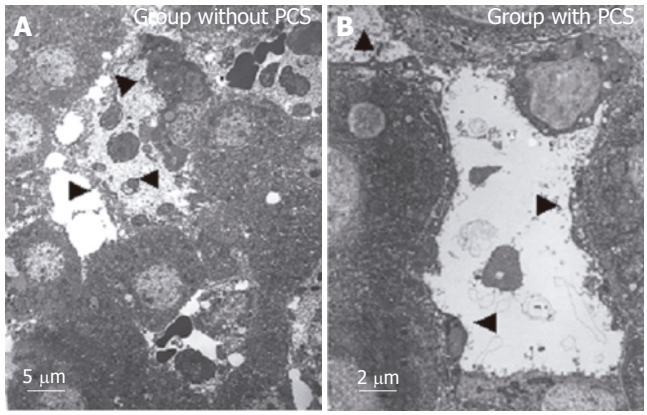

Figure 6 Transmission electron microscopical findings of the sinusoid after reperfusion. Arrowheads indicate the destroyed or preserved or detached sinusoidal endothelial cells into the sinusoidal space with destructed or intact Disse's spaces.

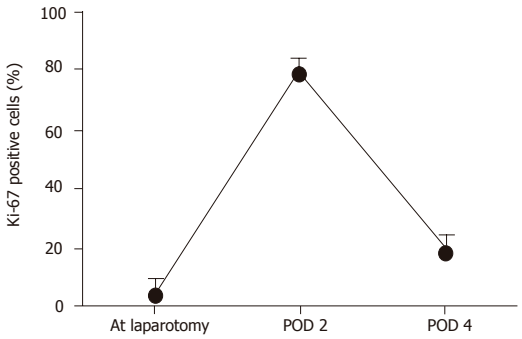

Figure 7 Ki-67 detection in the pigs that survived for more than 4 d in the group with PCS (n = 8).

Liver function

There were no significant differences in ALT, AST or T-Bil until POD 1 after reperfusion in either group (Table3). ALT and AST increased after reperfusion, taking a peak value on POD 2 and POD 1 and then decreased. However, T-Bil increased continuously until POD 4. AT-

Table 3 Changes of serum ALT, AST, T-Bil, and AT-III (mean±SD)

Parameters	Group	Preo	RP 3 h	RP 6 h	POD 1	POD 2	POD 3	POD 4
ALT (KU)	A	22±1	16±2	20±3	35±18	-	-	-
	B	25±7	18±5	25±9	33±13	38±15	30±11	27±10
AST (KU)	A	30±13	80±36	144±51	351±42	-	-	-
	B	32±19	78±38	172±37	306±36	293±46	217±21	152±48
T-Bil (mg/dL)	A	0.24±0.26	0.32±0.18	0.48±0.21	0.88±0.54	-	-	-
	B	0.10±0.07	0.27±0.16	0.48±0.31	0.83±0.24	1.39±0.37	1.75±0.71	1.79±0.86
AT-III (%)	A	122±26	69±19	57±23[a]	66±15a	-	-	-
	B	125±21	86±37	91±25	86±34	75±14	82±12	107±23

Preo: preoperation; RP 3 h: 3 h after reperfusion; RP 6 h: 6 h after reperfusion; POD: postoperative day; A: group without PCS; B: group with PCS; ALT: alanine aminotransferase; KU: karmen unit; AST: aspartate aminotransferase; T-Bil: total bilirubin; AT-III: anti-thrombin III. [a]$P<0.05$ *vs* the group with PCS.

III decreased after reperfusion in both groups. At 6 h after reperfusion and on POD 1, AT-III in the group with PCS was significantly higher than that in the group without PCS ($P<0.05$).

DISCUSSION

In clinical liver surgery, an extended hepatectomy of 80% or 85% of the whole liver can be tolerable in patients with a normal liver[16]. In previous reports, 70-75% hepatectomy in animals represents a model of critical residual liver volume and is used to study the mechanism of liver regeneration[17-19]. This means that 25-30% of the liver can sustain hepatic function. However, this cannot be translated directly into a minimum graft volume in small-for-size liver transplantation, in which grafts are subjected to cold and warm ischemia and subsequent reperfusion injury. This is why the minimum graft volume for successful liver transplantation is presumably higher than the residual liver volume in extended hepatectomy. Currently, experience with living-related and split-liver transplantation has demonstrated that the size of the graft required for a successful liver transplantation is at least 40% of the recipient's native liver volume and more than 0.8% of the recipient body weight[6,20]. This is associated with lack of portosystemic collateral circulation, which lessens the influence of a high portal flow on the grafts and prevents the development of severe portal hypertension[21]. The precise mechanism of graft injury in a small-for-size liver transplantation remains still unknown. But there is a case report of hemorrhagic necrosis secondary to excessive portal flow in an adult LDLT[22]. An adult LDLT with small-for-size graft has been successfully performed using a mesocaval shunt to avoid graft failure caused by portal hyperperfusion[23]. From these reports, we hypothesized that excessive portal flow could attribute to postoperative liver dysfunction caused by sinusoidal microcirculatory injury after small-for-size liver transplantation. In our experiment, we investigated the effect of PCS on excessive portal flow for the prevention of sinusoidal microcirculatory injury in extremely small-for-size liver transplantation in pigs, focusing on the prevention of primary graft dysfunction. We chose the pig model because the anatomy, metabolism, and physiology of the liver are similar to those in human beings. As a result, we clarified that PCS could prevent portal hypertension and excessive portal inflow in small-for-size liver transplantation.

The sinusoids are the principal vessels involved in the transvascular exchange between blood and the parenchymal cells and play an important role in hepatic microcirculation. In an experimental transplantation model using a small-for-size graft weighing less than 30% of the native liver, Asakura *et al*.[14] and Man *et al*.[24] demonstrated that portal hypertension is a determinant factor for the injury of sinusoidal endothelial cells and hepatic parenchyma. The portal flow through the reduced microvascular bed of the small-for-size graft after reperfusion is likely to induce injury of sinusoidal endothelial cells and activation of Kupffer's cells, which is similar to those after extended hepatectomy in rats reported by Panis *et al*.[19].

In this study, TLBF after reperfusion increased approximately twice in comparison to the flow at laparotomy in the group without PCS. The portal flow increased predominantly and HAF reduced. Histological findings clearly indicated disruption of the sinusoidal lining and disturbance of the sinusoidal microcirculation. Furthermore, the graft became swollen after reperfusion, progressing into severe bowel congestion and then blood oozing. These phenomena were associated with a poor survival rate in the group without PCS. On the other hand, in the group with PCS, graft inflow was modified by PCS which permitted a significantly lower portal flow and a higher HAF. The pathological findings of microcirculatory disturbance after reperfusion recognized in the group without PCS were not observed in the group with PCS. The results of our study strongly suggest that an excessive portal flow after reperfusion in small-for-size liver transplantation is one of the major factors that cause sinusoidal microcirculatory injury and result in graft failure.

With regard to the graft regeneration in the group with PCS, though the TLBF was low, the weight of the graft and Ki-67 index increased remarkably in the pigs that survived for more than 4 d. The decreased HAF subsequent to the excessive portal flow observed after reperfusion in the group without PCS was also believed to contribute to the poor regeneration of residual liver and the poor outcome. Sato *et al*.[25] reported that portal hypertension is a trigger of liver regeneration following partial hepatectomy. But surplus portal hypertension

induces liver dysfunction[25]. Results of our study support the hypothesis that portal flow controls liver regeneration in small-for-size liver transplantation and maintains liver function.

In conclusion, an extreme small-for-size graft weighing less than 25% of the native liver can be successfully transplanted with a PCS in pigs. Portal hyperperfusion in small-for-size liver transplantation appears to play a major role in aggravating microcirculatory injury of the graft and attenuation of portal hyperperfusion by PCS minimizes the injury and improves the survival. This study provides helpful information for transplant surgeons regarding the novel therapeutic strategies for the rescue of small-for-size liver grafts.

REFERENCES

1 **Strong RW,** Lynch SV, Ong TH, Matsunami H, Koido Y, Balderson GA. Successful liver transplantation from a living donor to her son. *N Engl J Med* 1990; **322:** 1505-1507

2 **Hashikura Y**, Makuuchi M, Kawasaki S, Matsunami H, Ikegami T, Nakazawa Y, Kiyosawa K, Ichida T. Successful living-related partial liver transplantation to an adult patient. *Lancet* 1994; **343:** 1233-1234

3 **Testa G,** Malago M, Broelsch CE. Living-donor liver transplantation in adults. Langenbecks *Arch Surg* 1999; **384:** 536-543

4 **Ito T,** Kiuchi T, Yamamoto H, Oike F, Ogura Y, Fujimoto Y, Hirohashi K, Tanaka AK. Changes in portal venous pressure in the early phase after living donor liver transplantation: pathogenesis and clinical implications. *Transplantation* 2003; **75:** 1313-1317

5 **Garcia-Valdecasas JC,** Fuster J, Charco R, Bombuy E, Fondevila C, Navasa M, Rodriguez-Laiz G, Ferrer J, Amador MA, Llovet JM, Forns X, Rimola A. Adult living donor liver transplantation. Analysis of the first 30 cases. *Gastroenterol Hepatol* 2003; **26:** 525-530

6 **Kawasaki S,** Makuuchi M, Matsunami H, Hashikura Y, Ikegami T, Nakazawa Y, Chisuwa H, Terada M, Miyagawa S. Living related liver transplantation in adults. *Ann Surg* 1998; **227:** 269-274

7 **Fan ST,** Lo CM, Liu CL. Technical refinement in adult-to-adult living donor liver transplantation using right lobe graft. *Ann Surg* 2000; **231:** 126-131

8 **Sugawara Y,** Makuuchi M. Small-for-size graft problems in adult-to-adult living-donor liver transplantation. *Transplantation* 2003; **75:** S20-22

9 **Emond JC, Renz JF,** Ferrell LD, Rosenthal P, Lim RC, Roberts JP, Lake JR, Ascher NL. Functional analysis of grafts from living donors. Implications for the treatment of older recipients. *Ann Surg* 1996; **224:** 544-52; discussion 552-554

10 **Nishizaki T,** Ikegami T, Hiroshige S, Hashimoto K, Uchiyama H, Yoshizumi T, Kishikawa K, Shimada M, Sugimachi K. Small graft for living donor liver transplantation. *Ann Surg* 2001; **233:** 575-580

11 **Kiuchi T,** Kasahara M, Uryuhara K, Inomata Y, Uemoto S, Asonuma K, Egawa H, Fujita S, Hayashi M, Tanaka K. Impact of graft size mismatching on graft prognosis in liver transplantation from living donors. *Transplantation* 1999; **67:** 321-327

12 **Lo CM,** Fan ST, Chan JK, Wei W, Lo RJ, Lai CL. Minimum graft volume for successful adult-to-adult living donor liver transplantation for fulminant hepatic failure. *Transplantation* 1996; **62:** 696-698

13 **Kelly DM,** Demetris AJ, Fung JJ, Marcos A, Zhu Y, Subbotin V, Yin L, Totsuka E, Ishii T, Lee MC, Gutierrez J, Costa G, Venkataraman R, Madariaga JR. Porcine partial liver transplantation: a novel model of the "small-for-size" liver graft. *Liver Transpl* 2004; **10:** 253-263

14 **Asakura T,** Ohkohchi N, Orii T, Koyamada N, Tsukamoto S, Sato M, Enomoto Y, Usuda M, Satomi S. Portal vein pressure is the key for successful liver transplantation of an extremely small graft in the pig model. *Transpl Int* 2003; **16:** 376-382

15 **Yanaga K,** Kishikawa K, Suehiro T, Nishizaki T, Shimada M, Itasaka H, Nomoto K, Kakizoe S, Sugimachi K. Partial hepatic grafting: porcine study on critical volume reduction. *Surgery* 1995; **118:** 486-492

16 **Starzl TE,** Putnam CW, Groth CG, Corman JL, Taubman J. Alopecia, ascites, and incomplete regeneration after 85 to 90 per cent liver resection. *Am J Surg* 1975; 129: 587-590

17 **Kahn D,** Hickman R, Terblanche J, von Sommoggy S. Partial hepatectomy and liver regeneration in pigs--the response to different resection sizes. *J Surg Res* 1988; **45:** 176-180

18 **Nagao M,** Isaji S, Iwata M, Kawarada Y. The remnant liver dysfunction after 84% hepatectomy in dogs. *Hepatogastroenterology* 2000; **47:** 1564-1569

19 **Panis Y,** McMullan DM, Emond JC. Progressive necrosis after hepatectomy and the pathophysiology of liver failure after massive resection. *Surgery* 1997; **121:** 142-149

20 **Garcia-Valdecasas JC,** Fuster J, Charco R, Bombuy E, Fondevila C, Ferrer J, Ayuso C, Taura P. Changes in portal vein flow after adult living-donor liver transplantation: does it influence postoperative liver function? *Liver Transpl* 2003; **9:** 564-569

21 **Smyrniotis V,** Kostopanagiotou G, Kondi A, Gamaletsos E, Theodoraki K, Kehagias D, Mystakidou K, Contis J. Hemodynamic interaction between portal vein and hepatic artery flow in small-for-size split liver transplantation. *Transpl Int* 2002; **15:** 355-360

22 **Ayata G,** Pomfret E, Pomposelli JJ, Gordon FD, Lewis WD, Jenkins RL, Khettry U. Adult-to-adult live donor liver transplantation: a short-term clinicopathologic study. *Hum Pathol* 2001; **32:** 814-822

23 **Boillot O,** Delafosse B, Mechet I, Boucaud C, Pouyet M. Small-for-size partial liver graft in an adult recipient; a new transplant technique. *Lancet* 2002; **359:** 406-407

24 **Man K,** Lo CM, Ng IO, Wong YC, Qin LF, Fan ST, Wong J. Liver transplantation in rats using small-for-size grafts: a study of hemodynamic and morphological changes. *Arch Surg* 2001; **136:** 280-285

25 **Sato Y,** Koyama S, Tsukada K, Hatakeyama K. Acute portal hypertension reflecting shear stress as a trigger of liver regeneration following partial hepatectomy. *Surg Today* 1997; **27:** 518-526

Science Editor Wang XL and Guo SY **Language Editor** Elsevier HK

PO Box 2345, Beijing 100023, China
www.wjgnet.com
wjg@wjgnet.com

ELSEVIER

World J Gastroenterol 2005;11(44):6960-6967
World Journal of Gastroenterology ISSN 1007-9327

• *BASIC RESEARCH* •

Nuclear factor-κB decoy oligodeoxynucleotides attenuates ischemia/reperfusion injury in rat liver graft

Ming-Qing Xu, Xiu-Rong Shuai, Mao-Lin Yan, Ming-Man Zhang, Lu-Nan Yan

Ming-Qing Xu, Mao-Lin Yan, Ming-Man Zhang, Lu-Nan Yan, Department of General Surgery, West China Hospital, Sichuan University, Chengdu 610041, Sichuan Province, China
Xiu-Rong Shuai, Department of General Surgery, Sichuan Provincial Hospital, Chinese People's Armed Police Forces, Leshan 640014, Sichuan Province, China
Supported by grants from China Postdoctoral Science Foundation, No. 2003033531
Correspondence to: Professor Lu-Nan Yan, Department of General Surgery, West China Hospital, Sichuan University, Chengdu 610041, Sichuan Province, China. xumingqing0018@163.com
Telephone: +86-28-85422476
Received: 2003-06-05 Accepted: 2003-08-16

Abstract

AIM: To evaluate the protective effect of NF-κB decoy oligodeoxynucleotides (ODNs) on ischemia/reperfusion (I/R) injury in rat liver graft.

METHODS: Orthotopic syngeneic rat liver transplantation was performed with 3 h of cold preservation of liver graft in University of Wisconsin solution containing phosphorothioated double-stranded NF-κB decoy ODNs or scrambled ODNs. NF-κB decoy ODNs or scrambled ODNs were injected intravenously into donor and recipient rats 6 and 1 h before operation, respectively. Recipients were killed 0 to 16 h after liver graft reperfusion. NF-κB activity in the liver graft was analyzed by electrophoretic mobility shift assay (EMSA). Hepatic mRNA expression of TNF-α, IFN-γ and intercellular adhesion molecule-1 (ICAM-1) were determined by semiquantitative RT-PCR. Serum levels of TNF-α and IFN-γ were measured by enzyme-linked immunosorbent assays (ELISA). Serum level of alanine transaminase (ALT) was measured using a diagnostic kit. Liver graft myeloperoxidase (MPO) content was assessed.

RESULTS: NF-κB activation in liver graft was induced in a time-dependent manner, and NF-κB remained activated for 16 h after graft reperfusion. NF-κB activation in liver graft was significant at 2 to 8 h and slightly decreased at 16 h after graft reperfusion. Administration of NF-κB decoy ODNs significantly suppressed NF-κB activation as well as mRNA expression of TNF-α, IFN-γ and ICAM-1 in the liver graft. The hepatic NF-κB DNA binding activity [presented as integral optical density (IOD) value] in the NF-κB decoy ODNs treatment group rat was significantly lower than that of the I/R group rat (2.16±0.78 *vs* 36.78 ±6.35 and 3.06±0.84 *vs* 47.62± 8.71 for IOD value after 4 and 8 h of reperfusion, respectively, $P<0.001$). The hepatic mRNA expression level of TNF-α, IFN-γ and ICAM-1 [presented as percent of β-actin mRNA (%)] in the NF-κB decoy ODNs treatment group rat was significantly lower than that of the I/R group rat (8.31 ±3.48 *vs* 46.37±10.65 and 7.46± 3.72 *vs* 74.82±12.25 for hepatic TNF-α mRNA, 5.58±2.16 *vs* 50.46±9.35 and 6.47±2.53 *vs* 69.72±13.41 for hepatic IFN-γ mRNA, 6.79 ±2.83 *vs* 46.23±8.74 and 5.28±2.46 *vs* 67.44±10.12 for hepatic ICAM-1 mRNA expression after 4 and 8 h of reperfusion, respectively, $P<0.001$). Administration of NF-κB decoy ODNs almost completely abolished the increase of serum level of TNF-α and IFN-γ induced by hepatic ischemia/reperfusion, the serum level (pg/mL) of TNF-α and IFN-γ in the NF-κB decoy ODNs treatment group rat was significantly lower than that of the I/R group rat (42.7±13.6 *vs* 176.7±15.8 and 48.4±15.1 *vs* 216.8±17.6 for TNF-α level, 31.5±12.1 *vs* 102.1±14.5 and 40.2±13.5 *vs* 118.6±16.7 for IFN-γ level after 4 and 8 h of reperfusion, respectively, $P<0.001$). Liver graft neutrophil recruitment indicated by MPO content and hepatocellular injury indicated by serum ALT level were significantly reduced by NF-κB decoy ODNs, the hepatic MPO content (A655) and serum ALT level (IU/L) in the NF-κB decoy ODNs treatment group rat was significantly lower than that of the I/R group rat (0.17±0.07 *vs* 1.12 ±0.25 and 0.46±0.17 *vs* 1.46±0.32 for hepatic MPO content, 71.7±33.2 *vs* 286.1±49.6 and 84.3±39.7 *vs* 467.8±62.3 for ALT level after 4 and 8 h of reperfusion, respectively, $P<0.001$).

CONCLUSION: The data suggest that NF-κB decoy ODNs protects against I/R injury in liver graft by suppressing NF-κB activation and subsequent expression of proinflammatory mediators.

Key words: Hepatic ischemia/reperfusion injury; NF-κB; Liver graft

Xu MQ, Shuai XR, Yan ML, Zhang MM, Yan LN. Nuclear factor-κB decoy oligodeoxynucleotides attenuates ischemia/reperfusion injury in rat liver graft. *World J Gastroenterol* 2005; 11(44): 6960-6967
http://www.wjgnet.com/1007-9327/11/6960.asp

INTRODUCTION

Liver transplantation is the only therapeutic strategy for many inherited and acquired disorders of the liver. The vulnerability of the transplantation liver to warm ischemia, cold preservation, and reperfusion injury is possibly associated with immediate posttransplant graft function loss, and graft damage caused by ischemia/reperfusion (I/R) is a serious problem after transplantation. Hepatic I/R injury still leads to primary graft nonfunction in about 4% of liver transplantation. Moreover, late consequences of ischemia injury include intrahepatic and extrahepatic biliary strictures, which further increase morbidity and jeopardize graft survival. Therefore, inhibition of I/R injury has become a more serious clinical interest.

Two distinct phases in the development of organ injury have been identified in experimental hepatic I/R injury animal models. During the initial phase of injury, Kupffer cells are activated and release reactive oxygen species and proinflammatory cytokines, including tumor necrosis factor (TNF)-α[1-4]. The enhanced production of TNF-α plays a more important role in the initiation of a cascade of events that causes significant liver injury mediated by neutrophils. One of the main functions of TNF-α is the up-regulation of adhesion molecules and neutrophil-attracting C-X-C chemokines[5,6]. The coordinated efforts of adhesion molecules and C-X-C chemokines mediate the recruitment of neutrophils into the liver. Sequestered neutrophils release protease and reactive oxygen intermediates (ROI), which directly damage hepatocytes and endothelial cells and also to capillary plugging causing hepatic hypoperfusion. The transcription factor nuclear factor (NF)-κB plays a key role in the regulation of genes that function in immune and inflammatory systems such as TNF-α, IFN-γ, chemokines and ICAM-1[7-15]. Previous studies suggested that NF-κB activation plays a deteriorative role during hepatic I/R injury[15-18]. In contrast to these studies, Bradham *et al.*[19] reported that NF-κB activation during orthotopic liver transplantation is protective.

In the present study, we have attempted to evaluate the exact effect of NF-κB activation on the I/R injury in liver graft after orthotopic liver transplantation in rats. For this aim, we used the recently developed technology of decoy ODNs. The original concept of using synthetic double-stranded ODN as "decoy" cis elements to block the binding of nuclear factors to promoter regions of target genes was introduced in 1990 by Sullenger *et al.* and Bielinska *et al.* In 1997, Morishita *et al.* reported the first *in vivo* application of this technology, they prevented myocardial infarction after reperfusion in rats by direct infusion of synthetic double-stranded 20-bp ODNs containing the NF-κB cis element into cannulated coronary arteries[20]. Subsequently, Kawamura *et al.* showed that the direct injection of NF-κB decoy ODNs into implanted tumors in mice inhibited cachexia, without affecting the tumor growth[21]. In 2000, Abeyama *et al.* reported that intraperitoneal and local administration of NF-κB decoy ODNs reduces the extent of UV-induced skin inflammation, and this is associated with NF-κB activation inhibition and decreased the transcription of inflammatory cytokines TNF-α and IL-1 and IL-6[22]. Here we report that the application of NF-κB decoy ODNs significantly attenuates the liver graft I/R injury in rats.

MATERIALS AND METHODS

NF-κB decoy ODNs and scrambled ODNs

Double-stranded NF-κB decoy ODNs were generated using equimolar amounts of single-stranded sense and antisense phosphorothioate-modified oligonucleotides containing two NF-κB binding sites(sense sequence 5' -AGGGACTTTCCGCTGGGGACTTTCC-3'; NF-κB binding sites bold and underlined)[23]. Scrambled ODNs (treatment control ODNs: 5'-TTGCCGTACCTGACTTAGCC-3')[22] were generated in the same way. Sense and antisense strands were mixed in the presence of 150 mmol PBS, heated to 100 ℃, and allowed to cool to room temperature to obtain double-stranded DNA .

Experimental design and liver transplantation

Male SD rats (220-250 g) were used for the liver graft I/R injury experiments. The animals were maintained with a 12-h light/dark cycle in a conventional animal facility with water and commercial chow provided *ad libitum*, with no fasting before the transplantation. The following experimental groups were compared: (1) the I/R group, in which orthotopic liver transplantation were performed with two-cuff method and liver graft reperfusion was initiated after 3 h of cold-preservation in chilled (4 ℃) University of Wisconsin (UW) solution containing NF-κB decoy ODNs or scrambled ODNs (5 μmol/L/mL); (2) the NF-κB decoy ODNs + I/R group, in which donor and recipient animals were injected intravenously through the penile vein with NF-κB decoy ODNs (1.0 mmol/L solution in PBS, 1 mL/rat) 6 and 1 h before liver harvesting or orthotopic liver transplantation; (3) the scrambled ODNs + I/R group in which donor and recipient animals were injected intravenously through the penile vein with scrambled ODNs (1.0 mmol/L solution in PBS, 1 mL/rat) 6 and 1 h before liver harvesting or orthotopic liver transplantation; (4) the sham control group in which rats only underwent a midline laparotomy. Orthotopic liver transplantation was performed according to the method described in our previous study[24]. All operations were performed under ether anesthesia in sterile conditions. The survival rate was >89% at 24 h after liver transplantation. Liver graft tissues and recipient blood samples (n = 5) were harvested at different time points (0, 0.5, 1, 2, 4, 8, and 16 h) after graft reperfusion and were immediately frozen in liquid nitrogen (only liver samples) and kept at -80 ℃ until use.

Myeloperoxidase assay

Liver myeloperoxidase (MPO) content was assessed by methods described elsewhere[15]. Briefly, liver tissue (50 mg) was homogenized in 2 mL of homogenization buffer (3.4 mmol/L KH_2HPO_4, 16 mmol/L Na_2HPO_4, pH 7.4).

After centrifugation for 20 min at 10 000 g, 10 volumes of resuspension buffer (43.2 mmol/L KH_2HPO_4, 6.5 mmol/L Na_2HPO_4, 10 mmol/L ethylenediaminetetraacetic acid, 0.5% hexadecyltrimethylammonium, pH 6.0) was added to the pellet and the samples were sonicated for 10 s. After heating for 2 h at 60 ℃, the supernatant was reacted with 3, 3', 3, 5'-tetramethylbenzidine (Sigma Chemicall Co.) and read at 655 nm.

Preparation of liver graft nuclear extract

Nuclear proteins from frozen liver graft tissue were extracted according to the method of Nanji[8]. One gram of liver tissue was homogenized in 5 mL buffer [0.32 mol/L sucrose, 50 mmol/L Tris-HCl (pH 7.5), 25 mmol/L KCl, 5 mmol/L $MgCl_2$, 0.5 mmol/L phenylmethylsulfonyl fluoride,10 μg/mL aprotinin, 10 μg/mL tosyllysylchloromethyl ketone(TLCK)] and centrifuged for 10 min at 600 r/min at 40 ℃. The pellet was resuspended in 2.5 mL of 2 mol/L sucrose-Tris HCl, KCl, and $MgCl_2$ (TKM) buffer and homogenized. The homogenate was centrifuged at 40 000 g at 4 ℃ for 2 h. The supernatant was carefully removed and the pellet containing the nuclear extract was resuspended in 40 μL of buffer A [10 mmol/L HEPES/KOH (pH 7.9), 2 mmol/L $MgCl_2$, 0.1 mmol/L ethylenediaminetetraacetic acid, 10 mmol/L KCl, 1 mmol/L dithiothreitol, 0.5 mmol/L phenylmethylsulfonyl fluoride] and left on ice for 10 min, mixed, and centrifuged at 15 000 g at 4 ℃ for 15 s. The pellet was then resuspended in 1.0 mL of buffer B [10 mmol/L HEPES/KOH (pH 7.9), 50 mmol/L KCl, 300 mmol/L NaCl, 0.1 mmol/L ethylenediaminetetraacetic acid, 10% (v/v) glycerol, 1 mmol/L dithiothreitol, 0.5 mmol/L phenylmethylsulfonyl fluoride, 10 μg/mL leupeptin, 10 μg/mL aprotinin, 10 μg/mL TPCK] and put on ice for 20 min. After centrifugation at 15 000 g at 4 ℃ for 5 min, the supernatant was stored at -80 ℃ as a nuclear extract. Before the experiments, the total protein concentration in the samples were determined according to the method of Bradford.

Electrophoretic mobility shift assay (EMSA) for hepatic NF-κB activity

NF-κB DNA binding activity was performed in a 10 μL binding reaction mixture containing 1×binding buffer [50 mg/L of double-stranded poly (dI-dC), 10 mmol/L Tris-HCl (pH 7.5), 50 mmol/L $NaCl_2$, 0.5 mmol/L EDTA, 0.5 mmol/L-1DTT, 1 mmol/L $MgCl_2$, and 100 mL/L glycerol], 5 μg of nuclear protein, and 35 fmol of double-stranded NF-κB consensus oligonucleotide (5' -AGTGAGGGGACTTTCCCAGGC -3') that was endly labeled with γ-^{32}P (111 TBq/mol/L at 370 GBq^{-1}) using T4 polynucleotide kinase. The binding reaction mixture was incubated at room temperature for 20 min and analyzed by electrophoresis on 7% nondenaturing polyacrylamide gels. After electrophoresis the gels were dried by Gel-Drier (Biol-Rad Laboratories, Hercules, CA, USA) and exposed to Kodak X-ray films at -70 ℃. NF-κB DNA binding activity was presented as integral optical density (OD) value.

Semiquantitative RT-PCR assay for hepatic expression of TNF-α, IFN-γ and ICAM-1 mRNA

Analysis of the expression of TNF-α, IFN-γ and ICAM-1 mRNA was determined by semiquantitative RT-PCR amplification in contrast with house-keeping gene β-actin. Total RNA from 10 mg liver graft tissue was extracted using Tripure™ reagent. First-strand cDNA was transcribed from 1 μg RNA using AMV and an oligo (dT15) primer. PCR was performed in a 25 μL reaction system. Specific primers used in PCR reaction were as follows: TNF-α, 5' primer 5'-AGCCCACGTAGCAAACCACCA-3' and 3' primer 5'-ACACCCATTCCCTTCACAGAGCAAT-3', to give a 446-bp product; $ICAM^{-1}$, 5' primer 5' -TGGAACTGCACGTGCTGTAT-3', 3' primer 5' -ACCATTCTGTTCAAAAGCAG-3', to give a 513-bp product; IFN-γ, 5' primer 5'-ACAATGAACGCTACACACTG-3', 3' primer 5'-TCAAACTTGGCAATACTCAT-3', to give a 362-bp product; β-actin, 5' primer 5' -ATGGATGATGATATCGCCGCG-3', 3' primer 5' -TGAAGGTAGTTTCGTGGATGC-3', to give a 813-bp product. PCR products of each sample were subjected to electrophoresis in a 15 g/L agarose gel containing 0.5 mg/L ethidium bromide. Densitometrical analysis using NIH image software was performed for semiquantification of PCR products, and mRNA expression was evaluated by the band-intensity ratio of TNF-α, IFN-γ and ICAM-1 to β-actin, and presented as percent of β-actin (%).

Blood assay for serum levels of TNF-α, IFN-γ and ALT

Blood was obtained by cardiac puncture at the time of killing. Serum samples were analyzed for TNF-α and IFN-γ by enzyme-linked immunosorbent assays (ELISA) according to the manufacturer's instructions. Serum samples were also analyzed for ALT level as indices of hepatocellular injury. Measurements of serum ALT level were made using a diagnostic kit from Sigma Chemical Co.

Statistical analysis

All data were expressed as mean±SE . Statistical analysis of data was performed using the Student's *t*-test; $P<0.05$ was considered statistically significant.

RESULTS

NF-κB activation in the liver graft

NF-κB activation in the liver graft at seven separate time points after reperfusion was determined by EMSA (as shown in Figure 1). NF-κB activation in the liver graft after reperfusion was induced in a time-dependent manner. Hepatic NF-κB activation was observed to start within 30 min after the initiation of reperfusion and continued for 16 h after liver graft reperfusion. NF-κB activation in the liver graft was significant at 2 to 8 h and slightly decreased at 16 h after graft reperfusion.

NF-κB decoy ODNs suppresses NF-κB activation in the liver graft

In the I/R + NF-κB decoy ODNs group rats, administration of NF-κB decoy ODNs group almost

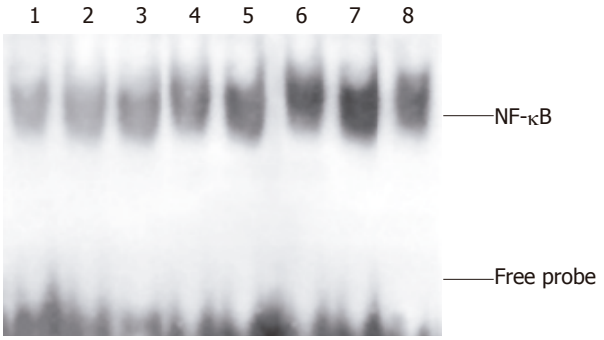

Figure 1 NF-κB activation in the liver graft. Lanes 1: Hepatic nuclear protein extracts from sham control rat; Lanes 2-8: Liver graft nuclear protein extracts on 0, 0.5, 1, 2, 4, 8 and 16 h after reperfusion.

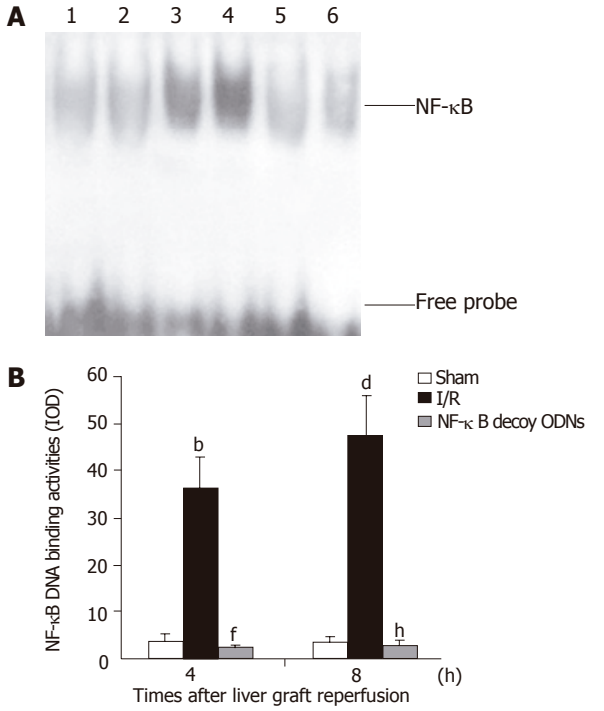

Figure 2 Hepatic NF-κB activation (**A**) and NF-κB DNA binding activities presented as IOD value (**B**). Lanes 1 and 2: Hepatic RNA extracts from sham control group. Lanes 3 and 4: Hepatic RNA extracts from I/R group. Lanes 5 and 6: Hepatic RNA extracts from I/R + NF-κB decoy ODNs group. [b, d]$P<0.001$ vs sham group, [f, h]$P<0.001$ *vs* I/R group.

completely abrogated NF-κB activation in the liver graft after 4 h and 8 h of reperfusion (as shown in Figure 2). Similar effects were observed at 0.5, 1, 2 or 16 h after hepatic reperfusion (data not shown). However, in the I/R + scrambled ODNs group rats, NF-κB activation in the liver graft were not significantly changed compared with the I/R group rats (data not shown).

NF-κB decoy ODNs suppresses hepatic mRNA expression of TNF-α, IFN-γ and ICAM-1

To investigate whether NF-κB decoy ODNs induced suppression of NF-κB was associated with reduced inflammatory mediator expression, mRNA expression of TNF-α, IFN-γ and ICAM-1 in the liver graft were assessed by RT-PCR. Hepatic ischemia/reperfusion increased hepatic mRNA expression of TNF-α, IFN-γ and ICAM-1. Administration of NF-κB decoy ODNs almost completely abrogated hepatic ischemia/reperfusion-induced increases of TNF-α, IFN-γ and ICAM-1 mRNA expression in the liver graft with reperfusion for 4 and 8 h (as shown in Figure 3). Similar effects were observed at 0.5, 1, 2 or 16 h after reperfusion (data not shown). However, administration of scrambled ODNs did not have any significant effect on the hepatic mRNA expression of these inflammatory mediators (data not shown). Thus, NF-κB decoy ODNs-mediated suppression of NF-κB activation in the liver graft is associated with the inhibited hepatic mRNA expression of these proinflammatory mediators.

NF-κB decoy ODNs reduces serum level of TNF- α and IFN-γ

To confirm the inhibitory effects of NF-κB decoy ODNs on the inflammatory mediator production, serum levels of TNF-α and IFN-γ were analyzed by ELISA. Serum levels of TNF-α and IFN-γ were significantly increased within 1 h and were maximal at 8 h after liver graft reperfusion. Administration of NF-κB decoy ODNs markedly reduced serum levels of TNF-α and IFN-γ ($P<0.001$) at every time point, respectively (Figure 4). However, administration of scrambled ODNs did not have any significant effect on the serum levels of TNF-α and IFN-γ (data not shown).

NF-κB decoy ODNs suppresses liver graft neutrophil recruitment and liver graft injury

Liver graft neutrophil recruitment was determined by liver MPO content and hepatocellular injury was assessed by serum level of ALT. Liver graft ischemia/reperfusion caused significant increases of liver MPO content and serum level of ALT compared with sham controls. In the presence of NF-κB decoy ODNs, the liver graft MPO content and the serum level of ALT were significantly reduced ($P<0.001$) (as shown in Figure 5), whereas administration of scrambled ODNs did not have any significant effect on the liver graft MPO content and serum level of ALT (data not shown).

DISCUSSION

Hepatic ischemia/reperfusion injury remains a significant problem and limitation of liver transplantation and may result in liver failure, remote organ failure, and death. Previous studies have identified many proinflammatory mediators (TNF-α, MIP-2, IFN-γ, KC, ENA-78, and ICAM-1) involved in the pathogenesis of hepatic ischemia/reperfusion injury, and production of TNF-α by activated Kupffer cells is central to this process[3,15, 6,25-27]. TNF-α enhances the inflammatory response in liver by inducing the expression of adhesion molecules on vascular endothelial cells and stimulating the production and release of neutrophil-attracting CXC chemokines[18,28]. TNF-α[29-33] and ICAM-1[15] also play significant roles in

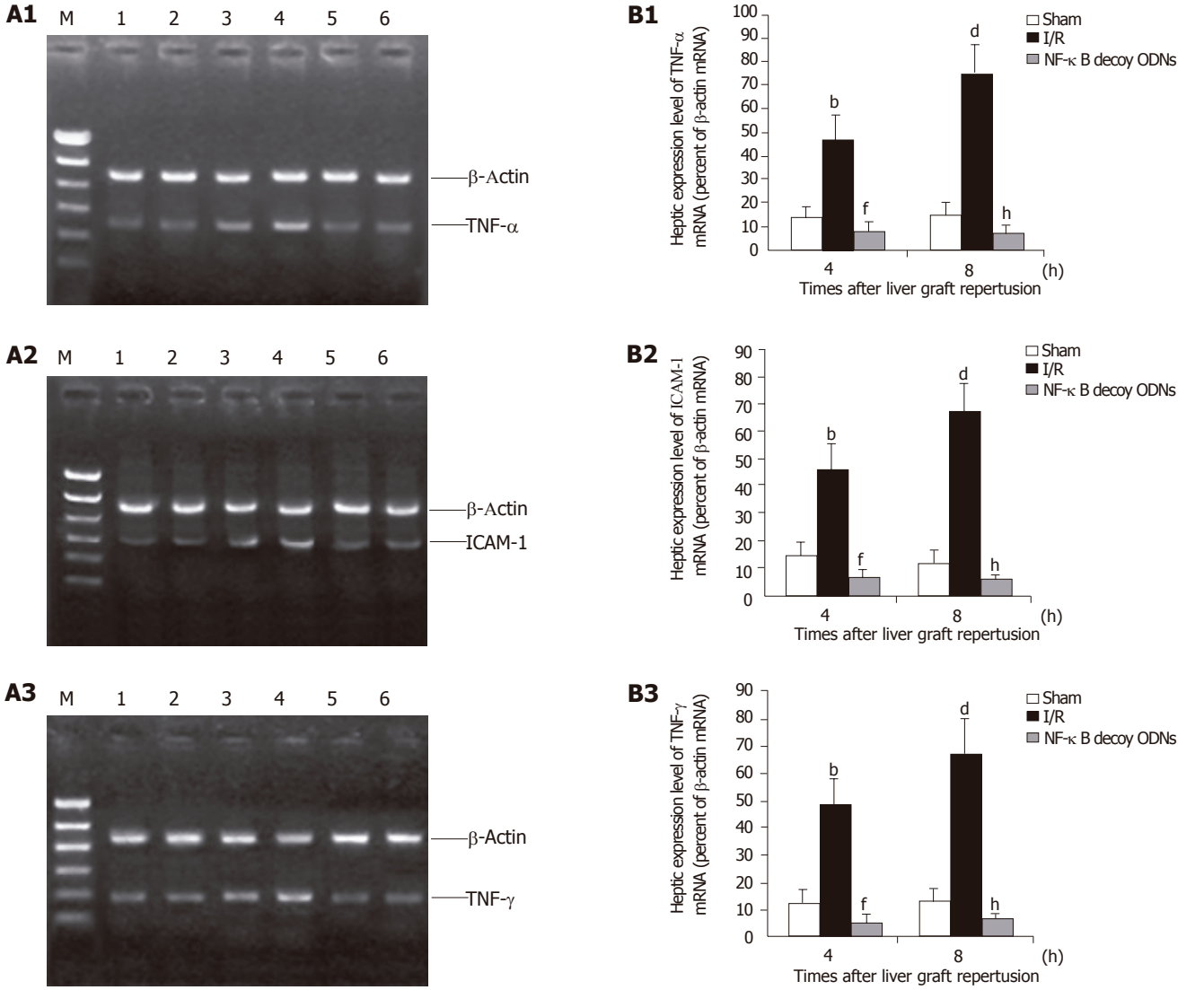

Figure 3 Hepatic expression (**A**) and the expression level (**B**) of cytokine mRNA after 4 and 8 h of reperfusion. Lanes 1 and 2: Hepatic RNA extracts from sham control group. Lanes 3 and 4: Hepatic RNA extracts from I/R group. Lanes 5 and 6: Hepatic RNA extracts from I/R + NF-κB decoy ODNs group. $^{b,d}P<0.001$ *vs* sham group; $^{f,h}P<0.001$ *vs* I/R group.

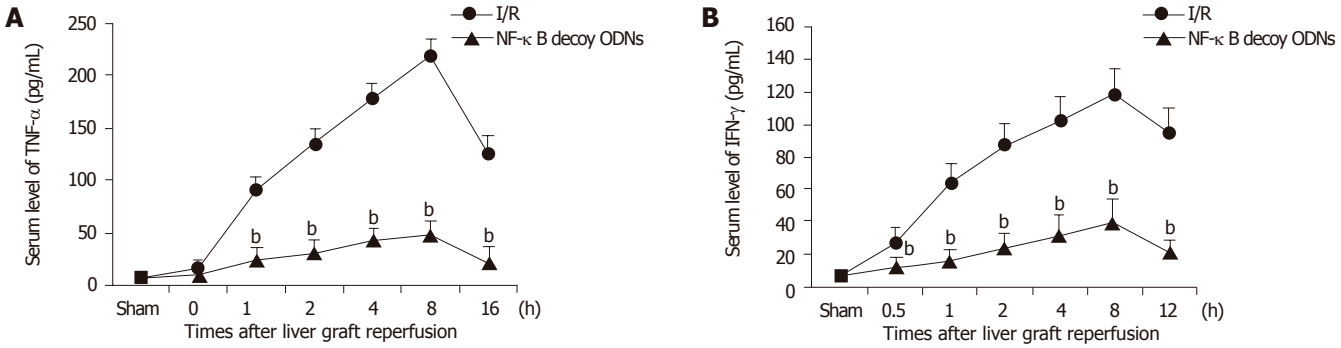

Figure 4 Serum levels of TNF-α (A) and IFN-γ (B) after hepatic ischemia/reperfusion. $^{b}P<0.001$ *vs* I/R group.

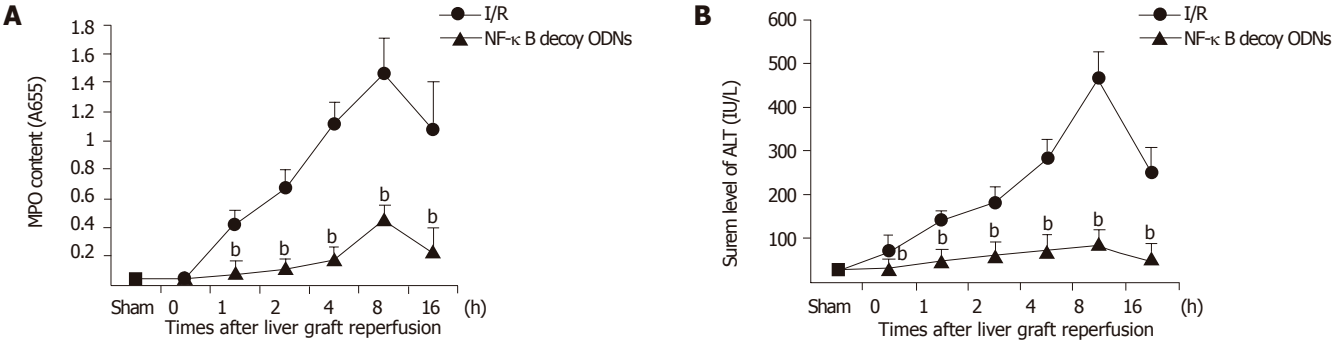

Figure 5 Hepatic MPO content (**A**) and serum level of ALT (**B**). $^{b}P<0.001$ *vs* I/R group.

the inflammatory and immune responses that mediate allograft rejection. Thus, they are important as they are against liver graft I/R injury and rejection to suppress the production of these proinflammatory mediators. Each of these mediators is controlled, at least in part, by the transcription factor, NF-κB. Yoshidome *et al.*[15] reported interleukin (IL)-10 protected against hepatic I/R injury by suppressing NF-κB activation and subsequent expression of proinflammatory mediators. Recent studies have confirmed that hepatic ischemic preconditioning (IPC) has protective effect on hepatic cold storage-reperfusion injury, including improved graft function, reduced graft circulatory impairment, enhanced bile production, augmented responses to a bile acid challenge, elevated O_2 consumption, improved hepatic tissue blood flow and decreased hepatic vascular resistance, reduced endothelial cell damage, suppressed Kupffer cell activation, decreased apoptosis of hepatocytes, and as a result, graft survival improves after liver transplantation[34-43]. The recent study have found out that attenuation of NF-κB activation and subsequent reduction in TNF-α production after sustained ischemia play important roles in the protective mechanism of IPC against hepatic I/R injury[16,44]. These data suggest a central role of NF-κB activation in the initiation of hepatic I/R injury, and NF-κB activation inhibition could protect against hepatic I/R injury. However, there are contrary reports about the role of NF-κB activation during I/R injury and liver transplantation. Maulik *et al.*[45] showed that IPC activated NF-κB, of which p38 mitogen-associated protein kinase (MAPK) might be upstream before sustained ischemia, and also that inhibitor of p38MAPK abolished preconditioning-induced cardioprotection. Teoh *et al.*[46] recently reported that the hepatoprotective effects of ischemic preconditioning are associated with the activation of NF-κB and SAPKs that are associated with entry of hepatocytes into the cell cycle, a critical biological effect that favors survival of the liver against ischemic and I/R injury. Bradham *et al.*[19] reported that the activation of NF-κB during orthotopic liver transplantation in rats is protective, inhibition of donor hepatic NF-κB activation by adenoviral-mediated IκB alpha superrepressor gene transfer resulted in increased serum ALT levels after 3 h of transplantation. In addition, the blockade of NF-κB resulted in increased histological tissue injury and increased hepatic terminal deoxyribonucleotide transferase-mediated deoxyuridine triphosphate nick end labeling (TUNEL) staining, indicating apoptosis.

To assess the role of NF-κB activation during liver transplantation, we examined the effect of NF-κB activation inhibition by NF-κB decoy ODNs containing two NF-κB binding sites on the liver graft I/R injury. We found that cold preservation-reperfusion of liver graft rapidly activated hepatic NF-κB and concomitantly elevated hepatic mRNA expression of TNF-α, INF-γ and ICAM-1 as well as serum levels of TNF-α and IFN-γ. Administration of NF-κB decoy ODNs almost completely abrogated the increased hepatic NF-κB activation, the up-regulated hepatic mRNA expression of the proinflammatory mediators, the elevated serum levels of TNF-α and IFN-γ as well as the increased hepatic neutrophil recruitment, and as a result, attenuated liver graft I/R injury. Liver I/R injury is considered to be primarily dependent on the activation of Kupffer cells, these cells are a major source of ROIs, proinflammatory cytokines or chemokines that promote neutrophils recruitment, adhesion, and activation eventually leading to organ injury. Bradham *et al.*[19] reported that the induction of TNF-α mRNA and serum protein during liver transplantation was unaffected by Kupffer cells depletion with $GdCl_3$. These results show that Kupffer cells are not the only major source of TNF-α production after liver transplantation and that stress-signaling protein activation occurs independently of Kupffer cells. A recent study reported that hepatic I/R injury critically depends on liver activated T cells[47,48]. Indeed, both cyclosporine and FK506, which are potent T cell-deactivating agents, were reported to decrease reperfusion injury after liver transplantation or warm ischemia compared with untreated controls. Besides the role of liver reside T cells, lymphocytes recruited from the circulatory cell pool within hours or days after reperfusion are also involved in the cascade of reperfusion in the kidney and in the liver[49, 50]. Circulating monocytes/macrophages are the primary systemic sources of TNF-α[51] in response to endotoxin stimulation. Previous studies showed that endotoxin in portal vein blood was significantly increased during portal vein occlusion and after liver transplantation, and the increased endotoxin could stimulat macrophages that reside in spleen, lung, and other organs, as well as circulating monocyte/

macrophage to produce TNF-α. Tsoulfas *et al*. have shown the LPS/CD14/LBP/NF-κB signaling pathway activation in hepatic transplantation preservation injury[52]. Thus, far besides Kupffer cells, T lymphocytes and monocytes/macrophages, either residing in the organ, or being recruited from the blood, should definitely be considered effector cells in I/R injury. IFN-γ released by activated T cells is able to prime macrophages/Kupffer cells for the production of proinflammatory cytokines like TNF, and to down-regulate the synthesis of IL-10, a protective cytokine which has been identified to protect against hepatic ischemia/reperfusion injury. Conversely, monomacrophages can also activate T cells and promote the synthesis of INF-γ through the release of cytokines like IL-12 and IL-18 and the engagement of costimulatory molecules[53]. In the present study, the administration of NF-κB decoy ODNs may attenuate not only donor hepatic Kupffer cells NF-κB activation, but also recipient monocytes/macrophages and T-cells NF-κB activation, and consequently decreases the hepatic mRNA expression of TNF-α and IFN-γ as well as the protein production of TNF-α and IFN-γ. Although blockade of NF-κB can result in increased hepatocytes apoptosis induced by TNF-α, the significantly decreased production of TNF-α by NF-κB decoy ODNs may attenuates the initiation of hepatocytes apoptosis. Thus, NF-κB decoy ODNs may protect against I/R injury in the transplanted liver graft by suppressing NF-κB activation and the subsequent production of TNF-α, ICAM-1 and IFN-γ.

REFERENCES

1 **Minor T,** Akbar S, Tolba R, Dombrowski F. Cold preservation of fatty liver grafts: prevention of functional and ultrastructural impairments by venous oxygen persufflation. *J Hepatol* 2000; **32:** 105-111

2 **Thurman RG,** Schemmer P, Zhong Z, Bunzendahl H, von Frankenberg M, Lemasters JJ. Kupffer cell-dependent reperfusion injury in liver transplantation: new clinically relevant use of glycine. *Langenbecks Arch Chir Suppl Kongressbd* 1998; **115**: 185-190

3 **Xu MQ,** Xue L, Gong JP. Significance of Kupffer cell NF-κB activation during hepatic ischemia-reperfusion in rats. *Shijie Huaren Xiaohua Zazhi* 2001; **9:** 1250-1253

4 **Iimuro Y,** Bradford BU, Yamashina S, Rusyn I, Nakagami M, Enomoto N, Kono H, Frey W, Forman D, Brenner D, Thurman RG. The glutathione precursor L-2-oxothiazolidine-4-carboxylic acid protects against liver injury due to chronic enteral ethanol exposure in the rat. *Hepatology* 2000; **31:** 391-398

5 **Colletti LM,** Cortis A, Lukacs N, Kunkel SL, Green M, Strieter RM. Tumor necrosis factor up-regulates intercellular adhesion molecule 1, which is important in the neutrophil-dependent lung and liver injury associated with hepatic ischemia and reperfusion in the rat. *Shock* 1998; **10:** 182-191

6 **Lentsch AB,** Yoshidome H, Cheadle WG, Miller FN, Edwards MJ. Chemokine involvement in hepatic ischemia/reperfusion injury in mice: roles for macrophage inflammatory protein-2 and KC. *Hepatology* 1998; **27:** 1172-1177

7 **Gong JP,** Liu CA, Wu CX, Li SW, Shi YJ, Li XH. Nuclear factor kB activity in patients with acute severe cholangitis. *World J Gastroenterol* 2002; **8:** 346-349

8 **Nanji AA,** Jokelainen K, Rahemtulla A, Miao L, Fogt F, Matsumoto H, Tahan SR, Su GL. Activation of nuclear factor kappa B and cytokine imbalance in experimental alcoholic liver disease in the rat. *Hepatology* 1999; **30:** 934-943

9 **Sakaguchi T,** Nakamura S, Suzuki S, Oda T, Ichiyama A, Baba S, Okamoto T. Participation of platelet-activating factor in the lipopolysaccharide-induced liver injury in partially hepatectomized rats. *Hepatology* 1999; **30:** 959-967

10 **Verhasselt V,** Vanden Berghe W, Vanderheyde N, Willems F, Haegeman G, Goldman M. N-acetyl-L-cysteine inhibits primary human T cell responses at the dendritic cell level: association with NF-kappaB inhibition. *J Immunol* 1999; **162:** 2569-2574

11 **Ouaaz F,** Arron J, Zheng Y, Choi Y, Beg AA. Dendritic cell development and survival require distinct NF-kappaB subunits. *Immunity* 2002; **16:** 257-270

12 **Grumont R,** Hochrein H, O'Keeffe M, Gugasyan R, White C, Caminschi I, Cook W, Gerondakis S. c-Rel regulates interleukin 12 p70 expression in CD8(+) dendritic cells by specifically inducing p35 gene transcription. *J Exp Med* 2001; **194:** 1021-1032

13 **Mann J,** Oakley F, Johnson PW, Mann DA. CD40 induces interleukin-6 gene transcription in dendritic cells: regulation by TRAF2, AP-1, NF-kappa B, AND CBF1. *J Biol Chem* 2002; **277:** 17125-17138

14 **Xu MQ,** Wang W, Xue L, Yan LN. NF-kappaB activation and zinc finger protein A20 expression in mature dendritic cells derived from liver allografts undergoing acute rejection. *World J Gastroenterol* 2003; **9:** 1296-1301

15 **Yoshidome H,** Kato A, Edwards MJ, Lentsch AB. Interleukin-10 suppresses hepatic ischemia/reperfusion injury in mice: implications of a central role for nuclear factor kappaB. *Hepatology* 1999; **30:** 203-208

16 **Funaki H,** Shimizu K, Harada S, Tsuyama H, Fushida S, Tani T, Miwa K. Essential role for nuclear factor kappaB in ischemic preconditioning for ischemia-reperfusion injury of the mouse liver. *Transplantation* 2002; **74:** 551-556

17 **Hiasa G,** Hamada M, Ikeda S, Hiwada K. Ischemic preconditioning and lipopolysaccharide attenuate nuclear factor-kappaB activation and gene expression of inflammatory cytokines in the ischemia-reperfused rat heart. *Jpn Circ J* 2001; **65:** 984-990

18 **Lentsch AB,** Kato A, Yoshidome H, McMasters KM, Edwards MJ. Inflammatory mechanisms and therapeutic strategies for warm hepatic ischemia/reperfusion injury. *Hepatology* 2000; **32:** 169-173

19 **Bradham CA,** Schemmer P, Stachlewitz RF, Thurman RG, Brenner DA. Activation of nuclear factor-kappaB during orthotopic liver transplantation in rats is protective and does not require Kupffer cells. *Liver Transpl Surg* 1999; **5:** 282-293

20 **Morishita R,** Sugimoto T, Aoki M, Kida I, Tomita N, Moriguchi A, Maeda K, Sawa Y, Kaneda Y, Higaki J, Ogihara T. In vivo transfection of cis element "decoy" against nuclear factor-kappaB binding site prevents myocardial infarction. *Nat Med* 1997; **3:** 894-899

21 **Kawamura I,** Morishita R, Tomita N, Lacey E, Aketa M, Tsujimoto S, Manda T, Tomoi M, Kida I, Higaki J, Kaneda Y, Shimomura K, Ogihara T. Intratumoral injection of oligonucleotides to the NF kappa B binding site inhibits cachexia in a mouse tumor model. *Gene Ther* 1999; **6:** 91-97

22 **Abeyama K,** Eng W, Jester JV, Vink AA, Edelbaum D, Cockerell CJ, Bergstresser PR, Takashima A. A role for NF-kappaB-dependent gene transactivation in sunburn. *J Clin Invest* 2000; **105:** 1751-1759

23 **Giannoukakis N,** Bonham CA, Qian S, Chen Z, Peng L, Harnaha J, Li W, Thomson AW, Fung JJ, Robbins PD, Lu L. Prolongation of cardiac allograft survival using dendritic cells treated with NF-kB decoy oligodeoxyribonucleotides. *Mol Ther* 2000; **1:** 430-437

24 **Xu MQ,** Yao ZX. Functional changes of dendritic cells derived from allogeneic partial liver graft undergoing acute rejection in rats. *World J Gastroenterol* 2003; **9:** 141-147

25 **Eckhoff DE,** Bilbao G, Frenette L, Thompson JA, Contreras JL. 17-Beta-estradiol protects the liver against warm ischemia/reperfusion injury and is associated with increased serum

nitric oxide and decreased tumor necrosis factor-alpha. *Surgery* 2002; **132:** 302-309
26 **Ben-Ari Z,** Hochhauser E, Burstein I, Papo O, Kaganovsky E, Krasnov T, Vamichkim A, Vidne BA. Role of anti-tumor necrosis factor-alpha in ischemia/reperfusion injury in isolated rat liver in a blood-free environment. *Transplantation* 2002; **73:** 1875-1880
27 **Zhu XH,** Qiu YD, Shen H, Shi MK, Ding YT. Effect of matrine on Kupffer cell activation in cold ischemia reperfusion injury of rat liver. *World J Gastroenterol* 2002; **8:** 1112-1116
28 **Kataoka M,** Shimizu H, Mitsuhashi N, Ohtsuka M, Wakabayashi Y, Ito H, Kimura F, Nakagawa K, Yoshidome H, Shimizu Y, Miyazaki M. Effect of cold-ischemia time on C-X-C chemokine expression and neutrophil accumulation in the graft liver after orthotopic liver transplantation in rats. *Transplantation* 2002; **73:** 1730-1735
29 **Fernandes H,** Koneru B, Fernandes N, Hameed M, Cohen MC, Raveche E, Cohen S. Investigation of promoter polymorphisms in the tumor necrosis factor-alpha and interleukin-10 genes in liver transplant patients. *Transplantation* 2002; **73:** 1886-1891
30 **Mazariegos GV,** Reyes J, Webber SA, Thomson AW, Ostrowski L, Abmed M, Pillage G, Martell J, Awad MR, Zeevi A.Cytokine gene polymorphisms in children successfully withdrawn from immunosuppression after liver transplantation. *Transplantation* 2002; **73:** 1342-1345
31 **Warle MC,** Farhan A, Metselaar HJ, Hop WC, van der Plas AJ, Kap M, de Rave S, Kwekkeboom J, Zondervan PE, IJzermans JN, Tilanus HW, Pravica V, Hutchinson IV, Bouma GJ. In vitro cytokine production of TNFalpha and IL-13 correlates with acute liver transplant rejection. *Hum Immunol* 2001; **62:** 1258-1265
32 **Grenz A,** Schenk M, Zipfel A, Viebahn R. TNF-alpha and its receptors mediate graft rejection and loss after liver transplantation. *Clin Chem Lab Med* 2000; **38:** 1183-1185
33 **Bathgate AJ,** Lee P, Hayes PC, Simpson KJ. Pretransplantation tumor necrosis factor-alpha production predicts acute rejection after liver transplantation. *Liver Transpl* 2000; **6:** 721-727
34 **Ricciardi R**, Schaffer BK, Kim RD, Shah SA, Donohue SE, Wheeler SM, Quarfordt SH, Callery MP, Meyers WC, Chari RS. Protective effects of ischemic preconditioning on the cold-preserved liver are tyrosine kinase dependent. *Transplantation* 2001; **72:** 406-412
35 **Peralta C,** Bartrons R, Serafin A, Blazquez C, Guzman M, Prats N, Xaus C, Cutillas B, Gelpi E, Rosello-Catafau J. Adenosine monophosphate-activated protein kinase mediates the protective effects of ischemic preconditioning on hepatic ischemia-reperfusion injury in the rat. *Hepatology* 2001; 34: 1164-1173
36 **Sindram D,** Rudiger HA, Upadhya AG, Strasberg SM, Clavien PA. Ischemic preconditioning protects against cold ischemic injury through an oxidative stress dependent mechanism. *J Hepatol* 2002; 36: 78-84
37 **Serafin A,** Rosello-Catafau J, Prats N, Xaus C, Gelpi E, Peralta C. Ischemic preconditioning increases the tolerance of Fatty liver to hepatic ischemia-reperfusion injury in the rat. *Am J Pathol* 2002; 161: 587-601
38 **Zhang X,** Cao H, Jiao Z, Ling W, Wu Z, Chen Z, Kuang Y. Effects of ischemic preconditioning on apoptosis of hepatocytes in liver transplantation in rats. *Zhonghua Gan Zang Bing Za Zhi* 2000; **8:** 221-213
39 **Arai M,** Thurman RG, Lemasters JJ. Contribution of adenosine A(2) receptors and cyclic adenosine monophosphate to protective ischemic preconditioning of sinusoidal endothelial cells against Storage/Reperfusion injury in rat livers. *Hepatology* 2000; **32:** 297-302
40 Totsuka E, Fung JJ, Urakami A, Moras N, Ishii T, Takahashi K, Narumi S, Hakamada K, Sasaki M. Influence of donor cardiopulmonary arrest in human liver transplantation: possible role of ischemic preconditioning. *Hepatology* 2000; **31:** 577-580
41 **Ricciardi R,** Meyers WC, Schaffer BK, Kim RD, Shah SA, Wheeler SM, Donohue SE, Sheth KR, Callery MP, Chari RS. Protein kinase C inhibition abrogates hepatic ischemic preconditioning responses. *J Surg Res* 2001; **97:** 144-149
42 **Fernandez L**, Heredia N, Grande L, Gomez G, Rimola A, Marco A, Gelpi E, Rosello-Catafau J, Peralta C. Preconditioning protects liver and lung damage in rat liver transplantation: role of xanthine/xanthine oxidase. *Hepatology* 2002; **36:** 562-572
43 **Yin DP,** Sankary HN, Chong AS, Ma LL, Shen J, Foster P, Williams JW. Protective effect of ischemic preconditioning on liver preservation-reperfusion injury in rats. *Transplantation* 1998; **66:** 152-157
44 **Ricciardi R,** Shah SA, Wheeler SM, Quarfordt SH, Callery MP, Meyers WC, Chari RS. Regulation of NFkappaB in hepatic ischemic preconditioning. *J Am Coll Surg* 2002; 195: 319-326
45 **Maulik N,** Sato M, Price BD, Das DK. An essential role of NFkappaB in tyrosine kinase signaling of p38 MAP kinase regulation of myocardial adaptation to ischemia. *FEBS Lett* 1998; **429:** 365-369
46 **Teoh N,** Dela Pena A, Farrell G. Hepatic ischemic preconditioning in mice is associated with activation of NF-kappaB, p38 kinase, and cell cycle entry. *Hepatology* 2002; **36:** 94-102
47 **Le Moine O,** Louis H, Demols A, Desalle F, Demoor F, Quertinmont E, Goldman M, Deviere J. Cold liver ischemia-reperfusion injury critically depends on liver T cells and is improved by donor pretreatment with interleukin 10 in mice. *Hepatology* 2000; 31: 1266-1274
48 **Shen XD,** Ke B, Zhai Y, Amersi F, Gao F, Anselmo DM, Busuttil RW, Kupiec-Weglinski JW. CD154-CD40 T-cell costimulation pathway is required in the mechanism of hepatic ischemia/reperfusion injury, and its blockade facilitates and depends on heme oxygenase-1 mediated cytoprotection. *Transplantation* 2002; **74:** 315-319
49 **Takada M,** Chandraker A, Nadeau KC, Sayegh MH, Tilney NL. The role of the B7 costimulatory pathway in experimental cold ischemia/reperfusion injury. *J Clin Invest* 1997; **100:** 1199-1203
50 **Zwacka RM,** Zhang Y, Halldorson J, Schlossberg H, Dudus L, Engelhardt JF. CD4(+) T-lymphocytes mediate ischemia/reperfusion-induced inflammatory responses in mouse liver. *J Clin Invest* 1997; **100:** 279-289
51 **Teramoto K,** Tanaka Y, Kusano F, Hara Y, Ishidate K, Iwai T, Sato C. Expression of tumor necrosis factor-alpha gene during allograft rejection following rat liver transplantation. *Liver* 1999; **19:** 19-24
52 **Tsoulfas G,** Takahashi Y, Ganster RW, Yagnik G, Guo Z, Fung JJ, Murase N, Geller DA. Activation of the lipopolysaccharide signaling pathway in hepatic transplantation preservation injury. *Transplantation* 2002; **74:** 7-13
53 **Okamura H,** Kashiwamura S, Tsutsui H, Yoshimoto T, Nakanishi K. Regulation of interferon-gamma production by IL-12 and IL-18. *Curr Opin Immunol* 1998; **10:** 259-264

Science Editor Ma JY **Language Editor** Elsevier HK

PO Box 2345, Beijing 100023, China
www.wjgnet.com
wjg@wjgnet.com

ELSEVIER

World J Gastroenterol 2005;11(44):6968-6974
World Journal of Gastroenterology ISSN 1007-9327

• *BASIC RESEARCH* •

Induction of pancreatic duct cells of neonatal rats into insulin-producing cells with fetal bovine serum: A natural protocol and its use for patch clamp experiments

San-Hua Leng, Fu-Er Lu

San-Hua Leng, Fu-Er Lu, Institute of Integrative Traditional Chinese and Western Medicine, Tongji Hospital, Tongji Medical College, Huazhong University of Science and Technology, Wuhan 430030, Hubei Province, China
Supported by the National Natural Science Foundation of China, No. 30472254
Correspondence to: Professor Fu-Er Lu, Institute of Integrative Traditional Chinese and Western Medicine, Tongji Hospital, Tongji Medical College, Huazhong University of Science and Technology, Wuhan 430030, Hubei Province, China. felu@tjh.tjmu.edu.cn
Telephone: +86-27-83662220 Fax: +86-27-83646605
Received: 2004-12-28 Accepted: 2005-03-24

Abstract

AIM: To induce the pancreatic duct cells into endocrine cells with a new natural protocol for electrophysiological study.

METHODS: The pancreatic duct cells of neonatal rats were isolated, cultured and induced into endocrine cells with 15% fetal bovine serum for a period of 20 d. During this period, insulin secretion, MTT value, and morphological change of neonatal and adult pancreatic islet cells were comparatively investigated. Pancreatic β-cells were identified by morphological and electrophysiological characteristics, while ATP sensitive potassium channels (K_{ATP}), voltage-dependent potassium channels (K_V), and voltage-dependent calcium channels (K_{CA}) in β-cells were identified by patch clamp technique.

RESULTS: After incubation with fetal bovine serum, the neonatal duct cells budded out, changed from duct-like cells into islet clusters. In the first 4 d, MTT value and insulin secretion increased slowly (MTT value from 0.024 ±0.003 to 0.028±0.003, insulin secretion from 2.6±0.6 to 3.1±0.8 mIU/L). Then MTT value and insulin secretion increased quickly from d 5 to d 10 (MTT value from 0.028 ±0.003 to 0.052±0.008, insulin secretion from 3.1±0.8 to 18.3±2.6 mIU/L), then reached high plateau (MTT value >0.052±0.008, insulin secretion >18.3±2.6 mIU/L). In contrast, for the isolated adult pancreatic islet cells, both insulin release and MTT value were stable in the first 4 d (MTT value from 0.029±0.01 to 0.031±0.011, insulin secretion from 13.9±3.1 to 14.3±3.3 mIU/L), but afterwards they reduced gradually (MTT value <0.031 ±0.011, insulin secretion <8.2±1.5 mIU/L), and the pancreatic islet cells became dispersed, broken or atrophied correspondingly. The differentiated neonatal cells were identified as pancreatic islet cells by dithizone staining method, and pancreatic β-cells were further identified by both morphological features and electrophysiological characteristics, i.e. the existence of recording currents from K_{ATP}, K_V, and K_{CA}.

CONCLUSION: Islet cells differentiated from neonatal pancreatic duct cells with the new natural protocol are more advantageous in performing patch clamp study over the isolated adult pancreatic islet cells.

Key words: Pancreatic duct cells; Pancreatic precursor cells; Insulin-producing cells; Patch clamp; Experimental protocol; ATP sensitive potassium channels; Voltage-dependent potassium channels; Voltage-dependent calcium channels

Leng SH, Lu FE. Induction of pancreatic duct cells of neonatal rats into insulin-producing cells with fetal bovine serum: A natural protocol and its use for patch clamp experiments. *World J Gastroenterol* 2005; 11(44): 6968-6974
http://www.wjgnet.com/1007-9327/11/6968.asp

INTRODUCTION

The pancreatic islets (containing α, β, and δ cells that produce glucagon, insulin, and somatostatin, respectively) are intensively involved in the regulation of physiological metabolic homeostasis[1]. Patch clamp technique is considered as a very important approach for studying the endocrine activities and mechanisms of these cells. The traditional method for the isolation of rat intact pancreatic islet cells[2] has been performed for almost 40 years, and is still the most widely acceptable method in electrophysiological study of pancreatic islet cells. Nevertheless, pancreatic islet cells usually survive poorly after isolation because the cells are fragile in the *in vitro* culture condition[3]. Thus, only the freshly isolated or shortly cultured islet cells can be introduced for patch clamp experiments. Furthermore, there are some disadvantages in performing patch clamp experiments with

isolated islet cells. The endocrine pancreas is considered as a slowly and continuously renewing tissue in the kinetic balance process of apoptosis and neogenesis[4]. Thus, pancreatic β cells isolated from adult rats are heterogeneous at different ages, including neonatal, adult, and senile cells. The isolated adult and senile β cells are more susceptible than neonatal β cells to the transition from the native living surroundings to the *in vitro* culture. Because the membrane of isolated adult β cells is fragile, it is difficult to manipulate gigaseal, a key step in patch clamp experiments.

Although there are other cell sources for performing patch clamp experiments without obvious problems mentioned above, such as β cell line and islet cells differentiated from marrow mesenchymal stem cells[5] or multipotent cells, and precursor cells of fetal pancreas, they still show considerable shortcomings. According to the reports, the β cell line only retains partial characteristics of primitive pancreatic islet cells, while the islet cells differentiated from marrow mesenchymal stem cells[6] and precursor cells of fetal pancreas[7-11] exhibit poor insulin secretory response to glucose. Therefore, it is essential to seek for more optimal cell sources and approaches suitable for patch clamp experiments.

Neonatal pancreatic duct cells are composed mainly of precursor cells[12,13] and can be induced into endocrine cells if appropriate morphogen stimuli are provided[10-13], and the induced endocrine cells are stable in culture condition[12,13], and their glucose-induced insulin secretion is evident[7-10]. Thus, we suppose that the neonatal pancreatic duct cells might be more suitable for patch clamp experiments.

Here the pancreatic duct cells were differentiated into endocrine islet cells with fetal bovine serum, a physiological nutrition[14]. The cell proliferation and insulin secretion of differentiated neonatal endocrine cells were compared to isolated adult endocrine islet cells. ATP sensitive potassium channels (K_{ATP}), voltage-dependent potassium channels (K_V) and voltage-dependent calcium channels (K_{CA}) of β cells were identified with patch clamp technique to prove the usefulness of this protocol.

MATERIALS AND METHODS

Reagents

Na_2-ATP, EGTA, HEPES, repaglinide, and diazoxide were purchased from Sigma Co. The other chemicals used were of analytical reagent grade.

Isolation and culture of pancreatic islet cells

Sprague-Dawley rats aged 1-3 and 50-60 d were obtained from Laboratory Animal Center, Tongji Medical College, Huazhong University of Science and Technology. Hubei Experimental Animal Association approved the experiments. The culture medium used for both neonatal and adult cells was RPMI 1640 medium (glucose 11.1 mmol/L) supplemented with 15% fetal bovine serum, 15 mmol/L HEPES buffer, pH 7.40, without any antibiotics (to eliminate its possible influence on the differentiation of precursor cells). The cells were cultured at 37 ℃ in the atmosphere containing 950 mL/L O_2+50 mL/L CO_2. The isolation of pancreatic islet cells from adult rats was performed as previously described[2]. The isolation and induction of duct cells were performed as follows: the pancreases were moved from 10 neonatal rats and thoroughly washed in KRBH solution containing (in mmol/L) 136 NaCl, 4.8 KCl, 1 $CaCl_2$, 1.2 $MgSO_4$, 1.2 KH_2PO_4, 5 $NaHCO_3$, 25 HEPES, 1% BSA, pH 7.40. The pancreases were minced into pieces of 1-2 mm in size. The minced pancreases were hand-shaken while being digested by 0.5 mg/mL type V collagenase in PBS (pH 7.40) for about 3-8 min in a 10-mL tube bathed in 37 ℃water. Then digestion was stopped by 4 ℃ KRBH. The production was centrifuged (50 r/min) thrice to eliminate collagenase and broken cells. Thereafter, the cells were suspended in the cell culture medium and seeded in plastic dishes (18 mm in diameter) with 2 mL culture medium in each dish. After being cultured for about 24 h, the culture medium was moved, and the duct cells were washed with KRBH solution five times to remove the floated cells thoroughly. Then the left cells were mostly duct cells (Figure 1). The cells were kept in the cell culture medium for 20 d, during which the dishes were replenished with a new medium every 2 d.

Morphology observation

The incubated cells were observed under inverted microscope each day. When the marked morphologic changes were observed, photograph of the cells was taken by phase difference microscopy.

Insulin measurement

All the isolated products from neonatal duct cells or adult pancreatic islet cells were equally seeded in gelatin-coated dishes (18 mm in diameter), and each dish contained 2 mL isolated products (about 10^4 cells). The supernatant of culture media in the five dishes was harvested every 2 d and kept at -20 ℃ for insulin determination by radioimmunoassay. The dishes were washed with KRBH solution twice, then 2 mL of the cell culture medium was added again for further culture.

MTT test

MTT assay was carried out as previously described[15]. The isolated products from neonatal or adult rats (about 10^5 cells) were equally seeded in 10 dishes (96 cells in each dish, and each cell containing 150 μL isolated products), one dish of cells was used every 2 d for MTT determination, and the remaining dishes were replenished with a new medium.

Identification of pancreatic islet cells

The pancreatic islet cells were identified by dithizone staining method[16]. The viable cells were determined by trypan blue exclusive test.

Identification of pancreatic β cells

Two steps were performed to identify pancreatic β cells from α and δ cells[17]. Therefore, only large cells with a capacitance of >5 pF were selected as β cells. Then

a depolarizing protocol was applied to the large cells to identify the properties of voltage-dependent Na^+ currents[18]. Thus, cells in which a Na^+ current could be activated by a small depolarizing pulse from a prolonged holding potential of -70 mV were discarded. By contrast, cells exhibiting a Na^+ current only after a hyperpolarizing pulse to -140 mV were considered to be β cells[19].

Patch clamp experiments

Patch clamp experiments were performed on β cells of isolated islet cells only in the first 4 d after the isolation, the β cells beyond this period of time could not be introduced into patch clamp experiments. The β cells differentiated from islet cells of neonatal rats were applied for patch clamp experiments from d 10 to d 16.

Rat pancreatic islet cells plated on the plastic dishes were placed in a recording chamber mounted on an inverted microscope (Olympus). Patch clamp recordings were done for cells that were not in contact with the other cells to avoid possible cell-cell coupling artifacts. For recording K_{ATP} currents, the solutions were as follows (in mmol/L): internal solution containing 140 KCl, 2 $CaCl_2$, 4 $MgCl_2$, 10 EGTA, 0.65 Na_2-ATP, and 20 HEPES (pH 7.15 with KOH); and external solution containing 140 NaCl, 5.6 KCl, 1.2 $MgCl_2$, 2.6 $CaCl_2$, 0.5 glucose and 10 HEPES (pH 7.4 with KOH). K_{ATP} currents were measured at a holding potential of -70 to -80 mV and -60 mV at 15-s intervals, and diazoxide (100 μmol/L) and repaglinide (100 μmol/L) were added respectively to further confirm whether it was K_{ATP} currents or not. For K_V currents recording, the solutions were the same as for recording K_{ATP} currents except that 100 μmol/L repaglinide was added into external solution to block K_{ATP} currents. The cells were held at -120 mV and depolarized at 15-s intervals to 30 mV to activate K_V currents. For K_{CA} recording, the solutions were as follows (in mmol/L): internal solution containing 70 CsCl, 1 $MgCl_2$, 4 ATP, 20 HEPES, 5 EGTA, pH 7.2; external solution containing 90 NaCl, 1 $MgCl_2$, 20 TEA-Cl, 10 HEPES, 20 $BaCl_2$, 5.6 KCl, 5 CsCl, pH 7.15. All cell membrane currents were measured using whole-cell mode of patch clamp technique at 22 ℃, using an EPC-9 patch clamp amplifier (Heka Electronics, Lambrecht/Pfalz, Germany) and the software Pulsefit. Patch clamp electrodes were made from borosilicate glass capillaries (Shanghai Physiology Institute, China) using a two-stage puller (PP-830, Narishige Co., Japan) to give a resistance of 4-5 MΩ.

RESULTS

Morphological evolvement and identification

The neonatal rat pancreatic duct cells were organized in duct-like cells when incubated for 3-4 d (Figure 1A). There were precursors of pancreatic islet cells among them. When cultured for 5-10 d, some duct cells changed into round cells organized as islet clusters, being similar to pancreatic islet cells *in vivo* (Figure 1B). Then the cells grew bigger and budded out (Figures 1C and 1D). The buds grew bigger and bigger and became new ground cells in clusters (Figure 1E), which were further identified as pancreatic islet cells by dithizone (Figure 1F), a chemical considered to selectively stain pancreatic islet cells[16].

In contrast, the freshly isolated pancreatic islet cells from adult rats were round, but gradually became dispersed, broken or atrophied. After being cultured for a week, the islet cells were dispersed to be single cells, and the cell number was greatly reduced (data not shown).

Insulin release

For neonatal pancreatic islet cells, the insulin concentration in

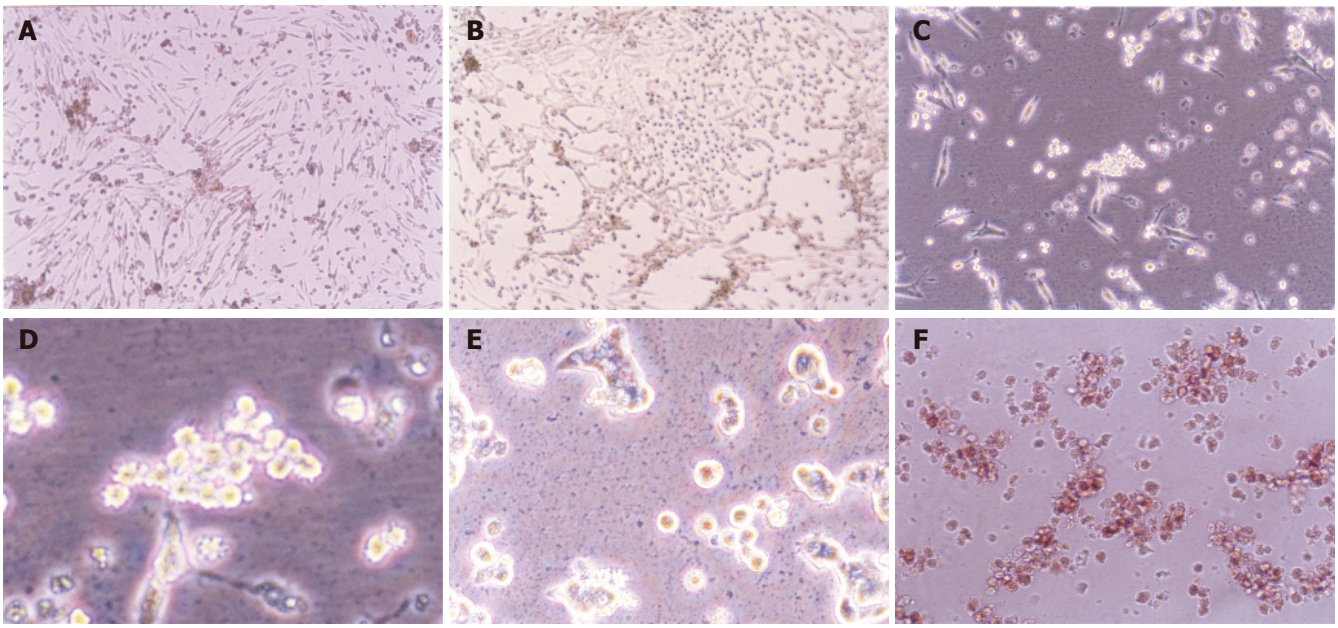

Figure 1 Morphological change of neonatal pancreatic duct cells cultured for 3-4 d (**A**), 5-7 d (**B**), 8-10 d (**C** and **D**) and more than 10 d (**E**), as well as identification of pancreatic islet cells by dithizone (**F**).

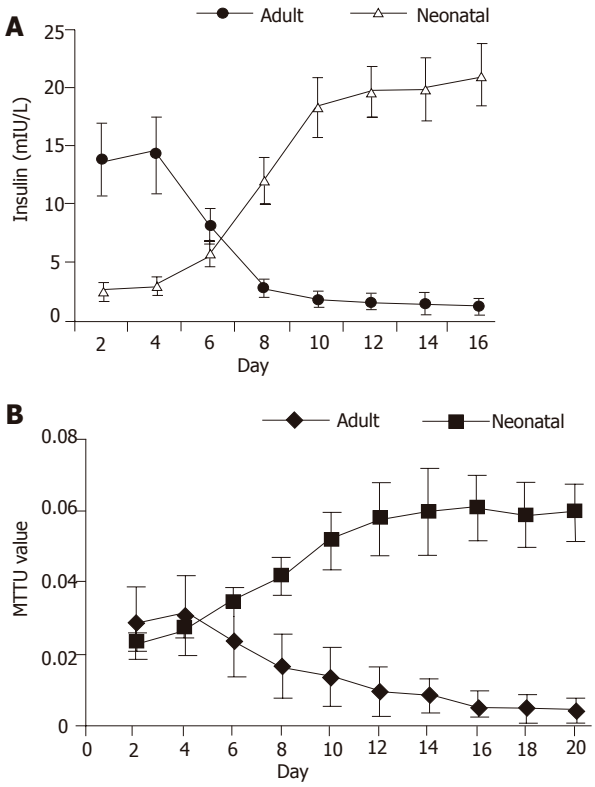

Figure 2 Insulin release curve (**A**) and MTT value curve (**B**) during the culture period of isolated adult islet cells and neonatal endocrine cells.

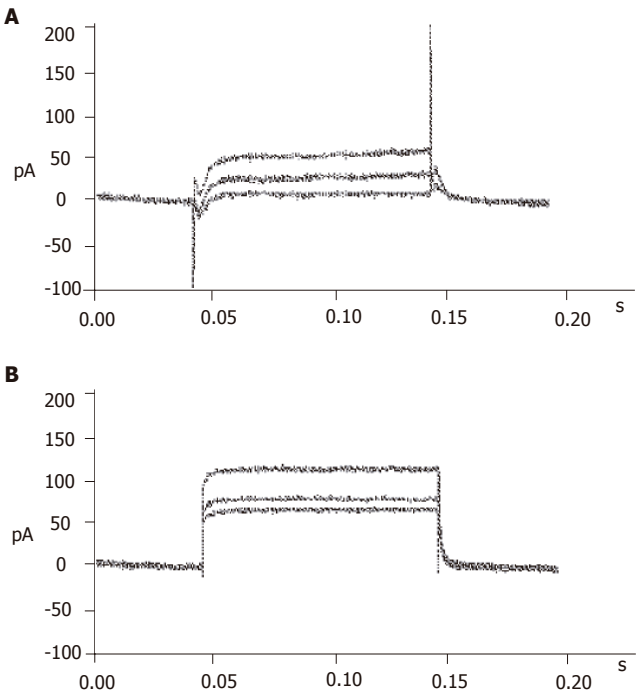

Figure 3 Identification of pancreatic β cells. **A:** Currents recorded from α or δ cells; **B:** currents recorded from β cells.

the cell culture medium was low (from 2.6±0.6 to 3.1±0.8 mIU/L) in the first 4 d, then quickly increased (from 3.1±0.8 to 12.1±2.1 mIU/L) from d 5 to d 10. Thereafter, the insulin release reached its high plateau (>18.3±2.6 mIU/L). For isolated pancreatic islet cells from adult rats, the insulin concentration was high (from 13.9±3.1 to 14.3±3.3 mIU/L) in the first 4 d, and gradually reduced (from 8.2±1.5 to 2.9 ±0.7 mIU/L) from d 5 to d 10. Then the insulin release was very low (<2.9±0.7 mIU/L) (Figure 2A).

MTT value

For neonatal pancreatic islet cells, the MTT value was low (0.024±0.003 to 0.028±0.003) in the first 4 d and gradually increased (0.028±0.003 to 0.052±0.008) from d 5 to d 10. Thereafter, the MTT value reached its high plateau (>0.052 ±0.008). For isolated pancreatic islet cells from adult rats, the MTT value was stable (from 0.029±0.01 to 0.031± 0.011) in the first 4 d and gradually reduced (0.031±0.01 to 0.014±0.008) from d 5 to d 10. Then the MTT value was very low (<0.014±0.008) (Figure 2B).

Identification of pancreatic islet cells and β cells

The big round cells (with a diameter >10 μm) were selected and their capacitance was determined (>5 pF). Then a depolarizing protocol was used to identify the properties of voltage-dependent Na^+ currents. The results showed that voltage-dependent Na^+ currents of selected cells could not be recorded at a holding potential of -70 mV (Figure 3B). On the contrary, the voltage-dependent Na^+ currents of small round cells (capacitance <5 pF) could be detected at a holding potential of -70 mV (Figure 3A). It was demonstrated that the big round cells were pancreatic β cells, while small round cells were not.

K_{ATP} current recording

With certain internal and external solutions and protocol, the currents recorded in pancreatic β cells were almost entirely K_{ATP} currents[19]. To verify this, 100 μmol/L diazoxide, a special opener of K_{ATP} channels, and 100 μmol/L repaglinide, a special antagonist of K_{ATP} channels, were added correspondingly. The results showed that diazoxide enhanced, while repaglinide reduced the currents greatly (Figure 4), suggesting that the detected currents were from K_{ATP} channels.

K_V current recording

Repaglinide was used in the external solution to block K_{ATP} currents. Then the currents recorded should be almost entirely K_V currents with the internal and external solutions and protocol. The recorded outward currents showed that the channels were inactive from -120 to -55 mV and active from -55 to 0 mV and the currents increased in proportion to voltage. When added with 100 μmol/L TEA, the currents could not be recorded, suggesting that the detected currents were from K_V channels (Figure 5).

K_{CA} current recording

To efficiently record K_{CA} currents, Cs^+ was added in the internal solution, while TEA and Ba^+ were added in the external solution to block voltage-dependent outward potassium currents. Meanwhile, Ba^+ enhanced

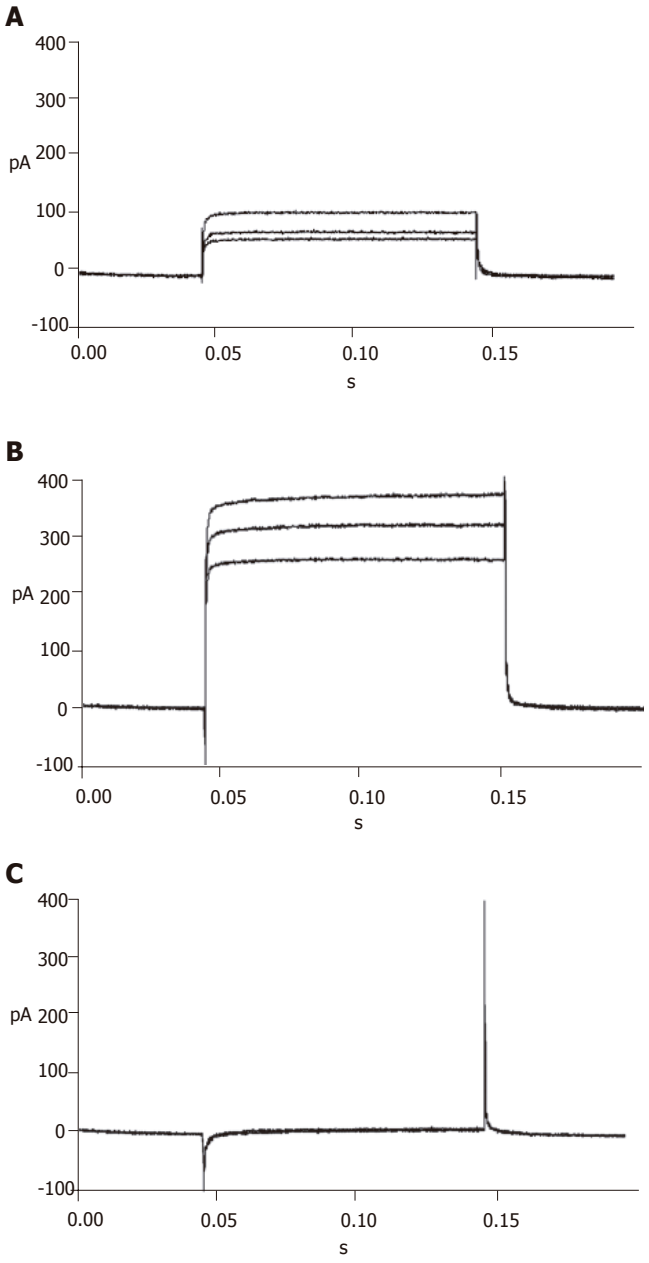

Figure 4 ATP sensitive potassium currents recorded in the absence (**A**), presence of diazoxide (**B**) and repaglinide (**C**).

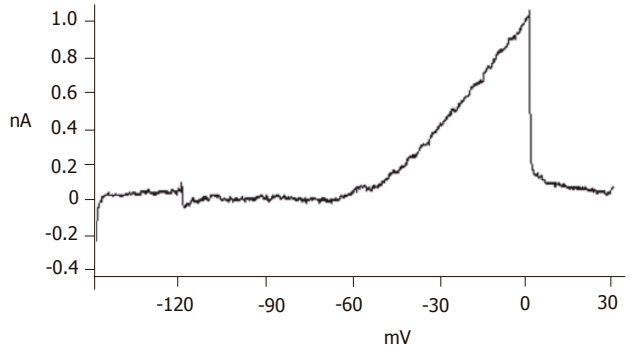

Figure 5 Voltage-dependent potassium currents recorded on neonatal pancreatic β cells.

K_{CA} currents. Inward currents were recorded at -40 mV and reached their peak at 0-10 mV, and then turned over at 50-60 mV. These dynamic electric patterns were characteristic of K_{CA} currents[20,21]. Furthermore, special opener and antagonist of K_{CA} channels were introduced to verify their existence. When added with 100 μmol/L Bay K8644, the currents enhanced greatly; while 100 μmol/L nifedipine was added, the currents reduced strikingly (Figure 6). These facts suggest that the detected currents were K_{CA} currents (mainly of L-type calcium currents).

DISCUSSION

It has been reported that pancreatic endocrine cells of neonatal rats can be used in long-term study of secretion and electrophysiology[22]. According to the experimental protocol, fibroblasts are cleared away by timerosal to enhance insulin release. However, the enhancing effect of

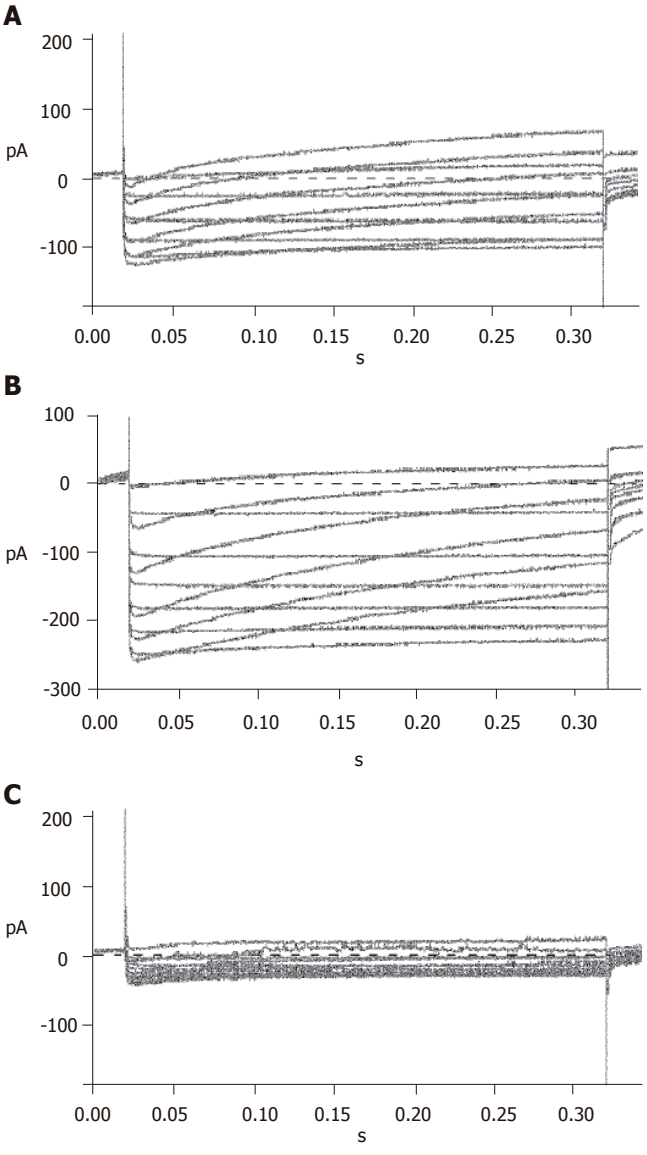

Figure 6 Voltage-dependent calcium currents recorded in the absence (**A**), presence of Bay K8644 (**B**) and nifedipine (**C**).

timerosal cannot be interpreted by the clearing away of fibroblasts, but might be produced due to the modified effects of timerosal on sulfonylurea receptor which regulates insulin release, because timerosal can modify mitochondrial sulfonylurea receptor[23]. Fibroblasts are present as the mesenchyme of islet cells, which may provide fibroblast growth factors and matrix to help the differentiation and replication of endocrine cells[24,25]. Therefore, alterations were made to optimize the experimental protocol correspondingly. Firstly, the fibroblasts in the pancreatic islet cells for the normal differentiation and replication of endocrine cells were retained. Secondly, timerosal was not introduced in our protocol to exclude its insulin regulating effect. Instead, fetal bovine serum, a physiological nutrition that does not intervene the normal neogenesis process, was administered in the cell incubation. With this natural protocol, the neonatal duct cells were successfully induced into endocrine cells.

It was reported that neonatal duct cells are composed mainly of precursor cells[12,13]. Thus, the harvested endocrine cells from neonatal rats should be mostly differentiated from precursor cells that lie in the pancreas duct tree. The harvested endocrine cells from the neonatal rats auto-organized as islet clusters (Figure 1B). Our observations that the islet cells changed from duct-like into round shape and that the round cells then budded outward *in vitro* culture, were in conformity with the report by Gershengorn *et al*.[26].

Gigaseal, the key step in patch clamp experiments, is difficult to perform on isolated islet cells because the membrane is fragile and easily gets broken by the electrode. Even when gigaseal was completed, the currents recorded may be deformed or lower than normal because there are tiny gaps between cell membrane and the electrode, through which the currents might leak out. However, we found that it was easy to manipulate gigaseal on islet cells differentiated with this natural protocol. To explain this phenomenon, we compared the morphological and functional characteristics of neonatal and adult pancreatic islet cells in culture condition. For differentiated neonatal islet cells, insulin release was low during the early phase, but increased rapidly from d 5 to d 10, and then kept in high plateau (Figure 2). Correspondingly, the cell mass grew much bigger. As for isolated islet cells from adult rats, insulin release was high in the first 4 d, but then reduced quickly (Figure 2). Correspondingly, the islet cells became dispersed, broken or atrophied. For neonatal endocrine islet cells, the MTT value increased quickly from d 5 to d 10 and then kept in high plateau. For isolated islet cells from adult rats, the MTT value was stable in the first 4 d and then reduced quickly (Figure 3). The data are in conformity with the idea that isolated islet cells survive poorly in culture condition[3] and support that neonatal pancreatic islet cells are more preferable for long-term and stable culture, thus more suitable for patch clamp experiments.

It was reported that the differentiated neonatal pancreatic islet cells have evident glucose-induced insulin secretion property[7-10]. To understand its mechanism, we investigated the electric activities of K_{ATP}, K_V, and K_{CA}, regulators of glucose-induced insulin secretion process. The role of K_{ATP} channels of β cells in glucose-induced insulinotropic process has been well demonstrated[27]; the K_{CA} and K_V channels are also suggested to couple with glucose-dependent insulinotropic effects[28-32]. Thus, the properties of these channels in differentiated islet cells were studied. The fact that K_{ATP}, K_V, and K_{CA} channels in differentiated islet β cells are sensitive to corresponding antagonist and/or opener (Figures 4-6) indicates that the differentiated islet cells have evident glucose-induced insulin secretion properties.

In conclusion, the natural protocol illustrated in this paper enables the long-term incubation of stable endocrine islet cells, which will greatly optimize and facilitate the performance of patch clamp experiments and other single cell studies.

ACKNOWLEDGMENTS

The authors thank Professor Yong-Jian Xu and technician Wang Ni (Respiratory Department of Tongji Hospital, Tongji Medical College, Huazhong University of Science and Technology) for their help in patch clamp technique.

REFERENCES

1 **Slack JM.** Developmental biology of the pancreas. *Development* 1995; **121:** 1569-1580
2 **Lacy PE,** Kostianovsky M. Method for the isolation of intact islets of Langerhans from the rat pancreas. *Diabetes* 1967; **16:** 35-39
3 **Brandhorst D,** Brandhorst H, Hering BJ, Bretzel RG. Long-term survival, morphology and in vitro function of isolated pig islets under different culture conditions. *Transplantation* 1999; **67:** 1533-1541
4 **Bonner-Weir S.** Perspective: Postnatal pancreatic beta cell growth. *Endocrinology* 2000; **141:** 1926-1929
5 **Lumelsky N,** Blondel O, Laeng P, Velasco I, Ravin R, McKay R. Differentiation of embryonic stem cells to insulin-secreting structures similar to pancreatic islets. *Science* 2001; **292:** 1389-1394
6 **Vogel G.** Developmental biology. Stem cells are coaxed to produce insulin. *Science* 2001; **292:** 615-617
7 **Asplund K,** Westman S, Hellerstrom C. Glucose stimulation of insulin secretion from the isolated pancreas of foetal and newborn rats. *Diabetologia* 1969; **5:** 260-262
8 **Asplund K.** Dynamics of insulin release from the foetal and neonatal rat pancreas. *Eur J Clin Invest* 1973; **3:** 338-344
9 **Rhoten WB**. Insulin secretory dynamics during development of rat pancreas. *Am J Physiol* 1980; **239:** E57-63
10 **Hole RL,** Pian-Smith MC, Sharp GW. Development of the biphasic response to glucose in fetal and neonatal rat pancreas. *Am J Physiol* 1988; **254:** E167-174
11 **Tuch BE,** Jones A, Turtle JR. Maturation of the response of human fetal pancreatic explants to glucose. *Diabetologia* 1985; **28:** 28-31
12 **Korbutt GS,** Elliott JF, Ao Z, Smith DK, Warnock GL, Rajotte RV. Large scale isolation, growth, and function of porcine neonatal islet cells. *J Clin Invest* 1996; **97:** 2119-2129
13 **Yoon KH,** Quickel RR, Tatarkiewicz K, Ulrich TR, Hollister-Lock J, Trivedi N, Bonner-Weir S, Weir GC. Differentiation and expansion of beta cell mass in porcine neonatal pancreatic cell clusters transplanted into nude mice. *Cell Transplant* 1999; **8:**

673-689
14 **Hulinsky I,** Hulinska H, Silink M. DNA synthesis in cultured neonatal rat islets--a comparison of two methods. *Diabetes Res Clin Prac*t 1995; **27:** 119-126
15 **Janjic D,** Wollheim CB. Islet cell metabolism is reflected by the MTT (tetrazolium) colorimetric assay. *Diabetologia* 1992; **35:** 482-485
16 **Fiedor P,** Rowinski W, Licinska I, Mazurek AP, Hardy MA. The survival identification of pancreatic islets of Langerhans. In vitro and in vivo effects of two dithizone preparations on staining of rat and human islets of Langerhans-preliminary study (Part I). *Acta Pol Pharm* 1995; **52:** 431-436
17 **Gopel SO,** Kanno T, Barg S, Rorsman P. Patch-clamp characterisation of somatostatin-secreting -cells in intact mouse pancreatic islets. *J Physiol* 2000; **528:** 497-507
18 **Plant TD.** Na+ currents in cultured mouse pancreatic B-cells. *Pflugers Arch* 1988; **411:** 429-435
19 **Jonas JC,** Plant TD, Henquin JC. Imidazoline antagonists of alpha 2-adrenoceptors increase insulin release in vitro by inhibiting ATP-sensitive K+ channels in pancreatic beta-cells. *Br J Pharmacol* 1992; **107:** 8-14
20 **Rorsman P,** Trube G. Calcium and delayed potassium currents in mouse pancreatic beta-cells under voltage-clamp conditions. *J Physiol* 1986; **374:** 531-550
21 **Satin LS,** Cook DL. Evidence for two calcium currents in insulin-secreting cells. *Pflugers Arch* 1988; **411:** 401-409
22 **Schwartz JL,** Mealing GA, Whitfield JF, Braaten JT. Long-term culture of neonatal rat pancreatic endocrine cells as model for insulin-secretion and ion-channel studies. *Diabetes* 1990; **39:** 1353-6130
23 **Szewczyk A,** Wojcik G, Lobanov NA, Nalecz MJ. Modification of the mitochondrial sulfonylurea receptor by thiol reagents. *Biochem Biophys Res Commun* 1999; **262:** 255-258
24 **Arany E, Hill DJ.** Ontogeny of fibroblast growth factors in the early development of the rat endocrine pancreas. *Pediatr Res* 2000; **48:** 389-403
25 **Hulinsky I,** Cooney S, Harrington J, Silink M. In vitro growth of neonatal rat islet cells is stimulated by adhesion to matrix. *Horm Metab Res* 1995; **27:** 209-215
26 **Gershengorn MC,** Hardikar AA, Wei C, Geras-Raaka E, Marcus-Samuels B, Raaka BM. Epithelial-to-mesenchymal transition generates proliferative human islet precursor cells. *Science* 2004; **306:** 2261-2264
27 **Schwanstecher C,** Schwanstecher M. Nucleotide sensitivity of pancreatic ATP-sensitive potassium channels and type 2 diabetes. *Diabetes* 2002; 51 Suppl **3:** S358-362
28 **Rorsman P.** The pancreatic beta-cell as a fuel sensor: an electrophysiologist's viewpoint. *Diabetologia* 1997; **40:** 487-495
29 **Lang J.** Molecular mechanisms and regulation of insulin exocytosis as a paradigm of endocrine secretion. *Eur J Biochem* 1999; **259:** 3-17
30 **MacDonald PE,** Sewing S, Wang J, Joseph JW, Smukler SR, Sakellaropoulos G, Wang J, Saleh MC, Chan CB, Tsushima RG, Salapatek AM, Wheeler MB. Inhibition of Kv2.1 voltage-dependent K+ channels in pancreatic beta-cells enhances glucose-dependent insulin secretion. *J Biol Chem* 2002; **277:** 44938-44945
31 **MacDonald PE,** Salapatek AM, Wheeler MB. Glucagon-like peptide-1 receptor activation antagonizes voltage-dependent repolarizing K(+) currents in beta-cells: a possible glucose-dependent insulinotropic mechanism. *Diabetes* 2002; 51 Suppl **3:** S443-447
32 **MacDonald PE,** Wang G, Tsuk S, Dodo C, Kang Y, Tang L, Wheeler MB, Cattral MS, Lakey JR, Salapatek AM, Lotan I, Gaisano HY. Synaptosome-associated protein of 25 kilodaltons modulates Kv2.1 voltage-dependent K(+) channels in neuroendocrine islet beta-cells through an interaction with the channel N terminus. *Mol Endocrinol* 2002; **16:** 2452-2461

Science Editor Wang XL **Language Editor** Elsevier HK

PO Box 2345, Beijing 100023, China
www.wjgnet.com
wjg@wjgnet.com

ELSEVIER

World J Gastroenterol 2005;11(44):6975-6980
World Journal of Gastroenterology ISSN 1007-9327

• *BASIC RESEARCH* •

Oral vaccination of mice against rodent malaria with recombinant *Lactococcus lactis* expressing MSP-1$_{19}$

Zhi-Hong Zhang, Pei-Hong Jiang, Ning-Jun Li, Mi Shi, Weida Huang

Zhi-Hong Zhang, Pei-Hong Jiang, Ning-Jun Li, Mi Shi, Weida Huang, Department of Biochemistry, School of Life Science, Fudan University, Shanghai 200433, China
Pei-hong Jiang, equal contribution as the first author
Supported by the UNDP/World Bank/WHO Special Programme for Research and Training in Tropical Diseases (TDR), No. 980198
Correspondence to: Weida Huang, Department of Biochemistry, Fudan University, 220 Han Dan Road, Shanghai 200433, China. whuang@fudan.edu.cn
Telephone: +86-21-65643446 Fax: +86-21-55522773
Received: 2004-09-18 Accepted: 2004-11-19

Abstract

AIM: To construct the recombinant *Lactococcus lactis* as oral delivery vaccination against malaria.

METHODS: The C-terminal 19-ku fragments of MSP1 (MSP-1$_{19}$) of *Plasmodium yoelii* 265-BY was expressed in *L. lactis* and the recombinant *L. lactis* was administered orally to BALB/c and C57BL/6 mice. After seven interval vaccinations within 4 wk, the mice were challenged with *P. yoelii* 265-BY parasites of erythrocytic stage. The protective efficacy of recombinant *L. lactis* was evaluated.

RESULTS: The peak parasitemias in average for the experiment groups of BALB/c and C57BL/6 mice were 0.8±0.4% and 20.8±26.5%, respectively, and those of their control groups were 12.0±0.8% and 60.8±9.6%, respectively. None of the BALB/c mice in both experimental group and control group died during the experiment. However, all the C57BL/6 mice in the control group died within 23 d and all the vaccinated mice survived well.

CONCLUSION: The results imply the potential of recombinant *L. lactis* as oral delivery vaccination against malaria.

Key words: Lactococcus lactis; Oral delivery vaccination; Malaria

Zhang ZH, Jiang PH, Li NJ, Shi M, Huang W. Oral vaccination of mice against rodent malaria with recombinant *Lactococcus lactis* expressing MSP-1$_{19}$. *World J Gastroenterol* 2005; 11(44): 6975-6980
http://www.wjgnet.com/1007-9327/11/6975.asp

INTRODUCTION

The development of efficacious vaccines against malaria is one of the greatest challenges for the application of current life sciences in infectious diseases. The easiness of administration of a vaccine provides an attractive alternative to continue drug treatments in a population exceeding hundreds of millions of people with limited health care resources. Merozoite surface protein 1 (MSP1) is present in all species of *Plasmodium*[1,2], and has been widely studied as the major candidate for vaccine against malaria[3-5]. The high level expression of MSP1 by *Plasmodium* in the asexual stage is closely related to its invasion into erythrocytes. MSP1 can be proteolytically cleaved into five fragments by two processing steps after the maturation of merozoite, with the carboxyl-terminal 19-ku fragment (MSP-1$_{19}$) remaining on the merozoite surface[6-8]. The MSP-1$_{19}$ comprises two epidermal growth factor (EGF)-like modules. Antibodies directed to this fragment have been shown to inhibit the invasion of *Plasmodium falciparum* into erythrocyte *in vitro*[9,10] and intranasal or subcutaneous immunization may protect mice against the challenge of *Plasmodium yoelii* asexual blood-stage parasite[11]. The recombinant MSP-1$_{19}$ has been expressed in several host organisms, such as *Escherichia coli*[12], *Saccharomyces cerivisae*[11], *Bacillus Calmette-Guerin* (BCG)[13], and Baculovirus[14]. It has also been proven to be immuno-effective against the challenge of parasite. In vaccination experiments with recombinant MPS-1$_{19}$ from *P. yoelii*, immunized mice were protected against challenge with blood-stage parasites, and the protection was confirmed to be largely mediated by antibodies[15-17].

The development of efficient mucosal vaccines is one of the hotspots in modern vaccinology. One approach to deliver the protective antigens to the mucosal surfaces is to use live bacteria carrying plasmids responsible for the expression of specific antigen. Until recently most of these are derived from attenuated pathogenic microorganisms, such as *Salmonella typhi*[18] and *chlorella*[19]. As an alternative to this strategy, non-pathogenic food grade bacteria such as lactic acid bacteria are being focused for their efficacy as live antigen carriers[20]. *Lactococcus lactis* has a long history of being used in food fermentations and has been, therefore, generally regarded as a safe (GRAS) status[21]. This food-grade lactic acid bacterium is able to survive through the gastrointestinal tract of human beings and other animals, with a retention time of 2-3 d, but it does not invade or colonize the mucous and does not evoke strong host im-

mune responses[21]. The availability of various food-grade genetic engineering systems for *L. lactis*[22] makes the bacteria a potentially functional food or medicines by expressing heterogeneous peptides. Recent report using *L. lactis* preloaded with a bacterial antigen, tetanus toxin fragment C of *Clostridium tetanus*, demonstrated the feasibility of this approach: a protective systemic antibody response was elicited after nasal or oral immunization of mice[21]. Similar study was carried out by Lee *et al*.[23], in which urease subunit B (UreB) gene of *Helicobacter pylori* was expressed in *L. lactis* MG1363 and the recombinant bacterium was used as an oral vaccine against *H pylori* infection in mice. However, in this case no protective effect was observed, which implied that the adjuvant effects of *L. lactis* are likely to be insufficient to produce an effective immune response to protect against *H pylori* challenge, when used to deliver a weak immunogen like UreB.

Since the use of oral (or other mucosal) routes for immunization against malaria is also desirable due to the easiness of administration, we attempted *L. lactis* as the live vehicle for vaccine development against malaria. In this work, we showed that the oral immunization, with recombinant *L. lactis* constitutively expressing MSP-1$_{19}$ antigen, could protect BALB/c and C57BL/6 mice against malaria parasites challenge.

MATERIALS AND METHODS

Genes, plasmids, bacteria, and malarial parasites

The DNA fragment encoding for MSP-1$_{19}$ domain was amplified from the genomic DNA of *P. yoelii*. Plasmid pTRKL2 was from Prof. Todd R. Klaenhammer at Food Science Center, North California University, USA[24]. Cloning vector pBluescriptSKII(+) was from Strategene (La Jolla, CA, USA), and fusion-protein expression vector pGEX-5X-3 was from Amersham Pharmacia. *L. lactis* LM2345 was from Prof. Keith Thompson at Agriculture and Food Science Center, Newforge Lane, Northern Ireland. *Lactobacillus brevis* (ATCC8287) and *Bacillus subtilis* BR151 (ATCC33677) were purchased from the American Type Culture Collection. *P. yoelii* 265-BY was by Professor Weibin Guan at Second Military Medical University, Shanghai, China.

Construction of expression vector

The plasmid for the expression of MSP-1$_{19}$ fragment was constructed by conventional DNA recombination manipulation. The promoter region and the first five amino acids of the signal peptide-coding region of S-layer protein A (*SlpA)* gene (nucleotides 1-282, GenBank Z14250) was amplified by polymerase chain reaction (PCR) from genomic DNA of *L. brevis* with forward primer GCTGAGCTCGATTACAAAGGCTTTAAGCAGGTTAGTGAC (with *Sac*I site) and reverse primer GTCGGATCCTAAACTTGATTGCATAATCTTTCTTCCTCC (with *Bam*HI site). The DNA fragment encoding MSP-1$_{19}$ (nucleotides 5 040-5 451, GenBank AF165928) was amplified from the genomic DNA of *P. yoelii* 265BY, with forward primer ACGGGATCCAA CACATAGCCTCAATAGCT (with *Bam*HI site) and reverse primer ACGGAATTCTAGCTGG AAGAACTACAGAA (with *Eco*RI site). The terminator of *N*-acetylmuramoyl-L-alanine amidase (*cwl*B) (nucleotides 2 187-2 471, GenBank M81324) was amplified from *Bacillus subtilis* BR151 by PCR with forward primer CTCGAGCTCCACAAGCTATTCATGAC (with *Xho*I site) and reverse primer GGTACCTCTCT GCACTCACTG ACACA (with *Kpn*I site). The PCR products were cloned on T-vector (Promega, USA) first, and then joined together in a tandem way on pBluescriptSKII(+) with restriction enzyme pairs of *Sac*I/BamHI, *Bam*HI/*Eco*RI, and *Xho*I/*Kpn*I respectively to obtain plasmid pSK-PSGT. For expression of MSP-1$_{19}$ in *L. lactis*, pSK-PSGT was then digested with *Pvu*II to release the 1.6-kb blunt-end fragment, which was then inserted into the *Eco*RV site of shuttle vector pTRKL2[24]. The final construct was referred as pL2-PSGT. For expression of fusion protein GST-MSP-1$_{19}$ in *E. coli*, the DNA fragment encoding MSP-1$_{19}$ was derived by PCR and joined to fusion protein expression vector pGEX-5X-3 with *Bam*HI and *Eco*RI sites. The derived plasmid was noted as pGEX-MSP-1$_{19}$.

Transformation

Electroporation[25] was used to transform *L. lactis* LM2345 with pL2-PSGT. $CaCl_2$ method was used to transform *E. coli* BL21 with plasmid pGEX-5X-3.

Preparation of antiserum against P. yoelii 265-BY

The antiserum against *P. yoelii* 265-BY was prepared from BALB/c mice infected with 10^4 asexual blood stage parasites. The serum was collected from the eye veins 4 d after burst with 10^4 parasites one month after infection, and stored at 4 ℃.

Expression and analysis of MSP-1$_{19}$ in E. coli and L. lactis

The BL21 transformant harboring plasmid pGEX-MSP-1$_{19}$ was cultured in L-broth to A_{600} around 1.0, and was treated with supplement containing 1.0 mmol/L of isopropylthio-β-galactoside (IPTG) for 3 h. The fusion protein GST-MSP-1$_{19}$ was purified from cell lysate by affinity chromatography of Glutathione Sepharose-4B according to manual instruction provided by the manufacturer. The purified fusion protein was used as positive control of immunoblotting. To express MSP-1$_{19}$ in *L. lactis*, the transformant harboring plasmid pL2-PSGT was cultured overnight in MRS medium[26] supplemented with 10 mg/L erythromycin. The cells were collected by centrifuge, and the lysates were analyzed by using SDS-polyacrylamide gel electrophoresis analysis followed with immunoblotting by using antiserum against *P. yoelii* 265-BY (1:500 dilution). All other operations were performed following standard protocols[27].

Oral immunization of BALB/c and C57BL/6 mice with recombinant L. lactis

Oral immunization experiments were performed according

to the protocol described by Robinson *et al*.[21]. The BALB/c and C57BL/6 mice were divided into groups of 10 mice and fed for 6-8 wk. The test group was administered with recombinant *L. lactis* constitutively expressing MSP-1$_{19}$, and the control groups were administered with free *L. lactis* bacteria or phosphate-buffered saline (PBS). For BALB/c mice, every dose containing 5×10^9 bacterial cells in the suspension buffer (0.2 mol/L sodium bicarbonate, 5% Casino acids, and 0.5% glucose); and for C57BL/6 mice (two dosage groups), every dose containing 5×10^9 or 1×10^8 cells were administered. All the groups were administered with recombinant *L. lactis* on d 1, 2, 3, 29, 30, 31, and 36, respectively.

Challenge infections and evaluation of protective efficacy

Mice in each group were challenged on d 49 with 1×10^5 asexual blood stage *P. yoelii* parasites obtained from a donor mouse. Parasitemia was monitored every two days after challenge using microscopic examination of blood film with Giemsa staining.

RESULTS

Expression of fusion protein GST-MSP-1$_{19}$ in E. coli

The fusion protein GST-MSP-1$_{19}$ was expressed in *E. coli* BL21 transformed with plasmid pGEX-MSP-1$_{19}$. The transformed BL21 cells were cultured in L-broth until the A_{600} reached 1.0, and then induced with 1.0 mmol/L IPTG for 3 h. Total proteins of BL 21 *E. coli* cells were analyzed by sodium dodecyl sulfate-polyacrylamide gel electrophoresis (SDS-PAGE). As shown in lane 4 of Figure 1, the thick band of the expressed protein showed a molecular weight of 45 ku, matching well with the theoretical value of fusion protein GST-MSP-1$_{19}$. The expressed fusion protein was about 40% of the total protein of *E. coli* cells. Most of the fusion protein was found in inclusion body, but a small fraction was soluble. Glutathione Sepharose-4B affinity chromatography was carried out with the soluble fraction of *E. coli* cell lysate, and the derived fusion protein was used as the positive control of immunoblotting.

Expression of MSP-1$_{19}$ in L. lactis

For the expression of MSP-1$_{19}$ in *L. lactis*, the transformant harboring plasmid pL2-PSGT was cultured overnight at 30 ℃ in MRS medium[26] supplemented with 10 mg/L erythromycin. The cells were collected by centrifuge, and the lysates were analyzed with SDS-PAGE. However, no obvious protein bands around 19 ku were detected. Immunoblotting with antiserum against *P. yoelii* 265-BY was applied to check if there was low-level expression of MSP-1$_{19}$. As a result, the presence of MSP-1$_{19}$ was confirmed by immunoblotting as shown in lane 3 of Figure 2. The stained protein band at 19 ku was a little bit broad. This might be the result of partial degradation of MSP-1$_{19}$ in *E coli* cells. At least part of the expressed MSP-1$_{19}$ was in its native structure, since the antiserum prepared by *P. yoelii* parasites infection is considered to preferentially recognize the MSP-1$_{19}$ fragment located on erythrocyte membrane with the native conformation.

In lane 2 of the positive control, two protein bands were stained: one was at 45 ku, and the other was slightly below 45 ku, but not detectable on SDS-PAGE with Coomassie brilliant blue staining. When fusion protein is isolated from inclusion body of corresponding *E. coli* and refolded by rapid dilution method, only one protein band could be stained (data not shown). Therefore, we concluded that the low molecular weight protein was the degraded fusion protein present in the soluble fraction of *E. coli*.

Evaluation of protective immunity induced by recombinant L. lactis

Previous work of Tian *et al*.[28] indicated that mice with different genetic backgrounds may have quite different responses to *P. yoelii* infection. C57BL/6 mice showed the highest level against challenge with infected erythrocytes after immunization with recombinant proteins consisting of the PyMSP-1 C terminus in adjuvants. In this work, two strains of mice, BALB/c and C57BL/6, were used for oral

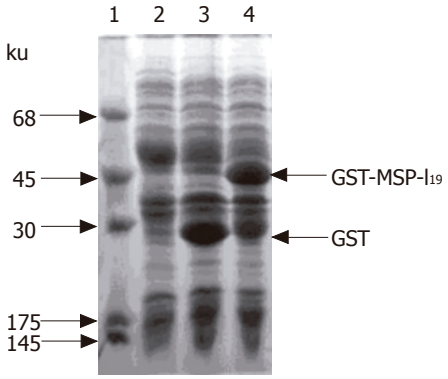

Figure 1 Expression of fusion protein in *E. coli* BL21 cells. Coomassie brilliant blue-stained 12% SDS-polyacrylamide gel. lane 1, protein markers; lane 2, total protein of BL21 cells; lane 3, total protein of *E. coli* BL21 transformed with plasmid pGEX-5X-3 with IPTG induction; lane 4, total protein of *E. coli* BL21 cells harboring plasmid pGEX-MSP-1$_{19}$ after with IPTG induction. The arrows indicate the positions of GST and fusion protein GST-MSP-1$_{19}$.

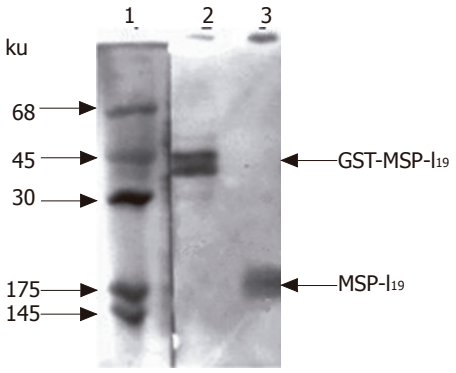

Figure 2 Immunoblotting analysis of MSP-1$_{19}$ expressed in *L. lactis*. Protein samples were first analyzed on 12% SDS-polyacrylamide gel and then transferred on nitrocellulose membrane followed by immunostaining with antiserum prepared by infecting mouse with *P. yoelii* parasites. lane 1, protein markers stained by amido black; lane 2, positive control of fusion protein GST-MSP-1$_{19}$ purified from *E. coli* cell lysate expressing the fusion protein by pGEX-MSP-1$_{19}$; lane 3, total protein of *L. lactis* cells harboring plasmid pL2-PSGT. The arrows indicate the position of fusion protein GST-MSP-1$_{19}$ and MSP-1$_{19}$.

immunization for comparison.

For BALB/c mice, two control groups were designed. Mice were administered with phosphate-buffered saline in control group 1, with 5×10^9 per dose of original *L. lactis* cells in control group 2, and with 5×10^9 per dose of *L. lactis* cells carrying pL2-PSGT construct in the test group, respectively. After seven doses of vaccination, each mouse was challenged with 1×10^5 asexual blood stage parasites. The parasitemias were measured from the next day of parasite challenging. The average and standard deviation of each group are shown in Figure 3. The peak p-arasitemias were 0.8±0.4% at d 4 for test group, 16.0±1.2% at d 8 for control group 1, and 12.0±0.8% at d 8 for control group 2, respectively. There was little difference between the peak parasitemias of the two control groups. Therefore, the non-specific immunity caused by the adjuvanticity of *L. lactis* was little. It should be noted that the appearance of parasitemia in the test group was one-day delayed compared with the control groups. None of the mice in any of the three groups died during the experiment. Overall, the BALB/c mice in all the three groups had the ability to scavenge *P. yoelii* parasites from their bodies by themselves.

For C57BL/6 mice, one control group and two test groups were designed. Mice were administered with 5×10^9 plasmid-harbored *L. lactis* cells per dose in test group 1, and 1×10^8 cells per dose in test group 2. Vaccination was performed by the same protocol for BALB/c mice, and the parasitemias were measured from the next day of parasite challenging. As shown in Figure 4A, the average peak parasitemias for the three groups were 60.8±9.6% for the control group, 41.6±8.8% for test group 1, and 20.8±26.5% for test group 2, respectively. Surprisingly, test group 2 administered with 1×10^8 bacterial cells per dose gained significantly stronger immune protection than test group 1, which was administered with 15 times more bacterial cells per dose. However, the standard deviation of test group 2 was remarkably bigger than the other two groups. This was largely due to the difference between individuals. Another important fact that should be noted was that all the mice in the control group died within 23 d after parasite infection, whereas all the vaccinated mice survived despite the high parasitemias (Figure 4B). After 30 d counting from the day of parasite challenging, malarial parasites were no more detectable in both of the two test groups (data not shown), implicating the complete elimination of the *P. yoelii* parasites.

We also checked the duration of recombinant bacteria in mice gut by investigation of the titers of recombinant bacterial cells in mice feces. After feeding of a single dose of 5×10^9 recombinant cells, the recombinant *L. lactis* reached a peak at 6 h with a density of 1×10^7 cells/g of feces, and then gradually decreased with time. The density of recombinant cells decreased to 1×10^4/g at 48 h, and 1×10^3/g at 72 h. Therefore, the interaction between the host and recombinant bacterial cell could be as long as 3 d per dose.

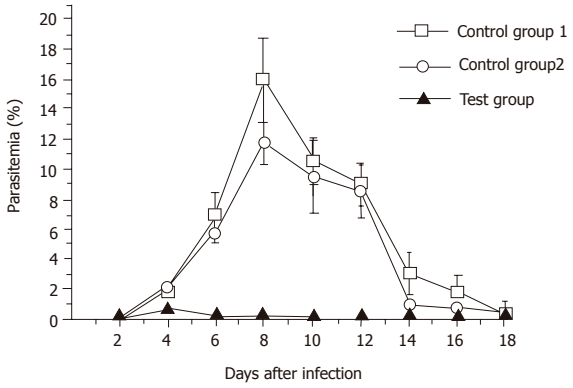

Figure 3 Blood-stage parasitemia of immunized BALB/c mice challenged with *P. yoelii* 265BY parasites. Mice were orally administered with PBS in the control group 1 (-□-), with 5×10^9 per dose of free *L. lactis* cells in the control group 2 (-○-), and with 5×10^9 per dose of *L. lactis* cells carrying pL2-PSGT construct in the test group (-▲-), respectively. Immunization procedure is described in Materials and Methods, and each mouse was challenged with 1×10^5 asexual blood-stage *P. yoelii* parasites.

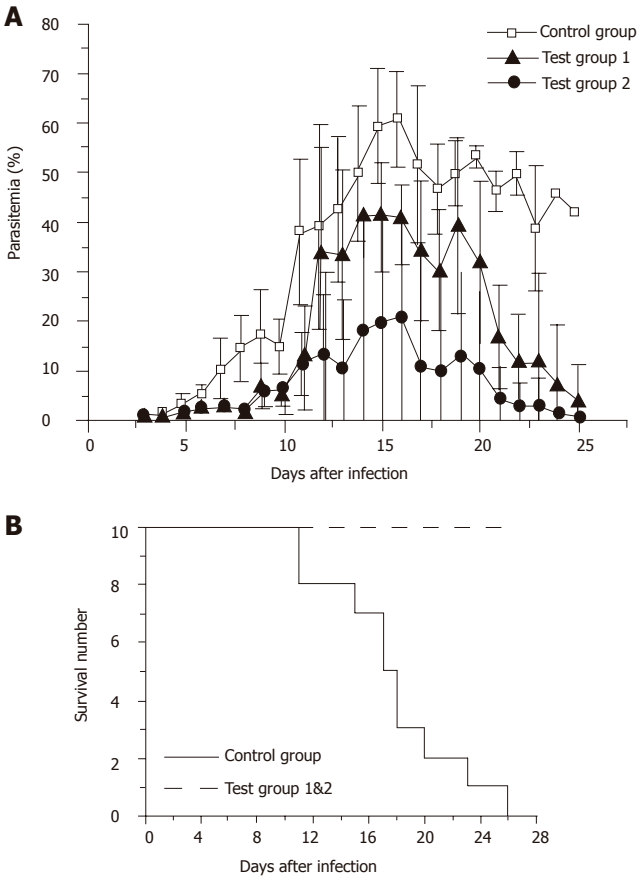

Figure 4 (**A**) Blood-stage parasitemia of immunized C57BL/6 mice challenged with *P. yoelii* 265BY parasites. Mice were orally administered with 5×10^9 per dose of free *L. lactis* cells in the control group (-□-), with 5×10^9 pL2-PSGT plasmid-harbored *L. lactis* cells per dose in the test group 1 (-▲-), and with 1×10^8 cells per dose of pL2-PSGT plasmid-harbored *L. lactis* cells in the test group 2 (-●-). Immunization procedure is described in Materials and Methods, and each mouse was challenged with 1×10^5 asexual blood-stage *P. yoelii* parasites. (**B**) Time course of survivals of the mice in the three groups is indicated in A.

DISCUSSION

It is known that the immunogenicity of soluble protein is low when administered orally but when expressed by genetically engineered bacteria and can be considerably enhanced. To achieve this goal, promoters that can drive the expression of a gene constitutively are essential. S-layer protein is a protein that forms regular crystalline arrays on prokaryotic cell surface. The *slp*A promoter can express the β-lactamase constitutively at a high level in *L. lactis*[27]. However, it failed to express MSP-1$_{19}$ with high efficiency in this study. The expression of MSP-1$_{19}$ in *L. lactis* could be detected only by immunoblotting; therefore, it was estimated at the level of several nanograms per 10^7 bacterial cells.

Unexpectedly, the low-level expression of MSP-1$_{19}$ in *L. lactis* was still able to elicit strong protection against *P. yoelii* infection on both BALB/c and C57BL/6 mice by oral administration. Although BALB/c mice seemed to be able to scavenge the malarial parasites by themselves, the parasitemia was reduced more than 10-folds (less than 1%) in the test group compared with the control groups. In the case of C57BL/6 strain, all the members in the control group died within 26 d after the infection, whereas all the members in the two test groups survived, and the parasites disappeared from both groups one month after the parasite challenging.

The different immune responses of the two C57BL/6 test groups also support the point of view that the expression level of MSP-1$_{19}$ is not critical for the elicitation of immune response, i.e., the group administered with a low dose of the recombinant bacterium gained stronger protection than the group administered with a high dose. The reason for the difference between the two groups is not clear at present; however, this might be partially due to immune tolerance caused by overdose. In the study by Robinson *et al*.[21], expression of tetanus toxin fragment C of *C. tetanus* in the intracellular accumulation of *L. lactis* was up to 3% of soluble cellular protein, and 5×10^9 cells were orally administered per dose to gain complete protection of mice from tetanus. Therefore, the optimal dose and the time schedule for oral administration should be carefully determined for each antigen.

It is striking to find the difference in immune response between the two strains of mice, BACL/c and C57BL/6. Our results partially support the report by Tian *et al*.[28] that C57BL/6 mice are most sensitive to *P. yoelii* infection. In most cases, BALB/c and C3H/He mice are used for protection test of a vaccine. Our results suggest that at least for protection experiments, C57BL/6 mice are better to be used in parallel.

In vaccination experiments with recombinant MPS-1$_{19}$ of *P. yoelii*, the protection effect has been found to be mediated by humoral immune response[15-17]. Robinson *et al*.[21] also reported high titers of IgG against tetanus toxin. We also tried immunoblotting and ELISA test with sera from the survivals of C57BL/6 mice in the test groups (data not shown). Nearly all the mice generated IgG against MSP-1$_{19}$, and there were no significant differences between the two test groups at the titers of IgG. In general, the titers were between 5×10^2 and 3×10^3, lower than the titers reported by Robinson *et al*. On the other hand, Lee *et al*.[23] measured the antigen-specific IgG titers in monkeys immunized with recombinant *L. lactis* bacterium expressing *H pylori UreB* gene, and titers as high as 1×10^5 were detected. However, despite the presence of high-titer antigen-specific IgG, all monkeys were infected after *H pylori* challenge, and there were no differences in the density of colonization. Taking our results obtained from low-dose test group of C57BL/6, we suggest that high-titer antigen-specific IgG should not be considered as the major indicator of the protective immune response. The role of cell-mediated immunity played in live bacteria vaccine should be focused.

ACKNOWLEDGMENTS

The authors thank Professor Weibin Guan of Second Military Medical University for his advices and kind instruction on *P. yoelii* culture. The authors are also grateful to Dr WeiQing Pan of Second Military Medical University for providing monoclonal antibody.

REFERENCES

1 **Cooper JA.** Merozoite surface antigen-1 of *Plasmodium*. Parasitol. *Today* 1993; **9:** 50-54
2 **Holder AA,** Blackman MJ. What is the function of MSP-1 on the malaria merozoite. Parasitol. *Today* 1994; **10:** 182-184
3 **Holder AA,** Freeman RR. Immunization against blood-stage rodent malaria using purified parasite antigens. *Nature* 1981; **294:** 361-364
4 **Siddiqui WA,** Tam LQ, Kramer KJ, Hui GS, Case SE, Yamaga KM, Chang SP, Chan EB, Kan SC. Merozoite surface coat precursor protein completely protects Aotus monkeys against Plasmodium falciparum malaria. *Proc Natl Acad Sci USA* 1987; **84:** 3014-3018
5 **Tian JH,** Kumar S, Kaslow DC, Miller LH. Comparison of protection induced by immunization with recombinant proteins from different regions of merozoite surface protein 1 of Plasmodium yoelii. *Infect Immun* 1997; **65:** 3032-3036
6 **Holder AA,** Sandhu JS, Hillman Y, Davey LS, Nicholls SC, Cooper H, Lockyer MJ. Processing of the precursor to the major merozoite surface antigens of Plasmodium falciparum. *Parasitology* 1987; **94**: 199-208
7 **Blackman MJ,** Ling IT, Nicholls SC, Holder AA. Proteolytic processing of the Plasmodium falciparum merozoite surface protein-1 produces a membrane-bound fragment containing two epidermal growth factor-like domains. *Mol Biochem Parasitol* 1991; **49:** 29-33
8 **Blackman MJ,** Heidrich HG, Donachie S, McBride JS, Holder AA. A single fragment of a malaria merozoite surface protein remains on the parasite during red cell invasion and is the target of invasion-inhibiting antibodies. *J Exp Med* 1990; **172:** 379-382
9 **Miller LH,** Roberts T, Shahabuddin M, McCutchan TF. Analysis of sequence diversity in the Plasmodium falciparum merozoite surface protein-1 (MSP-1). *Mol Biochem Parasitol* 1993; **59:** 1-14
10 **Kang Y,** Long CA. Sequence heterogeneity of the C-terminal, Cys-rich region of the merozoite surface protein-1 (MSP-1) in field samples of Plasmodium falciparum. *Mol Biochem Parasitol* 1995; **73:** 103-110
11 **Renia L,** Ling IT, Marussig M, Miltgen F, Holder AA, Mazier

D. Immunization with a recombinant C-terminal fragment of Plasmodium yoelii merozoite surface protein 1 protects mice against homologous but not heterologous P. yoelii sporozoite challenge. *Infect Immun* 1997; **65:** 4419-4423

12 **Matsumoto S,** Yukitake H, Kanbara H, Yamada T. Recombinant Mycobacterium bovis bacillus Calmette-Guerin secreting merozoite surface protein 1 (MSP1) induces protection against rodent malaria parasite infection depending on MSP1-stimulated interferon gamma and parasite-specific antibodies. *J Exp Med* 1998; **188:** 845-854

13 **Tian JH,** Kumar S, Kaslow DC, Miller LH. Comparison of protection induced by immunization with recombinant proteins from different regions of merozoite surface protein 1 of Plasmodium yoelii. *Infect Immun* 1997; **65:** 3032-3036

14 **Perera KL,** Handunnetti SM, Holm I, Longacre S, Mendis K. Baculovirus merozoite surface protein 1 C-terminal recombinant antigens are highly protective in a natural primate model for human Plasmodium vivax malaria. *Infect Immun* 1998; **66:** 1500-1506

15 **Calvo PA,** Daly TM, Long CA. *Plasmodium yoelii:* the role of the individual epidermal growth factor-like domains of the merozoite surface protein-1 in protection from malaria. *Exp. Parasitol* 1996; **82:** 54-64

16 **Daly TM,** Long CA. Humoral response to a carboxyl-terminal region of the merozoite surface protein-1 plays a predominant role in controlling blood-stage infection in rodent malaria. *J Immunol* 1995; **155:** 236-243

17 **Ling IT,** Ogun SA, Holder AA. The combined epidermal growth factor-like modules of Plasmodium yoelii Merozoite Surface Protein-1 are required for a protective immune response to the parasite. *Parasite Immunol* 1995; **17:** 425-433

18 **Hackett J.** Use of Salmonella for heterologous gene expression and vaccine delivery systems. *Curr Opin Biotechnol* 1993; **4:** 611-615

19 **Holmgren J,** Czerkinsky C. Cholera as a model for research on mucosal immunity and development of oral vaccines. *Curr Opin Immunol* 1992; **4:** 387-391

20 **Mercenier A,** Muller-Alouf H, Grangette C. Lactic acid bacteria as live vaccines. Curr Issues *Mol Biol* 2000; **2:** 17-25

21 **Robinson K,** Chamberlain LM, Schofield KM, Wells JM, Le Page RW. Oral vaccination of mice against tetanus with recombinant Lactococcus lactis. *Nat Biotechnol* 1997; **15:** 653-657

22 **de Vos WM.** Gene expression systems for lactic acid bacteria. *Curr Opin Microbiol* 1999; **2:** 289-295

23 **Lee MH,** Roussel Y, Wilks M, Tabaqchali S. Expression of Helicobacter pylori urease subunit B gene in Lactococcus lactis MG1363 and its use as a vaccine delivery system against H. pylori infection in mice. *Vaccine* 2001; **19:** 3927-3935

24 **O'Sullivan DJ,** Klaenhammer TR. High- and low-copy-number Lactococcus shuttle cloning vectors with features for clone screening. *Gene* 1993; **137:** 227-231

25 **Posno M,** Leer RJ, Luijk N, Giezen MJF, Heuvelmans PTH. M, Lokman BC, Pouwels PH. Incompatibility of *Lactobacillus* vectors with replicons derived from small cryptic lactobacillus plasmids and segregational instability of the introduced vectors. *Applied and Environmental Microbiology* 1991; **57**:1822-1828

26 **Harlow E,** Lane D. Antibodies: a laboratory manual. Cold Spring Harbor: Cold Spring Harbor Lab press 198827. Savijoki K, Kahala M, Palva A. High level heterologous protein production in Lactococcus and Lactobacillus using a new secretion system based on the Lactobacillus brevis S-layer signals. *Gene* 1997; **186:** 255-262

28 **Tian JH,** Miller LH, Kaslow DC, Ahlers J, Good MF, Alling DW, Berzofsky JA, Kumar S. Genetic regulation of protective immune response in congenic strains of mice vaccinated with a subunit malaria vaccine. *J Immunol* 1996; **157:** 1176-1183

Science Editor Wang XL and Li WZ **Language Editor** Elsevier HK

PO Box 2345, Beijing 100023, China
www.wjgnet.com
wjg@wjgnet.com

ELSEVIER

World J Gastroenterol 2005;11(44):6981-6987
World Journal of Gastroenterology ISSN 1007-9327

• *BASIC RESEARCH* •

Exogenous acid fibroblast growth factor inhibits ischemia-reperfusion-induced damage in intestinal epithelium via regulating P53 and P21WAF-1 expression

Wei Chen, Xiao-Bing Fu, Shi-Li Ge, Wen-Juan Li, Tong-Zhu Sun, Zhi-Yong Sheng

Wei Chen, Xiao-Bing Fu, Wen-Juan Li, Tong-Zhu Sun, Zhi-Yong Sheng, Key Research Laboratory of Wound Repair, Burns Institute, 304th Clinical Department, General Hospital of PLA, Beijing 100037, China
Shi-Li Ge, Institute of Radiation Medicine, Beijing 100850, China
Supported by the National Natural Science Foundation of China, No. 30400172, 30230370, and the National Basic Science and Development programme (973 programme, 2005 CB 522603)
Correspondence to: Professor Xiao-Bing Fu, MD, Key Research Laboratory of Wound Repair, Burns Institute, 304th Clinical Department, General Hospital of PLA, 51 Fu cheng Road, Beijing 100037, China. fuxb@cgw.net.cn
Telephone: +86-10-66867396 Fax: +86-10-88416390
Received: 2004-11-12 Accepted: 2005-02-18

Abstract

AIM: To detect the effect of acid fibroblast growth factor (aFGF) on P53 and P21WAF-1 expression in rat intestine after ischemia-reperfusion (I-R) injury in order to explore the protective mechanisms of aFGF.

METHODS: Male rats were randomly divided into four groups, namely intestinal ischemia-reperfusion group (R), aFGF treatment group (A), intestinal ischemia group (I), and sham-operated control group (C). In group I, the animals were killed after 45 min of superior mesenteric artery (SMA) occlusion. In groups R and A, the rats sustained for 45 min of SMA occlusion and were treated with normal saline (0.15 mL) and aFGF (20 μg/kg, 0.15 mL), then sustained at various times for up to 48 h after reperfusion. In group C, SMA was separated, but without occlusion. Apoptosis in intestinal villi was determined with terminal deoxynucleotidyl transferase-mediated dUTP-biotin nick-end labeling technique (TUNEL). Intestinal tissue samples were taken not only for RT-PCR to detect P53 and P21WAF-1 gene expression, but also for immunohistochemical analysis to detect P53 and P21WAF-1 protein expression and distribution.

RESULTS: In histopathological study, ameliorated intestinal structures were observed at 2, 6, and 12 h after reperfusion in A group compared to R group. The apoptotic rates were (41.17±3.49)%, (42.83±5.23)%, and (53.33±6.92)% at 2, 6, and 12 h after reperfusion, respectively in A group, which were apparently lower than those in R group at their matched time points (50.67±6.95)%, (54.17±7.86)%, and (64.33±6.47)%, respectively, (P<0.05)). The protein contents of P53 and P21WAF-1 were both significantly decreased in A group compared to R group (P<0.05) at 2-12 h after reperfusion, while the mRNA levels of P53 and P21WAF-1 in A group were obviously lower than those in R group at 6-12 h after reperfusion (P<0.05).

CONCLUSION: P53 and P21WAF-1 protein accumulations are associated with intestinal barrier injury induced by I-R insult, while intravenous aFGF can alleviate apoptosis of rat intestinal cells by inhibiting P53 and P21WAF-1 protein expression.

Key words: Acid fibroblast growth factor; Ischemia; Reperfusion; P53 gene; P21WAF-1 gene

Chen W, Fu XB, Ge SL, Li WJ, Sun TZ, Sheng ZY. Exogenous acid fibroblast growth factor inhibits ischemia-reperfusion-induced damage in intestinal epithelium via regulating P53 and P21WAF-1 expression. *World J Gastroenterol* 2005; 11(44): 6981-6987
http://www.wjgnet.com/1007-9327/11/6981.asp

INTRODUCTION

Intestinal ischemia-reperfusion (I-R) injury is characterized histologically by inflammation, villus abscission, and mucosal epithelial cell apoptosis[1]. Agents can modulate or prevent apoptosis after I-R[2-6]. Though the mechanisms of action are diverse, all these agents ultimately show their potent antiapoptotic properties that account, at least in part, for their protective effects. Accumulation of P53 protein, which is well known as a tumor suppressor gene product, plays a central role as the initiator of the intrinsic apoptotic cascade triggered by a wide variety of insults[7-10]. In addition, a role of P53 in regulating the extrinsic receptor-mediated apoptotic pathway has also been reported[11]. P21WAF-1, which is a downstream mediator of P53 function, plays a key role in determining the ultimate sensitivity of cells to myriad stimuli and insults that induce apoptosis[12-14]. Thus, P53 and P21WAF-1 are poised as the ideal candidates for mediating apoptosis after I-R, a setting

where many insults coexist.

Acid fibroblast growth factor (aFGF) is a mitogen *in vitro* for most of the ectoderm- and mesoderm-derived cell lines. In addition, this factor shows a wide range of endocrine-like activities[15,16]. As a multiple function growth factor, aFGF is involved in embryo development and tissue repair[17,18]. Previous studies have shown that intravenous administration of exogenous aFGF could improve the physiological functions of intestine after I-R injury[19,20]. Since the mechanism by which aFGF inhibits apoptosis is unknown, we investigated the effects of aFGF on gene expression and protein contents of P53 and P21WAF-1 underlying the protective mechanisms of aFGF against intestinal I-R injury.

MATERIALS AND METHODS

Animal model and experimental design

Healthy male Wistar rats weighing 220±20 g (Animal Centre, Academy of Military Medical Sciences, Beijing) were used in this study. Animals were housed in wire-bottomed cages placed in a room illuminated from 08:00 to 20:00 (12:12-h light-dark cycle) and maintained at 21±1 ℃. Rats were allowed free access to water and food. The animals were anesthetized with 3% sodium pentobarbital (40 mg/kg) and underwent laparotomy. The superior mesenteric artery (SMA) was identified and freed by blunt dissection. A micro-bulldog clamp was placed at the root of SMA to cause complete cessation of blood flow for 45 min, and thereafter the clamp was loosened to form reperfusion injury. The animals were randomly divided into four groups, namely intestinal ischemia-reperfusion group (R), intestinal ischemia group (I), reconstructive aFGF treatment group (A) and sham-operated control group (C). In group I, the animals were killed after 45 min of SMA occlusion. In groups R and A, the rats sustained for 45 min of SMA occlusion and were treated with 0.15 mL normal saline and 0.15 mL saline plus aFGF (20 μg/kg) injected from tail vein, then sustained for 15, 30 min, 1, 2, 6, 12, 24, and 48 h of reperfusion respectively. In C group, SMA was separated, but without occlusion, and samples were taken after exposure of SMA for 45 min. In groups R and A, rats were killed at different time points after reperfusion, and intestinal tissue biopsies were taken. Six specimens of the intestine were obtained at each time point from six rats. When any rat died during the study, additional rats were used until six specimens could be obtained from six rats at each time point. A small part of the intestine specimen was fixed with 10% neutral buffered formalin for immunohistochemical detections of intestinal epithelial apoptosis, and protein expression of P53 and P21WAF-1. The remaining tissue samples were placed in liquid nitrogen for RT-PCR to detect P53 and P21WAF-1 gene expression.

Histopathological study

Formalin-fixed, paraffin-embedded intestinal samples were cut into 5-μm-thick sections, deparaffinized in xylene, rehydrated in graded ethanol, and then stained with hematoxylin-eosin (HE) for histological observation under light microscope.

In situ detection of cell death

The apoptotic cells in intestinal tissues were detected by the terminal deoxynucleotidyl transferase (TdT)-mediated dUTP-biotin nick-end labeling (TUNEL) method. Specimens were dewaxed and immersed in phosphate-buffered saline containing 0.3% hydrogen peroxide for 10 min and then incubated with 20 μg/mL proteinase K for 15 min. Seventy-five microliters of equilibration buffer was applied directly onto the specimens for 10 min, followed by 55 μL of TdT enzyme and incubation, which were then incubated at 37 ℃ for 1 h. The reaction was terminated by transferring the slides to prewarmed stop/wash buffer for 30 min at 37 ℃. The specimens were covered with a few drops of rabbit serum and incubated for 20 min and then covered with 55 μL of anti-digoxigenin peroxidase and incubated for 30 min. Specimens were then soaked in Tris buffer containing 0.02% diaminobenzidine and 0.02% hydrogen peroxide for 1 min to achieve color development. Finally, the specimens were counterstained by immersion in hematoxylin. The cells with clear nuclear labeling were defined as TUNEL-positive cells. The results of positive cells and their distribution were observed under 400× microscope. Sixty intestinal villi per time point were required for counting, and then the apoptotic ratios were calculated and analyzed.

Immunohistochemistry

Immunostaining for proteins of P53 and P21WAF-1 was performed in paraffin sections with a high-temperature antigen-unmasking method in citrate buffer and ABC peroxidase, using P21WAF-1 monoclonal mouse antibody (Santa Cruz Cor, sc-6246) and P53 polyclonal rabbit antibody (Santa Cruz Cor, sc-6243) against antigens (1:100 in PBS). Tissues were fixed overnight in 4% paraformaldehyde, dehydrated, and embedded in paraffin. Five-micrometer thick sections were deparaffinized and rehydrated using graded alcohol concentrations. Antigen retrieval was performed by incubation in 100 mmol/L sodium citrate, pH 6.0, at 90 ℃for 20 min. Then, sections were blocked with 5% normal swine serum in PBS for 30 min at 25 ℃, followed by incubation with primary antibodies at a concentration of 5 μg/mL overnight at 4 ℃. Control slides were incubated with PBS without primary antibodies. Tissue sections were then incubated for 60 min with biotinylated secondary antibody. After being washed in PBS, the sections were exposed to acidin-biotin complex for 60 min, reacted with 0.05% (wt/vol) DAB in 50 mmol/L Tris-HCl (pH 7.4) with 0.1% (vol/vol) hydrogen peroxide for 5 min and counterstained with hematoxylin. The results of positive staining cells and their distribution were observed under 400× microscope. Sixty intestinal villi per time point were required for counting, and then the ratio of positive cells was calculated and analyzed.

RNA extraction and RT-PCR analysis

Tissue total RNA was extracted using TRIzol reagent

(Gibco BRL, USA). RNA was serially diluted with water containing 1 unit RNase inhibitor per μL and 3 mmol/L dithiothreitol (DTT). One microliter RNA, 1 μL oligo (dT12-18), 1 μL avian myeloblastosis virus reverse transcriptase (AMV-RT), 2 μL 10 mmol/L deoxynucleoside triphosphate (dNTP), 2 μL 0.1 mol/L DTT, 4 μL 5× buffer, and sterilized distilled water up to a total volume of 20 μL were incubated at 37 ℃ for 60 min. Subsequently, 2 μL of each reaction product was amplified in 50 μL of a PCR mixture. Then 29 cycles were performed with a Perkin-Elmer Cetus/DNA thermal cycler (Takara Shuzo Co., Tokyo, Japan) at 94 ℃ for 1 min, at 50 ℃ for 1 min, at 72 ℃for 1 min, and then at 72 ℃ for 10 min at the end of the procedure. In this study, β-actin, which is ubiquitously expressed, was used as a positive control in a pilot study before formal experimentation, and PCR reaction for each primer set was repeated four times to verify the reproducibility of results. After PCR, 5-μL sample aliquots was electrophoresed on a 2% agarose gel for 30 min, stained with ethidium bromide and photographed. Densitometry was done with a Bechman densitometer. The level of gene transcription was expressed as the ratio of gray density of the gene to β-actin.

Statistical analysis

All values were expressed as mean±SD. The statistical significance was determined by one-way analysis of variance (ANOVA) followed by the Student's and Newman-Keuls multiple comparison tests. $P<0.05$ was considered statistically significant.

RESULTS

Histopathological findings

After the SMA was clamped near its origin from the aorta, the entire small intestine showed a dark purple, cyanotic color within 45 min. The histological evaluation revealed that damage to the small intestine in I group was small, with slightly edematous villus tips and intact crypts just after the ischemic period. Two hours after reperfusion, partial loss of the mucosa could be observed. During 6-12 h after reperfusion, the damage of intestinal epithelial cells, hemorrhage and apoptosis could be found accompanied with inflammatory cells infiltrated into the intestinal wall, and the crypt-villus structure was seriously spoiled. In the period of 24-48 h after reperfusion, the mucosal integrity was partially restored. Histological structure of the intestinal mucosa was markedly improved after administration of aFGF. The protective function of aFGF on intestinal mucosa was very effective 2-12 h after reperfusion. The structures of crypt and villus were both guarded, with less damage of intestinal mucosa in A group compared to R group.

Change of cellular apoptotic rates

To quantify the extent of apoptosis after ischemia and reperfusion, TUNEL reaction was performed in serial sections prepared from the middle quarter of the small intestine (jejunum). The time, when the animals were killed after a 45-min SMA occlusion followed by reperfusion, varied to further define the apoptotic response. Statistically significant increase in TUNEL-positive cells was not detectable until 1 h after reperfusion and reached its peak at 12 h. The cellular apoptotic rate in intestinal mucosa at 12 h after reperfusion was 3.3 times of that in C group. After reperfusion for 24 and 48 h, the mucosal apoptotic rates were restored to the level of C group. Administration of aFGF resulted in statistically significant decrease of the apoptotic rates compared to R group 2-12 h after reperfusion ($P<0.05$). No statistically significant decrease of apoptotic rates was observed at 24 and 48 h after reperfusion (Table 1).

Table 1 Effect of aFGF on apoptotic rates in intestinal mucosa after ischemia-reperfusion insult (n = 6, mean±SD, %)

Groups	R group	A group
C group	19.67±3.50	19.67±3.50
I group	27.67±9.63	27.67±9.63
15 min after reperfusion	29.50±5.61	25.17±6.43
30 min after reperfusion	28.00±7.02	26.00±4.86
1 h after reperfusion	34.67±5.47[a]	29.83±7.08
2 h after reperfusion	50.67±6.95[a]	41.17±3.49[ac]
6 h after reperfusion	54.17±7.86[a]	42.83±5.23[ac]
12 h after reperfusion	64.33±6.47[a]	53.33±6.92[ac]
24 h after reperfusion	28.50±5.47	23.33±3.83
48 h after reperfusion	26.00±5.76	22.00±4.60

[a]$P<0.05$ *vs* C group; [c]$P<0.05$ *vs* R group at matched time point.

Expression characteristics of P53 and P21WAF-1 proteins

Quantitative immunohistochemical results for P53 and P21WAF-1 proteins are summarized in Table 2. Protein expression levels of P53 were weaker in the sham-operated intestinal and ischemic tissues, and positive particles were mainly located in the epithelial cells of the upper part of villi. However, the positive cellular rates elevated with the increment of duration after reperfusion injury. In the period of 1-12 h after reperfusion, P53 protein was expressed at a dramatically higher level in comparison to C group ($P<0.05$) and the maximum level was 2.1-fold of C group at 6 h after reperfusion. The positive signals of P53 were mostly distributed in the nuclei and cytoplasm of epithelial cells of villi and crypts. At 24-48 h after reperfusion, the positive cellular rates were not substantially changed compared to C group. Treatment with aFGF could apparently inhibit the protein contents of P53 in intestinal mucosal epithelial cells 2-12 h after reperfusion in comparison to R group at different matched time points ($P<0.05$, Figures 1A-1C). The levels of P21WAF-1 protein were also significantly increased 2-12 h after reperfusion with a peak at 12 h after reperfusion (1.5-fold of C group, $P<0.05$). The positive particles of P21WAF-1 were mainly localized in the cytoplasm and nuclei of intestinal epithelial cells (Figures 1D-1F). By 24-48 h after I-R, the P21WAF-1 levels tended to normalize back to baseline of C group ($P>0.05$). Compared to the saline-treated group, the positive cellular rates of P21WAF-1 were significantly

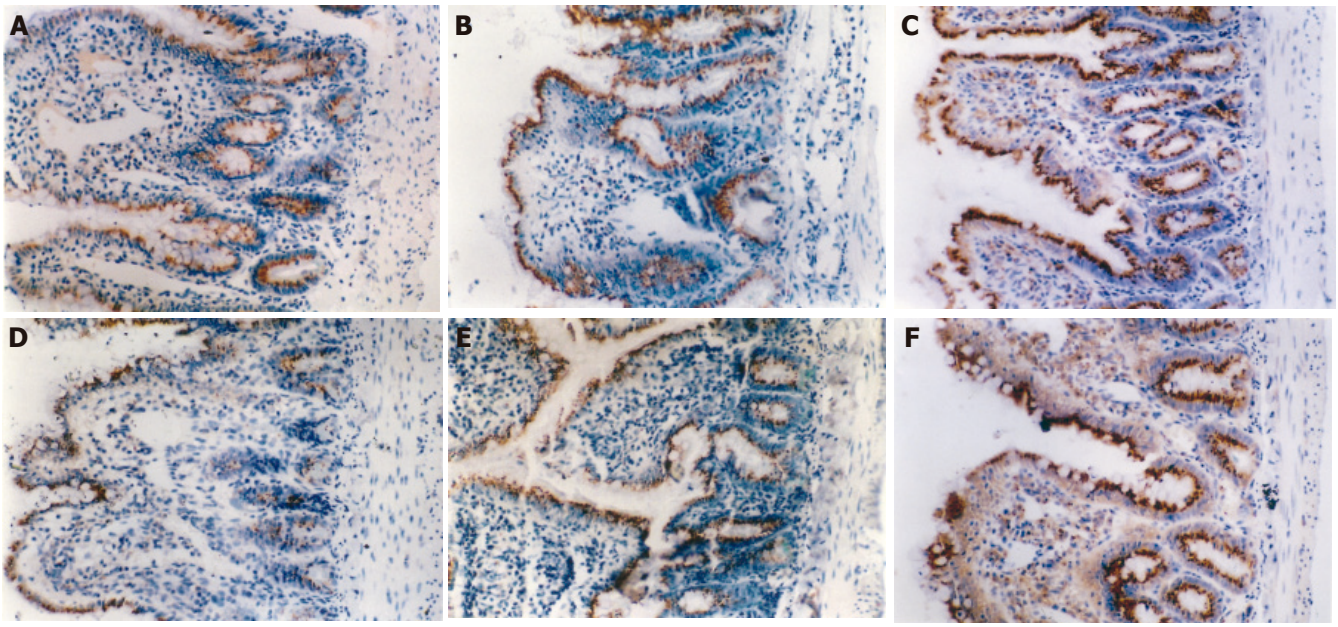

Figure 1 Expression of P53 and P21^{WAF-1} protein in C group (**A** and **D**, respectively), A group (**B** and **E**, respectively) and R group (**C** and **F**, respectively).

Table 2 Effect of aFGF on protein expression of P53 and P21WAF-1 in intestinal mucosa after ischemia-reperfusion (n = 6, mean±SD, %)

Groups	P53		P21WAF-1	
	R group	A group	R group	A group
C group	23.67±4.55	23.67±4.55	32.50±3.94	32.50±3.94
I group	29.17±4.45	29.17±4.45	35.83±4.83	35.83±4.83
15 min after reperfusion	27.00±3.90	23.83±5.08	34.67±4.76	31.50±4.37
30 min after reperfusion	30.67±3.98	26.67±3.78	36.17±3.31	37.00±4.86
1 h after reperfusion	33.17±3.19[a]	32.50±3.27[a]	39.83±4.58	37.83±4.36
2 h after reperfusion	40.33±3.50[a]	33.83±5.04[a,c]	49.33±4.18[a]	41.83±6.65[a,c]
6 h after reperfusion	50.50±4.23[a]	42.67±3.88[a,c]	53.00±4.39[a]	44.67±4.46[a,c]
12 h after reperfusion	45.67±5.65[a]	37.50±4.81[a,c]	57.50±3.62[a]	49.33±3.78[a,c]
24 h after reperfusion	30.00±6.13	25.33±3.33	34.50±6.02	30.00±3.79
48 h after reperfusion	28.17±8.89	25.67±4.32	33.83±7.31	30.67±4.18

[a]P<0.05 *vs* C group; [c]P<0.05 *vs* R group at matched time point.

Table 3 Effect of aFGF on mRNA contents of P53 and P21WAF-1 genes in intestinal mucosa after ischemia-reperfusion (n = 6, mean±SD, %)

Groups	P53		P21WAF-1	
	R group	A group	R group	A group
C group	23.5±6.0	22.4±2.5	26.7±2.0	24.6±4.1
I group	38.9±5.1[a]	34.8±4.2[a]	32.6±2.0[a]	31.7±2.0[a]
15 min after reperfusion	53.9±3.9[a]	45.8±10.7[a]	33.4±2.3[a]	24.0±3.4[c]
30 min after reperfusion	34.0±4.4[a]	41.9±5.2[a,c]	23.3±4.2	22.9±2.0
1 h after reperfusion	48.5±3.2[a]	44.7±5.4[a]	24.8±2.3	23.8±3.2
2 h after reperfusion	46.7±5.4[a]	41.3±6.3[a]	26.5±2.7	24.9±3.0
6 h after reperfusion	48.8±5.2[a]	38.3±4.7[a,c]	30.8±3.0[a]	20.9±2.6[c]
12 h after reperfusion	51.0±4.5[a]	34.1±4.8[a,c]	32.7±1.6[a]	21.9±2.8[c]
24 h after reperfusion	55.3±7.3[a]	56.9±5.3[a]	28.8±3.1	28.5±5.0
48 h after reperfusion	56.4±8.3[a]	61.0±4.0[a]	29.0±2.3	28.9±3.8

[a]P<0.05 *vs* C group; [c]P<0.05 *vs* R group at matched time point.

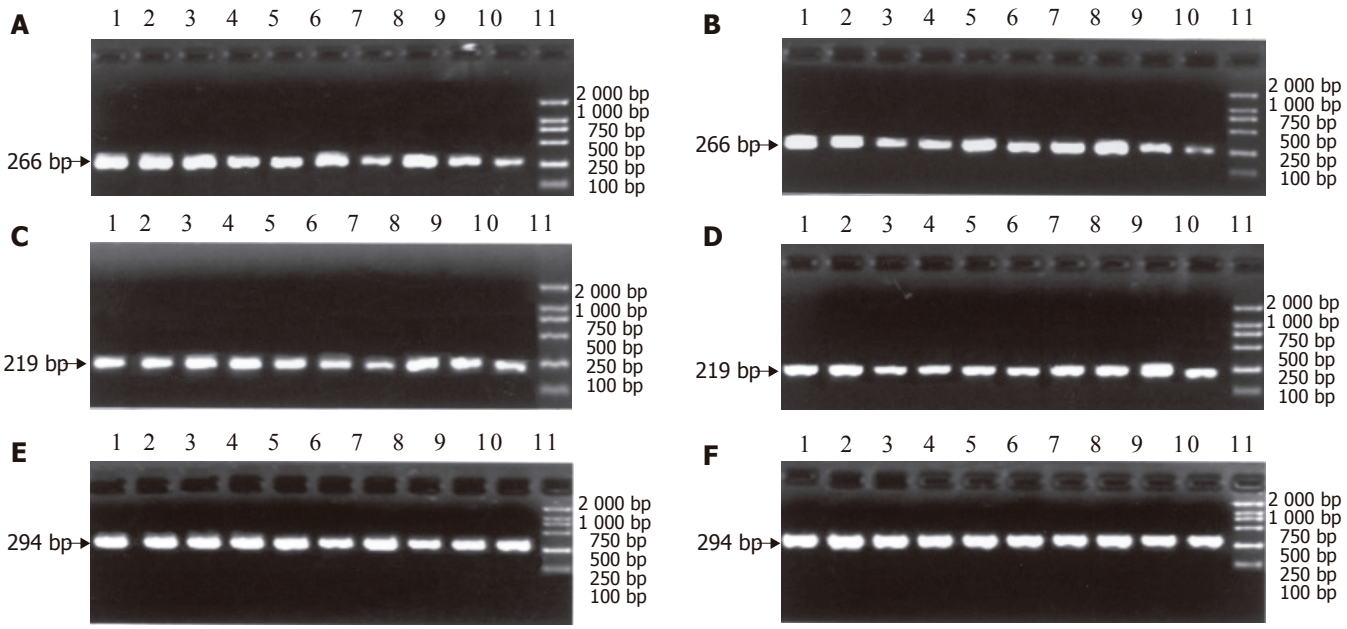

Figure 2 Expression of P53, $P21^{WAF-1}$, and β-actin genes in normal saline-treated (**A**, **C**, **E**, respectively) and aFGF treated (**B**, **D**, **F**, respectively) rat intestinal villi. Bar indicates the size of RT-PCR cDNA products. Lanes 1-8: 48, 24, 12, 6, 2, 1 h, and 30, 15 min after reperfusion; lane 9: ischemia group; lane 10: sham-operated control group; lane 11: DL 2000 marker.

lower 2 to 12 h after reperfusion in aFGF-treated group ($P<0.05$, Table 2).

Expression characteristics of P53 and P21WAF-1mRNA

We investigated the gene expression of P53 and P21WAF-1 in differentially treated intestinal villi through RT-PCR analysis (Table 3). The P53 gene amplification product was composed of 266 bp (Figures 2A-2C). Expression of this gene was remarkably and rapidly increased in intestinal mucosa after ischemia during the whole period of reperfusion. After aFGF administration, the mRNA level of P53 in villus cells was lower than that in normal saline-treated group. Especially at 30 min, 6 and 12 h after reperfusion, the discrepancy of P53 expression levels between the two groups was apparent ($P<0.05$, Table 3). Figures 2D-2F show that the length of RT-PCR products of P21WAF-1 was 219 bp. The P21WAF-1 gene was expressed at a pronounced high level in villi compared to sham-operated group at 15 min, 6 and 12 h after reperfusion ($P<0.05$). After treatment with aFGF, although P21WAF-1 gene expression was not substantially decreased after reperfusion in A group compared to C group, the content of P21WAF-1 gene transcript were markedly reduced at 15 min, 6 and 12 h after reperfusion in A group compared to R group ($P<0.05$, Table 3).

DISCUSSION

The major clinical disorders involving gastrointestinal circulation are hemorrhage and ischemia. It is well recognized that the small intestine is extremely sensitive to the deleterious effects of I-R, and it has been clearly demonstrated that I-R causes both mucosal and vascular injury within the small intestine[21,22]. Intestinal I-R injury may also cause release of bacteria and toxins from the gut into the host blood circulation and changes of inflammatory factors, cytokines, and growth factors, resulting in damage to the intestinal barrier. In the current study, we found that I-R, following occlusion of the SMA, induced apoptosis in the intestinal mucosal cells. Results of TUNEL method displayed that the apoptotic rate increased during ischemia and peaked at 12 h after reperfusion. The locations of apoptotic cells were extended from villus tip in sham-operated rats to the whole structure of mucosa in rats insulted by I-R. The quantification of apoptosis was corroborated with histological examination using HE staining. It was also found that administration of exogenous aFGF could reduce the intestinal injury caused by I-R insult. The antiapoptotic effect of aFGF was achieved by inhibiting the expression of some apoptosis-related genes. Previous experimental data showed that the change of expression of apoptosis-related genes played a pivotal role in alleviating cardiac, myocardial[23], cerebral[24,25], muscular[26], cutaneous[27], and adrenal cortex[28] apoptosis induced by I-R, which was in agreement with our results that I-R promoted P53 and P21WAF-1 expression.

After 45 min of ischemia, although gene expression of P53 was quickly increased, and lasted for the whole period after reperfusion, P21WAF-1 gene was only strongly expressed at 15 min, 6 h, and 12 h after reperfusion. The difference of time in the kinetics between these two genes may indicate that P21WAF-1 gene transcription might be activated in a P53-independent manner. Moreover, although protein levels of P53 and P21WAF-1 accumulated after reperfusion, there was a time lag in the

onset of elevation and the peak time point between these two proteins. These results indicate that the P21WAF-1 translation is activated by the elevated P53 protein contents. In this current study, we also found that the kinetics between the levels of P21WAF-1 and P53 protein expression and the apoptotic rate were similar, suggesting that protein levels of P21WAF-1 and P53 might be related to cell apoptosis. When severe histological damage of intestinal villi 2-12 h after reperfusion is considered, DNA damage in the intestinal cells cannot be repaired, resulting in cell apoptosis. Our study also found that the rate of apoptosis in intestinal villi insulted by I-R was significantly decreased by aFGF administration. aFGF could inhibit the increments of P21WAF-1 and P53 protein expression 2-12 h after reperfusion in comparison to normal saline treatment, suggesting that the decrement of P21WAF-1 and P53 protein contents caused by aFGF might be one of the mechanisms attenuating ischemia-reperfusion-induced apoptosis.

Studies have demonstrated that the activated neutrophils and oxygen free radicals produced in ischemic tissue during reperfusion play an important role in developing the injury of the intestine[26,28]. Free radicals are produced mainly by the activated neutrophils and xanthine dehydrogenase/xanthine oxidase enzyme system after reperfusion, but the free radicals produced from the neutrophils play a more important role than xanthine oxidase in mediating tissue-destroying events[29]. Our histopathological study showed that leukocyte sequestration into the villi was evident 6-12 h after reperfusion, and exogenous aFGF could alleviate leukocyte infiltration into intestinal villi. It is well known that free radicals cause DNA damage, and the series of cell reactions mediated by P53 might be investigated by free radicals produced during the reperfusion process. The protective mechanism of aFGF might inhibit P53 and P21WAF-1 protein translation by scavenging free radicals. The current study also demonstrated that apoptosis occurred 1 h after reperfusion and returned to baseline values after 24 h, suggesting that I-R-induced intestinal apoptosis and mucosal recovery is a rapid process. The mechanism underlying this interesting kinetics of induction of mucosal cell apoptosis and restoration is unclear. A time-dependent increment in protein expression of apoptosis-promoting factors including P53 and P21WAF-1 during ischemia and early phases of reperfusion, and decrement with prolonged reperfusion might be an alternative cause. Therefore, the protective effect of aFGF against intestinal I-R insult might be not only associated with inhibiting epithelial cell apoptosis but also related to inducing mucosal cell restoration.

In conclusion, the protective effects of aFGF against I-R in rat intestinal villi might be partially due to its ability to inhibit I-R-induced apoptosis. aFGF exerts its antiapoptotic effect via regulating P53 and P21WAF-1gene transcription and translation. The precise mechanisms of aFGF underlying the inhibition of intestinal I-R injury and attenuation of apoptosis need further investigation.

REFERENCES

1 **Fu XB,** Yang YH, Sun TZ, Chen W, Li JY, Sheng ZY. Rapid mitogen-activated protein kinase by basic fibroblast growth factor in rat intestine after ischemia/reperfusion injury. *World J Gastroenterol* 2003; **9:** 1312-1317

2 **Palmen M,** Daemen MJ, De Windt LJ, Willems J, Dassen WR, Heeneman S, Zimmermann R, Van Bilsen M, Doevendans PA. Fibroblast growth factor-1 improves cardiac functional recovery and enhances cell survival after ischemia and reperfusion: a fibroblast growth factor receptor, protein kinase C, and tyrosine kinase-dependent mechanism. *J Am Coll Cardiol* 2004; **44:** 1113-1123

3 **Kohda Y,** Chiao H, Star RA. alpha-Melanocyte-stimulating hormone and acute renal failure. *Curr Opin Nephrol Hypertens* 1998; **7:** 413-417

4 **Oskarsson HJ,** Coppey L, Weiss RM, Li WG. Antioxidants attenuate myocyte apoptosis in the remote non-infarcted myocardium following large myocardial infarction. *Cardiovasc Res* 2000; **45:** 679-687

5 **Schierle GS,** Hansson O, Leist M, Nicotera P, Widner H, Brundin P. Caspase inhibition reduces apoptosis and increases survival of nigral transplants. *Nat Med* 1999; **5:** 97-100

6 **Daemen MA,** de Vries B, Buurman WA. Apoptosis and inflammation in renal reperfusion injury. *Transplantation* 2002; **73:** 1693-1700

7 **Kelly KJ,** Plotkin Z, Vulgamott SL, Dagher PC. P53 mediates the apoptotic response to GTP depletion after renal ischemia-reperfusion: protective role of a p53 inhibitor. *J Am Soc Nephrol* 2003; **14:** 128-138

8 **Shirangi TR,** Zaika A, Moll UM. Nuclear degradation of p53 occurs during down-regulation of the p53 response after DNA damage. *FASEB J* 2002; **16:** 420-442

9 **Chen W,** Fu X, Sun TZ, Sun XQ, Zhao ZL, Sheng ZY. Different expression of p53 and c-myc in hypertrophic scars versus normal skins and their effects on apoptosis in scars. *Zhongguo Wei Zhong Bing Ji Jiu Yi Xue* 2002; **14:** 100-103

10 **Chen W,** Fu X, Sun TZ, Sun XQ, Zhao ZL, Sheng ZY. Characteristics of proliferating cell nuclear antigen and p53 expression in fetal and postnatal skins and their biological significance. *Zhongguo Wei Zhong Bing Ji Jiu Yi Xue* 2002; **14:** 654-657

11 **Ryan KM,** Ernst MK, Rice NR, Vousden KH. Role of NF-kappaB in p53-mediated programmed cell death. *Nature* 2000; **404:** 892-897

12 **Corbucci GG,** Perrino C, Donato G, Ricchi A, Lettieri B, Troncone G, Indolfi C, Chiariello M, Avvedimento EV. Transient and reversible deoxyribonucleic acid damage in human left ventricle under controlled ischemia and reperfusion. *J Am Coll Cardiol* 2004; **43:** 1992-1999

13 **Laubriet A,** Fantini E, Assem M, Cordelet C, Teyssier JR, Athias P, Rochette L. Changes in HSP70 and P53 expression are related to the pattern of electromechanical alterations in rat cardiomyocytes during simulated ischemia. *Mol Cell Biochem* 2001; **220:** 77-86

14 **Didenko VV,** Wang X, Yang L, Hornsby PJ. Expression of p21(WAF1/CIP1/SDI1) and p53 in apoptotic cells in the adrenal cortex and induction by ischemia/reperfusion injury. *J Clin Invest* 1996; **97:** 1723-1731

15 **Cuevas P,** Carceller F, Martinez-Coso V, Asin-Cardiel E, Gimenez-Gallego G. Fibroblast growth factor cardioprotection against ischemia-reperfusion injury may involve K+ ATP channels. *Eur J Med Res* 2000; **5:** 145-149

16 **Cuevas P,** Carceller F, Martinez-Coso V, Cuevas B, Fernandez-Ayerdi A, Reimers D, Asin-Cardiel E, Gimenez-Gallego G. Cardioprotection from ischemia by fibroblast growth factor: role of inducible nitric oxide synthase. *Eur J Med Res* 1999; **4:** 517-524

17 **Chen W,** Fu XB, Ge SL, Zhou G, Han B, Sun TZ, Sheng ZY. Gene expression of angiogenesis-related factors in fetal skin at

different developmental stages and childhood skin. *Zhongguo Wei Zhong Bing Ji Jiu Yi Xue* 2004; **16:** 85-89
18 **Cuevas P,** Martinez-Coso V, Fu X, Orte L, Reimers D, Gimenez-Gallego G, Forssmann WG, Saenz De Tejada I. Fibroblast growth factor protects the kidney against ischemia-reperfusion injury. *Eur J Med Res* 1999; **4:** 403-410
19 **Weng LX,** Fu XB, Li XX, Sun TZ, Zheng SY, Chen W. Effects of acidi fibroblast growth factor on hepatic and renal functions after intestinal ischemia/reperfusion injury. *Zhongguo Wei Zhong Bing Ji Jiu Yi Xue* 2004; **16:** 19-21
20 **Fu X,** Cuevas P, Gimenez-Gallego G, Wang Y, Sheng Z. The effects of fibroblast growth factors on ischemic kidney, liver and gut injuries. *Chin Med J (Engl)* 1998; **111:** 398-403
21 **Itoh H,** Yagi M, Hasebe K, Fushida S, Tani T, Hashimoto T, Shimizu K, Miwa K. Regeneration of small intestinal mucosa after acute ischemia-reperfusion injury. *Dig Dis Sci* 2002; **47:** 2704-2710
22 **Itoh H,** Yagi M, Fushida S, Tani T, Hashimoto T, Shimizu K, Miwa K. Activation of immediate early gene, c-fos, and c-jun in the rat small intestine after ischemia/reperfusion. *Transplantation* 2000; **69:** 598-604
23 **Chang TH,** Liu XY, Zhang XH, Wang HL. Effects of dl-praeruptorin A on interleukin-6 level and Fas, bax, bcl-2 protein expression in ischemia-reperfusion myocardium. *Acta Pharmacol Sin* 2002; **23:** 769-774
24 **Zhou H,** Ma Y, Zhou Y, Liu Z, Wang K, Chen G. Effects of magnesium sulfate on neuron apoptosis and expression of caspase-3, bax and bcl-2 after cerebral ischemia-reperfusion injury. *Chin Med J (Engl)* 2003; **116:** 1532-1534
25 **Wang Y,** Hayashi T, Chang CF, Chiang YH, Tsao LI, Su TP, Borlongan C, Lin SZ. Methamphetamine potentiates ischemia/reperfusion insults after transient middle cerebral artery ligation. *Stroke* 2001; **32:** 775-782
26 **Hatoko M,** Tanaka A, Kuwahara M, Yurugi S, Iioka H, Niitsuma K. Difference of molecular response to ischemia-reperfusion of rat skeletal muscle as a function of ischemic time: study of the expression of p53, p21(WAF-1), Bax protein, and apoptosis. *Ann Plast Surg* 2002; **48:** 68-74
27 **Hatoko M,** Tanaka A, Kuwahara M, Yurugi S. Molecular response to ischemia-reperfusion of rat skin: study of expression of p53, p21WAF-1, and Bax proteins, and apoptosis. *Ann Plast Surg* 2001; **47:** 425-430
28 **Baskin DS,** Ngo H, Didenko VV. Thimerosal induces DNA breaks, caspase-3 activation, membrane damage, and cell death in cultured human neurons and fibroblasts. *Toxicol Sci* 2003; **74:** 361-368
29 **Kerrigan CL,** Stotland MA. Ischemia reperfusion injury: a review. *Microsurgery* 1993; **14:** 165-175

Science Editor Wang XL, Li WZ and Guo SY **Language Editor** Elsevier HK

PO Box 2345, Beijing 100023, China
www.wjgnet.com
wjg@wjgnet.com

ELSEVIER

World J Gastroenterol 2005;11(44):6988-6994
World Journal of Gastroenterology ISSN 1007-9327

• *CLINICAL RESEARCH* •

Anti-*Saccharomyces cerevisiae* antibody titers are stable over time in Crohn's patients and are not inducible in murine models of colitis

Stefan Müller, Maya Styner, Beatrice Seibold-Schmid, Beatrice Flogerzi, Michael Mähler, Astrid Konrad, Frank Seibold

Stefan Müller, Maya Styner, Beatrice Seibold-Schmid, Beatrice Flogerzi, Astrid Konrad, Frank Seibold, Division of Gastroenterology, Department of Clinical Research, University Hospital Bern
Michael Mähler, Central Animal Facility and Institute for Laboratory Animal Science, Medical School Hannover, Germany
Supported by the Swiss National Science Foundation grant n° SNSF 31-59031.99 to F. Seibold
Co-first-authors: Stefan Müller and Maya Styner
Co-correspondence: Stefan Müller, stefan.mueller@dkf.unibe ch
Correspondence to: Professor Frank Seibold, University Hospital Bern, Department of Gastroenterology, Freiburgstr. 10, 3010 Bern, Switzerland. frank.seibold@insel.ch
Telephone: +41-31-6328025 Fax: +41-31-6323671
Received: 2005-03-11 Accepted: 2005-07-01

Abstract

AIM: To investigate ASCA production over time in CD and murine colitis in order to further our understanding of their etiology.

MATERIALS AND METHODS: Sixty-six CD patients were compared to ulcerative colitis (UC) and irritable bowel syndrome patients with respect to ASCA production as measured by ELISA. ASCA IgG or IgA positivity as well as change in titers over a period of up to 3 years ($\Delta_{IgG/A}$) was correlated with clinical parameters such as CD activity index (CDAI) and C-reactive protein levels (CRP). Moreover, two murine models of colitis (DSS and IL-10 knock out) were compared to control animals with respect to ASCA titers after oral yeast exposure.

RESULTS: ASCA IgG and IgA titers are stable over time in CD and non-CD patients. Fistular disease was associated with a higher rate of ASCA IgA positivity (P = 0.014). Ileal disease was found to have a significant influence on the Δ_{IgG} of ASCA (P = 0.032). There was no correlation found between ASCA positivity or $\Delta_{IgG/A}$ and clinical parameters of CD: CDAI and CRP. In mice, neither healthy animals nor animals with DSS-induced or spontaneous colitis exhibited a marked increase in ASCA titers after high-dose yeast exposure. On the other hand, mice immunized intraperitoneally with mannan plus adjuvant showed a marked and significant increase in ASCA titers compared to adjuvant-only immunized controls (P = 0.014).

CONCLUSION: The propensity to produce ASCA in a subgroup of CD patients is largely genetically predetermined as evidenced by their stability and lack of correlation with clinical disease activity parameters. Furthermore, in animal models of colitis, mere oral exposure of mice to yeast does not lead to the induction of marked ASCA titers irrespective of concomitant colonic inflammation. Hence, environment may play only a minor role in inducing ASCA.

Key words: Crohn's disease; Anti-*Saccharomyces cerevisiae* antibodies; Colitis

Müller S, Styner M, Seibold-Schmid B, Flogerzi B, Mähler M, Konrad A, Seibold F. Anti-*Saccharomyces cerevisiae* antibody titers are stable over time in Crohn's patients and are not inducible in murine models of colitis. *World J Gastroenterol* 2005; 11(44): 6988-6994
http://www.wjgnet.com/1007-9327/11/6988.asp

INTRODUCTION

Much attention has been focused on serologic markers in inflammatory bowel disease (IBD). The anti-*Saccharomyces cerevisiae* antibody (ASCA) is one such marker, which possesses an intermediate sensitivity and a high specificity for Crohn's disease (CD)[1-5]. Antibodies to *S cerevisiae* in CD were first described by Main *et al*.[6], using whole killed yeast cells as antigens. Sendid *et al*.[3] demonstrated greater diagnostic value for CD with *S cerevisiae* Su1, a strain of brewer's yeast, and identified the antigenic oligomannosidic epitopes of this organism. Subsequent work demonstrated that CD patients develop antibodies to a variety of baker's and brewer's yeast strains[4]. The antigen reacting with ASCA is a phosphopeptidomannan, a component of the *S. cerevisiae* cell wall[3].

Aside from the diagnostic role performed by ASCA, uncertainty remains as to whether they possess a pathophysiologic significance. One can argue for a genetic origin due to ASCA presence in 20-25% of unaffected first-degree family members[7-10]. Healthy monozygotic twins of CD patients also demonstrate increased IgA, IgG, and IgM ASCA levels[11]. In one study of non-IBD families,

ASCA were found to be familial with a vertical transmission pattern[12]. ASCA stability over time and independence from disease activity further indicate a genetic link[11,13]. Moreover, we have shown that T cells from ASCA-positive patients proliferated upon stimulation with mannan[14]. We were able to show that mannan binding lectin (MBL) deficient patients were significantly more frequently ASCA-positive and showed an enhanced T cell proliferation upon mannan stimulation compared to MBL wildtype patients[15]. These results further support the importance of genetic determination of ASCA.

Nevertheless, some of the familial studies have yielded conflicting data. For example, one group showed increased ASCA production in familial *vs* sporadic CD[7], but others have shown equal or increased ASCA prevalence for sporadic CD[9,16-18]. Thus, the case for an environmental etiology for ASCA has been articulated as well. For instance, a decline in ASCA levels has been observed post-surgically in a pediatric CD population[5]. Another group demonstrated lower ASCA titers in CD patients taking mesalazine than in CD patients not taking mesalazine[19]. Additionally, both brewing and baking strains of *S cerevisiae* provoke an antibody response in CD, implicating dietary antigens in disease pathogenesis[4]. One group has noted higher ASCA IgG antibody levels in patients with small bowel Crohn's disease *vs* those with colonic disease[18]. This same study found high levels of ASCA IgG but not IgA in celiac disease, indistinguishable from levels seen in CD. It was, thus, concluded that ASCA may result from a mucosal permeability defect. However, Vermeire *et al*.[20] were not able to show a correlation between ASCA and intestinal permeability.

In this study, our aim was to characterize ASCA over time in patients with IBD in order to further our understanding of their etiology. Furthermore, we assessed the possibility to induce an ASCA response in animal models.

MATERIALS AND METHODS

Patients

Sixty-six Crohn's disease (CD) patients, 29 ulcerative colitis (UC) patients, and 10 irritable bowel syndrome (IBS) patients with informed consent were enrolled in the study, and the study was approved by the ethical committee of the local authorities. Patient serum samples were drawn during routine outpatient visits (Gastroenterology clinic, University Hospital, Bern, Switzerland) for ASCA IgG and IgA analysis. Diagnosis of CD and UC was established by endoscopic, histological, and clinical criteria. Diagnosis of IBS was established by the Rome criteria[21].

A subgroup of CD (73 sera from 29 patients), UC (26 sera from 12 patients) and IBS (22 sera from 10 patients) patients, whose serum samples were drawn on at least 2 consecutive (maximally 4 consecutive) routine out-patient visits, were retrospectively selected for ASCA IgG and IgA titer analysis. An assessment of the Crohn's disease activity index (CDAI) was obtained at each CD patient's visit to the clinic[22]. The serum CRP levels were obtained at each clinic visit as well. Three patients with stoma were excluded from the CDAI analysis. One patient was excluded from the clinical analysis, since this patient's CDAI and CRP could not be obtained.

Mice

Four to six-weeks-old female interleukin-10 knockout mice (*Il10*^{tm1Cgn}; henceforth abbreviated as IL-10$^{0/0}$) on a C3H/HeJBir background were obtained from the University of Bern breeding facility (Bern, Switzerland) and housed under specified pathogen-free conditions. Four to six-week-old BALB/c mice were obtained from Harlan (Horst, The Netherlands). All procedures involving animals were performed in compliance with the local authorities on the use of animals in research.

ASCA ELISA for mouse and human sera

Investigators were blinded to disease status when performing the ELISA. Phosphopeptidomannans from baker's yeast (Hefe Vital Gold, Deutsche Hefewerke, Nürnberg, Germany) were extracted as previously described[8,23]. Ninety-six well ELISA plates (MaxiSorb, Nunc, Wiesbaden, Germany) were coated with 100 μL of 0.25 μg/mL phosphopeptidomannans in carbonate-bicarbonate buffer, pH 9.6 and incubated overnight at 4 °C. Serum diluted 1/1 000 was applied to the coated plates in triplicates. The plates were incubated for 1 h at 37 °C. Secondary antibody was added and plates were incubated for 1 h at RT. The secondary antibodies (Sigma, Buchs Switzerland) were as follows: goat anti-mouse polyvalent immunoglobulin peroxidase conjugate at 1/1 000; goat anti-human IgA (alpha-chain specific) peroxidase conjugate; and goat anti-human IgG (Fc specific) peroxidase conjugate, both at 1/5 000. The plates were developed using TMB substrate (Sigma) and the reaction was stopped with sulfuric acid. The absorbance at 450 nm (reference filter = 490 nm) was read by an EL 800 microplate reader (Bio-Tek Instruments, Winooski, Vermont). The mean absorbance value for the healthy control sera plus two standard deviations was used to discriminate between positive and negative subjects. Absorbance units equal to or above this value were considered positive for ASCA antibodies. A patient was considered ASCA$^+$, when positive for ASCA IgG, IgA or both.

For the human ELISA, one serum highly positive for ASCA was used to obtain a standard curve at dilutions ranging from 1/100 to 1/102 400. The curve was fitted using a four parameter logistic function to the logarithmically scaled dilutions. Human titers are expressed as dilution units from this curve. We computed the average change of IgG and IgA ($\Delta_{IgG/A}$) in human ASCA titer as our main variable of interest. An increase of $\Delta_{IgG/A}$ represents a decrease in ASCA levels and vice versa. Of the CD patients, two patient's IgG titer and one patient's IgA titer could not be reliably calculated from the standard curve after two repeated assays and thus were excluded from the IgG/A titer analysis. The murine ASCA titers are expressed as optical density (OD).

Preparation of yeast solution

Baker's yeast (Hefe Vital Gold, Deutsche Hefewerke, Nürnberg, Germany) was freshly grown in YPD broth

(Becton Dickinson, Le Pont de Claix, France) for 12 h at 30 ºC in a shaker at 200 r/min. The yeast solution was centrifuged at 2 000 r/min for 5 min. The cellular pellet was washed twice, resuspended in sterilized water and sonicated at 100 W for 2 min. Protein concentration was determined using the Bradford reagent (Sigma, Buchs, Switzerland).

Induction of chronic dextran sulfate sodium-induced (DSS) colitis, oral yeast administration and histological assessment

The previously described model of chronic DSS colitis was adapted from Mähler *et al*.[24]. Briefly, Balb/c mice were given three 5-day cycles of 3% DSS (DSS salt, MW= 36 000-50 000, ICN Biomedicals, Inc., Ohio), each interrupted by the 7th d without DSS. All mice received yeast *ad libitum* at a protein concentration of 100 or 500 μg/mL for the entire experiment. Murine serum samples were drawn on d 0 and the day of killing (d 36) for ASCA immunoglobulin analysis.

Mice were euthanized via CO_2 asphyxiation. Colons were harvested, fixed in 4% phosphate-buffered formaldehyde, embedded *in toto* and H&E-stained sections were examined by a pathologist (Mähler) blinded to the code. The sections were scored on a previously described[24] scale ranging from 0 (no inflammation) to 4 (severe inflammation). A total colonic inflammation score was obtained by averaging the individual scores of the proximal, middle, and distal colon.

Immunizations

Balb/c mice from our central animal facility were intraperitoneally injected with 50 μg phosphopeptidomannans or ovalbumin (Sigma, Gaithersburg, MD) mixed 1:1 (v/v) with GERBU adjuvant (GERBU, Gaiberg, Germany). Injection was repeated after two weeks and mice were killed for analysis one week later. Serum samples were obtained before primary immunization by tail tip bleeding and after euthanization by puncture of the caval vein.

Statistical analysis

We analyzed the CD population in regard to ASCA IgG and IgA positivity to test for a significant influence of the following patient variables: age, gender, anatomical location of disease, medication, fistulae, and extra-intestinal manifestations. Significance of each variable was computed via unpaired, two-tailed Student's *t*-test assuming equal variances if the additional *F*-test was non-significant. We analyzed the titer subgroup in respect to ASCA IgG and ASCA IgA positivity to test for a significant influence of the above-mentioned variables and additionally CD activity index (CDAI) and C-reactive protein (CRP) levels.

In order to qualitatively assess the amplitude and distribution of IgG and IgA, the respective $\Delta_{IgG/A}$ histograms for the CD, UC, and IBS titer subgroups were computed. The quantitative assessment is shown via the mean, SD and 95% confidence interval of each $\Delta_{IgG/A}$ distribution and via unpaired, two-tailed Student's *t*-tests. We also employed Student's *t*-tests for testing $\Delta_{IgG/A}$ differences with regard to gender, anatomical location of disease, fistulae, extra-intestinal manifestations, and medication. To assess the differences between the three patient groups with regard to IgG and IgA $\Delta_{IgG/A}$, we applied the one-way ANOVA test. The correlation coefficients between $\Delta_{IgG/A}$ and the two clinical parameters, change in CDAI (Δ_{CDAI}) and change in CRP (Δ_{CRP}), were also computed.

The differences between the mice groups on day 36 were statistically assessed using the unpaired, two-tailed Student's *t*-test. Significance level for all tests was 0.05.

RESULTS

ASCA positivity in the study population

Thirty-five of sixty-six CD patients, 4 of 29 UC patients and 3 of 10 IBS patients were ASCA positive. The sensitivity, specificity, and positive predictive value of the ASCA assay in distinguishing CD from UC are 53%, 86%, and 90%, respectively.

Fistular disease is associated with higher rate of ASCA IgA positivity

The baseline clinical characteristics of the patients and controls can be seen in Table 1. None of the following clinical characteristics had a significant effect on ASCA IgG and IgA positivity in the Crohn's disease patients: age, gender, anatomical locations of disease, medication, and extra-intestinal manifestations. Patients with fistular disease were significantly more likely to possess ASCA IgA positivity (P = 0.014, 71% *vs* 32%) than patients with non-fistular disease.

ASCA IgG and IgA titers are stable over time in CD and non-CD patients

ASCA IgG and IgA titers in the CD subgroup, expressed as logarithmically (ln) scaled dilutions of a high positive control, have been plotted over a time-period of up to 3 years (Figure 1). The change in titers did not vary significantly as can be seen in the Gaussian distribution in the histogram, which is centered close to zero for all patient groups with respect to both IgG and IgA titers (Figure 2). The means, standard deviations and 95% confidence intervals of $\Delta_{IgG/A}$ are shown in Table 2 and indicate stable titers over time. Nevertheless, the patient groups are significantly different in regard to Δ_{IgA} values (P<0.05, ANOVA), specifically between CD and UC patients (P<0.05, ANOVA *post hoc*). This suggests that patients with UC were more likely to experience a decrease in IgA ASCA levels over time than patients with CD. The patient groups are not significantly different with regard to Δ_{IgG} values.

Anatomic location of disease significantly influences the Δ_{IgG} of ASCA

Of the clinical parameters assessed upon entry, ileal disease was found to have a significant influence on the Δ_{IgG} of ASCA (Table 3). The mean Δ_{IgG} value for patients with ileal disease *vs* those without ileal disease was 0.13 and -0.34, respectively. This suggests that patients without ileal

Table 1 Baseline characteristics of the study populations tested for anti-*Saccharomyces cerevisiae* IgG and IgA antibodies. Unless otherwise indicated values are numbers of patients (%)

Study population	Crohn's disease (n = 66)	Ulcerative colitis (n = 29)	Healthy controls (n = 18)	IBS patients (n = 10)
Age, yr				
Mean±SD	38±16	37±15	40±13	57±13
Range	14-82	16-78	17-74	41-81
Male sex	32 (48)	15 (52)	10 (56)	6 (60)
Disease location				
Colonic	58 (88)	29 (100)		
Ileal	45 (68)			
Upper gastrointestinal involvement	3 (5)			
Presence of fistulae	15 (23)	1 (3)		
Extraintestinal manifestations	4 (6)	0 (0)		
Medical therapy				
Azathioprine	22 (33)	9 (31)		
Infliximab	5 (8)	3 (10)		
5-ASA compounds	4 (6)	11 (38)		
Methotrexate	4 (6)	0 (0)		
Oral steroids	29 (44)	15 (52)		
None of the above	19 (29)	7 (24)		

Table 2 Mean, standard deviation (SD) and the 95% confidence interval of the mean of the change in ASCA IgG and IgA titers

	Δ_{IgG}			Δ_{IgA}		
	Mean	SD	95%CI	Mean	SD	95%CI
CD	0.01	0.56	(-0.20, 0.22)	-0.04	0.25	(-0.13, 0.05)
UC	0.05	0.15	(-0.03, 0.14)	0.16	0.24	(0.02, 0.29)
IBS	0.05	0.08	(-0.003, 0.09)	-0.01	0.12	(-0.08, 0.06)

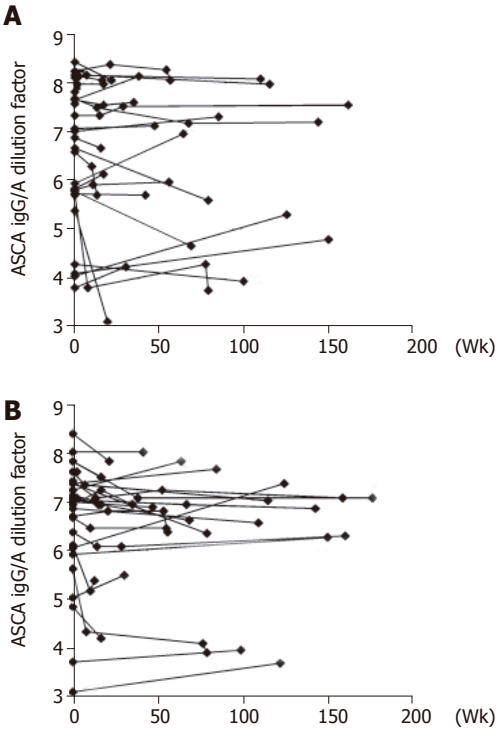

Figure 1 Anti-*Saccharomyces cerevisiae* (**A**) IgG and (**B**) IgA antibody titers in ASCA-positive patients with Crohn's disease expressed as a logarithmically (ln) scaled dilution unit of a highly positive control over a time-period of up to 3 years.

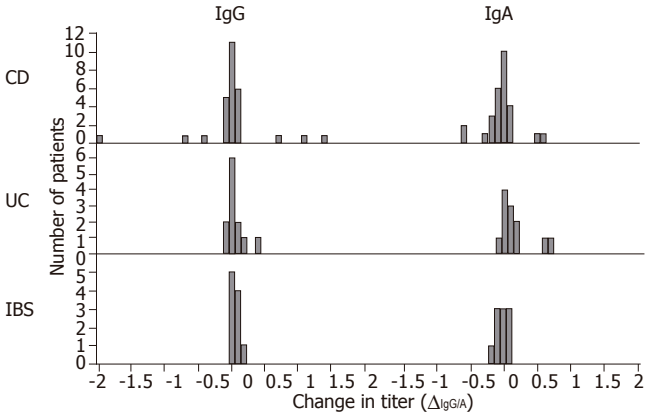

Figure 2 Histogram of change in ASCA IgA and IgG titers (ΔIgG/A) in patients with Crohn's disease (CD), ulcerative colitis (UC) and irritable bowel syndrome (IBS). CD patients demonstrate higher variability as compared to UC and IBS.

disease were more likely to experience an increase in ASCA level as opposed to patients with ileal disease. All other tested clinical parameters did not significantly influence the $\Delta_{IgG/A}$ of ASCA. Regarding the clinical parameters of disease, no strong corre=lation was found between the Δ_{CDAI} and Δ_{IgG} (c = -0.086) and Δ_{IgA} (c = -0.127). Moreover, no strong correlation was found between the Δ_{CRP} and Δ_{IgG} (c = 0.424) and Δ_{IgA} (c = -0.245).

Anti-S cerevisiae antibodies are not efficiently induced upon oral yeast administration, irrespective of concomitant induction of colitis in Balb/c or IL-10$^{0/0}$ mice

All mice given yeast lysate and unfed controls exhibited slightly increased ASCA titers at the end of the experimental period compared with values obtained at the beginning of the experiment. A slight increase in ASCA titers was observed in mice exposed to 500 μg/mL yeast lysate in their drinking water when compared with mice exposed to 100 μg/mL (Figure 3A). Concomitant DSS-

Table 3 Effect of the CD clinical characteristics on the following parameters: ASCA IgG and IgA positivity and change in IgG and IgA ASCA titers. Results are expressed as *P*-values of the mean-difference tests or as correlation coefficients (*c*)

Clinical characteristics	ASCA IgG	ASCA IgA	ΔIgG	ΔIgA
Correlation with age	*c* = –0.140	*c* = 0.198	*c* = –0.340	*c* = –0.197
Male *vs* female	0.881	0.881	0.089	0.571
Disease Location				
Colonic *vs* non-colonic	0.667	0.169	0.203	0.289
Ileal *vs* non-ileal	0.285	0.285	0.032[a]	0.395
Fistular *vs* Non-fistular disease	0.152	0.075	0.499	0.907
Medical therapy				
Azathioprine	0.881	0.881	0.749	0.375
Infliximab	0.233	0.233	0.870	0.844
5-ASA compounds	0.806	0.233	0.903	0.491
Oral steroids	0.512	0.385	0.475	0.531
None of the above medical therapy *vs* medical therapy	0.285	0.577	0.438	0.117

[a]*P*<0.05.

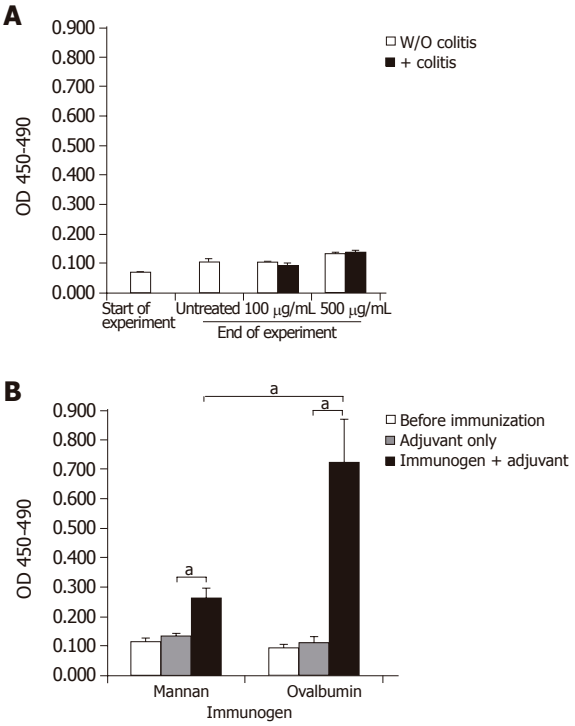

Figure 3 OD at 450 nm representing relative levels of polyclonal anti-*Saccharomyces cerevisiae* antibody (ASCA) (**A**) in control Balb/c mice (empty columns) or mice with DSS-induced experimental colitis (shaded columns). Basal ASCA titers were determined at the start of the experiment. During the experiment, mice received water containing 100 μg/mL or 500 μg/mL yeast solution *ad libitum*. (**B**) Balb/c mice were immunized with water or 50μg yeast mannan or ovalbumin mixed 1:1 (v:v) in GERBU adjuvant. After 2 wk, mice received a booster injection and ASCA or anti ovalbumin antibodies were determined 7 d later. [a]*P*<0.05.

treatment (Figure 3A) or onset of colitis in IL-10$^{0/0}$ mice (data not shown) did not lead to a further increase in ASCA titers. Development of colitis was evidenced by the observation of clinical signs such as soft stools and in some cases anal ulcerations and bloody stools. The average histological score±SD was as follows: 1.056±0.25 for the DSS-treated Balb/c group, 0±0 for the non-DSS-treated Balb/c group, and 1.5±0.19 for the IL-10$^{0/0}$ group.

ASCA titers are induced in mice after immunization with yeast mannan

Groups of Balb/c mice were immunized with adjuvant alone, or with adjuvant plus yeast mannan or, as a positive control, ovalbumin (Figure 3B). Mannan-immunized mice showed an average two-fold increase in ASCA titers when compared with mice receiving adjuvant only (P = 0.014). Mannan was poorly immunogenic compared to ovalbumin (P = 0.038) since specific serum antibody titers after ovalbumin plus adjuvant-immunization increased about seven-fold over adjuvant-only injected controls (P = 0.015).

DISCUSSION

Antibodies to the *S cerevisiae* cell wall mannans have been widely studied as a diagnostic tool to distinguish CD from UC. In this study, the rates of CD patient ASCA positivity correlate well with our previous results[8] as well as those cited in the literature[7,10,13]. Of all the clinical variables tested, fistular Crohn's disease was found to be associated with ASCA IgA positivity. This study is not the first to demonstrate such an association. Others have shown that the subgroup of CD patients with high levels of IgG and IgA ASCA has more aggressive, small-bowel fistulizing disease[25].

Our study was the first to assess time-period streamlined ASCA titers. We found no association between the change in ASCA titers and the following clinical characteristics: age, gender, presence of fistulae, medical therapy, CDAI or CRP levels. Of the clinical parameters tested, patients without ileal disease were more likely to encounter an increase in their ASCA titers over time as compared with CD patients with ileal disease. There is no good explanation why anatomic location of CD should provoke an increase or decrease in ASCA titers. It should be noted that Giaffer *et al.* noted increased ASCA IgG positivity association with small bowel disease as compared to

colonic disease[18]. Nevertheless, this study does not explain why these patient's titers were more likely to change over time. Also of special interest is the lack of association between Δ_{CDAI} and $\Delta_{IgG/A}$ and Δ_{CRP} and $\Delta_{IgG/A}$. ASCA stability over time in relation to the changes in CDAI was demonstrated by Landers *et al*.[13], utilizing a time period of at least 4 mo. Recently, Teml *et al*. established ASCA stability during a course of steroid or 5-ASA therapy[26]. Our data further strengthen this stability and lack of association with CDAI or medical therapy with the addition of CRP as a serologic marker of disease. This lack of association with clinical activity leads others and us away from thinking of ASCA as a subclinical marker of disease activity as it does not follow CD clinical status variations.

In line with the results obtained with human sera, the murine ASCA titers were rather stable, at least during the time of the experimental procedure (36 d). This is the first study to investigate murine ASCA production in the setting of DSS and IL-$10^{0/0}$ colitis. After oral treatment with a high antigen dose (500 μg/mL), we observed a slight increase of ASCA titers compared to untreated controls or mice treated with 100 μg/mL. Interestingly, we observed slightly lower ASCA titers in young untreated mice compared to untreated mice at the end of the experiment. It is very likely that ASCA titers in mice may slightly vary between the breeder company and our animal facility as a consequence of differential exposure to yeast-antigens depending on the hygiene status of the animal facility and/or the composition of food pellets. We did not, however, observe a further increase upon induction of colitis. Therefore, the impairment of mucosal barrier during inflammation and/or the enhanced presence of immune competent cells alone does not lead to markedly enhanced ASCA generation.

In contrast, systemic immunization of mice with phosphopeptidomannans in the context of appropriate adjuvant leads to a significant increase in ASCA titers. However, the increase of ASCA titers is much less pronounced than that of anti-ovalbumin antibodies after ovalbumin immunization. Thus, these data show that mannans are not very efficient antigens when used for immunization, further indicating that normally mice and human beings are tolerant to mannans. Local inflammation during colitis is not sufficient to break this tolerance. In our recent study we were able to show that ASCA positivity was associated with MBL deficiency[15]. Furthermore, family studies show an increased incidence of ASCA in healthy family members[7,8,20]. Thus, generation of ASCA in a subgroup of CD patients and healthy family members may be mainly a result of a genetic predisposition, although biochemical and genetic analyses supporting this notion are not currently available.

In conclusion, we have demonstrated the stability of the ASCA titers over time and their lack of association with clinical activity in the form of CDAI and CRP. These findings are in line with the observation that ASCA are only marginally inducible in mice via high dose oral exposure, and are not further influenced by concomitant induction of colitis. Hence, we speculate that the propensity to produce ASCA in a subgroup of CD patients is largely genetically predetermined and, thus, may reflect a predisposition of distinct genetic backgrounds to establish immune responses against normally tolerated antigens.

ACKNOWLEDGMENTS

We are grateful to Dr A Sergew and Dr M Weber for their editorial assistance. Dr MA Styner is acknowledged for insightful discussions regarding statistical analysis.

REFERENCES

1 **Quinton JF**, Sendid B, Reumaux D, Duthilleul P, Cortot A, Grandbastien B, Charrier G, Targan SR, Colombel JF, Poulain D. Anti-Saccharomyces cerevisiae mannan antibodies combined with antineutrophil cytoplasmic autoantibodies in inflammatory bowel disease: prevalence and diagnostic role. *Gut* 1998; **42**: 788-791

2 **Sandborn WJ**, Loftus EV Jr, Colombel JF, Fleming KA, Seibold F, Homburger HA, Sendid B, Chapman RW, Tremaine WJ, Kaul DK, Wallace J, Harmsen WS, Zinsmeister AR, Targan SR. Evaluation of serologic disease markers in a population-based cohort of patients with ulcerative colitis and Crohn's disease. *Inflamm Bowel Dis* 2001; **7**: 192-201

3 **Sendid B**, Colombel JF, Jacquinot PM, Faille C, Fruit J, Cortot A, Lucidarme D, Camus D, Poulain D. Specific antibody response to oligomannosidic epitopes in Crohn's disease. *Clin Diagn Lab Immunol* 1996; **3**: 219-226

4 **McKenzie H**, Main J, Pennington CR, Parratt D. Antibody to selected strains of Saccharomyces cerevisiae (baker's and brewer's yeast) and Candida albicans in Crohn's disease. *Gut* 1990; **31**: 536-538

5 **Ruemmele FM**, Targan SR, Levy G, Dubinsky M, Braun J, Seidman EG. Diagnostic accuracy of serological assays in pediatric inflammatory bowel disease. *Gastroenterology* 1998; **115**: 822-829

6 Main **J**, McKenzie H, Yeaman GR, Kerr MA, Robson D, Pennington CR, Parratt D. Antibody to Saccharomyces cerevisiae (bakers' yeast) in Crohn's disease. *BMJ* 1988; **297**: 1105-1106

7 **Annese V**, Andreoli A, Andriulli A, Dinca R, Gionchetti P, Latiano A, Lombardi G, Piepoli A, Poulain D, Sendid B, Colombel JF. Familial expression of anti-Saccharomyces cerevisiae Mannan antibodies in Crohn's disease and ulcerative colitis: a GISC study. *Am J Gastroenterol* 2001; **96**: 2407-2412

8 **Seibold F**, Stich O, Hufnagl R, Kamil S, Scheurlen M. Anti-Saccharomyces cerevisiae antibodies in inflammatory bowel disease: a family study. *Scand J Gastroenterol* 2001; **36**: 196-201

9 **Sendid B**, Quinton JF, Charrier G, Goulet O, Cortot A, Grandbastien B, Poulain D, Colombel JF. Anti-Saccharomyces cerevisiae mannan antibodies in familial Crohn's disease. *Am J Gastroenterol* 1998; **93**: 1306-1310

10 **Sutton CL**, Yang H, Li Z, Rotter JI, Targan SR, Braun J. Familial expression of anti-Saccharomyces cerevisiae mannan antibodies in affected and unaffected relatives of patients with Crohn's disease. *Gut* 2000; **46**: 58-63

11 **Lindberg E**, Magnusson KE, Tysk C, Jarnerot G. Antibody (IgG, IgA, and IgM) to baker's yeast (Saccharomyces cerevisiae), yeast mannan, gliadin, ovalbumin and betalactoglobulin in monozygotic twins with inflammatory bowel disease. *Gut* 1992; **33**: 909-913

12 **Poulain D**, Sendid B, Fajardy I, Danze PM, Colombel JF. Mother to child transmission of anti-S cerevisiae mannan antibodies (ASCA) in non-IBD families. *Gut* 2000; **47**: 870-871

13 **Landers CJ**, Cohavy O, Misra R, Yang H, Lin YC, Braun J, Targan SR. Selected loss of tolerance evidenced by Crohn's disease-associated immune responses to auto- and microbial antigens. *Gastroenterology* 2002; **123**: 689-699

14 **Konrad A**, Rutten C, Flogerzi B, Styner M, Goke B, Seibold F. Immune sensitization to yeast antigens in ASCA-positive patients with Crohn's disease. *Inflamm Bowel Dis* 2004; **10**: 97-105

15 **Seibold F**, Konrad A, Flogerzi B, Seibold-Schmid B, Arni S, Juliger S, Kun JF. Genetic variants of the mannan-binding lectin are associated with immune reactivity to mannans in Crohn's disease. *Gastroenterology* 2004; **127**: 1076-1084

16 **Halme L**, Turunen U, Helio T, Paavola P, Walle T, Miettinen A, Jarvinen H, Kontula K, Farkkila M. Familial and sporadic inflammatory bowel disease: comparison of clinical features and serological markers in a genetically homogeneous population. *Scand J Gastroenterol* 2002; **37**: 692-698

17 **Barnes RM**, Allan S, Taylor-Robinson CH, Finn R, Johnson PM. Serum antibodies reactive with Saccharomyces cerevisiae in inflammatory bowel disease: is IgA antibody a marker for Crohn's disease? *Int Arch Allergy Appl Immunol* 1990; **92**: 9-15

18 **Giaffer MH**, Clark A, Holdsworth CD. Antibodies to Saccharomyces cerevisiae in patients with Crohn's disease and their possible pathogenic importance. *Gut* 1992; **33**: 1071-1075

19 **Oshitani N**, Hato F, Matsumoto T, Jinno Y, Sawa Y, Hara J, Nakamura S, Seki S, Arakawa T, Kitano A, Kitagawa S, Kuroki T. Decreased anti-Saccharomyces cerevisiae antibody titer by mesalazine in patients with Crohn's disease. *J Gastroenterol Hepatol* 2000; **15**: 1400-1403

20 **Vermeire S**, Peeters M, Vlietinck R, Joossens S, Den Hond E, Bulteel V, Bossuyt X, Geypens B, Rutgeerts P. Anti-Saccharomyces cerevisiae antibodies (ASCA), phenotypes of IBD, and intestinal permeability: a study in IBD families. *Inflamm Bowel Dis* 2001; **7**: 8-15

21 **Thompson WG**. The road to Rome. i1999; **45** Suppl 2: II80

22 **Best WR**, Becktel JM, Singleton JW, Kern F Jr. Development of a Crohn's disease activity index. National Cooperative Crohn's Disease Study. *Gastroenterology* 1976; **70**: 439-444

23 **Kocourek J**, Ballou CE. Method for fingerprinting yeast cell wall mannans. *J Bacteriol* 1969; **100**: 1175-1181

24 **Mähler M**, Bristol IJ, Leiter EH, Workman AE, Birkenmeier EH, Elson CO, Sundberg JP. Differential susceptibility of inbred mouse strains to dextran sulfate sodium-induced colitis. *Am J Physiol* 1998; **274**: G544- G551

25 **Vasiliauskas EA**, Plevy SE, Landers CJ, Binder SW, Ferguson DM, Yang H, Rotter JI, Vidrich A, Targan SR. Perinuclear antineutrophil cytoplasmic antibodies in patients with Crohn's disease define a clinical subgroup. *Gastroenterology* 1996; **110**: 1810-1819

26 **Teml A**, Kratzer V, Schneider B, Lochs H, Norman GL, Gangl A, Vogelsang H, Reinisch W. Anti-Saccharomyces cerevisiae antibodies: a stable marker for Crohn's disease during steroid and 5-aminosalicylic acid treatment. *Am J Gastroenterol* 2003; **98**: 2226-2231

Science Editor Guo SY **Language Editor** Elsevier HK

PO Box 2345, Beijing 100023, China
www.wjgnet.com
wjg@wjgnet.com

ELSEVIER

World J Gastroenterol 2005;11(44):6995-7000
World Journal of Gastroenterology ISSN 1007-9327

• *CLINICAL RESEARCH* •

Computer-aided morphometry of liver inflammation in needle biopsies

N Dioguardi, B Franceschini, C Russo, F Grizzi

N Dioguardi, B Franceschini, C Russo, F Grizzi, Scientific Direction, Istituto Clinico Humanitas, Rozzano, Milan, Italy and "Michele Rodriguez" Foundation, Institute for Quantitative Measures in Medicine, Milan, Italy
Supported by the "Michele Rodriguez" Foundation, Institute for Quantitative Measures in Medicine, Milan, Italy
Correspondence to: Nicola Dioguardi, MD, Scientific Direction, Istituto Clinico Humanitas, Via Manzoni 56, 20089 Rozzano MI, Italy. nicola.dioguardi@humanitas.it
Telephone: +39-02-82244501 Fax: +39-02-82244590
Received: 2005-03-24 Accepted: 2005-04-18

Abstract

AIM: To introduce a computer-aided morphometric method for quantifying the necro-inflammatory phase in liver biopsy specimens using fractal geometry and Delaunay's triangulation.

METHODS: Two-micrometer thick biopsy sections taken from 78 chronic hepatitis C virus-infected patients were immunohistochemically treated to identify the inflammatory cells. An automatic computer-aided image analysis system was used to define the inflammatory cell network defined on the basis of Delaunay's triangulation, and the inflammatory cells were geometrically classified as forming a cluster (an aggregation of a minimum of three cells) or as being irregularly distributed within the tissue. The phase of inflammatory activity was estimated using Hurst's exponent.

RESULTS: The proposed automatic method was rapid and objective. It could not only provide rigorous results expressed by scalar numbers, but also allow the state of the whole organ to be represented by Hurst's exponent with an error of no more than 12%.

CONCLUSION: The availability of rigorous metrical measures and the reasonable representativeness of the status of the organ as a whole raise the question as to whether the indication for hepatic biopsy should be revised by establishing clear rules concerning the contraindications suggested by its invasiveness and subjective interpretation.

Key words: Biopsy; Grading; Image analysis; Fractal geometry; Topography; Delaunay

Dioguardi N, Franceschini B, Russo C, Grizzi F. Computer-aided morphometry of liver inflammation in needle biopsies. *World J Gastroenterol* 2005; 11(44): 6995-7000
http://www.wjgnet.com/1007-9327/11/6995.asp

INTRODUCTION

The antiviral treatment of chronic hepatitis C is expensive, efficacious in only 50% of cases, and has sometimes major undesired effects. The criteria for selecting the patients to treat are therefore a central problem and its solution is sought by evaluating the inflammatory lesions (grading) and fibrosis (staging) histologically observed in bioptic specimens.

A single bioptic sample is still the most effective means of obtaining the greatest amount of information for formulating a diagnosis of chronic hepatitis, excluding other diseases, hypothesizing the prognosis, and defining therapeutic indications[1-4]. However, taking a bioptic sample is expensive, carries a certain risk, and the results are not reliable insofar as they do not express real measures, but only semi-quantitative categories of severity, and its evaluation entirely depends on the subjective skill and experience of the pathologist[5-9]. It therefore follows that such semi-quantitative data cannot be used for statistical purposes[10,11].

The recently proposed alternative methods of estimating hepatic tissue inflammation by measuring the blood levels of molecules associated with the evolution of liver inflammation (including the extremely and widely used measurement of transaminase levels) have not shown any sure correspondence with actual tissue status[12-16].

It is therefore necessary to develop more rigorous and objective morphometric methods capable of providing scalars for the metrical quantification of inflammation structures within a liver biopsy sample. We have herein described the first results of our metrical measurements of the *fractal spaces* covered by necro-inflammatory lesions observed in the biopsies of consecutive chronic hepatitis C patients, and obtained by means of a totally computerized analysis that excludes any subjective influence.

The phase of inflammatory activity in the examined samples has been estimated using Hurst's exponent (*H*). *H* was first excogitated in the middle of the last century in order to study the local variations in water flow in the branches of the Nile delta during the construction of the Aswan dam[17]. Further refined in 1965 and 1969, it can

now be drawn from the fractal dimension (D)[18,19]. As it can describe even subtle quantitative differences in the smoothness of the configurations of natural objects with fractal properties, we used it to describe the phase of the inflammatory process on the basis of the fractal space occupied by inflammatory cells. In our case, a high H value indicates a small number of inflammatory cells within the tissue (i.e. the natural state), and a low value indicates the presence of many inflammatory cells (i.e. severe inflammatory states). H can be considered as a quantitative descriptor of the configuration pattern expressing the phase of the inflammatory process, and thus gives inflammatory cell density, the significance of a physical variable.

MATERIALS AND METHODS

Biopsy specimens

The study was conducted in accordance with the guidelines of the Ethics Committee of Istituto Clinico Humanitas, Rozzano, Milan, Italy.

The 72 liver specimens (>10 mm long) came from 43 male and 29 female chronic hepatitis C patients (mean age 50.3±14 years; range 25-77 years) admitted to our Hepato-gastroenterology Unit.

Histochemistry

Two consecutive 2-μm-thick sections were cut from the formalin-fixed and paraffin-embedded specimens. One was subsequently stained with hematoxylin-eosin (HE) solution, and the other was used for immunohistochemistry. HE stained sections were graded by two hepato-pathologists using a semi-quantitative scoring system.

Immunohistochemistry

In order to classify the inflammatory cells, the histological sections were treated with primary antibodies raised against human leukocyte common antigen (LCA, monoclonal mouse anti-LCA) for 1 h at room temperature, 1 mg/mL mouse IgG1 (Dako, Milan, Italy) was used as a negative control.

In order to distinguish settled macrophagic mesenchymal Kupffer cells from recruited inflammatory T cells, a further section was immersed in an antigen retrieval bath (Dako, Milan, Italy) for 30 min at 98 °C in 1 mmol/L of a freshly made EDTA solution. The inflammatory T cells were classified using primary antibodies raised against human CD3 (Dako, Milan, Italy), and the Kupffer cells by treatment with primary antibodies raised against human CD68 (Dako, Milan, Italy) at room temperature, or with 1 mg/mL mouse IgG1 (Dako, Milan, Italy) as a negative control.

The sections were then incubated with the DAKO Envision Doublestain System (Dako, Milan, Italy). Fast red was used as a chromogen to yield the red reaction products for CD68, and 3,3'-diaminobenzidine tetrahydrochloride (DAB, Sigma Ltd, MO, USA) to yield the brown reaction products for LCA and CD3.

The nuclei were lightly counterstained with Harris's hematoxylin solution (Medite, Bergamo, Italy).

Quantitative image analysis

The histological sections were digitized using an image analysis system consisting of a Leica DMLA microscope (Leica, Italy) equipped with an *x-y* translator table, a digital camera (Leica DC200, Leica, Italy), and an Intel dual Pentium IV, 660 MHz computer with incorporated *ad hoc* constructed image analysis software[20].

The computer program automatically selected the surface covered by the whole LCA-immunopositive inflammatory system. In this paper, the term *true area* indicates the surface of the liver tissue section without unfilled natural holes, vascular and biliary cavities, sinusoidal spaces or artificial spaces due to the needle excision and histological manipulations[20]. All the measurements were made at an objective magnification of ×20.

Determination of Hurst's exponent

This was obtained using the general relationship:

$$H=E+1-D \quad (1)$$

where E indicates the Euclidean topological dimension and D the fractal dimension of the surface covered by the whole LCA-immunopositive inflammatory system.

D was automatically estimated using the box-counting method and the formula:

$$D_B = \lim_{\varepsilon \to 0} \frac{\log N(\varepsilon)}{\log(1/\varepsilon)} \quad (2)$$

where D_B is the box-counting fractal dimension of the object, ε the side length of the box, and $N(\varepsilon)$ the smallest number of boxes of side ε required to cover the surface of the object completely, i.e. the whole LCA-immunopositive inflammatory system. As the zero limit cannot be applied to biological objects, the dimensions were calculated as $D=d$, where d is the slope of the graph of log $[N(\varepsilon)]$ against log $1/\varepsilon$. The log-log graphs were plotted and the linear segments were identified using least squares regression. Their gradients were calculated using an iterative resistant line method[20-28].

On the basis of the H value, two categories were considered. The first included all the samples characterized by $0.5<H<1.0$, and the second included all the samples verifying the relationship $0<H<0.5$.

Dynamic side of the shapes of chronic liver inflammation

The pictures indicating chronic liver inflammation appeared as portal, periportal, and perilobular aggregations of lymphocytes, plasma cells, and monocytes/macrophages (Figure 1). The extent of intralobular focal necro-inflammation varied with the severity of the disease, with confluent necrosis expressing its most severe clinical exacerbation[29-33].

These cell conglomerates arose when the viral etiological agent shaped critical points in the liver tissue consistent with hepatocyte necrosis. Each critical point acted as an attractor of the inflammatory cells naturally present within the liver tissue and recruited lymphocytes,

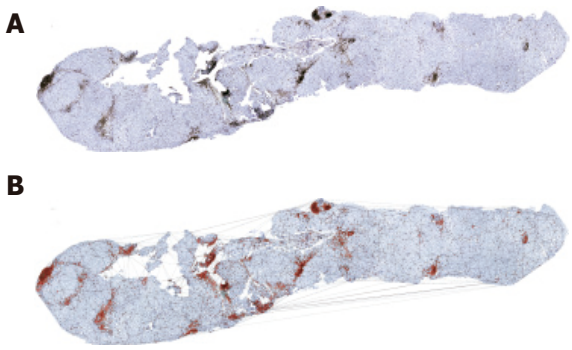

Figure 1 Liver biopsy section immunohistochemically treated with antibodies against LCA (**A**) and computer-aided recognition of the inflammatory cell network (**B**).

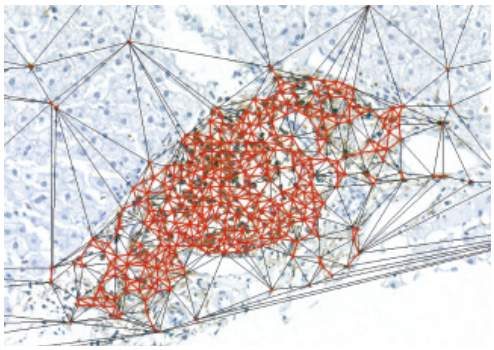

Figure 2 Border of clustered and non-clustered inflammatory cells.

plasma cells and other white blood cells. The trajectories of the inflammatory cells would die inside the attraction basin created by the necro-inflammatory process, where the motion of the recruited cells came to an end, and they formed a *cluster* marking the metrical space covered by the inflammation basin. The cell density of the cluster was transient and depended on the evolution of the inflammation connected to necrosis healing.

Definition of cluster outlines

As the cells of a cluster were not settled in tasseled forms, they were not bounded by a distinguishable contour. This meant that, in order to measure the fractal spaces they covered, the canonical step was to fix their bounds. To this end, we used a triangulation method based on the principles of Delaunay's tessellation[34-37], which can be very efficiently adapted to cluster geometry and involves the metrical measurement of the *distances* between the cells belonging to the whole inflammatory system.

Each inflammatory cell on the surface of the histological specimen was considered as a node of a continuous framework covering the entire section characterized by very irregular triangular windows in which any two triangles have one common side (Figure 1).

The border of the cluster (Figure 2) was arbitrarily fixed at the level of the continuous line formed by the set of the most external triangle sides with a length of ≤20 μm, corresponding to about twice the mean diameter of a lymphocyte (7-12 μm)[38]. All the points within this border were considered as belonging to the subset of cluster-resident cells, and those connected by longer segments as belonging to the non-clustered subset of inflammatory cells.

Geometrical structure of inflammatory clusters

The dynamics of the necro-inflammation shaping a cluster generate metrical spaces covered by two overlapping components. One belonged to the entire attraction basin of hepatocyte necrosis bounded by the cluster contour drawn by the triangulation, the other belonged to the sum of the surfaces of the inflammatory cells residing within the attraction (necro-inflammation) basin. The outline of the true area of the biopsy sample was indicated by the symbol A_B, the area of the triangulation-defined cluster (necrosis attraction zone) was indicated by the symbol A_C, and the sum of the areas of cluster-resident inflammatory cells was indicated by the symbol A_{CINF} (Figure 3). The dispersed cells were indicated by the symbol A_{PINF}, and their areas added to the area of resident inflammatory cells provided the area covered by the inflammation system as a whole, which was indicated by the symbol A_{TINF}

Physical parameters of inflammation

The physical parameters of inflammation were taken from analyses of the clusters consisting of at least three inflammatory cells. Smaller aggregates were considered as randomly united cells.

In the two dimensions of a histological section, we obtained the following physical parameters relating to the state of inflammation: (1) cluster extension: the area of the necro-inflammation basins identified by means of Delaunay's triangulation; (2) the area covered by the inflammatory cells resident within the cluster perimeter: i.e. the intracluster mass of inflammatory cells; (3) the whole area occupied by all the inflammatory parenchymal cells not residing inside the clusters; (4) the A_C/A_{CINF} ratio; (5) the extent of inflammatory tissue as a whole ($A_{CINF}+A_{PINF}$); (6) the discrimination of inflammatory T cells from Kupffer cells; (7) Hurst's exponent in order to evaluate the spatial heterogeneity of the chronic inflammatory process, i.e. the phase of the inflammatory process.

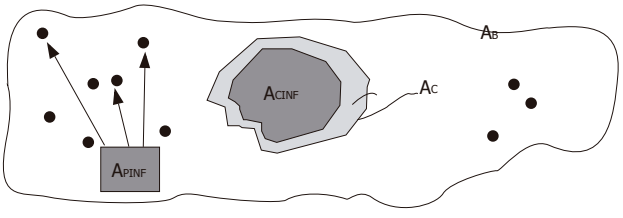

Figure 3 Geometrical structure of clustered inflammatory cells. A_B=true area of the biopsy sample; A_C=area of the triangulation-defined cluster (necrosis attraction zone); A_{CINF}=sum of the areas of cluster-resident inflammatory cells; A_{PINF}=dispersed non-clustered cells.

Statistical analysis

All the data were expressed as mean±SD.

RESULTS

Cluster extension

The area of the necro-inflammation basins obtained by Delaunay's triangulation ranged from 0.010% to 33.74% (mean 5.22±6.5%) of the area of the histological section. This area was a perceptible and measurable marker of the necrosis subtending each cluster. The sum of these areas could express the overall extension of the necrotic process in the evaluated section.

Area covered by clustered inflammatory cells

This area ranged from 0.021% to 15.36% (mean 2.22 ±2.9%) of the area of the histological section. As it represented effective inflammatory activity, its measure indicated the inflammatory potential of the set of clusters identified in the biopsy section.

Area of dispersed inflammatory cells

The area covered by the whole set of LCA-immunopositive inflammatory cells lying outside the clusters recognized in the histological sections ranged from 0.024% to 3.93% (mean 0.91±0.83%).

A_C/A_{CINF} ratio

This parameter, which expresses the density of the inflammatory cells lying within the clusters, ranged from 0.34 to 3.28 (mean 0.56±0.35).

Extension of inflammatory tissue

This area was drawn from the sum of the clustered and dispersed inflammatory cells immunopositive for LCA, and ranged from 0.045% to 18.58% (mean 3.13±3.30%).

Discrimination of recruited inflammatory T cells from resident macrophagic Kupffer cells

The whole LCA-immunopositive inflammatory area was shared by recruited blood cells (lymphocytes, monocytes, plasma cells, mast cells) and settled macrophagic Kupffer cells (Figure 4). The different range of the areas of Kupffer cells suggested that the number of Kupffer cells potentially capable of being activated might explain the distinction between fast and slow fibrosis. It is worth mentioning that this preliminary study found a high percentage of macrophages among the dispersed cells and a very low percentage in the clusters, which mainly consisted of lymphocytes and other recruited blood inflammation cells (Figure 4).

Quantification of spatial histological heterogeneity of chronic inflammatory process

This was evaluated using Hurst's exponent, the values of which range from 0 to 1 and indicate the actual phase of the inflammatory process. *H* coefficients of >0.5 were considered as belonging to tendentially less severe inflammatory pictures, and those of <0.5 as belonging to more severe pictures. The mean *H* value of all the cases was 0.67±0.14 (range 0.36-1).

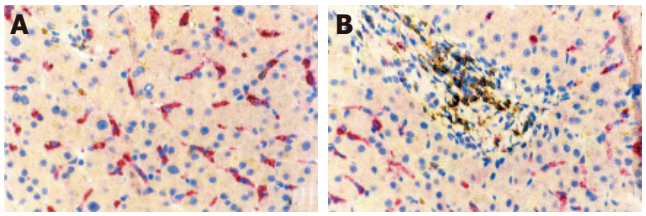

Figure 4 High percentage of macrophages among dispersed cells (**A**) and low percentage in clusters of lymphocytes and other inflammatory cells (**B**).

DISCUSSION

Given a hierarchy of logical concepts going from the purely qualitative or classificatory, to the semi-quantitative or ordering, and finally to the entirely quantitative or metrical (i.e. scientific variables), it is not a prejudice to consider that the maturity of a discipline is reflected by the number of quantitative concepts it adopts.

From this viewpoint, the phasing out of the clinical use of qualitative and semi-quantitative methods when evaluating the extension of chronic inflammatory lesions can be correlated with the maturity of hepatological disciplines. In this study, we used measurement theory, which forms the basis of our concrete knowledge of the real world and discriminates the specificity of its interrelationships, to construct a method of evaluating the different pictures of chronic liver inflammation.

Studying the measurement of inflammation (or the intensity of a process) obliged us to think in different terms from those that we were used to. In order to express new facts in intelligible terms, the confusion generated by the vague and emotive semi-quantitative definitions dictated by an observer's skill must be removed from every conceptual structure.

The method adopted by us is highly objective insofar as it is entirely computerized. Its foundations lie in the theory of measurement, a basic point of reference for all conceptual structures organizing knowledge[39].

The liver tissue lesions related to the inflammatory process at any given time caused variations in the concentrations of some specific blood molecules. These have been grouped and proposed as disease indices despite the fact that their concentrations depend not only on their production, but also on the rate of their metabolism in the bloodstream, thus depriving them of much of their significance as a quantitative index of the hepatic structure producing them. The changes in the concentrations of these blood indices over time can be described by the general equation:

$$dx_i/dt = f_i(x_1, x_2, \ldots, x_n) \quad (3)$$

where x_i denotes the blood concentration of the molecular species used, t is time, and the functions f_i are determined by the specific reactions of each x_i with the environmental factors in the bloodstream that affect their mean life (many

of which are unknown).

This makes these blood molecules independent variables that are incapable of expressing the state conditions of hepatic tissue even when the most sophisticated statistical methods are used. Similar conclusions can be made concerning the figured elements of blood (granulocytes, red cells, and platelets), and the characteristics of independent variables can also be found in the case of hepatofuge circulations (esophageal, gastric, hemorrhoidal, and umbilical varices). It therefore follows that the only variables describing the state of a chronic necro-inflammatory hepatic tissue lesion are those obtained by measuring their characteristics in the tissue in which they occur.

Since all theoretical hepatologists freely admit that the forms of chronic viral inflammation are so numerous and that they elude a complete verbal description, metrical measurements estimating the size of the true area covered by inflammatory cells and the density of the cells occupying it are the most real means of defining the stage of the process.

In practical terms, measuring chronic hepatitis B and C virus-related inflammation on the basis of a histological section of liver tissue is a problem of estimating the density of the points aggregated in clusters and those isolated in the interstitium of the hepatic parenchyma. As the points of the former (lymphocytes, monocytes, plasma cells) and the latter (which also include Kupffer cells) have the same mesenchymal nature and a similar capacity of activation during disease, it can be reasonably presumed that the degree of activity of the chronic viral process can be estimated by measuring the metrical spaces occupied by these cells and their density within them.

Whatever the method used, it is always difficult to determine the density of the punctiform particles representing the recruited inflammatory blood cells in a cluster because it depends on what is assumed to be the boundary of these basic elements of the chronic hepatitis virus-related process of liver tissue inflammation. After repeated tests (not described here), we decided to use cell sequences characterized by intercellular distances of $\leq$20 μm. Although this resolved our case, it certainly did not provide definitive solutions.

One basic question raised by our study is how much new knowledge of inflammation we have acquired after recognizing, measuring and classifying it. A first reply can be that we are able to acquire rigorous and repeatable metrical data concerning the anatomical (i.e. physical) state of the lesions induced by the etiological agent, which can be used as a reference point to give some significance to the hematological indices of disease whose uncertainty is always due to partially unknown factors. No other method of tissue or hematological analysis offers a result that is so near to reality.

Furthermore, using the same equation (4), we can now geometrically describe the morphometry of the histological picture offered by a liver biopsy. In this case, x_i represents the observable (i.e. measurable) quantities indicating the phase of the dynamic state of the inflammatory lesions that directly mark the evolution of the disease, t is time, and the functions f_i are determined by both viral and immune activity.

We included in x_i the observable, directly perceivable and metrically quantifiable measures that can change the blood concentrations of the individual molecules indicative of chronic liver disease.

Tissue and hematological indices can both be seen as dynamic variables and written using the same formula, but the hematological indices described by equation (3) are completely different functions (f_i) from those determining the dynamics of anatomical lesions. It therefore follows that blood indices cannot be used to validate the results of our method, and that the changes in hematological indices are due to the action of very different independent factors. At this point, it may be wondered what qualitative differences distinguish our method from previous recognition/classification and evaluation procedures. The most immediate reply is the rigorousness of the results expressed by scalar numbers, but it should also be added that our method allows the state of the whole organ to be represented by Hurst's exponent with an error of no more than 12% (manuscript in preparation).

The availability of rigorous metrical measures and the reasonable representativeness of the status of the organ as a whole raise the question as to whether the indication for hepatic biopsy should be reviewed by establishing clear rules in relation to the contraindications suggested by its invasiveness.

REFERENCES

1 **Kleiner DE**. The liver biopsy in chronic hepatitis C: a view from the other side of the microscope. *Semin Liver Dis* 2005; **25**: 52-64
2 **Desmet VJ**. Liver tissue examination. *J Hepatol* 2003; **39**: 43- 49
3 **Bravo AA**, Sheth SG, Chopra S. Liver biopsy. *N Engl J Med* 2001; **344**: 495-500
4 **Brunt EM**. Liver biopsy interpretation for the gastroenterologist. *Curr Gastroenterol Rep* 2000; **2**: 27-32
5 **Brunt EM**. Grading and staging the histopathological lesions of chronic hepatitis: the Knodell histology activity index and beyond. *Hepatology* 2000; **31**: 241-246
6 **Hubscher SG**. Histological grading and staging in chronic hepatitis: clinical applications and problems. *J Hepatol* 1998; **29**: 1015-1022
7 **Scheuer PJ**. Assessment of liver biopsies in chronic hepatitis: how is it best done? *J Hepatol* 2003; **38**: 240-242
8 **Rosenberg WM**. Rating fibrosis progression in chronic liver diseases. *J Hepatol* 2003; 38: 357-360
9 **Guido M**, Rugge M. Liver biopsy sampling in chronic viral hepatitis. *Semin Liver Dis* 2004; **24**: 89-97
10 **Lagging LM**, Westin J, Svensson E, Aires N, Dhillon AP, Lindh M, Wejstal R, Norkrans G. Progression of fibrosis in untreated patients with hepatitis C virus infection. *Liver* 2002; **22**: 136-144
11 **Svensson E**. Ordinal invariant measures for individual and group changes in ordered categorical data. *Stat Med* 1998; **17**: 2923-2936
12 **Poynard T**, Imbert-Bismut F, Munteanu M, Messous D, Myers RP, Thabut D, Ratziu V, Mercadier A, Benhamou Y, Hainque B. Overview of the diagnostic value of biochemical markers of liver fibrosis (FibroTest, HCV FibroSure) and necrosis (ActiTest) in patients with chronic hepatitis C. *Comp Hepatol* 2004; **3**: 8
13 **Silva IS**, Ferraz ML, Perez RM, Lanzoni VP, Figueiredo VM,

Silva AE. Role of gamma-glutamyl transferase activity in patients with chronic hepatitis C virus infection. *J Gastroenterol Hepatol* 2004; **19**: 314-318

14 **Myers RP**, Tainturier MH, Ratziu V, Piton A, Thibault V, Imbert-Bismut F, Messous D, Charlotte F, Di Martino V, Benhamou Y, Poynard T. Prediction of liver histological lesions with biochemical markers in patients with chronic hepatitis B. *J Hepatol* 2003; **39**: 222-230

15 **He QY**, Lau GK, Zhou Y, Yuen ST, Lin MC, Kung HF, Chiu JF. Serum biomarkers of hepatitis B virus infected liver inflammation: a proteomic study. *Proteomics* 2003; **3**: 666-674

16 **Lichtinghagen R**, Bahr MJ. Noninvasive diagnosis of fibrosis in chronic liver disease. *Expert Rev Mol Diagn* 2004; **4**: 715-726

17 **Hurst HE**. Long-term storage capacity of reservoirs. *Trans Amer Soc Civ Eng* 1951; **116**: 770-808

18 **Hurst HE**, Black RP, Simaiki YM. Long-term storage: an experimental study. London: Constable, 1965

19 **Bassingthwaighte JB**, Raymond GM. Evaluation of the dispersional analysis method for fractal time series. *Ann Biomed Eng* 1995; **23**: 491-505

20 **Bassingthwaighte JB**, Liebovitch LS, West BJ: Fractal physiology. New York: Oxford University Press, 1994

21 **Dioguardi N**, Franceschini B, Aletti G, Russo C, Grizzi F. A fractal dimension rectified meter for quantification of liver fibrosis and other irregular microscopy objects. *Anal Quant Cytol Histol* 2003; **25**: 312-320

22 **Dioguardi N**, Grizzi F, Bossi P, Roncalli M. Fractal and spectral dimension analysis of liver fibrosis in needle biopsy specimens. *Anal Quant Cytol Histol* 1999; **21**: 262-266

23 **Hastings HM**, Sugihara G. Fractals. A User's Guide for the Natural Sciences. Oxford: Oxford Science Publications, 1993.

24 **Nonnenmacher TF**, Baumann G, Barth A, Losa GA: Digital image analysis of self-similar cell profiles. *Int J Biomed Comput* 1994; **37**: 131-138

25 **Losa GA**, Nonnenmacher TF: Self-similarity and fractal irregularity in pathologic tissues. *Mod Pathol* 1996; **9**: 174-182

26 **Cross SS**: Fractals in pathology. *J Pathol* 1988; **182**: 1-8

27 **Grizzi F**, Dioguardi N. A fractal scoring system for quantifying active collagen synthesis during chronic liver disease. *Int J Chaos Theo Appl* 1999 **4**; 39-44,

28 **Dioguardi N**, Grizzi F. Fractal dimension exponent for quantitative evaluation of liver collagen in bioptic specimens. In "Mathematics and Biosciences in interaction" ,Basel, Boston, Berlin: Birkhauser Press, 2001: 113-120

29 **Ishak KG**. Pathologic features of chronic hepatitis. A review and update. *Am J Clin Pathol* 2000; **113**: 40-55. PMID: 10631857

30 **Nathan C**. Points of control in inflammation. *Nature* 2002; **420**: 846-852

31 **Baptista A**, Bianchi L, De Groote J, Desmet VJ, Ishak KG, Korb G, MacSween RN, Popper H, Poulsen H, Scheuer PJ, et al. The diagnostic significance of periportal hepatic necrosis and inflammation. *Histopathology* 1988; **12**: 569-579

32 **Ishak K**, Baptista A, Bianchi L, Callea F, De Groote J, Gudat F, Denk H, Desmet V, Korb G, MacSween RN, et al. Histological grading and staging of chronic hepatitis. *J Hepatol* 1995; **22**: 696-699

33 **Villari D**, Raimondo G, Brancatelli S, Longo G, Rodino G, Smedile V. Histological features in liver biopsy specimens of patients with acute reactivation of chronic type B hepatitis. *Histopathology* 1991; **18**: 73-77

34 **Wallet F**, Dussert C. Multifactorial comparative study of spatial point pattern analysis methods. *J Theor Biol* 1997; **187**: 437-447

35 **Fortune S**. A Sweepline Algorithm for Voronoi Diagrams. *Algorithmica* 1987; 2: 153-174

36 **Fitzsimons CJ**, Nikjoo H, Bolton CE, Goodhead DT. A novel algorithm for tracing the interaction of a track with molecular targets-use of Delaunay triangulation. *Math Biosci* 1998; **154**: 103-115

37 **Bostick D**, Vaisman II. A new topological method to measure protein structure similarity. *Biochem Biophys Res Commun* 2003; **304**: 320-325

38 **Weiler-Normann C**, Rehermann B. The liver as an immunological organ. *J Gastroent Hepatol* 2004; **19**: S279-S283

39 **Rosen R**. Fundamentals of measurements and representation of natural systems. Amsterdam: North-Holland, 1978

Science Editor Wang XL and Guo SY **Language Editor** Elsevier HK

PO Box 2345, Beijing 100023, China
www.wjgnet.com
wjg@wjgnet.com

ELSEVIER

World J Gastroenterol 2005;11(44):7001-7006
World Journal of Gastroenterology ISSN 1007-9327

• *CLINICAL RESEARCH* •

Open label trial of granulocyte apheresis suggests therapeutic efficacy in chronically active steroid refractory ulcerative colitis

Wolfgang Kruis, Axel Dignass, Elisabeth Steinhagen-Thiessen, Julia Morgenstern, Joachim Mössner, Stephan Schreiber, Maurizio Vecchi, Alberto Malesci, Max Reinshagen, Robert Löfberg

Wolfgang Kruis, Julia Morgenstern, Evangelisches Krankenhaus Kalk, Innere Abteilung, Universität zu Köln, Germany
Axel Dignass, Elisabeth Steinhagen-Thiessen, Medizinische Klinik für Hepatologie und Gastroenterologie, Campus Virchow-Klinikum, Universitätsklinikum, Charité, Berlin, Germany
Joachim Mössner, Medizinische Klinik und Poliklinik II, Universitätsklinikum Leipzig, Germany
Stephan Schreiber, Medizinische Klinik, Universität Kiel, Germany
Maurizio Vecchi, Dep of Int Medicine IRCCS Ospedale Policlinico, University of Milano, Italy
Alberto Malesci, Istituto Clinico Humanitas, Milano, Italy
Max Reinshagen, Innere Medizin, Universitätsklinikum Ulm, Germany
Robert Löfberg, Karolinska Institute at the IBD unit, Sophia Hemmet, Stockholm, Sweden
Correspondence to: Wolfgang Kruis, MD, Professor of Medicine, Evangelisches Krankenhaus Kalk. Buchforststr. 2, 51103 Cologne (Köln), Germany. ansorg@evkk.de
Telephone: +49-2-21-8289-5289 Fax: +49-2-21-8289-5291
Received: 2005-04-04 Accepted: 2005-04-18

Abstract

AIM: To study the efficacy, safety, and feasibility of a granulocyte adsorptive type apheresis system for the treatment of patients with chronically active ulcerative colitis despite standard therapy.

METHODS: An open label multicenter study was carried out in 39 patients with active ulcerative colitis (CAI 6-8) despite continuous use of steroids (a minimum total dose of 400 mg prednisone within the last 4 wk). Patients received a total of five aphereses using a granulocyte adsorptive technique (Adacolumn®, Otsuka Pharmaceutical Europe, UK). Assessments at wk 6 and during follow-up until 4 mo comprised clinical (CAI) and endoscopic (EI) activity index, histology, quality of life (IBDQ), and laboratory tests.

RESULTS: Thirty-five out of thirty-nine patients were qualified for intent-to-treat analysis. After the apheresis treatment at wk 6, 13/35 (37.1%) patients achieved clinical remission and 10/35 (28.6%) patients had endoscopic remission (CAI<4, EI<4). Quality of life (IBDQ) increased significantly (24 points, $P<0.01$) at wk 6. Apheresis could be performed in all but one patient. Aphereses were well tolerated, only one patient experienced anemia.

CONCLUSION: In patients with steroid refractory ulcerative colitis, five aphereses with a granulocyte/monocyte depleting filter show potential short-term efficacy. Tolerability and technical feasibility of the procedure are excellent.

Key words: Steroid; Refractory colitis; Ulcerative colitis; Granulocyte; Apheresis

Kruis W, Dignass A, Steinhagen-Thiessen E, Morgenstern J, Mössner J, Schreiber S, Vecchi M, Malesci A, Reinshagen M, Löfberg R. Open label trial of granulocyte apheresis suggests therapeutic efficacy in chronically active steroid refractory ulcerative colitis. *World J Gastroenterol* 2005; 11(44): 7001-7006
http://www.wjgnet.com/1007-9327/11/7001.asp

INTRODUCTION

Systemically acting corticosteroids are mainstay in the treatment of patients with severely active ulcerative colitis (UC). But steroid free remission cannot be achieved in up to 40% of these selected patients[1,2]. Thus, there is a need of alternative treatment options.

Etiology of inflammatory bowel disease (IBD) is still unknown, but the pathogenesis is thought to comprise interaction between genetic factors, intestinal flora, and immunomediated tissue injury[3] Extravasation of a large number of granulocytes and macrophages into the mucosa plays a major role in the release of proinflammatory cytokines[4,5], reactive oxygen derivatives[6-9], and degradative proteases[10]. Accordingly, immunosuppressive therapy has been introduced for refractory patients. Azathioprine/6-mercaptopurine, cyclosporin, and tacrolimus are widely used at present. But drawbacks such as delayed efficacy, adverse events, and costs are currently still limiting the clinical success in severely ill patients and proctocolectomy is necessary in about one-third of these patients. The search for a better treatment strategy has failed as yet. Trials with methotrexate, infliximab, and interferon have shown no convincing effects.

In view of the pathogenetic key role of granulocytes and macrophages, it makes sense to focus on therapeutic goals here. A recently developed adsorptive carrier-based granulocyte and monocyte apheresis device has demonstrated significant effects on inflammatory processes both *in vivo* and *in vitro*[11]. Preliminary data have shown promising therapeutic efficacy in IBD, rheumatoid arthritis, and other conditions[11]. Expanding on these findings, we have reported the results of an open label study on the efficacy of granulocyte apheresis treatment in severely ill patients with chronically active UC despite high doses of systemic corticosteroids.

MATERIALS AND METHODS

This was a prospective and open label trial investigating the efficacy, safety, and feasibility of therapeutic apheresis in patients with active UC despite chronic intake of high doses of systemic corticosteroids. The study was conducted in eight European gastrointestinal (GI) referral centers (Germany, Sweden, Italy, Spain) according to the Declaration of Helsinki (as amended in Edinburgh) and the good clinical practice (GCP) guidelines. The study was approved by the "Ethikkommission der Ärztekammer Nordrhein", Germany as well as local ethics committees of the participating centers. All patients received materials in their own language and gave written consent.

Patients were included if they were aged between 18 and 75 years and diagnosed with active disease (clinical activity index/CAI$\geqslant$6 and $\leqslant$8, and endoscopic index/EI>4)[12]. Additional inclusion criteria were as follows: patients who were dependent on steroids and relapsed despite continuous use of steroids (a minimum total dose of 400 mg prednisone or equivalent within the last 4 wk, dose of steroids was not changed 2 wk prior to the study), history of at least one previous attack with an unsuccessful attempt to taper corticosteroids, immunosuppressants, and aminosalicylates were constant, 3 mo and 4 wk prior to the study, respectively.

Exclusion criteria were patients with severe activity (CAI>8); pregnancy, nursing; arterial hypotension/systolic pressure <11.97 kPa and/or diastolic pressure <8.645 kPa or hypertension (systolic pressure >23.94 kPa or diastolic pressure >15.96 kPa); serious renal, hepatic or cardiovascular disease; laboratory abnormalities such as neutrophils $<1\times10^9$/L, platelets $<100\times10^9$/L, hemoglobin <10 g/L, aPT >1.25 times upper range, aPTT >1.66 times upper normal range, AST or ALT >3 times upper normal range, total bilirubin >2.5 times upper normal range, creatinine >1.8 mg/L; allergy to heparin; viral infection within 4 wk prior to the study; positive stool microbiology; major bowel resection.

Study treatment

Each patient was intended to receive a total of five apheresis sessions, each per week for 5 consecutive weeks. An apheresis session lasted for 60 min at a flow rate of 30 mL/min. Most treatments were performed in an outpatient clinic, partly in dialysis units and also in apheresis non-specialized settings.

The apheresis system used consists of a pump with an integrated monitor (Adamonitor®, manufactured by Otsuka Electronics, Japan) and a single use polycarbonate column (Adacolumn®, CE-Mark; EC certificate GI030136676005, TUV) with a capacity of about 335 mL, filled with 220 g cellulose acetate beads (about 35 000 pieces) of 2 mm in diameter (carriers) bathed in physiological saline and steam sterilized (manufactured by JIMRO, Japan).

Concomitant medication according to inclusion criteria was permitted.

Study design

The aim of this open label pilot study was to investigate the therapeutic effects of a granulocyte adsorptive type apheresis system in patients with chronically active UC despite high doses of corticosteroids. Clinical efficacy as well as feasibility and safety of the procedure were evaluated.

Clinical examination and laboratory tests

Assessments were performed at the beginning and end of the study as well as after 1, 2, 3, 4, and 5 wk of treatment. Clinical (clinical activity index, CAI) and endoscopic (endoscopic index, EI) findings were defined according to Rachmilewitz[12]. Endoscopies were performed at the beginning and the end of study. Histology was reviewed by pathologists who were blinded to the study. Clinical remission was defined by a score of CAI$\leqslant$4, while clinical response was defined as a drop of CAI$\geqslant$3. Endoscopic remission was defined by an EI$\leqslant$4, while endoscopic response was defined as a drop of EI$\geqslant$2. In addition, quality of life was assessed according to the IBDQ scoring system[13]. IBDQ was not assessed in Italian patients (n = 5). Physician's global assessment was asked for and the consumption of steroids was noted.

Laboratory tests included a differential blood count, hemoglobin, hematocrit, fibrinogen, aPT, aPTT, ESR, CRP, orosomucoid, calcium, sodium, potassium, phosphorus, creatinine, BUN/urea, uric acid, bilirubin, total protein albumin, alpha1-antitrypsin, haptoglobin, alkaline phosphatase, AST, ALT, GGT, LDH, and standard urine analyses.

Statistical analysis

The primary objective of this open multicenter study was to find the number of patients achieving clinical remission (CAI$\leqslant$4) at the end of the treatment (wk 6). Because of the uncontrolled pilot characteristics of the study, only descriptive statistical analyses were performed. Sample size was set at 35 patients. Two groups of patients were analyzed. The intent-to-treat (ITT) population consisted of all patients who experienced at least one complete (60 min) treatment of apheresis. Only patients who fulfilled the protocol without major violations were included into the per-protocol (PP) population. Comparisons were made using Wilcoxon signed rank test.

If not otherwise mentioned, data were expressed as mean$\pm$SE. P<0.05 was considered statistically significant.

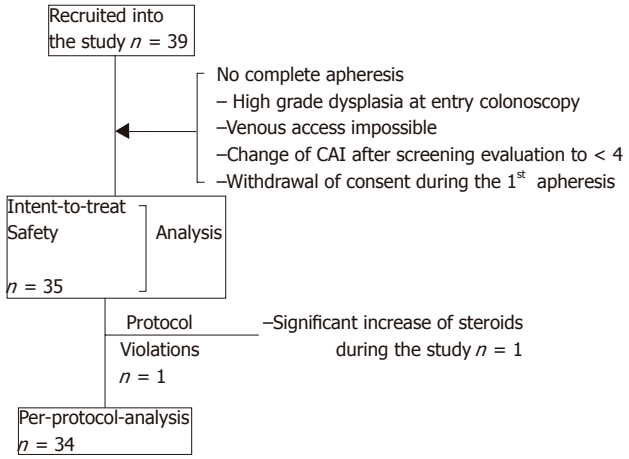

Figure 1 Patients: Analysis sets and drop outs.

Table 1 Biographical and clinical characteristics of the patients studied (intent-to-treat population[1])

Patients (ITT analysis)	*n* = 35	
Age: median/range (yr)	35	(20-72)
Female *n* (%)	10	(28.6)
Smoker *n* (%)	2	(5.7)
Ex-smoker *n* (%)	19	(54.3)
Disease: duration (mean+SE, yr) 7.2+0.8		
Site of disease: extent *n* (%):		
Proctosigmoiditis	3	(8.6)
Left sided	9	(25.7)
Pancolitis	23	(65.7)
Pretreatment (all patients had steroids)		
Aminosalicylates *n* (%)	25	(74.4%)
Immunosuppressants *n* (%)	13	(37.1%)

[1]Note: Per-protocol population comprised all but one ITT patient.

RESULTS

According to the inclusion criteria a total of 39 patients were recruited. Among the patients who underwent proctocolectomy, one patient received surgery before he started apheresis therapy because high grade dysplasia was found in the initial colonoscopy, the other two patients were operated upon because of refractory disease at wk 6 during the follow-up period. Figure 1 displays the different analysis sets and reasons for exclusion. Biographic and clinical characteristics are listed in Table 1. Suitable venous access could not be accomplished in one patient. All the other patients who started treatment received five treatments with apheresis. A total of 176 apheresis procedures could be performed without major technical difficulties. The majority of the patients (18/35) were treated in GI units, while 17/35 patients were treated in specialized dialysis units. Aphereses lasted for 60±3 min in 90.3% of the procedures and were prematurely stopped (50-55 min) in 1.7% procedures and the respective apheresis exceeded (65-91 min) in 8.0% procedures.

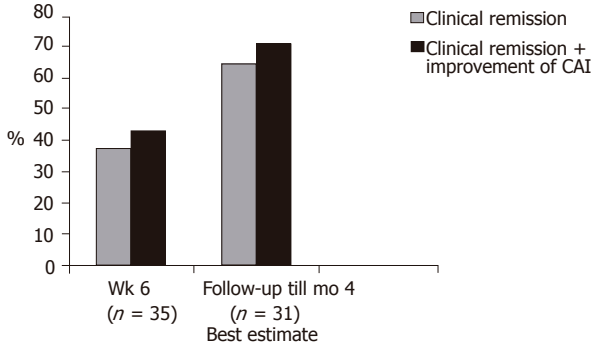

Figure 2 Patients (ITT analysis) in clinical remission or improved during a 4-mo follow-up period without additional apheresis therapy.

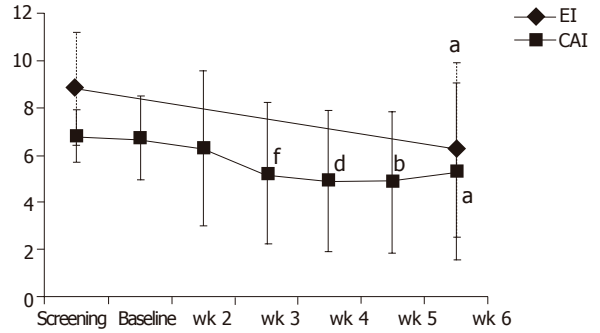

Figure 3 Course of clinical and endoscopic activity indices (CAI, EI) throughout the apheresis treatment. [a]*P*<0.05 *vs* Et at wk 6, [b]*P*<0.01 *vs* Et at wk 5, [d]*P*<0.01 *vs* Et at wk 4, [f]*P*<0.05 *vs* Et at wk 3.

Intent-to-treat analysis

At the end of the treatment period (at wk 6) 13/35 patients (37.1%) achieved clinical remission (CAI≤4). Remission or clinical improvement was observed in 15/35 (42.8%) of the patients. During a follow-up period (up to 4 mo), the number of patients achieving clinical remission increased to 20/31 patients (65%) (best estimate) (Figure 2). Except for doses of steroids no other relevant changes in medication occurred during the follow-up. Four patients lost the follow-up. The clinical remission rate of patients with concomitant immunosuppressants was 23% (3/13 patients) at wk 6 and 54.5% (6/11 patients) at the end of the follow-up. Figure 3 displays the course of clinical (CAI) and endoscopic (EI) activity. Both indices dropped significantly between the beginning and end (at wk 6) of the treatment period.

Endoscopic remission (EI<4) was observed at wk 6 in 10/35 (28.6%) patients. Mucosal healing (vulnerability of mucosa and mucosal damage scores) was improved in 19 patients, unchanged in 13 patients and deteriorated in 3 patients (P<0.001).

Between wk 0 and 6, changes in histology improved in 14 (44%) patients, no change in 16 (50%) and deteriorated in 2 (6%) patients (P<0.002).

Quality of life of the 30 non-Italian patients (IBDQ) improved rapidly by 17 points within 3 wk of treatment (P<0.01) and reached 162±6.4 points at wk 6 which was

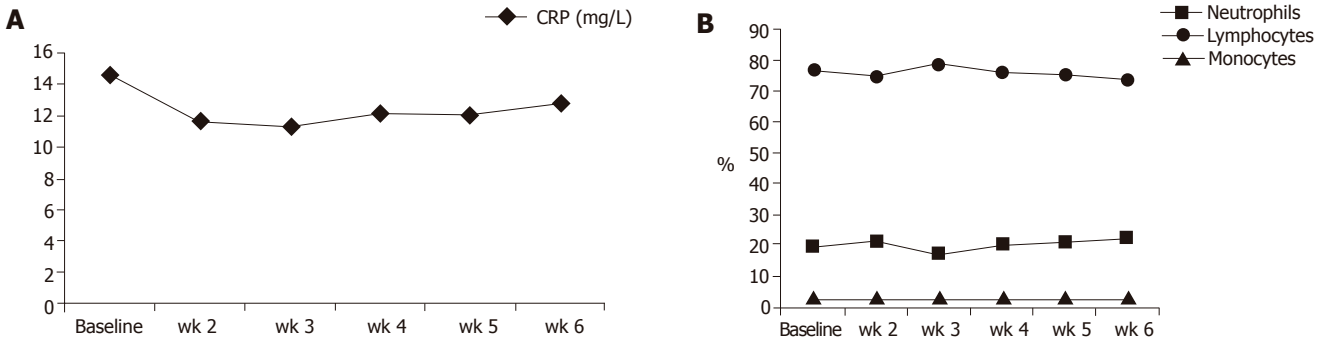

Figure 4 Course of neutrophil, lymphocyte, and monocyte counts as well as CRP between the beginning and wk 6 of the study (numbers are given as means; no significant differences).

significantly ($P<0.01$) better than that at the beginning of the study (138.1±4.8 points).

Physician's global assessment at wk 6 was 'very much improved' (11.4%), 'much improved' (37.1%), 'minimally improved' (25.7%), 'no change' (20.0%), 'minimally worse' (5.7%) and 'much worse' (0%).

Figure 4 displays the results of blood cell counts and CRP serum concentrations between the beginning and wk 6 of the study. With the exception of the lymphocyte count all other numbers dropped, but none of those changes reached statistical significance.

Consumption of systemic steroids decreased significantly ($P<0.05$) throughout the whole treatment period. The median total dose of systemic steroids was decreased from 20.0 mg/d at baseline to 15.0 mg/d at wk 6. The means were 26.1±18.04 mg/d and 16.5±15.56 mg/d, respectively. At the end of 4-mo follow-up period, the median daily dose of steroids was 6.5 mg (mean daily dose: 14.6±16.8 mg).

Per-protocol analysis

One patient of the ITT patient group experienced several changes of his dose of steroids (increase or decrease >10 mg) throughout the study. He was, therefore, excluded from the per-protocol analysis. The patient did not achieve clinical remission but had clinical improvement.

Safety analysis

No unexpected adverse events occurred. The 35 patients included experienced a total of 46 adverse events (AEs) in 65 episodes recorded. Three events were serious: thrombosis of the lower leg, worsening of UC, and a significant drop of hemoglobin which could not be explained despite extensive investigations (the patient recovered quickly). The causality was judged as unlikely, none and possible, respectively. All other AEs were judged as non-serious and mild or moderate. Ten had no causal relationship to the study treatment, 38 had a possible, and 3 had a probable relationship. The three AEs probably related to the therapy were finger edema, right arm phlebitis, and paresthesia of the left hand. All of them were classified as mild. The 38 events judged as possibly related were headache, abdominal disorder, dysesthesia, dizziness, nausea, flush, muscle cramps, fatigue, vegetative dystonia, mood alteration, prostate inflammation, and urinary tract infection. They were judged as mild (28) or moderate (10). Those events classified as unlikely related to the study treatment were oral aphthae, vertigo, headache, common cold, cramps, thrombosis, arthralgia, meralgia, ankle swelling, and bronchopneumonia. Laboratory testing as mentioned in Methods did not reveal any significant alterations.

DISCUSSION

Granulocyte apheresis application with five scheduled sessions strongly suggests efficacy in chronically active steroid refractory UC in the study reported here. A short treatment period of 5 wk resulted not only in significant clinical but also in significant endoscopic and histological improvements. Moreover, when aphereses were stopped, further beneficial effects could be observed. A follow-up period of 4 mo demonstrated carryover effects of the initial treatment leading to clinical remission in three out of four patients. Apheresis treatment was safe and well tolerated.

These very good results must be critically seen in the light of the open uncontrolled study design. Extracorporal treatment, apparently different from medicinal or surgical therapy, is a new method also for 'experienced' patients, a fact which may hold some placebo effects. Other studies demonstrated that the placebo effect is up to 30% in similar patient groups (e.g. 14) but to our knowledge, none of those trials allowed ongoing intensive treatment (dose of steroids, immunosuppressants) at entry to the study as in the present study. All patients kept on having their initial unsuccessful treatment with steroids and in part with immunosuppressants. Recent results of other studies support our findings. Yamamoto *et al*.[15] described 70% clinical remission in 30 patients with active distal UC and Naganuma *et al*.[16] found a remission rate of 55% in either steroid refractory or dependent patients. Both trials used a similar treatment protocol.

The apheresis system is used to remove excess and activated leukocytes from peripheral blood. The release of proinflammatory cytokines in the peripheral blood such as tumor necrosis factor-α (TNF-α), interleukin-1β (IL-

1β), IL-6, and IL-8 is suppressed as well as the leukocyte adhesion molecules (L-selectin) and neutrophil adhesion to IL-1β-activated endothelial cells are downregulated[17-20]. In addition, it exerts antioxidant effects[21] and the production of anti-inflammatory substances such as IL-1 receptor antagonist (IL-1ra), IL-10, and soluble TNF-α receptors I and II (sTNF-α RI and sTNF-α RII) is increased[22,23]. UC patients with high mucosal content of IL-8mRNA responding well to granulocyte apheresis and mucosal IL-8mRNA can be significantly reduced[24]. Granulocyte apheresis seems also to modulate apoptosis[17]. These far reaching interventions on inflammatory immune reactions may explain the carryover effects of granulocyte apheresis, when its application is stopped and standard treatment is continued.

Adsorption techniques may lead to a decrease of circulating blood cells. Indeed peripheral granulocytes decrease significantly by 22% after a 60-min apheresis application in UC patients, but no granulocytopenia occurs[18]. Measurements of pre- and post-column blood cell counts have demonstrated adsorption of 65% of granulocytes, 55% of monocytes, and 2% of lymphocytes, but the number of peripheral leukocytes does not fall below the normal level[19]. Flow cytometry has shown an increase in the number of immature circulating granulocytes (CD 10^- neutrophils) which should be less proinflammatory[17]. The modest effect of apheresis on blood cell counts may prevent dangerous immunosuppressive adverse events seen in systemically acting immunosuppressants.

The protocol of our study prescribed 5-wk apheresis sessions with a duration of 60 min and a flow rate of 30 mL/min, a procedure which is based on empiricism. Intensification of this low exchange technique might create more rapid and/or more favorable therapeutic results. In a large trial in patients with rheumatoid arthritis the protocol here was compared to apheresis twice per week and no therapeutic advantage of intense treatment could be observed[20]. In a small study in patients with UC, intensified apheresis revealed more rapid but not superior therapeutic effects[25]. As yet the most effective procedure remains unclear. Another way to intensify the effects of apheresis is to increase the exchange of blood per time by augmenting the flow rate during the procedure. This may create technical difficulties. The easy technical success of the protocol as it occurred in the present study is based on the low exchange protocol. Simple handling is a prerequisite of the method for its introduction to non specialized (apheresis) units.

In conclusion, granulocyte apheresis seems to be a very promising treatment, particularly in severely ill patients with UC. For patients refractory to standard therapies, it could offer an alternative which is safe and well tolerated. Controlled studies are urgently warranted.

REFERENCES

1 **Allison MC**, Dhillon AP, Lewis WG, Pounder RE (eds). Inflammatory Bowel Disease. London: Mosby, 1998

2 **Jarnerot G**, Rolny P, Sandberg-Gertzen H. Intensive intravenous treatment of ulcerative colitis. *Gastroenterology* 1985; **89:** 1005-1013

3 **Shanahan F**. Crohn's disease. *Lancet* 2002; **359:** 62-69

4 **van Dullemen HM**, van Deventer SJ, Hommes DW, Bijl HA, Jansen J, Tytgat GN, Woody J. Treatment of Crohn's disease with anti-tumor necrosis factor chimeric monoclonal antibody (cA2). *Gastroenterology* 1995; **109:** 129-135

5 **Lloyd AR**, Oppenheim JJ. Poly's lament: the neglected role of the polymorphonuclear neutrophil in the afferent limb of the immune response. *Immunol Today* 1992; **13:** 169-172

6 **Yamada T,** Volkmer C, Grisham MB. Antioxidant properties of 5-aminosalicylic acid: Potential mechanism for its anti-inflammatory activity. In: Trends in Inflammatory Bowel Disease Therapy. CN Williams (ed) Boston: *Kluwer Academic Publishers,* 1990: 73-84

7 **Yamada T,** Grisham MB. Role of neutrophil-derived oxidants in the pathogenesis of intestinal inflammation. *Klin Wochenschr* 1991; **69:** 988-994

8 **Grisham MB**, Yamada T. Neutrophils, nitrogen oxides, and inflammatory bowel disease. *Ann N Y Acad Sci* 1992; **664:** 103-115

9 **Kurtel H**, Granger DN, Tso P, Grisham MB. Vulnerability of intestinal interstitial fluid to oxidant stress. *Am J Physiol* 1992; **263:** G573-G578

10 **Grisham MB**, Granger N. Mechanisms of neutrophil-mediated tissue injury. In: Inflammatory Bowel Disease. RP MacDermott, WF Stenson (eds.) New York: *Elsevier*, 1992: 225-239

11 **Saniabadi AR,** Hanai H, Takeuchi K, Umemura K, Nakashima M, Adachi T, Shima C, Bjarnason I, Loefberg R. Adacolumn, an adsorptive carrier based granulocyte and monocyte apheresis device for the treatment of inflammatory and refractory diseases associated with leukocytes. *Ther Apher Dial* 2003; **7:** 48-59

12 **Rachmilewitz D.** Coated mesalazine (5-aminosalicylic acid) versus sulphasalazine in the treatment of active ulcerative colitis: a randomised trial. *BMJ* 1989; **298:** 82-86

13 **Irvine EJ**, Feagan B, Rochon J, Archambault A, Fedorak RN, Groll A, Kinnear D, Saibil F, McDonald JW. Quality of life: a valid and reliable measure of therapeutic efficacy in the treatment of inflammatory bowel disease. Canadian Crohn's Relapse Prevention Trial Study Group. *Gastroenterology* 1994; **106:** 287-296

14 **Probert CS**, Hearing SD, Schreiber S, Kuhbacher T, Ghosh S, Arnott ID, Forbes A. Infliximab in moderately severe glucocorticoid resistant ulcerative colitis: a randomised controlled trial. *Gut* 2003; **52:** 998-1002

15 **Yamamoto T**, Umegae S, Kitagawa T, Yasuda Y, Yamada Y, Takahashi D, Mukumoto M, Nishimura N, Yasue K, Matsumoto K. Granulocyte and monocyte adsorptive apheresis in the treatment of active distal ulcerative colitis: a prospective, pilot study. *Aliment Pharmacol Ther* 2004; **20:** 783-792

16 **Naganuma M**, Funakoshi S, Sakuraba A, Takagi H, Inoue N, Ogata H, Iwao Y, Ishi H, Hibi T. Granulocytapheresis is useful as an alternative therapy in patients with steroid-refractory or -dependent ulcerative colitis. *Inflamm Bowel Dis* 2004; **10:** 251-257

17 **Kashiwagi N,** Sugimura K, Koiwai H, Yamamoto H, Yoshikawa T, Saniabadi AR, Adachi M, Shimoyama T. Immunomodulatory effects of granulocyte and monocyte adsorption apheresis as a treatment for patients with ulcerative colitis. *Dig Dis Sci* 2002; **47:** 1334-1341

18 **Shimoyama T**, Sawada K, Hiwatashi N, Sawada T, Matsueda K, Munakata A, Asakura H, Tanaka T, Kasukawa R, Kimura K, Suzuki Y, Nagamachi Y, Muto T, Nagawa H, Iizuka B, Baba S, Nasu M, Kataoka T, Kashiwagi N, Saniabadi AR. Safety and efficacy of granulocyte and monocyte adsorption apheresis in patients with active ulcerative colitis: a multicenter study. *J Clin Apher* 2001; **16:** 1-9

19 **Ohara M,** Saniabadi AR, Kokuma S, Hirata I, Adachi M, Agishi T, Kasukawa R. Granulocytapheresis in the treatment of patients with rheumatoid arthritis. *Artif Organs* 1997; **21:** 989-994

20 **Kashiwagi N**, Hirata I, Kasukawa R. A role for granulocyte and monocyte apheresis in the treatment of rheumatoid arthritis. *Ther Apher* 1998; **2:** 134-141

21 **Hirayama A**, Nagase S, Ueda A, Ishizu T, Taru Y, Yoh K, Hirayama K, Kobayashi M, Koyama A. Oxidative stress during leukocyte absorption apheresis. *J Clin Apher* 2003; 18: 61-66

22 **Hanai H,** Takeuchi K, Iida T, Tanaka T, Tozawa K, Watanabe F, Maruyama Y, Yamada M, Iwaoka Y, Satou Y, Matsushita I, Saniabadi A. Release of IL-10, IL-1 receptor antagonist, soluble TNF-α receptors I and II during adsorptive granulocyte and monocyte/macrophage reduction therapy of patients with active ulcerative colitis. *Gastroenterology* 2004; **126 (Suppl 2):** A 567

23 **Takeda Y,** Hiraishi K, Takeda H, Shiobara H, Saniabadi AR, Adachi M, Kawata S. Cellulose acetate beads induce release of interleukin-1 receptor antagonist, but not tumour necrosis factor-α or interleukin-1β in human peripheral blood, *Inflamm Res* 2003; **52:** 287-290

24 **Tsukada Y,** Nakamura T, Iimura M, Iizuka BE, Hayashi N. Cytokine profile in colonic mucosa of ulcerative colitis correlates with disease activity and response to granulocytapheresis. *Am J Gastroenterol* 2002; **97:** 2820-2828

25 **Sakuraba A,** Naganuma M, Hibi T. Intensive therapy of granulocyte and adsorption apheresis induces rapid remission in patients with ulcerative colitis. *Gastroenterology* 2003; **124 (Suppl 1):** A 522

Science Editor Wang XL and Guo SY **Language Editor** Elsevier HK

PO Box 2345, Beijing 100023, China
www.wjgnet.com
wjg@wjgnet.com

ELSEVIER

World J Gastroenterol 2005;11(44):7007-7013
World Journal of Gastroenterology ISSN 1007-9327

• *CLINICAL RESEARCH* •

Appropriateness of indication and diagnostic yield of colonoscopy: First report based on the 2000 guidelines of the American Society for Gastrointestinal Endoscopy

Iqbal Siddique, Krishna Mohan, Fuad Hasan, Anjum Memon, Istvan Patty, Basil Al-Nakib

Iqbal Siddique, Fuad Hasan, Basil Al-Nakib, Department of Medicine, Faculty of Medicine, Kuwait University, Kuwait
Iqbal Siddique, Krishna Mohan, Fuad Hasan, Istvan Patty, Basil Al-Nakib, Thunayan Al-Ghanim Gastroenterology Center, Al-Amiri Hospital, Kuwait
Anjum Memon, Department of Public Health and Primary Care, Institute of Public Health, University of Cambridge, Cambridge, United Kingdom
Correspondence to: Dr Iqbal Siddique, Department of Medicine, Faculty of Medicine, Kuwait University, PO Box 24923, Safat 13110, Kuwait. isiddique@hsc.edu.kw
Telephone: +965-5319596 Fax: +965-5338907
Received: 2005-03-17 Accepted: 2005-06-09

Abstract

AIM: To assess the appropriateness of referrals and to determine the diagnostic yield of colonoscopy according to the 2000 guidelines of the American Society for Gastrointestinal Endoscopy (ASGE).

METHODS: A total of 736 consecutive patients (415 males, 321 females; mean age 43.6±16.6 years) undergoing colonoscopy during October 2001-March 2002 were prospectively enrolled in the study. The 2000 ASGE guidelines were used to assess the appropriateness of the indications for the procedure. Diagnostic yield was defined as the ratio between significant findings detected on colonoscopy and the total number of procedures performed for that indication.

RESULTS: The large majority (64%) of patients had colonoscopy for an indication that was considered "generally indicated", it was "generally not indicated" for 20%, and it was "not listed" for 16% in the guidelines. The diagnostic yield of colonoscopy was highest for the "generally indicated" (38%) followed by "not listed" (13%) and "generally not indicated" (5%) categories. In the multivariable analysis, the diagnostic yield was independently associated with the appropriateness of indication that was "generally indicated" (odds ratio=12.3) and referrals by gastroenterologist (odds ratio =1.9).

CONCLUSION: There is a high likelihood of inappropriate referrals for colonoscopy in an open-access endoscopy system. The diagnostic yield of the procedure is dependent on the appropriateness of indication and referring physician's specialty. Certain indications "not listed" in the guidelines have an intermediate diagnostic yield and further studies are required to evaluate whether they should be included in future revisions of the ASGE guidelines.

Key words: Colonoscopy; Indications; Diagnostic yield; Guidelines; Appropriateness

Siddique I, Mohan K, Hasan F, Memon A, Patty I, Al-Nakib B. Appropriateness of indication and diagnostic yield of colonoscopy: First report based on the 2000 guidelines of the American Society for Gastrointestinal Endoscopy. *World J Gastroenterol* 2005; 11(44): 7007-7013
http://www.wjgnet.com/1007-9327/11/7007.asp

INTRODUCTION

Over the last two decades, there has been a remarkable advancement in gastrointestinal endoscopy, and colonoscopy has become the most commonly performed procedure for the diagnosis and treatment of diseases of the large intestine as well as screening for colon cancer[1,2]. The increasing availability of colonoscopy, however, has also led to an inappropriate referral and overuse of this procedure, which is reported to range between 15% and 35% in different studies[3-6]. Consensus-based guidelines for appropriate referral of both upper and lower gastrointestinal endoscopic procedures have been developed by several expert panels[7,8]. The American Society for Gastrointestinal Endoscopy (ASGE) has also developed and periodically reviews the guidelines on the appropriate use of these procedures with the latest update made in the year 2000[9].

The diagnostic yield of an endoscopic procedure is defined as its capacity for identifying a lesion that is potentially important to patient care and has been reported for both upper and lower endoscopy in relation to the appropriateness of the indication[8]. For colonoscopy, it is reported to range 40-45% for procedures that are referred for appropriate indications, and 15-20% for those with inappropriate indications[3,6,8,10].

The objectives of this study were to evaluate the appropriateness of referrals for colonoscopy based on

the 2000 ASGE guidelines on the appropriate use of gastrointestinal endoscopy, and to assess the diagnostic yield of the procedure according to these guidelines.

MATERIALS AND METHODS

For administrative purposes, Kuwait with its population of about 2.2 million is divided into six districts, each with a well-defined area and population. Medical services in each district comprise a network of primary care clinics and a general public hospital. In addition, there are a number of centralized specialty hospitals. Our study was conducted at the Thunayan Al-Ghanim Gastroenterology Center, which offers modern facilities in gastrointestinal endoscopy, and treatment and follow-up of gastroenterology and hepatology patients. The center provides open access endoscopy services for five out of six general public hospitals in Kuwait. Primary care physicians and specialists working in hospitals can directly refer patients for endoscopy. The majority of endoscopies are performed without prior consultation with a gastroenterologist.

This study was carried out prospectively between October 2001 and March 2002. Demographic data, in/outpatient status, specialty of the referring physician, indications for the procedure, and results of colonoscopy (including histologic reports, if any) were recorded in a standardized form specifically developed for this study. The year 2000 ASGE guidelines were used to determine the appropriateness of indication(s) for the procedure. These guidelines were printed on the form used for data collection, but the headings "generally indicated" and "generally not indicated" were omitted to avoid bias. Before starting the colonoscopy, the endoscopist obtained a brief history from the patient to confirm the indications for the procedure and to exclude any contraindications. If the indications were not listed in the ASGE guidelines, the endoscopist was asked to record it separately on the form. If the patient had more than one indication for colonoscopy and at least one of these was "generally indicated" by the guidelines, then the procedure was considered appropriate.

Diagnostic yield in relation to each indication was defined as the ratio between significant findings detected on colonoscopy and the total number of procedures performed for that indication. Based on the criteria followed in previous studies[3,6,11], the presence of any of the following lesions was considered as a significant finding on colonoscopy: a pre-malignant or malignant lesion, inflammatory bowel disease (IBD) (either newly diagnosed or a more precise diagnosis or determination of the extent of the disease that influenced immediate management of the disease), angiodysplasia, stricture (benign or malignant), other colitides (infectious, ischemic, eosinophilic, microscopic), and diverticulosis (as a definite or presumptive cause of acute hematochezia)[12]. The following were not considered as significant findings: normal colonoscopy, hemorrhoids, anal fissures, previously established IBD, uncomplicated diverticulosis, and nonadenomatous polyps. The study was carried out in accordance with the ethical standards of our institution and the Helsinki Declaration as revised in 1989.

We used Student's *t*-test to compare the difference between two means and the normal *Z* test to assess the significant difference between two proportions. Multiple logistic regression analysis was performed to study the clinical parameters independently associated with diagnostic yield of colonoscopy. $P<0.05$ was considered statistically significant. All *P* values presented are two sided. The data were analyzed using SPSS 13.0 for Windows software (SPSS Inc., Chicago, IL, USA).

RESULTS

A total of 759 patients were referred for colonoscopy during the study period. Colonoscopy could not be performed in 23 of these patients because of inadequate bowel preparation. None of the patients had any contraindications for the procedure. Table 1 shows the demographic and clinical characteristics of the 736 patients (415 males, 321 females) who were prospectively enrolled in the study. The mean age of the patients was 43.6±16.6 years (range 1-90 years), and the large majority (82.3%) were outpatients. The majority of the patients were referred by general physicians (34.6%) and surgeons (33.4%).

Table 1 Demographic and clinical characteristic of 736 patients undergoing colonoscopy in Kuwait

Characteristic	*n* (%)
Gender	
Male	415 (56.4)
Female	321 (43.6)
Age (yr)	
Mean age (SD)	43.6 (16.6)
<15	31 (4.2)
15-49	441 (59.9)
⩾50	264 (35.9)
Referring clinician	
General physician	255 (34.6)
Surgeon	246 (33.4)
Gastroenterologist	205 (27.9)
Pediatric gastroenterologist	22 (3.0)
Other[1]	8 (1.1)
Clinical status	
Inpatient	130 (17.7)
Outpatient	606 (82.3)

[1]Oncologist (6), gynecologist (2).

Indications for colonoscopy

Of the 736 patients, 468 (63.6%) had colonoscopy for an indication that was considered appropriate according to the ASGE guidelines (Table 2). The two most common indications were "hematochezia" and "diarrhea of

Table 2 Indications for colonoscopy among 468 patients referred for reasons generally indicated according to the 2000 ASGE guidelines[1]

Indication	*n* (%)
1 Hematochezia	151 (20.5)
2 Clinically significant diarrhea of unexplained origin	65(8.8)
3 Irritable bowel syndrome or chronic abdominal pain: colonoscopy done once to rule out organic disease	48(6.5)
4 Chronic inflammatory bowel disease of the colon, if more precise diagnosis or determination of the extent of activity of disease will influence immediate management	34 (4.6)
5 Unexplained iron deficiency anemia	27 (3.7)
6 Following adequate clearance of neoplastic polyp(s) survey at 3-5 year intervals	24 (3.3)
7 Colonoscopy to remove synchronous neoplastic lesions at or around time of curative resection of cancer followed by colonoscopy at 3 years and 3-5 years thereafter to detect metachronous cancer	23 (3.1)
8 Evaluation of an abnormality on barium enema or other imaging study, which is likely to be clinically significant, such as a filling defect or stricture	19 (2.6)
9 Presence of fecal occult blood	12 (1.6)
10 Examination to evaluate the entire colon for synchronous cancer or neoplastic polyps in a patient with treatable cancer or neoplastic polyp	11 (1.5)
11 Excision of colonic polyp	9 (1.2)
12 Balloon dilation of stenotic lesions (e.g., anastomotic strictures)	9 (1.2)
13 Melena after an upper GI source has been excluded	8 (1.1)
14 In patients with ulcerative or Crohn's pancolitis eight or more years' duration or left sided colitis 15 or more years' duration every 1-2 years with systematic biopsies to detect dysplasia	8 (1.1)
15 Treatment of bleeding from such lesions as vascular malformation, ulceration, neoplasia, and polypectomy site (e.g., electrocoagulation, heater probe, laser or injection therapy)	7 (1.0)
16 Family history of sporadic colorectal cancer before the age of 60: colonoscopy every 5 years beginning at the age of 10 years earlier than the affected relative or every three years if adenoma is found	6 (0.8)
17 Intraoperative identification of a lesion not apparent at surgery (e.g., polypectomy site, location of a bleeding site)	3 (0.4)
18 Family history of hereditary non-polyposis colorectal cancer: colonoscopy every two years beginning at the age of 25, or five years younger than the earliest age of diagnosis of colorectal cancer. Annual colonoscopy beginning at the age of 40	2 (0.3)
19 Palliative treatment of stenosing or bleeding neoplasms (e.g., laser, electrocoagulation, stenting)	2 (0.3)

[1]According to 2000 American Society for Gastrointestinal Endoscopy (ASGE) guidelines on appropriate use of gastrointestinal endoscopy[9].

unexplained etiology". Whereas, 149 (20.2%) patients underwent colonoscopy for an indication, which was "generally not indicated" (Table 3), and for 119 (16.2%) patients the indication for colonoscopy was not listed in the guidelines (Table 4). The most common indications for patients in these two categories were "chronic, stable, irritable bowel syndrome or chronic abdominal pain", and "constipation", respectively.

Table 5 shows the appropriateness of indications for colonoscopy in relation to patients' gender, age, admission status, and specialty of the referring physician. There was no material difference in the appropriateness of indications between males and females or in- and out-patients. The mean age of patients who had colonoscopy for an indication that was "generally not indicated" was significantly lower than those who had the procedure for an indication that was "generally indicated" or "not listed" in the guidelines (38.2 *vs* 44.7 years, $P<0.0001$). Patients aged <15 years and those >50 years had a higher proportion of procedures for an indication that was considered "generally indicated" by the guidelines (77.4% and 74.6%, respectively). On the other hand, 29.5% of the patients aged 15-49 years had a significantly higher proportion of colonoscopies for an indication that was considered "generally not indicated" ($P<0.0001$). There was no real difference in the age groups when the procedure was performed for an indication that was "not listed" in the guidelines.

Pediatric gastroenterologists referred the highest proportion of patients (81.8%) for colonoscopy for an indication that was considered "generally indicated", followed by adult gastroenterologists (66.8%), surgeons (62.2%) and general physicians (60.4%). Among other specialists, general physicians referred the highest proportion of patients for colonoscopy for a reason that was considered "generally not indicated", while surgeons referred the highest proportion of patients for a "not listed" indication.

Diagnostic yield of colonoscopy

A total of 200 patients had one or more significant findings on colonoscopy giving an overall diagnostic yield of 27.2%. The most common significant findings were adenomatous polyps (29.5%), new diagnosis or more precise determination of the extent of IBD (23.5%) and colorectal cancer (12.0%). The yield of the procedures performed for "generally indicated" category was 37.8%, which was significantly higher than "generally not indicated" (4.7%, $P<0.0001$) and "not listed" (13.4%, $P<0.0001$) categories in the ASGE guidelines (Table 5). The yield of the procedures performed for "not listed" indications was also significantly higher than that for "generally not indicated" procedures (13.4% *vs* 4.7%, $P<0.05$). Inpatients had a higher diagnostic yield of

Table 3 Indications for colonoscopy among 149 patients referred for reasons generally not indicated according to the 2000 ASGE guidelines[1]

Indication	*n* (%)
1 Chronic, stable, irritable bowel syndrome or chronic abdominal pain	117 (15.9)
2 Routine follow-up of inflammatory bowel disease	15 (2.0)
3 Acute diarrhea	7 (1.0)
4 Metastatic adenocarcinoma of unknown primary site in the absence of colonic signs or symptoms when it will not influence management	6 (0.8)
5 Upper GI bleeding or melena with a demonstrated upper gastrointestinal source	4 (0.5)

[1]According to 2000 American Society for Gastrointestinal Endoscopy (ASGE) guidelines on appropriate use of gastrointestinal endoscopy[9].

Table 4 Indications for colonoscopy among 119 patients referred for reasons not listed in the 2000 ASGE guidelines[1]

Indication	*n* (%)
1 Constipation	71 (9.6)
2 Unexplained weight loss	14 (1.9)
3 Normochromic anemia	7 (1.0)
4 Perianal abscess or fistula	6 (0.8)
5 Abdominal mass of unknown origin	4 (0.5)
6 Periodic follow up of healed benign lesions	4 (0.5)
7 Surveillance after resection of colonic polyps or cancer, at different intervals from those recommended	3(0.4)
8 Intestinal obstruction	2 (0.3)
9 Routine examination of the colon in patients with no colon-related signs or symptoms about to have elective abdominal surgery for non-colonic disease	2 (0.3)
10 Others	6 (0.8)

[1]According to 2000 American Society for Gastrointestinal Endoscopy (ASGE) guidelines on appropriate use of gastrointestinal endoscopy[9].

Table 5 Appropriateness of indication and diagnostic yield of colonoscopy according to patients' characteristics

Characteristic (no. of patients)	Appropriateness of referral[1] *n* (%)			Diagnostic yield (%)
	Generally indicated	Generally not indicated	Not listed	
All patients (736)	468 (63.6)	149 (20.2)	119 (16.2)	27.2
Diagnostic yield	37.8%	4.7%	13.4%	-
Gender				
Male (415)	263(63.4)	87 (21.0)	65 (15.7)	28.0
Female (321)	205 (63.9)	62 (19.3)	54 (16.8)	26.2
Age (yr)				
Mean age (SD)	44.7 (17.3)	38.2 (12.1)	46.3 (17.3)	
<15 (31)	24 (77.4)	2 (6.5)	5 (16.1)	48.4
15-49 (441)	247 (56.0)	130 (29.5)	64 (14.5)	22.2
⩾50 (264)	197 (74.6)	17 (6.4)	50 (18.9)	33.0
Referring clinician				
General physician (255)	154 (60.4)	63 (24.7)	38 (14.9)	18.0
Surgeon (246)	153 (62.2)	34 (13.8)	59 (24.0)	27.6
Gastroenterologist (205)	137 (66.8)	49 (23.9)	19 (9.3)	36.6
Pediatric gastroenterologist (22)	18 (81.8)	1 (4.5)	3 (13.6)	50.0
Other[2] (8)	6 (75.0)	2 (25.0)	0	0
Clinical status				
Inpatient (130)	89 (68.5)	19 (14.6)	22 (16.9)	35.4
Outpatient (606)	379 (62.5)	130 (21.5)	97 (16.0)	25.4

[1]According to 2000 American Society for Gastrointestinal Endoscopy (ASGE) guidelines on appropriate use of gastrointestinal endoscopy[9]. [2]Oncologist (6), gynecologist (2).

Table 6 Clinical findings on colonoscopy by appropriateness of referral

	Appropriateness of referral[1] *n* (%)		
	Generally indicated	Generally not indicated	Not listed
Cancer	21 (4.5)	0[a]	3 (2.5)
Adenoma	54 (11.5)	1 (0.7)[c]	4 (3.4)[a]
IBD[2]	62 (13.2)	6 (4.0)[c]	8 (6.7)
Other colitides[3]	36 (1.3)	0	1 (0.8)
Angiodysplasia	5 (1.1)	0	0

[1]According to 2000 American Society for Gastrointestinal Endoscopy (ASGE) guidelines on appropriate use of gastrointestinal endoscopy[9].
[2]IBD, inflammatory bowel disease.
[3]Non-specific colitis (3), infectious colitis (3), eosinophilic colitis (1).
[a]$P<0.05$ compared to "Generally indicated".
[c]$P<0.005$ compared to "Generally indicated".

Table 7 Odds ratios (OR) and 95% confidence intervals (95% CI) for association between selected clinical parameters and diagnostic yield of colonoscopy

Parameter (*n*)	Diagnostic yield (%)	OR[1] (95% CI[2])	*P*
Gender			
Female (321)	26.2	1.0 -	
Male (415)	28.0	1.1 (0.8-1.5)	>0.50
Age (years)			
<50 (472)	23.9	1.0 -	
≥50 (264)	33.0	1.6 (1.1-2.2)	<0.05
Clinical status			
Outpatient (606)	25.4	1.0 -	
Inpatient (130)	35.4	1.6 (1.1-2.4)	<0.05
Referring clinician			
Other (531)	23.5	1.0 -	
Gastroenterologist (205)	36.6	1.9 (1.3-2.7)	<0.001
Appropriateness of indication[3]			
Generally not indicated (149)	4.7	1.0 -	
Not listed (119)	13.4	3.2 (1.3-7.9)	<0.05
Generally indicated (468)	37.8	12.3 (5.7-27.0)	<0.001

[1]OR, odds ratio.
[2]CI, confidence interval.
[3]According to 2000 American Society for Gastrointestinal Endoscopy (ASGE) guidelines on appropriate use of gastrointestinal endoscopy[9].

colonoscopy compared to outpatients (35.4% *vs* 25.4%, $P<0.05$). The highest diagnostic yield was obtained in those aged <15 years, and in those who were referred by a gastroenterologist.

Table 6 lists some of the significant findings on colonoscopy by appropriateness of referrals. Colorectal cancer, adenomatous polyps, and IBD were more likely to be detected, if the colonoscopy was performed for a "generally indicated" reason. The colon was reported as completely normal in 82.6% of the patients in the "generally not indicated" and 73.9% in "not listed" groups, compared to 51.7% in the "generally indicated" group.

Determinants of diagnostic yield

Table 7 shows the association between selected clinical parameters and diagnostic yield of colonoscopy. The probability of finding a clinically significant lesion was significantly higher in patients aged ⩾50 years (odds ratio = 1.6), inpatients (odds ratio = 1.6), those referred by gastroenterologists (odds ratio = 1.9), and those who had the colonoscopy for "generally indicated" (odds ratio = 12.3) or "not listed" (odds ratio = 3.2) categories. After adjustment for the other variables, appropriateness of indications for colonoscopy according to the ASGE guidelines and referrals by gastroenterologist were the two independent parameters associated with the diagnostic yield.

DISCUSSION

To our knowledge, this is the first study to assess the appropriateness of referrals for colonoscopy and to determine the diagnostic yield according to the year 2000 ASGE guidelines. About 64% of our patients had an indication for colonoscopy that was appropriate or

"generally indicated", according to the ASGE guidelines. This finding is similar to the 61-66% rate reported from open-access colonoscopy settings in the United States, Italy and Switzerland[3,5,6,8]. A higher rate (81%) has been reported in a study from the United States, where the referring physicians were instructed on the accepted indications for gastrointestinal endoscopy[4]. All these studies were based on the 1992 version of the ASGE guidelines. The year 2000 guidelines include several new conditions for which colonoscopy is now considered "generally indicated" such as all patients presenting with hematochezia, while the older guidelines only considered colonoscopy to be appropriate, if the hematochezia was not thought to be from the rectum or a perianal source. In addition, screening of asymptomatic, average risk patients for colonic neoplasia and seven new therapeutic indications have been included in the new guidelines. Inclusion of these additional indications means that a higher proportion of the patients referred for open-access colonoscopy should have an appropriate indication for the procedure. In our study, the overall rate of "generally indicated" colonoscopies was comparable to the studies based on the 1992 guidelines. It is noteworthy that our patients were relatively younger than those in other studies. Compared to an average age of 53-62 years in other studies, the average age of our patients was about 44 years and 60% were aged between 15 and 49 years. This may be the reason why we did not have a higher proportion of patients referred for appropriate indications even though we used more "liberal" ASGE guidelines. We did, however, observe a higher rate of "generally indicated" colonoscopy for patients aged <15 years (77%), which is not unexpected as colonoscopy is usually not performed in children unless an appropriate indication is present, and for those aged >50 years (75%).

We found no real difference between various specialties when patients were referred for a "generally indicated" colonoscopy. As for "generally not indicated" procedure, the rate was lowest for surgeons, while that for gastroenterologists was similar to general physicians. This finding is consistent with a study of open-access colonoscopy from Italy which reported similar rates of "generally not indicated" colonoscopy between gastroenterologists and family physicians[5], but is in contrast with studies of open access upper gastrointestinal endoscopy[13]. The majority (80%) of "generally not indicated" colonoscopies requested by gastroenterologists in our study were for chronic stable abdominal pain or irritable bowel syndrome (IBS), while the other 20% were for routine follow-up of IBD. This high referral rate of colonoscopy for chronic stable abdominal pain or IBS by gastroenterologists may be because in Kuwait many such patients after failing to respond to therapy are referred to the gastroenterology clinics by primary care physicians. When these patients were excluded from the analysis, the rate of "generally indicated" colonoscopy for gastroenterologists increased to about 83%, which was higher than that for all other specialties.

In our study, the definition of significant findings was based on certain positive results on colonoscopy. A normal colonoscopy was not considered significant, although this may be relevant to patient care as it may rule out a serious disease in the colon. Our results show that the diagnostic yield of colonoscopy was independently associated with appropriateness of indications and referrals by gastroenterologists. Our findings are consistent with studies conducted in Europe and the United States[3,6,11], but the difference between the yield of "generally indicated' and "generally not indicated' procedures (37.8% *vs* 4.7%) is much higher than reported in these studies. Charles *et al*.[3] reported that 40% of patients who have colonoscopy for an ASGE (1992 version) approved indication have a significant pathological finding compared to 22% of those who do not meet the guidelines. Similarly, Morini *et al*.[6] have reported a diagnostic yield of 43% for "generally indicated" and 16% for "generally not indicated" categories. De Bosset *et al*.[11], using the Swiss criteria developed by the Rand Corporation/University of California at Los Angeles (RAND/UCLA) panel, have reported a diagnostic yield of 26% for patients who have colonoscopy for an appropriate or uncertain indication and 17% for those with an inappropriate indication. The higher difference in the diagnostic yield of colonoscopy for a "generally indicated" and "generally not indicated" category seen in our study suggests that the 2000 ASGE guidelines for appropriate use of gastrointestinal endoscopy are more efficient in discriminating indications for colonoscopy than the earlier versions or the Swiss (RAND/UCLA) criteria.

The year 2000 ASGE guidelines clearly differentiate between the "generally indicated" and "generally not indicated" colonoscopies in terms of the diagnostic yield of the procedure. Clinicians can therefore predict the expected yield of colonoscopy as long as the indications for the procedure can clearly be classified as "generally indicated' or "generally not indicated". However, in clinical practice there are always some patients who undergo colonoscopy for indications that cannot be clearly classified into either of these two categories. It has been reported that about 12-28% of the patients undergoing colonoscopy have indications that are not listed in the ASGE guidelines[5,6,8]. In our study, the proportion of patients in "not listed' category was about 16% with a diagnostic yield of 13.4%, being about three times higher than the diagnostic yield of colonoscopy which is "generally not indicated". Among the patients in the "not listed' category, three were diagnosed with colorectal cancer compared to none in the "generally not indicated" group and the proportion of patients diagnosed with adenomatous polyps and IBD was also higher. The ASGE guidelines appear to be deficient with regard to these "not listed" indications, but it is acknowledged that clinical considerations may occasionally justify a course of action at variance with the recommendations of the ASGE. The two most frequent unlisted indications in our study were constipation and unexplained weight loss, and all three cases of colorectal cancer were found in patients who underwent colonoscopy for constipation. Clear recommendations are needed for such common unlisted

indications such as constipation as provided in the Swiss and American panel-based guidelines[8]. Further studies are needed to identify other common but unlisted indications that may be included in future versions of the ASGE guidelines.

In summary, the results of this prospective study demonstrate that a large proportion of colonoscopies performed in an open-access system in Kuwait is for the indications considered inappropriate by, or not listed in the 2000 guidelines of the ASGE on appropriate use of gastrointestinal endoscopy. The probability of identifying a significant finding on colonoscopy is particularly higher when the indications for the procedure are judged to be appropriate by the ASGE guidelines, but a proportion of patients who undergo colonoscopy for an unlisted indication also have significant findings. Further studies are required to evaluate these unlisted indications to determine whether they should be included in future revisions of the guidelines. General physicians need further edification for appropriate referrals of patients for colonoscopy.

REFERENCES

1 **Karasick S**, Ehrlich SM, Levin DC, Harford RJ, Rosetti EF, Ricci JA, Beam LM, Gigliotti JV. Trends in use of barium enema examination, colonoscopy, and sigmoidoscopy: is use commensurate with risk of disease? *Radiology* 1995; **195**: 777-784

2 **Scott B**. Endoscopic demands in the 90's. *Gut* 1990; **31**: 125-126

3 **Charles RJ**, Chak A, Cooper GS, Wong RC, Sivak MV Jr. Use of open access in GI endoscopy at an academic medical center. *Gastrointest Endosc* 1999; **50**: 480-485

4 **Mahajan RJ**, Barthel JS, Marshall JB. Appropriateness of referrals for open-access endoscopy. How do physicians in different medical specialties do? *Arch Intern Med* 1996; **156**: 2065-2069

5 **Minoli G**, Meucci G, Bortoli A, Garripoli A, Gullotta R, Leo P, Pera A, Prada A, Rocca F, Zambelli A. The ASGE guidelines for the appropriate use of colonoscopy in an open access system. *Gastrointest Endosc* 2000; **52**: 39-44

6 **Morini S**, Hassan C, Meucci G, Toldi A, Zullo A, Minoli G. Diagnostic yield of open access colonoscopy according to appropriateness. *Gastrointest Endosc* 2001; **54**: 175-179

7 **Burnand B**, Vader JP, Froehlich F, Dupriez K, Larequi-Lauber T, Pache I, Dubois RW, Brook RH, Gonvers JJ. Reliability of panel-based guidelines for colonoscopy: an international comparison. *Gastrointest Endosc* 1998; **47**: 162-166

8 **Froehlich F**, Pache I, Burnand B, Vader JP, Fried M, Beglinger C, Stalder G, Gyr K, Thorens J, Schneider C, Kosecoff J, Kolodny M, DuBois RW, Gonvers JJ, Brook RH. Performance of panel-based criteria to evaluate the appropriateness of colonoscopy: a prospective study. *Gastrointest Endosc* 1998; **48**: 128-136

9 Appropriate use of gastrointestinal endoscopy. American Society for Gastrointestinal Endoscopy. *Gastrointest Endosc* 2000; **52:** 831-837

10 **Berkowitz I**, Kaplan M. Indications for colonoscopy. An analysis based on indications and diagnostic yield. *S Afr Med J* 1993; **83**: 245-248

11 **De Bosset V**, Froehlich F, Rey JP, Thorens J, Schneider C, Wietlisbach V, Vader JP, Burnand B, Muhlhaupt B, Fried M, Gonvers JJ. Do explicit appropriateness criteria enhance the diagnostic yield of colonoscopy? *Endoscopy* 2002; **34**: 360-368

12 **Jensen DM**, Machicado GA, Jutabha R, Kovacs TO. Urgent colonoscopy for the diagnosis and treatment of severe diverticular hemorrhage. *N Engl J Med* 2000; **342**: 78-82

13 **Minoli G**, Prada A, Gambetta G, Formenti A, Schalling R, Lai L, Pera A. The ASGE guidelines for the appropriate use of upper gastrointestinal endoscopy in an open access system. *Gastrointest Endosc* 1995; **42**: 387-389

Science Editor Wang XL and Guo SY **Language Editor** Elsevier HK

PO Box 2345, Beijing 100023, China
www.wjgnet.com
wjg@wjgnet.com

ELSEVIER

World J Gastroenterol 2005;11(44):7014-7017
World Journal of Gastroenterology ISSN 1007-9327

• *RAPID COMMUNICATION* •

Treatment for isolated loco-regional recurrence of gastric adenocarcinoma: Does surgery play a role?

Fabio Carboni, Pasquale Lepiane, Roberto Santoro, Riccardo Lorusso, Pietro Mancini, Massimo Carlini, Eugenio Santoro

Fabio Carboni, Pasquale Lepiane, Roberto Santoro, Riccardo Lorusso, Pietro Mancini, Eugenio Santoro, Department of Digestive Surgery and Liver Transplantation, Regina Elena Cancer Institute, Rome, Italy
Massimo Carlini, Division of General A.T. Surgery, St. Eugenio Hospital, Rome, Italy
Correspondence to: Fabio Carboni, MD, PhD, Department of Digestive Surgery and Liver Transplantation, Regina Elena Cancer Institute, via Elio Chianesi 53, 00144, Rome, Italy. fabiocarb@tiscali.it
Telephone: +39-6-52666789 Fax: +39-6-52662338
Received: 2005-01-14 Accepted: 2005-04-26

Key words: Gastric adenocarcinoma; Recurrence; Diagnosis; Surgery

Carboni F, Lepiane P, Santoro R, Lorusso R, Mancini P, Carlini M, Santoro E. Treatment for isolated loco-regional recurrence of gastric adenocarcinoma: Does surgery play a role? *World J Gastroenterol* 2005; 11(44): 7014-7017
http://www.wjgnet.com/1007-9327/11/7014.asp

Abstract

AIM: To evaluate the role of surgical treatment for isolated loco-regional recurrences of operated gastric adenocarcinoma.

METHODS: Among the 837 patients operated for gastric adenocarcinoma between December 1979 and April 2004, 713 (85%) underwent resection with curative intent. A retrospective review of a prospectively collected gastric cancer database was carried out. Overall recurrence rate was 44% (315 cases), with 75% occurring within the first 2 years from the operation. Isolated L-R recurrences were observed in 38 (12%) patients. Symptomatic lesions were observed in 27 (71%).

RESULTS: Six (16%) patients were macroscopically resected with curative intent. The recurrence was located in the gastric stump after a STG in three patients, in the esophagojejunal anastomosis after a TG in two patients and in the gastric bed after a TG in one patient. Surgical procedures consisted of three secondary TG, two esophagojejunal resection and one excision of an extraluminal recurrence. Postoperative complications occurred in two patients (33%), including one anastomotic leakage and one hemorrhage. The latter patient died of sepsis 35 d after the surgery (mortality rate 17%). All patients died of recurrent gastric cancer: 2 within 1 year from surgery (8 and 11 mo, respectively), 2 after 16 and 17 mo respectively and 1 after 28 mo from the second operation.

CONCLUSION: Surgery plays a very limited role in the treatment for isolated loco-regional recurrence of gastric adenocarcinoma.

INTRODUCTION

Despite the decreasing overall incidence, gastric adenocarcinoma is still one of the most common causes of death for cancer worldwide. Even after curative gastrectomy, disease recurrence occurs in 22-50% of patients, mostly within two years from the operation[1-5].

Loco-regional (L-R) recurrence results from lymphatic spread or direct tumor propagation within the abdominal cavity[6]. Several series tried to clarify the relationship between clinicopathologic features of the primary tumor and failure patterns[1-5,7-11]. In any case, effective therapies are lacking and surgical resection is only rarely possible.

The aim of this study was to retrospectively analyze our experience with the surgical treatment of L-R recurrence in patients operated for gastric cancer.

MATERIALS AND METHODS

Out of the 905 patients submitted to gastric resections between December 1979 and April 2004, 837 with adenocarcinoma were entered and followed in a prospectively recorded database. Among these, 713 (85%) underwent resection with curative intent, consisting of 392 total gastrectomies (TG) and 321 proximal or subtotal distal gastrectomies (STG). Standard D2 lymph node dissection was performed in most patients, with D3 dissection performed for curative intent in selected cases. Pathologic stage distribution, according to the 1997 TNM classification[12], included stages IA (11%), IB (13%), II (14%), IIIA (15%), IIIB (16%), and IV (31%). All stages up to IV were due to N category or T4 classification in the presence of positive nodes. The most common histological type was intestinal (53%), according to Lauren's criteria.

All patients were included in a prospectively collected database. Follow-up examinations were performed 1 mo

Table 1 Resected patients' background at the time of the primary operation

Sex	Age	Staging	Operation	Adjuvant therapy	Histology	Tumor-free interval (mo)
1 M	72	T3N2M0	STG	CHT	Diffuse	9
2 F	60	T3N0M0	STG	–	Diffuse	21
3 M	49	T3N2M0	STG	CHT	Intestinal	12
4 M	63	T3N2M0	TG	CHT	Diffuse	16
5 M	66	T4N1M0	TG	CHT	Diffuse	24
6 F	58	T2N1M0	TG	–	Intestinal	50

after the surgery, once in every 3 mo during the first 2 years, every 6 mo for the first 5 years and yearly thereafter. Follow-up program included physical examination, laboratory analysis including serum tumor markers (CEA, CA 19-9, and CA 72-4) at each visit, abdominal ultrasound or computed tomography (CT) and chest radiograph every 6 mo and endoscopy once a year. Follow-up information was regularly obtained from outpatient clinical visits, from the time of surgery to May 2004 or until death. Median follow-up was 13 mo (range 1 mo to 163 mo).

Recurrences were classified according to the definition of Lenhert *et al*. as distant metastasis and L-R recurrences, including local lymph nodes metastasis, extraluminal recurrence, recurrence within the gastric remnant after STG and esophagojejunal anastomosis recurrence after TG[6].

Overall recurrence rate was 44% (315 cases), with 75% occurring within the first 2 years from the operation. Disease recurrence was rare after 5 years (5%). Isolated L-R recurrences were observed in 38 (12%) patients, while distant metastasis only in 167 (53%) and combined in the remaining 110 (35%). Symptomatic lesions were observed in 27 (71%), mostly including upper digestive obstruction and pain. In the asymptomatic patients, the recurrence was incidentally discovered during routine follow-up, most commonly by CT scan and occasionally by endoscopy or tumor markers elevation.

RESULTS

Six (16%) patients were macroscopically resected with curative intent, representing 4% only of all observed L-R recurrences. The other 32 patients underwent conservative treatment in 25 cases (66%), laparotomy only in five cases (13%) and by-pass procedure in two cases (5%). Resected patients' background at the time of the primary operation is shown in Table 1. Mean tumor-free interval was 22 mo.

The recurrence was located in the gastric stump after a STG in three patients, in the esophagojejunal anastomosis after a TG in two patients and in the gastric bed after a TG in one patient. Surgical procedures consisted of three secondary TG, two esophagojejunal resection and one excision of an extraluminal recurrence. Postoperative complications occurred in two patients (33%), including one anastomotic leakage and one hemorrhage. The latter patient died of sepsis 35 d after the surgery (mortality rate 17%). Three patients received adjuvant chemotherapy (CHT) after the second operation, in two combined with intraoperative radiation therapy (IORT). Clinical course of the resected cases is described in Table 2.

Table 2 Clinical course in resected cases

Case	Recurrent site	Operation	Adjuvant therapy	Survival (mon)	Recurrence
1	Gastric stump	TG-liver segmentectomy	–	16	Distant
2	Gastric stump	TG-splenectomy	CHT+IORT	28	Distant
3	Gastric stump	TG-liver segmentectomy	CHT+IORT	17	Combined
4	Esophagojejunal anastomosis	Resection	–	1	–
5	Esophagojejunal anastomosis	Resection	–	8	Combined
6	Gastric bed	Excision	CHT	11	Loco-regional

All patients died of recurrent gastric cancer: 2 within 1 year from surgery (8 and 11 mo, respectively), 2 after 16 and 17 mo respectively and 1 after 28 mo from the second operation (Table 2). Mean survival of the palliated or non-resected patients was 8 mo.

DISCUSSION

Despite considerable improvement in the surgical treatment of gastric adenocarcinoma, recurrences still constitute the main cause of death in operated patients. Recent series showed overall incidence rates of 22-50% after curative surgery, mostly (75-80%) occurring within 2 years[1-5,7-11]. Our 44% recurrence rate is probably due to the high incidence (62%) of advanced operated gastric cancer cases, as for most Western experience. Moreover, our results confirm that recurrences beyond 5 years are rare (3-9%)[1,4,5,10,13]. Median survival from the time of recurrence is approximately 6 mo[1,2,7,10,13].

Gastric cancer recurrence include: L-R recurrence (regional lymph nodes, perianastomotic region, gastric bed, and stump), peritoneal recurrence and hematogenous metastasis (liver, lungs, bones, brain, and skin)[2,3,5,7-11]. As confirmed by our experience, combined recurrences are frequently observed and hematogenous or lymphatic spread without intra-abdominal metastases occur rarely[2,6-8]. An isolated L-R recurrence is reported in 6-46% of patients[1-3,7,8,10,11,13] and they were 12% in our series. Such differences may be explained by variations in the presentation of data, the definition of recurrence, as well as the mode and timing of detection[6,7,10,11].

Clinicopathologic features of the primary tumor that predict L-R recurrences are: proximal location, older age and male gender, advanced stage of disease (T3-4, N+), infiltrative growth, diffuse type and stromal reaction[2-5,7-11]. Although not statistically significant, almost all our cases were males, with advanced age (median 61 years), T4 N+ and diffuse type. Even though advanced stage of the disease is a common risk factor, early gastric cancer (EGC) may relapse in 1.4-6.4% of patients, mostly being hematogenous metastasis, but in approximately 20% of cases, L-R recurrences[2,14].

Diagnosis is improved with modern imaging and

mainly suggested by tumor markers elevation, endoscopy, and CT scan. As occurred in our experience, most patients are symptomatic and diagnosis is earlier in such cases[10,13]. Since early detection of recurrence do not improve overall survival of patients; however, according to some authors, until the development of a more effective treatment, routine follow-up is not indicated and should be reserved for symptomatic patients and to provide psychological support[1,13,15].

Some retrospective and small series showed the usefulness of CEA, CA 19-9 and CA 72-4 monitoring in detecting the recurrence of operated gastric cancer[16,17]. However, their elevation is often seen much later than detection of recurrence by imaging, especially in patients with low preoperative levels.

Endoscopic surveillance is the most accurate method to identify anastomotic or gastric stump recurrences after STG, allowing early diagnosis and radical treatment in highly selected cases[18], as it occurred for one patient of our series. Helical CT scan is the most commonly employed diagnostic tool in such cases, but its sensitivity is very low because of the limit in differentiating recurrent tumor from postoperative fibrotic and inflammatory changes[1,19,20].

Once the diagnosis of L-R recurrence has been made, curative surgical resection is only rarely possible. Available data in the literature do not allow a valid interpretation with respect to the different types of recurrence[6]. Excluding anecdotal cases of local lymph nodes or extraluminal recurrence excision[21-23], it appears that a curative resection is possible when a partial gastrectomy was previously performed. Approximately 20% of patients undergo surgical resection but in 2-6% only it may be considered curative, with a mean survival lower than 2 years[1,2,6,13,17,21]. In our series, the resection rate was extremely low. In fact, considering the 38 patients with isolated L-R recurrence, only six (16%) were resected. The remaining group was excluded from surgery mostly because the recurrences were not considered amenable to a curative resection or to the poor general condition. According to some authors, adjuvant chemoradiotherapy has a potential effect on improving prognosis[6,21,23].

Palliative resections are indicated in highly selected symptomatic patient, mainly to restore the food passage, while tumor reduction is of minor importance[2,6]. In those with poor general conditions and a short life expectancy, placement of covered expandable metallic stents is technically feasible and clinically effective[24,25].

In conclusion, surgery plays a very limited role in the treatment for isolated L-R recurrences of gastric cancer. In low-risk patients, especially if symptomatic, an attempt at resection may be justified in specialized center with acceptable postoperative mortality and morbidity, as there are no effective alternative therapies. At present, however, prevention or reduction of the frequency of recurrence, with more extended lymph nodal resection and the combination of perioperative adjuvant treatment[2,4,6,7,10,11], seem more important than the early detection and surgical treatment.

REFERENCES

1 **Bohner H**, Zimmer T, Hopfenmuller W, Berger G, Buhr HJ. Detection and prognosis of recurrent gastric cancer. Is routine follow-up after gastrectomy worthwhile ? *Hepato-Gastroenterol* 2000; **47**: 1489-1494

2 **Yoo CH**, Noh SH, Shin DW, Choi SH, Min JS. Recurrence following curative resection for gastric carcinoma. *Br J Surg* 2000; **87**: 236-242

3 **Maehara Y**, Hasuda S, Koga T, Tokunaga E, Kakeji Y, Sugimachi K. Postoperative outcome and sites of recurrence in patients following curative resection of gastric cancer. *Br J Surg* 2000; **87**: 353-357

4 **Shiraishi N**, Inomata M, Osawa N, Yasuda K, Adachi Y, Kitano S. Early and late recurrence after gastrectomy for gastric carcinoma. Univariate and multivariate analyses. *Cancer* 2000; **89:** 255-261

5 **Marrelli D**, Roviello F, de Manzoni G, Morgagni P, Di Leo A, Saragoni L, De Stefano A, Folli S, Cordiano C, Pinto E. Different patterns of recurrence in gastric cancer depending on Lauren's histological type: longitudinal study. *World J Surg* 2002; **26:** 1160-1165

6 **Lehnert T**, Rudek B, Buhl K, Golling M. Surgical therapy for loco-regional recurrence and distant metastasis of gastric cancer. *Eur J Surg Oncol* 2002; **28:** 455-461

7 **Schwarz RE**, Zagala-Nevarez K. Recurrence patterns after radical gastrectomy for gastric cancer: prognostic factors and implications for postoperative adjuvant therapy. *Ann Surg Oncol* 2002; **9**: 394-400

8 **Wu CW**, Lo SS, Shen KH, Hsieh MC, Chen JH, Chiang JH, Lin HJ, Li AF, Lui WY. Incidence and factors associated with recurrence patterns after intended curative surgery for gastric cancer. *World J Surg* 2003; **27:** 153-158

9 **Otsuji E**, Kuriu Y, Ichikawa D, Okamoto K, Ochiai T, Hagiwara A, Yamagishi H. Time to death and pattern of death in recurrence following curative resection of gastric carcinoma: analysis based on depth of invasion. *World J Surg* 2004; **28**: 866-869

10 **D'Angelica M**, Gonen M, Brennan MF, Turnbull AD, Bains M, Karpeh MS. Patterns of initial recurrence in completely resected gastric adenocarcinoma. *Ann Surg* 2004; **240:** 808-816

11 **Lim DH**, Kim DY, Kang MK, Kim YI, Kang WK, Park CK, Kim S, Noh JH, Joh JW, Choi SH, Sohn TS, Heo JS, Park CH, Park JO, Lee JE, Park YJ, Nam HR, Park W, Ahn YC, Huh SJ. Patterns of failure in gastric carcinoma after D2 gastrectomy and chemoradiotherapy: a radiation oncologist's view. *Br J Cancer* 2004; **91:** 11-17

12 **Sobin LH**, Wittekind C. International Union Against Cancer (UICC) TNM Classification of Malignant Tumours. 5th ed. *New York: Wiley-Liss* 1997: 59-62

13 **Kodera Y**, Ito S, Yamamura Y, Mochizuki Y, Fujiwara M, Hibi K, Ito K, Akiyama S, Nakao A. Follow-up surveillance for recurrence after curative gastric cancer surgery lacks survival benefit. *Ann Surg Oncol* 2003; **10:** 898-902

14 **Lee HJ**, Kim YH, Kim WH, Lee KU, Choe KJ, Kim JP, Yang HK. Clinicopathological analysis for recurrence of early gastric cancer. *Jpn J Clin Oncol* 2003; **33**: 209-214

15 **Huguier M**, Houry S, Lacaine F. Is the follow-up of patients operated on for gastric carcinoma of benefit to the patient? *Hepatogastroenterology* 1992; **39:** 14-16

16 **Takahashi Y**, Takeuchi T, Sakamoto J, Touge T, Mai M, Ohkura H, Kodaira S, Okajima K, Nakazato H. The usefulness of CEA and/or CA19-9 in monitoring for recurrence in gastric cancer patients: a prospective clinical study. *Gastric Cancer* 2003; **6:** 142-145

17 **Marrelli D**, Pinto E, De Stefano A, Farnetani M, Garosi L, Roviello F. Clinical utility of CEA, CA 19-9, and CA 72-4 in the follow-up of patients with resectable gastric cancer. *Am J Surg* 2001; **181:** 16-19

18 **Hosokawa O**, Kaizaki Y, Watanabe K, Hattori M, Douden

K, Hayashi H, Maeda S. Endoscopic surveillance for gastric remnant cancer after early cancer surgery. *Endoscopy* 2002; **34:** 469-473

19 **Jadvar H**, Tatlidil R, Garcia AA, Conti PS. Evaluation of recurrent gastric malignancy with [F-18]-FDG positron emission tomography. *Clin Radiol* 2003; **58:** 215-221

20 **Kim KA**, Park CM, Park SW, Cha SH, Seol HY, Cha IH, Lee KY. CT findings in the abdomen and pelvis after gastric carcinoma resection. *AJR Am J Roentgenol* 2002; **179:** 1037-1041

21 **Takeyoshi I**, Ohwada S, Ogawa T, Kawashima Y, Ohya T, Kawate S, Nakasone Y, Arai K, Ikeya T, Morishita Y. The resection of non-hepatic intraabdominal recurrence of gastric cancer. *Hepatogastroenterology* 2000; **47:** 1479-1481

22 Nashimoto A, Sasaki J, Sano M, Tanaka O, Tsutsui M, Tsuchiya Y, Makino H. Disease-free survival for 6 years and 4 months after dissection of recurrent abdominal paraaortic nodes (no. 16) in gastric cancer: report of a case. *Surg Today* 1997; **27**: 169-173

23 **Inada T**, Ogata Y, Andoh J, Ozawa I, Matsui J, Hishinuma S, Shimizu H, Kotake K, Koyama Y. Significance of para-aortic lymph node dissection in patients with advanced and recurrent gastric cancer. *Anticancer Res* 1994; **14:** 677-682

24 **Jeong JY**, Kim YJ, Han JK, Lee JM, Lee KH, Choi BI, Yang HK, Lee KU. Palliation of anastomotic obstructions in recurrent gastric carcinoma with the use of covered metallic stents: clinical results in 25 patients. *Surgery* 2004; **135:** 171-177

25 Park KB, Do YS, Kang WK, Choo SW, Han YH, Suh SW, Lee SJ, Park KS, Choo IW. Malignant obstruction of gastric outlet and duodenum: palliation with flexible covered metallic stents. *Radiology* 2001; **219**: 679-683

Science Editor Guo SY **Language Editor** Elsevier HK

PO Box 2345, Beijing 100023, China
www.wjgnet.com
wjg@wjgnet.com

ELSEVIER

World J Gastroenterol 2005;11(44):7018-7023
World Journal of Gastroenterology ISSN 1007-9327

• *RAPID COMMUNICATION* •

Hemoconcentration is a poor predictor of severity in acute pancreatitis

José M. Remes-Troche, Andrés Duarte-Rojo, Gustavo Morales, Guillermo Robles-Díaz

José M. Remes-Troche, Andrés Duarte-Rojo, Gustavo Morales, Department of Gastroenterology, Instituto Nacional de Ciencias Médicas y Nutrición Salvador Zubirán, Vasco de Quiroga # 15, Colonia Seccion XVI, Tlalpan, CP 14000, Mexico City, Mexico
Guillermo Robles-Díaz, Department of Experimental Medicine, Facultad de Medicina, Universidad Nacional Autónoma de México, Hospital General de México, Dr Balmis # 148, Colonia de los Doctores, CP 06726, México City, Mexico
Co-first-authors: José M. Remes-Troche and Guillermo Robles-Díaz
Co-correspondent: José M. Remes-Troche
Correspondence to: Professor Guillermo Robles-Díaz, Department of Experimental Medicine, Facultad de Medicina, Universidad Nacional Autónoma de México, Hospital General de México, Dr Balmis # 148, Colonia de los Doctores, CP 06726, México City, Mexico. guiberodi@yahoo.com.mx
Telephone: +52-55-56232673 Fax: +52-55-56232673
Received: 2005-04-07 Accepted: 2005-04-26

Abstract

AIM: To determine whether the hematocrit (Hct) at admission or at 24 h after admission was associated with severe acute pancreatitis (AP), organ failure (OF), and pancreatic necrosis.

METHODS: A total of 336 consecutive patients with a first AP episode were studied. Etiology, Hct values at admission and at 24 h, development of severe AP according to Atlanta's criteria, pancreatic necrosis, OF and mortality were recorded. Hemoconcentration was defined as Hct level >44% for males and >40% for females. The *t*-test and χ^2 test were used to assess the association of hemoconcentration to the severity, necrosis and OF. Diagnostic accuracy was also determined.

RESULTS: Biliary disease was the most frequent etiology (n = 148). Mean Hct levels at admission were 41±6% for females and 46±7% for males (P<0.01). Seventy-eight (23%) patients had severe AP, and OF developed in 45 (13%) patients. According to contrast-enhanced computed tomography scan, 36% (54/150) patients showed pancreatic necrosis. Hct levels were elevated in 58% (55/96) and 61% (33/54) patients with interstitial and necrotizing pancreatitis, respectively. Neither Hct levels at admission nor hemoconcentration at 24 h were associated with the severity, necrosis or OF. Sensitivity, specificity and positive predictive values for both determinations were very low; and negative predictive values were between 61% and 86%, being the highest value for OF.

CONCLUSION: Hct is not a useful marker to predict a worse outcome in acute pancreatitis. In spite of the high negative predictive value of hemoconcentration, the prognosis gain is limited due to an already high incidence of mild disease.

Key words: Acute pancreatitis; Hematocrit; Hemoconcentration; Severity; Necrosis

Remes-Troche JM, Duarte-Rojo A, Morales G, Robles-Díaz G. Hemoconcentration is a poor predictor of severity in acute pancreatitis. *World J Gastroenterol* 2005; 11(44): 7018-7023
http://www.wjgnet.com/1007-9327/11/7018.asp

INTRODUCTION

Acute pancreatitis (AP) is an inflammatory process of the pancreas with variable involvement of peripancreatic tissues or remote organ systems. Mostly, it develops as a mild and auto-limited disease, but around 25% of patients present the severe form with an elevated mortality rate (30%), when compared with overall mortality (2-16%)[1,2]. This worrisome condition is due to the eventual development of organ failure (OF) and sepsis[3,4], both complications are associated with the concurrent development of necrotizing pancreatitis that occurs in 20-30% of the cases[2,5]. Severity is currently defined according to the Atlanta International Symposium on AP by the presence of local complications (pancreatic necrosis, pancreatic pseudocyst, and pancreatic abscess) and/or OF (cardiovascular, pulmonary or renal insufficiency, and gastrointestinal bleeding)[6]. Several efforts have been made to describe prognostic factors that could help for the identification of high risk patients in order to maintain a closer vigilance, thereby providing a more aggressive medical treatment and an earlier admittance to the intensive care unit[7].

The usefulness of multiple clinical and laboratory tests to predict severe and/or necrotizing pancreatitis has been studied[8]. Ranson's criteria are most widely accepted for the assessment of high risk patients; however numerous parameters need to be measured during the first 48 h after admission[9,10]. Other scales like Glasgow or APACHE II are commonly used, but these also require several measurements and have not been proven superior to Ranson's criteria[11,12]. More recently, biochemical

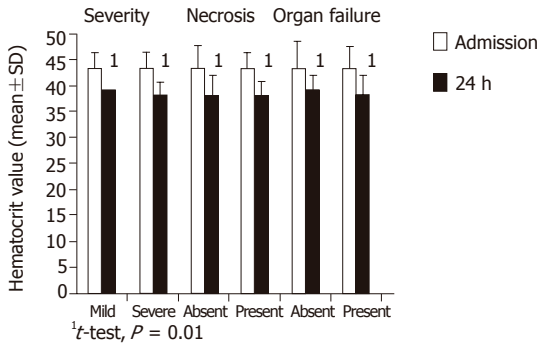

Figure 1 Mean hematocrit values at admission and 24 h later.

markers, such as C-reactive protein[13], polymorphonuclear elastase[14], interleukin-6 and trypsinogen activation peptide[15,16], have been used as predictors of severity in AP. C-reactive protein is a useful marker only 48 h after the onset of acute episodes[13,14] and overall usefulness of the remaining markers is restricted by their limited availability or elevated cost. Thus, so far, no early, accessible and economical predictive marker for severe AP has yet been described.

Hematocrit (Hct) is routinely assessed in every AP case at admission and is an accessible and low-cost test. Recent studies have proposed that hemoconcentration may constitute a good marker for severity of AP, but others were unable to find a significant correlation with the development of OF, pancreatic necrosis or death[17-20]. Thus, the value of hemoconcentration in the initial assessment of AP patients and its implications in prognosis remain controversial. We, therefore, aimed to determine whether hemoconcentration at admission and in the following 24 h was associated with the development of severe AP, pancreatic necrosis and/or OF.

MATERIALS AND METHODS

Patients with a first AP episode admitted consecutively to a tertiary medical center between June 1998 and December 2001 were included in this study. AP diagnosis was confirmed by typical clinical presentation and an increase in amylase or lipase concentration at least thrice the upper limit of normal, and/or evidence of pancreatic inflammation revealed by contrast-enhanced abdominal computed tomography[21]. Medical records of all the patients were reviewed retrospectively for the following variables: gender, age, etiology, Hct level at admission, Hct level at 24 h after admission, development of OF, and severity of AP (both defined according to Atlanta' s criteria)[6], evidence of necrosis in contrast-enhanced abdominal computed tomography, total hospital stay and mortality. Exclusion criteria included patients with previous AP episode(s) or with a first AP episode previously treated in other institutions.

Hematocrit levels at admission and 24 h later were compared with the severity of the pancreatitis, the presence of necrosis or OF. Categorical variables are expressed as absolute and relative frequencies and continuous variables as mean±SD. Receiver operator characteristic (ROC) curves were plotted for the range of Hct levels. Hemoconcentration was defined as an Hct level >44% for male and >40% for female patients[17-20]. The *t* test was used to analyze continuous variables, whereas the χ^2 or *F* tests were used on categorical variables, when appropriate. A *P* value <0.05 was considered statistically significant. Statistical analysis was performed using commercially statistical software SPSS 10 (SPSS, Chicago, IL, USA) and NCSS-2000 (NCSS, Kaysville, UT, USA).

RESULTS

Three hundred and thirty-six AP cases were included in the current study. Mean age was 45±17 (range, 15-90 years) years and 55% (*n* = 185) of patients were females. Sixteen patients (4.7%) were anemic according to reference values established for our population[22]. Mean Hct levels at admission were 41±6 for women and 46±7 for men (*P* = 0.00001). Biliary disease was the most common cause of the acute episode (*n* = 148, 44%), followed by alcohol abuse (*n* = 48, 14%). Other causes included: hypertriglyceridemia (9%), post endoscopic retrograde cholangiopancreatography (7%), drugs-induced (5%), post surgery (4%), obstructive disease (3%), hypercalcemia (1%), trauma (1%) and vasculitis (1%). Thirty-eight events were considered idiopathic (11%). When divided according to gender, biliary disease was more frequent in women and alcoholic pancreatitis was more frequent in men [odds ratio (OR) = 2.16; 95%CI 1.3-3.5 and OR = 40; 95%CI 9.7-243, respectively].

A mild AP episode was diagnosed in 258 (77%) patients, while the remaining 78 (23%) suffered from a severe attack. Organ failure developed in 45 (13%) patients. A contrast-enhanced abdominal computed tomography was performed during the first week after admission to assess the presence of necrosis in 150 cases. The Hct was determined in 233 (69%) patients 24 h after admission; of these, 183 patients (79%) presented with mild AP and 50 (21%) with severe AP. No differences were found in Hct levels at admission regardless of the presence of severe AP, necrosis or OF. A significant decrease in Hct levels was noted in all the patients at 24 h after admission, which was found to be independent of the severity status (Figure 1). There were no differences between the necrotizing and interstitial pancreatitis groups in terms of the fall in Hct levels after admission (7.5±4% *vs* 6.5±4%, respectively).

A ROC curve analysis for several cut offs of Hct levels at admission failed to show a single point combining good sensitivity, specificity, positive and negative predictive values for the detection of severe AP, necrotizing pancreatitis or OF (Figure 2).

However, the optimal cut-off values of Hct were similar to those used to define hemoconcentration (>44% for males and >40% for females). Neither the presence nor the absence of hemoconcentration at admission was associated to severity, necrosis or OF (Table 1). Hemoconcentration was present in 58% (55/96) and 61% (33/54) of patients with interstitial and necrotizing

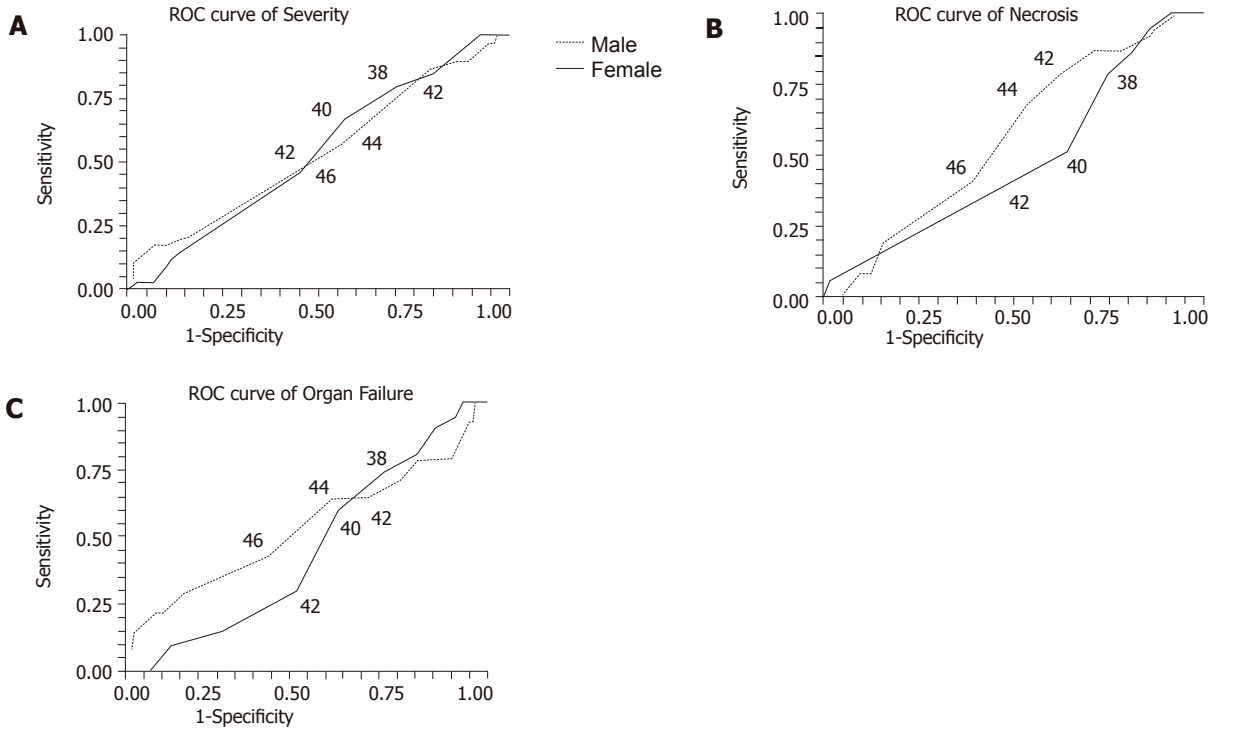

Figure 2 Receiver operating characteristic (ROC) curves for several hematocrit cut-off levels on admission as prognostic factors for severity (**A**), pancreatic necrosis (**B**) and organ failure (**C**).

Table 1 Hemoconcentration at admission as a marker for severe acute pancreatitis (AP), necrotizing AP and organ failure

	Hemoconcentration (Hct≥44% M, Hct≥40% F)[1]	No hemoconcentration (Hct <44% M, Hct <40% F)	Odds ratio (95%CI)	*P* value (χ^2)
Severe AP (*n* = 336)				
No	168	90	0.77	0.32
Yes	46	32	(0.4-1.3)	
Necrotizing AP (*n* = 150)				
No	55	41	1.17	0.64
Yes	33	21	(0.5-2.4)	
Organ failure (*n* = 336)				
No	187	104	0.83	0.58
Yes	27	18	(0.4-1.7)	

[1]Hct: hematocrit; M: male; F: female.

pancreatitis, respectively. Hemoconcentration at 24 h was not associated to severity, necrosis or OF (Table 2). Hemoconcentration at admission and 24 h later had very low sensitivity, specificity, and positive predictive values for severity, necrosis or OF. Better results were obtained for negative predictive values (Table 3).

Hospital and intensive care unit stays were higher in patients with severe AP than mild cases (18±15 and 8±3 d *vs* 10±7 and 0.5±0.1 d, $P<0.05$). Mortality was significantly higher in patients with severe AP (13% *vs* 0.03%, $P = 0.001$).

DISCUSSION

One of the most important actions to cope with patients suffering from AP is to quickly and accurately assess the severity of the attack. Earlier identification of patients at risk of developing pancreatic necrosis and OF potentially improves their care via prompt admission to intensive care unit[23-25].

Besides the development of several prognostic systems for severity in AP, there are multiple biochemical tests[13-16] and clinical parameters[8,9,26-29] proposed as single markers for severe or necrohemorrhagic pancreatitis. Most of the laboratory assays have significant limitations in clinical practice mainly because they are expensive and not widely available. The clinical features might be the most economical and easily available parameters because they result from routine patient assessment. Among them, the presence of older age[8], alcohol etiology[9], time interval between onset of symptoms and admission[26], rebound tenderness/guarding[27], obesity[28], and android fat distribution[29] have been associated with the subsequent development of severe AP. The identification of these parameters as risk factors for the development of severe AP contributed to the understanding of the disease, but their impause of several drawbacks, such as biased clinical

Table 2 Hemoconcentration at 24 h as a marker for severe acute pancreatitis (AP), necrotizing AP and organ failure

	Hemoconcentration (Hct≥44% M, Hct≥40% F)[1]	No hemoconcentration (Hct <44% M, Hct <40% F)	Odds ratio (95%CI)	*P* value(χ^2)
Severe AP (*n* = 233)				
No	125	58	0.64	0.23
Yes	29	21	(0.3–1.2)	
Necrotizing AP (*n* = 100)				
No	39	24	0.9	0.97
Yes	22	15	(0.4–2)	
Organ failure (*n* = 233)				
No	139	68	0.68	0.47
Yes	15	11	(0.3–1.5)	

[1]Hct: hematocrit; M: male; F: female.

Table 3 Accuracy of hemoconcentration at admission and at 24 h later as a marker for severe acute pancreatitis (AP), necrotizing AP and organ failure

Groups	Sensitivity (%)		Specificity (%)		PPV (%)		NPV(%)	
	Admission	24 h	Admission	24 h	Admission	24 h	Admission	24 h
Severe AP	59	58	35	31	21	18	74	73
Necrotizing AP	61	59	42	38	37	36	66	61
Organ failure	60	58	36	32	13	10	85	86

PPV: positive predictive value; NPV: negative predictive value.

Table 4 Prognostic values of hemoconcentration in previous studies

Studies	*n*	Prognostic criteria	sensitivy (%)	specificity (%)	PPV (%)	NPV (%)
		Necrosis				
Baillargeon *et al*.[17]	64	≥47% at admission	34	91	44	87
		Failure to decrease at 24 h	81	88		
		Necrosis				
Brown *et al*.[18]	128	>44% at admission	72	83	68	85
		Failure to decrease at 24 h	94	69	61	96
		Organ failure				
		>44% at admission	60	75	26	93
		Failure to decrease at 24 h	87	65	27	97
		Necrosis				
Goulis *et al*.[37]	63	>44% at admission	78	83	50	94
		Necrosis				
Lankisch *et al*.[20]	316	>43% for male and >39.6% for female at admission	74	45	24	88
		Necrosis				
Pezzilli *et al*.[36]	158	>43.8 at admission	52.3	74.6		
		Severity				
Khan *et al*. [16]	58	>47% at admission	0	92	0	65
		>44% at admission	32	82	46	71
		Hct not decreasing	21	66	24	63
Present study	336	Severity				
		>44% for male and 40% for female at admission	59	35	21	74
		Necrosis				
		>44% for male and 40% for female at admission	61	42	37	66
		Organ failure				
		>44% for male and 40% for female at admission	60	36	13	85

data obtainment, controversial results and low sensitivity and/or specificity, and the results have been controversial.

AP is considered as a consequence from an insult to the pancreatic parenchyma that generates a local inflammatory reaction which then propagates and gives place to a generalized inflammatory response. Multiple studies have underlined the role of cytokines (e.g., tumor necrosis factor-α and interleukin-1, -6, and -8) and other inflammatory response mediators (e.g., platelet activating factor) in this propagating process[30]. Interestingly, the inflammatory response is always accompanied by the increase in vascular permeability that produces extravasation of

intravascular fluid into the peritoneal cavity[31,32]. The fluid loss significantly decreases the perfusion pressure into the pancreas leading to microcirculatory changes that contribute to pancreatic necrosis[33]. Thus, it has been proposed that hemoconcentration resulting from this fluid loss might well be associated with AP severity.

Gray and Rosenman[34] in 1965 reported that hemoconcentration at admission was a poor prognostic sign in patients with AP, but Talamini *et al*.[35] did not find significant differences of Hct levels obtained within 24 h of admission in survivors and non-survivors of AP. On the other hand, the classic study of Ranson[10] found that a fall in Hct level by greater than 10% during the initial 48 h of therapy correlates with severity and mortality. Thereafter, Baillargeon *et al*.[17] in a retrospective study reported that an admission Hct ⩾47% or, opposed to Ranson's finding, a failure of Hct to decrease at 24 h were predictive of necrosis but not of OF. The same group of authors in a subsequent prospective study of 128 patients with AP established an admission Hct ⩾44% and a failure to decrease after 24 h as the best binary predictor for necrosis and OF[18]. Both studies may have a referral bias in patient selection because the included patients transferred from other hospitals may correspond to sicker cases with a delay or less vigorous hydration. In some of the subsequent studies[36,37], elevated values of admission Hct were reported in necrotizing pancreatitis and also associated with serious complications but in all the studies, neither hemoconcentration at admission nor an Hct not decreasing after 24 h were able to predict severity (Table 4). In the current study, we could not find differences in the admission Hct between severe and mild cases. In every case, independently of the presence or absence of necrosis and/or systemic complications, there was a significant decrease in Hct levels at 24 h after admission. This finding might be explained by the common practice of aggressive fluid resuscitation in most of our patients with AP. The mean Hct fall at 24 h was under 10%, being non-significantly lower in necrotizing pancreatitis as expected in agreement with Ranson. According to our results, the accuracy of hemoconcentration at admission and at 24 h later as a marker for severe AP, necrotizing pancreatitis or OF lies in its high negative predictive value, mainly for OF (85% and 86%, respectively), as has been found in the previous reports (Table 4).

We analyzed a series of consecutive patients, including 4.7% of them with anemia, in order to test the utility of the Hct in a realistic clinical setting as was done by Khan *et al*.[16]. Our results were similar to those found by them, unlike our higher mean Hct levels. Admission Hct was analyzed separately in males and females as done by Lankisch *et al*.[20], but in addition to their approach, we also analyzed the Hct at 24 h after admission. Since Hct levels may differ according to atmospheric oxygen pressure (higher in high altitudes) and to gender (lower in females)[22], we constructed ROC curves that displayed cut-off values of Hct to define hemoconcentration at risk for severity in agreement with those previously reported by others[17-20]. Thus, anemia does not seem to play a role in the poor predictive accuracy of Hct in our study.

Our study is the only one that proves that hemoconcentration analyzed according to gender at admission and at 24 h is not a good predictor for severity in AP. We consider that our findings of the poor prognostic value of Hct at admission in AP cannot be attributed to sample bias. However, this is a retrospective study and only 69% of the patients had Hct determination at 24 h after admission; thus the lack of utility of the Hct at this time cannot be established strongly.

In conclusion, the sole clinical application that follows from the current study and several previous reports could be that patients without hemoconcentration have a very low likelihood of developing pancreatic necrosis or organ failure. However, we consider that in spite of the consistent findings of high negative predictive value of hemoconcentration for necrosis and/or OF, there is no prognostic gain because of the pre-existing 75% prevalence of mild AP.

REFERENCES

1 **Halonen KI**, Leppaniemi AK, Puolakkainen PA, Lundin JE, Kemppainen EA, Hietaranta AJ, Haapiainen RK. Severe acute pancreatitis: prognostic factors in 270 consecutive patients. *Pancreas* 2000; **21:** 266-271

2 **Tenner S**, Sica G, Hughes M, Noordhoek E, Feng S, Zinner M, Banks PA. Relationship of necrosis to organ failure in severe acute pancreatitis. *Gastroenterology* 1997; **113**: 899-903

3 **Sakorafas GH**, Tsiotou AG. Etiology and pathogenesis of acute pancreatitis: current concepts. *J Clin Gastroenterol* 2000; **30:** 348-356

4 **Steinberg W**, Tenner S. Acute pancreatitis. *N Engl J Med* 1994; **330:** 1198-1210

5 **Baron TH,** Morgan DE. Acute necrotizing pancreatitis. *N Engl J Med* 1999; **340**: 1412-1417

6 **Bradley EL 3rd**. A clinically based classification system for acute pancreatitis. Summary of the International Symposium on Acute Pancreatitis, Atlanta, Ga, September 11 through 13, 1992. *Arch Surg* 1993; **128:** 586-590

7 **McKay CJ**, Imrie CW. Staging of acute pancreatitis. Is it important? *Surg Clin North Am* 1999; **79:** 733-743

8 **Lankisch PG**, Blum T, Maisonneuve P, Lowenfels AB. Severe acute pancreatitis: when to be concerned? *Pancreatology* 2003; **3:** 102-110

9 **Ranson JH,** Rifkind KM, Roses DF, Fink SD, Eng K, Spencer FC. Prognostic signs and the role of operative management in acute pancreatitis. *Surg Gynecol Obstet* 1974; **139**: 69-81

10 **Ranson JH**. Etiological and prognostic factors in human acute pancreatitis: a review. *Am J Gastroenterol* 1982; **77**: 633-638

11 **Blamey SL**, Imrie CW, O'Neill J, Gilmour WH, Carter DC. Prognostic factors in acute pancreatitis. *Gut* 1984; **25:** 1340-1346

12 **Wilson C,** Heath DI, Imrie CW. Prediction of outcome in acute pancreatitis: a comparative study of APACHE II, clinical assessment and multiple factor scoring systems. *Br J Surg* 1990; **77**: 1260-1264

13 **Chen CC**, Wang SS, Lee FY, Chang FY, Lee SD. Proinflammatory cytokines in early assessment of the prognosis of acute pancreatitis. *Am J Gastroenterol* 1999; **94**: 213-218

14 **Ikei S**, Ogawa M, Yamaguchi Y. Blood concentrations of polymorphonuclear leucocyte elastase and interleukin-6 are indicators for the occurrence of multiple organ failures at the early stage of acute pancreatitis. *J Gastroenterol Hepatol* 1998; **13:** 1274-1283

15 **Neoptolemos JP**, Kemppainen EA, Mayer JM, Fitzpatrick JM, Raraty MG, Slavin J, Beger HG, Hietaranta AJ, Puolakkainen PA. Early prediction of severity in acute pancreatitis by urinary trypsinogen activation peptide: a multicentre study. *Lan-*

cet 2000; **355:** 1955-1960
16 **Khan Z**, Vlodov J, Horovitz J, Jose RM, Iswara K, Smotkin J, Brown A, Tenner S. Urinary trypsinogen activation peptide is more accurate than hematocrit in determining severity in patients with acute pancreatitis: a prospective study. *Am J Gastroenterol* 2002; **97:** 1973-1977
17 **Baillargeon JD**, Orav J, Ramagopal V, Tenner SM, Banks PA. Hemoconcentration as an early risk factor for necrotizing pancreatitis. *Am J Gastroenterol* 1998; **93:** 2130-2134
18 **Brown A**, Orav J, Banks PA. Hemoconcentration is an early marker for organ failure and necrotizing pancreatitis. *Pancreas* 2000; **20**: 367-372
19 **Whitcomb DC,** Pedroso M, Oliva J, Venkatesan T,Ulrich C, Saul M. An admission hematocrit of 40 or less predicts a low risk of pancreatic necrosis and may reduce the need for diagnostic CT scan. *Gastroenterology* 1999; **116**: A1176, G 50967
20 **Lankisch PG**, Mahlke R, Blum T, Bruns A, Bruns D, Maisonneuve P, Lowenfels AB. Hemoconcentration: an early marker of severe and/or necrotizing pancreatitis? A critical appraisal. *Am J Gastroenterol* 2001; **96**: 2081-2085
21 **Balthazar EJ**, Ranson JH, Naidich DP, Megibow AJ, Caccavale R, Cooper MM. Acute pancreatitis: prognostic value of CT. *Radiology* 1985; **156:** 767-772
22 **Ruiz-Arguelles GJ**, Sanchez-Medal L, Loria A, Piedras J, Cordova MS. Red cell indices in normal adults residing at altitude from sea level to 2670 meters. *Am J Hematol* 1980; **8:** 265-271
23 **Klar E**, Foitzik T, Buhr H, Messmer K, Herfarth C. Isovolemic hemodilution with dextran 60 as treatment of pancreatic ischemia in acute pancreatitis. Clinical practicability of an experimental concept. *Ann Surg* 1993; **217:** 369-374
24 **Bassi C**, Falconi M, Talamini G, Uomo G, Papaccio G, Dervenis C, Salvia R, Minelli EB, Pederzoli P. Controlled clinical trial of pefloxacin versus imipenem in severe acute pancreatitis. *Gastroenterology* 1998; **115:** 1513-1517
25 **Pederzoli P**, Bassi C, Vesentini S, Campedelli A. A randomized multicenter clinical trial of antibiotic prophylaxis of septic complications in acute necrotizing pancreatitis with imipenem. *Surg Gynecol Obstet* 1993; **176**: 480-483
26 **McMahon MJ**, Playforth MJ, Pickford IR. A compaative study of methods for the prediction of severity of attacks of acute pancreatitis. *Br J Surg* 1980; **67:** 22-25
27 **Werner H-M,** Blum T, Haack U, Mahlke R, Lübbers H, Struckmann K, Brinkmann G, Maisonneuve P, Lowenfels AB, Lankisch PG. Acute pancreatitis: Limited value of physical examination for the prediction of pancreatic necrosis. *Pancreatology* 2002; **2**: 295-296
28 **Suazo-Barahona J**, Carmona-Sanchez R, Robles-Diaz G, Milke-Garcia P, Vargas-Vorackova F, Uscanga-Dominguez L, Pelaez-Luna M. Obesity: a risk factor for severe acute biliary and alcoholic pancreatitis. *Am J Gastroenterol* 1998; **93:** 1324-1328
29 **Mery CM,** Rubio V, Duarte-Rojo A, Suazo-Barahona J, Pelaez-Luna M, Milke P, Robles-Diaz G. Android fat distribution as predictor of severity in acute pancreatitis. *Pancreatology* 2002; **2**: 543-549
30 **Gomez-Cambronero LG,** Sabater L, Pereda J, Cassinello N, Camps B, Vina J, Sastre J. Role of cytokines and oxidative stress in the pathophysiology of acute pancreatitis: therapeutical implications. *Curr Drug Targets Inflamm Allergy* 2002; **1**: 393-403
31 **Eibl G**, Hotz HG, Faulhaber J, Kirchengast M, Buhr HJ, Foitzik T. Effect of endothelin and endothelin receptor blockade on capillary permeability in experimental pancreatitis. *Gut* 2000; **46:** 390-394
32 **Foitzik T**, Eibl G, Hotz HG, Faulhaber J, Kirchengast M, Buhr HJ. Endothelin receptor blockade in severe acute pancreatitis leads to systemic enhancement of microcirculation, stabilization of capillary permeability, and improved survival rates. *Surgery* 2000; **128:** 399-407
33 **Bassi D**, Kollias N, Fernandez-del Castillo C, Foitzik T, Warshaw AL, Rattner DW. Impairment of pancreatic microcirculation correlates with the severity of acute experimental pancreatitis. *J Am Coll Surg* 1994; **179:** 257-263
34 **Gray SH**, Rosenman LD. Acute pancreatitis. The significance of hemoconcentration at admission to the hospital. *Arch Surg* 1965; **91:** 485-489
35 **Talamini G**, Bassi C, Falconi M, Sartori N, Frulloni L, Di Francesco V, Vesentini S, Pederzoli P, Cavallini G. Risk of death from acute pancreatitis. Role of early, simple "routine" data. *Int J Pancreatol* 1996; **19:** 15-24
36 **Pezzilli R,** Morselli-Labate AM**.** Hematocrit determination (HCT) as an early marker associated with necrotizing pancreatitis and organ failure. *Pancreas* 2001; **4**: 433-435
37 **Goulis IG**, Koumpoudis P, Arvanitakis C. Hemoconcentration is an early marker of severe and/or necrotizing pancreatitis. *Gastroenterology* 2002; **122**: A366

Science Editor Kumar M and Guo SY **Language Editor** Elsevier HK

PO Box 2345, Beijing 100023, China
www.wjgnet.com
wjg@wjgnet.com

ELSEVIER

World J Gastroenterol 2005;11(44):7024-7027
World Journal of Gastroenterology ISSN 1007-9327

• *RAPID COMMUNICATION* •

Catheter tract implantation metastases associated with percutaneous biliary drainage for extrahepatic cholangiocarcinoma

Jun Sakata, Yoshio Shirai, Toshifumi Wakai, Tatsuya Nomura, Eiko Sakata, Katsuyoshi Hatakeyama

Jun Sakata, Yoshio Shirai, Toshifumi Wakai, Tatsuya Nomura, Eiko Sakata, Katsuyoshi Hatakeyama, Division of Digestive and General Surgery, Niigata University Graduate School of Medical and Dental Sciences, Niigata, Japan
Correspondence to: Yoshio Shirai, MD, PhD, Division of Digestive and General Surgery, Niigata University Graduate School of Medical and Dental Sciences, 1-757 Asahimachi-dori, Niigata City 951-8510, Japan. shiray@med.niigata-u.ac.jp
Telephone: +81-25-227-2228 Fax: +81-25-227-0779
Received: 2005-04-07 Accepted: 2005-07-15

Key words: Neoplasm seeding; Extrahepatic cholangiocarcinoma; Percutaneous transhepatic biliary drainage; Malignant biliary obstruction; Surgery; Prognosis

Sakata J, Shirai Y, Wakai T, Nomura T, Sakata E, Hatakeyama K. Catheter tract implantation metastases associated with percutaneous biliary drainage for extrahepatic cholangiocarcinoma. *World J Gastroenterol* 2005; 11(44): 7024-7027
http://www.wjgnet.com/1007-9327/11/7024.asp

Abstract

AIM: To estimate the incidence of catheter tract implantation metastasis among patients undergoing percutaneous transhepatic biliary drainage (PTBD) for extrahepatic cholangiocarcinoma, and to provide data regarding the management of this unusual complication of PTBD by reviewing cases reported in the literature.

METHODS: A retrospective analysis of 67 consecutive patients who underwent PTBD before the resection of extrahepatic cholangiocarcinoma was conducted. The median follow-up period after PTBD was 106 mo. The English language literature (PubMed, National Library of Medicine, Bethesda, MD, USA), from January 1966 through December 2004, was reviewed.

RESULTS: Catheter tract implantation metastasis developed in three patients. The cumulative incidence of implantation metastasis reached a plateau (6%) at 20 mo after PTBD. All of the three patients with implantation metastasis died of tumor progression at 3, 9, and 20 mo after the detection of this complication. Among the 10 reported patients with catheter tract implantation metastasis from extrahepatic cholangiocarcinoma (including our three patients), two survived for more than 5 years after the excision of isolated catheter tract metastases.

CONCLUSION: Catheter tract implantation metastasis is not a rare complication following PTBD for extrahepatic cholangiocarcinoma. Although the prognosis for patients with this complication is generally poor, the excision of the catheter tract may enable survival in selected patients with isolated metastases along the catheter tract.

INTRODUCTION

Percutaneous transhepatic biliary drainage (PTBD) has been widely employed as a biliary decompression procedure for malignant biliary obstruction[1-5]. It may cause implantation metastasis along the catheter tract, which has generally been considered as an unusual and lethal complication[6,7]. Although sporadic cases of such implantation metastasis have been reported[6-10], the incidence of this complication following PTBD is yet to be determined. Also, there is a paucity of data regarding the management of this complication. Taken together, these facts prompted us to conduct the current study.

The aims of this study were to estimate the incidence of catheter tract implantation metastasis among patients undergoing PTBD for extrahepatic cholangiocarcinoma, and to provide data regarding the management of this unusual complication by reviewing cases reported in the literature.

MATERIALS AND METHODS

Patient population

A total of 87 patients with carcinoma arising from the extrahepatic bile ducts (extrahepatic cholangiocarcinoma) underwent resection with curative intent at our department during the 15-year period between January 1988 and December 2002. Carcinoma arising from the cystic duct was categorized as extrahepatic cholangiocarcinoma according to the tumor-node-metastasis staging system[14]. Three patients who also had gallbladder carcinoma were excluded. Of the remaining 84 patients, 67 jaundiced patients underwent PTBD before the resection. They formed the basis of this retrospective study, and included 39 men and 28 women with a median age of 65 years (range: 35-88 years). All patients were Japanese.

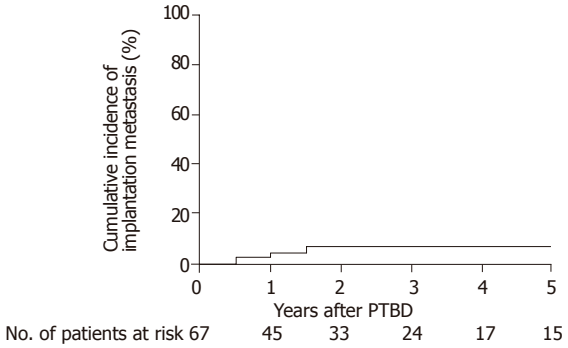

Figure 1 The cumulative incidence of catheter tract implantation metastasis after percutaneous transhepatic biliary drainage among 67 patients who underwent resection of extrahepatic cholangiocarcinoma.

Resectional procedure of the primary tumor

The resectional procedures were chosen according to the primary tumor location. Forty-one patients with hilar cholangiocarcinoma underwent a hepatectomy with bile duct resection, 12 with non-hilar tumor underwent a Whipple procedure or a pylorus-preserving pancreaticoduodenectomy, six underwent a bile duct resection, and eight underwent a combination of hepatectomy and pancreaticoduodenectomy. Regional lymphadenectomy was performed in all patients.

Pathologic examination

The resected specimens were submitted to the Department of Surgical Pathology at our hospital for histologic evaluation. The histologic findings were described according to the tumor-node-metastasis staging system[14]. The histologic grade was determined based on the areas of the tumor with the highest grade[14]. Adenocarcinoma was identified as the primary tumor in 64 patients and adenosquamous carcinoma was identified in three patients.

Patient follow-up

Patients were followed up regularly at outpatient clinics every 3 mo. The median follow-up period after PTBD was 106 mo (range: 4 to 186 mo). By the time of disease status assessment, 38 patients had died of tumor recurrence. Seven patients had died of other causes with no evidence of tumor recurrence. One patient was alive with recurrent disease, and the remaining 21 patients were alive without disease.

Review of the literature

The English language literature (PubMed, National Library of Medicine, Bethesda, MD, USA), from January 1966 through December 2004, was reviewed, and revealed that a total of seven patients undergoing resection of extrahepatic cholangiocarcinoma suffered from catheter tract implantation metastasis following PTBD[7-13].

Statistical analysis

Medical records and survival data were obtained for all the 67 patients. The causes of death were determined based on the medical records. The follow-up period was defined as the interval between the date of PTBD and that of the last follow-up. The Kaplan-Meier method was used to estimate both the cumulative incidence of catheter tract implantation metastasis and the cumulative patient survival rates. The differences in survival were evaluated using the log rank test. All statistical evaluations were performed using the SPSS 11.5J software package (SPSS Japan Inc., Tokyo, Japan). All tests were two-sided, and the differences with P values of <0.05 were considered statistically significant.

RESULTS

The incidence of catheter tract implantation metastasis after PTBD in the current series

Catheter tract implantation metastasis after PTBD presented as a subcutaneous nodule in 3 of the 67 patients during the follow-up period. The interval between PTBD and the detection of implantation metastases was 7, 14, and 20 mo for those 3 patients. The cumulative incidence of this complication reached a plateau (6%) at 20 mo after PTBD (Figure 1).

Of the three patients with implantation metastases, one underwent a resection of the catheter tract (patient 9 in Table 1), one underwent local radiation (patient 8), and the other received the best supportive care (patient 10). They died of disease at 3, 9, and 20 mo after the detection of this complication.

A review of the literature on catheter tract implantation metastasis from extrahepatic cholangiocarcinoma

An analysis of the 10 reported patients (including our three patients; Table 1) with catheter tract implantation metastasis revealed that the histologic grade of the primary tumor was well differentiated in four patients, moderately differentiated in three, poorly differentiated in one, and not documented in two. The median interval between PTBD and the detection of this complication was 14 mo (range: 3 to 45 mo).

Catheter tract implantation metastasis was isolated (without recurrences at other sites) in six patients, whereas it was non-isolated (with recurrences at other sites) in the other 4 patients (Table 1). Although the survival after the detection of implantation metastasis was generally poor, two patients who underwent excision of isolated implantation metastases survived for more than five years. Among the nine patients with documented outcomes, those with isolated implantation metastases survived longer than those with non-isolated implantation metastases ($P = 0.0457$; Figure 2).

DISCUSSION

The incidence of catheter tract implantation metastasis after PTBD has been reported to range from 0.6 to 6% in patients with malignant biliary obstruction due to tumors of various origins[7,11,15-17]. Nimura *et al*.[18] have reported

Table 1 Implantation metastases along the PTBD tract among patients who underwent a resection for extrahepatic cholangiocarcinoma

n	First author	Sex/age (yr)	Histology of the primary tumor		Detection of implantation metastases after PTBD (mo)	Sites of recurrences other than the PTBD tract	Management of implantation metastases	Outcome after the detection of implantation metastases (mo)
			Type	Grade				
1	Sano[7]	M/68	Adeno	G1	45	–	Hx	100; NED
2	Inagaki[8]	F/51	As	nd	6	–	Hx, EAW	65; NED
3	Matsumoto[9]	F/61	Adeno	G2	21	–	Hx	24; NED
4	Shimizu[10]	M/75	Adeno	G2	16	–	Hx	14; NED
5	Tersigni[11]	M/66	Adeno	G1	13	–	RTx, CTx	4; DOD
6	Omokawa[12]	M/45	Adeno	nd	3	-	Hx	nd; nd
7	Uenishi[13]	F/57	Adeno	G1	14	Pleura (right)	Pleuropneum-onectomy, ECW[2]	21; DOD
8	Sakata1	F/63	Adeno	G1	14	Bone, Local	RTx	20; DOD
9	Sakata1	M/70	Adeno	G2	20	Peritoneum	EAW	9; DO
10	Sakata1	M/76	Adeno	G3	7	Local	BSC	3; DOD

PTBD: percutaneous transhepatic biliary drainage; Adeno: adenocarcinoma; As: adenosquamous carcinoma; G1: well differentiated; G2: moderately differentiated; G3: poorly differentiated; Hx: hepatectomy; EAW: excision of the abdominal wall; RTx: radiotherapy; CTx: chemotherapy; ECW: excision of the chest wall, BSC: best supportive care; NED: (alive with) no evidence of disease; DOD: died of disease; nd: not documented. [1]Present case. [2]A PTBD catheter had been introduced transphrenically via the right pleural cavity in this patient.

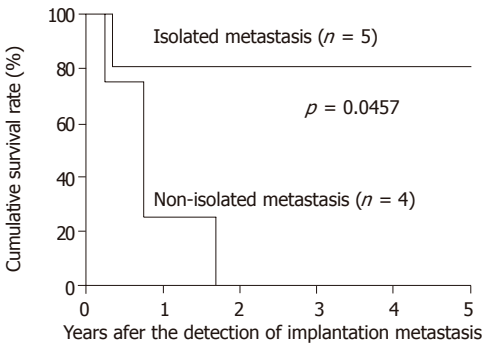

Figure 2 Kaplan-Meier estimates of survival after the detection of catheter tract implantation metastasis among nine patients with documented outcomes (Table 1). The median survival time was not reached with a cumulative 1-year survival rate of 80% in patients with isolated implantation metastasis, whereas it was 9 mo with that of 25% in patients with non-isolated metastasis. Patients with isolated implantation metastases survived longer than patients with non-isolated implantation metastases (P = 0.0457).

a 3% incidence of such implantation metastasis among 133 patients with hilar cholangiocarcinoma. In the current series, the cumulative incidence of this complication increased with time and reached a plateau (6%) 20 mo after PTBD (Figure 2). The above data suggests that catheter tract implantation is not a rare complication following PTBD for extrahepatic cholangiocarcinoma.

Uesaka *et al*.[19] have reported that catheter tract implantation metastasis from hilar cholangiocarcinoma occurred more frequently in patients with well differentiated tumors. Among the 10 reported patients with this complication (Table 1), only one had a poorly differentiated tumor, implying that differentiated tumors may be more related to the development of this complication than poorly differentiated ones. The association between implantation metastasis after PTBD and the histologic grade of extrahepatic cholangiocarcinoma warrants further investigation.

Although Sano *et al*.[7] have reported the occurrence of a late implantation metastasis arising 46 mo after PTBD for extrahepatic cholangiocarcinoma, most of our collected patients suffered from this complication within 21 mo after PTBD (Table 1). Thus, patients undergoing PTBD for extrahepatic cholangiocarcinoma should be monitored for catheter tract implantation for around 2 years.

The survival of patients with catheter tract implantation metastasis from extrahepatic cholangiocarcinoma was found to be generally poor (Table 1), as with our patients. Despite the metastatic nature of this condition, surprisingly, the outcome after the excision of the implantation metastasis was not so dismal in some patients with isolated implantation metastases (patients 1-4). The possibility that the course of deceased patients is unlikely to be reported (a publication bias) may, in part, explain this. In order to excise catheter tract metastases following PTBD, a hepatectomy is usually required, because the catheter tract runs through the liver parenchyma; in some patients, a local excision of the abdominal wall is also required. Two of the five patients who underwent a hepatectomy, with or without a local excision of the abdominal wall, for isolated implantation metastases (patients 1 and 2) survived for more than 5 years with no evidence of the disease. This clearly demonstrates that excision of the metastases offers the only chance for long-term survival.

The issue how to prevent catheter tract implantation metastasis following PTBD is yet to be resolved. Although excision of the catheter tract along with the resection of the primary tumor appears to be effective, it is practically difficult to excise the whole catheter tract between the surface of the skin and the punctured intrahepatic bile ducts. Some authors have advocated ethanol injection into the catheter tract to prevent cancer implantation[10,19,20]. However, Shimizu and colleagues have reported a case of implantation metastasis following ethanol injection[10]. Further investigation is warranted to conclude the effects of this procedure.

In conclusion, catheter tract implantation metastasis is not a rare complication following PTBD for extrahepatic

cholangiocarcinoma. Although the prognosis for patients with this complication is generally poor, excision of the catheter tract, which usually requires a hepatectomy, enables long-term survival in selected patients with isolated implantation metastases.

REFERENCES

1 **Takada T,** Hanyu F, Kobayashi S, Uchida Y. Percutaneous transhepatic cholangial drainage: direct approach under fluoroscopic control. *J Surg Oncol* 1976; **8**: 83-97

2 **Hatfield AR**, Tobias R, Terblanche J, Girdwood AH, Fataar S, Harries-Jones R, Kernoff L, Marks IN. Preoperative external biliary drainage in obstructive jaundice. A prospective controlled clinical trial. *Lancet* 1982; **2:** 896-899

3 **Nimura Y**, Hayakawa N, Kamiya J, Kondo S, Shionoya S. Hepatic segmentectomy with caudate lobe resection for bile duct carcinoma of the hepatic hilus. *World J Surg* 1990; **14:** 535-543; discussion 544

4 **Nagino M,** Hayakawa N, Nimura Y, Dohke M, Kitagawa S. Percutaneous transhepatic biliary drainage in patients with malignant biliary obstruction of the hepatic confluence. *Hepatogastroenterology* 1992; **39:** 296-300

5 **Wakai T**, Shirai Y, Moroda T, Yokoyama N, Hatakeyama K. Impact of ductal resection margin status on long-term survival in patients undergoing resection for extrahepatic cholangiocarcinoma. *Cancer* 2005; **103**: 1210-1216

6 **Chapman WC**, Sharp KW, Weaver F, Sawyers JL. Tumor seeding from percutaneous biliary catheters. *Ann Surg* 1989; **209:** 708-713; discussion 713-715

7 **Sano T,** Nimura Y, Hayakawa N, Kamiya J, Kondo S, Nagino M, Kanai M, Miyachi M, Uesaka K. Partial hepatectomy for metastatic seeding complicating pancreatoduodenectomy. *Hepatogastroenterology* 1997; **44**: 263-267

8 **Inagaki M,** Yabuki H, Hashimoto M, Maguchi M, Kino S, Sawa M, Ojima H, Tokusashi Y, Miyokawa N, Kusano M, Kasai S. Metastatic seeding of bile duct carcinoma in the transhepatic catheter tract: report of a case. *Surg Today* 1999; **29**: 1260-1263

9 **Matsumoto A,** Imamura M, Akagi Y, Kaibara A, Ohkita A, Mizobe T, Isomoto H, Aoyagi S. A case report of disseminated recurrence of inferior bile duct carcinoma in PTCD fistula. *Kurume Med* J 2002; **49**: 71-75

10 **Shimizu Y,** Yasui K, Kato T, Yamamura Y, Hirai T, Kodera Y, Kanemitsu Y, Ito S, Shibata N, Yamao K, Ohhashi K. Implantation metastasis along the percutaneous transhepatic biliary drainage sinus tract. *Hepatogastroenterology* 2004; **51**: 365-367

11 **Tersigni R,** Rossi P, Bochicchio O, Cavallini M, Ambrogi C, Bufalini G, Alessandroni L, Arena L, Armeni O, Miraglia F, Stipa S. Tumor extension along percutaneous transhepatic biliary drainage tracts. *Eur J Radiol* 1986; **6:** 280-282

12 **Omokawa S,** Hashizume T, Ohsato M, Nanjo H, Asanuma Y, Koyama K. Insemination of bile duct carcinoma to the liver after insertion of percutaneous biliary endoprosthesis. *Gastroenterol Jpn* 1991; **26**: 678-682

13 **Uenishi T,** Hirohashi K, Inoue K, Tanaka H, Kubo S, Shuto T, Yamamoto T, Kaneko M, Kinoshita H. Pleural dissemination as a complication of preoperative percutaneous transhepatic biliary drainage for hilar cholangiocarcinoma: report of a case. *Surg Today* 2001; **31**: 174-176

14 **Greene FL,** Page DL, Fleming ID, Fritz AG, Balch CM, Haller DG, Morrow M. American Joint Committee on Cancer (AJCC) Staging Manual. 6th ed. *New York: Springer-Verlag* 2002: 145-150

15 **Oleaga JA**, Ring EJ, Freiman DB, McLean GK, Rosen RJ. Extension of neoplasm along the tract of a transhepatic tube. *AJR Am J Roentgenol* 1980; **135:** 841-842

16 **Shorvon PJ**, Leung JW, Corcoran M, Mason RR, Cotton PB. Cutaneous seeding of malignant tumours after insertion of percutaneous prosthesis for obstructive jaundice. *Br J Surg* 1984; **71:** 694-695

17 **Kim WS,** Barth KH, Zinner M. Seeding of pancreatic carcinoma along the transhepatic catheter tract. *Radiology* 1982; **143**: 427-428

18 **Nimura Y,** Kamiya J, Kondo S, Nagino M, Uesaka K, Oda K, Sano T, Yamamoto H, Hayakawa N. Aggressive preoperative management and extended surgery for hilar cholangiocarcinoma: Nagoya experience. *J Hepatobiliary Pancreat Surg* 2000; **7**: 155-162

19 **Uesaka K**, Kamiya J, Nagino M, Yuasa N, Sano T, Oda K, Kanai M, Hayakawa N, Yamamoto H, Yokoi S, Nimura Y. [Treatment of recurrent cancer after surgery for biliary malignancies] *Nippon Geka Gakkai Zasshi* 1999; **100:** 195-199

20 **Kondo S,** Nimura Y, Hayakawa N, Kamiya J, Shionoya S. Ethanol injection for prevention of seeding metastasis along the tract after percutaneous transhepatic biliary drainage. *J Jpn Bil Assoc* 1989; **3:** 100-105 (in Japanese with English abstract)

Science Editor Guo SY **Language Editor** Elsevier HK

PO Box 2345, Beijing 100023, China
www.wjgnet.com
wjg@wjgnet.com

ELSEVIER

World J Gastroenterol 2005;11(44):7028-7032
World Journal of Gastroenterology ISSN 1007-9327

• *RAPID COMMUNICATION* •

Upper gastrointestinal carcinoid tumors incidentally found by endoscopic examinations

Seng-Kee Chuah, Tsung-Hui Hu, Chung-Mou Kuo, King-Wah Chiu, Chung-Huang Kuo, Keng-Liang Wu, Yeh-Pin Chou, Sheng-Nan Lu, Shue-Shian Chiou, Chi-Sin Changchien, Hock-Liew Eng

Seng-Kee Chuah, Tsung-Hui Hu, Chung-Mou Kuo, King-Wah Chiu, Chung-Huang Kuo, Keng-Liang Wu, Yeh-Pin Chou, Sheng-Nan Lu, Shue-Shian Chiou, Chi-Sin Changchien, Department of Hepato-Gastroenterology, Chang Gung Memorial Hospital, 123, Ta-Pei Road, Niao-sung Hsiang, Kaohsiung Hsien, Taiwan, China
Hock-Liew Eng, Department of Pathology, Chang Gung Memorial Hospital, 123, Ta-Pei Road, Niao-sung Hsiang, Kaohsiung Hsien, Taiwan, China
Co-first authors: Seng-Kee Chuah and Tsung-Hui Hu
Correspondence to: Shue-Shian Chiou, Department of Gastroenterology, Chang Gung Memorial Hospital, Kaohsiung Medical Center, 123, Ta-Pei Road, Niao-sung Hsiang, Kaohsiung Hsien, Taiwan, China. chuahsk@seed.net.tw
Telephone: +886-7-7317123 ext. 8301 Fax: +886-7-7322402
Received: 2005-03-27 Accepted: 2005-07-20

Abstract

AIM: This study shares Asian clinical experiences of carcinoid tumors that originated in the upper gastrointestinal tract.

METHODS: From May 1987 to June 2002, we had found only 13 cases of histologically confirmed carcinoid tumors in the upper gastrointestinal tract by endoscopic examinations. There were eight males and five females. The mean age was 53.16±20.51 years that ranged from 26 to 82 years. Each of their clinical presentations, locations, tumor morphology, and size and the treatment outcome were analyzed and discussed.

RESULTS: One patient had a polypoid lesion at the lower esophagus, nine were stomach lesions and three located at the duodenum. All patients with polypoid and submucosal tumor types were of small size (<1.7 cm) and all patients survived after simple excision or polypectomy. Four of the five patients in tumor mass forms died and the tumors were more than 2.0 cm in size.

CONCLUSION: Carcinoid tumors rarely originated from the upper gastrointestinal tract and are usually found accidentally after endoscopic study. Bigger size (more than 2 cm) tumor masses may indicate a more severe disease and poor prognosis.

Key words: Upper gastrointestinal carcinoid tumors; Tumor morphology; Sizes; Treatment courses; Prognosis

Chuah SK, Hu TH, Kuo CM, Chiu KW, Kuo CH, Wu KL, Chou YP, Lu SN, Chiou SS, Changchien CS, Eng HL. Upper gastrointestinal carcinoid tumors incidentally found by endoscopic examinations. *World J Gastroenterol* 2005; 11(44): 7028-7032
http://www.wjgnet.com/1007-9327/11/7028.asp

INTRODUCTION

Carcinoid tumors are a type of very slow-growing neuroendocrine tumors that originate from the embryonic neural crest. Their prominent feature is the production of multiple hormones[1]. The incidence is increasing at rates around 24.7-44.8 cases per million in the United States each year. Over 90% of all carcinoid tumors originate in the GI tract. Most carcinoid tumors are GI in origin, yet they only account for 1.5% of all gastrointestinal neoplasms. Most carcinoids are, in fact, found incidentally. Neither cytology nor histology can determine if the lesion is benign or malignant. Only the presence of distant metastases confirms malignancy.

However, all carcinoids must be considered malignant when found because of the high threat of metastasis. Although carcinoids <1 cm in diameter are unlikely to metastasize, a wide excision is recommended[1]. Five-year survival rates of patients with a local excision of carcinoid are >95%, metastases to the liver constitute a dismal 20% 5-year survival rate. Therefore, early detection as with most cancers is, desirable. In the past 15 years, we found only 13 cases of upper gastrointestinal tract carcinoid tumors by endoscopic examination. We tried to analyze and correlate the clinical settings, the sizes of tumors, their morphology, and the outcome of the disease.

MATERIALS AND METHODS

The medical records of these 13 patients who were diagnosed as upper GI carcinoid tumors at Chang Gung Memorial Hospital, Kaohsiung Center, Taiwan from May 1987 to June 2002 were reviewed. We excluded all the cases with an uncertain diagnosis, small-bowel cancers found in the GI tract but thought to have metastasized there from an extra-abdominal primary site, and patients were operated on for periampullary tumors. The final study population composed of 13 patients who were treated. There

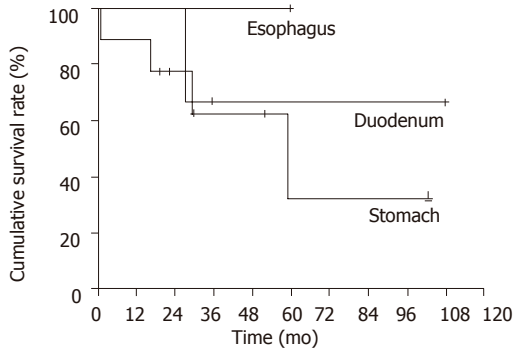

Figure 1 Cumulative survival of the upper gastrointestinal carcinoid tumors.

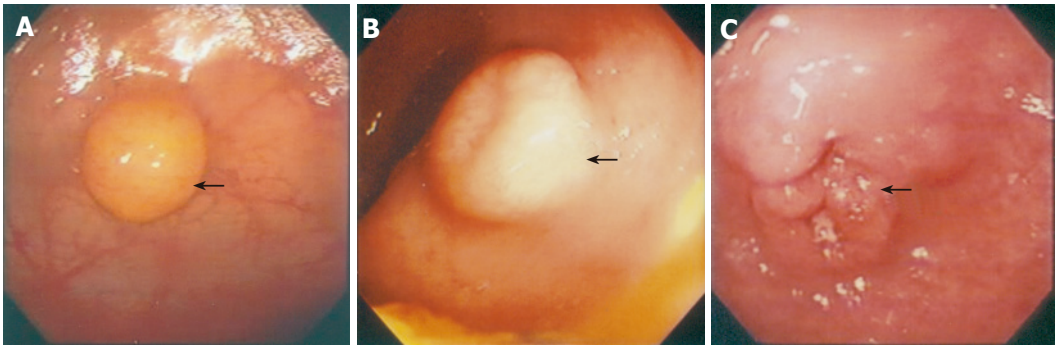

Figure 2 Subject **A:** A polypoid carcinoid lesion at the gastric fundus site about 0.8 cm with typical yellowish color of the lesion; **B:** A submucosal carcinoid lesion at the duodenal bulb about 1.7 cm; **C:** A carcinoid tumor with ulceration, at the antrum site, about 4.0 cm in size.

Table 1 Demographic data, morphology, sizes, treatment and outcome of patients with upper gastrointestinal carcinoid tumors

Patients	Age (yr)	Sex	Symptom	Location	Morphology	Size(cm)	Treatment	Outcome
1	26	Male	GI bleeding	Esophagus	Polyp	0.7	Polypectomy	(Survive)
2	81	Female	GI bleeding	Stomach	Polyp	0.4	Polypectomy	(Survive)
3	33	Female	Epigastralgia	Stomach	ST	0.9	Polypectomy	(Survive)
4	26	Female	Epigastralgia	Stomach	ST	1.0	Polypectomy	(Survive)
5	70	Female	Epigastralgia	Stomach	Polyp	0.5	Polypectomy	(Survive)
6	63	Male	Abdominal pain	Stomach	Tumor	10	Surgery	(Expired)
7	46	Male	GI bleeding	Stomach	ST	4.3	Surgery	(Survive)
8	62	Male	GI bleeding	Stomach	Tumor	4.0	Surgery	(Expired)
9	68	Male	Epigastralgia	Stomach	Tumor	1.5	Surgery	(Survive)
10	30	Male	Epigastralgia	Stomach	Tumor	>4.0	Supportive care	(Expired)
11	64	Female	Epigastralgia	Duodenum (bulb)	Polyp	0.9	Polypectomy	(Survive)
12	40	Male	Epigastralgia	Duodenum (bulb)	ST	1.7	Duodenectomy	(Survive)
13	82	Male	Jaundice	Duodenum (second portion)	Tumor	>2.0	Stenting	(Expired)

ST: submucosal tumor; All patients with polypoid and submucosal tumor types were of small size (<1.7 cm) and all survived. Four of the five patients in tumor mass form died and were more than 2.0 cm.

were eight males and five females. The mean age was 53.15 ±20.51 years ranging from 26 to 82 years (Figure 1).

The morphology of the tumors observed by endoscopic examinations was divided into three main categories: polypoid (Figure 2A), submucosal (Figure 2B), tumor-like (Figure 2C) lesions. A single surgical pathologist reviewed pathological specimens and histological features. Routine hematoxylin-eosin stains, immunohistochemistry, or elevated urinary 5-hydroxyindole acetic acid levels established the diagnosis of carcinoid tumor. Survival duration was measured from the time of diagnosis to the last follow-up evaluation or death. The follow-up observations were obtained from the medical records of the patients or direct contact with the patients, their relatives, or primary care physician. The endoscopic observations of the lesions such as the morphologic appearance and the sizes were analyzed in correlation to the treatment course and prognosis of each recorded patient (Table 1).

RESULTS

This study group included eight men and five women, with the median follow-up duration of 36 mo. The most common symptom was abdominal pain (53%), followed by weight loss (38.5%), GI tract bleeding (23%) and jaundice (7.7%). Some patients had more than one symptom or physical finding, though no combination of signs, symptoms, or acuity of presentation was thought to have any influence on the prognosis.

Only one 26-year-old male patient had a 0.7-cm esophageal carcinoid lesion, polypoid in appearance and located at the lower esophagus. Polypectomy was done for him and no signs of recurrence for more than 5 years. Nine patients suffered from gastric carcinoid tumors and three of them died. All these three patients had gastric tumor masses of at least 4 cm in size found by endoscope. One patient had tumor involving colon, spleen, and pancreas, while the other had metastatic mesenteric lymphnodes. Both underwent surgery but still failed to survive due to sepsis and organ failure.

A 30-year-old female had a huge mass over the pelvis extended to almost the whole of the left side abdomen. Endoscope showed a 4.0-cm ulcerated mass over the cardiac portion and fundus. Carcinoid tumor was proven by snare biopsy. She also suffered from a septic right knee. Due to the poor general condition, she received supportive treatment only. One 68-year-old male patient had a 1.5-cm tumor mass at gastric antrum who received complete resection already and survived for 6 years. One 46-year-old male patient had been suffering from repeated gastroduodenal ulcers bleeding. Scope reviewed a more than 4 cm slightly elevated submucosal lesion at the antrum. Computer tomography and angiography showed a tumor mass bulging out posterior to the stomach. He had been well after surgical resection of the antrum.

All four patients who had gastric carcinoid lesions smaller than 1.0 cm survived, and the morphology were polypoid (n = 2) and appearance of submucosa (n = 2). Two received polypectomies and two mucosectomies and there are no signs of recurrence so far.

Three patients had duodenal carcinoid lesions, two located in the duodenal bulb and one in the second portion of the duodenum. One 64-year-old female patient had a 0.9-cm polypoid lesion at the bulb portion, and polypectomy was performed. The other 40-year-old male patient who had a 1.7-cm submucosal lesion at bulb received duodenectomy. Both of them are still alive and disease-free at 4 and 6 years status post therapy. However, one 82-year-old female patient who suffered from obstructive jaundice by a carcinoid tumor mass at the duodenal second portion was not as fortunate. Stent was placed by using endoscope to relieve her obstructive jaundice but she still died because of sepsis shortly after.

The cumulative 5-year survival rate was 64% in the carcinoid tumor. Gastric carcinoid had the worse prognosis in this study with 5-year survival of less than 40%. Duodenal carcinoid tumor had a 5-year survival of about 60%. Only one case was found with a carcinoid in the esophagus and the patient is still surviving but the total number of patients is too small to come to any conclusion.

DISCUSSION

Carcinoid tumor of the esophagus is exceedingly rare, and the knowledge about this tumor is based primarily on case reports[2]. Several case reports have emphasized that esophageal carcinoid tumors are associated with a poor prognosis[2]. Primary endocrine tumors of the esophagus are rare tumors that include small cell carcinoma, large cell neuroendocrine carcinoma, atypical carcinoid tumor, classical carcinoid tumor, and combined endocrine tumor and adenocarcinoma[2]. Small cell carcinoma of the esophagus accounts for 1% of all esophageal tumors, and the overall median survival is 3.1 mo[3]. The only one case, who had a small polyp at distal esophagus, still survives, 50 mo after endoscopic polypectomy. Although only one case was treated, it supported that esophageal carcinoid tumors are not always associated with a poor prognosis probably as a non-small cell carcinoma.

Three types of gastric carcinoids have been described[4,5]. Type I is associated with chronic atrophic body-fundus gastritis type A. Type II is seen in Zollinger-Ellison syndrome/multiple endocrine neoplasia type I (MEN-1) syndrome. Type III is a sporadic tumor[6]. Gastric carcinoids arise from endocrine cells in gastric mucosa and recent reports indicate that 10-30% of all gastrointestinal carcinoids occur in the stomach[6].

Type I gastric carcinoids is the most frequent type encountered in about 65% of cases[7]. The tumors are usually small (<1 cm) polypoid lesions located in the gastric body or fundus[8]. Adjacent atrophic mucosa contains foci of precursor lesions, which are at different stages of ECL cell hyperplasia, dysplasia, and neoplasia. Hypergastrinemia is usually present[6]. Nodal metastasis is reported in up to 16% of cases and hepatic metastasis, in up to 4%[9]. Endocrine symptoms are rare; 5-year survival is high in our series, four gastric carcinoids were less than 1.0 cm in size, either in polypoid or submucosal in morphology endoscopically. Polypectomies and endoscopic mucosectomy were performed smoothly and they still survive.

One of our patients who belonged to type II gastric carcinoids suffered from repeated GI bleeding and hypergastrinemia. After receiving operation, he is still healthy. The adjacent mucosa is non-atrophic and entirely comprised precursor lesions[6]. Prognosis is intermediate, between types I and III[7].

Type III gastric lesions make about 20% of gastric carcinoids[6]. Forty percent occur in the antropyloric area[6] when discovered; they are usually single tumor more than 2 cm. They arise from ECL, EC, or X cells. There is no hypergastrinemia and no precursor lesions. They can cause either a classic syndrome of facial flushing, abdominal cramps, diarrhea, left-sided endocardial fibrosis, and 24 h urinary 5-HIAA more than 10 mg, or an atypical carcinoid syndrome associated with vasoactive substances and

polypeptide hormone production[6]. Nodal metastasis is reported in 55% of patients and liver metastases, in 25% of patients[5]. Five-year survival is only 50%[7]. All the four of our patients with gastric tumor masses of more than 4 cm in size were associated with adjacent and distant metastasis. Two had carcinoid syndrome. Three received surgical intervention and one had supportive care. Three of them expired.

Schneider *et al*.[10] showed that the patients with gastric carcinoids had an eight times higher risk of developing a secondary malignancy as compared with the normal population. None of our gastric carcinoids had secondary carcinomas so far.

The management of gastric carcinoids depends on the type; presence of symptoms, or metastases spread, size, and number of tumors[6]. Although multiple studies have been published, the treatment in many cases still remains controversial. Most agreed on the management of type III (or sporadic) carcinoids, which have the worst prognosis and the highest rate of metastasis and associated carcinoid syndrome[6]. The recommended therapy is *en bloc* surgical resection with regional lymph node dissection, especially for lesions of more than 2 cm[5,11,12]. If the tumor penetrated the serosa, gastrectomy is also recommended[13].

For the patients with liver metastasis, surgical resection of tumor foci or selective hepatic artery ligation or embolization may reduce the symptoms and improve survival[6]. Chemotherapy of disseminated disease with streptozocin, 5-FU, cyclophosphamide, and doxorubicin were reported to produce a 20-40% response rate[6]. Leukocyte interferon produced a temporary response in some patients[5]. Somatostatin analogs, octreotide, and lanreotide have been used successfully in recent years to relieve the symptoms of carcinoid syndrome[14]. Recently, the results of trials with long-acting formulations octreotide-LAR (10, 20, or 30 mg every 28 d) and lanreotide-PR (30 mg every 2 wk) were published and demonstrated effectiveness and convenience of the treatment[15-18].

The optimal management of the types I and II gastric carcinoids is less clear[6]. Many authors base their recommendations on the size and number of the tumors[6]. For lesions less than 1 cm in diameter and less than 3-5 in number, endoscopic removal and semiannual EGD surveillance is recommended[6]. If there is a recurrence, or if the lesions are larger than 1 cm or more than 3-5 in number, then antrectomy with endoscopic excision is recommended[5,13].

Type I is considered as the most benign type of gastric carcinoids, rarely affecting the 5-year survival[8]. There are strong arguments supporting surgery[6]. Although type I carcinoid is the most benign type, it is still associated with some incidence of lymph node and liver metastasis[7,8]. Most gastric carcinoids regress after antrectomy[12,19-21]. In contrast, improved overall survival for metastatic neuroendocrine tumors after the complete resection of primary and hepatic metastases is accomplished, with an actuarial 5-year survival rate of 70%.

Carcinoid tumor was the most common small bowel tumor. It occurred in 24% of patients. Forty-six percent of patients were asymptomatic during life, the tumors being found either at autopsy or during other surgical procedures. Of those that were symptomatic, half presented with intestinal obstruction and the rest with long-standing symptoms. An abdominal mass, which occurred in 14% of cases, is an uncommon physical finding since the majority present as small submucosal tumors. Fifty-eight percent overall and 72% of those having surgery had evidence of regional spread, either by local invasion or in the form of regional nodal involvement. Seven percent of patients have died because of their disease. Excision surgery should be performed for all cases where feasible, and repeated for recurrent symptoms[22].

Ampullary carcinoids are rare tumors. Like the 82-year-old male in our series, they most commonly present with obstructive symptoms like jaundice and nonspecific abdominal discomfort. They are difficult to diagnose preoperatively secondary to their relatively small size and submucosal location. Rarely, ulcerated duodenal carcinoids can present as a source of significant gastrointestinal bleeding. Overall, approximately 80-90% of all carcinoids secrete serotonin or its precursor 5-hydroxy tryptophan, and other tumors rarely do so. Measurements of serotonin and its metabolites like urinary 5-hydroxy indole acetic acid (5-HIAA) have been described to be very helpful in the diagnosis and postresection follow-up of carcinoids. In our patient, those levels were not obtained preoperatively as the patient did not have any signs, symptoms, or histologic evidence to suggest a diagnosis of carcinoid tumor[23].

In conclusion, carcinoid tumors rarely originated from the upper gastrointestinal tract in the eastern countries and are usually found incidentally after endoscopic study. Bigger size (more than 2 cm) tumor mass form may indicate a more severe disease and poor prognosis.

REFERENCES

1 **Onaitis MW**, Kirshbom PM, Hayward TZ, Quayle FJ, Feldman JM, Seigler HF, Tyler DS. Gastrointestinal carcinoids: characterization by site of origin and hormone production. *Ann Surg* 2000; **232:** 549-556

2 **Hoang MP**, Hobbs CM, Sobin LH, Albores-Saavedra J. Carcinoid tumor of the esophagus: a clinicopathologic study of four cases. *Am J Surg Pathol* 2002; **26:** 517-522

3 **Law SY**, Fok M, Lam KY, Loke SL, Ma LT, Wong J. Small cell carcinoma of the esophagus. *Cancer* 1994; **73:** 2894-2899

4 **Rindi G**, Luinetti O, Cornaggia M, Capella C, Solcia E. Three subtypes of gastric argyrophil carcinoid and the gastric neuroendocrine carcinoma: a clinicopathologic study. *Gastroenterology* 1993; **104:** 994-1006

5 **Creutzfeldt W**. The achlorhydria-carcinoid sequence: role of gastrin. *Digestion* 1988; **39**: 61-79

6 **Rybalov S**, Kotler DP. Gastric carcinoids in a patient with pernicious anemia and familial adenomatous polyposis. *J Clin Gastroenterol* 2002; **35:** 249-252

7 **Ahlman H**, Kolby L, Lundell L, Olbe L, Wangberg B, Granerus G, Grimelius L, Nilsson O. Clinical management of gastric carcinoid tumors. *Digestion* 1994; **55 Suppl 3:** 77-85

8 **Borch K**. Atrophic gastritis and gastric carcinoid tumours. *Ann Med* 1989; **21**: 291-297

9 **Higham AD**, Dimaline R, Varro A, Attwood S, Armstrong G, Dockray GJ, Thompson DG. Octreotide suppression test

predicts beneficial outcome from antrectomy in a patient with gastric carcinoid tumor. *Gastroenterology* 1998; **114:** 817-822
10 **Schneider C**, Wittekind C, Kockerling F. An unusual incidence of carcinoid tumors and secondary malignancies. *Chirurg* 1995; **66:** 607-611
11 **Modlin IM**, Gilligan CJ, Lawton GP, Tang LH, West AB, Darr U. Gastric carcinoids. The Yale Experience. *Arch Surg* 1995; **130:** 250-255; discussion 255-256
12 **Thirlby RC**. Management of patients with gastric carcinoid tumors. *Gastroenterology* 1995; **108**: 296-297
13 **Ahren B**, Borch K. Multiple gastric carcinoid tumours. *Eur J Surg* 1995; **161:** 375
14 **O'Toole D**, Ducreux M, Bommelaer G, Wemeau JL, Bouche O, Catus F, Blumberg J, Ruszniewski P. Treatment of carcinoid syndrome: a prospective crossover evaluation of lanreotide versus octreotide in terms of efficacy, patient acceptability, and tolerance. *Cancer* 2000; **88:** 770-776
15 **Bajetta E**, Bichisao E, Artale S, Celio L, Ferrari L, Di Bartolomeo M, Zilembo N, Stani SC, Buzzoni R. New clinical trials for the treatment of neuroendocrine tumors. *Q J Nucl Med* 2000; **44:** 96-101
16 **Ricci S**, Antonuzzo A, Galli L, Orlandini C, Ferdeghini M, Boni G, Roncella M, Mosca F, Conte PF. Long-acting depot lanreotide in the treatment of patients with advanced neuroendocrine tumors. *Am J Clin Oncol* 2000; **23:** 412-415
17 **Anthony LB**. Long-acting formulations of somatostatin analogues. *Ital J Gastroenterol Hepatol* 1999; **31 Suppl 2:** S216-S218
18 **Tomassetti P**, Migliori M, Corinaldesi R, Gullo L. Treatment of gastroenteropancreatic neuroendocrine tumours with octreotide LAR. *Aliment Pharmacol Ther* 2000; **14:** 557-560
19 **Hirschowitz BI**, Griffith J, Pellegrin D, Cummings OW. Rapid regression of enterochromaffinlike cell gastric carcinoids in pernicious anemia after antrectomy. *Gastroenterology* 1992; **102:** 1409-1418
20 **Richards AT**, Hinder RA, Harrison AC. Gastric carcinoid tumours associated with hypergastrinaemia and pernicious anaemia--regression of tumors by antrectomy. A case report. *S Afr Med J* 1987; **72:** 51-3
21 **Hirschowitz BI**, Griffith J, Pellegrin D, Cummings OW. Rapid regression of enterochromaffinlike cell gastric carcinoids in pernicious anemia after antrectomy. *Gastroenterology* 1992; **102:** 561-566
22 **O'Rourke MG**, Lancashire RP, Vattoune JR. Carcinoid of the small intestine. *Aust N Z J Surg* 1986; **56:** 405-8
23 **Singh VV**, Bhutani MS, Draganov P. Carcinoid of the minor papilla in incomplete pancreas divisum presenting as acute relapsing pancreatitis. *Pancreas* 2003; **27:** 96-97

Science Editor Guo SY **Language Editor** Elsevier HK

PO Box 2345, Beijing 100023, China
www.wjgnet.com
wjg@wjgnet.com

ELSEVIER

World J Gastroenterol 2005;11(44):7033-7035
World Journal of Gastroenterology ISSN 1007-9327

• *RAPID COMMUNICATION* •

Cell cycle and radiosensitivity of progeny of irradiated primary cultured human hepatocarcinoma cells

Zhi-Zhong Liu, Wen-Ying Huang, Ju-Sheng Lin, Xiao-Sheng Li, Kuo-Huan Liang, Jia-Long Huang

Zhi-Zhong Liu, Ju-Sheng Lin, Kuo-Huan Liang, Jia-Long Huang, Institute of Liver Diseases, Tongji Hospital, Tongji Medical College, Huazhong University of Science and Technology, Wuhan 430030, Hubei Province, China
Wen-Ying Huang, The People's Hospital of Chenzhou City, Chenzhou 423000, Hunan Province, China
Xiao-Sheng Li, Xiehe Hospital, Tongji Medical College, Huazhong University of Science and Technology, Wuhan 430030, Hubei Province, China
Correspondence to: Zhi-Zhong Liu, Institute of Liver Diseases, Tongji Hospital, Tongji Medical College, Huazhong University of Science and Technology, Wuhan 430030, Hubei Province, China. whzzl@163.net
Telephone: +86-27-13554460933
Received: 2004-06-18 Accepted: 2004-08-20

Abstract

AIM: To evaluate the change of growth characteristics and radiosensitivity of irradiated primary cultured human hepatocarcinoma cells.

METHODS: All tumor tissue samples were obtained from 39 hepatocarcinoma patients with a mean age of 49.6 years (range 22-76 years). We divided the samples into irradiated group and non-irradiated group and measured their plating efficiency (PE), population doubling time (PDT), radiosensitivity index SF2 and cell cycle.

RESULTS: The PDT of primary culture of hepatocarcinoma cells was 91.0±6.6 h, PE was 12.0±1.4%, SF2 was 0.41±0.05%. The PDT of their irradiated progeny was 124.8±5.8 h, PE was 5.0±0.7%, SF2 was 0.65±0.09%. The primary cultured human hepatocarcinoma cells showed significant S reduction and G^2 arrest in a dose-dependent manner. The progeny of irradiated primary cultured hepatocarcinoma cells grew more slowly and its radiosensitivity increased.

CONCLUSION: The progeny of irradiated primary cultured human hepatocarcinoma cells grows more slowly and its radiosensitivity increases.

Key words: Hepatocarcinoma; Cell cycle; Population doubling time; Radiosensitivity

Liu ZZ, Huang WY, Lin JS, Li XS, Liang KH, Huang JL. Cell cycle and radiosensitivity of progeny of irradiated primary cultured human hepatocarcinoma cells. *World J Gastroenterol* 2005; 11(44): 7033-7035
http://www.wjgnet.com/1007-9327/11/7033.asp

INTRODUCTION

Hepatocarcinoma cells have a better reaction to X-rays. The mechanism of radiosensitivity of hepatocarcinoma cells after radiotherapy is not very clear. In this study, we have used primary cultured human hepatocarcinoma cells *in vitro* to evaluate the change of growth characteristics and radiosensitivity of progeny of irradiated primary hepatocarcinoma cells.

MATERIALS AND METHODS

Specimens

All tumor tissue specimens were obtained from 39 hepatocarcinoma patients with a mean age of 49.6 years (range 22-76 years).

Cell culture

Primary hepatocarcinoma tissue specimens were obtained from hepatocarcinoma patients. The volume of the sample was 1.5 cm^3. Cells were grown in Dulbecco's minimal essential medium (DMEM) containing 25% fetal calf serum and incubated at 37 °C in 50 mL/L CO_2. Most cells were anchored after inoculation for 16 h and the cell growth could be seen after inoculation for 48 h. Then the primary cultured human hepatocarcinoma cells entered the experimental growth phase. The proliferation was very productive and ended 7-8 d after incubation. The density of cells was 50-95% in flask with a few fibroblasts. The time was the best opportunity for irradiation in flask.

Irradiation condition

The samples were divided into irradiated group and non-irradiated group. Cells in the experimental growth phase were irradiated with 2-8 Gy of X-ray at a dose rate of 200 cGy/min and divided into five groups (0-8 Gy). The lucite was placed in dishes.

Population doubling time (PDT)

Cells in the experimental growth phase were digested into single-cell suspension by 2.5 g/L trypsin. *In vitro* transduction was performed by plating 1×10^5 cells in 6-cm^2 flasks. Cells were digested after being irradiated for 48, 72, 96, 120, 144 h and counted. The experiment was repeated thrice. The cell growth curve was drawn and the cell PDT was calculated.

Table 1 PDT and PE between irradiated and non-irradiated human hepatocarcinoma cells (mean±SD)

Dose (Gy)	PDT (PDT) (t/h)	PE (%)
0	91.0±6.6	12.0±1.4
2	104.7±2.1	10.2±0.6
4	120.4±2.8	8.2±0.4
6	133.5±1.4	6.0±1.1
8	141.8±5.8[a]	5.0±0.7[b]

[a]P<0.05, [b]P<0.01 *vs* 0 Gy.

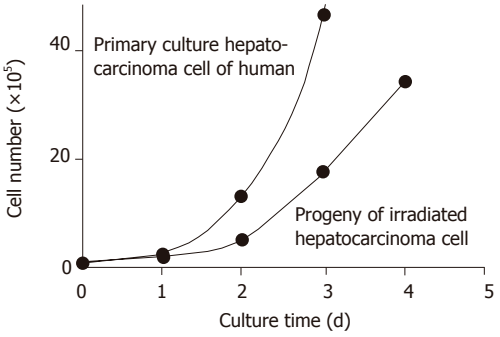

Figure 1 Cell growth curve and irradiated progeny of primary cultured human hepatocarcinoma cells.

Colony assay

Cells in the experimental growth phase were digested into single-cell suspension by 2.5 g/L trypsin. *In vitro* transduction was performed by plating 1×10^5 cells in 3-cm^2 flasks. Cells were irradiated with 2-8 Gy. After 12-15 d of plating, the culture was ended. Cells were fixed by formaldehyde and stained with Giemsa. The number of colonies exceeding 50 was defined as positive. The survival fraction rate was the colony rate. Three parallel samples were set in each dosage point and the experiment was repeated thrice. The formulations [SF2 = e-($aD+\beta D2$)] (the secondary equation) and [(S = 1-(1–e-KD)N)] (the multi-target click model) were used to simulate the cell survival curve of hepatocarcinoma cells. The radiosensitivity parameters such as SF2, α, D_0, and N were calculated.

Detection of cell cycle

Cells in the experimental growth phase were irradiated with 2-8 Gy (Linear Accelerator Saturn 43 type). Cells after being irradiated were retrieved at five time points (0, 6, 12, 24, 36 h) and centrifuged (800 r/min). Then the cells were washed twice with PBS. The single-cell suspension was fixed in 80% ethanol and then treated with RNase. At last, the cells were resuspended and incubated for 30 min at 4 ℃. Cellular fluorescence was measured by FASort flow cytometry (Becton Dickinson). The data were analyzed by CELLQuest software.

Statistical analysis

Using the SPSS 10.0 statistical analysis software, cell growth curve and cell survival curve were simulated by square regression. The cell cycle ratio and radiosensitivity parameters were expressed as mean±SD. Student's t-test was used to compare the difference between the two groups.

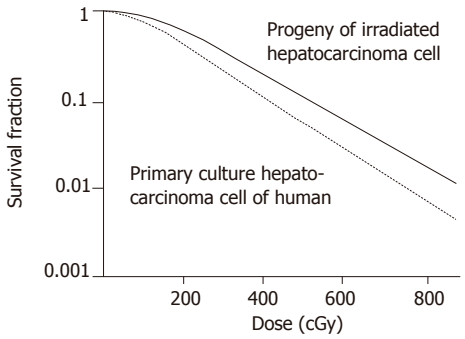

Figure 2 Cell survival curve of primary human hepatocarcinoma cells and irradiated progeny.

RESULTS

Plating efficiency (PE) and cell population doubling time of irradiated progeny

The plating efficiency (PE) of primary cultured human hepatocarcinoma cells was 12.0 ± 1.4%, the irradiated progeny was 5.0±0.7%, being significantly higher than that of non-irradiated cells (t = 8.547, P<0.01). The cell PDT of progeny of irradiated human hepatocarcinoma cells was longer than that of non-irradiated ones. The cell PDT of primary cultured human hepatocarcinoma cells was 91.0 ±6.6 h. The PDT difference between irradiated progeny and non-irradiated cells was significant (t = 3.672, P<0.05; Table 1 and Figure 1).

Radiosensitivity of irradiated progeny

The survival curve and irradiated progeny of human hepatocarcinoma cells are shown in Figure 2. SF2, α, D_0, and N of primary human hepatocarcinoma cells were 0.41±0.05, 0.37/Gy, 0.43 Gy, 2.52, respectively. SF2, α, D_0, and N of irradiated progeny were 0.65±0.09, 0.10/Gy, 0.61 Gy, 1.08, respectively (t = 3.863, P<0.05). The difference was significant. Both SF2 and radiosensitivity of hepatocarcinoma cells were increased in human hepatocarcinoma cells and irradiated progeny.

Detection of cell cycle

Cells in the experimental growth phase were irradiated with 2-8 Gy (Linear Accelerator Saturn 43 type). The cells decreased in S phase and increased in G_2/M phase in a dose-dependent manner (P<0.05). The DNA synthesis time was shorter and mitosis was delayed. The cells after mitosis entering G_0/G_1 phase decreased in a dose-dependent manner (Table 2).

DISCUSSION

The results of radiosensitivity *in vitro* of carcinoma cells are closely related with the clinical effect of carcinoma

Table 2 Cells in S and G2/M phase of irradiated progeny (mean±SD)

Dose (Gy)	SPF (%)	G2/M (%)
0	66.10±0.75	0.91±0.19
2	61.52±0.22	1.73±0.53
4	50.15±0.68	3.32±0.68
6	43.35±0.24	4.51±0.92
8	33.32±0.51[a]	6.48±0.57[a]

[a]$P<0.05$ *vs* oGy.

radiotherapy. But most studies showed that there have been great differences in radiosensitivity of identical carcinomas[1-2]. Studies indicate that radiation can lead to the instability of cell genes and survived progeny will occur[3]. It was reported that irradiated progeny produces resistance after radiation or DNA damage[4-5].

There is evidence that carcinoma is a cell cycle disease. The malignant level of carcinoma is closely related with cell cycle. The carcinoma cells in different cell cycle phases have different radiosensitivity to chemotherapy drugs. Proliferating cells have a good radiosensitivity. Radiotherapy can change the processes of cell cycle. It displays G_0, G_2/M, and S arrest. To study the alteration of cell cycle after radiation is of great significance in choosing suitable chemotherapy drugs after radiotherapy.

Our study indicated that the growth characteristics of progeny of human hepatocarcinoma cells were changed after being irradiated with 2-8 Gy. The growth speed was delayed, the PE was decreased and the radiosensitivity was increased. The radiosensitivity of irradiated progeny was related with G_2/M arrest and cells in S phase reduced in a dose-dependent manner. The radiosensitivity of cells in S phase was the highest due to decreased progeny of irradiated human hepatocarcinoma cells and PE as well as delayed PDT cell reaction in S phase and G_2/M arrest[6].

In conclusion, stereotactic radiotherapy can achieve better results in the treatment of hepatocarcinoma.

REFERENCES

1 **Xia YF**, Li MZ, Huang B, Chen JJ, Li ZQ, Wang HM, Brook WA. Cellular radiobiological characteristics of human nasopharyngeal carcinoma cell lines. *Ai Zheng* 2001; **20:** 683
2 **Hu B**, Zhou XY, Wang X, Zeng ZC, Iliakis G, Wang Y. The radioresistance to killing of A1-5 cells derives from activation of the Chk1 pathway. *J Biol Chem* 2001; **276:** 17693-17698
3 **Shi WM**, Fan YX, Chen LH. The study of radiosensitivity of two human being hepatocacinoma cell lines in vitro. *Zhongguo Xiandai Yixue* 2001; **11:** 6-7
4 **Pitot HC**, Hikita H, Dragan Y, Sargent L, Haas M. Review article: the stages of gastrointestinal carcinogenesis--application of rodent models to human disease. *Aliment Pharmacol Ther* 2000; **14 Suppl 1:** 153-160
5 **Zhang XW**, Zhang LZ, Zhou XM, Wu SY, Wang YP, Zhang W. The relationship between hydatidiform mole canceration and Y chromatosome. *Beijing Yixue* 2002; **24:** 82-83
6 **Ku JL**, Yoon KA, Kim IJ, Kim WH, Jang JY, Suh KS, Kim SW, Park YH, Hwang JH, Yoon YB, Park JG. Establishment and characterisation of six human biliary tract cancer cell lines. *Br J Cancer* 2002; **87:** 187-193

Science Editor Wang XL and Guo SY **Language Editor** Elsevier HK

PO Box 2345, Beijing 100023, China
www.wjgnet.com
wjg@wjgnet.com

ELSEVIER

World J Gastroenterol 2005;11(44):7036-7039
World Journal of Gastroenterology ISSN 1007-9327

• *RAPID COMMUNICATION* •

Prediction value of radiosensitivity of hepatocarcinoma cells for apoptosis and micronucleus assay

Zhi-Zhong Liu, Wen-Ying Huang, Xiao-Sheng Li, Ju-Sheng Lin, Xiao-Kun Cai, Kuo-Huang Lian, He-Jun Zhou

Zhi-Zhong Liu, Ju-Sheng Lin, Xiao-Kun Cai, Kuo-Huang Lian, He-Jun Zhou, Tongji Hospital, Tongji Medical College, Huazhong University of Science and Technology, Wuhan 430030, Hubei Province, China
Wen-Ying Huang, The People's Hospital of Chenzhou City, Chenzhou 423000, Hunan Province, China
Xiao-Sheng Li, Xiehe Hospital, Tongji Medical College, Huazhong University of Science and Technology, Wuhan 430030, Hubei Province, China
Correspondence to: Dr Zhi-Zhong Liu, Institute of Liver Diseases, Tongji Hospital, Tongji Medical College, Huazhong University of Science and Technology, Wuhan 430030, Hubei Province, China. whzzl@163.net
Telephone: +86-27-13554460433
Received: 2004-05-07 Accepted: 2004-08-18

Abstract

AIM: To investigate the prediction value of radiosensitivity of hepatocarcinoma cells for apoptosis and micronucleus assay.

METHODS: Clonogenic assay, flow cytometry, and CB micronuclei assay were used to survey the cell survival rate, radiation-induced apoptosis and micronucleus frequency of hepatocarcinoma cell lines SMMC-7721, HL-7702, and HepG2 after being irradiated by X-ray at the dosage ranging 0-8 Gy.

RESULTS: After irradiation, there was a dose-effect relationship between micronucleus frequency and radiation dosage among the three cell lines ($P<0.05$). A positive relationship was observed between apoptosis and radiation dosage among the three cell lines. The HepG2 cells had a significant correlation ($P<0.05$) but apoptosis incidence had a negative relationship with micronucleus frequency. There was a positive relationship between apoptosis and radiation dosage and the correlation between SMMC-7721 and HL-7702 cell lines had a significant difference ($P<0.01$). After irradiation, a negative relationship between cell survival rate and radiation dosages was found among the three cell lines ($P<0.01$). There was a positive relationship between cell survival rate and micronucleus frequency ($P<0.01$). No correlation was observed between apoptosis and cell survival rate.

CONCLUSION: The radiosensitivity of hepatocarcinoma cells can be reflected by apoptosis and micronuclei. Detection of apoptosis and micronuclei could enhance the accuracy for predicting radiosensitivity.

Key words: Hepatocarcinoma cell; Micronuclei; Apoptosis; Radiosensitivity

Liu ZZ, Huang WY, Li XS, Lin JS, Cai XK, Lian KH, Zhou HJ. Prediction value of radiosensitivity of hepatocarcinoma cells for apoptosis and micronucleus assay. *World J Gastroenterol* 2005; 11(44): 7036-7039
http://www.wjgnet.com/1007-9327/11/7036.asp

INTRODUCTION

The prediction of cell radiosensitivity is a main content in radiobiology and carcinoma treatment. Apoptosis of carcinoma cells can be induced by radiotherapy. Micronucleus is a product of abnormal mitosis. Studies have verified that micronucleus analysis can predict radiosensitivity of cells[1,2]. It was reported that apoptosis is correlated with cell survival[3,4]. Apoptosis and micronuclei occur after the first mitosis and are related with the damage in heredity substance. To investigate apoptosis and micronucleus assay is of significance in predicting radiosensitivity.

This study focused on the relationship among apoptosis, micronuclei, and cell survival rate of three hepatic cell lines (HL-7702, HepG2, SMMC-7721). The prediction value of radiosensitivity for apoptosis and micronucleus assay of hepatocarcinoma cells was investigated *in vitro*.

MATERIALS AND METHODS

Three hepatic carcinoma cell lines (HL-7702, HepG2, SMMC-7721) were cultured at 37 ℃ in RPMI 1640 medium supplemented with 10% fetal bovine serum and divided into irradiated group and non-irradiated group. Cells in experimental growth phase were irradiated by X-ray at a dose of 2-8 Gy (Linear Accelerator Saturn 43 type) with a dose rate of 200 cGy/min. The lucite was placed in dishes.

Cells in the experimental growth phase were digested by 2.5 g/L trypsin into a single-cell suspension. *In vitro* transduction was performed by plating 1×10^5 cells in 3-cm^2 flasks. Cells were irradiated with 2-8 Gy. After 12-15 d of plating, the culture was stopped. Cells were fixed by formaldehyde and stained with Giemsa. The number

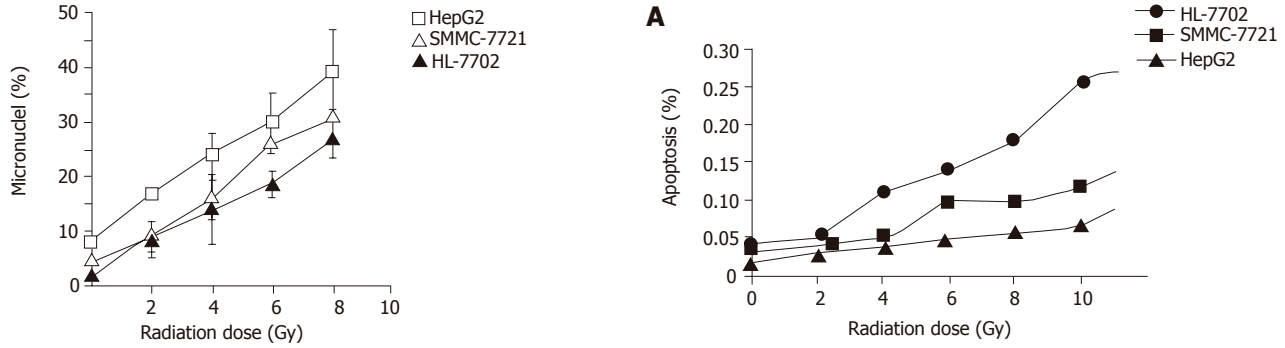

Figure 1 Micronucleus frequency of three cell lines.

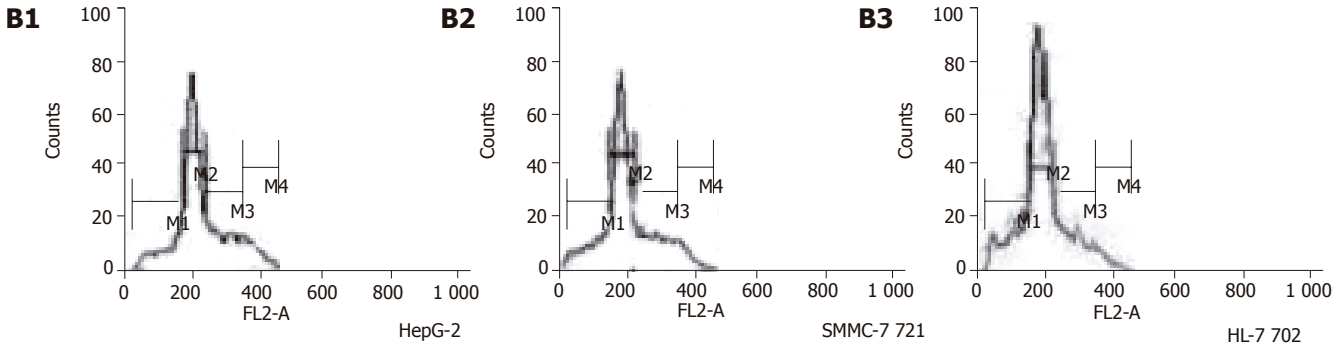

Figure 2 Apoptosis incidence (**A**) and DNA content (**B**) in three cell lines.

of colonies exceeding 50 was defined as positive. The survival fraction rate amounted to colony formation rate in irradiation group. Three parallel samples were set in each dosage point and repeated thrice.

Cells in the experimental growth phase were digested by 2.5 g/L trypsin into single-cell suspension at the concentration of 3×10^4 μg/mL and inoculated in petri dishes. When the cells were attached to the wall, they were cultured for 2 days and then irradiated with 2-8 Gy. After irradiation, samples were added in 2 μg/mL cytochalasin-B, and cultured for 48 h, and then stained *in situ*. The number of micronuclei in double nuclear cells was counted. At least 1 000 double nuclear cells were calculated. Each dosage had three parallel exponents and the experiment was repeated thrice.

Cells were centrifuged and washed 2-3 times with PBS and then fixed in 80% ethanol at -20 ℃. The samples were centrifuged for 5 min (800 r/min) and washed with PBS, mixed into mono cell suspension and diluted at 1:400 in PBS. The cells were treated with RNase for 30 min, resuspended in 10 μg/mL of PI and incubated overnight at 4 ℃. Cellular fluorescence was measured by FASort flow cytometry (Becton Dickinson, San Jose, CA, USA). We collected the data by CELLQuest software and analyzed the cell cycle by ModFit2.0.

Statistical analysis

Correlation analysis was made using the SPSS statistical analysis software.

RESULTS

After being irradiated with 2-8 Gy, the micronucleus frequency of HepG2, SMMC-7721, and HL-7702 was related with radiation dosage. The relationship between the micronucleus frequency of HepG2 and radiation dosage was significant ($P<0.05$, Figure 1).

After being irradiated with 2-8 Gy, a positive relationship was observed between apoptosis incidence and radiation dosages. The relationship between micronucleus frequency of HepG2, SMMC-7721 and radiation dosage was significant ($P<0.01$, Figure 2). But apoptosis incidence was negatively related with micronucleus frequency.

After being irradiated with 2-8 Gy, the cell survival rate of three cell lines was decreased ($P<0.05$, Tables 1 and 2).

After being irradiated with 2-8 Gy, a positive relationship was found between micronucleus frequency and cell survival rate ($P<0.01$, Figure 3) .

The relationship between micronucleus frequency and apoptosis of three cell lines was not significant ($P>0.05$).

DISCUSSION

Hepatocarcinoma is a common malignant tumor. Stereotactic radiotherapy of hepatocarcinoma can achieve better effects. Hepatocarcinoma cells may have corresponding radiosensitivity.

Micronucleus is a product of abnormal mitosis and consists of chromatosome fragments that cannot enter the

Table 1 Cell survival rate of three cell lines (mean±SD)

Cells	Radiation dose (Gy)			
	2	4	6	8
HepG2	0.45±0.08	0.22±0.02	0.06±0.02	0±0
SMMC-7721	0.72±0.05	0.29±0.05	0.08±0.05	0±0
HL-7702	0.79±0.02	0.31±0.09	0.11±0.06	0±0

Table 2 SF2 of three cell lines (mean±SD)

Cells	Do	Dq	*n*	SF_2
HepG2	1.5	0.8	1.7	0.45±0.08
SMMC-7721	1.8	1.5	2.5	0.72±0.05
HL-7702	2.0	1.8	3.0	0.79±0.02

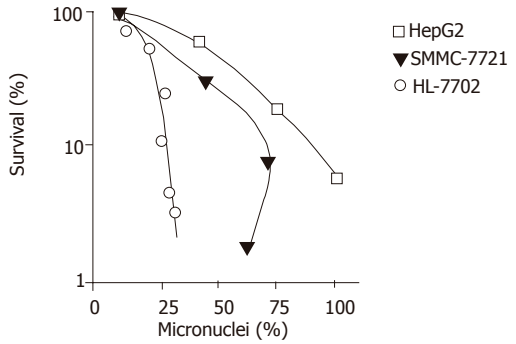

Figure 3 Relationship between micronucleus frequency and cell survival rate.

core nuclei when cells undergo mitosis. Micronucleus analysis is a method to detect cell radiosensitivity. Widel *et al*.[5] found that micronucleus frequency can be used as a marker to predict prognosis of hepatocarcinoma patients. Kolotas *et al*.[6] showed that the prognosis is better in patients with a higher micronucleus frequency than in those with a lower micronucleus frequency. But we found that micronucleus frequency of radiation-resistant cell lines was not related with cell survival rate. It is usually believed that micronuclei induced by X-ray express only in sensitive cells. Micronucleus frequency of sensitive cells is higher than that of radiation-resistant cells. Therefore, micronuclei as a marker to predict cell radiosensitivity of all cells needs to be studied further.

Apoptosis of carcinoma cells can be induced by radiotherapy. The sensitivity to apoptosis and X-ray of carcinoma cells is coincident. Studies showed that apoptosis index of carcinoma cells increases after radiation. The rate of apoptosis induced by radiotherapy increases after radiation, indicating that apoptosis can be used as a marker to predict radiosensitivity.

In this experiment, radiation dose was related with micronucleus frequency in three cell lines. There was a positive relationship between the micronucleus frequency and cell survival rate, suggesting that micronucleus frequency can be used as a marker to predict the radiosensitivity of hepatic carcinoma cells. Radiation dose was related with apoptosis incidence in three cell lines. The apoptosis incidence of HL-7702 and SMMC-7721 was higher than that of HepG2, suggesting that apoptosis incidence can be used as a marker to predict the radiosensitivity of hepatocarcinoma cells.

In this experiment, no significant difference was found between apoptosis incidence induced by radiotherapy and cell survival rate in three cell lines, indicating that the damage induced by radiotherapy is different from apoptosis of hepatic carcinoma cells and that response of radiation-resistant cells occurs due to apoptosis.

Masunaga *et al*.[10] showed that micronucleus frequency and apoptosis incidence can predict radiosensitivity of carcinoma cells. Our study confirmed that micronucleus frequency was negatively related with apoptosis incidence of three cell lines. Apoptosis resulted from cell damage. The impaired cells express apoptosis or micronuclei. This result supports that once apoptosis occurs, the cells lose the segregating opportunity, thus affecting micronucleus formation. Apoptosis may be an important factor affecting micronucleus frequency.

REFERENCES

1 **Vijayalaxmi**, Bisht KS, Pickard WF, Meltz ML, Roti Roti JL, Moros EG. Chromosome damage and micronucleus formation in human blood lymphocytes exposed in vitro to radiofrequency radiation at a cellular telephone frequency (847.74 MHz, CDMA). *Radiat Res* 2001; **156:** 430-432

2 **Bhattathiri VN**, Bindu L, Remani P, Chandralekha B, Davis CA, Nair MK. Serial cytological assay of micronucleus induction: a new tool to predict human cancer radiosensitivity. *Radiother Oncol* 1996; **41:** 139-142

3 **Kirsch-Volders M**, Elhajouji A, Cundari E, Van Hummelen P. The in vitro micronucleus test: a multi-endpoint assay to detect simultaneously mitotic delay, apoptosis, chromosome breakage, chromosome loss and non-disjunction. *Mutat Res* 1997; **392:** 19-30

4 **Levine EL**, Renehan A, Gossiel R, Davidson SE, Roberts SA, Chadwick C, Wilks DP, Potten CS, Hendry JH, Hunter RD. Apoptosis, intrinsic radiosensitivity and prediction of radiotherapy response in cervical carcinoma. *Radiother Oncol* 1995; **37:** 1-9

5 **Widel M**, Kolosza Z, Jedrus S, Lukaszczyk B, Raczek-Zwierzycka K, Swierniak A. Micronucleus assay in vivo provides significant prognostic information in human cervical carcinoma; the updated analysis. *Int J Radiat Biol* 2001; **77:** 631-636

6 **Kolotas C**, Tonus C, Baltas D, Cernea M, Vogt HG, Martin T, Strassmann G, Zamboglou N. Clinical relevance of tumor ploidy and micronucleus formation for oral cavity cancer. *Tumori* 1999; **85:** 253-258

7 **Guo GZ**, Sasai K, Oya N, Shibata T, Shibuya K, Hiraoka M. A significant correlation between clonogenic radiosensitivity and the simultaneous assessment of micronucleus and apoptotic cell frequencies. *Int J Radiat Biol* 1999; **75:** 857-864

8 **Pervan M**, Pajonk F, Sun JR, Withers HR, McBride WH. Molecular pathways that modify tumor radiation response. *Am J Clin Oncol* 2001; **24:** 481-485

9 **Kim JY**, Cho HY, Lee KC, Hwang YJ, Lee MH, Roberts SA, Kim CH. Tumor apoptosis in cervical cancer: its role as a prognostic factor in 42 radiotherapy patients. *Int J Cancer* 2001; **96:** 305-312

10 **Masunaga SI**, Ono K, Suzuki M, Nishimura Y, Kinashi Y, Takagaki M, Hori H, Nagasawa H, Uto Y, Tsuchiya I, Sadahiro S, Murayama C. Radiosensitization effect by combination with paclitaxel in vivo, including the effect on intratumor quiescent cells. *Int J Radiat Oncol Biol Phys* 2001; **50:** 1063-1072

11 **Kirsch-Volders M**, Elhajouji A, Cundari E, Van Hummelen

P. The in vitro micronucleus test: a multi-endpoint assay to detect simultaneously mitotic delay, apoptosis, chromosome breakage, chromosome loss and non-disjunction. *Mutat Res* 1997; **392:** 19-30

Science Editor Wang XL and Guo SY **Language Editor** Elsevier HK

PO Box 2345, Beijing 100023, China
www.wjgnet.com
wjg@wjgnet.com

ELSEVIER

World J Gastroenterol 2005;11(44):7040-7043
World Journal of Gastroenterology ISSN 1007-9327

• *RAPID COMMUNICATION* •

Cell survival curve for primary hepatic carcinoma cells and relationship between SF_2 of hepatic carcinoma cells and radiosensitivity

Zhi-Zhong Liu, Wen-Ying Huang, Ju-Sheng Lin, Xiao-Sheng Li, Xiao Lan, Xiao-Kun Cai, Kuo-Huan Liang, Hai-Jun Zhou

Zhi-Zhong Liu, Ju-Sheng Lin, Xiao-Kun Cai, Kuo-Huan Liang, Tongji Hospital, Tongji Medical College, Huazhong University of Science and Technology, Wuhan 430030, Hubei Province, China
Wen-Ying Huang, Hai-Jun Zhou, The People's Hospital of Chenzhou, Chenzhou 423000, Hunan Province, China
Xiao-Sheng Li, Xiao Lan, Xiehe Hospital, Tongji Medical College, Huazhong University of Science and Technology, Wuhan 430030, Hubei Province, China
Correspondence to: Dr Zhi-Zhong Liu, Institute of Liver Diseases, Tongji Hospital, Tongji Medical College, Huazhong University of Science and Technology, Wuhan 430030, Hubei Province, China. whzzl@163.net
Telephone: +86-27-13554460933
Received: 2004-06-18 Accepted: 2004-08-12

Abstract

AIM: To establish the cell survival curve for primary hepatic carcinoma cells and to study the relationship between SF_2 of primary hepatic carcinoma cells and radiosensitivity.

METHODS: Hepatic carcinoma cells were cultured *in vitro* using 39 samples of hepatic carcinoma at stages II-IV. Twenty-nine samples were cultured successfully in the fifth generation cells. After these cells were radiated with different dosages, the cell survival ratio and SF_2 were calculated by clonogenic assay and SF_2 model respectively. The relationship between SF_2 and the clinical pathological feature was analyzed.

RESULTS: Twenty-nine of thirty-nine samples were successfully cultured. After X-ray radiation of the fifth generation cells with 0, 2, 4, 6, 8 Gy, the cell survival rate was 41%, 36.5%, 31.0%, 26.8%, and 19%, respectively. There was a negative correlation between cell survival and irradiation dosage (r = -0.973, P<0.05). SF_2 ranged 0.28-0.78 and correlated with the clinical stage and pathological grade of hepatic carcinoma (P<0.05). There was a positive correlation between SF_2 and D0.5 (r = 0.773, P<0.05).

CONCLUSION: SF_2 correlates with the clinical stage and pathological grade of hepatic carcinoma and is a marker for predicting the radiosensitivity of hepatic carcinomas.

Key words: Hepatocarcinoma; SF_2; Radiosensitivity; D0.54

Liu ZZ, Huang WY, Lin JS, Li XS, Lan X, Cai XK, Liang KH, Zhou HJ. Cell survival curve for primary hepatic carcinoma cells and relationship between SF_2 of hepatic carcinoma cells and radiosensitivity. *World J Gastroenterol* 2005; 11(44): 7040-7043
http://www.wjgnet.com/1007-9327/11/7040.asp

INTRODUCTION

Hepatic carcinoma is the most common malignant tumors in China. Radiotherapy is its main therapy. But owing to the influence of radiosensitivity and other factors, the effect of radiotherapy on hepatic carcinoma is not obvious. About 40% of hepatic carcinoma patients do not respond to radiotherapy.

The cell survival curve is a curve that describes the relationship between radiation dose and survival cells.

In general, the proliferation ability of survival cells decreases with the increasing of radiation dose. Detecting the SF_2 is a reliable index to predict the radiosensitivity of tumors.

In this experiment, we used the primary cell culture and the clone-formation technique to establish the reliable cell survival curve for hepatic carcinoma. By application of the multi-target click model and calculation of SF_2, we studied the relationship between SF_2 and D0.5. The value of SF_2 for the prediction of the prognosis of hepatic carcinoma was evaluated.

MATERIALS AND METHODS

Source of samples

Thirty-nine fresh specimens were taken from hepatic carcinoma patients at stages II-IV. All the patients had their final diagnosis in Tongji Hospital and did not receive any therapy. Their average age was 49.6 years (22-76 years). All the cases were diagnosed by pathology. Twenty-four specimens of hepatocellular carcinoma and 15 samples of bile duct epithelial carcinoma were taken. Nine were in stage IIB (23%), 25 in stage IIIB (64.1%) and 5 in stage IV (12.9%). The maximum diameter of local carcinoma was <4 cm in 22 specimens (56.9%) and >4 cm

in 17 specimens (43.1%). The specimens were put into RPMI-1640 medium containing 25% fetal calf serum.

Reagents

RPMI-1640 medium, bovine trypsin (1:250), insulin, poly-lysine, and hydrocortisone were purchased from JingMei Company, Shenzhen, China. Agarose was purchased from DIFCO Company.

Irradiation condition

The specimens were irradiated by 6 MV X-ray at the doses of 0, 2, 4, 6, and 8 Gy. The irradiation field was 10 cm ×10 cm. The source skin distance (SSD) was 100 cm. The absorbed dose was 200 cGy/min. The culture bottle was covered with 1.5-cm lucite plate.

Primary culture of hepatic carcinoma cells

The specimens were rinsed 2-3 times with PBS containing streptomycin and penicillin. Blood, fibrous and necrosed tissue were removed. Then a small quantity of PBS was added and the tissue was cut into micro-blocks. The micro-blocks of tissue and PBS were left in the plate and incubated in a 50 mL/L CO_2 incubator. The plate was kept in inversion status for 4-6 h. The anchoring condition of cells was observed under a microscope. If the cells in the tissue were in good condition, RPMI-1640 medium containing 15-25% fetal calf serum was added. The anchoring condition of cells was observed under a microscope on the next day and poly-lysine was added. The poly-lysine promoted the anchoring of cells. In order to provide the cells a better growing condition, we could also add some stimulation factors such as hydrogenated cortadren (4 μg/mL) and insulin (4 μg/mL) on the third and fourth culture days. The culture medium was changed after 5 d, and then every 2-3 d. After incubation for about 14 d, the cultured cells were digested for future generation.

Clone formation rate of hepatic carcinoma cells detected by soft agarose cloning technique[1]

The fifth generation of hepatic carcinoma cells in logarithmic growth phase was digested by 0.25% trypsinogen and counted. Then the cells were inoculated into cell suspension containing 35% soft agarose. According to the irradiation dosage, the cell suspension was put into glass plates. The culture medium was changed after irradiation for about 12 h. The inoculated cells were divided into five groups and irradiated, and then cultured for 10-14 h. The surface culture medium of the plate was stained with hematoxylin and observed under invert microscope and the number of colonies was more than 50. The clone formation rate (SF) after irradiation was assayed thrice to obtain the mean value.

Drawing cell survival curve for hepatic carcinoma cells

Three petri dishes were selected from each dosage group to obtain the mean value. O Gy group was used in every experiment and the colony formation rate (SF) was calculated. On the basis of different dosage irradiation and different incubation time, the cell number was used as the ordinate and the irradiation dosage as the abscissa to draw the growth curve for hepatic carcinoma cells. SF_2 was calculated by the formula [$SF = 1-(1-e^{-D/D_0})^N$] (the multi-target click model)[2].

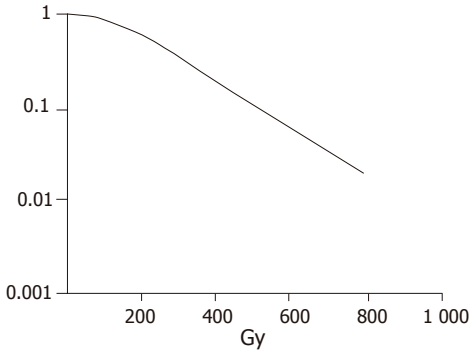

Figure 1 Survival curve of hepatic carcinoma cells.

Regression of hepatic carcinoma in vivo

The patients were examined once a week before and during radiotherapy. The stage plate was used to measure the size of carcinoma. The volume of tumor was calculated to describe the volume-dosage curve and the dosage decreasing tumor size of 50% (D0.5) was calculated.

Determination of colony formation

The fibroblasts were diffusely distributed in petri dishes after the culture medium was changed before one week. A small quantity of colony formation was also seen. The cell distribution in the center of colony was close. The surrounding cells were distributed outward. The cell density decreased. Different cell colonies had different sizes. Only a few cells could be seen in some new colonies. After 14 d, the fibroblasts in petri dishes increased and their diameter became bigger. The cell distribution in the center of the colony was dense. The diameter of the biggest colony was 8 mm.

Statistical analysis

Student's *t* test was used for the statistical analysis using SPSS 10.0.

RESULTS

After hepatic carcinoma tissue was primarily cultured for about 14-20 d, primary cell culture technique was established in 29 of 39 samples.

The survival curve was drawn after different dosage irradiation of hepatic carcinoma cells. The hepatic carcinoma cells were moderately radiosensitive cells (Figure 1).

The cell survival rate was 41%, 36.5%, 31.0%, 26.8%, and 19%, respectively, after irradiated at the dose of 0, 2, 4, 6, and 8 Gy, respectively. The survival rate of hepatic carcinoma cells had a significantly negative relationship with the irradiation dosage ($r = -0.973$, $P<0.05$, Figure 2).

SF_2 of hepatic carcinoma cells was 0.28-0.78, which

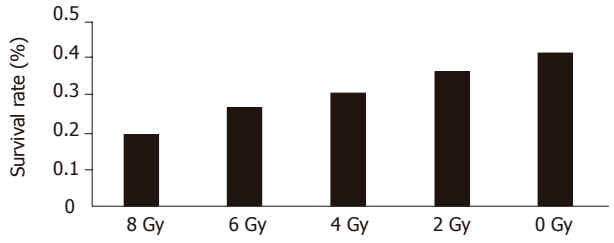

Figure 2 Relationship between survival rate of hepatic carcinoma cells and irradiation dosage.

Table 1 SF_2 of hepatic carcinoma in different clinical stages and pathological types

	Clinical stage		
	IIb	IIIb	IV
Pathology typing			
Hepatocellular carcinoma	0.28	0.47	0.61
Bile duct epithelial carcinoma	0.41	0.57	0.78

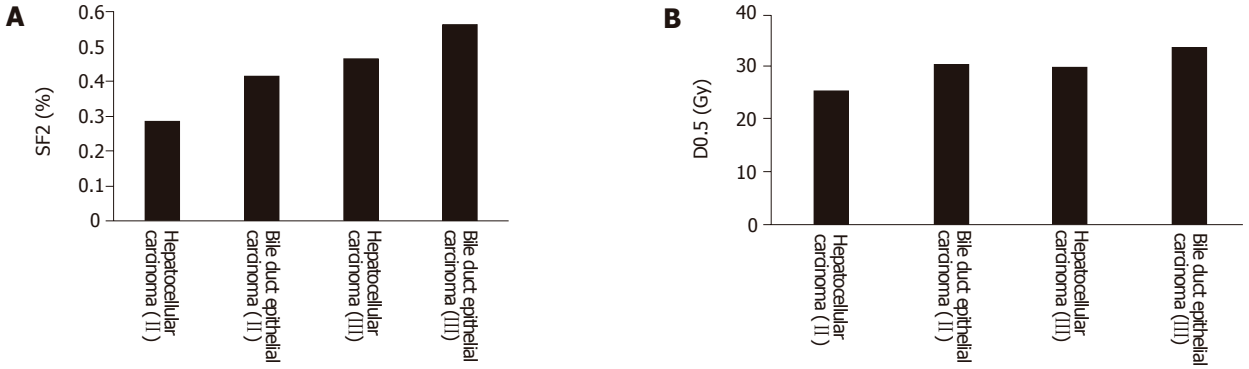

Figure 3 Relationship between the SF2 (**A**) and D0.5 (**B**) in different clinical stages and pathological typing.

was related with the clinical stage of hepatic carcinoma. The more advanced the clinical stage was, the higher the SF_2. SF_2 was also related with the pathological typing of hepatic carcinoma. SF_2 of bile duct epithelial carcinoma was higher than that of hepatocellular carcinoma (Table 1).

SF_2 had a positive relationship with D0.5 ($r = 0.773$, $P<0.05$). SF_2 in different clinical stages of hepatic carcinoma was also related with D0.5. SF_2 in different pathological types of hepatic carcinoma was correlated with D0.5 (Figures 3A and 3B).

DISCUSSION

The determination of radiosensitivity for tumor cells is an important component of tumor radiobiology. The final objective of tumor radiotherapy is to eradicate tumor. But the objective of clinical radiotherapy is to prevent tumor from growth and to eradicate the tumor. Based on the definition of cell survival, the judge of radiotherapy result is based on whether the cells proliferate or not. The survived cells are the main factor for the failure of radiotherapy[3].

Radiosensitivity of hepatic carcinoma cells is a main factor influencing the prognosis of radiotherapy for hepatic carcinoma. To predict the radiosensitivity of hepatic carcinoma cells before and during the therapy, individualization of reasonable and effective therapy is always the direction of tumor investigation.

Primary tumor cell culture *in vitro* has some difficulties such as longer time consumption, high cost, and easy contamination. Based on the past experience, the chief key point to the success of this technique is to draw the materials from tissue because it is closely related with the culture. Aseptic technique is one of the important factors for the success of culture.

It was reported that radiosensitivity is different in different hepatic carcinoma cells and that the local control rate of hepatic carcinoma with its SF_2 <0.55 is higher than that with its SF_2 >0.05[4,5]. SF_2 is related with the staging and pathological typing of tumor but not related with the age of patients and the diameter of tumor. SF_2 is also correlated with pathological typing and clinical stage of tumor. SF_2 for hepatic carcinoma cells in different clinical pathological typing and clinical stage has some differences. It is due to the necessity for individualized treatment of hepatic carcinoma in different clinical pathological typing and clinical stages.

The reports regarding the relationship between SF2 and radiosensitivity have different conclusions. But most experiments showed that SF_2 is negatively related with cell radiosensitivity[6]. SF_2 can be used as a marker for predicting the local control of head and neck tumor. It was reported that SF_2 can predict the reaction after radiotherapy[7]. SF_2 is related with the clinical prognosis of tumor[8]. In our study, SF_2 was significantly related with the radiosensitivity of hepatic carcinoma cells, suggesting that SF_2 can reflect the radiosensitivity of hepatic carcinoma cells.

In conclusion, SF_2 is a reliable marker for predicting the radiosensitivity of hepatic carcinoma cells before and during the therapy.

REFERENCES

1 **Tamamoto T**, Ohnishi K, Takahashi A, Wang X, Yosimura H, Ohishi H, Uchida H, Ohnishi T. Correlation between gamma-ray-induced G2 arrest and radioresistance in two human cancer cells. *Int J Radiat Oncol Biol Phys* 1999; **44**: 905-909

2 **Vral A**, Thierens H, Baeyens A, De Ridder L. Chromosomal aberrations and in vitro radiosensitivity: intra-individual versus inter-individual variability. *Toxicol Lett* 2004; **149:** 345-352

3 **Bedford JS**, Dewey WC. Radiation Research Society. 1952-2002. Historical and current highlights in radiation biology: has anything important been learned by irradiating cells? *Radiat Res* 2002; **158:** 251-291

4 **West CM**, Davidson SE, Roberts SA, Hunter RD. Intrinsic radiosensitivity and prediction of patient response to radiotherapy for carcinoma of the cervix. *Br J Cancer* 1993; ***68:*** 819-23

5 **West CM**, Davidson SE, Roberts SA, Hunter RD. The independence of intrinsic radiosensitivity as a prognostic factor for patient response to radiotherapy of carcinoma of the cervix. *Br J Cancer* 1997; **76:** 1184-1190

6 **Bjork-Eriksson T**, West C, Karlsson E, Mercke C. Tumor radiosensitivity (SF2) is a prognostic factor for local control in head and neck cancers. *Int J Radiat Oncol Biol Phys* 2000; **46:** 13-19

7 **Britten RA**, Evans AJ, Allalunis-Turner MJ, Franko AJ, Pearcey RG. Intratumoral heterogeneity as a confounding factor in clonogenic assays for tumour radioresponsiveness. *Radiother Oncol* 1996; **39:** 145-153

8 **Stausbol-Gron B**, Overgaard J. Relationship between tumour cell in vitro radiosensitivity and clinical outcome after curative radiotherapy for squamous cell carcinoma of the head and neck. *Radiother Oncol* 1999; **50:** 47-55

Science Editor Wang XL **Language Editor** Elsevier HK

PO Box 2345, Beijing 100023, China
www.wjgnet.com
wjg@wjgnet.com

ELSEVIER

World J Gastroenterol 2005;11(44):7044-7047
World Journal of Gastroenterology ISSN 1007-9327

• *CASE REPORT* •

A case of bowel schistosomiasis not adhering to endoscopic findings

Manfredi Rizzo, Pasquale Mansueto, Daniela Cabibi, Elisabetta Barresi, Kaspar Berneis, Mario Affronti, Gabriele Di Lorenzo, Sergio Vigneri, Giovam Battista Rini

Manfredi Rizzo, Pasquale Mansueto, Mario Affronti, Gabriele Di Lorenzo, Sergio Vigneri, Giovam Battista Rini, Department of Clinical Medicine and Emerging Diseases, University of Palermo, Italy
Daniela Cabibi, Elisabetta Barresi, Institute of Pathological Anatomy, University of Palermo, Italy
Kaspar Berneis, Medical University Clinic, Bruderholz, Switzerland
Correspondence to: Dr Manfredi Rizzo, Dipartimento di Medicina Clinica e delle Patologie Emergenti, Universita' di Palermo, Via del Vespro, 141, 90127 Palermo, Italy. mrizzo@unipa.it
Telephone: +39-091-6552945 Fax: +39-091-6552945
Received: 2005-04-03 Accepted: 2005-05-03

Abstract

Schistosomiasis is a chronic worm infection caused by a species of *trematodes,* the *Schistosomes*. We may distinguish a urinary form from *Schistosomes haematobium* and an intestinal-hepatosplenic form mainly from *Schistosomes mansoni* characterized by nausea, meteorism, abdominal pain, bloody diarrhea, rectal tenesmus, and hepatosplenomegaly. These infections represent a major health issue in Africa, Asia, and South America, but recently *S mansoni* has increased its prevalence in other continents, such as Europe and North America, due to international travelers and immigrants, with several diagnostic and prevention problems. We report a case of a 24-year-old patient without HIV infection, originated from Ghana, admitted for an afebrile dysenteric syndrome. All microbiologic studies were negative and colonoscopy revealed macroscopic lesions suggestive of a bowel inflammatory chronic disease. Since symptoms became worse, a therapy with mesalazine (2 g/d) was started, depending on the results of a bowel biopsy, but without any resolution. The therapy was stopped after 2 wk when the following result was available: a diagnosis of "intestinal schistosomiasis" was done (two *Schistosoma* eggs were detected in the colonic mucosa) and this was confirmed by the detection of *Schistosoma* eggs in the feces. Therapy was therefore changed to praziquantel (40 mg/kg, single dose), a specific anti-parasitic agent, with complete recovery. Schistosomiasis shows some peculiar difficulties in terms of differential diagnosis from the bowel inflammatory chronic disease, as the two disorders may show similar colonoscopic patterns. Since this infection has recently increased its prevalence worldwide, it has to be considered in the differential diagnosis of our patients with gastrointestinal symptoms.

Key words: Schistosomiasis; Chronic inflammatory bowel disease; Ulcerative colitis; Granuloma

Rizzo M, Mansueto P, Cabibi D, Barresi E, Berneis K, Affronti M, Di Lorenzo G, Vigneri S, Rini GB. A case of bowel schistosomiasis not adhering to endoscopic findings. *World J Gastroenterol* 2005; 11(44): 7044-7047
http://www.wjgnet.com/1007-9327/11/7044.asp

INTRODUCTION

Schistosomiasis or Bilharziasis is a chronic worm infection caused by a species of t*rematodes*, the *Schistosomes*, which are blood flukes that parasitize the venous channels of definitive human hosts. The infection is transmitted by fresh-water snails. Based on their organ localization, we may distinguish a urinary form from *Schistosomes haematobium*, and an intestinal or hepatosplenic form from *Schistosomes mansoni*, *Schistosomes japonicum*, *Schistosomes mekongi,* and *Schistosomes intercalatum*[1,2].

S mansoni, a main agent of the intestinal form, is a *trematode* which infects human beings more frequently and also infects other primates too. Adult females of *S mansoni* deposit the eggs in the small veins around the large intestine of infected individuals. Some of the eggs may be trapped in the gut wall or break loose into it and are then eliminated by defecation. The eggs trapped in the gut wall are responsible for inflammatory and immunopathologic responses, leading to erythema, edema, granulomas, ulcerations, hemorrhages, and fibrosis. The infection is characterized by nausea, meteorism, abdominal pain, bloody diarrhea, rectal tenesmus, and hepatosplenomegaly[3,5].

Infection with *S mansoni* is still a major health issue in Africa, Asia, and South America[6-10], but recent epidemiological studies showed that its prevalence increases in Europe[11-15] and USA[16,17], due to international travelers and immigrants. In our country, the presence of acute *S mansoni* infection with progression to chronic lesions has been reported in a group of Italian travelers returning from Africa, showing both diagnostic and preventive problems[18].

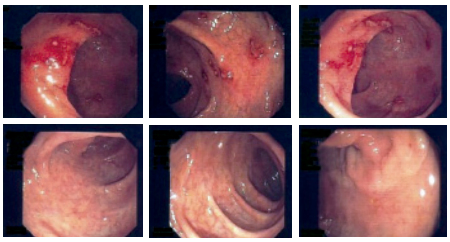

Figure 1 Colonoscopy before (**A**) and after (**B**) therapy.

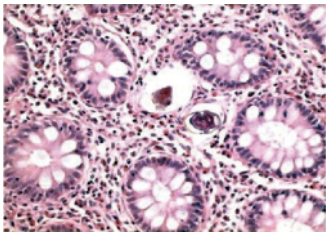

Figure 2 *Schistosoma* eggs detected in colonic mucosa.

Therefore, this infection was considered in the differential diagnosis of our patient with gastrointestinal symptoms. In particular, it is often hard to distinguish this infection from the bowel inflammatory chronic disease, since these two disorders may show similar colonoscopic patterns[19,20]. However, the contemporary presence of the two disorders (usually a chronic schistosomiasis precede the inflammatory disease in the same patient) represents a rare event[21,22].

We report a case of a 24-year-old patient without HIV infection, living in our region who immigrated from Ghana, and was admitted for an afebrile dysenteric syndrome. All microbiologic studies were negative and colonoscopy revealed macroscopic lesions suggestive of a bowel inflammatory chronic disease, and then treated with mesalazine, but without resolution. Further studies by bowel biopsy and feces examination revealed a *Schistosoma* infection, which was treated with praziquantel, a specific anti-parasitic agent and had a complete recovery.

CASE REPORT

A 24-year-old non-HIV patient immigrated from Ghana for economic reasons. He had pain in the left testicle 2 years ago and was hospitalized in his own country, where he was wrongly diagnosed and was given an unknown therapy. However, the pain occasionally recurred with exacerbation after the therapy. The patient was admitted to our hospital for diffuse abdominal pain with occasional bloody diarrhea and vomiting. Hematologic laboratory tests revealed no abnormalities; chest X-ray, and hepatosplenic ultrasonography were normal. The patient had no signs of distress but pain in epigastric and mesogastric regions. Small lymph nodes were observed in the latero-cervix area. All microbiologic studies were negative and colonoscopy revealed macroscopic lesions suggestive of a bowel inflammatory chronic disease reacutization (Figure 1A), like ulcerative colitis or a Crohn's disease. During the colonoscopy, a bowel biopsy was done. Since symptoms became worse, we started a therapy with mesalazine (2 g/d), pending the results of the intestinal biopsy. One week later, a second colonoscopy documented a minor improvement in the endoscopic pattern and the therapy with mesalazine was continued.

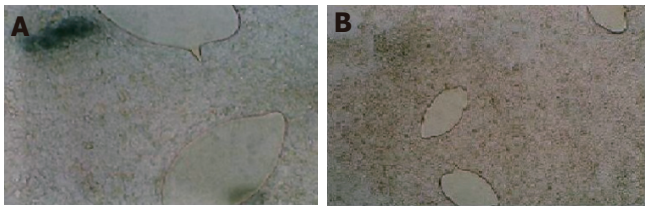

Figure 3 *Schistosoma mansoni* isolated in feces.

Two weeks later, the result of the bowel biopsy was available but did not support a diagnosis of a bowel inflammatory chronic disease, as suggested by the endoscopic patterns. The histopathological findings in colonic biopsies were negative for a bowel inflammatory chronic disease. Glands were regular in shape, with a normal amount of cytoplasmic mucous and without crypt abscesses. By contrast, the number of inflammatory cells increased in the *Lamina propria*, mostly eosinophils. These aspects, together with the clinical symptoms and the nationality of the patient, suggested that a searching for a parasitic infestation should be made. We were able to detect two *Schistosoma* eggs in the colonic mucosa, both of them were surrounded by a granuloma's reaction (Figure 2). Therefore, a diagnosis of "intestinal schistosomiasis" was made and was confirmed by the detection of *S mansoni* eggs in the feces (Figure 3).

On this basis, after two weeks, mesalazine was changed to praziquantel (40 mg/kg, single dose). Three weeks later, a third colonoscopy documented a significant improvement (data not shown). Therefore, the therapy with praziquantel was continued at the same dosage, and further improvement of the colonoscopy pattern was documented one month later (Figure 1B). Nothing was found in the other laboratory or radiographic tests, except of a weak plasma eosinophilia.

DISCUSSION

Schistosomiasis is an infectious disease, which affects more than 200 million people worldwide. Since it is endemic in at least three continents, Africa, Asia, and South America, it represents the most important public health problem of the tropical and sub-tropical areas[1,2]. In particular, Ghana is one of the African countries where schistosomiasis is more prevalent in both the urinary and intestinal forms[23,24].

Since the transmission of schistosomiasis is linked to the intermediate snail hosts, in the endemic countries the disease is more prevalent in subjects whose skin is more susceptible to contacts with water in rivers, lakes, swamps or artificial irrigation systems. This may occur frequently

in water-related activities of boatmen, fishermen, and rice workers. The infection is also promoted by unsanitary disposal of urine and feces and can occur in animals, such as dogs and cows[3,4,25].

S mansoni, a main agent of the intestinal form, together with *S japonicum*, *S mekongi,* and *S intercalatum*, is a trematode which parasitizes in human beings and also in other primates. *Schistosoma* eggs, upon deposition in the feces, mature in suitable environmental conditions (such as fresh water), giving rise to its larval forms (miracidia). These swimming forms reach and infect snails, species of the genus *Biomphalaria* (intermediate hosts), and mature in cercarie[26,27]. The cercarie are the infective forms for human beings and come out from the snails under specific conditions of light and temperature and infect men through the skin. During penetration, the cercarie shake off their tails and change into the next stage of the life cycle, the schistosomula, that reach the lungs and the liver. In the intrahepatic portal system, the worms complete the sexual stages of their development. Then, the adult females deposit the eggs in the small veins around the large intestine. Some of the eggs may be trapped in the gut wall or break loose into it and are then eliminated by feces. The eggs trapped in the gut wall are responsible for the inflammatory and immunopathologic responses, leading to erythema, edema, granulomas, ulcerations, hemorrhages, and fibrosis[28,29]. Regarding the pathogenesis of the disease, recent studies have dramatically changed the acknowledgment in this field. The T helper (Th) CD4+/CD8- cells, derived from hepatic granulomas of infected mice, may produce cytokines such as interleukin-2, interleukin-4, interferon-γ, with a type Th0 immunomediate response. After a longer period of infection, the murine models could show a type Th2 response[30-33].

The symptoms of our patient included nausea, meteorism, abdominal pain, bloody diarrhea, rectal tenesmus, and hepatosplenomegaly, which are consistent with those already reported[5]. The case showed some difficulties in terms of differential diagnosis of a chronic inflammatory bowel disease, since anatomical pathologic reports, in relation to the immediate endoscopic evidence, were not available.

Previous studies stated that colonoscopic findings are suggestive of schistosomiasis in about 45.3% of patients, but *S mansoni* eggs in feces are detectable in only 11.1% of the patients with colonic biopsies positive for *S mansoni*[34,35]. Endoscopic findings may not be typical and it is often hard to distinguish *Schistosoma* infection from a chronic inflammatory bowel disease, since these two disorders may show similar patterns, as shown in our patient[19,20].

Moreover, cystoscopy or rectosigmoidal endoscopy may be useful. In our case, the first probable diagnosis of bowel schistosomiasis was made by the detection of two *Schistosoma* eggs in the colonic mucosa, surrounded by a granuloma's reaction. During the disease's acute phase, the histological examination may show the presence of eggs on the ulcerated lesions as well as polyps-like forms on the bowel mucosa[36,37]. However, these aspects may be macroscopically and microscopically evocative of other disorders, such as chronic inflammatory bowel disease and infective colitis[38,39]. Therefore, diagnosis of schistosomiasis can be made by urine and feces examination and isolation of the agent.

When the correct diagnosis is made, the complete recovery of the patient can be achieved using a specific anti-parasitic therapy with praziquantel[40,41]. The intimate relationship between human beings and infected water leads to schistosomiasis elevated prevalence. Elimination of the intermediate hosts and avoiding the contact with infected water sources are the measures to prevent schistosomiasis[42]. For the treatment, current drugs include praziquantel, metriphonate[43], and oxamniquine[44].

We reported in this paper a case of an unsuspicious schistosomiasis, initially treated with mesalazine, for its peculiar difficulties in terms of differential diagnosis from a chronic inflammatory bowel disease. We suggest that the detection of the *Schistosoma* eggs in feces should always anticipate the colonoscopy examination. Since the prevalence of schistosomiasis has been increasing in Europe and USA, due to international travelers and immigrants[16-18,45], schistosomiasis should be considered in the differential diagnosis of patients with gastrointestinal symptoms.

REFERENCES

1 **Sturrock RF**. Schistosomiasis epidemiology and control: how did we get here and where should we go? *Mem Inst Oswaldo Cruz* 2001; **96 Suppl:** 17-27

2 **Goodburn EA**, Ross DA. Young people's health in developing countries: a neglected problem and opportunity. *Health Policy Plan* 2000; **15:** 137-144

3 **Ripert C**. [Schistosomiasis: diagnosis and treatment] *Presse Med* 2000; **29:** 1583-1585

4 **Ranque S**, Dessein A. [Schistosoma mansoni schistosomiasis] *Rev Prat* 2001; **51:** 2099-2103

5 **Schafer TW**, Hale BR. Gastrointestinal complications of schistosomiasis. *Curr Gastroenterol Rep* 2001; **3:** 293-303

6 **Erko B**, Medhin G, Berhe N, Abebe F, Gebre-Michael T, Gundersen SG. Epidemiological studies on intestinal schistosomiasis in Wondo Genet, southern Ethiopia. *Ethiop Med J* 2002; **40:** 29-39

7 **Lansdown R**, Ledward A, Hall A, Issae W, Yona E, Matulu J, Mweta M, Kihamia C, Nyandindi U, Bundy D. Schistosomiasis, helminth infection and health education in Tanzania: achieving behaviour change in primary schools. *Health Educ Res* 2002; **17:** 425-433

8 **Keiser J**, N'Goran EK, Traore M, Lohourignon KL, Singer BH, Lengeler C, Tanner M, Utzinger J. Polyparasitism with Schistosoma mansoni, geohelminths, and intestinal protozoa in rural Cote d'Ivoire. *J Parasitol* 2002; **88:** 461-466

9 **Zhou X**, Acosta L, Willingham AL 3rd, Leonardo LR, Minggang C, Aligui G, Zheng F, Olveda R. Regional Network for Research, Surveillance and Control of Asian Schistosomiasis (RNAS). *Acta Trop* 2002; **82:** 305-311

10 **Leonardo LR**, Acosta LP, Olveda RM, Aligui GD. Difficulties and strategies in the control of schistosomiasis in the Philippines. *Acta Trop* 2002; **82:** 295-299

11 **Roca C**, Balanzo X, Gascon J, Fernandez-Roure JL, Vinuesa T, Valls ME, Sauca G, Corachan M. Comparative, clinico-epidemiologic study of Schistosoma mansoni infections in travellers and immigrants in Spain. *Eur J Clin Microbiol Infect Dis* 2002; **21:** 219-223

12 **Kager PA**, Schipper HG. [Acute schistosomiasis: fever and eosinophilia, with or without urticaria, after a trip to Africa] *Ned Tijdschr Geneeskd* 2001; **145:** 220-225 (Dutch)
13 **Whitty CJ**, Mabey DC, Armstrong M, Wright SG, Chiodini PL. Presentation and outcome of 1107 cases of schistosomiasis from Africa diagnosed in a non-endemic country. *Trans R Soc Trop Med Hyg* 2000; **94:** 531-534
14 **Whitty CJ**, Carroll B, Armstrong M, Dow C, Snashall D, Marshall T, Chiodini PL. Utility of history, examination and laboratory tests in screening those returning to Europe from the tropics for parasitic infection. *Trop Med Int Health* 2000; **5:** 818-823
15 **Lademann M**, Burchard GD, Reisinger EC. Schistosomiasis and travel medicine. *Eur J Med Res* 2000; **5:** 405-410
16 **Adair R**, Nwaneri O. Communicable disease in African immigrants in Minneapolis. *Arch Intern Med* 1999; **159:** 83-85
17 **Ganem JP**, Marroum MC. Schistosomiasis of the urinary bladder in an African immigrant to North Carolina. *South Med J* 1998; **91:** 580-583
18 **Raglio A**, Russo V, Swierczynski G, Sonzogni A, Goglio A, Garcia LS. Acute Schistosoma mansoni infection with progression to chronic lesion in Italian travelers returning from Cameroon, West Africa: a diagnostic and prevention problem. *J Travel Med* 2002; **9:** 100-102
19 **Waye JD**, Hunt RH. Colonoscopic diagnosis of inflammatory bowel disease. *Surg Clin North Am* 1982; **62:** 905-913
20 **Tedesco FJ**, Moore S. Infectious diseases mimicking inflammatory bowel disease. *Am Surg* 1982; **48:** 243-249
21 **Torres EA**, Acosta H, Cruz M, Weinstock J, Hillyer GV. Seroprevalence of Schistosoma mansoni in Puerto Ricans with inflammatory bowel disease. *P R Health Sci J* 2001; **20:** 211-214
22 **Eaden JA**, Pararajasingam R, MacKay H, Thomas WM, Mayberry JF. Chronic schistosomiasis: an incidental finding in new onset ulcerative colitis. *Eur J Gastroenterol Hepatol* 1999; **11:** 443-445
23 **Brooker S**, Marriot H, Hall A, Adjei S, Allan E, Maier C, Bundy DA, Drake LJ, Coombes MD, Azene G, Lansdown RG, Wen ST, Dzodozmenyo M, Cobbinah J, Obro N, Kihamia CM, Issae W, Mwanri L, Mweta MR, Mwaikemwa A, Salimu M, Ntimbwa P, Kiwelu VM, Turuka A, Nkungu DR, Magingo J. Community perception of school-based delivery of anthelmintics in Ghana and Tanzania. *Trop Med Int Health* 2001; **6:** 1075-1083
24 The cost of large-scale school health programmes which deliver anthelmintics to children in Ghana and Tanzania. The Partnership for Child Development. *Acta Trop* 1999; **73:** 183-204
25 **Boisier P**, Ramarokoto CE, Ravoniarimbinina P, Rabarijaona L, Ravaoalimalala VE. Geographic differences in hepatosplenic complications of schistosomiasis mansoni and explanatory factors of morbidity. *Trop Med Int Health* 2001; **6:** 699-706
26 **Morgan JA**, Dejong RJ, Snyder SD, Mkoji GM, Loker ES. Schistosoma mansoni and Biomphalaria: past history and future trends. *Parasitology* 2001; 1**23 Suppl:** S211- S228
27 **Mavarez J**, Amarista M, Pointier JP, Jarne P. Fine-scale population structure and dispersal in Biomphalaria glabrata, the intermediate snail host of Schistosoma mansoni, in Venezuela. *Mol Ecol* 2002; **11:** 879-889
28 **Silva LM**, Fernandes AL, Barbosa A Jr, Oliveira IR, Andrade ZA. Significance of schistosomal granuloma modulation. *Mem Inst Oswaldo Cruz* 2000; **95:** 353-361
29 **Abdel-Hadi AM**, Talaat M. Histological assessment of tissue repair after treatment of human schistosomiasis. *Acta Trop* 2000; **77:** 91-96
30 **Yoshida A**, Maruyama H, Yabu Y, Amano T, Kobayakawa T, Ohta N. Immune response against protozoal and nematodal infection in mice with underlying Schistosoma mansoni infection. *Parasitol Int* 1999; **48:** 73-79
31 **Park MK**, Hoffmann KF, Cheever AW, Amichay D, Wynn TA, Farber JM. Patterns of chemokine expression in models of Schistosoma mansoni inflammation and infection reveal relationships between type 1 and type 2 responses and chemokines in vivo. *Infect Immun* 2001; **69:** 6755-6768
32 **Fallon PG**, Smith P, Richardson EJ, Jones FJ, Faulkner HC, Van Snick J, Renauld JC, Grencis RK, Dunne DW. Expression of interleukin-9 leads to Th2 cytokine-dominated responses and fatal enteropathy in mice with chronic Schistosoma mansoni infections. *Infect Immun* 2000; **68:** 6005-6011
33 **Almeida CA**, Leite MF, Goes AM. Signal transduction events in human peripheral blood mononuclear cells stimulated by Schistosoma mansoni antigens. *Hum Immunol* 2001; **62:** 1159-1166
34 **Yasawy MI**, El Shiekh Mohamed AR, Al Karawi MA. Comparison between stool examination, serology and large bowel biopsy in diagnosing Schistosoma mansoni. *Trop Doct* 1989; **19:** 132-134
35 **Mohamed AR**, al Karawi M, Yasawy MI. Schistosomal colonic disease. *Gut* 1990; **31:** 439-442
36 **Ricosse JH**, Emeric R, Courbil LJ. Anatomopathological aspects of schistosomiasis. A study of 286 pathological specimens. *Med Trop (Mars)* 1980; **40:** 77-94
37 **Geboes K**, el-Deeb G, el-Haddad S, Amer G, el-Zayadi AR. Vascular alterations of the colonic mucosa in schistosomiasis and portal colopathy. *Hepatogastroenterology* 1995; **42:** 343-347
38 **Sanguino J**. Schistosomiasis of the colon and rectum. *Hepatogastroenterology* 1994; **41:** 506
39 **Sanguino J**, Peixe R, Guerra J, Rocha C, Quina M. Schistosomiasis and vascular alterations of the colonic mucosa. *Hepatogastroenterology* 1993; **40:** 184-187
40 **Sturrock RF**, Davis A. Efficacy of praziquantel against Schistosoma mansoni in northern Senegal. *Trans R Soc Trop Med Hyg* 2002; **96:** 105; author reply 105-106
41 **Filho SB**, Gargioni C, Silva Pinto PL, Chiodelli SG, Gurgel Vellosa SA, da Silva RM, da Silveira MA. Synthesis and evaluation of new oxamniquine derivatives. *Int J Pharm* 2002; **233:** 461-471
42 **Lambertucci JR**, Serufo JC, Gerspacher-Lara R, Rayes AA, Teixeira R, Nobre V, Antunes CM. Schistosoma mansoni: assessment of morbidity before and after control. *Acta Trop* 2000; **77:** 101-109
43 **Stephenson I**, Wiselka M. Drug treatment of tropical parasitic infections: recent achievements and developments. *Drugs* 2000; **60:** 985-995
44 **Filho SB**, Gargioni C, Silva Pinto PL, Chiodelli SG, Gurgel Vellosa SA, da Silva RM, de Silveira MA. Synthesis and evaluation of new oxamniquine derivatives. *Int J Pharm* 2002; **233:** 35-41
45 **Grobusch MP**, Muhlberger N, Jelinek T, Bisoffi Z, Corachan M, Harms G, Matteelli A, Fry G, Hatz C, Gjorup I, Schmid ML, Knobloch J, Puente S, Bronner U, Kapaun A, Clerinx J, Nielsen LN, Fleischer K, Beran J, da Cunha S, Schulze M, Myrvang B, Hellgren U. Imported schistosomiasis in Europe: sentinel surveillance data from TropNetEurop. *J Travel Med* 2003; **10:** 164-169

Science Editor Wang XL and Guo SY **Language Editor** Elsevier HK

PO Box 2345, Beijing 100023, China
www.wjgnet.com
wjg@wjgnet.com

ELSEVIER

World J Gastroenterol 2005;11(44):7048-7050
World Journal of Gastroenterology ISSN 1007-9327

• *CASE REPORT* •

Gastric cancer occurring in a patient with Plummer-Vinson syndrome: A case report

Ki-Han Kim, Min-Chan Kim, Ghap-Joong Jung

Ki-Han Kim, Min-Chan Kim, Ghap-Joong Jung, Department of Surgery, Dong-A University College of Medicine, Busan, South Korea
Correspondence to: Ghap-Joong Jung, Department of Surgery, Dong-A University College of Medicine, 3-1 Dongdaeshin-Dong, Seo-Gu, Busan 602-715, South Korea. gjjung@donga.ac.kr
Telephone: +82-51-2405147 Fax: +82-51-2479316
Received: 2005-05-01 Accepted: 2005-06-09

Abstract

Plummer-Vinson syndrome (sideropenic dysphagia) is characterized by dysphagia due to an upper esophageal or hypopharyngeal web in patients with chronic iron deficiency anemia. The main cause of dysphagia is the presence of the web in the cervical esophagus, and abnormal motility of the pharynx or esophagus is also found to play a significant role in this condition. This syndrome is thought to be precancerous because squamous cell carcinoma of hypopharynx, oral cavity or esophagus takes place in 10% of those patients suffering from this malady, but it is even more unusual that Plummer-Vinson syndrome should be accompanied by gastric cancer. We have reported here a case of a 43-year-old woman with Plummer-Vinson syndrome who developed stomach cancer and recovered after a radical total gastrectomy with D2 nodal dissection.

Key words: Plummer-Vinson syndrome; Gastric cancer; Esophageal web

Kim KH, Kim MC, Jung GJ. Gastric cancer occurring in a patient with Plummer-Vinson syndrome: A case report. *World J Gastroenterol* 2005; 11(44): 7048-7050
http://www.wjgnet.com/1007-9327/11/7048.asp

INTRODUCTION

Plummer-Vinson syndrome is characterized by dysphagia due to upper esophageal or hypopharyngeal web in patients with chronic iron deficiency anemia[1,2]. It is also combined with iron deficiency anemia, mucosal lesion of oral cavity or pharynx. This syndrome has been reported since 1893 in various literatures describing its specific symptoms. In 1926, Sir Arthur Hurst designated this symptom complex as Plummer-Vinson syndrome[1]. This syndrome is also referred to as Paterson-Kelly syndrome or sideropenic dysphagia. The main cause of dysphagia is the presence of a web in the cervical esophagus, and the abnormal motility of pharynx or esophagus is also found to play a significant role in the above causes[1,2]. It is well known that this syndrome is associated with an increased incidence of hypopharyngeal or cervical esophageal cancer. However, it is even more unusual that this syndrome is combined with gastric cancer[3]. So, we have reported a case of a 43-year-old woman who was initially diagnosed as Plummer-Vinson syndrome 2 years ago, and recently developed stomach cancer, which was managed successfully by surgery.

CASE REPORT

A 43-year-old woman was admitted to our hospital with symptoms of nausea, dysphagia and general weakness. She was diagnosed as Plummer-Vinson syndrome in April 2002, and has been managed conservatively on routine follow-ups. In August 2003, her nausea and dysphagia were aggravated. Her past history and family history were not specific. On admission, she complained about general weakness, mild abdominal pain and vomiting. The blood pressure was 0.247 kPa, pulse rate 90 bpm and body temperature 36.4 °C. The laboratory findings were consistent with microcystic, hypochronic iron deficiency anemia with 62 g/L hemoglobin, 22.2% hematocrit, 76.8 fL MCV, 21.5 pg MCH, 279 g/L MCHC, 325 000/μL platelet, 46 μg/dL serum iron, 271 μg/dL total iron binding capacity (TIBC), and 11.33 ng/mL serum ferritin. Urine analysis, serum liver function test (LFT), and serum electrolytes were unremarkable.

A gastrointestinal radiographic series indicated a linear filling defect (1.5 cm length) in the upper esophagus, which suggested an esophageal web (Figure 1). Contrast-enhanced abdominal CT scan showed diffuse irregular wall thickening with multiple calcifications at the body and antrum of the stomach. The CT scan also showed lymph node enlargement in the perigastric area and a mild enlargement of the spleen (Figure 2).

Esophagogastroduodenoscopic findings showed a web at 16 cm from the incisors. Upon endoscopic procedure for esophageal bougienage, we found a lesion at the cardia suspecting gastric cancer involving the upper body and the esophagogastric junction. Endoscopic biopsy proved to be a poorly differentiated adenocarcinoma. On surgical exploration, the serosa of the stomach was not invaded

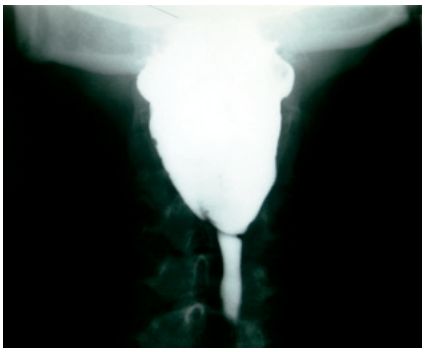

Figure 1 Esophagography showing a linear filling defect (1.5 cm length) at the upper esophagus, suggesting esophageal web.

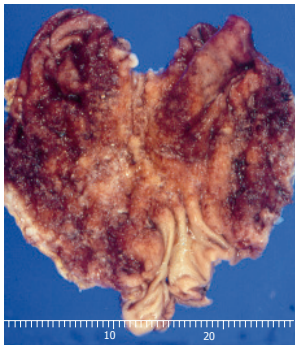

Figure 3 Macroscopic appearance of resected stomach showing a diffuse large Borrmann type 4 cancer in the whole body and cardia.

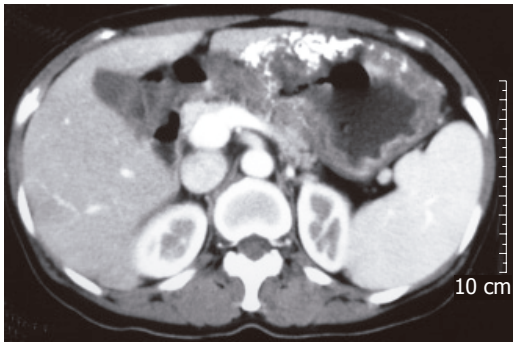

Figure 2 Contrast-enhanced abdominal CT scan showing diffuse irregular wall thickness with multiple calcifications at the body and antrum of the stomach.

macroscopically by cancer, but hilar lymph nodes of the spleen were grossly enlarged, suspecting tumor metastasis. The patient underwent a radical total gastrectomy with D2 nodal dissection. The spleen was taken out along with lymph node #10 and lymph node #11 d. No transfusion was required during and after the surgery. Excised surgical specimen demonstrated that the tumor size was 22 cm×18 cm, and both resection margins were tumor-free. The lesion was histologically confirmed as mucinous adenocarcinoma, Borrmann type IV, and it had infiltrated into the serosa with nodal metastasis of 33 out of 62 nodes. The TMN stage was T3N3M0 (Stage IV) (Figure 3). Iron supplemented soft diet was commenced on the 6th postoperative day. Peripheral blood findings improved within 2 wk after the surgery: 87 g/L hemoglobin, 28.5% hematocrit, 81.9 fL MCV, 25.0 pg MCH, 30.5 g/dL MCHC, and 1 186 000/μL platelets. The patient was discharged on the 19th postoperative day with no remarkable surgical complications except a mild nausea and surgical wound discomfort.

DISCUSSION

Plummer-Vinson syndrome, also known as Paterson-Kelly syndrome or sideropenic dysphagia[1], is characterized by dysphagia, iron deficiency anemia, and mucosal lesion of the oral cavity or pharynx. In 1893, Blackenstein reported a case with anemia, spasmodic stenosis of cervical esophagus and dysphagia[1]. The patient's symptoms were improved by endoscopic bougienage. In 1911, an another case with dysphagia due to upper esophageal web was reported, which was also alleviated by endoscopic bougienage. In 1912, Plummer[2] also reported cases with upper esophageal rigidity that the patients had iron deficiency anemia and splenomegaly. In 1922, Vinson named a series of patients with dysphagia, anemia, and splenomegaly as hysterical dysphagia[1]. In 1926, Sir Arthur Hurst designated similar cases of the syndrome as Plummer-Vinson syndrome[1].

The incidence of the Plummer-Vinson syndrome has recently decreased because of nutritional improvement, advanced health care, a decreased incidence of pregnancy and improved care programs for pregnant women. Moreover, this syndrome is now thought to be associated with the deficient intake of vitamins and iron[1,3,4]. Most patients are women aged over 40 years, and this group accounts for 75% in number[5,6]. The syndrome is usually asymptomatic, but the patients sometimes develop dysphagia, weight loss, and weakness. Other symptoms may include nail deformation of the hand and foot, cheilosis, atrophic glossitis, early loss of teeth, conjunctivitis, dermatitis seborrheica, hyperkeratosis, keratitis, blepharitis, visual disturbances and 30% of cases accompany splenomegaly[1]. The diagnosis of upper esophageal web is confirmed by radiologic methods or endoscopy. The radiologic method, however, is more suitable because endoscopy can sometimes miss the point of benign stricture, and does not verify most of the motility disorders[7]. On esophagography, the web is usually detected at the upper esophagus below the cricoid by showing a thin membrane across esophagus[8]. Pathologic finding of upper esophageal web shows hypertrophy or atrophy of squamous cells and it is sometimes combined with chronic inflammation[1].

Plummer-Vinson syndrome is known to be associated with an increased risk of upper alimentary tract cancers, and the incidence rate of upper esophageal cancer in this syndrome is 3-15%[6]. In Sweden, the incidence of upper alimentary tract cancer and hypopharyngeal cancer in Plummer-Vinson syndrome is decreasing along with that of the syndrome itself[3]. However, it is more unusual for

this syndrome to be accompanied by gastric cancer. Only two cases were reported in the literature, in which gastric cancer developed in the lower portion of the stomach[9,10]. In our case, the gastric cancer developed in the upper portion of the stomach involving esophagogastric junction.

It is not clear why Plummer-Vinson syndrome can exceptionally be associated with stomach cancer. However, it is widely accepted that atrophic mucosal change of alimentary tract due to iron deficiency anemia may lead to cancer development of the upper esophagus or hypopharynx. Therefore, careful examinations of hypopharynx, upper esophagus and stomach are of crucial importance for early detection of cancer development in this syndrome.

REFERENCES

1 **Lichtenstein GR**. Esophageal rings, webs, and diverticula. In: Haubrich WS, ed. Bockus gastroenterology. Volume 1.5th ed. *Philadelphia: WB Saunders Company*, 1994: 518-523

2 **Plummer HS**. Diffuse dilatation of the esophagus without anatomic stenosis (cardiospasm): Report of 91 cases. *JAMA* 1912; **58**: 2013-2015

3 **Larsson LG**, Sandstrom A, Westling P. Relationship of Plummer-Vinson disease to cancer of the upper alimentary tract in Sweden. *Cancer Res* 1975; **35**: 3308-3316

4 **Chen TS**, Chen PS. Rise and fall of the Plummer-Vinson syndrome. *J Gastroenterol Hepato*l 1994; **9:** 654-658

5 **Rosof BM**, Nagler RW. Plummer-Vinson syndrome. Revisited. *N Y State J Med* 1975; **75**: 414-415

6 **Chisholm M**. The association between webs, iron and post-cricoid carcinoma. *Postgrad Med J* 1974; **50**: 215-219

7 **Halpert RD**, Feczko PJ, Spickler EM, Ackerman LV. Radiological assessment of dysphagia with endoscopic correlation. *Radiology* 1985; **157**: 599-602

8 **SHAMMA'A MH**, BENEDICT EB. Esophageal webs; a report of 58 cases & an attempt at classification. *N Engl J Med* 1958; **259:** 378-384

9 **Nagai T**, Susami E, Ebihara T. Plummer-Vinson syndrome complicated by gastric cancer: a case report. *Keio J Med* 1990; **39**: 106-111

10 **Kitabayashi K**, Akiyama T, Tomita F, Saitoh H, Kosaka T, Kita I, Takashima S. Gastric cancer occurring in a patient with Plummer-Vinson syndrome: report of a case. *Surg Today* 1998; **28**: 1051-1055

Science Editor Kumar M and Guo SY **Language Editor** Elsevier HK

PO Box 2345, Beijing 100023, China
www.wjgnet.com
wjg@wjgnet.com

ELSEVIER

World J Gastroenterol 2005;11(44):7051-7053
World Journal of Gastroenterology ISSN 1007-9327

• *CASE REPORT* •

Very high alpha-fetoprotein in a young man due to concomitant presentation of hepatocellular carcinoma and Sertoli cell testis tumor

Ozdal Ersoy

Ozdal Ersoy, Sisili Etfal Education and Research Hospital, Kocamancur sok, Sisili
Correspondence to: Ozdal Ersoy, Sisili Etfal Education and Research Hospital, Kocamancur sok 16/6 80240, Sisili. ozdal@dr.com
Telephone: +90-2122413741
Received: 2004-12-16 Accepted: 2005-01-05

Abstract

Studies reported that there is a close relationship between hepatocellular carcinoma (HCC) and testis carcinoma. Both tumors can be presented as synchronal tumors, or as testicular metastases of HCC or as hepatic metastases of testicular tumor[7]. HCC is one of the most common malignancies worldwide and the incidence of HCC increases with age[8]. The relationship between hepatitis B incidence and HCC rates is also well recognized. Alpha fetoprotein (AFP) is produced by 70% of HCC. Though a level of AFP >400 ng/mL is diagnostic for HCC, in the presence of active hepatitis B infection, the cut-off level should be considered to be at least 1 000-4 000 ng/mL. Like HCC, germ cell tumors of the testis also release AFP; but it is shown that some of Sertoli cell tumors of testis can also release AFP[10]. Herein we have reported about the first case of HCC in the literature which is presented concomitantly with Sertoli-Leydig tumor of testis, leading to extremely high level of AFP in a 21-year-old man.

Key words: Hepatocellular carcinoma; Sertoli-Leydig cell tumor; AFP; Cirrhosis; Hypercholesterolemia

Ersoy O. Very high alpha-fetoprotein in a young man due to concomitant presentation of hepatocellular carcinoma and Sertoli cell testis tumor. *World J Gastroenterol* 2005; 11(44): 7051-7053
http://www.wjgnet.com/1007-9327/11/7051.asp

INTRODUCTION

Studies have reported that there is a close relationship between hepatocellular carcinoma (HCC) and testis carcinoma. Both tumors can be presented as synchronal tumors[1,2], or as testicular metastases of HCC[3-5] or as hepatic metastases of testicular tumor[6,7].

HCC is one of the most common malignancies worldwide and the incidence of HCC increases with age[8]. Alpha fetoprotein (AFP) is produced by 70% of HCC. Like HCC, germ cell tumors of the testis also release AFP[9]; but it is shown that some of Sertoli cell tumors of testis can also release AFP[10]. Herein we have reported the first case of HCC in the literature which is presented concomitantly with Sertoli-Leydig tumor of testis, leading to extremely high level of AFP in a 21-year-old man.

CASE REPORT

A 21-year-old man was admitted to our clinic in May 2002, with complaints of fatigue, nausea, vomiting, abdominal distention and weight loss. The patient was well before two months. His mother died of cirrhosis due to hepatitis B. His two sisters were HBsAg seropositive. On physical examination minimal ascites was detected and the abdomen was tender on palpation. The liver was palpated under the rib margin as 10 cm and was also tender. The spleen was palpated as 6 cm. Other systems were normal on examination. On admission, laboratory tests performed reported ALT: 64 IU/L (0-41), AST: 44 IU/L (0-37), fasting plasma glucose: 94 mg/dL, urea: 21 mg/dL, serum creatinine: 0.65 mg/dL, LDH: 500 IU/mL (240-480), GGT: 161 U/L (0-49), ALP: 372 U/L, T prot: 67 g/L, alb: 36 g/L, glob: 31 g/L, D bil: 0.76 mg/dL, I bil: 1.09 mg/dL, total cholesterol: 463 mg/dL, triglyceride: 130 mg/dL, LDL: 413 mg/dL, HDL: 24 mg/dL, VLDL: 38.2 mg/dL, Na: 138 mmol/L, K: 3.9 mmol/L, Ca: 9.4 mmol/L, Fe: 43 μg/dL, total iron binding capacity: 396 μg/dL, hemoglobin:11.5 g/dL, hematocrit: 34.8%, white blood cell: 2 700, platelet: 215 000, MCV: 83 fL, erythrocyte sedimentation rate: 12 mm/h. Markers of viral hepatitis were HBsAg (+), antiHBs (-), antiHCV -), HbeAg (-), antiHBe (-).

On ultrasonographic examination, the liver was heterogenous and there were multiple hypodense lesions in the right and left liver lobes. Thromboses were seen in both hepatic and portal veins in Doppler ultrasound. The AFP level was 5 181 000/mL (0-10) and beta-HCG was 0.5 mIU/mL (normal range: 5-10 mIU/mL). Computerized abdominal tomography showed that the craniocaudal sizes of the liver and spleen were 25 and 22 cm respectively. The liver margin was irregular, the right and

left lobes of the liver contained multiple hypodense lesions resembling metastasis or primary HCC. A liver biopsy was done to identify the hypodense lesions of the liver. Diffuse fibrosis and HCC were reported from the histopathological examination. Hepatocytes were positive for keratin and AFP, but negative for vimentin. Because of the young age of the patient, the presence of multiple hepatic hypodense lesions resembling metastasis and the extremely high AFP level, an examination of the testis was also done to exclude a testicular tumor. Physical examination of the testis revealed a painless mass on the left testis. Ultrasound sonography showed a hypoechoic lesion (19 mm× 18 mm×17 mm in size) in the left testis. High inguinal orchiectomy was performed. The tumor within the testis was histopathologically diagnosed as Sertoli cell testis tumor. Leydig cells were negative for keratin but positive for vimentin. Finally, the patient who had primary HCC and primary Sertoli cell tumor of the testis (two primary tumors concomitantly presented) was referred to the oncology clinic for further evaluation and therapy.

DISCUSSION

HCC is one of the commonest malignant diseases in the world and the majority of cases of HCC arise in individuals with chronic hepatitis B or C virus infections[11]. All ages can be affected by HCC. The mean age at diagnosis is 53 years in Asia and 62 years in the United States. Recently, an analysis of 76 HCC cases investigated by Butt *et al*.[8] showed that the mean age is 52.2±11.3 years and the mean AFP level is 142±155 ng/mL. In contrary, our patient was very young and the AFP level was very high. Transmission of hepatitis B virus from his mother at the very early time of his life might be the cause of HCC development at the very young age.

AFP continues to be the best marker for early diagnosis of HCC. In adults the value of AFP up to 20 ng/mL is considered to be normal. Patients with hepatitis B virus-related cirrhosis having AFP level greater than 100 ng/mL are in the very high risk group for HCC. The AFP level usually correlates with tumor size[12]. Thus, the very high level of AFP in our patient may be due to the large tumor size, which was multifocal in both lobes of the liver.

Extremely high AFP levels are found in endodermal sinus tumors (yolk sac tumors) also[13]. Such neoplasms occur in testis, ovary and extragonadal sites. Typically they occur in young subjects. Hence we also examined the testis in our patient and performed orchiectomy after we palpated a testicular mass. The histopathological result was a Sertoli cell tumor of the testis, which was a testicular gonadal stromal tumor. Sertoli cell tumor (SCT) is very rare among testis tumors accounting for lower than 1% of primary testicular neoplasms. It is subclassified into three groups: classic, large cell calcifying (LCCSCT), and sclerosing. Most SCTs are benign, metastases are the only reliable indicator of malignancy, occurring in lower than 10% of cases. The most common sites for metastatic spread are retroperitoneal lymph nodes, lungs, liver, and bone. LCCSCT and sclerosing SCT have minimal metastatic potential[14].

The risk for liver cancer is very high in cirrhotic liver. There is also evidence that the risk for extrahepatic cancers increases in patients with cirrhosis. The reason of the increased extrahepatic malignancy risk in cirrhosis is not clear but may be due to many abnormal and metabolic alterations in cirrhosis like hyperestrogenism, alterations in metabolism of lipid and water-soluble drugs and other chemicals, alterations in immune functions and risk of infections in cirrhosis[15]. In this cohort study, Sorensen *et al*.[15] also reported that the occurrence of liver cancer, tobacco- and alcohol-related cancers, testicular cancer, stomach and colon cancer is significantly higher in cirrhosis than expected. This study may explain two primary cancers in our young patient which were thought to be cirrhotic due to chronic hepatitis B infection.

Though our case was in a state of decompensated liver failure, he had hypercholesterolemia which was parallel to the change in serum AFP. Hwang *et al*.[16] also observed that HCC patients with hypercholesterolemia have significantly higher mean serum levels of albumin, triglyceride, and AFP compared with age-sex-tumor volume-matched HCC patients without hypercholesterolemia. It was reported that 11% of HCC patients have hypercholesterolemia, which can be explained by the possible result from the absence of dietary cholesterol suppression feedback regulation in the damaged liver[17].

In conclusion, this case is an example showing the increased risk of hepatic and extrahepatic tumors in cirrhosis. In the presence of HCC in a cirrhotic patient, there might be multiple primary cancers. The possibility of second primary malignancy in a patient with HCC should be kept in mind especially when a very high level of AFP is encountered and this second primary malignancy may be a kind of a very rare tumor. However, the co-existence of HCC and testis tumor is very rare. As far as we know, this is the first case report showing the co-existence of HCC and SCT in a young boy presented with an extremely high level of AFP.

REFERENCES

1 **Hiraki Y**, Nakajo M, Uchiyama N. [A case of multiple primary cancers, hepatoma and seminoma, detected by 67Ga citrate and 99mTc-HIDA scintigraphy] *Kaku Igaku* 1991; **28:** 1497-1502
2 **Yamauchi M**, Yoshigoe F, Mera F, Ogura K, Kameda H, Nakada J, Takasaka S, Machida T, Fukunaga M. An autopsy case of double cancer (Hepatocellular carcinoma and mixed germ cell tumor of the testis)--significance of alpha-fetoprotein and human chorionic gonadotropin as tumor markers. *Gan No Rinsho* 1983; **29:** A-22, 349-352
3 **Young RH**, Van Patter HT, Scully RE. Hepatocellular carcinoma metastatic to the testis. *Am J Clin Pathol* 1987; **87:** 117-120
4 **Fukuda T**, Ohnishi Y, Miyazaki Y, Ohnuki K, Tachikawa S. Clear cell hepatocellular carcinoma with abundant myxoid stroma. *Acta Pathol Jpn 1992*; **42:** 897-903
5 **Horie Y**, Kato M. Hepatoid variant of yolk sac tumor of the testis. *Pathol Int* 2000; **50:** 754-758
6 **de Boer HD**, Haerkens MH, van der Stappen W, van Ingen G, Wobbes T. Testicular carcinoma: postmortem diagnosis after a car accident. *Lancet* 2002; **359:** 1666

7 **Minowada S,** Okano Y, Miyazaki J, Homma Y, Kitamura T. Multidisciplinary treatment of advanced testicular tumor with bulky liver metastasis. *Urol Int* 2001; **67:** 178-180
8 **Butt AK,** Khan AA, Alam A, Ahmad S, Shah SW, Shafqat F, Naqvi AB. Hepatocellular carcinoma: analysis of 76 cases. *J Pak Med Assoc* 1998; **48:** 197-201
9 **Ganz M**, Joller-Jemelka HI, Grob PJ. [Severely increased alpha fetoprotein and associated diseases] *Schweiz Med Wochenschr* 1979; **109:** 1314-1322
10 **Taniyama K**, Suzuki H, Hara T, Yokoyama S, Tahara E. [An alpha-fetoprotein producing Sertoli-Leydig cell tumor--a case report] *Gan No Rinsho* 1989; **35:** 107-113
11 **Izzo F**, Cremona F, Delrio P, Leonardi E, Castello G, Pignata S, Daniele B, Curley SA. Soluble interleukin-2 receptor levels in hepatocellular cancer: a more sensitive marker than alfa fetoprotein. *Ann Surg Oncol* 1999; **6:** 178-185
12 **Sherlock S,** Dooley J.Hepatic tumours. Diseases of the liver and biliary system, 10th ed. *Massachusetts* 1997; 531-559
13 **Talerman A**, Haije WG, Baggerman L. Serum alphafetoprotein (AFP) in patients with germ cell tumors of the gonads and extragonadal sites: correlation between endodermal sinus (yolk sac) tumor and raised serum AFP. *Cancer* 1980; **46:** 380-385
14 **Rosl GJ**, Bajorin DF, Sheinfeld J, Motzer RJ, and Chaganti RSK. Cancer of the testis. In: DeVita VT, Hellman S and Rosenberg SA, eds. Cancer, 6th ed. Philadelphia: Lippincott Williams & Wilkins, 2001: 1491-1518
15 **Sorensen HT**, Friis S, Olsen JH, Thulstrup AM, Mellemkjaer L, Linet M, Trichopoulos D, Vilstrup H, Olsen J. Risk of liver and other types of cancer in patients with cirrhosis: a nationwide cohort study in Denmark. *Hepatology* 1998; **28:** 921-925
16 **Hwang SJ**, Lee SD, Chang CF, Wu JC, Tsay SH, Lui WY, Chiang JH, Lo KJ. Hypercholesterolaemia in patients with hepatocellular carcinoma. *J Gastroenterol Hepatol* 1992; **7:** 491-496
17 **Goldberg RB**, Bersohn I, Kew MC. Hypercholesterolaemia in primary cancer of the liver. *S Afr Med J* 1975; **49:** 1464-1466

Science Editor Wang XL and Guo SY **Language Editor** Elsevier HK

PO Box 2345, Beijing 100023, China
www.wjgnet.com
wjg@wjgnet.com

ELSEVIER

World J Gastroenterol 2005;11(44):7054-7056
World Journal of Gastroenterology ISSN 1007-9327

Immunosurveillance function of human mast cell?

Öner Özdemir

Öner Özdemir, Department of Pediatrics, Division of Allergy/Immunology, Louisiana State University Health Sciences Center, New Orleans, LA, United States
Correspondence to: Öner Özdemir, MD, Department of Pediatrics, Division of Allergy/Immunology, LSUHSC, New Orleans, LA, United States. ozdemir_oner@hotmail.com
Telephone: +1- 5045682578 Fax: +1- 504 5687598
Received: 2005-05-24 Accepted: 2005-07-08

Abstract

Mast cell (MC) is so widely recognized as a critical effector in allergic disorders that it can be difficult to think of MC in any other context. Indeed, MCs are multifunctional and recently shown that MCs can also act as antigen presenters as well as effector elements of human immune system. First observations of their possible role as anti-tumor cells in peri- or intra-tumoral tissue were mentioned five decades ago and a high content of MCs is considered as a favorable prognosis, consistent with this study. Believers of this hypothesis assumed them to be inhibitors of tumor development through their pro-apoptotic and -necrolytic granules e.g., granzymes and TNF-α. However, some still postulate them to be enhancers of tumor development through their effects on angiogenesis due to mostly tryptase. There are also some data suggesting increased MC density causes tumor development and indicates bad prognosis. Furthermore, since MC-associated mediators have shown to influence various aspects of tumor biology, the net effect of MCs on the development/progression of tumors has been difficult to evaluate. For instance, chymase induces apoptosis in targets; yet, tryptase, another MC protease, is a well-known mitogen. MCs with these various enzyme expression patterns may mediate different functions and the predominant MC type in tissues may be determined by the environmental needs. The coexistence of tryptase-expressing MCs (MC_T) and chymase and tryptase-expressing MCs (MC_{TC}) in physiological conditions reflects a naturally occurring balance that contributes to tissue homeostasis. We have recently discussed the role and relevance of MC serine proteases in different bone marrow diseases.

Key words: Mast cell; Immunosurveillance; Tryptase-chymase; Cytotoxicity; Tumors

Özdemir Ö. Immunosurveillance function of human mast cell? *World J Gastroenterol* 2005; 11(44): 7054-7056
http://www.wjgnet.com/1007-9327/11/7054.asp

LETTER TO THE EDITOR

I read the article by Tan *et al*.[1] describing `prognostic significance of cell infiltrations of immunosurveillance in colorectal cancer with great interest. My interest in this study is that we have recently demonstrated human mast cell (MC) mediated cytotoxicity against different human leukemia and lymphoma tumor cells *in vitro*[2-4]. Our *in vitro* results seem to support their study conclusion of MC cytotoxicity against tumor cells that might contribute to immunosurveillance *in vivo*. The genuine role of MC in tumor stroma has been a very controversial topic for the past five decades and needs still further clarification. Here, I have discussed further primarily the anti-tumor effects of MC in the light of recent literature and our findings.

MC is so widely recognized as a critical effector in allergic disorders that it can be difficult to think of MC in any other context. Indeed, MCs are multifunctional and recently shown that MCs can also act as antigen presenters as well as effector elements of human immune system. First observations of their possible role as anti-tumor cells in peri- or intra-tumoral tissue were mentioned five decades ago and a high content of MCs is considered as a favorable prognosis, consistent with this study[1,5,6]. Believers of this hypothesis assumed them to be inhibitors of tumor development through their pro-apoptotic and -necrolytic granules e.g. granzymes and TNF-α. However, some still postulate them to be enhancers of tumor development through their effects on angiogenesis due to mostly tryptase. There are also some data suggesting that increased MC density causes tumor development and indicates bad prognosis[7,8]. MCs with these various enzyme expression patterns may mediate different functions and the predominant MC type in tissues may be determined by the environmental needs. Furthermore, since MC-associated mediators have shown to influence various aspects of tumor biology, the net effect of MCs on the development/progression of tumors has been difficult to evaluate. For instance, chymase induces apoptosis in targets; yet, tryptase, another MC protease, is a well-known mitogen. We have recently discussed the role and relevance of MC serine proteases in different bone marrow diseases[9]. The coexistence of tryptase-expressing MCs (MC_T) and chymase and tryptase-expressing MCs (MC_{TC}) in physiological conditions reflects a naturally occurring balance that contributes to tissue homeostasis.

In the past two decades, it was believed that murine MC has natural cytotoxicity in the long term (>24 h) against murine tumor cells (WEHI-164, L929, etc.) by different mechanisms e.g. TNF-α dependent and non-TNF-α dependent[10]. Recent studies suggested that MC

can kill targets through degranulation of serine proteases, cathepsin G, leukotrienes and NO. Lately, MCs have been shown to contain granzyme B[11] and express Fas ligand[12], which are the most important components of cell mediated cytotoxicity. Chymase was also demonstrated to induce apoptosis in neonatal rat cardiomyocytes and human vascular smooth muscle cells[13]. Thus, MC mediated cytotoxicity seems to be operated by at least 2 pathways: by secretory pathways via exocytosis of granules containing serine proteases such as granzymes, chymase and soluble TNF-α; and nonsecretory (cell-to-cell contact) pathways via membranous TNF-α and FasL. We are the first to show human MC cytotoxicity against NK-sensitive/resistant human leukemia/lymphoma cells in short and long term by our established flow cytometric method[2-4]. Our studies suggested that increased chymase content of MCs in long-term culture could have played a role to mediate cytotoxicity.

Tan *et al.* demonstrated in this study that both MCT and MCTC may equally proliferate or infiltrate in colorectal cancer similar to hepatocellular carcinoma and intrahepatic cholangiocarcinoma, consistent with some earlier literature[14]. In contrast to these reports, in some malignant lesions, MCT`s were found to be concentrated at the tumor edge, i.e., the "invasion zone," whereas MCTCs were not increased in this area[15-17]. For instance, a significant increase of MCT phenotype was observed in the invasive carcinoma of the cervix throughout the different stages of malignant transformation. Furthermore, an abundant MCT (but not MCTC) increase was detected infiltrating the tumors in sections of invasive carcinoma although the number of MCT was shown to be similar to that of MCTC in benign lesions. Malignant tumors had 2 to 3 times more MCT than MCTC and the number of MCT was noted to be significantly higher in malignant than benign lesions.

Our studies and past literature review suggest that increase of MC density in tumor stroma is as important as the phenotypic change[18,19] causing predominance of one phenotype. Consistent with this study, if chymase containing MCs (MCTC/MCC) were dominant over MCT in tumor stroma, this would usually be predictor of good prognosis such as in localized bronchioloalveolar carcinoma[20] and human renal tumors[21]. In contrast to this opinion, there are a few data suggesting that MCTC/MCC are related to a bad prognosis e.g. lip and some gastrointestinal cancers[22,23]. Nevertheless, overall chymase content of granules in MCs as well as timing of biopsy and other factors could be also important in these exceptional cases. If MCT`s were dominant over MCCT/MCC, this would be a bad prognostic factor such as in cervix cancer, B-cell non-Hodgkin's lymphoma and others[24,25]. Mounting evidence certainly indicates that MCs accumulate around the tumors and could either promote or inhibit tumor growth depending on the local stromal conditions[26]. These findings overall emphasize the role of MCT type in the tumor development rather than chymase containing MCs (MCC and/or MCCT) but this requires further studies and clarification. My personal conclusion is that inhibitory or proliferative effects of MCs depend on multiple interactions among MC, tumor type and the environment.

REFERENCES

1 **Tan SY**, Fan Y, Luo HS, Shen ZX, Guo Y, Zhao LJ. Prognostic significance of cell infiltrations of immunosurveillance in colorectal cancer. *World J Gastroenterol* 2005; **11**: 1210-1214
2 **Özdemir Ö**, Ravindranath Y, Savasan S. Evaluation of long-term liquid culture grown human bone marrow mast cell cytotoxicity against human leukemia cells. *Blood* 2002; **100**, 45b, abstract # 3642
3 **Özdemir Ö**, Moore C, Ravindranath Y, Savasan S. Can Mast Cells Mediate Natural Cytotoxicity in Short Term Culture? *Ann Allergy Asthma Immunol* 2004; **94**: 185, abstract # 216
4 **Özdemir Ö**, Ravindranath Y, Savasan S. Short Term Mast Cell Natural Cell-Mediated Cytotoxicity. *Ann Allergy Asthma Immunol* 2004; **94**: 186-187, abstract # 220
5 **Aaltomaa S**, Lipponen P, Papinaho S, Kosma VM. Mast cells in breast cancer. *Anticancer Res* 1993; **13**: 785-788
6 **Ueda T**, Aozasa K, Tsujimoto M, Yoshikawa H, Kato T, Ono K, Matsumoto K. Prognostic significance of mast cells in soft tissue sarcoma. *Cancer* 1988; **62**: 2416-2419
7 **Grimbaldeston MA**, Skov L, Baadsgaard O, Skov BG, Marshman G, Finlay-Jones JJ, Hart PH. Communications: high dermal mast cell prevalence is a predisposing factor for basal cell carcinoma in humans. *J Invest Dermatol* 2000; **115:** 317–320
8 **Roche WR**. The nature and significance of tumour-associated mast cells. *J Pathol* 1986; **148**: 175-182
9 **Özdemir Ö**, Savaşan S. The role of mast cells in bone marrow diseases. *J Clin Path* 2004; **57**: 108-109
10 **Ghiara P**, Boraschi D, Villa L, Scapigliati G, Taddei C, Tagliabue A. In vitro generated mast cells express natural cytotoxicity against tumour cells. *Immunology* 1985; **55**: 317-324
11 **Kataoka TR**, Morii E, Oboki K, Kitamura Y. Strain-dependent inhibitory effect of mutant mi-MITF on cytotoxic activities of cultured mast cells and natural killer cells of mice. *Lab Invest* 2004; **84:** 376-384
12 **Wagelie-Steffen AL**, Hartmann K, Vliagoftis H, Metcalfe DD. Fas ligand (FasL, CD95L, APO-1L) expression in murine mast cells. *Immunology* 1998; **94:** 569-574
13 **Leskinen MJ**, Lindstedt KA, Wang Y, Kovanen PT. Mast cell chymase induces smooth muscle cell apoptosis by a mechanism involving fibronectin degradation and disruption of focal adhesions. *Arterioscler Thromb Vasc Biol* 2003; **23**: 238-243
14 **Terada T**, Matsunaga Y. Increased mast cells in hepatocellular carcinoma and intrahepatic cholangiocarcinoma. *J Hepatol* 2000; **33**: 961-966
15 **Kankkunen JP**, Harvima IT, Naukkarinen A. Quantitative analysis of tryptase and chymase containing mast cells in benign and malignant breast lesions. *Int J Cancer* 1997; **72**: 385-388
16 **Cabanillas-Saez A**, Schalper JA, Nicovani SM, Rudolph MI. Characterization of mast cells according to their content of tryptase and chymase in normal and neoplastic human uterine cervix. *Int J Gynecol Cancer* 2002; **12:** 92-98
17 **Benitez-Bribiesca L**, Wong A, Utrera D, Castellanos E. The role of mast cell tryptase in neoangiogenesis of premalignant and malignant lesions of the uterine cervix. *J Histochem Cytochem* 2001; **49:** 1061-1062
18 **de Rey BM**, Palmieri MA, Duran HA. Mast cell phenotypic changes in skin of mice during benzoyl peroxide-induced tumor promotion. *Tumour Biol* 1994; **15**: 166-174
19 **Yang M**, Zhang X, He A. [Mast cells in the labial cancer: histochemical and electron microscopical study] *Zhonghua Kouqiang Yixue Zazhi* 1997; **32:** 13-15
20 **Nagata M**, Shijubo N, Walls AF, Ichimiya S, Abe S, Sato N. Chymase-positive mast cells in small sized adenocarcinoma of

the lung. *Virchows Arch* 2003; **443**: 565-573

21 **Beil WJ**, Fureder W, Wiener H, Grossschmidt K, Maier U, Schedle A, Bankl HC, Lechner K, Valent P. Phenotypic and functional characterization of mast cells derived from renal tumor tissues. *Exp Hematol* 1998; **26**: 158-169

22 **Gulubova MV**. Structural examination of tryptase- and chymase-positive mast cells in livers, containing metastases from gastrointestinal cancers. *Clin Exp Metastasis* 2003; **20**: 611-620

23 **Rojas IG**, Spencer ML, Martinez A, Maurelia MA, Rudolph MI. Characterization of mast cell subpopulations in lip cancer. *J Oral Pathol Med* 2005; **34**: 268-273

24 **Welle M**. Development, significance, and heterogeneity of mast cells with particular regard to the mast cell-specific proteases chymase and tryptase. *J Leukoc Biol* 1997; **61:** 233–245

25 **Ribatti D**, Vacca A, Marzullo A, Nico B, Ria R, Roncali L, Dammacco F. Angiogenesis and mast cell density with tryptase activity increase simultaneously with pathological progression in B-cell non-Hodgkin's lymphomas. *Int J Cancer* 2000; **85**: 171–175

26 **Theoharides TC**, Conti P. Mast cells: the Jekyll and Hyde of tumor growth. *Trends Immunol* 2004; **25**: 235-241

Science Editor and Guo SY **Language Editor** Elsevier HK

PO Box 2345, Beijing 100023, China
www.wjgnet.com
wjg@wjgnet.com

ELSEVIER

World J Gastroenterol 2005;11(44):7057
World Journal of Gastroenterology ISSN 1007-9327

Hormone receptor status of primary tumor as a prognostic factor in patients with liver metastases from breast cancer treated with transcatheter arterial chemoembolization

Kadri Altundag, Ozden Altundag, Serdal Aktolga, Ozlem Yavas, Cem Boruban

Kadri Altundag, Department of Medical Oncology, Hacettepe University Faculty of Medicine, Ankara, Turkey
Ozden Altundag, 8181 Fannin Street No. 728 Houston, Texas, United States
Serdal Aktolga, Department of Internal Medicine, Marmara University School of Medicine, Istanbul, Turkey
Ozlem Yavas, Cem Boruban, Department of Medical Oncology, Selcuk University Faculty of Medicine, Konya, Turkey
Correspondence to: Kadri Altundag, 8181 Fannin Street No. 728, Houston, Texas 77054,
United States. altundag@sbcglobal.net
Telephone: +1-713-563-0909 Fax: +1-713-794-4385
Received: 2005-06-27 Accepted: 2005-07-20

TO THE EDITOR

We read with great interest the article by XP *et al*.[1] They reported the results of their experience with transcatheter arterial chemoembolization (TACE) and systemic chemotherapy for forty-five patients with liver metastases from breast cancer and evaluate the prognostic factors. In their study, the response and survival rates were significantly better in TACE group than in chemotherapy group. The lymph node status of the primary cancer, the clinical stage of liver metastases, the Child-Pugh grade, loss of weight were found to be significantly associated with survival in both univariate and multivariate and analyses. However, they did not mention hormone receptor status of the patients that might have an effect on the survival rate. Elias *et al*.[2] in their study evaluated 54 breast cancer patients with liver metastases as the sole site of metastatic disease (except for bone metastases in 3 patients) that underwent hepatectomy. They showed that the only factor influencing survival in both the univariate and multivariate analyses was the hormone receptor status ($P = 0.03$), and the relative risk of death increased by 3.5-fold when hormone receptor was negative. Moreover, Mack *et al* [3] reported excellent local tumor control and survival rates achieved by laser induced interstitial thermotherapy (LITT) in breast cancer patients with liver metastases. Regarding the prognostic and predictive factors related to primary tumor, they found no statistically significant difference in terms of mean survival between the patients with N0-N1 lymph nodes and N2-N3 lymph nodes. However, they found that the hormone receptor status is a significant ($P<0.05$) prognostic factor on both mean and median survival. The mean survival in patients with positive hormone receptor status was 5.5 years (95%CI: 4.8-6.3 years, median survival 4.7 years) starting the calculation at the date of diagnosis of the metastases treated with LITT. The mean survival in patients with negative hormone receptor status was 3.7 years (95%CI: 2.8-4.6 years, median survival 5.1 years)[4].

In the light of the above information, hormone receptor status of primary tumor should also be evaluated as a prognostic factor in patients with breast cancer and liver metastases treated with TACE and systemic chemotherapy.

REFERENCES

1 **Li XP**, Meng ZQ, Guo WJ, Li J. Treatment for liver metastases from breast cancer: results and prognostic factors. *World J Gastroenterol* 2005; **11**: 3782-3787
2 **Elias D**, Maisonnette F, Druet-Cabanac M, Ouellet JF, Guinebretiere JM, Spielmann M, Delaloge S. An attempt to clarify indications for hepatectomy for liver metastases from breast cancer. *Am J Surg* 2003; **185**: 158-164
3 **Mack MG**, Straub R, Eichler K, Sollner O, Lehnert T, Vogl TJ. Breast cancer metastases in liver: laser-induced interstitial thermotherapy--local tumor control rate and survival data. *Radiology* 2004; **233:** 400-409
4 **Altundag K**, Altundag O, Morandi P, Gunduz M. Hormone receptor status in patients with breast cancer and liver metastases treated with laser-induced intersititial thermotherapy. *Radiology* 2005; **235:** 339; author reply 339-340

Science Editor Guo SY **Language Editor** Elsevier HK

PO Box 2345, Beijing 100023, China
www.wjgnet.com
wjg@wjgnet.com

ELSEVIER

World J Gastroenterol 2005;11(44):7058
World Journal of Gastroenterology ISSN 1007-9327

Acknowledgments to Reviewers of World Journal of *Gastroenterology*

Many reviewers have contributed their expertise and time to the peer review, a critical process to ensure the quality of *World Journal of Gastroenterology*. The editors and authors of the articles submitted to the journal are grateful to the following reviewers for evaluating the articles (including those were published and those were rejected in this issue) during the last editing period of time.

Luigi Bonavina, Professor
Department of Surgery, Policlinico San Donato, University of Milano, via Morandi 30, Milano 20097, Italy

Yusuf Bayraktar, Professor
Department of Gastroenterology, School of Medicine, Hacettepe University, Ankara 06100, Turkey

David L Carr-Locke, M.D.
Director of Endoscopy, Brigham and Women's Hospital, Endoscopy Center, Brigham and Women's Hospital, 75 Francis St, Boston MA, 02115, United States

Da-Jun Deng, Professor
Department of Cancer Etiology, Peking University School of Oncology, 1 Da-Hong-Luo-Chang Street, Western District, Beijing 100034, China

Fabio Farinati, M.D.
Surgical And Gastroenterological Sciences, University of Padua, Via Giustiniani 2, Padua 35128, Italy

Burkhard Göke, Professor
Internal Medicine II, University of Munich, Marchioninistr. 15, Munich 81377, Germany

Edoardo G Giannini, Assistant Professor
Department of Internal Medicine, Gastroenterology Unit, Viale Benedetto XV, no. 6, Genoa, 16132, Italy

Fu-Lian Hu, Professor
Department of Gastroenterology, Peking University First Hospital, 8 Xishiku St, Xicheng District, Beijing 100034, China

Hiroyuki Hanai, Director
Director of Department of Endoscopic and Photodynamic Medicine,Hamamatsu University School of Medicine, 1-20-3 Izumi, Hamamatsu 433-8124, Japan

Robin G Lorenz, Associate Professor
Department of Pathology, University of Alabama at Birmingham, 845 19th Street South BBRB 730, Birmingham, AL 35294-2170, United States

Shou-Dong Lee, Professor
epartment of Medicine, Taipei Veterans General Hospital, 201 Shih-Pai Road, Sec. 2. Taipei 112, Taiwan, China

Hisataka S Moriwaki, Professor
Department Of Medicine, Gifu University, 1-1 Yanagido, Gifu 501-1194, Japan

Hisato Nakajima, M.D.
Department of Gastroenterology and Hepatology, The Jikei University School of Medicine, 3-25-8, Nishi-Shinbashi, Minato-ku, Tokyo 105-8461, Japan

James Neuberger, Professor
Liver Unit, Queen Elizabeth Hospital, Birmingham B15 2TH, United Kingdom

CS Pitchumoni, Professor
Robert Wood Johnson School of Medicine, Robert Wood Johnson School of Medicine, New Brunswiuc NJ D8903, United States

Gustav Paumgartner, Professor
University of Munich, Klinikum Grosshadern, Marchioninistr. 15, Munich, D-81377, Germany

Ian C Roberts-Thomson, Professor
Department of Gastroenterology and Hepatology, The Queen Elizabeth Hospital, 28 Woodville Road, Woodville South 5011, Australia

Chifumi Sato, Professor
Department of Analytical Health Science, Tokyo Medical and Dental University, Graduate School of Health Sciences, 1-5-45 Yushima, Bunkyoku, Tokyo 113-8519, Japan

Shingo Tsuji, Professor
Department of Internal Medicine and Therapeutics, Osaka University Graduate School of Medicine(A8), 2-2 Yamadaoka, Suita, Osaka 565-0871, Japan

Chun-Yang Wen, M.D.
Department of Molecular Pathology, Atomic Bomb Disease Institute, Nagasaki University Graduate School of Biomedical Sciences. 1-12-4 Sakamoto, Nagasaki 852-8523, Japan

Ming_shiang Wu, Dr, Associate Professor
Internal Medicine, National Taiwan University Hospital, No 7,Chung-Shan S. Rd., Taipei 100, Taiwan, China

Shinichi Wada, M.D.
Department of Gastroenterology, Jichi Medical School, Minamikawachimachi,Kwachi-gun, Tochigi-ken, Tochigi 329-0498, Japan

Masahide Yoshikawa, M.D.
Department of Parasitology, Nara Medical University, Shijo-cho 840, Kashihara 634-8521, Japan

Takayuki Yamamoto, M.D.
Inflammatory Bowel Disease Center, Yokkaichi Social Insurance Hospital, 10-8 Hazuyamacho, Yokkaichi 510-0016, Japan

PO Box 2345, Beijing 100023, China
www.wjgnet.com
wjg@wjgnet.com

ELSEVIER

World J Gastroenterol 2005;11(44):7059
World Journal of Gastroenterology ISSN 1007-9327

Meetings

MAJOR MEETINGS COMING UP

American College of Gastroenterology Annual Scientific Meeting
October 28 -November 2, 2005
annualmeeting@acg.gi.org
www.acg.gi.org

EVENTS AND MEETINGS IN THE UPCOMING 6 MONTHS

ISGCON2005
November 11-15, 2005
isgcon2005@yahoo.co.in
isgcon2005.com

II Latvian Gastroenterology Congress
November 29, 2005
gec@stradini.lv
www.gastroenterologs.lv

70th ACG Annual Scientific Meeting and Postgraduate Course
October 28-November 2, 2005

Advanced Capsule Endoscopy Users Course
November 18-19, 2005
www.asge.org/education

2005 CCFA National Research and Clinical Conference - 4th Annual Advances in the Inflammatory Bowel Diseases
December 1-3, 2005
c.chase@imedex.com
www.imedex.com/calendars/therapeutic.htm

EVENTS AND MEETINGS IN 2005

XIII Argentine Hepatology Congress
XIII Congreso Argentino de HepatologÃa
June 10-13, 2005
mci@mcimeetings.com
www.hepatologia.org

9th Annual Coolum Update in Gastroenterology & Hepatology
June 11-13, 2005
info@e-Kiddna.com.au

Canadian Digestive Disease Week Conference
February 26-March 6, 2005
www.cag-acg.org

2005 World Congress of Gastroenterology
September 12-14, 2005
wcog2005@congrex.nl

International Colorectal Disease Symposium 2005
February 3-5, 2005
info@icds-hk.org

15th World Congress of the International Association of Surgeons and Gastroenterologists
September 7-10, 2005
iasg2005@guarant.cz
www.iasg2005.cz

7th International Workshop on Therapeutic Endoscopy
September 10-12, 2005
alfa@alfamedical.com
www.alfamedical.com

EASL 2005 the 40th annual meeting
April 13-17, 2005
www.easl.ch/easl2005/

ISGCON2005
November 11-15, 2005
isgcon2005@yahoo.co.in
isgcon2005.com

Pediatric Gastroenterology, Hepatology and Nutrition
March 13, 2005

II Latvian Gastroenterology Congress
November 29, 2005
gec@stradini.lv
www.gastroenterologs.lv

21st annual international congress of Pakistan society of Gastroenterology & GI Endoscopy
March 25-27, 2005
psgc05@hotmail.com
www.psgc2005.com

8th Congress of the Asian Society of HepatoBiliary Pancreatic Surgery
February 10-13, 2005

1º Workshop de Gastrenterologia para Clínica Geral
April 29, 2005
luis.m.lopes@sapo.pt

APDW 2005 - Asia Pacific Digestive Week 2005
September 25-28, 2005
asiapdw@kornet.net
www.apdw2005.org

World Congress on Gastrointestinal Cancer
June 15-18, 2005
meetings@imedex.com

British Society of Gastroenterology Conference
March 14-17, 2005
www.bsg.org.uk

Training Director's Workshop:Developing and Teaching Principles in the New Era of GI Training
February 4-6, 2005
www.asge.org/education

The Pharmacological, Surgical and Endoscopic Management of GERD
April 8-9, 2005
www.asge.org/education

Digestive Disease Week
DDW 106th Annual Meeting
May 15-18, 2005
ddwadmin@gastr.org
www.ddw.org

ASGE Advanced Endscopy Skills Hands-on Sessions
May 15, 2005
www.asge.org/education

ASGE GERD Hands-on Session
May 17, 2005
www.asge.org/education

Annual Postgraduate Course
May 18-19, 2005
www.asge.org/education

Advanced Capsule Endoscopy Users Course
June 4-5, 2005
www.asge.org/education

Advanced Capsule Endoscopy Users Course
August 12-13, 2005
www.asge.org/education

GI Practice Management Symposium: Solutions for a Successful Practice
August 18, 2005
www.asge.org/education

70th ACG Annual Scientific Meeting and Postgraduate Course
October 28-November 2, 2005

Advanced Capsule Endoscopy Users Course
November 18-19, 2005
www.asge.org/education

2005 CCFA National Research and Clinical Conference - 4th Annual Advances in the Inflammatory Bowel Diseases
December 1-3, 2005
c.chase@imedex.com
www.imedex.com/calendars/therapeutic.htm

EVENTS AND MEETINGS IN 2006

10th World Congress of the International Society for Diseases of the Esophagus
February 22-25, 2006
isde@sapmea.asn.au
www.isde.net

Easl 2006 - The 41st Annual Meeting
April 26-30, 2006

Canadian Digestive Disease Week Conference
March 4-12, 2006
www.cag-acg.org

XXX pan-american congress of digestive diseases
XXX congreso panamericano de anfermedades digestivas
November 25-December 1, 2006
amg@gastro.org.mx
www.gastro.org.mx

World Congress on Gastrointestinal Cancer
June 14-17, 2006
c.chase@imedex.com

7th World Congress of the International Hepato-Pancreato-Biliary Association
September 3-7, 2006
convention@edinburgh.org
www.edinburgh.org/conference

Annual Postgraduate Course
May 25-26, 2006
www.asge.org/education

71st ACG Annual Scientific Meeting and Postgraduate Course
October 20-25, 2006

PO Box 2345, Beijing 100023, China
www.wjgnet.com
wjg@wjgnet.com

ELSEVIER

World J Gastroenterol 2005;11(44):7060-7061
World Journal of Gastroenterology ISSN 1007-9327

Instructions to authors

GENERAL INFORMATION

World Journal of Gastroenterology (*WJG,* ISSN 1007-9327 CN 14-1219/R) is a weekly journal of more than 48 000 circulation, published on the 7th, 14th, 21st and 28th of every month.

Original Research, Clinical Trials, Reviews, Comments, and Case Reports in esophageal cancer, gastric cancer, colon cancer, liver cancer, viral liver diseases, *etc*., from all over the world are welcome on the condition that they have not been published previously and have not been submitted simultaneously elsewhere.

Published jointly by
The WJG Press and Elsevier Inc.

SUBMISSION OF MANUSCRIPTS

Manuscripts should be typed double-spaced on A4 (297×210 mm) white paper with outer margins of 2.5 cm. Number all pages consecutively, and start each of the following sections on a new page: Title Page , Abstract, Introduction, Materials and Methods, Results, Discussion, Acknowledgements, References, Tables, Figures and Figure Legends. Neither the Editors nor the Publisher is responsible for the opinions expressed by contributors. Manuscripts formally accepted for publication become the permanent property of The WJG Press and Elsevier Inc., and may not be reproduced by any means, in whole or in part without the written permission of both the Authors and the Publisher. We reserve the right to put onto our website and copy-edit accepted manuscripts. Authors should also follow the guidelines for the care and use of laboratory animals of their institution or national animal welfare committee.

Authors should retain one copy of the text, tables, photographs and illustrations, as rejected manuscripts will not be returned to the author(s) and the editors will not be responsible for the loss or damage to photographs and illustrations.

Online submission
Online submission is strongly advised. Manuscripts should be submitted through the Online Submission System at: http://www.wjgnet.com/index.jsp. Authors are highly recommended to consult the ONLINE INSTRUCTIONS TO AUTHORS (http://www.wjgnet.com/wjg/help/instructions.jsp) before attempting to submit online. Authors encountering problems with the Online Submission System may send an email describing the problem to wjg@wjgnet.com for assistance. If you submit manuscript online, do not make a postal contribution. A repeated online submission for the same manuscript is strictly prohibited.

Postal submission
Send 3 duplicate hard copies of the full-text manuscript typed double-spaced on A4(297×210 mm) white paper together with any original photographs or illustrations and a 3.5 inch computer diskette or CD-ROM containing an electronic copy of the manuscript including all the figures, graphs and tables in native Microsoft Word format or *.rtf format to:

World Journal of Gastroenterology
Apartment 1066 Yishou Garden,
58 North Langxinzhuang Road,
PO Box 2345, Beijing 100023, China
E-mail: wjg@wjgnet.com
http: //www.wjgnet.com

MANUSCRIPT PREPARATION

All contributions should be written in English. All articles must be submitted using a word-processing software. All submissions must be typed in 1.5 line spacing and in word size 12 with ample margins. The letter font is Tahoma. For authors originating from China, one copy of the Chinese translation of the manuscript is also required (excluding references). Style should conform to our house format. Required information for each of the manuscript sections is as follows:

Title page
Full manuscript title, running title, all author(s) name(s), affiliations, institution(s) and/or department(s) where the work was accomplished, disclosure of any financial support for the research, and the name, full address, telephone and fax numbers and email address of the corresponding author should be involved. Titles should be concise and informative (removing all unnecessary words), emphasize what is NEW, and avoid abbreviations. A short running title of less than 40 letters should be provided. List the author(s)' name(s) as follows: initials and/or first name, middle name or initial(s) and full family name.

Abstract
An informative, structured abstract of no more than 250 words should accompany each manuscript. Abstracts for original contributions should be structured into the following sections: AIM: Only the purpose should be included. METHODS: The materials, techniques, instruments and equipments, and the experimental procedures should be included. RESULTS: The observatory and experimental results, including data, effects, outcome, *etc*. should be included. Authors should present *P* value where necessary, and the significant data should accompany. CONCLUSION: Accurate view and the value of the results should be included.

The format of structured abstracts is at: http://www.wjgnet.com/wjg/help/11.doc

Key words
Please list 3-10 key words that could reflect content of the study.

Text
For most article types, the main text should be structured into the following sections: INTRODUCTION, MATERIALS AND METHODS, RESULTS and DISCUSSION, and should include appropriate Figures and Tables. Data should be presented in the body text or Figures and Tables, not both.

Illustrations
Figures should be numbered as 1, 2, 3 and so on, and mentioned clearly in the main text. Provide a brief title for each figure on a separate page. No detailed legend should be involved under the figures. This part should add into the text where the figures are applicable. Digital images: black and white photographs should be scanned and saved in TIFF format at a resolution of 300 dpi; color images should be saved as CMYK (print files) and not RGB (screen-viewing files). Place each photograph in a separate file. Print images: supply images of size no smaller than 126× 76 mm printed on smooth surface paper; label the image by writing the Figure number and orientation using an arrow. Photomicrographs: indicate the original magnification and stain in the legend. Digital Drawings: supply files in EPS if created by Freehand and Illustrator, or TIFF from Photoshop. EPS files must be accompanied by a version in native file format for editing purposes. Scans of existing line drawings should be scanned at a resolution of 1200 dpi and as close as possible to the size at which they will appear when printed, not smaller. Please use uniform legends for the same subjects. For example: Figure 1 Pathological changes of atrophic gastritis after treatment. A: ...; B: ...;C: ...; D: ...; E: ...; F: ...; G: ...

Tables
Three-line tables should be numbered as 1, 2, 3 and so on, and mentioned clearly in the main text. Provide a brief title for each table. No detailed legend should be involved under the tables. This part should add into the text where the tables are applicable. The information should complement but not duplicate that contained in the text. Use one horizontal line under the title, a second under the column heads, and a third below the Table, above any footnotes. Vertical and italic lines should be omitted.

Notes in tables and illustrations
Data which is not statistically significant should not be noted. $^{a}P<0.05$, $^{b}P<0.01$ ($P>0.05$ should not be noted). If there are other series of *P* values, $^{c}P<0.05$ and $^{d}P<0.01$ are used; Third series of *P* values can be expressed as $^{e}P<0.05$ and $^{f}P<0.01$. Other notes in tables or under illustrations should be expressed as ^{1}F, ^{2}F, ^{3}F; or some other symbols with a superscript (Arabic

numerals) in the upper left corner. In a multi-curve illustration, each curve should be labeled with ●, ○, ■, □, ▲, △, *etc*. in a certain sequence.

Acknowledgments

Brief acknowledgments of persons who have made genuine contributions to the manuscripts and who endorse the data and conclusions are included. Authors are responsible for obtaining written permission to use any copyrighted text and/or illustrations.

References

Cited references should mainly be drawn from journals covered in the Science Citation Index (http://www.isinet.com) and/or Index Medicus (http://www.ncbi.nlm.nih.gov/PubMed) databases. Mention all references in the text, tables and figure legends, and set off by consecutive, superscripted Arabic numerals. References should be numbered consecutively in the order in which they appear in the text. Abbreviate journal title names according to the Index Medicus style (http://www.ncbi.nlm.nih.gov/entrez/query.fcgi?db=journals). Unpublished observations and personal communications are not listed as references. The style and punctuation of the references conform to ISO standard and the Vancouver style (5th edition); see examples below. Reference lists not conforming to this style could lead to delayed or even rejected publication status. Examples:

Standard jounal article (list all authors and include the PubMed ID [PMID] where applicable)

1 **Das KM,** Farag SA. Current medical therapy of inflammatory bowel disease. *World J Gastroenterol* 2000; 6: 483-489 [PMID: 11819634]

2 **Pan BR**, Hodgson HJF, Kalsi J. Hyperglobulinemia in chronic liver disease: Relationships between *in vitro* immunoglobulin synthesis, short lived suppressor cell activity and serum immunoglobulin levels. *Clin Exp Immunol* 1984; 55: 546-551 [PMID: 6231144]

3 **Lin GZ,** Wang XZ, Wang P, Lin J, Yang FD. Immunologic effect of Jianpi Yishen decoction in treatment of Pixu-diarrhoea. *Shijie Huaren Xiaohua Zazhi* 1999; 7: 285-287 [CMFAID:1082371101835979]

Books and other monographs (list all authors)

4 **Sherlock S,** Dooley J. Diseases of the liver and billiary system. 9th ed. Oxford: Blackwell Sci Pub, 1993: 258-296

Chapter in a book (list all authors)

5 **Lam SK.** Academic investigator's perspectives of medical treatment for peptic ulcer. In: Swabb EA, Azabo S. Ulcer disease: investigation and basis for therapy. New York: Marcel Dekker, 1991: 431-450

Electronic journal (list all authors)

6 **Morse SS.** Factors in the emergence of infectious diseases. Emerg Infect Dis serial online, 1995-01-03, cited 1996-06-05; 1(1):24 screens. Available from: URL: http//www.cdc.gov/ncidod/EID/eid.htm

PMID requirement

From the full reference list, please submit a separate list of those references embodied in PubMed, keeping the same order as in the full reference list, with the following information only: (1) abbreviated journal name and citation (e.g. *World J Gastroenterol* 2003;9(11):2400-2403; (2) article title (e.g. Epidemiology of gastroenterologic cancer in Henan Province, China; (3) full author list (e.g. Lu JB, Sun XB, Dai DX, Zhu SK, Chang QL, Liu SZ, Duan WJ; (4) PMID (e.g. 14606064). Provide the full abstracts of these references, as quoted from PubMed on a 3.5 inch disk or CD-ROM in Microsoft Word format and send by post to The *WJG* Press. For those references taken from journals not indexed by *Index Medicus*, a printed copy of the first page of the full reference should be submitted. Attach these references to the end of the manuscript in their order of appearance in the text.

Inappropriate references

Authors should always cite references that are relevant to their article, and avoid any inappropriate references. Inappropriate references include those that are linked with a hyphen and the difference between the two numbers at two sides of the hyphen is more than 5. For example, [1-6], [2-14] and [1, 3, 4-10, 22] are all considered as inappropriate references. Authors should not cite their own unrelated published articles.

Statistical data

Present as mean±SD and mean±SE.

Statistical expression

Express *t* test as *t*(in italics), *F* test as *F*(in italics), chi square test as χ^2(in Greek), related coefficient as *r*(in italics), degree of freedom as γ (in Greek), sample number as *n*(in italics), and probability as *P*(in italics).

Units

Use SI units. For example: body mass, m(B) = 78 kg; blood pressure, p(B)=16.2/12.3 kPa; incubation time, t(incubation)=96 h, blood glucose concentration, c(glucose) 6.4±2.1 mmol/L; blood CEA mass concentration, p(CEA) = 8.6 24.5 μg/L; CO_2 volume fraction, 50 mL/L CO_2 not 5% CO_2; likewise for 40 g/L formaldehyde, not 10% formalin; and mass fraction, 8 ng/g, *etc*. Arabic numerals such as 23,243,641 should be read 23 243 641.

The format about how to accurately write common units and quantum is at: http://www.wjgnet.com/wjg/help/15.doc

Abbreviations

Standard abbreviations should be defined in the abstract and on first mention in the text. In general, terms should not be abbreviated unless they are used repeatedly and the abbreviation is helpful to the reader. Permissible abbreviations are listed in Units, Symbols and Abbreviations: A Guide for Biological and Medical Editors and Authors (Ed. Baron DN, 1988) published by The Royal Society of Medicine, London. Certain commonly used abbreviations, such as DNA, RNA, HIV, LD50, PCR, HBV, ECG, WBC, RBC, CT, ESR, CSF, IgG, ELISA, PBS, ATP, EDTA, mAb, can be used directly without further mention.

Italicization

Quantities: *t* time or temperature, *c* concentration, *A* area, *l* length, *m* mass, *V* volume.

Genotypes: *gyr*A, *arg* 1, *c myc*, *c fos*, *etc*.

Restriction enzymes: *Eco*RI, *Hin*dI, *Bam*HI, *Kbo* I, *Kpn* I, *etc*.

Biology: *Helicobacter pylori, H pylori, E coli, etc*.

SUBMISSION OF THE REVISED MANUSCRIPTS AFTER ACCEPTED

Please revise your article according to the revision policies of *WJG*. The revised version including manuscript and high-resolution image figures (if any) should be copied on a floppy or compact disk. Author should send the revised manuscript, along with printed high-resolution color or black and white photos, copyright transfer letter, the final check list for authors, and responses to reviewers by a courier (such as EMS) (submission of revised manuscript by e-mail or on the WJG Editorial Office Online System is NOT available at present).

Language evaluation

The language of a manuscript will be graded before sending for revision. (1) Grade A: priority publishing; (2) Grade B: minor language polishing; (3) Grade C: a great deal of language polishing; (4) Grade D: rejected. The revised articles should be in grade B or grade A.

Copyright assignment form

It is the policy of WJG to acquire copyright in all contributions. Papers accepted for publication become the copyright of WJG and authors will be asked to sign a transfer of copyright form. All authors must read and agree to the conditions outlined in the Copyright Assignment Form (which can be downloaded from http://www.wjgnet.com/wjg/help/9.doc).

Final check list for authors

The format is at: http://www.wjgnet.com/wjg/help/13.doc

Responses to reviewers

Please revise your article according to the comments/suggestions of reviewers. The format for responses to the reviewers' comments is at: http://www.wjgnet.com/wjg/help/10.doc

Proof of financial support

For paper supported by a foundation, authors should provide a copy of the document and serial number of the foundation.

Publication fee

Authors of accepted articles must pay publication fee.

PO Box 2345, Beijing 100023, China
www.wjgnet.com
wjg@wjgnet.com

ELSEVIER

World J Gastroenterol 2005;11(44):7062
World Journal of Gastroenterology ISSN 1007-9327

World Journal of Gastroenterology standard of quantities and units

Number	Nonstandard	Standard	Notice
1	4 days	4 d	In figures, tables and numerical narration
2	4 days	four days	In text narration
3	day	d	After Arabic numerals
4	Four d	Four days	At the beginning of a sentence
5	2 hours	2 h	After Arabic numerals
6	2 hs	2 h	After Arabic numerals
7	hr, hrs,	h	After Arabic numerals
8	10 seconds	10 s	After Arabic numerals
9	10 year	10 years	In text narration
10	Ten yr	Ten years	At the beginning of a sentence
11	0,1,2 years	0,1,2 yr	In figures and tables
12	0,1,2 year	0,1,2 yr	In figures and tables
13	4 weeks	4 wk	
14	Four wk	Four weeks	At the beginning of a sentence
15	2 months	2 mo	In figures and tables
16	Two mo	Two months	At the beginning of a sentence
17	10 minutes	10 min	
18	Ten min	Ten minutes	At the beginning of a sentence
19	50% (*V/V*)	500 mL/L	
20	50% (m/*V*)	500 g/L	
21	1 M	1 mol/L	
22	10 μM	10 μmol/L	
23	1N HCl	1 mol/L HCl	
24	1N H_2SO_4	0.5 mol/L H_2SO_4	
25	4rd edition	4^{th} edition	
26	15 year experience	15- year experience	
27	18.5 kDa	18.5 ku,18 500u or M_r18 500	
28	25 $g.kg^{-1}/d^{-1}$	25 g/(kg·d) or 25 g/kg per day	
29	6900	6 900	
30	1000 rpm	1 000 r/min	
31	sec	s	After Arabic numerals
32	1 pg·L^{-1}	1 pg/L	
33	10 kilograms	10 kg	
34	13 000 rpm	13 000 *g*	High speed; *g* should be in italic and suitable conversion.
35	1000 *g*	1 000 r/min	Low speed. *g* cannot be used.
36	Gene bank	GenBank	International classified genetic materials collection bank
37	Ten L	Ten liters	At the beginning of a sentence
38	Ten mL	Ten milliliters	At the beginning of a sentence
39	umol	μmol	
40	30 sec	30 s	
41	1 g/dl	10 g/L	10-fold conversion
42	OD_{260}	A_{260}	"OD" has been abandoned.
43	One g/L	One microgram per liter	At the beginning of a sentence
44	*A*260 nm	A_{260} nm	*A* should be in italic.
	^{b}P<0.05	^{a}P<0.05	In Table, no note is needed if there is no significance in statistics: ^{a}P<0.05, ^{b}P<0.01 (no note if P>0.05). If there is a second set of P value in the same table, ^{c}P<0.05 and ^{d}P<0.01 are used for a third set: ^{e}P<0.05, ^{f}P<0.01.
45	**F*=9.87, $^{\S}F$=25.9, $^{\#}F$=67.4	^{1}F=9.87,^{2}F=25.9, ^{3}F=67.4	Notices in or under a table
46	KM	km	kilometer
47	CM	cm	centimeter
48	MM	mm	millimeter
49	Kg, KG	kg	kilogram
50	Gm, gr	g	gram
51	nt	N	newton
52	l	L	liter
53	db	dB	decibel
54	rpm	r/min	rotation per minute
55	bq	Bq	becquerel, a unit symbol
56	amp	A	ampere
57	coul	C	coulomb
58	HZ	Hz	
59	w	W	watt
60	KPa	kPa	kilo-pascal
61	p	Pa	pascal
62	ev	EV	volt (electronic unit)
63	Jonle	J	joule
64	J/mmol	kJ/mol	kilojoule per mole
65	10×10×$10cm^3$	10 cm×10 cm×10 cm	
66	N·km	KN·m	moment
67	$\bar{x}$±s	mean±SD	In figures, tables or text narration
68	Mean±SEM	mean±SE	In figures, tables or text narration
69	*im*	im	intramuscular injection
70	*iv*	iv	intravenous injection
71	Wang et al	Wang *et al.*	
72	EcoRI	*Eco*RI	*Eco* in italic and RI in positive. Restriction endonuclease has its prescript form of writing.
73	Ecoli	*E.coli*	Bacteria and other biologic terms have their specific ex pression.
74	Hp	*H pylori*	
75	Iga	*Iga*	writing form of genes
76	*igA*	IgA	writing form of proteins
77	-70 kDa	~70 ku	